frontiers | Research Topics

Industrial and health applications of lactic acid bacteria and their metabolites, volume II

Edited by
Paloma López and Giuseppe Spano

Published in
Frontiers in Microbiology

ISSN 1664-8714
ISBN 978-2-8325-3031-3
DOI 10.3389/978-2-8325-3031-3

About Frontiers

Frontiers is more than just an open access publisher of scholarly articles: it is a pioneering approach to the world of academia, radically improving the way scholarly research is managed. The grand vision of Frontiers is a world where all people have an equal opportunity to seek, share and generate knowledge. Frontiers provides immediate and permanent online open access to all its publications, but this alone is not enough to realize our grand goals.

Frontiers journal series

The Frontiers journal series is a multi-tier and interdisciplinary set of open-access, online journals, promising a paradigm shift from the current review, selection and dissemination processes in academic publishing. All Frontiers journals are driven by researchers for researchers; therefore, they constitute a service to the scholarly community. At the same time, the *Frontiers journal series* operates on a revolutionary invention, the tiered publishing system, initially addressing specific communities of scholars, and gradually climbing up to broader public understanding, thus serving the interests of the lay society, too.

Dedication to quality

Each Frontiers article is a landmark of the highest quality, thanks to genuinely collaborative interactions between authors and review editors, who include some of the world's best academicians. Research must be certified by peers before entering a stream of knowledge that may eventually reach the public - and shape society; therefore, Frontiers only applies the most rigorous and unbiased reviews. Frontiers revolutionizes research publishing by freely delivering the most outstanding research, evaluated with no bias from both the academic and social point of view. By applying the most advanced information technologies, Frontiers is catapulting scholarly publishing into a new generation.

What are Frontiers Research Topics?

Frontiers Research Topics are very popular trademarks of the *Frontiers journals series*: they are collections of at least ten articles, all centered on a particular subject. With their unique mix of varied contributions from Original Research to Review Articles, Frontiers Research Topics unify the most influential researchers, the latest key findings and historical advances in a hot research area.

Find out more on how to host your own Frontiers Research Topic or contribute to one as an author by contacting the Frontiers editorial office: frontiersin.org/about/contact

Industrial and health applications of lactic acid bacteria and their metabolites, volume II

Topic editors

Paloma López — Margarita Salas Center for Biological Research, Spanish National Research Council (CSIC), Spain

Giuseppe Spano — University of Foggia, Italy

Citation

López, P., Spano, G., eds. (2023). *Industrial and health applications of lactic acid bacteria and their metabolites, volume II*. Lausanne: Frontiers Media SA.

doi: 10.3389/978-2-8325-3031-3

Table of contents

frontiers | Frontiers in Microbiology

TYPE Editorial
PUBLISHED 04 July 2023
DOI 10.3389/fmicb.2023.1242253

OPEN ACCESS

EDITED AND REVIEWED BY
Aldo Corsetti,
University of Teramo, Italy

*CORRESPONDENCE
Paloma López
✉ plg@cib.csic.es

RECEIVED 18 June 2023
ACCEPTED 21 June 2023
PUBLISHED 04 July 2023

CITATION
López P and Spano G (2023) Editorial: Industrial and health applications of lactic acid bacteria and their metabolites, volume II.
Front. Microbiol. 14:1242253.
doi: 10.3389/fmicb.2023.1242253

Editorial: Industrial and health applications of lactic acid bacteria and their metabolites, volume II

Paloma López[1]* and Giuseppe Spano[2]

[1]Departamento de Biotecnología Microbiana y de Plantas, Centro de Investigaciones Biológicas Margarita Salas, CSIC, Madrid, Spain, [2]Department of Agriculture Food Natural Science Engineering, University of Foggia, Foggia, Italy

KEYWORDS

Lactic Acid Bacteria, probiotic, postbiotic, bacteriocin, exopolysaccharides, antioxidant activity, anti-gout activity

Editorial on the Research Topic
Industrial and health applications of lactic acid bacteria and their metabolites, volume II

Lactic acid bacteria (LAB) are a heterogeneous group of species, which synthesize lactic acid as the major product of sugar fermentations. LAB are an industrially important group of microorganisms used throughout the world for a large variety of food fermentations, such as those of dairy, wine, bread, and vegetables. The European Food Safety Agency (EFSA) has introduced a system for a premarket safety assessment of selected taxonomic groups of microorganisms leading to a "Qualified Presumption of Safety" (QPS), the European equivalent of the Generally Recognized As Safe (GRAS) status. Several species of food associated LAB have obtained a QPS status. The adaptability of LAB to fermentation processes, their biosynthetic capacity and metabolic versatility, are some of the principal features that facilitate the application of LAB as microbial starters for producing, releasing and/or increasing specific beneficial compounds in fermented food. In addition, LAB produce compounds related to the food safety which just prevent the growth of pathogens (e.g., antimicrobial peptides) or conversely generating compounds which can cause serious health problems in humans (e.g., biogenic amines). Therefore, characterization and usage of new bacteriocins and antifungal compounds for food preservation by LAB are subjects of current studies in the field. LAB are also natural members of the human gastrointestinal microbiota and several strains are considered beneficial to the host and have been selected for probiotic applications. Likewise, there are a number of metabolites produced by these organisms, such as vitamins, polyphenols and gamma-aminobutyric acid (postbiotic and/or antioxidants) as well as certain polysaccharides (prebiotics and postbiotics) whose functions, among others, are to enhance the development of a microbiota that is beneficial to the human and animal gastrointestinal tract, as well as possibly possessing an immunomodulating effect. These aspects constitute an important field of research that could lead to the production of fermented functional foods (and beverages) which benefit human health.

In this context, the special issue received several contributions on the health applications of lactic acid bacteria (LAB) and their metabolites. The beneficial effect of LAB on two human trials have been reported in this special issue. First, Mozota et al. studied at the metataxonomic level the influence of *Ligilactobacillus salivarius* CECT administration during a period of 4 months in the functional, nutritional, and immunological status

of elderly people living in a nursing home greatly affected by the COVID-19 pandemic. The obtained results indicated that the LAB colonized temporally the intestinal tract of the treated elderly improving the above mentioned status without altering the structure of their nasal and fecal bacteriomes at the genus level. Second, Rodríguez J. M. et al. explored the usage of LAB for alleviation of gout symptoms. The authors analyzed the capability of 13 *Ligilactobacillus salivarius* strains to degrade purines. Among them, *Ligilactobacillus salivarius CECT* 3063 showed the best ability to consume purines with no significant production of uric acid. Thus, this LAB was investigated in a randomized pilot trial on hyperuremic patients. The results showed, among other beneficial effects, a significant reduction of the gout episodies, and in the use of drugs for hyperuremic treatments.

Also, in this special issue LAB have been tested using a rat model, Jeong et al. evaluated the combination of different commercial probiotic mix (including 4 lactobacilli as well as strains belonging to the *Streptococcus thermophilus* (1) and *Bifidobacterium animalis* (1) species) on the reduction of loperamide-induced constipation. The results indicated that the probiotic mix reduce the constipation symtoms by improving the intestinal microbiota through an alteration of the levels of serotonin, mucin and short-chain fatty acids.

Many LAB have probiotic properties and they contribute to improve the properties of food during fermentation. In this context, Rodríguez J. et al. investigated the behavior of *Lactococcus lactis* LA1, *Lactococcus cremoris* LA10 and *Lactiplantibacillus plantarum* LA30 as a consortium in a fermented dairy product, performing the study by means of metabolic analysis correlated with genomic analysis.

Extracellular vesicles (EVs) present in milk or produced by probiotic bacteria have beneficial health properties. Thus, Perez Martínez et al. has investigated the protein content of EV produced by *Lacteicaseibacillus paracasei* produced in fermented dairy products.

Some compounds produced by LAB, such as exopolysaccharides (EPS) and vitamins, can act as postbiotics and immunomodulators with beneficial effects for health when produced by the bacteria *in situ* during elaboration of fermented foods. Thus, Díez-Ozaeta et al. isolated and characterized riboflavin (vitamin B_2)-overproducing *Weissella cibaria* spontaneous mutants obtained by treatment of dextran (a EPS)- and riboflavin-producing parental strains isolated from rye sourdoughs with roseoflavin. Also, the authors proposed an *in silico* and *in vitro* procedure to detect riboflavin-overproducing mutants prior their isolation. In addition, to understand how to improve EPS production, Besrour-Ouam et al. performed a proteomic analysis of the role of the dextran production in the adaptation of the bacteria to temperature changes using as a model system *Leuconostoc lactis* AV1n isolated from avocado. A review article was presented by Pérez-Alvarado et al., in which on the basis of current knowledge the authors proposed an overview of the postbiotic-like relevance of LAB and yeasts from sourdough in breadmaking.

Hu et al. explored the antioxidant potential and probiotic properties of 15 LAB isolated from "Jiangshui" and pickled foods. Among them, two *Lactobacillus fermentans* strains (J2-5, and J2-9) shown to be the best candidates for potential future application in functional food design and healthcare.

LAB use many mechanisms for adaptation to changes in the environment and Acciarri et al. chose *Enterococcus faecalis*, a commensal bacterium of the digestive tract, to study and interrelate, its two potassium transporters with the bacterial response to alkaline and hyperosmotic stresses. High adhesion capability of probiotic bacteria could improve their beneficial effect in the gut, and Racioppo et al. has shown that ultrasound pretreatment of *Lactiplantibacillus plantarum* (but not of bifidobacteria) enhance the LAB capability to form biofilm.

In several cases, the health application of LAB deals with the antimicrobial activities of molecules produced by the tested bacteria. Vitale et al. assessed the antibiofilm activity of cell-free supernatant (CFS) of *Limosilactobacillus reuteri* DSM 17938 cultures on pathogenic microorganisms (*Escherichia coli* ATCC 25922, *Pseudomonas aeruginosa* ATCC 27853, *Staphylococcus aureus* ATCC 29213, *Streptococcus mutants* UA 159 and *Fusobacterium nucleatum* ATCC 25586 and carried out an NMR-based metabolomic exploration of the target matrix. The results of this study revealed a promising potential of the CFS and the subfractions of *Limosilactobacillus reuteri* DSM 17938 for eradication of biofilm in nosocomial and oral infections. In addition, Vanitha et al. investigated the activity of 20 LAB isolated from Haria, (a fermented rice beverage) against the dermatophyte fungus, *Trichophyton tonsurans*. Among these, the *Lactiplantibacillus plantarum* MYSN7 strain showed probiotic properties, and its CFS showed the best antifungal activity. Thus, this LAB could have a potential use as an antidermatophytic formulation. Bengoa et al. proposed the exploitation of exopolysaccharide-producing *Lacticaseibacillus paracasei* strains isolated from kefir for the production of fermented milk with antagonistic activity against intestinal pathogens. Chen et al. using cold-smoked salmon as model system, analyzed the effect of nisin on survival of three *Listeria monocytogenes* serotypes during storage. The results showed variations within *L. monocytogenes* depending on serotype, nisin concentration and temperature of storage. In addition, Nie et al. performed transcriptomic and proteomic analyses to get insight into the mechanisms involved in the enhancement of plantaricin production by *Lactiplantibacillus paraplantarum* RX-8 as a response to exposure of the BAL to the yeast *Wickerhamomyces anomalus* Y-5 by co-culture. The results showed an increase of the expression of the *L. paraplantarum plnABCDEF* cluster in the presence of the fungus as well as activation of various metabolic pathways that could provide energy for the plantaricin synthesis. Furthermore, Cebrian et al. reviewed the possible therapeutic use of AS-48, a head-to-tail cyclized cationic bacteriocin, produced by *Enterococcus faecalis*.

Finally, as an application of industrial interest, Sharma et al. reviewed the current knowledge on mechanisms of spoilage during storage of chicken and seafood products and methods for their preservation. In view of the state of the art, it is proposed the combination of LAB with essential oils as green preservative solutions for these types of food products. However, the authors state that the incorporation of these anti-spoilage agents requires assessment of their potential to alter food properties and of their possible risks.

Author contributions

GS wrote the draft of the editorial. PL corrected the draft and generate the final version. All authors contributed to the article and approved the submitted version.

Conflict of interest

The authors declare that the research was conducted in the absence of any commercial or financial relationships that could be construed as a potential conflict of interest.

Publisher's note

frontiers | Frontiers in Microbiology

TYPE Original Research
PUBLISHED 06 September 2022
DOI 10.3389/fmicb.2022.930400

OPEN ACCESS

EDITED BY
Paloma López,
Margarita Salas Center for Biological Research (CSIC), Spain

REVIEWED BY
Beatriz Martínez,
Spanish National Research Council, Spain
Gonçalo Nieto Almeida,
Instituto Nacional Investigaciao Agraria e Veterinaria (INIAV), Portugal

*CORRESPONDENCE
Ruixi Chen
rc836@cornell.edu

SPECIALTY SECTION
This article was submitted to Food Microbiology, a section of the journal Frontiers in Microbiology

RECEIVED 27 April 2022
ACCEPTED 01 July 2022
PUBLISHED 06 September 2022

CITATION
Chen R, Skeens JW, Wiedmann M and Guariglia-Oropeza V (2022) The efficacy of nisin against *Listeria monocytogenes* on cold-smoked salmon at natural contamination levels is concentration-dependent and varies by serotype. *Front. Microbiol.* 13:930400. doi: 10.3389/fmicb.2022.930400

The efficacy of nisin against *Listeria monocytogenes* on cold-smoked salmon at natural contamination levels is concentration-dependent and varies by serotype

Ruixi Chen*, Jordan William Skeens, Martin Wiedmann and Veronica Guariglia-Oropeza

Department of Food Science, Cornell University, Ithaca, NY, United States

Cold-smoked salmon is a ready-to-eat food product capable of supporting *Listeria monocytogenes* growth at refrigeration temperatures. While the FDA-approved antimicrobial nisin can be used to mitigate *L. monocytogenes* contamination, stresses associated with cold-smoked salmon and the associated processing environments may reduce nisin efficacy. A previous study in our laboratory showed that, at high inoculation levels, pre-exposure of *L. monocytogenes* to sublethal concentrations of quaternary ammonium compounds had an overall detrimental effect on nisin efficacy. The objective of this study was to investigate the impact of nisin concentration and storage temperature on nisin efficacy against *L. monocytogenes* inoculated on salmon at natural contamination levels. Three *L. monocytogenes* strains were pre-grown in the presence of sublethal levels of benzalkonium chloride prior to inoculation at ~10^2CFU/g on salmon slices that were pre-treated with either 0, 25, or 250ppm nisin, followed by vacuum-packing and incubation at 4 or 7°C for up to 30days. *L. monocytogenes* was enumerated on days 1, 15, and 30 using direct plating and/or most probable number methods. A hurdle model was constructed to describe the odds of complete elimination of *L. monocytogenes* on salmon and the level of *L. monocytogenes* when complete elimination was not achieved. Our data showed that (i) nisin efficacy (defined as *L. monocytogenes* reduction relative to the untreated control) was concentration-dependent with increased efficacy at 250ppm nisin, and that (ii) 250ppm nisin treatments led to a reduction in *L. monocytogenes* prevalence, independent of storage temperature and serotype; this effect of nisin could only be identified since low inoculation levels were used. While lower storage temperatures (i.e., 4°C) yielded lowered absolute *L. monocytogenes* counts on days 15 and 30 (as compared to 7°C), nisin efficacy did not differ between these two temperatures. Finally, the serotype 1/2b strain was found to be more susceptible to nisin compared with serotype 1/2a and 4b strains on samples incubated at 7°C or treated with 25ppm nisin. This variation of nisin susceptibility across serotypes,

which is affected by both the storage temperature and nisin concentration, needs to be considered while evaluating the efficacy of nisin.

KEYWORDS

***Listeria monocytogenes*, nisin, cold-smoked salmon, antimicrobial concentration, serotype**

Introduction

Listeria (*L.*) *monocytogenes* is a Gram-positive human pathogen, which can cause listeriosis, a potentially life-threatening disease that primarily affects pregnant women (who can pass it on to their newborns), the elderly, and immunocompromised individuals (Farber and Peterkin, 1991; Center for Disease Control, 2020). Since 99% of the human listeriosis cases in the US can be attributed to consumption of contaminated foods (Scallan et al., 2011), controlling *L. monocytogenes* in foods is of crucial importance. However, prevention of *L. monocytogenes* contamination remains extremely challenging due to the wide distribution of *L. monocytogenes* in natural as well as urban environments (Nightingale et al., 2004; Sauders et al., 2012), food processing facilities (Møretrø and Langsrud, 2004; Ferreira et al., 2014), and consumer homes (Ding et al., 2013).

Listeria monocytogenes contamination represents a particular concern and economic burden for the cold-smoked salmon industry. *L. monocytogenes* has been reported to be frequently found in raw materials (i.e., salmon; Eklund et al., 1995; Di Ciccio et al., 2012) and smoked seafood processing environments (Dauphin et al., 2001; Vogel et al., 2001; Di Ciccio et al., 2012; Nakari et al., 2014). Importantly, the process of cold smoking (usually at a temperature less than 30°C) does not represent an effective kill step for *L. monocytogenes* (Eklund et al., 1995; Cornu et al., 2006). Although the initial *L. monocytogenes* contamination levels are usually low (Rørvik, 2000), samples with *L. monocytogenes* levels exceeding 10^6 CFU/g have been reported (Acciari et al., 2017), as the time and temperature of storage (Kang et al., 2012) as well as the intrinsic characteristics of smoked fish (e.g., water activity, pH, and salt content) normally fall within a range that allows for growth of *L. monocytogenes* (Seeliger and Jones, 1984). Consequently, cold-smoked salmon products have been associated with a number of listeriosis outbreaks and food recalls worldwide (Goetz, 2013; Nakari et al., 2014; Gillesberg Lassen et al., 2016; Schjørring et al., 2017; Vincent and Merchant, 2018).

One possible strategy to control *L. monocytogenes* contamination of cold-smoked salmon products is the application of FDA-approved, Generally Recognized As Safe (GRAS) bacteriocins (Mokoena, 2017). Nisin, a bacteriocin naturally produced by some strains of *Lactococcus lactis*, exhibits antimicrobial activity against a broad range of Gram-positive spoilage microorganisms and foodborne pathogens, including *L. monocytogenes* (Singh, 2018). Nisin kills bacterial cells mainly by recognizing and binding to lipid II in cell membrane, which is used as a "docking molecule" to assemble and form pores efficiently, leading to dissipation of the proton motive force (Brötz et al., 1998; Breukink et al., 1999; Breukink and de Kruijff, 2006).

Commercialized nisin has been used for controlling *L. monocytogenes* on cold-smoked salmon products (Neetoo and Mahomoodally, 2014), and while a specific limit has not been stipulated for cold-smoked salmon, the maximum limit of nisin in pasteurized processed cheese spreads has been set to 10,000 IU/g (250 ppm) by FDA (Cleveland et al., 2001). The efficacy of nisin treatments against *L. monocytogenes* on cold-smoked salmon, either by itself or in synergy with other treatments, has been extensively studied at various antimicrobial concentrations and storage temperatures. Several studies were consistent in showing that when challenged with up to 50 ppm nisin on cold-smoked salmon, *L. monocytogenes* experienced an initial decrease in level, followed by a potential regrowth of the population to higher levels (Tang et al., 2013; Kang et al., 2014; Chen et al., 2020). Furthermore, the susceptibility of *L. monocytogenes* to nisin treatments has been reported to be affected by pre-growth condition in growth media (Kang et al., 2015) and by both pre-growth condition and strain diversity on cold-smoked salmon (Chen et al., 2020). Consistent with this, incorporating multiple strains and pre-growth conditions in challenge studies associated with foodborne pathogens has also been suggested by Harrand et al. (2019) and the EURL *Lm* Technical Guidance Document on challenge tests and durability studies for assessing shelf-life of ready-to-eat foods related to *L. monocytogenes* (Bergis et al., 2021). Notably, the aforementioned challenge studies (Tang et al., 2013; Kang et al., 2014; Chen et al., 2020) on cold-smoked salmon were conducted at 7°C (mimicking a slight temperature abuse at the consumer phase) and with high inoculum levels (10^4–10^6 CFU/g). Since storage temperature and inoculum level have been reported to impact the apparent efficacy of nisin treatments (Neetoo et al., 2008), it is essential to validate efficacy of nisin treatments against *L. monocytogenes* on cold-smoked salmon at natural contamination levels and lower temperatures. Moreover, the efficacy of nisin treatments at concentrations higher than 50 ppm for controlling *L. monocytogenes* on cold-smoked salmon remains to be explored.

The objectives of this study were to (i) validate nisin efficacy for controlling *L. monocytogenes* on cold-smoked salmon at low contamination levels (i.e., 10^2 CFU/g) that are more reflective of

natural contamination (European Food Safety Authority, 2013, 2014), as the use of artificially high contamination levels (e.g., 10^6 CFU/g) may not be reflective of the real-world industries and may sometimes overestimate the efficacy of antimicrobial treatments (Yoon et al., 2005; NACMCF, 2010; Spanu et al., 2014), and (ii) explore the impact of antimicrobial concentration and storage temperature on nisin efficacy, under a worst-case scenario (i.e., pre-exposure to sublethal concentrations of quaternary ammonium compounds, which has been shown to decrease nisin susceptibility) that is universally applicable to different *L. monocytogenes* strains (Chen et al., 2020).

Materials and methods

Bacterial strains and culture preparation

Three *L. monocytogenes* strains (Table 1) were selected for this study because they (i) represented the serotypes (i.e., 1/2a, 1/2b, and 4b) commonly associated with human listeriosis and cold-smoked salmon production (Farber and Peterkin, 1991; Clark et al., 2010; Di Ciccio et al., 2012; Vongkamjan et al., 2013), (ii) were isolated from smoked fish finished products, and (iii) were reported to show high, medium, and low nisin susceptibility in previous challenge studies for *L. monocytogenes* on cold-smoked salmon (Tang et al., 2013; Kang et al., 2014; Chen et al., 2020). These strains were preserved in Brain Heart Infusion (BHI) broth with 15% (v/v) glycerol at −80°C. Prior to experiments on cold-smoked salmon, frozen stock cultures were streaked on BHI agar plates, followed by incubation at 37°C for 20–24 h. Inoculum preparation was performed as previously described (Chen et al., 2020) to simulate pre-exposure of *L. monocytogenes* to sublethal concentrations of quaternary ammonium compounds; this pre-exposure was selected as a worst-case scenario as it has been reported (Chen et al., 2020) to reduce nisin efficacy. Briefly, for each strain, single colonies from freshly streaked plates (less than 7 days old) were inoculated into 5 ml BHI broth, followed by incubation with shaking (200 rpm) at 37°C for 18 h. Bacterial cultures were then sub-cultured (1:100) into BHI broth with benzalkonium chloride (final concentration: 0.5 μg/ml) and subsequently incubated at 7°C until mid-logarithmic phase, as previously detailed (Chen et al., 2020).

Nisin stock solution preparation

A commercial preparation of nisin (Nisaplin, containing 2.5% nisin) was provided by DuPont (DuPont, Wilmington, DE). Immediately prior to each experiment, Nisaplin powder (500 mg or 5,000 mg) was added to ultrapure water (15 ml) in a 50 ml centrifuge tube, followed by vortexing until complete dissolution. The nisin concentrations of the stock solution were approximately 833.3 and 8333.3 ppm, which corresponded to a final concentration of 25 and 250 ppm on salmon, respectively, when adding 300 μl of the stock solution onto a 10 ± 0.5 g salmon slice.

Cold-smoked salmon sample preparation

Pre-sliced, vacuum-packed cold-smoked salmon containing celery extract as the nitrite source was provided by Acme Smoked Fish Corporation. A single batch of salmon (300 g per package) was shipped frozen to our laboratory and stored at −20°C. Prior to each experiment, one package was thawed at 4°C overnight. For each *L. monocytogenes* strain, a bacterial culture was prepared as described in section 2.1, and salmon inoculation was performed as previously reported (Kang et al., 2014; Chen et al., 2020). Briefly, for each experiment, 10 ± 0.5 g salmon slices were prepared aseptically for inoculation with each of the three *L. monocytogenes* strains as well as a uninoculated control, two treatments (untreated and treated with either 25 or 250 ppm nisin), and three sampling days during storage (days 1, 15, and 30) for a total of 24 samples. For each of the nisin-treated samples, 300 μl nisin stock solution prepared as described in section 2.2 was evenly distributed on the surface of the salmon slice and further spread with a sterile spreader. The samples were incubated in a biosafety cabinet (NuAire, Inc., Plymouth, MN) for 30 min to facilitate complete absorption of nisin to the surface of salmon. For each *L. monocytogenes* strain, the OD_{600} value of bacterial culture was measured to confirm that mid-logarithmic growth phase was reached. The bacterial culture was subsequently diluted and inoculated onto the surface of salmon slices at a final concentration of ~10^2 CFU/g. The inoculated samples were incubated in a biosafety cabinet for another 30 min, vacuum-packed in Whirl-Pak® filter bags (0.33 mm pore size; oxygen transmission

TABLE 1 *Listeria monocytogenes* strains used in this study.

FSL number[a]	Lineage	Serotype	Ribotype	Source of isolation	Year	References
FSL F2-0237	II	1/2a	DUP-1062D	Finished RTE food product (salmon)	1999	Sauders et al., 2012
FSL L3-0051	I	1/2b	DUP-1042C	Finished RTE food product (salmon)	2002	Sauders et al., 2012
FSL F2-0310	I	4b	DUP-1038B	Finished RTE food product (salmon)	2000	Sauders et al., 2012

[a]Food Safety Lab (FSL) strain information can be found on Food Microbe Tracker, available at: http://www.foodmicrobetracker.com/.

rate: 149.9 cc/in^2/24 h; North American Sales Company, Inc., Pacific Palisades, CA), and incubated at 4 or 7°C for up to 30 days. Three biological replicates were conducted for each combination of nisin concentration (25 ppm vs. 250 ppm) and storage temperature (4°C vs. 7°C).

Evaluation of nisin efficacy against *Listeria monocytogenes* on cold-smoked salmon

For each experiment, *L. monocytogenes* enumeration was performed on days 1, 15, and 30 of incubation, using direct plating on selective and differential media and/or the most probable number (MPN) technique. MPN was used for enumerating *L. monocytogenes* numbers on samples processed on day 1 due to the low inoculation level used. On days 15 and 30, *L. monocytogenes* levels were estimated based on the data obtained from previous experiments; one or both enumeration method(s) were used for each sample such that the range of measurement would most likely cover the actual level of *L. monocytogenes*. Both enumeration methods (MPN and direct plating) are further described in the following sections. Uninoculated samples (negative controls) were processed on each day of enumeration to monitor natural contamination of salmon samples with *L. monocytogenes*, following the FDA bacteriological analytical manual (BAM) procedures for enrichment and isolation of *L. monocytogenes* in food (US Food and Drug Administration, 2017). None of the negative controls in this study yielded colonies with typical *Listeria* morphology, suggesting (i) no natural and cross contamination of the samples with *L. monocytogenes* and (ii) the salmon native microbiota did not contain organisms that share similar morphologies as *L. monocytogenes* on the selective and differential media used.

Quantification by MPN

MPN was performed as described in BAM with modifications (US Food and Drug Administration, 2017). Briefly, each sample was diluted with 90 ml of Buffered *Listeria* Enrichment Broth (BLEB) containing selective agents (acriflavine: 10 mg/l; cycloheximide: 40 mg/l; and sodium nalidixic acid: 50 mg/l) and stomached in the filter bag for 1 min at 260 rpm using a Seward stomacher 400 circulator (Seward Limited, Worthing, United Kingdom). A 4-dilution, 3-tube MPN was then prepared in BLEB containing selective agents using the salmon homogenate (obtained from the clean side of the filter bags used); the 4 dilutions were set up to represent appropriate 10-fold dilutions of the salmon homogenate. The MPN enrichment aliquots were incubated at 30°C for 48 h, along with the rest of the salmon homogenate to achieve an overall detection limit of 0.1 MPN/g. Following incubation, samples were streaked (20 µl) onto Modified Oxford Agar (MOX) plates in duplicate to determine the presence/absence of typical *L. monocytogenes* colonies. All MOX plates were incubated at 30°C for 48 h. For each sample, aliquots that tested positive for *L. monocytogenes* were recorded, followed by calculation of *L. monocytogenes* levels (MPN/g) using the MPN v 0.3.0 package (Ferguson and Ihrie, 2019) in R Statistical Programming Environment (R) v 3.5.2 (R Core Team, 2020).

Quantification by direct plating

For direct plating, each sample was diluted (1:10) and stomached in the filter bag for 1 min at 260 rpm. Subsequently, salmon homogenate was serially diluted with 1% peptone water and appropriate dilutions were spread-plated onto MOX plates in duplicate. All MOX plates were incubated at 30°C for 48 h, followed by enumeration of typical *L. monocytogenes* colonies using a Sphereflash® Automated Colony Counter (Neutec, Albuquerque, NM) to determine *L. monocytogenes* levels (CFU/g).

Statistical analysis

All statistical analyses were performed in R (R Core Team, 2020); raw data and R codes are available on Github.[1] The threshold of significance for all statistical tests was set to $p = 0.05$. Raw *L. monocytogenes* enumeration data estimated using direct plating (CFU/g) and MPN (MPN/g) were decimal log transformed into $\log_{10}$(CFU/g) and $\log_{10}$(MPN/g), respectively. Due to the superior performance of MPN in estimating viable number of bacterial cells at low concentrations, the $\log_{10}$(MPN/g) estimate was primarily used to represent *L. monocytogenes* levels on salmon samples. For samples where $\log_{10}$(MPN/g) estimates were not available or beyond the quantifiable range, $\log_{10}$(CFU/g) was converted to $\log_{10}$(MPN/g) using equation (1), which was generated by fitting a simple linear regression model to preliminary enumeration data of *L. monocytogenes* on samples analyzed by both enumeration methods (Supplementary Figure 1). Consistent with a number of previous studies, the reduction in $\log_{10}$(MPN/g) between untreated and nisin-treated samples (hereafter referred to as "log reduction") was used to infer the overall efficacy of nisin treatments to reduce *L. monocytogenes* levels on salmon; this log reduction could be a result of (i) reductions of *L. monocytogenes* prevalence/levels during the initial killing phase and/or (ii) reduced *L. monocytogenes* growth in the following regrowth phase.

$$\log_{10}(\mathrm{MPN/g}) = 1.007 \times \log_{10}(\mathrm{CFU/g}) + 0.035 \quad (1)$$

It was assumed that *L. monocytogenes* levels on nisin-treated samples were governed by two distinct processes; one process determined whether *L. monocytogenes* was present or not, while the other process determined the distribution of detectable counts

1 https://github.com/FSL-MQIP/LowInoculation_Listeria_Nisin.git

of *L. monocytogenes*. To be able to investigate both processes, a hurdle model was constructed, which comprised (i) mixed effects logistic models for describing the odds of complete elimination of *L. monocytogenes* due to 250 ppm nisin treatments and (ii) a mixed effects linear model for describing *L. monocytogenes* levels when complete elimination was not achieved. As all inoculated samples that tested negative for *L. monocytogenes* were treated with 250 ppm nisin, the Chi-Square test of independence was first performed to assess the association between the complete elimination of *L. monocytogenes* (i.e., absence in the complete 10 g sample) and 250 ppm nisin treatments. To investigate the odds of the complete elimination of *L. monocytogenes*, 250 ppm nisin-treated samples inoculated with the same strain and stored at the same temperature, regardless of storage days, were treated as replicates. The data of 250 ppm nisin-treated samples were fitted with two mixed effects logistic models (the Serotype Elimination Model and the Temperature Elimination Model) using the lme4 v 1.1.21 package (Bates et al., 2015) to assess the impact of serotype and storage temperature on the odds of complete elimination, respectively. For both models, the outcome specified whether *L. monocytogenes* was completely eliminated, and the random effect was the "age" (i.e., duration of frozen storage at −20°C prior to experiment) of the salmon samples. The fixed effect was serotype (reference level: 1/2a) for the Serotype Elimination Model and storage temperature (reference level: 4°C) for the Temperature Elimination Model. For each model, adding additional variables or interactions did not significantly improve the performance according to the likelihood ratio test. For the primary variable of interest (i.e., the fixed effect) of each model, the odds ratio as well as the 95% confidence interval (CI) were estimated, using the broom.mixed v 0.2.6 package (Bolker and Robinson, 2020) for each alternative level in comparison with the reference level. In addition, a mixed effects logistic model specifying storage day as the fixed effect (reference level: day 1) was also constructed (the Day Elimination Model), and the odds ratios and CIs were estimated as part of the justification for treating samples from different storage days as replicates. A *post hoc* sample size calculation was performed to determine the number of 250 ppm nisin-treated samples necessary for obtaining significant odds ratios.

Due to the reduction in *L. monocytogenes* prevalence among 250 ppm nisin-treated samples, to estimate the theoretical initial log reduction that can be achieved, the following equation described by Pouillot et al. (2015) was used.

$$P_{new} = P_{original}\left(\left(1-10^{-D}\right)^{N_0}\right) \quad (2)$$

where $P_{original}$ and P_{new} are the prevalence of *L. monocytogenes* among salmon samples before and after the nisin treatment, respectively, N_0 is the number of *L. monocytogenes* on samples prior to the nisin treatment, and D is the theoretical reduction in $\log_{10}$(MPN/g) that can be achieved by nisin treatments.

To investigate the effect of different factors on *L. monocytogenes* levels on cold-smoked salmon when complete elimination was not achieved, the data for samples with detectable levels of *L. monocytogenes* were fitted with a mixed effects linear model (the Level Model). The outcome of the model was the $\log_{10}$(MPN/g) of *L. monocytogenes* on the samples. Fixed effects included in the model were: (i) nisin concentration, (ii) storage temperature, (iii) serotype, and (iv) day in storage; two-way interactions included were those between (i) nisin concentration and serotype, (ii) nisin concentration and day in storage, (iii) storage temperature and serotype, and (iv) storage temperature and day in storage. All fixed effects were considered as primary variables of interest, and a backwards stepwise selection was performed to determine the interactions to be retained using (i) the F test and (ii) the likelihood ratio test. The "age" of the salmon samples was included in the model as a random effect. A two-way ANOVA was performed on the model to evaluate the impact of the main effects as well as the interactions on the outcome. *Post hoc* pairwise comparison (i.e., Tukey's HSD test) was performed, using the emmeans v 1.4.4 package (Lenth, 2020), for the main effects and interactions that significantly affected the outcome.

Results

The effect of 250 ppm nisin against *Listeria monocytogenes* on cold-smoked salmon involves a stochastic process of complete elimination, which was not affected by storage temperature or serotype

Treatment of cold-smoked salmon with 250 ppm nisin resulted in one of two scenarios: (i) complete elimination of *L. monocytogenes* or (ii) incomplete elimination, recovery, and growth of *L. monocytogenes*. Untreated or 25 ppm nisin-treated samples, on the other hand, all tested positive for *L. monocytogenes*. A Chi-Square test of independence indicated a significant association ($p < 0.001$) between the complete elimination and the 250 ppm nisin treatments. To investigate the odds of complete elimination due to 250 ppm nisin treatment, we assumed that this event occurred within the first 24 h post-inoculation based on two pieces of evidence. Firstly, growth curves of *L. monocytogenes* on 50 ppm nisin-treated salmon retrieved from Tang et al. (2013) suggested nisin was most efficient in killing *L. monocytogenes* at or around 0.44–2.25 days post-inoculation. Since the current study involved a lower inoculum size (10^2 CFU/g instead of 10^4 CFU/g) and a much higher nisin concentration (250 ppm instead of 50 ppm) compared with Tang et al. (2013), it is likely that the complete elimination would be achieved within the first 24 h. Secondly, according to the Day Elimination Model, the odds of complete elimination on days 15 and 30 were not significantly different compared to day 1 (Table 2). Therefore, 250 ppm nisin-treated samples inoculated with a given *L. monocytogenes* strain

TABLE 2 Odds ratios and 95% confidence intervals (CIs) with respect to factors associated with the complete elimination of *Listeria monocytogenes* on cold-smoked salmon samples due to 250 ppm nisin treatments.

Factors (levels)[a]	Odds ratio	95% confidence interval	*p* value
Serotype			
1/2a	1.00	–	–
1/2b	1.26	0.33, 4.74	0.735
4b	0.79	0.20, 3.07	0.729
Storage temperature			
4°C	1.00	–	–
7°C	2.21	0.72, 6.75	0.166
Storage day			
1	1.00	–	–
15	1.27	0.33, 4.97	0.729
30	1.60	0.41, 6.18	0.495

[a]The impact of each factor on the complete elimination was assessed using a mixed effects logistic model at the univariable level. One of the levels was selected as the reference level for calculating odds ratios and CIs.

and stored at the same temperature were considered as replicates for calculating the odds of complete elimination. At a lower detection limit of 0.1 MPN/g, *L. monocytogenes* was undetectable on 21 (39%) of the 54 samples, indicating the potential of highly concentrated nisin treatments to reduce the prevalence of *L. monocytogenes* contamination. For a given combination of serotype and storage temperature, the proportion of samples that showed complete *L. monocytogenes* elimination ranged from 1/9 for serotype 4b at 4°C to 5/9 for serotype 1/2b at 4°C and serotype 1/2a as well as 4b at 7°C (Figure 1). The Temperature Elimination Model estimated an odds ratio of 2.21 (95% CI: 0.72, 6.75; $p = 0.166$) for 7°C in comparison with 4°C, and the Serotype Elimination Model estimated odds ratios of 1.26 (95% CI: 0.33, 4.74; $p = 0.735$) and 0.79 (95% CI: 0.20, 3.07; $p = 0.729$) for serotype 1/2b and 4b, respectively, in comparison with serotype 1/2a (Table 2), indicating that the odds of complete elimination of *L. monocytogenes* on cold-smoked salmon were not significantly affected by strain serotype and storage temperature.

Nisin reduces the level of *Listeria monocytogenes* on cold-smoked salmon in a concentration-dependent manner throughout the storage

In 25 ppm nisin-treated samples and 250 ppm nisin-treated samples in which complete elimination was not achieved, a nisin concentration-dependent reduction in *L. monocytogenes* numbers was observed throughout the storage (Figure 2 and Supplementary Table 1). Specifically, the $\log_{10}$(MPN/g) of *L. monocytogenes* on 0, 25, and 250 ppm nisin-treated samples, averaged over serotypes and temperatures, was 6.82, 5.13, and 1.55 on day 15 and 8.74, 7.78, and 5.50 on day 30. Compared to days 15 and 30, however, the efficacy of nisin treatments for reducing *L. monocytogenes* levels was less pronounced on day 1, as the $\log_{10}$(MPN/g) was only reduced from 2.24 in samples with 0 ppm nisin to 1.72 and 0.59 in samples with 25 and 250 ppm nisin, respectively. In addition, leveraging the *L. monocytogenes* prevalence reduction (from 100 to 61%) among samples treated with 250 ppm nisin, the theoretical initial log reduction due to 250 ppm nisin treatments was estimated to be 3.025. Altogether, these results suggest that 250 ppm nisin treatments have a higher efficacy, compared to 25 ppm nisin treatments, in reducing *L. monocytogenes* levels on cold-smoked salmon.

A mixed effects linear model (the Level Model) was developed to describe the effect of nisin concentration, serotype, storage temperature, day in storage, and four two-way interactions on the levels of *L. monocytogenes* on cold-smoked salmon (see Table 3 for summary statistics of the two-way ANOVA). According to the F tests, all main effects as well as two-way interactions included in the model were significant ($p < 0.05$). However, interpretation was only deemed appropriate for the two-way interactions, which involved each of the main effects. The two-way interaction between nisin concentration and day in storage was determined to be significant ($p < 0.001$), suggesting the impact of nisin concentration on *L. monocytogenes* levels (represented by $\log_{10}$(MPN/g)) on salmon varied across different days in storage. A pairwise comparison analysis using Tukey's HSD test was performed to compare the model-reported estimated marginal means of the *L. monocytogenes* level (hereafter referred to as "EMMLM"), averaged over serotypes and storage temperatures, across different nisin concentrations on each day in storage. The EMMLM for the 250 ppm nisin treatment was significantly lower (adj. $p < 0.05$) compared to 0 and 25 ppm nisin treatments for all days in storage (Figure 3A). Compared to untreated samples, the samples treated with 25 ppm nisin showed a significantly lower EMMLM on days 15 and 30 (adj. $p < 0.05$), with no significant differences observed for day 1 (Figure 3A). These results confirm that the 250 ppm nisin treatment has a higher efficacy in reducing *L. monocytogenes* levels on cold-smoked salmon throughout the storage as compared to the 25 ppm nisin treatment.

Lower storage temperature is associated with reduced *Listeria monocytogenes* level, but does not affect nisin efficacy on cold-smoked salmon

In the Level Model (Table 3), the two-way interaction between storage temperature and day in storage was significant ($p < 0.001$), indicating that the effect of storage temperature on *L. monocytogenes* levels on salmon was dependent on days in storage. Specifically, although no difference in *L. monocytogenes* levels on salmon was observed on day 1, for both days 15 and 30 salmon stored at 4°C showed significantly lower *L. monocytogenes* levels (adj. $p < 0.001$) as compared to salmon stored at 7°C, as

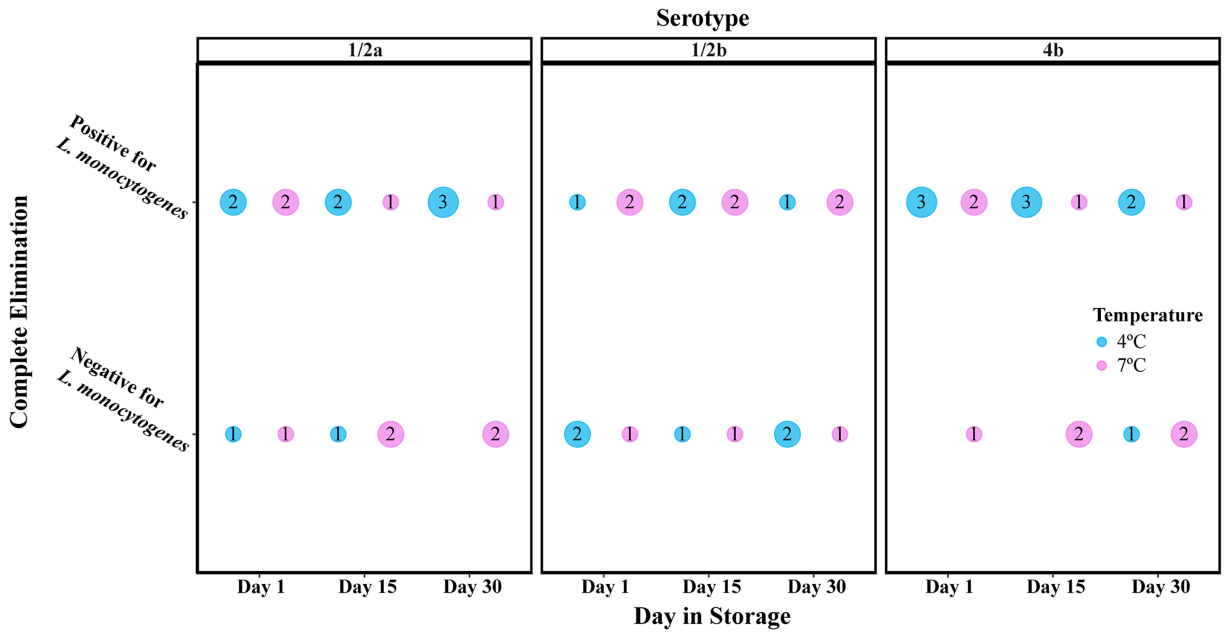

FIGURE 1
Presence/absence of *Listeria monocytogenes* on 10-g cold-smoked salmon samples treated with 250ppm nisin. For each combination of storage temperature, serotype, and day in storage, the number of samples positive and negative for *L. monocytogenes* are indicated in the center of the circles. The size of the circles is in proportion to the number of samples.

indicated by the EMMLM averaged over serotypes and nisin concentrations (Figure 3B). While these data supported more rapid growth of *L. monocytogenes* on salmon stored at 7°C (as compared to 4°C), storage temperature (i.e., 4 or 7°C) did not seem to affect the overall efficacy (i.e., *L. monocytogenes* reduction relative to the untreated controls) of nisin treatment throughout storage, since neither the two-way interaction between nisin concentration and storage temperature nor the three-way interaction between nisin concentration, storage temperature, and day in storage were identified as significant and retained in the Level Model. Importantly, this may suggest that (i) storage at mildly abusive temperature has limited impact on the log reduction achieved during the initial killing phase and (ii) the effect of temperature on *L. monocytogenes* growth does not differ substantially between untreated and nisin-treated samples.

The effect of serotype on *Listeria monocytogenes* levels on cold-smoked salmon is dependent on nisin concentration and storage temperature

Significant interactions were identified between serotype and nisin concentration ($p = 0.015$) as well as between serotype and storage temperature ($p = 0.027$), indicating that *L. monocytogenes* strains from different serotypes grew to different levels in a nisin concentration and storage temperature dependent manner. Compared with the strains representing serotypes 1/2a (FSL F2-0237) and 4b (FSL F2-0310), the EMMLM was significantly lower for the serotype 1/2b strain (FSL L3-0051) on salmon treated with 25 ppm nisin (averaged over storage temperatures and days in storage) or on salmon stored at 7°C (averaged over nisin concentrations and days in storage; Figures 3C,D, respectively). Overall, this indicates that the 1/2b strain was more susceptible to 25 ppm nisin treatment or grew with a slower rate at 7°C compared to the strains from other serotypes. While the three-way interaction between serotype, nisin concentration, and storage temperature was not found to be significant, the raw data suggested *L. monocytogenes* levels on salmon treated with 25 ppm nisin, averaged over days in storage, were consistently lower for the serotype 1/2b strain [$\log_{10}$(MPN/g) = 4.33], compared with the strains from serotypes 1/2a and 4b [$\log_{10}$(MPN/g) = 5.86 and 6.12 for the 1/2a and 4b strains, respectively], following incubation at 7°C (Supplementary Table 1). This difference was not as apparent when the samples were stored at 4°C [$\log_{10}$(MPN/g) = 4.08, 4.74 and 4.15 for the 1/2b, 1/2a, and 4b strains, respectively]. This suggests that the susceptibility of *L. monocytogenes* to 25 ppm nisin may differ across serotypes at 7°C but to a lesser extent at 4°C. Notably, the observed serotype-dependent nisin susceptibility of *L. monocytogenes* may represent strain differences, since only one strain was included in this study to represent each of the serotypes.

Discussion

Assessments of nisin efficacy in reducing *L. monocytogenes* levels on cold-smoked salmon have typically been conducted

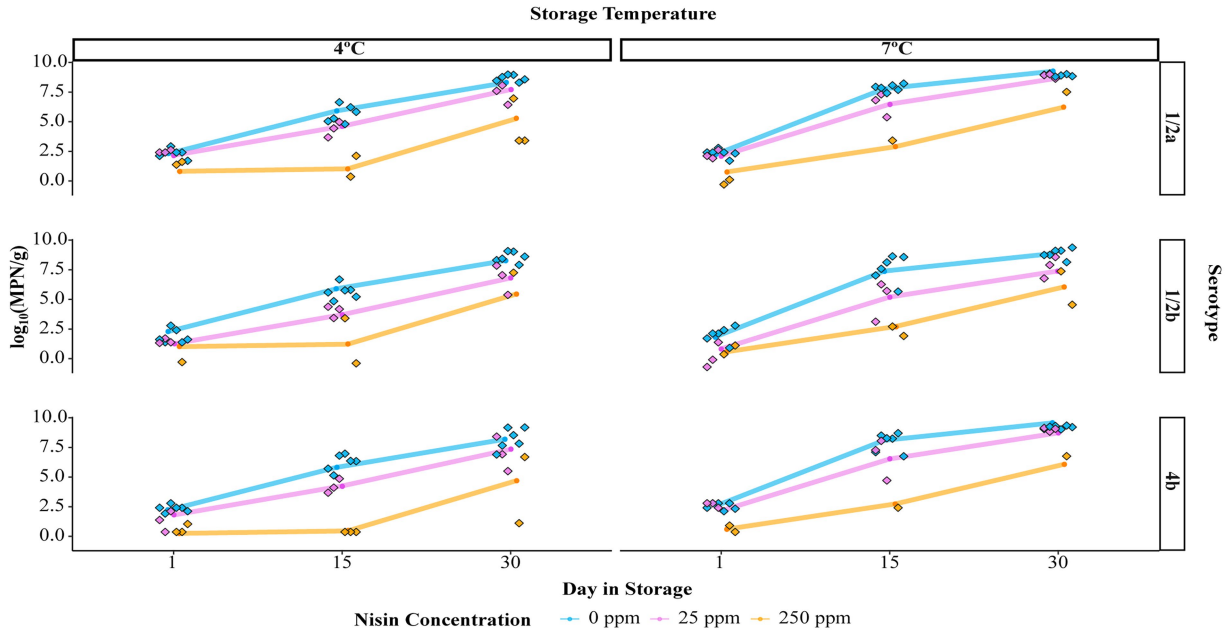

FIGURE 2
Levels of *Listeria monocytogenes* [in $\log_{10}$(MPN/g)] on cold-smoked salmon treated with different concentrations of nisin and stored for up to 30 days. The results are displayed by storage temperature (4°C or 7°C) and serotype of *L. monocytogenes* (1/2a, 1/2b, or 4b). Raw data points are plotted as standalone diamonds and estimated marginal means of the *L. monocytogenes* level (EMMLM) obtained from the mixed effects linear model (the Level Model) are displayed as colored dots connected by solid lines.

TABLE 3 Two-way ANOVA summary of the mixed effects linear model (Level Model).

	Sum sq[a]	Mean sq[a]	NumDF[a]	DenDF[a]	*F* value[a]	Pr(>F)[a]
Nisin concentration	248.58	124.29	2	130.58	186.59	<0.001
Storage temperature	20.38	20.38	1	9.89	30.60	<0.001
Serotype	4.72	2.36	2	169.91	3.54	0.031
Day in storage	869.13	434.57	2	166.69	652.39	<0.001
Nisin concentration: Serotype	8.44	2.11	4	169.03	3.17	0.015
Nisin concentration: Day in storage	50.49	12.62	4	166.46	18.95	<0.001
Storage temperature: Serotype	4.94	2.47	2	167.02	3.71	0.027
Storage temperature: Day in storage	29.94	14.97	2	165.90	22.47	<0.001

[a]Two-way ANOVA statistics of the mixed effects linear model by reference coding (R default). Sum sq.: the sum of squares due to the factor or two-way interaction; Mean sq.: mean of the sum of squares due to the factor or two-way interaction; NumDF: numerator degree of freedom; DenDF: denominator degree of freedom; *F* value: the F-statistic; Pr(>F): the *p* value.

with high inoculation levels, at least in part due to the increased enumeration errors associated with low bacterial concentrations (Spanu et al., 2014). However, it is important to validate the efficacy of nisin treatments at natural contamination levels to better assess their "real world" efficacy. In the current study, the efficacy of nisin treatments to control *L. monocytogenes* on cold-smoked salmon was thus assessed at an inoculum level that resembles natural contamination levels. To reduce enumeration errors associated with low *L. monocytogenes* numbers, we used a combination of MPN and direct plating approaches to achieve an overall lower detection limit of 0.1 MPN/g. Our results suggest that (i) treatments with high levels of nisin can reduce the *L. monocytogenes* prevalence among cold-smoked salmon products; (ii) nisin efficacy against *L. monocytogenes* on cold-smoked salmon does not appear to be reduced by storage at mildly abusive temperature (i.e., 7°C); and (iii) serotype/strain diversity needs to be considered in challenge studies as nisin efficacy varies depending on serotype; the variation in nisin efficacy by serotype is in turn affected by antimicrobial concentration and storage temperature.

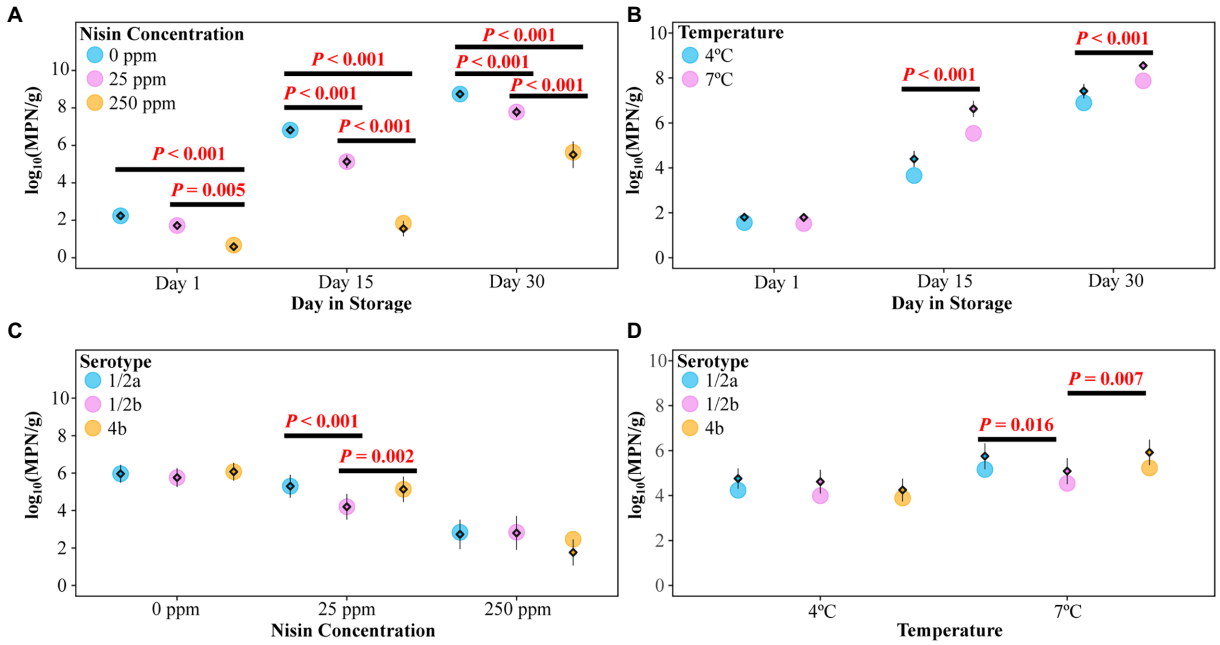

FIGURE 3
Listeria monocytogenes levels [in $\log_{10}$(MPN/g)] on cold-smoked salmon treated with different nisin concentrations and tested on days 1, 15, and 30. Within each panel, raw data points are summarized as means (standalone diamonds)±standard errors (shown as error bars, which sometimes are not visible due to their small values, e.g., the day 1 data shown in panel A) and estimated marginal means of the *L. monocytogenes* level (EMMLM) obtained from the mixed effects linear model (the Level Model) were plotted as circles. **(A)** EMMLMs (averaged over serotypes and storage temperatures) compared across different nisin concentrations on each day in storage. **(B)** EMMLMs (averaged over nisin concentrations and serotypes) compared between storage temperatures on each day in storage. **(C)** EMMLMs (averaged over storage temperatures and days in storage) compared across different serotypes for each nisin concentration. **(D)** EMMLMs (averaged over nisin concentrations and days in storage) compared across different serotypes for each storage temperature. Pairwise comparison of the EMMLMs (within each category shown on the X axis of each panel) was performed using the Tukey's HSD test (overall α=0.05). Significant differences were indicated by the *p* values above horizontal lines.

Treatment with high levels of nisin can reduce the *Listeria monocytogenes* prevalence among cold-smoked salmon products

Our data revealed that increasing nisin concentrations from 25 to 250 ppm significantly increased the efficacy of nisin against *L. monocytogenes*. Although a number of studies have assessed nisin efficacy against *L. monocytogenes* on cold-smoked salmon (Nilsson et al., 1997; Neetoo et al., 2008; Ye et al., 2008; Tang et al., 2013; Kang et al., 2014; Chen et al., 2020), none of them investigated the ability of nisin to lower the prevalence of *L. monocytogenes* contamination. In the current study, *L. monocytogenes* was recovered from 33 (61%) of the 54 salmon samples treated with 250 ppm nisin (as compared to 100% of the samples treated with 25 ppm nisin), indicating the potential of highly concentrated nisin treatments to reduce *L. monocytogenes* prevalence. While our statistical analyses indicated that the odds of complete elimination were independent of storage temperature and serotype, the odds of complete elimination were numerically greater (i.e., 2.21 times greater) for salmon stored at 7°C as compared to 4°C. The fact that the difference in odds of complete elimination between storage temperatures was insignificant (*p* value = 0.166) may be due to a relatively small number of samples tested. Assuming the proportions of 250 ppm nisin-treated samples that tested negative (i.e., 8/27 and 13/27 for 4°C and 7°C, respectively) were realistic, a *post hoc* sample size calculation (Dean et al., 2013) indicated we would have needed 214 salmon samples treated with 250 ppm nisin to identify a significant difference (α = 0.05; power = 80%) in the odds of complete elimination achieved at different storage temperatures. This calculation can be used to estimate sample sizes for possible follow-up studies that would specifically assess the ability of high levels of nisin to eliminate *L. monocytogenes* contamination of smoked salmon.

Given the fact that *L. monocytogenes* prevalence was lowered from 100 to 61% in the 250 ppm nisin-treated samples, the theoretical initial log reduction that could be achieved by 250 ppm nisin treatments was estimated to be 3.025. Various studies have investigated the efficacy of nisin to inactivate *L. monocytogenes* on cold-smoked salmon at similar storage temperatures and initial contamination levels (Nilsson et al., 1997; Neetoo et al., 2008). For salmon inoculated with 2.7 $\log_{10}$(CFU/cm^2) *L. monocytogenes* and stored at 4°C, the initial log reduction in *L. monocytogenes* induced by 12.5 ppm and 50 ppm was <1 and 2.7, respectively (Neetoo et al., 2008). In a

separate study with an inoculum level of 3.2 $\log_{10}$(CFU/g) and a storage temperature of 5°C, the initial log reduction in *L. monocytogenes* following 25 ppm nisin treatment was around 2.2 (Nilsson et al., 1997). This study, for the first time, explored the efficacy of nisin treatment at the maximum allowable level to reduce *L. monocytogenes* on cold-smoked salmon at natural contamination levels, and estimated a theoretical log reduction of 3.025 as well as the possibility of prevalence reduction that could be achieved by this treatment. The results of our study and the previous studies are consistent in suggesting that the nisin efficacy on cold-smoked salmon contaminated with *L. monocytogenes* at natural contamination levels increases in a concentration-dependent manner (higher nisin concentrations lead to higher efficacy). Furthermore, while reduction in prevalence was based on absence of *L. monocytogenes* in 10 g samples, which is lower than both the typical sample size used for testing and the typical package size, our data were also based on (i) an initial inoculation level that could be considered the higher end of natural contamination levels and (ii) *L. monocytogenes* pre-grown under a worst-case scenario (i.e., worst foreseeable conditions that conferred enhanced nisin resistance; Chen et al., 2020). In order to address the impact of different parameters on the complete elimination of *L. monocytogenes*, which could be important in characterizing both public health and recall risks (Pouillot et al., 2007, 2009), the data reported here (and potential new additional data) should be used to conduct risk assessments that model realistic package sizes and include realistic distributions for initial contamination levels.

While our use of low inoculum levels allowed us to identify the potential of treatment with high nisin levels to eliminate *L. monocytogenes*, we also found that nisin efficacy in samples that did not show complete *L. monocytogenes* elimination was overall comparable between low and high *L. monocytogenes* inoculum levels. More specifically, our study here found 0.52, 1.68 and 0.96 log lower *L. monocytogenes* levels on days 1, 15, and 30, respectively, on salmon treated with 25 ppm nisin as compared to the untreated controls, while a previous study conducted in our lab following similar experimental settings (e.g., pre-growth condition, storage temperature, and nisin concentration) but with an inoculum size of 10^6 CFU/g showed 1.07, 1.06, and 0.57 log lower *L. monocytogenes* levels, also for days 1, 15, and 30, respectively (Chen et al., 2020). Hence, for each day we saw a < 0.7 log difference between the low and high inoculation level experiments. Admittedly, the agreement between the results of this study and our previous study may be due in part to the inclusion of the same set of strains. However, high and low inoculation studies need to be performed with the same set of strains for the comparisons of results to be deemed appropriate since strain variability with respect to nisin susceptibility has been reported by previous studies (Rasch and Knøchel, 1998; Katla et al., 2003; Chen et al., 2020) and observed in this study, as further discussed in sections below. Therefore, our findings suggest that the nisin efficacy determined in challenge studies using high inoculation levels can be properly used for guiding industry practices and incorporated in risk assessments for predicting public health and/or recall risks.

Nisin efficacy against *Listeria monocytogenes* on cold-smoked salmon appears to not be impacted by storage at mildly abusive temperature (i.e., 7°C)

Not surprisingly, our data confirmed reduced growth of *L. monocytogenes* on salmon stored at 4°C relative to 7°C, consistent with a number of previous studies (Cornu et al., 2006; Hwang, 2007). Importantly, however, we found no difference in the efficacy of nisin (defined as the log reduction in *L. monocytogenes* numbers in nisin-treated salmon samples relative to the untreated controls) at 4 and 7°C, as supported by the observation that the interaction between nisin concentration and storage temperature was not significant. This finding is consistent with a previous challenge study of *L. monocytogenes* on cold-smoked salmon; when inoculated at 2.7 $\log_{10}$(CFU/cm^2) and challenged with nisin at 12.5 or 50 μg/cm^2, the reduction in *L. monocytogenes* levels on samples stored at 4°C was equal to or lower than on samples stored at 10°C at the end of storage (Neetoo et al., 2008). Different from these findings, an increased nisin sensitivity of *L. monocytogenes* at low temperatures has also been reported. Li et al. (2002) specifically showed that, compared with 30°C, growth of *L. monocytogenes* at 10°C induced an increase in cell membrane fluidity through elevating the percentage of shorter, branched-chain fatty acids and the ratio of anteiso- to iso-configured fatty acids, which was suggested to render the membrane more sensitive to nisin. Increased nisin efficacy against *L. monocytogenes* has also been reported in growth media when temperature was lowered from 12°C to 4°C (Szabo and Cahill, 1998) and in a laboratory-scale cheese model following incubation at 6°C, compared with 14°C and 22°C (Henderson et al., 2020). Many of these studies, however, only identified a reduced nisin efficacy at temperatures typically considered above the typical exposure temperatures of commercially distributed salmon. We thus conclude that nisin appears to maintain the relative added margin of safety at mildly abusive temperatures, which we consider as up to 7°C and possibly up to 10°C, as supported by Neetoo et al. (2008). At abusive temperatures above 10°C one, however, would have to expect a reduced efficacy of nisin. Further studies with larger sample sizes (and *a priori* sample size calculations) may, however, be needed to further clarify the impact of storage temperature on nisin sensitivity.

Biologically, the absence of the impact of storage temperature on nisin efficacy observed here could be attributed to a variety of reasons. Firstly, the temperature difference investigated in this study (4°C versus 7°C) is relatively small and may have limited impact on the fluidity of

cell membrane. By comparison, other studies, as detailed above, evaluated nisin sensitivity at wider temperature ranges where differences in membrane fluidity are larger. Secondly, an overall reduction in nisin activity on salmon (relative to other, low-fat matrices, e.g., BHI) may render the difference in nisin efficacy between storage temperatures less apparent. Nisin has been shown to be less effective in inhibiting *L. monocytogenes* in ice cream and fluid milk with higher fat content (Jung et al., 1992; Dean and Zottola, 1996); similarly, binding of nisin molecules to the fat components of salmon could reduce the efficacy of the antimicrobial. Finally, the bacterial culture used in this study was pre-adapted to 0.5 μg/ml benzalkonium chloride, a pre-growth condition that was reported to provide cross-protection for *L. monocytogenes* against the subsequent nisin treatments (Chen et al., 2020), which also could reduce the effect of temperature differences on nisin sensitivity.

Strain diversity needs to be considered in challenge studies as efficacy of nisin treatments varies depending on serotype, which is affected by antimicrobial concentration and storage temperature

A significant effect of serotype on *L. monocytogenes* levels on salmon was shown for (i) samples treated with 25 ppm nisin and (ii) samples stored at 7°C, as supported by significant two-way interactions between serotype and nisin concentration and between serotype and storage temperature, respectively. Specifically, our data suggests that 1/2b strains may be more susceptible to 25 ppm nisin following incubation at 7°C, as compared to serotypes 1/2a and 4b strains. Similarly, our previous study on salmon conducted with a high inoculation level also demonstrated a higher susceptibility of 1/2b strains to 25 ppm nisin at 7°C, as compared to the serotype 1/2a and 4b strains (Chen et al., 2020). These findings are consistent with a number of studies showing that *L. monocytogenes* from different serotypes can differ in their tolerance to various types of stresses (Lianou et al., 2006; Van Der Veen et al., 2008; Ribeiro and Destro, 2014; Hingston et al., 2017). For instance, serotype 4b strains have been shown to be less susceptible to salt stress (Ribeiro and Destro, 2014), but more susceptible to cold stress (Lianou et al., 2006), compared with strains from serotypes 1/2a and 1/2b. With regard to nisin, different associations between *L. monocytogenes* serotype and nisin susceptibility have been reported. Both serotype 1/2a (Buncic et al., 2001; Szendy et al., 2019) and 4b strains (Ukuku and Shelef, 1997; Henderson et al., 2020) have been reported to be more resistant to nisin, as compared to serotype 1/2b strains, consistent with our results reported here. Some other studies, however, found no effect of serotype on nisin susceptibility (Ferreira and Lund, 1996; Rasch and Knøchel, 1998; Martínez and Rodríguez, 2005). Despite the reported inconsistent results, which could be attributed to the considerable within-serotype strain diversity, the data generated to date suggest that serotype 1/2b strains are in general more susceptible to nisin as compared to strains from serotypes 4b and 1/2a. Hence, our study further emphasizes the importance of using multiple strains encompassing different serovars in challenge studies, which is in line with the suggestions of the "EURL *Lm* Technical Guidance Document on challenge tests and durability studies for assessing shelf-life of ready-to-eat foods related to *L. monocytogenes*" (Bergis et al., 2021), and more specifically stresses that use of solely a serotype 1/2b strain (or strains) may lead to overestimation of the efficacy of nisin treatments. That being the case, the use of one strain from each of the three serotypes in this study by no means represented the entire diversity of *L. monocytogenes* strains. Although hundreds of *L. monocytogenes* strains have been characterized for their natural susceptibility to nisin in culture medium (Rasch and Knøchel, 1998; Katla et al., 2003), we are not aware of similar large-scale studies on cold-smoked salmon. As nisin susceptibility has been reported to differ by matrices (e.g., culture medium vs. salmon), we deliberately selected strains that showed the highest (FSL L3-0051) and lowest (FSL F2-0310) susceptibility to nisin on cold-smoked salmon across different conditions, as suggested by our previous study (Chen et al., 2020). Therefore, the main conclusions of this study regarding nisin efficacy and its variation due to the impact of different factors should be robust and appropriate to support decision making with regard to nisin use on commercial cold-smoked salmon.

Conclusion

The current study demonstrates the concentration-dependent efficacy of nisin treatments against *L. monocytogenes* at natural contamination levels on cold-smoked salmon and highlights the potential of highly concentrated nisin (250 ppm) to reduce the prevalence of *L. monocytogenes* contamination among the salmon products. Our study also supports that a thorough consideration of inoculum size, storage temperature, strain or serotype diversity, and worst-case scenarios that may confer cross-protection is important when assessing the efficacy of nisin treatments at a given concentration. The information gathered in the current study, such as those regarding odds of complete elimination of *L. monocytogenes* on salmon and *L. monocytogenes* levels on salmon under different combinations of storage temperature and antimicrobial concentration, may also be incorporated into existing and new risk assessment models for a better prediction of the reduction in risks of human listeriosis or food recalls that can be achieved by nisin treatments.

Data availability statement

The datasets presented in this study can be found in the GitHub online repositories under the direct link: https://github.com/FSL-MQIP/LowInoculation_Listeria_Nisin.git (Name: LowInoculation_Listeria_Nisin).

Author contributions

RC and JS performed experiments. RC performed statistical analysis. MW and VG-O conceived the study. RC, MW, and VG-O wrote the manuscript. All authors contributed to the article and approved the submitted version.

Funding

This publication is a product resulting from project R/SHH-18 funded under award NA18OAR4170096 from the National Sea Grant College Program of the US Department of Commerce's National Oceanic and Atmospheric Administration, to the Research Foundation for State University of New York Sea Grant. The statements, findings, conclusions, views, and recommendations are those of the author(s) and do not necessarily reflect the views of any of those organizations.

Acknowledgments

The authors thank Maureen Gunderson, Alan Bitar, and Liping Wei for the technical assistance.

Conflict of interest

The authors declare that the research was conducted in the absence of any commercial or financial relationships that could be construed as a potential conflict of interest.

Publisher's note

Supplementary material

The Supplementary material for this article can be found online at: https://www.frontiersin.org/articles/10.3389/fmicb.2022.930400/full#supplementary-material

References

Acciari, V. A., Torresi, M., Iannetti, L., Scattolini, S., Pomilio, F., Decastelli, L., et al. (2017). *Listeria monocytogenes* in smoked salmon and other smoked fish at retail in Italy: frequency of contamination and strain characterization in products from different manufacturers. *J. Food Prot.* 80, 271–278. doi: 10.4315/0362-028X.JFP-15-599

Bates, D., Maechler, M., Bolker, B., and Walker, S. (2015). Fitting linear mixed-effects models using lme4. *J. Stat. Softw.* 67, 1–48. doi: 10.18637/jss.v067.i01

Bergis, H., Bonanno, L., Asséré, A., and Lombard, B. (2021). EURL Lm technical guidance document on challenge tests and durability studies for assessing shelf-life of ready-to-eat foods related to *Listeria monocytogenes*. Available at: https://ec.europa.eu/food/system/files/2021-07/biosafety_fh_mc_tech-guide-doc_listeria-in-rte-foods_en_0.pdf (Accessed June 7, 2021).

Bolker, B., and Robinson, D. (2020). "broom. mixed": tidying methods for mixed models. *R package version 0.2.6.* Available at: https://CRAN.R-project.org/package=broom.mixed (Accessed March 1, 2022).

Breukink, E., Wiedemann, I., Van Kraaij, C., Kuipers, O. P., Sahl, H.-G., and de Kruijff, B. (1999). Use of the cell wall precursor lipid II by a pore-forming peptide antibiotic. *Science* 286, 2361–2364. doi: 10.1126/science.286.5448.2361

Breukink, E., and de Kruijff, B. (2006). Lipid II as a target for antibiotics. *Nat. Rev. Drug Discov.* 5, 321–323. doi: 10.1038/nrd2004

Brötz, H., Josten, M., Wiedemann, I., Schneider, U., Götz, F., Bierbaum, G., et al. (1998). Role of lipid-bound peptidoglycan precursors in the formation of pores by nisin, epidermin and other lantibiotics. *Mol. Microbiol.* 30, 317–327. doi: 10.1046/j.1365-2958.1998.01065.x

Buncic, S., Avery, S. M., Rocourt, J., and Dimitrijevic, M. (2001). Can Food-Related Environmental Factors induce different Behaviour in two key Serovars, 4b and 1r2a, of Listeria monocytogenes? *Int. J. Food Microbiol.* 65, 201–212. doi: 10.1016/S0168-1605(00)00524-9

Center for Disease Control (2020). *Listeria* (Listeriosis). Available at: https://www.cdc.gov/listeria/index.html (Accessed July 26, 2020).

Chen, R., Skeens, J., Orsi, R. H., Wiedmann, M., and Guariglia-Oropeza, V. (2020). Pre-growth conditions and strain diversity affect nisin treatment efficacy against *Listeria monocytogenes* on cold-smoked salmon. *Int. J. Food Microbiol.* 333:108793. doi: 10.1016/j.ijfoodmicro.2020.108793

Clark, C. G., Farber, J., Pagotto, F., Ciampa, N., Doré, K., Nadon, C., et al. (2010). Surveillance for *Listeria monocytogenes* and listeriosis, 1995–2004. *Epidemiol. Infect.* 138, 559–572. doi: 10.1017/S0950268809990914

Cleveland, J., Montville, T. J., Nes, I. F., and Chikindas, M. L. (2001). Bacteriocins: safe, natural antimicrobials for food preservation. *Int. J. Food Microbiol.* 71, 1–20. doi: 10.1016/S0168-1605(01)00560-8

Cornu, M., Beaufort, A., Rudelle, S., Laloux, L., Bergis, H., Miconnet, N., et al. (2006). Effect of temperature, water-phase salt and phenolic contents on *Listeria monocytogenes* growth rates on cold-smoked salmon and evaluation of secondary models. *Int. J. Food Microbiol.* 106, 159–168. doi: 10.1016/j.ijfoodmicro.2005.06.017

Dauphin, G., Ragimbeau, C., and Malle, P. (2001). Use of PFGE typing for tracing contamination with *Listeria monocytogenes* in three cold-smoked salmon processing plants. *Int. J. Food Microbiol.* 64, 51–61. doi: 10.1016/S0168-1605(00)00442-6

Dean, A. G., Sullivan, K. M., and Soe, M. M. (2013). OpenEpi: open source epidemiologic statistics for public health. Available at: www.OpenEpi.com (Accessed January 2, 2021).

Dean, J. P., and Zottola, E. A. (1996). Use of nisin in ice cream and effect on the survival of *Listeria monocytogenes*. *J. Food Prot.* 59, 476–480. doi: 10.4315/0362-028X-59.5.476

Di Ciccio, P., Meloni, D., Festino, A. R., Conter, M., Zanardi, E., Ghidini, S., et al. (2012). Longitudinal study on the sources of *Listeria monocytogenes* contamination in cold-smoked salmon and its processing environment in Italy. *Int. J. Food Microbiol.* 158, 79–84. doi: 10.1016/j.ijfoodmicro.2012.06.016

Ding, T., Iwahori, J., Kasuga, F., Wang, J., Forghani, F., Park, M.-S., et al. (2013). Risk assessment for *Listeria monocytogenes* on lettuce from farm to table in Korea. *Food Control* 30, 190–199. doi: 10.1016/j.foodcont.2012.07.014

Eklund, M. W., Poysky, F. T., Paranjpye, R. N., Lashbrook, L. C., Peterson, M. E., and Pelroy, G. A. (1995). Incidence and sources of *Listeria monocytogenes* in cold-smoked fishery products and processing plants. *J. Food Prot.* 58, 502–508. doi: 10.4315/0362-028X-58.5.502

European Food Safety Authority (2013). Analysis of the baseline survey on the prevalence of *Listeria monocytogenes* in certain ready-to-eat foods in the EU, 2010–2011 part A: *Listeria monocytogenes* prevalence estimates. *EFSA J.* 11, 3241. doi: 10.2903/j.efsa.2013.3241

European Food Safety Authority (2014). Analysis of the baseline survey on the prevalence of *Listeria monocytogenes* in certain ready-to-eat foods in the EU, 2010–2011 part B: analysis of factors related to prevalence and exploring compliance. *EFSA J.* 12, 3810. doi: 10.2903/j.efsa.2014.3810

Farber, J. M., and Peterkin, P. I. (1991). *Listeria monocytogenes*, a food-borne pathogen. *Microbiol. Rev.* 55, 476–511. doi: 10.1128/mr.55.3.476-511.1991

Ferguson, M., and Ihrie, J. (2019). MPN: most probable number and other microbial enumeration techniques. *R package version 0.3.0.* Available at: https://CRAN.R-project.org/package=MPN (Accessed March 1, 2022).

Ferreira, M. A., and Lund, B. M. (1996). The effect of nisin on *Listeria monocytogenes* in culture medium and long-life cottage cheese. *Lett. Appl. Microbiol.* 22, 433–438. doi: 10.1111/j.1472-765X.1996.tb01197.x

Ferreira, V., Wiedmann, M., Teixeira, P., and Stasiewicz, M. J. (2014). *Listeria monocytogenes* persistence in food-associated environments: epidemiology, strain characteristics, and implications for public health. *J. Food Prot.* 77, 150–170. doi: 10.4315/0362-028X.JFP-13-150

Gillesberg Lassen, S., Ethelberg, S., Björkman, J. T., Jensen, T., Sørensen, G., Kvistholm Jensen, A., et al. (2016). Two *Listeria* outbreaks caused by smoked fish consumption—using whole-genome sequencing for outbreak investigations. *Clin. Microbiol. Infect.* 22, 620–624. doi: 10.1016/j.cmi.2016.04.017

Goetz, G. (2013). String of smoked salmon products recalled for Listeria potential. Food Safety News. Available at: https://www.foodsafetynews.com/2013/01/another-smoked-salmon-recall-for-potential-Listeria-contamination/ (Accessed July 26, 2020).

Harrand, A. S., Kovac, J., Carroll, L. M., Guariglia-Oropeza, V., Kent, D. J., and Wiedmann, M. (2019). Assembly and characterization of a pathogen strain collection for produce safety applications: pre-growth conditions have a larger effect on peroxyacetic acid tolerance than strain diversity. *Front. Microbiol.* 10:1223. doi: 10.3389/fmicb.2019.01223

Henderson, L. O., Erazo Flores, B. J., Skeens, J., Kent, D., Murphy, S. I., Wiedmann, M., et al. (2020). Nevertheless, she resisted – role of the environment on *Listeria monocytogenes* sensitivity to nisin treatment in a laboratory cheese model. *Front. Microbiol.* 11:635. doi: 10.3389/fmicb.2020.00635

Hingston, P., Chen, J., Dhillon, B. K., Laing, C., Bertelli, C., Gannon, V., et al. (2017). Genotypes associated with *Listeria monocytogenes* isolates displaying impaired or enhanced tolerances to cold, salt, acid, or desiccation stress. *Front. Microbiol.* 8:369. doi: 10.3389/fmicb.2017.00369

Hwang, C.-A. (2007). Effect of salt, smoke compound, and storage temperature on the growth of *Listeria monocytogenes* in simulated smoked salmon. *J. Food Prot.* 70, 2321–2328. doi: 10.4315/0362-028X-70.10.2321

Jung, D.-S., Bodyfelt, F. W., and Daeschel, M. A. (1992). Influence of fat and emulsifiers on the efficacy of nisin in inhibiting *Listeria monocytogenes* in fluid milk. *J. Dairy Sci.* 75, 387–393. doi: 10.3168/jds.S0022-0302(92)77773-X

Kang, J., Stasiewicz, M. J., Boor, K. J., Wiedmann, M., and Bergholz, T. M. (2014). Optimization of combinations of bactericidal and bacteriostatic treatments to control *Listeria monocytogenes* on cold-smoked salmon. *Int. J. Food Microbiol.* 179, 1–9. doi: 10.1016/j.ijfoodmicro.2014.03.017

Kang, J., Tang, S., Liu, R. H., Wiedmann, M., Boor, K. J., Bergholz, T. M., et al. (2012). Effect of curing method and freeze-thawing on subsequent growth of *Listeria monocytogenes* on cold-smoked salmon. *J. Food Prot.* 75, 1619–1626. doi: 10.4315/0362-028X.JFP-11-561

Kang, J., Wiedmann, M., Boor, K. J., and Bergholz, T. M. (2015). VirR-mediated resistance of *Listeria monocytogenes* against food antimicrobials and cross-protection induced by exposure to organic acid salts. *Appl. Environ. Microbiol.* 81, 4553–4562. doi: 10.1128/AEM.00648-15

Katla, T., Naterstad, K., Vancanneyt, M., Swings, J., and Axelsson, L. (2003). Differences in susceptibility of *Listeria monocytogenes* strains to sakacin P, sakacin A, pediocin PA-1, and nisin. *Appl. Environ. Microbiol.* 69, 4431–4437. doi: 10.1128/AEM.69.8.4431-4437.2003

Lenth, R. (2020). Emmeans: estimated marginal means, aka least-squares means. *R package version 1.4.8.* Available at: https://CRAN.R-project.org/package=emmeans (Accessed March 1, 2022).

Li, J., Chikindas, M. L., Ludescher, R. D., and Montville, T. J. (2002). Temperature- and surfactant-induced membrane modifications that alter *Listeria monocytogenes* nisin sensitivity by different mechanisms. *Appl. Environ. Microbiol.* 68, 5904–5910. doi: 10.1128/AEM.68.12.5904-5910.2002

Lianou, A., Stopforth, J. D., Yoon, Y., Wiedmann, M., and Sofos, J. N. (2006). Growth and stress resistance variation in culture broth among *Listeria monocytogenes* strains of various serotypes and origins. *J. Food Prot.* 69, 2640–2647. doi: 10.4315/0362-028X-69.11.2640

Martínez, B., and Rodríguez, A. (2005). Antimicrobial susceptibility of nisin resistant *Listeria monocytogenes* of dairy origin. *FEMS Microbiol. Lett.* 252, 67–72. doi: 10.1016/j.femsle.2005.08.025

Mokoena, M. P. (2017). Lactic acid bacteria and their bacteriocins: classification, biosynthesis and applications against uropathogens: a mini-review. *Molecules* 22, 1255. doi: 10.3390/molecules22081255

Møretrø, T., and Langsrud, S. (2004). *Listeria monocytogenes*: biofilm formation and persistence in food-processing environments. *Biofilms* 1, 107–121. doi: 10.1017/S1479050504001322

NACMCF (2010). Parameters for determining inoculated pack/challenge study protocols. *J. Food Prot.* 73, 140–202. doi: 10.4315/0362-028X-73.1.140

Nakari, U. M., Rantala, L., Pihlajasaari, A., Toikkanen, S., Johansson, T., Hellsten, C., et al. (2014). Investigation of increased listeriosis revealed two fishery production plants with persistent *Listeria* contamination in Finland in 2010. *Epidemiol. Infect.* 142, 2261–2269. doi: 10.1017/S095026881300349X

Neetoo, H., and Mahomoodally, F. (2014). Use of antimicrobial films and edible coatings incorporating chemical and biological preservatives to control growth of *Listeria monocytogenes* on cold smoked salmon. *Biomed. Res. Int.* 2014, 1–10. doi: 10.1155/2014/534915

Neetoo, H., Ye, M., Chen, H., Joerger, R. D., Hicks, D. T., and Hoover, D. G. (2008). Use of nisin-coated plastic films to control *Listeria monocytogenes* on vacuum-packaged cold-smoked salmon. *Int. J. Food Microbiol.* 122, 8–15. doi: 10.1016/j.ijfoodmicro.2007.11.043

Nightingale, K. K., Schukken, Y. H., Nightingale, C. R., Fortes, E. D., Ho, A. J., Her, Z., et al. (2004). Ecology and transmission of *Listeria monocytogenes* infecting ruminants and in the farm environment. *Appl. Environ. Microbiol.* 70, 4458–4467. doi: 10.1128/AEM.70.8.4458-4467.2004

Nilsson, L., Henrik Huss, H., and Gram, L. (1997). Inhibition of *Listeria monocytogenes* on cold-smoked salmon by nisin and carbon dioxide atmosphere. *Int. J. Food Microbiol.* 38, 217–227. doi: 10.1016/S0168-1605(97)00111-6

Pouillot, R., Chen, Y., and Hoelzer, K. (2015). Modeling number of bacteria per food unit in comparison to bacterial concentration in quantitative risk assessment: impact on risk estimates. *Food Microbiol.* 45, 245–253. doi: 10.1016/j.fm.2014.05.008

Pouillot, R., Goulet, V., Delignette-Muller, M. L., Mahé, A., and Cornu, M. (2009). Quantitative risk assessment of *Listeria monocytogenes* in French cold-smoked salmon: II. Risk characterization. *Risk Anal.* 29, 806–819. doi: 10.1111/j.1539-6924.2008.01200.x

Pouillot, R., Miconnet, N., Afchain, A.-L., Delignette-Muller, M. L., Beaufort, A., Rosso, L., et al. (2007). Quantitative risk assessment of *Listeria monocytogenes* in French cold-smoked salmon: I. quantitative exposure assessment. *Risk Anal.* 27, 683–700. doi: 10.1111/j.1539-6924.2007.00921.x

R Core Team (2020). *R: a Language and Environment for Statistical Computing*. Vienna, Austria: R Foundation for Statistical Computing.

Rasch, M., and Knøchel, S. (1998). Variations in tolerance of *Listeria monocytogenes* to nisin, pediocin PA-1 and bavaricin A. *Lett. Appl. Microbiol.* 27, 275–278. doi: 10.1046/j.1472-765X.1998.00433.x

Ribeiro, V. B., and Destro, M. T. (2014). *Listeria monocytogenes* serotype 1/2b and 4b isolates from human clinical cases and foods show differences in tolerance to refrigeration and salt stress. *J. Food Prot.* 77, 1519–1526. doi: 10.4315/0362-028X.JFP-13-548

Rørvik, L. (2000). *Listeria monocytogenes* in the smoked salmon industry. *Int. J. Food Microbiol.* 62, 183–190. doi: 10.1016/S0168-1605(00)00334-2

Sauders, B. D., Overdevest, J., Fortes, E., Windham, K., Schukken, Y., Lembo, A., et al. (2012). Diversity of *Listeria* species in urban and natural environments. *Appl. Environ. Microbiol.* 78, 4420–4433. doi: 10.1128/AEM.00282-12

Scallan, E., Hoekstra, R. M., Angulo, F. J., Tauxe, R. V., Widdowson, M.-A., Roy, S. L., et al. (2011). Foodborne illness acquired in the United States—major pathogens. *Emerg. Infect. Dis.* 17, 7–15. doi: 10.3201/eid1701.P11101

Schjørring, S., Gillesberg Lassen, S., Jensen, T., Moura, A., Kjeldgaard, J. S., Müller, L., et al. (2017). Cross-border outbreak of listeriosis caused by cold-smoked salmon, revealed by integrated surveillance and whole genome sequencing (WGS), Denmark and France, 2015 to 2017. *Euro Surveill.* 22:762. doi: 10.2807/1560-7917.ES.2017.22.50.17-00762

Seeliger, H. P. R., and Jones, D. (1984). "Genus *Listeria*," in *Bergey's Manual of Systematic Bacteriology*. eds. P. H. A. Sheath, N. S. Maier, M. E. Sharpeand and J. G. Holt (Baltimore, MD: Williams & Wilkins), 1235–1245.

Singh, V. P. (2018). Recent approaches in food bio-preservation: a review. *Open Vet. J.* 8, 104–111. doi: 10.4314/ovj.v8i1.16

Spanu, C., Scarano, C., Ibba, M., Pala, C., Spanu, V., and De Santis, E. P. L. (2014). Microbiological challenge testing for *Listeria monocytogenes* in ready-to-eat food: a practical approach. *Ital. J. Food Saf.* 3, 4518. doi: 10.4081/ijfs.2014.4518

Szabo, E. A., and Cahill, M. E. (1998). The Combined Affects of Modified Atmosphere, Temperature, nisin and ALTATM 2341 on the Growth of *Listeria monocytogenes*. *Int. J. Food Microbiol.*, 43, 21–31.

Szendy, M., Kalkhof, S., Bittrich, S., Kaiser, F., Leberecht, C., Labudde, D., et al. (2019). Structural change in GadD2 of *Listeria monocytogenes* field isolates supports nisin resistance. *Int. J. Food Microbiol.* 305:108240. doi: 10.1016/j.ijfoodmicro.2019.108240

Tang, S., Stasiewicz, M. J., Wiedmann, M., Boor, K. J., and Bergholz, T. M. (2013). Efficacy of different antimicrobials on inhibition of *Listeria monocytogenes* growth in laboratory medium and on cold-smoked salmon. *Int. J. Food Microbiol.* 165, 265–275. doi: 10.1016/j.ijfoodmicro.2013.05.018

Ukuku, D. O., and Shelef, L. A. (1997). Sensitivity of six strains of *Listeria monocytogenes* to nisin. *J. Food Prot.* 60, 867–869. doi: 10.4315/0362-028X-60.7.867

US Food and Drug Administration (2017). BAM Chapter 10: detection of *Listeria monocytogenes* in foods and environmental samples, and enumeration of *Listeria monocytogenes* in foods. Available at: https://www.fda.gov/media/90488/download (Accessed June 7, 2021).

Van Der Veen, S., Moezelaar, R., Abee, T., and Wells-Bennik, M. H. J. (2008). The growth limits of a large number of *Listeria monocytogenes* strains at combinations of stresses show serotype- and niche-specific traits. *J. Appl. Microbiol.* 105, 1246–1258. doi: 10.1111/j.1365-2672.2008.03873.x

Vincent, A., and Merchant, R. (2018). Joint EFSA and ECDC 2018 workshop on preparedness for a multi-national food safety/public health incident. *EFSA Support. Publ.* 15, 1480E. doi: 10.2903/sp.efsa.2018.EN-1480

Vogel, B. F., Jørgensen, L. V., Ojeniyi, B., Huss, H. H., and Gram, L. (2001). Diversity of *Listeria monocytogenes* isolates from cold-smoked salmon produced in different smokehouses as assessed by random amplified polymorphic DNA analyses. *Int. J. Food Microbiol.* 65, 83–92. doi: 10.1016/S0168-1605(00)00503-1

Vongkamjan, K., Roof, S., Stasiewicz, M. J., and Wiedmann, M. (2013). Persistent *Listeria monocytogenes* subtypes isolated from a smoked fish processing facility included both phage susceptible and resistant isolates. *Food Microbiol.* 35, 38–48. doi: 10.1016/j.fm.2013.02.012

Ye, M., Neetoo, H., and Chen, H. (2008). Effectiveness of chitosan-coated plastic films incorporating antimicrobials in inhibition of *Listeria monocytogenes* on cold-smoked salmon. *Int. J. Food Microbiol.* 127, 235–240. doi: 10.1016/j.ijfoodmicro.2008.07.012

Yoon, Y., Calicioglu, M., Kendall, P. A., Smith, G. C., and Sofos, J. N. (2005). Influence of inoculum level and acidic marination on inactivation of *Escherichia coli* O157:H7 during drying and storage of beef jerky. *Food Microbiol.* 22, 423–431. doi: 10.1016/j.fm.2004.09.012

frontiers | Frontiers in Microbiology

TYPE Review
PUBLISHED 08 September 2022
DOI 10.3389/fmicb.2022.969460

OPEN ACCESS

EDITED BY
Giuseppe Spano,
University of Foggia,
Italy

REVIEWED BY
Mercedes Tamame,
Staff Scientist of CSIC, Spain
Mariagiovanna Fragasso,
Council for Agricultural and Economics Research (CREA), Italy

*CORRESPONDENCE
Tomás García-Cayuela
tomasgc@tec.mx

SPECIALTY SECTION
This article was submitted to Food Microbiology, a section of the journal Frontiers in Microbiology

RECEIVED 15 June 2022
ACCEPTED 18 August 2022
PUBLISHED 08 September 2022

CITATION
Pérez-Alvarado O, Zepeda-Hernández A, Garcia-Amezquita LE, Requena T, Vinderola G and García-Cayuela T (2022) Role of lactic acid bacteria and yeasts in sourdough fermentation during breadmaking: Evaluation of postbiotic-like components and health benefits. *Front. Microbiol.* 13:969460. doi: 10.3389/fmicb.2022.969460

Role of lactic acid bacteria and yeasts in sourdough fermentation during breadmaking: Evaluation of postbiotic-like components and health benefits

Omar Pérez-Alvarado[1], Andrea Zepeda-Hernández[1], Luis Eduardo Garcia-Amezquita[1], Teresa Requena[2], Gabriel Vinderola[3] and Tomás García-Cayuela[1]*

[1]Tecnologico de Monterrey, Escuela de Ingeniería y Ciencias, Food and Biotech Lab, Zapopan, Jalisco, Mexico, [2]Department of Food Biotechnology and Microbiology, Institute of Food Science Research, CIAL (CSIC), Madrid, Spain, [3]Faculty of Chemical Engineering, Instituto de Lactología Industrial (CONICET-UNL), National University of Litoral, Santa Fe, Argentina

Sourdough (SD) fermentation is a traditional biotechnological process used to improve the properties of baked goods. Nowadays, SD fermentation is studied for its potential health effects due to the presence of postbiotic-like components, which refer to a group of inanimate microorganisms and/or their components that confer health benefits on the host. Some postbiotic-like components reported in SD are non-viable microorganisms, short-chain fatty acids, bacteriocins, biosurfactants, secreted proteins/peptides, amino acids, flavonoids, exopolysaccharides, and other molecules. Temperature, pH, fermentation time, and the composition of lactic acid bacteria and yeasts in SD can impact the nutritional and sensory properties of bread and the postbiotic-like effect. Many *in vivo* studies in humans have associated the consumption of SD bread with higher satiety, lower glycemic responses, increased postprandial concentrations of short-chain fatty acids, and improvement in the symptoms of metabolic or gastrointestinal-related diseases. This review highlights the role of bacteria and yeasts used for SD, the formation of postbiotic-like components affected by SD fermentation and the baking process, and the implications of functional SD bread intake for human health. There are few studies characterizing the stability and properties of postbiotic-like components after the baking process. Therefore, further research is necessary to develop SD bread with postbiotic-related health benefits.

KEYWORDS

sourdough, postbiotics, functional bread, backslopping, baking

Introduction

Sourdough (SD) fermentation is a well-known biotechnological process that has been in use for 5,000 years and has shown the ability to improve the sensory, rheological, and shelf-life properties of baked goods. This biotechnology process encompasses a great variety of lactic acid bacteria (LAB) and yeast interactions (Poutanen et al., 2009). Sourdough is the result of fermenting a mixture of flour, water, and other ingredients by LAB and yeasts naturally occurring in the flour. Sourdough is propagated during backslopping process, in which a new mixture of flour and water is fermented by using as a starter the SD from a previous fermentation batch (Rizzello et al., 2019). From a microbiological point of view, SD is an ecosystem characterized by an environment with a low pH, high carbohydrate concentration, oxygen limitation, and a LAB cell count exceeding that of yeasts (De Vuyst et al., 2014). Lactic acid bacteria dominate the mature SD, while the yeast content is one/two logarithmic cycles lower (Rizzello et al., 2019). The major metabolic activities of the SD microbiota are acidification (LAB), flavor formation (LAB and yeasts), and leavening (yeasts and heterofermentative LAB species; De Vuyst et al., 2014). Even though LAB and yeasts originate principally from the flour and environmental microbiota, the process of microbiota maturation during SD fermentation depends on various factors such as temperature, the chemical and enzymatic composition of the flour, redox potential, water content, and time (Rizzello et al., 2019).

Nowadays, the culture-based techniques used to characterize SD microbial diversity across studies investigating the distribution of SD bacterial and fungal taxa are variable and biased (De Vuyst et al., 2014; Michel et al., 2019; Landis et al., 2021). Sourdough starters are maintained in many households, but these differ from those in bakeries due to heterogeneity among environments, production practices, and ingredients (Landis et al., 2021). The types/origins of the flours and baking procedures seem to affect mainly the SD biodiversity. Different SDs from the same region may be similar in composition due to the response to regional microclimates or the restricted dispersion of microbes (Landis et al., 2021). Bread producers often attribute distinct regional properties to their breads, giving credit to the environment for their unique characteristics (Landis et al., 2021). Some of the microorganisms identified from SD microbiota characterization studies are shown in Table 1, differentiated by LAB (homofermentative, obligate heterofermentative, and facultative heterofermentative) and yeasts (De Vuyst and Neysens, 2005; Chavan and Chavan, 2011; Gänzle and Gobbetti, 2013; De Vuyst et al., 2017; Papadimitriou et al., 2019; Preedy and Watson, 2019; Arora et al., 2021).

Fermented foods and functional ingredients (such as probiotics, prebiotics, and synbiotics) can be used as dietary interventions seeking health benefits. Probiotics are live microorganisms that confer a health benefit when administered in adequate amounts. Probiotic products may also deliver significant amounts of non-viable cells due to cell death during storage (Salminen et al., 2021). The interest in the potential effect of non-viable microorganisms and their components on health is rising. Fermented foods can contain numerous non-viable cells, especially after prolonged storage, thermal treatments, or processes (such as pasteurization or baking). Fermentation mediated by LAB produces different cellular structures and metabolites, such as cell surface components, lactic acid, short-chain fatty acids (SCFAs), and bioactive peptides, among other effector molecules associated with benefits to human health (Salminen et al., 2021).

New terms have been used to name these non-viable microbial cells and metabolites in recent years, including paraprobiotics, parapsychobiotics, ghost probiotics, metabiotics, tyndallized probiotics, and bacterial lysates. However, the concept of postbiotics to promote health is emerging as an important microorganism-derived tool (Salminen et al., 2021). The term postbiotic can be considered as a composite of biotic, defined as "relating to or resulting from living organisms," and post, which refers to "after life," implying that postbiotics are non-living microorganisms. Thus, postbiotics are defined as a preparation of inanimate microorganisms and/or their components that provides benefits to the host's health (Salminen et al., 2021). The definition of postbiotics requires identification to the strain level of the microbe/s used for their preparation, a deliberate termination of cell viability step, and the demonstration of a health benefit in a well-designed and conducted efficacy trial in the target host (Salminen et al., 2021). Since SD fermentation is performed by microbes that occur naturally in the flours used to prepare the dough, and even though the baking step represents a deliberate termination of cell viability, the presence of a consortium of unidentified microbes prevents SD from being regarded as a postbiotic. Nevertheless, metagenomic/metataxonomic techniques based in Next Generation Sequencing are now widely used to identify the microbiota of SDs worldwide and, in this sense, the microbes would be not "completely unidentified. Moreover, in inoculated SDs some postbiotic-like substances can be correlated or assigned to specific dominant or co-dominant LAB and/or yeast strains that are imposed on the native microbiota. Based on the above mentioned, the term "postbiotic-like" will be used in this review. This term has recently employed to refer the use of cell-free supernatants of lactic acid bacteria (Spaggiari et al., 2022).

The advantage of postbiotic over probiotic microorganisms is that they present little or no interaction with the different compounds in the food matrix, which increases shelf-life and maintains the same sensory and physicochemical properties. Other advantages are that they remain stable over a wide range of pH and temperature, which allows ingredients with higher acidity to be added and treated by thermal processing in a way that their functionality is not compromised, minimizing the chances of microbial contamination after packaging and during storage (Nataraj et al., 2020). Currently, researchers are particularly focused on the discovery and characterization of new LAB strains able to biosynthesize active compounds such as exopolysaccharides (EPS), antimicrobial compounds, bioactive peptides, and SCFAs

TABLE 1 Lactic acid bacteria (LAB) and yeasts found in different types of sourdough.

Homofermentative LAB	Obligate heterofermentative LAB	Facultative heterofermentative LAB	Yeasts
Enterococcus casseliflavus	*Levilactobacillus acidifarinae, Levilactobacillus*	*Companilactobacillus alimentarius*	*Saccharomyces cerevisiae*
Enterococcus durans	*brevis, Limosilactobacillus fermentum*	*Companilactobacillus paralimentarius*	*Saccharomyces bayanus*
Enterococcus faecalis	*Limosilactobacillus reuteri, Limosilactobacillus*	*Lactiplantibacillus plantarum*	*Kazachstania exigua*
Enterococcus faecium	*pontis, Furfurilactobacillus rossiae*	*Lacticaseibacillus casei, Lacticaseibacillus*	*Kazachstania humilis*
Lactobacillus amylovorus	*Limosilactobacillus panis, Companilactobacillus*	*paracasei Lacticaseibacillus rhamnosus*	*Kazachstania servazzi*
Lactobacillus amylolyticus	*crustorum*	*Levilactobacillus spicheri*	*Kazachstania exigua*
Lactobacillus delbrueckii	*Latilactobacillus curvatus*	*Lactiplantibacillus xiangfangensis*	*Pichia kudriavzevii*
Lactobacillus acidophilus	*Limosilactobacillus frumenti, Fructilactobacillus*	*Limosilactobacillus coleohominis*	*Torulaspora delbrueckii*
Companilactobacillus farciminis	*fructivorans*	*Companilactobacillus kimchii*	*Wickerhamomyces anomalus*
Lactobacillus johnsonii	*Levilactobacillus hammesii*	*Lactiplantibacillus pentosus*	*Pichia kudriavzevii*
Companilactobacillus crustorum	*Levilactobacillus koreensis, Levilactobacillus*	*Schleiferilactobacillus perolens*	*Candida tropicalis*
Companilactobacillus heilongjiangensis	*namurensis*	*Latilactobacillus sakei*	*Candida glabrata*
Companilactobacillus mindensis	*Companilactobacillus*	*Pediococcus acidilactici*	*Candida krusei*
Companilactobacillus nantensis	*nodensis*	*Lapidilactobacillus dextrinicus*	*Candida pelicullosa*
Companilactobacillus nodensis	*Limosilactobacillus oris, Lentilactobacillus*	*Pediococcus pentosaceus*	*Yarrowia keelungensis*
Lactobacillus crispatus	*parabuchneri*		*Torulaspora delbrueckii*
Lactobacillus gallinarum	*Fructilactobacillus sanfranciscensis*		*Rhodotorula mucilaginosa*
Lactobacillus gasseri	*Limosilactobacillus secaliphilus*		
Lactobacillus helveticus	*Furfurilactobacillus siliginis*		
Liquorilactobacillus nagelii	*Lentilactobacillus buchneri, Fructilactobacillus*		
Ligilactobacillus salivarius, Streptococcus	*fructivorans*		
constellatus	*Lentilactobacillus hilgardii*		
Streptococcus equinus	*Fructilactobacillus fructivorans*		
Streptococcus suis	*Lentilactobacillus kefiri, Apilactobacillus*		
	kunkeei, Fructilactobacillus lindneri		
	Limosilactobacillus mucosae, Limosilactobacillus		
	fermentum, Secundilactobacillus collinoides		
	Limosilactobacillus vaginalis, Levilactobacillus		
	zymae, Leuconostoc citreum		
	Leuconostoc gelidum		
	Leuconostoc mesenteroides		
	Weissella cibaria		
	Weissella confusa		
	Weissella hellenica		
	Weissella kandleri		

The microorganisms in the table were compiled from the following sourdough microbiota characterization: De Vuyst and Neysens (2005), Chavan and Chavan (2011), Gänzle and Gobbetti (2013), De Vuyst et al. (2017), Papadimitriou et al. (2019), Preedy and Watson (2019), and Arora et al. (2021).

to exploit their functional properties in food (Păcularu-Burada et al., 2020b). Moreover, the selection of LAB and yeast strains (Table 1) to further design starter cultures must also consider important features, such as the preservation technologies and overall nutritional-functional aspects of the final fermented products. This review focuses on the roles of LAB and yeasts in SD in the production of baked goods with enhanced properties and the presence of postbiotic-like components. The role of LAB in the formation of postbiotic-like components during SD fermentation and baking, as well as the health benefits of SD bread, are also explored. In this respect, the timeline for the literature search was set to the last 10 and 20 years using "postbiotic" and "sourdough" as main keywords, respectively. The screening strategy included full text research articles dealing with microbiological, biochemical, technological and/or health features of traditional SD baked goods.

Role of sourdough fermentation in the production of baked goods

Bread is one of the most important staple foods consumed in the world (Koistinen et al., 2018). Its recipe comprises cereal flour and can include pseudocereals and/or legumes, water, salt, other minor ingredients, and a leavening agent (Rizzello et al., 2019). Cereals and legumes are valuable sources of proteins, fats, and

dietary fiber. Through lactic acid fermentation, the properties of these ingredients can be improved, and the sensory characteristics of the final products enhanced. In recent years, the use of SD has become increasingly standardized, and the interaction among microbial cultures has been studied with the aim of employing fermentation in baking for leavening, flavor formation, and improving stability (Gobbetti et al., 2019). Moreover, SD fermented with LAB is a source of proteolytic enzymes, activated by acid production, that are likely to eliminate gluten toxicity during bread making (Fekri et al., 2020). Furthermore, the phytic acid and other antinutritional factors from cereals and legumes are reduced by specific enzymes produced during fermentation, resulting in higher bioavailability of important minerals in baked goods (Fekri et al., 2020).

Nowadays, four types of SD can be made depending on the inocula and the final desired properties of baked goods, such as flavor, texture, smell, stability, and nutritional properties: types I, II, III, and IV (Figure 1; Galli et al., 2019). The type I or traditional SD process depends on the backslopping technique at a low incubation temperature (20°C–24°C), which relies on a repeated cyclic of re-inoculation (6–24 h) with a new batch of flour and water from a previous one derived from a mother dough (Figure 1I). This type of SD is a pure craft, and the dough can be maintained for years. In terms of microbiology, type I SD harbors mixtures of distinctive yeast and LAB species or strains, representing a large diversity of natural SD starters. Backslopping results in the prevalence of the species/strains best adapted to the SD ecosystem. The type of flour used, and its enzymatic, microbiological, nutritional, and textural qualities are of the utmost importance since these factors will determine the stability of the mature doughs (De Vuyst et al., 2014). The main drawback of the type I process is that it cannot be scaled up for industrial exploitation; moreover, it is time-consuming, requires trained and qualified staff, and is not fully controllable (Galli et al., 2019).

In the case of the type II process, doughs are characterized by fermentation with specific LAB strains (Figure 1II). Type II SD is generally not suitable for dough leavening but is used for dough acidification and as a flavor enhancer. This process is shorter than that of type I, with a unique fermentation step of 15–20 h, followed by a storage period of many days. The SD is generally liquid, and fermentation occurs in bioreactors or tanks. Thus, type II SD can be scaled to an industrial level (Corsetti, 2013). In this case,

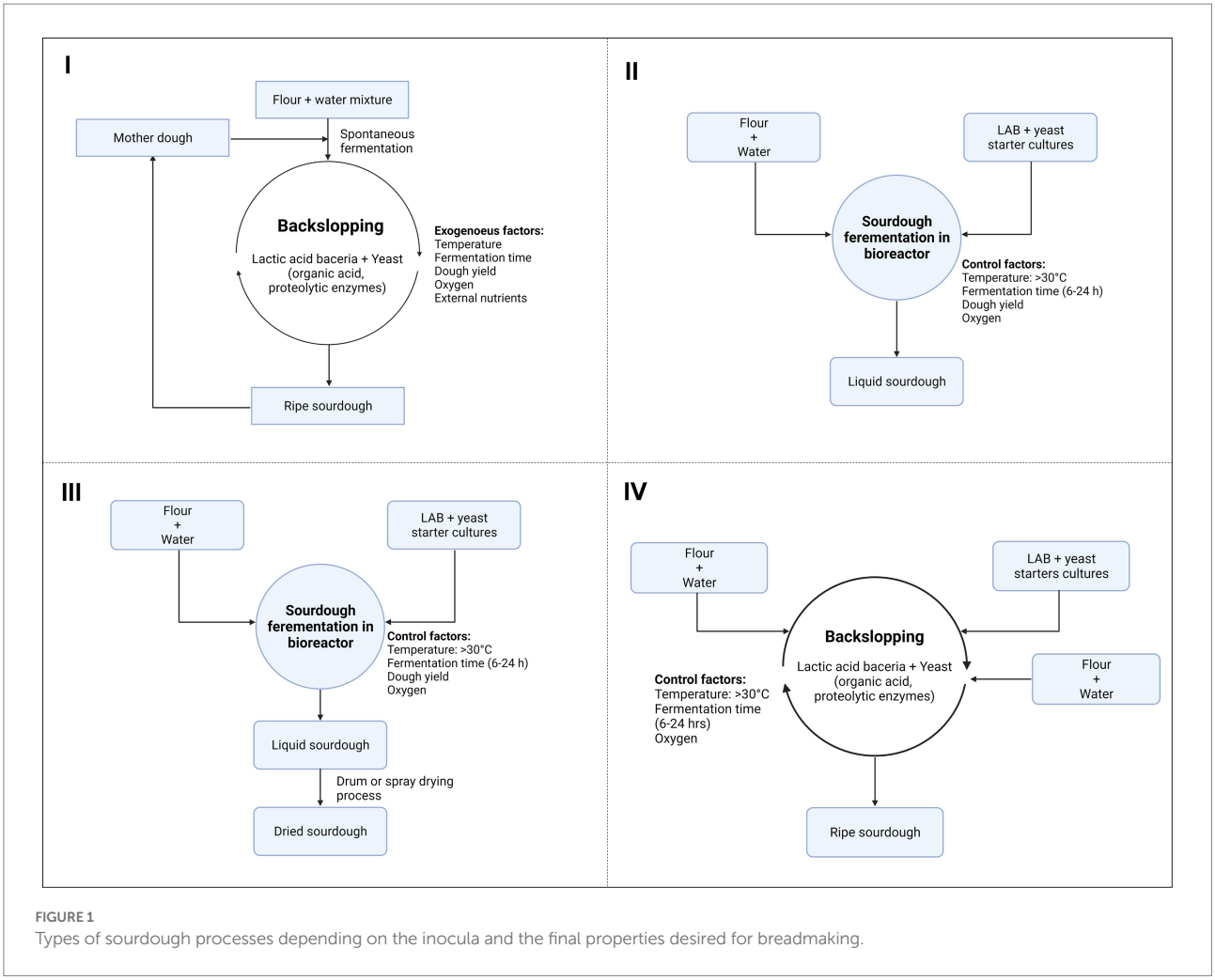

FIGURE 1
Types of sourdough processes depending on the inocula and the final properties desired for breadmaking.

defined acid-tolerant LAB starter cultures are used (e.g., strains of *Levilactobacillus brevis*, *Limosilactobacillus fermentum*, *Lactiplantibacillus plantarum*, *Limosilactobacillus reuteri*, or *Fructilactobacillus sanfranciscensis*), accompanied or not by yeasts, most commonly *Saccharomyces cerevisiae*, which is often added to the final stage but also can be added along with the LAB. Most strains are selected on the basis of their potential to quickly cause acidification of the dough and/or generate specific flavor compounds. These two properties offer a clear added value, which is reflected in the commercialization of dried SD powders used as flavorings in bread production (De Vuyst et al., 2017).

Type III SD is remarkably similar to type II, with the difference being in the dehydration or pasteurization of the liquid-stabilized SD (Figure 1III). Various dehydration techniques can be applied, with drum and spray drying being the most common ones. The starter cultures are selected on the basis of their high acidification capacity, ability to produce flavor compounds, and resistance to the drying procedure. The most common species include heterofermentative *L. brevis* and facultative heterofermentative *Pediococcus pentosaceus* and *L. plantarum* strains (Papadimitriou et al., 2019). Type III SD presents several advantages, such as a long shelf life, a smaller volume, and ease of handling for transportation and storage, which makes it more convenient for industrial bakeries, and finally, the production of standardized end-products. Generally, type III SD is used as an acidifier or as a bread improver (Corsetti, 2013).

Type IV SD is initiated with a LAB starter culture, followed by traditional backslopping as in type I SD (Figure 1IV; Preedy and Watson, 2019). This starter culture-backslopped SD approach is equally characterized by a pattern of three-step succession of LAB communities. However, competition frequently occurs between the added LAB starter culture and the spontaneously growing microorganisms. Differences in stress tolerance may lead the predominance of the autochthonous LAB species and elimination of the LAB starter culture. This may occur because the starter culture is not well adapted to the SD ecosystem and the prevailing conditions (De Vuyst et al., 2017).

Type II and III SD can simplify the production process, but they do not guarantee the same distinctive properties as type I SD; nevertheless, they contain only LAB and require the addition of bakery yeasts as a second step. Recently, liquid SD has been introduced in bakeries as a new technology trend. This type of SD allows the addition of both LAB and yeasts in a single step and thus meets the industrial demand for a more controllable and large-scale SD process (Galli et al., 2019).

Role of LAB in sourdough fermentation

Sourdough is a very complex ecosystem, where heterofermentative LAB are the dominant organisms and co-exist synergistically with yeasts, which are well adapted to the prevailing acidic environment and can grow to high concentrations [10^7 colony forming units (CFU)/g], albeit lower than those of LAB (10^8 CFU/g; De Vuyst et al., 2014). More than 90 different LAB species have already been isolated from SD, including obligately and facultatively heterofermentative species and some homofermentative species, as shown in Table 1.

The fermentation process generates mainly acids, alcohols, aldehydes, esters, and ketones; it is the primary route of volatile compound formation in SD and bread crumb (Limbad et al., 2020). The contribution of LAB to the flavor of SD bread is associated with the production of lactic acid (fresh acidity) and acetic acid (sharp acidity). That also contributes to the amino acid accumulation (e.g., accumulation of glutamate, which is responsible for the umami taste), and the generation of 2-acetyl-1-pyrroline as an end metabolite that is responsible for the aroma of the crust and formed through the Maillard reaction of ornithine in the arginine deiminase (ADI) pathway. Additionally, LAB activity is involved in the accumulation of peptides such as glutathione and glutamyl dipeptides, responsible for the kokumi taste (De Vuyst et al., 2017). The conversion of amino acids such as phenylalanine (sweet), isoleucine (acidic), glycine, serine, and alanine (vinegar/sour) to aldehydes and ketones can form additional flavor compounds (Limbad et al., 2020).

Regarding the metabolic pathways of LAB, the ones that influence bread quality are linked to central carbon flux and limited by cofactor availability, which affects the redox potential of the environment and inside the cell. Homo-and heterofermentative LAB differ fundamentally in the reduced cofactors they regenerate, such as nicotinamide adenine dinucleotide (NAD) or nicotinamide adenine dinucleotide phosphate (NADP). Furthermore, the use of co-substrates, such as oxygen or fructose, as electron acceptors by obligate heterofermentative LAB is coupled with an increase in acetate production in doughs. Thus, the different metabolic requirements of homo-and heterofermentative LAB produce other effects on the redox reactions in SD that influence the quality of the final bread beyond the formation of acetate (Chavan and Chavan, 2011).

The available carbohydrates in wheat flour are maltose, followed by sucrose, glucose, and fructose, along with some trisaccharides such as maltotriose and raffinose. The glucose concentration increases during fermentation because other complex carbohydrates are metabolized by LAB and yeasts; however, yeasts cannot ferment the disaccharide maltose, which is instead fermented by LAB (Chavan and Chavan, 2011). Starting from glucose, homofermentative LAB produce lactic acid through glycolysis, while heterofermentative LAB generate, besides lactic acid, CO_2, acetic acid, and/or ethanol (De Vuyst et al., 2017). Moreover, carbohydrate metabolism leads to the development of antimicrobials, flavor compounds, and EPS.

On the other hand, the generation of oligopeptides and amino acids is made possible by endogenous flour proteases that become activated at low pH and reduce the gluten disulfide bonds caused by LAB acidification and glutathione reductase activity (De Vuyst et al., 2017). As described earlier, amino acid conversion contributes to the acid stress response, redox balancing, and flavor

formation. Protein acid accumulation due to peptide hydrolysis stimulates SD flavor formation and nutrient enrichment (Gobbetti et al., 2014). Phenolic compounds and lipids are only minor compounds in cereal flours. Nevertheless, some LAB species catalyze the release of bound phenolic compounds through feruloyl esterase, tannase (tannin acyl hydrolase), and glycosyl hydrolases, which hydrolyze esters of ferulic acid, galloyl esters of gallotannins, and flavonoid hexoxides, respectively. Phenolic compounds and flavonoids can be further converted into flavor precursors; these conversions are grounded in specific phenolic acid decarboxylases and cinnamic acid reductases of LAB that are associated with cereal flours (De Vuyst et al., 2017). Sorghum and millet flours contain a high level of polyphenols. Their use is suggested for the metabolism of phenolic compounds by microorganisms, specifically by LAB species capable of degrading these compounds, such as *L. brevis, L. helveticus, L. plantarum,* and *P. pentosaceus* (Gänzle, 2014). Regarding fatty acids, fatty acid hydratases can transform oleic acid and linoleic acid into hydroxy fatty acid chains (Gänzle, 2014), whereas phytase hydrolysis, which releases inorganic phosphate and makes minerals bioavailable during the SD process, is primarily dependent on endogenous cereal phytases that become activated by acidification; LAB of the SD microbiota have also been shown to possess phytase activity (De Vuyst et al., 2017).

Role of yeasts in sourdough fermentation

Yeasts, by producing CO_2, act as the primary leavening agents in bread products. Baker's yeasts exhibit a rapid fermentative metabolism and are resistant to many stress factors that are present during breadmaking. The properties of these microorganisms, mainly *S. cerevisiae,* have significant economic and technological value (Chiva et al., 2021). The stability of the SD process depends on cooperation between certain species of LAB and yeasts (Palla et al., 2020). The use of baker's yeast as a leavening agent has been developed as an alternative for elaborating SD in industrial bread production, where time and speed of production are important factors. Nowadays, baker's yeast is sold as various product types with improved shelf-life, osmotolerant properties, retention of activity at low temperatures, and flavor generation. The presentation of yeasts includes liquid cream or small granules, compressed as blocks, and dried yeasts that may be dry active or dry frozen (De Vuyst et al., 2017). The yeast variability in SD is affected by dough hydration, type of cereal, and leavening temperature, among others (Chavan and Chavan, 2011; Urien et al., 2019).

The carbohydrates present in flour are fermented *via* glycolysis and further pyruvate breakdown to generate CO_2 and ethanol. Ethanol also impacts the dough properties, strengthening the gluten network, but a significant proportion evaporates during baking (Rezaei et al., 2015). Both glycerol and succinate are SD osmoprotectants, reducing pH and influencing dough rheology by improving gas retention and gluten formation (De Vuyst et al., 2021). Besides their leavening ability and influence on the strength of the gluten network, yeasts contribute largely to flavor development in bread. This depends not only on one yeast strain but also on symbiosis with the LAB strains present in the matrix (De Vuyst et al., 2017). Yeasts can, for instance, generate flavor metabolites *via* the Ehrlich pathway by converting branched-chain amino acids into higher alcohols and their esters (Pico et al., 2015). Additionally, yeasts produce low levels of organic acids, such as acetic and succinic acids, that contribute to slight acidification of the leavened dough and affect the final flavor (Jayaram et al., 2013). Furthermore, yeasts contribute to antioxidant activity based on the availability of phenols in the flour cereal (Wang et al., 2014). The dephosphorylation of phytate *via* the action of phytases and the antifungal activities of yeast due to the generation of ethyl acetate lead to the release of phenolic compounds (De Vuyst and Neysens, 2005). Moreover, yeasts can also increase the polyphenol content in cereal products by releasing bound and conjugated phenolic acids to free forms after cell wall degradation processes (Palla et al., 2020).

As well, yeasts in SD may present phytase activities which contribute to enhancing the bioavailability of minerals (calcium, iron, zinc, and magnesium), by degrading the phytate-mineral complex that is an antinutritional factor abundant in wholemeal flours (Chiva et al., 2021). Another activity related with the metabolism of yeasts in SD is their ability to increase the content of vitamin B_2 (riboflavin) in doughs and breads, specifically when *S. cerevisiae* is used as starter culture (Batifoulier et al., 2005). Likewise, baker yeast (*S. cerevisiae*) has been exploited by the potential of synthesize Vitamin D. Concentration of vitamin B_9 has also been reported to increase during SD fermentation of oat, barley, and rye, particularly by the presence of *S. cerevisiae* and *K. humilis* as starter cultures (Kariluoto et al., 2014). Yeasts also improves the digestibility of bread by the presence of proteases, since during dough fermentation, the proteolysis release small peptides and free amino acids, which are important for rapid microbial growth, acidification, as precursors for the flavor development of leavened baked products, and better protein digestibility (Kaur et al., 2008). Additionally, this proteolytic activity might be used as a tool to reduce certain allergen compounds like gluten, since cereal proteins are one of the most frequent causes of food allergies (Poutanen et al., 2009).

Presence of postbiotic-like components in sourdough fermentation

In the fermentation process of SD, the microorganisms involved produce a significant quantity of cells and metabolites, which can be in the intracellular or extracellular matrix, and such microorganisms can potentially benefit the consumer, even when present in their non-viable form after baking (Barros et al., 2020). Furthermore, during the baking process, the cell

lysis of microorganisms delivers cellular debris that may also have beneficial properties (Sadeghi et al., 2019). Besides whole non-viable microbes, among the examples of postbiotic-like compounds present in SD are SCFAs, secreted proteins/peptides, bacteriocins, secreted biosurfactants, amino acids, flavonoids, EPSs, vitamins, organic acids, and other widely diverse molecules. Other potential postbiotics are residues of the cell debris such as peptidoglycan-derived muropeptides, surface-protruding molecules (pili, fimbriae, flagella), cell-surface associated proteins, cell wall-bound biosurfactants, and cell supernatants (Nataraj et al., 2020). Table 2 presents the main postbiotic components that may occur in foods and the potential health benefits in the host.

The formation of postbiotic-like compounds during SD fermentation has mostly been described for LAB. Many metabolic pathways are activated during fermentation to produce bioactive substances that inhibit pathogenic bacterial growth and prevent bacterial toxin formation. Moreover, LAB produce low-molecular-weight organic components from the metabolism of carbohydrates, amino acids, vitamins, organic acids, and fatty acids. The LAB strain diversity and metabolic capability of generating a variety of bioactive compounds depend on many fermentation parameters, such as pH, time, and temperature. In the case of pH, many differences between SD with a pH of 4.0 and those with a lower pH have been described. When the pH is maintained at 4.0, the presence of lactic acid isomers and ethanol increases the metabolic activity of different LAB and the production of postbiotic-like compounds. By contrast, lower pH values lead to the accumulation of flavor-enhancing volatile compounds. Therefore, optimization of SD pH is a critical determinant of the type of dough obtained, depending on whether the aim is to produce a certain flavor or desired metabolites (Păcularu-Burada et al., 2020b).

Baking is carried out at a temperature up to 200°C–250°C and for an average duration of 1 h (Petrova and Petrov, 2020). Thermal treatment for the generation of postbiotic-like components may be influenced by the type of microorganisms, growth stage, prior exposure to stress, pH value, water activity, and heating mode (conduction, convection, and/or radiation), among other factors. Regarding postbiotics, thermal treatments have been reported to increase cell coarseness and roughness, influencing the immune-modulating properties. The higher the temperature applied, the greater the roughness and degree of coarseness of the cell-surface compared to that of viable cells. Furthermore, adhesion is another property affected by the temperature; when the temperature is higher, the adhesion capacity is reduced. These findings are relevant to the development of processes for postbiotic generation because they indicate that each potential microorganism demands a different temperature and time for inactivation (de Almada et al., 2016).

Several studies have reported the possible postbiotic components in foods (Table 2); however, very few have detailed the functionality and health benefits in the context of SD. Therefore, we will focus on specific compounds such as EPSs, antimicrobial molecules, and fatty acids. The most relevant studies addressing this topic are shown in Table 3.

Exopolysaccharides are often produced during the SD process. The EPS yield can be correlated to many factors, such as the composition of macronutrients and micronutrients of the substrate, temperature, pH, agitation, and the bacterial strains with defined biochemical properties (Păcularu-Burada et al., 2020a). The EPSs generated by LAB during SD have techno-functional aspects related to their ability to bind water and retain moisture. In the last decade, the use of EPS-producing cultures has attracted the attention of the bakery industry because of the hydrocolloid nature of these polysaccharides, as well as their health benefits, including anticarcinogenic effects (Lynch et al., 2018). Screening of EPS-producing SD strains is limited to wheat and rye fermentations. The SD process offers a convenient means by which the EPS-producing nature of LAB can be exploited to produce baked goods with enhanced quality (Lynch et al., 2018). This is typically achieved by adding a pre-fermented SD starter with defined EPS-producing strains, commonly on a 10%–40% (w/w) flour basis, to the final bread dough mix (Galle and Arendt, 2014).

Exopolysaccharide from SD provides an opportunity to improve consumers' health. These compounds stimulate carbohydrate fermentation to SCFAs by the intestinal microbiota. For example, dextran is metabolized by gut microbes to acetate, butyrate, and propionate. Propionate has been postulated to have several beneficial effects, such as reducing cholesterol and triglyceride levels, and increasing insulin sensitivity. Furthermore, oligosaccharides can act as soluble receptor analogs of epithelial cell-surface carbohydrates and inhibit pathogens or bacterial toxin adhesion to epithelial surfaces, an initial stage of an infective process. Thus, the large variety of oligosaccharides produced by LAB enzymes, also involved in EPS production, makes LAB potential candidates for preventing infection or inflammatory bowel diseases (Galle and Arendt, 2014). Several factors, such as dough yield, fermentation time, pH, sucrose content, and the fermentation substrate, influence the amount of EPS formed *in situ*. It was reported that glucan formation by *L. reuteri* from sucrose was higher in softer doughs, probably because of better diffusion of the substrates and extracellular glycansucrases (Seitter et al., 2019). Exopolysaccharides yield was also improved when sucrose was added stepwise (fed-batch) to the fermenting dough. Furthermore, with the pH adjusted to a constant value of 4.7, the EPS level increased. Interestingly, fermentation with wheat flour, a rye–wheat mixture, or rye bran with 10% sucrose addition showed that EPS production was the most efficient and fastest when rye bran was supplied as a substrate (Di Monaco et al., 2015).

Some examples of LAB metabolites with antimicrobial activity are bacteriocins, organic acids, bacteriocin-like inhibitory substances, and others. Bacteriocins are well-known peptides/proteins synthesized by bacterial ribosomes, and their function is to either kill or inhibit the growth of closely related bacteria. These antimicrobial molecules produced by LAB are usually regulated by environmental conditions and the productive strain growth

TABLE 2 Health benefits and characteristics of the main postbiotic components.

Postbiotic	Main description	Health benefits in the host	Reference
Biosurfactants	Molecules synthesized during the late log or early stationary phase of the growth cycle. Amphiphilic molecules that are composed of glycolipids, lipopeptides, phospholipids, neutral lipids, polysaccharide-protein complexes, and free fatty acids	Disruption and prevention of biofilm formation by pathogenic microorganisms. Wetting, foaming, and emulsification properties, which help the pathogen to adhere, establish itself, and subsequently communicate in biofilms	Nataraj et al., 2020
Exopolysaccharides	Extracellular biopolymers synthesized or secreted by microorganisms during the exponential phase. Based on their monosaccharide composition, exopolysaccharides are further classified into homopolysaccharides and heteropolysaccharides	Biofunctional attributes such as antioxidant, cholesterol-lowering, immunomodulatory, and anti-aging effects; gut microbiota modulation; and anti-toxic, anti-biofilm, and antitumoral effects in preclinical trials	Lynch et al., 2018 and Nataraj et al., 2020
Short-chain fatty acids	Fatty acids with fewer than six carbon atoms in their chains. The most common are acetate, propionate, formate, and butyrate. LAB synthesize SCFAs from non-digestible carbohydrates. Also, bifidobacteria can synthesize short-chain fatty acids, for example acetate and formate	Management of inflammatory bowel disease and colorectal cancer due to their potentiality to overcome the inflammation and proliferation of cancerous cells	Gill et al. (2018) and Nataraj et al. (2020)
Teichoic acids	These are anionic glycopolymers that play key roles in determining the cell shape, regulation of cell division, and other fundamental metabolic aspects of cell physiology. Teichoic acids are generally of two kinds: lipoteichoic acids and wall teichoic acids	Antibiofilm actions against oral and enteric pathogens, immunomodulatory potential, and decreased leaky gut and inflammation	Barros et al., 2020 and Nataraj et al., 2020
Bacteriocins	LAB produce an array of extracellular antimicrobials that inhibit both pathogenic and spoilage-causing microorganisms	Inhibitory potential against various urogenital and antibiotic-resistant pathogens	Bartkiene et al., 2020 and Nataraj et al., 2020
Cell-free supernatant	Cell-free supernatant of LAB is a consortium of low-molecular-weight (hydrogen peroxide, organic acids, carbon dioxide, and di-acetylene) and high-molecular-weight (bacteriocins) compounds	Bioliquid-detergent that reduces the adhesion and biofilm formation of pathogens to various surfaces	de Almada et al., 2016 and Nataraj et al., 2020
Peptidoglycan	Peptidoglycan is a linear glycan strand cross-linked by peptides. The strands are constructed by bonding N-acetylglucosamine and N-acetylmuramic acid	Immunomodulatory, anti-proliferative, and anti-tumor effects	Nataraj et al., 2020
Cell-surface proteins	Proteins that are found in the plasma membrane or in the cell wall. They can be classified into four categories: proteins anchored to the cytoplasmic membrane, lipoproteins, proteins containing a C-terminal motif, and non-covalently bound proteins associated with the cell wall	Immunomodulatory action, secretion of antibacterial peptides, anti-inflammatory effects, anti-adhesion effects, strengthening of epithelial barrier properties, and biosorption of toxic heavy metals	Shigwedha et al., 2014 and Nataraj et al., 2020

phase. Bacteriocin production is initiated in the early log phase, suggesting that bacteriocin is a primary metabolite. In the case of other antimicrobial compounds from LAB, it is very important to emphasize that these metabolites are released after 48 h of fermentation (Păcularu-Burada et al., 2020b). The inhibitory effect on pathogenic or spoilage microorganisms varies widely. The effects of some antimicrobial metabolites produced by two LAB (*L. plantarum* and *Lactobacillus delbrueckii*) cultivated on wheat dough extracts were studied. The species *L. plantarum* had a stronger inhibitory effect against *Penicillium* spp., whereas weaker

TABLE 3 Compounds synthetized during sourdough fermentation and in the final bread.

Compounds	Findings	Species	Source	Reference
Exopolysaccharides	Maximum value of exopolysaccharides synthesized in sourdough with ~22 g/L	*Lactobacillus* spp. *Leuconostoc* spp.	Whole wheat flour Sesame seeds	Păcularu-Burada et al., 2020b
Antibacterial compounds	Inhibitory properties of LAB species against the 15 pathogenic and opportunistic bacterial strains tested through diameter of inhibition zones	*Lactiplantibacillus plantarum* *Lacticaseibacillus casei* *Latilactobacillus curvatus* *Lacticaseibacillus paracasei* *Loigolactobacillus coryniformis*	Rye wheat flour	Bartkiene et al., 2020
Antifungal compounds	Most of the isolated sourdough LAB displayed antifungal activities against seven selected mold strains	*Lactobacillus* spp. *Leuconostoc* spp. *Enterococcus* spp. *Pediococcus* spp.	Rye wheat flour	Bartkiene et al., 2020
Acidification capacity	Strains of *Lactobacillus* spp. showed the highest acidification capacity	*Lactobacillus* spp.	Whole wheat flour	Păcularu-Burada et al., 2020b
Bacteriocins	Five strains were found to produce distinct bacteriocin-like inhibitory substances, but *L. lactis* showed a broader inhibitory range	*Lactiplantibacillus pentosus* *Lactiplantibacillus plantarum*	Rye wheat flour	Gomaa 2013
Fatty acids	*L. hammesii* converts linoleic acid in sourdough, and the resulting monohydroxy octadecenoic acid exerts antifungal activity in bread	*Levilactobacillus hammesii*	Wheat flour	Black et al., 2013
Vitamin B_2	Strains of *Meyerozyma* spp. overproduce vitamin B_2 and may increase the nutritional value of the doughs	*Meyerozyma* spp.	Wheat flour	Chiva et al., 2021
Phytase activity	*S. cerevisiae* IMA L15Y and L10Y showed the highest phytase activity when inoculated in the red-grained wheat	*S. cerevisiae* IMA L15Y and L10Y	Red-grained wheat	Palla et al., 2020

inhibition was observed against *Aspergillus niger*. These LAB species were also used to produce SD bread, where good resistance against fungal contamination was observed. Another study with isolated LAB strains from spontaneous rye SD (belonging to species such as *Leuconostoc mesenteroides, Latilactobacillus curvatus,* and *Levilactobacillus brevis*) showed no inhibitory effect against *Aspergillus* spp. and weak inhibition of *Penicillium* spp. However, it was found that all strains showed satisfactory inhibition of *Bacillus cereus* (Păcularu-Burada et al., 2020b).

In the case of fatty acids, many LAB can produce SCFA, especially acetate, propionate, and butyrate, with potential therapeutic effects on depression, autism, anxiety, and stress (Gill et al., 2018; Păcularu-Burada et al., 2020a). Additionally, metabolites from the conversion of fatty acids by specific LAB strains may contribute to the prolonged storage life of sourdough bread. Black et al. (2013) demonstrated that *Levilactobacillus hammesii* converts linoleic acid to a monohydroxy octadecenoic acid, preventing fungal spoilage of bread without adversely impacting on the sensory properties. This conversion was observed in SD fermentation supplemented with linoleic acid as a substrate (Black et al., 2013). These conversions from fatty acids have not been fully explored in SD. It remains unknown whether hydroxy fatty acids produced by LAB could have a specific positive impact on health.

Effect of heat treatment on microbial viability

The application of probiotics in bread is unlikely because the high temperature and dehydration that occur during the baking process terminate cell viability. Besides, to ensure the benefits of probiotics, the number of LAB must exceed 10^6 CFU/ml or per gram at the time of consumption (Zhang et al., 2016, 2018). The factors that affect the behavior of probiotics during baking include the temperature, moisture content, and structure of the matrix. Many studies have been performed to determine the effect of thermal and dehydration kinetics on the inactivation of the microorganisms in SD bread during baking. Furthermore, most research mainly studied the impact of the baking conditions,

storage, and composition on the technological quality of the baked bread instead of the microbiological quality (Duc Thang et al., 2019).

The kinetics of bread baking is an essential factor in the formation of the crust and the crumb, which give bread its textural and sensory properties. The minimum time required for baking bread is when 98% of the starch in the dough is completely gelatinized, and this time decreases as the baking temperature increases. For example, the baking time for a dough of 60 g at 175°C is 9 min. Under the same conditions, but at a temperature of 200°C, the minimum baking time is reduced to 6 min. However, when the temperature increases to 235°C, the baking time decreases by only 1 min. The viability of microorganisms is affected by the minimum baking time because of the heat and dehydration stresses to which they are exposed. If the baking time is shortened by increasing the baking temperature or reducing the bread size, higher residual viability of LAB species may be obtained after baking (Debonne et al., 2018).

Zhang et al. (2018) evaluated the viability of *L. plantarum* at three different baking temperatures (174°C, 200°C, and 235°C). The results showed that the viable *L. plantarum* counts were reduced by up to 4–5 log CFU/g, while the initial viable count in the dough was 8.8 log CFU/g (Zhang et al., 2018). The kinetics of the baking process showed that in the first 2 min, the microorganisms were only slightly inactivated, with a reduction of <0.5 log CFU/g; between minutes two and six, the reduction in the bacteria count was exponential, with a decrease of 3 log CFU/g; and in the last 2 min, the kinetic changed into a stationary phase with a maximum decrease of 1 log CFU/g (Zhang et al., 2016, 2018). In the case of yeasts, Debonne et al. (2018) found that the yeast count decreased from an initial value of 9 log CFU/g to 4 log CFU/g with baking at 200°C for 13 min. Under different conditions, 150°C for 8 min, the yeast count was reduced by only 2–3 log CFU/g, impacting the product's shelf life. Debonne et al. (2018) observed that the use of SD resulted in negligible detection of spore-forming bacteria, with 3 log CFU/g being the highest recorded value, after heat treatment (150°C, 8 min).

In vitro metabolic studies on the effect of thermal treatment on the viability of microorganisms and the functionality of their components already exist, but they are scarce. Nachtigall et al. (2021) examined the impact of thermal treatment on the molecular mass of EPS synthetized by *Streptococcus thermophilus*. The EPS solution was analyzed at 60°C, 80°C, and 90°C for 10, 30, and 60 min each and cooled to room temperature in an ice bath. When the EPS was untreated, the average molecular mass was 2.90×10^6 Da. In the case of thermal treatment at 60°C and 80°C for up to 60 min, the molecular mass of the EPS was not significantly affected. Similar behavior occurred at 90°C and 10 min residence time, with no reduction of the molecular mass. However, after 30 min of residence time, the molecular mass decreased significantly to 2.40×10^6 Da, and after 60 min, to 2.40×10^6 Da (Nachtigall et al., 2021). Therefore, a prolongated thermal treatment affects the molecular composition of EPS. Unfortunately, there is scarce information about EPS stability at baking temperatures (160°C–220°C). More studies are necessary to determine if the functionality of EPS in bread is compromised by the thermal treatment.

The functionality of antimicrobial compounds has also been analyzed by exposure to high temperatures. Păcularu-Burada et al. (2020b) evaluated the functionality of antibacterial and antifungal compounds treated at 60°C, 80°C, and 121°C for 15 min, forming inhibitory ratios or halo zones. The antimicrobial-compound-producing LAB were grown in three different types of flour extract: buckwheat, chickpea, and quinoa. *Bacillus* spp. was used as the pathogen for antibacterial activity, and *A. niger, Aspergillus flavus,* and *Penicillium* spp. were the microorganisms assessed for antifungal activity. The stability test showed that the antifungal capacity after the thermal treatments differed depending on the type of flour used. In the case of chickpea flour, neither strain inhibited the three fungal species. For buckwheat treated at 80°C, various heat-stable compounds with an inhibitory effect against *Penicillium* spp. were present. The fermented quinoa flour extract showed the highest inhibition ratio of 17% after thermal treatment at 60°C (15 min). However, at 121°C, an inhibitory effect against *A. niger* was observed with an inhibition ratio of 7.20% (Păcularu-Burada et al., 2020a). This result is in line with those obtained by Varsha et al. (2014), who concluded that antifungal compounds produced during fermentation are resistant to sterilization temperatures and have a high value in the baking industry (Varsha et al., 2014). Regarding antibacterial activity, the flour extracts fermented with both strains showed thermally stable antibacterial compounds that inhibited *Bacillus* spp. (Varsha et al., 2014). Similar results were found by Cizeikiene et al. (2013), who concluded that many antibacterial compounds, especially bacteriocins, are resistant to thermal treatment and may have many functions in foods that are exposed to high temperatures, such as baked goods (Cizeikiene et al., 2013). However, experimentation with higher temperatures, up to 220°C, is needed to evaluate the stability of the antifungal and antibacterial activity.

In the case of other compounds (e.g., biosurfactants, cell-surface proteins, cell-free supernatants, SCFAs, etc.), there are not sufficient studies to describe their properties and stability after thermal treatment. Therefore, further research is necessary to understand the functionality of these compounds after a baking process using *in vitro* and *in vivo* models.

Effects of sourdough bread on health

Different studies evaluated the potential health benefits of sourdough bread (SDB) consumption in healthy volunteers and in subjects with metabolic or gastrointestinal diseases. Table 4 summarizes some studies of SDB with different formulations and doses that evaluated the impact of their ingestion in healthy volunteers and patients with pathologies such as irritable bowel syndrome (IBS), among others. The administration of different SDB formulations resulted in reduced glycemic responses

TABLE 4 Evaluation of the benefits of sourdough bread in human health and disease.

Product	Dose	Model	Findings	Reference
Two SDB (different fermentation times: 4 h and 24 h) compared with yeast-fermented bread	One slice of bread (80 g) at 3-week intervals	**Clinical trial** (36 healthy volunteers aged 20–31 years) Double-blind	Highest satiety with SDB fermented for 24 h. In both SDB: faster gastric emptying, lower glycemic responses, higher concentration of total free amino acids and better digestibility	Rizzello et al., 2019
SDB (>12 h fermentation) compared with yeast-fermented bread	Six slices of the study bread (150 g)/day for 7 days	**Clinical trial** (26 patients with IBS aged 18–65 years) Double-blind	Higher reduction in ATIs to their monomeric form Lower levels of FODMAPs	Laatikainen et al., 2017
Whole-grain rye SDB (40 h of fermentation) compared with yeast-fermented crispbread and unfermented rye crispbread	One slice (59.4 g)	**Clinical trial** (24 healthy adults aged 18–70 years) Single-blind, cross-over trial	Higher satiety and degradation of β-glucans	Zamaratskaia et al., 2017
SDB with low FODMAPs against regular rye SDB	3.5–4 slices (105–120 g) of each bread/day in the 1st week 7–8 slices of SDB (210–240 g) per day from the 2nd to the 4th week	**Clinical trial** (87 patients with IBS aged 18–65 years) Double-blind, placebo-controlled cross-over study	Control of IBS symptoms and reduction of gastrointestinal gas accumulation Increase in dietary fiber intake and good acceptance	Laatikainen et al., 2016
Whole-grain rye SDB compared with WB and rye-bran-enriched WB	6–10 slices (25–30 g/slice) In two 4-week test periods	**Clinical trial** (21 healthy subjects with mild gastrointestinal symptoms aged 38–65 years); Cross-over study	Lower postprandial insulin concentration Improvement in the first-phase of insulin secretion Increase in postprandial concentrations of SCFAs	Lappi et al., 2014
Wholegrain wheat SDB against WB	6 slices (for women) and 7 (for men) of SDB per day (162.5 g) for 6 weeks	**Clinical trial** (14 normoglycemic/normoinsulinemic adults and 14 hyperglycemic/hyperinsulinemic adults aged 43–70 years); Crossover study	Improvement in glucose iAUC in response to an OGTT within hyperglycemic/hyperinsulinemic subjects	MacKay et al., 2012
Endosperm rye SDB compared with standard WB	One portion (50 g) at intervals of 1–2 weeks	***In vitro*** Starch and protein hydrolysis **Clinical trial** (16 healthy subjects aged 23 ± 3.7 years)	Higher levels of total fiber and phenolic acids and a higher starch hydrolysis rate Lower postprandial insulin response Beneficial changes in plasma amino acids and their metabolites	Bondia-Pons et al., 2011
Wholemeal wheat SDB (19.5 h fermentation) compared with WB, wholemeal wheat, and wholemeal wheat + xylanase	One slice with crust (50 g) of the test breads	**Clinical trial** (11 insulin-resistant subjects, aged 40–65 years)	Lowest postprandial glucose and insulin responses	Lappi et al., 2010
Two SDB compared with yeast-fermented wholemeal bread and yeast fermented WB	One slice (50 g)	***In vitro*** Starch hydrolysis **Clinical trial** (8 healthy volunteers aged 23–25 years)	Significantly lower glycemic responses in SDB Resistant starch levels were higher in the SDB	Scazzina et al., 2009
Whole wheat SDB (3 h fermentation) compared with whole wheat barley bread and WB	One slice (50 g)	**Clinical trial** (10 overweight male subjects) Single-blind, cross-over	Lower overall glucose and GLP-1 responses Lower glucose iAUC	Najjar et al., 2008

(Continued)

TABLE 4 Continued

Product	Dose	Model	Findings	Reference
SDB (24 h fermentation) with 4 flours compared with yeast-fermented 4-flour bread	A portion of 80 g for 2 days	**Clinical trial** (17 celiac sprue patients) Double-blind	Intestinal permeability not significantly different from baseline in 13 of the 17 patients	Di Cagno et al. (2004)

SDB, Sourdough bread; WB, white bread; IBS, irritable bowel syndrome; ATIs, alpha-amylase/trypsin inhibitors; FODMAPs, Fermentable, Oligo-, Di-, and Mono-saccharides and Polyols; SCFAs, short-chain fatty Acids; OGTT, oral glucose tolerance test; iAUC, incremental area under the curve; GLP-1, glucagon-like peptide 1.

compared with a traditional white wheat bread leavened with *S. cerevisiae*, where the content of blood glucose after 120 min of digestion was 125 mmol/L for white bread and 90 mmol/L for SDB (Scazzina et al., 2009; Bondia-Pons et al., 2011). Scazzina et al. (2009) evaluated the influence of SD on starch digestibility in bread. Four experimental formulations made from two wheat flours by two leavening techniques (SD and with *S. cerevisiae*) were analyzed. Sourdough bread showed higher resistant starch levels and significantly lower glycemic responses in young, healthy subjects. The reduction in the glycemic response was not related to the starch hydrolysis rate; however, organic acids produced by the SD microbiota might delay gastric emptying without affecting starch accessibility (Scazzina et al., 2009). Likewise, in Bondia-Pons et al. (2011), SD fermented rye bread was tested in healthy subjects. Sourdough bread contained a higher level of total fiber and free phenolic acids, a higher starch hydrolysis rate, and a lower postprandial insulin response. Sourdough bread altered plasma amino acids and their metabolites. The increase in tryptophan precursors following consumption of SD rye bread might stimulate a higher tryptophan concentration, resulting in lower appetite and food intake. Likewise, the levels of picolinic acid, which catabolizes the tryptophan metabolism associated with pro-inflammatory functions, significantly decreased after SD rye bread intake (Bondia-Pons et al., 2011).

Moreover, SDB elicited a weaker insulin response in overweight human males, as well as insulin-resistant, and hyperglycemic/hyperinsulinemic patients (Najjar et al., 2008; Lappi et al., 2010; MacKay et al., 2012). Najjar et al. (2008) analyzed the effect of SD-fermented whole wheat bread in overweight male patients. Sourdough bread was associated with the least disturbance in carbohydrate homeostasis, as well as lower overall glucose and glucagon-like peptide-1 (GLP-1) responses, indicating that its consumption could promote the prevention and management of metabolic disorders associated with type 2 diabetes (Najjar et al., 2008). Lappi et al. (2010) evaluated the postprandial insulin response to five different bread formulations in insulin-resistant patients. Sourdough bread (19.5 h of fermentation) showed the lowest postprandial glucose and insulin responses. The proteolysis in SD may be the contributory factor (Lappi et al., 2010). Finally, MacKay et al. (2012) reported that SDB showed an improvement in incremental area under the glucose curve in response to an oral glucose tolerance test (OGTT) in patients with hyperglycemia/hyperinsulinemia, which represents a potential to positively influence postprandial glucose responses in people at risk of cardiovascular disease (MacKay et al., 2012).

Moreover, SDB can increase the postprandial concentrations of SCFAs (Lappi et al., 2014). Sourdough has been shown to change the nutritional quality and health effects of grain ingredients (Lappi et al., 2014). Lappi et al. (2014) compared the impact of three bread formulations (SD rye bread, white bread with rye bran, and white bread) on glucose metabolism and SCFA plasma levels in healthy subjects with mild gastrointestinal symptoms. Sourdough rye bread lowered the postprandial insulin concentration and improved first-phase insulin secretion. The improvement in first-phase insulin secretion and the reduction of hyperinsulinemia in the later postprandial phase may prevent alterations in glucose metabolism. The consumption of both rye bran formulations improved subjects' gastrointestinal quality of life. Additionally, SD rye bran bread increased postprandial concentrations of butyrate and propionate (Lappi et al., 2014).

Sourdough bread is also considered to have beneficial effects on postprandial satiety (Zamaratskaia et al., 2017; Rizzello et al., 2019). Rizzello et al. (2019) and Zamaratskaia et al. (2017) tested the impact of SDB in healthy subjects and obtained the highest satiety response; however, only Rizzello et al. (2019) showed a lower glycemic response. Wholegrain SD rye bread led to the highest satiety (Zamaratskaia et al., 2017). Wholegrain rye bread is linked to a reduced molecular weight of arabinoxylans and β-glucans. Fibers with high solubility and low molecular weight might increase their fermentability and satiety. Additionally, organic acids produced in SD could affect satiety (Zamaratskaia et al., 2017). Rizzello et al. (2019) evaluated two SDBs with different fermentation times (4 and 24 h) in healthy subjects. Results showed that SDB fermented for 24 h obtained the highest fullness perception in the shortest time. Furthermore, both SDBs exhibited faster gastric emptying, a lower glycemic response, a higher total free amino acid concentration, and better digestibility than yeast-fermented bread (Rizzello et al., 2019).

Additionally, SDB has the potential benefit of improving some enteropathies such as celiac sprue (CS) or irritable bowel syndrome (IBS; Di Cagno et al., 2004; Laatikainen et al., 2016, 2017). Di Cagno et al. (2004) evaluated SDB formulations for tolerance by CS patients, while Laatikainen et al. (2016, 2017) focused on specific characteristics of SD that would benefit IBS patients. Di Cagno et al. (2004) included selected SD lactobacilli

for their ability to hydrolyze albumin, globulin, and gliadin fractions during SD fermentation in SDB formulated with four flours (wheat, oat, millet, and buckwheat flour). The result was improved tolerance of SDB with 30% wheat flour and no significant alterations in the intestinal permeability values in 13 of the 17 patients (Di Cagno et al., 2004). In the case of IBS patients, Fermentable, Oligo, Di-, and Mono- saccharides, and Polyols (FODMAPs) are considered triggers of IBS symptoms. Low-FODMAP SDB was administered and evaluated against regular SDB. Low-FODMAPs SDB improved IBS symptoms and reduced gastrointestinal gas accumulation, presenting lower fermentation in the colon, flatulence, abdominal pain, and stomach rumbling; it also increased dietary fiber intake and was well accepted by patients (Laatikainen et al., 2016). Likewise, SDB presented a greater reduction in alpha-amylase/trypsin inhibitors (ATIs) to their monomeric form and showed lower levels of FODMAPs than yeast-fermented bread; ATIs and other non-gluten proteins are associated with a pro-inflammatory effect on intestinal epithelial cells, which could cause gastrointestinal symptoms (Laatikainen et al., 2017). Sourdough bread applications have been demonstrated to improve health and even to aid in the management of symptoms of sensitive pathologies such as CS and IBS. However, further studies are needed to characterize and elucidate the mechanisms of action of these benefits and to perform additional clinical trials considering other diseases and a more diverse demographic.

Future perspectives

Recent studies are attempting to characterize the different compounds and cell debris present in SD. Among the examples are SCFAs, EPSs, biosurfactants, bacteriocins, cell-free supernatants, and cell-surface proteins, and the main health benefits are anti-immunomodulatory, antioxidant, and antimicrobial effects.

The potential health benefits promote consumer preference for foods prepared with LAB. This increasing need for the formulation of functional food products containing LAB starter cultures from sources such as kefir, yogurt, or kombucha, which have reported health benefits, has led to the application of different consortiums as mixed starters for SD breadmaking (Limbad et al., 2020; Plessas et al., 2020). Starters have a key role in the physical characteristics of SDB, modifying raw bread dough and cooked bread products (extensibility, elasticity, viscosity, and the organoleptic properties of the final bread; Fujimoto et al., 2019; Reese et al., 2020; Landis et al., 2021). There are numerous microbial consortiua with potential health benefits that need to be assessed. Another research opportunity is related to ingredients. Organic farming and products are gaining increasing consumer demand due to their association with sustainable production. Recent studies tested the impact of flour selection by evaluating new organic flour options created to meet consumers' needs (Urien et al., 2019; Pontonio et al., 2021). The use of organic flours may offer better functional characteristics, such as a higher total free amino acid content, than non-organic flour (Pontonio et al., 2021). Likewise, researchers are analyzing the effect of ingredients and the environment on the SD microbiota. Factors such as the bakers' skin microbiota may have an important role in the composition of bacteria and fungi in starters (Reese et al., 2020). Also, cereal fermentation may potentially improve nutritional quality and health effects; there is a wide variety of cereals and pseudocereals that can be combined and evaluated to obtain different profiles for fiber content and potential postbiotic-like components (Koistinen et al., 2018; Păcularu-Burada et al., 2020a). However, a noticeable challenge is to reach a consensus for applying standardized culture-based techniques to characterize SD microbial diversity to minimize the variability and biases among studies and define criteria for evaluation of SD starters and their bread products.

Conclusion

Postbiotic-like components in SD provide potential beneficial health properties such as better digestibility, satiety, antioxidant properties, among others. More studies are needed with a defined microbiological consortium and ingredients, to generate a SD able to apport specific nutrients and health benefits; therefore, it is imperative that the different postbiotic forms present in the final dough be characterized, their yield measured, and their potential health properties probed by *in vitro* and *in vivo* studies.

Author contributions

TG-C: conceptualization and final supervision. OP-A and AZ-H: investigation and writing and original draft preparation. OP-A and TG-C: visualization. LG-A, TR, GV, and TG-C: review and editing. All authors contributed to the article and approved the submitted version.

Funding

The authors acknowledge the financial support by Tecnologico de Monterrey within the funding program "Fund for financing the publication of Scientific Articles." This work was also supported by i-Link+2019 program from the Spanish National Research Council (CSIC) and Tecnologico de Monterrey (Project: LINKB20023).

Acknowledgments

OP-A and AZ-H thank CONACyT Mexico for scholarship funding and Tecnologico de Monterrey for academic support.

Conflict of interest

The authors declare that the research was conducted in the absence of any commercial or financial relationships that could be construed as a potential conflict of interest.

The reviewer MT declared a shared parent affiliation with the author TR to the handling editor at the time of review.

Publisher's note

References

Arora, K., Ameur, H., Polo, A., Di Cagno, R., Rizzello, C. G., and Gobbetti, M. (2021). Thirty years of knowledge on sourdough fermentation: a systematic review. *Trends Food Sci. Technol.* 108, 71–83. doi: 10.1016/J.TIFS.2020.12.008

Barros, C. P., Guimarães, J. T., Esmerino, E. A., Duarte, M. C. K., Silva, M. C., Silva, R., et al. (2020). Paraprobiotics and postbiotics: concepts and potential applications in dairy products. *Curr. Opin. Food Sci.* 32, 1–8. doi: 10.1016/J.COFS.2019.12.003

Bartkiene, E., Lele, V., Ruzauskas, M., Domig, K. J., Starkute, V., Zavistanaviciute, P., et al. (2020). Lactic acid bacteria isolation from spontaneous sourdough and their characterization including antimicrobial and antifungal properties evaluation. *Microorganisms* 8:64. doi: 10.3390/MICROORGANISMS8010064

Batifoulier, F., Verny, M. A., Chanliaud, E., Rémésy, C., and Demigné, C. (2005). Effect of different breadmaking methods on thiamine, riboflavin and pyridoxine contents of wheat bread. *J. Cereal Sci.* 42, 101–108. doi: 10.1016/J.JCS.2005.03.003

Black, B. A., Zannini, E., Curtis, J. M., and Gänzle, M. G. (2013). Antifungal hydroxy fatty acids produced during sourdough fermentation: microbial and enzymatic pathways, and antifungal activity in bread. *Appl. Environ. Microbiol.* 79, 1866–1873. doi: 10.1128/AEM.03784-12/SUPPL_FILE/ZAM999104185SO1.PDF

Bondia-Pons, I., Nordlund, E., Mattila, I., Katina, K., Aura, A. M., Kolehmainen, M., et al. (2011). Postprandial differences in the plasma metabolome of healthy Finnish subjects after intake of a sourdough fermented endosperm rye bread versus white wheat bread. *Nutr. J.* 10, 1–10. doi: 10.1186/1475-2891-10-116/TABLES/3

Chavan, R. S., and Chavan, S. R. (2011). Sourdough technology—a traditional way for wholesome foods: a review. *Compr. Rev. Food Sci. Food Saf.* 10, 169–182. doi: 10.1111/J.1541-4337.2011.00148.X

Chiva, R., Celador-Lera, L., Uña, J. A., Jiménez-López, A., Espinosa-Alcantud, M., Mateos-Horganero, E., et al. (2021). Yeast biodiversity in fermented Doughs and raw cereal matrices and the study of technological traits of selected strains isolated in Spain. *Microorganisms* 9:47. doi: 10.3390/MICROORGANISMS9010047

Cizeikiene, D., Juodeikiene, G., Paskevicius, A., and Bartkiene, E. (2013). Antimicrobial activity of lactic acid bacteria against pathogenic and spoilage microorganism isolated from food and their control in wheat bread. *Food Control* 31, 539–545. doi: 10.1016/J.FOODCONT.2012.12.004

Corsetti, A. (2013). Technology of sourdough fermentation and sourdough applications. *Handbook on Sourdough Biotechnology*, 85–103. doi: 10.1007/978-1-4614-5425-0_4

de Almada, C. N., Almada, C. N., Martinez, R. C. R., and Sant'Ana, A. S. (2016). Paraprobiotics: evidences on their ability to modify biological responses, inactivation methods and perspectives on their application in foods. *Trends Food Sci. Technol.* 58, 96–114. doi: 10.1016/J.TIFS.2016.09.011

De Vuyst, L., Comasio, A., and Kerrebroeck, S. V. (2021). Sourdough production: fermentation strategies, microbial ecology, and use of non-flour ingredients. *Crit. Rev. Food Sci. Nutr.* 1–33. doi: 10.1080/10408398.2021.1976100

De Vuyst, L., and Neysens, P. (2005). The sourdough microflora: biodiversity and metabolic interactions. *Trends Food Sci. Technol.* 16, 43–56. doi: 10.1016/J.TIFS.2004.02.012

De Vuyst, L., Van Kerrebroeck, S., Harth, H., Huys, G., Daniel, H. M., and Weckx, S. (2014). Microbial ecology of sourdough fermentations: diverse or uniform? *Food Microbiol.* 37, 11–29. doi: 10.1016/J.FM.2013.06.002

De Vuyst, L., Van Kerrebroeck, S., and Leroy, F. (2017). Microbial ecology and process technology of sourdough fermentation. *Adv. Appl. Microbiol.* 100, 49–160. doi: 10.1016/BS.AAMBS.2017.02.003

Debonne, E., Van Bockstaele, F., Van Driessche, M., De Leyn, I., Eeckhout, M., and Devlieghere, F. (2018). Impact of par-baking and packaging on the microbial quality of par-baked wheat and sourdough bread. *Food Control* 91, 12–19. doi: 10.1016/J.FOODCONT.2018.03.033

Di Cagno, R., De Angelis, M., Auricchio, S., Greco, L., Clarke, C., De Vincenzi, M., et al. (2004). Sourdough bread made from wheat and nontoxic flours and started with selected lactobacilli is tolerated in celiac Sprue patients. *Appl. Environ. Microbiol.* 70, 1088–1096. doi: 10.1128/AEM.70.2.1088-1096.2004

Di Monaco, R., Torrieri, E., Pepe, O., Masi, P., and Cavella, S. (2015). Effect of sourdough with exopolysaccharide (EPS)-producing lactic acid bacteria (LAB) on sensory quality of bread during shelf life. *Food Bioprocess Technol.* 8, 691–701. doi: 10.1007/S11947-014-1434-3

Duc Thang, T., Thi Hanh Quyen, L., Thi Thuy Hang, H., Thien Luan, N., Thi Kim Thuy, D., and My Dong, L. (2019). Turkish journal of agriculture-food science and technology survival survey of lactobacillus acidophilus in additional probiotic bread. *Turkish J. Agric.-Food Sci. Technol.* 7, 588–592. doi: 10.24925/turjaf.v7i4.588-592.2247

Fekri, A., Torbati, M., Yari Khosrowshahi, A., Bagherpour Shamloo, H., and Azadmard-Damirchi, S. (2020). Functional effects of phytate-degrading, probiotic lactic acid bacteria and yeast strains isolated from Iranian traditional sourdough on the technological and nutritional properties of whole wheat bread. *Food Chem.* 306:125620. doi: 10.1016/J.FOODCHEM.2019.125620

Fujimoto, A., Ito, K., Narushima, N., and Miyamoto, T. (2019). Identification of lactic acid bacteria and yeasts, and characterization of food components of sourdoughs used in Japanese bakeries. *J. Biosci. Bioeng.* 127, 575–581. doi: 10.1016/J.JBIOSC.2018.10.014

Galle, S., and Arendt, E. K. (2014). Exopolysaccharides from sourdough lactic acid bacteria. *Crit. Rev. Food Sci. Nutr.* 54, 891–901. doi: 10.1080/10408398.2011.617474

Galli, V., Venturi, M., Pini, N., Guerrini, S., Granchi, L., and Vincenzini, M. (2019). Liquid and firm sourdough fermentation: microbial robustness and interactions during consecutive backsloppings. *LWT* 105, 9–15. doi: 10.1016/J.LWT.2019.02.004

Gänzle, M., and Gobbetti, M. (2013). Physiology and Biochemistry of Lactic Acid Bacteria. *Handbook on Sourdough Biotechnology*, 183–216. doi: 10.1007/978-1-4614-5425-0_7

Gänzle, M. G. (2014). Enzymatic and bacterial conversions during sourdough fermentation. *Food Microbiol.* 37, 2–10. doi: 10.1016/J.FM.2013.04.007

Gill, P. A., van Zelm, M. C., Muir, J. G., and Gibson, P. R. (2018). Review article: short chain fatty acids as potential therapeutic agents in human gastrointestinal and inflammatory disorders. *Aliment. Pharmacol. Ther.* 48, 15–34. doi: 10.1111/APT.14689

Gobbetti, M., De Angelis, M., Di Cagno, R., Calasso, M., Archetti, G., and Rizzello, C. G. (2019). Novel insights on the functional/nutritional features of the sourdough fermentation. *Int. J. Food Microbiol.* 302, 103–113. doi: 10.1016/J.IJFOODMICRO.2018.05.018

Gobbetti, M., Rizzello, C. G., Di Cagno, R., and De Angelis, M. (2014). How the sourdough may affect the functional features of leavened baked goods. *Food Microbiol.* 37, 30–40. doi: 10.1016/J.FM.2013.04.012

Gomaa, E. Z. (2013). Antimicrobial and anti-adhesive properties of biosurfactant produced by lactobacilli isolates, biofilm formation and aggregation ability. *J. Gen. Appl. Microbiol.* 59, 425–436. doi: 10.2323/JGAM.59.425

Jayaram, V. B., Cuyvers, S., Lagrain, B., Verstrepen, K. J., Delcour, J. A., and Courtin, C. M. (2013). Mapping of Saccharomyces cerevisiae metabolites in fermenting wheat straight-dough reveals succinic acid as pH-determining factor. *Food Chem.* 136, 301–308. doi: 10.1016/J.FOODCHEM.2012.08.039

Kariluoto, S., Edelmann, M., Nyström, L., Sontag-Strohm, T., Salovaara, H., Kivelä, R., et al. (2014). In situ enrichment of folate by microorganisms in beta-glucan rich oat and barley matrices. *Int. J. Food Microbiol.* 176, 38–48. doi: 10.1016/J.IJFOODMICRO.2014.01.018

Kaur, P., Kunze, G., and Satyanarayana, T. (2008). Yeast phytases: present scenario and future perspectives. *Crit. Rev. Biotechnol.* 27, 93–109. doi: 10.1080/07388550701334519

Koistinen, V. M., Mattila, O., Katina, K., Poutanen, K., Aura, A. M., and Hanhineva, K. (2018). Metabolic profiling of sourdough fermented wheat and rye bread. *Sci. Rep.* 8, 5684–5611. doi: 10.1038/s41598-018-24149-w

Laatikainen, R., Koskenpato, J., Hongisto, S. M., Loponen, J., Poussa, T., Hillilä, M., et al. (2016). Randomised clinical trial: low-FODMAP rye bread vs. regular rye bread to relieve the symptoms of irritable bowel syndrome. *Aliment. Pharmacol. Ther.* 44, 460–470. doi: 10.1111/APT.13726

Laatikainen, R., Koskenpato, J., Hongisto, S. M., Loponen, J., Poussa, T., Huang, X., et al. (2017). Pilot study: comparison of sourdough wheat bread and yeast-fermented wheat bread in individuals with wheat sensitivity and irritable bowel syndrome. *Nutrients* 9:1215. doi: 10.3390/NU9111215

Landis, E. A., Oliverio, A. M., McKenney, E. A., Nichols, L. M., Kfoury, N., Biango-Daniels, M., et al. (2021). The diversity and function of sourdough starter microbiomes. *elife* 10, 1–24. doi: 10.7554/ELIFE.61644

Lappi, J., Mykkänen, H., Knudsen, K. E. B., Kirjavainen, P., Katina, K., Pihlajamäki, J., et al. (2014). Postprandial glucose metabolism and SCFA after consuming wholegrain rye bread and wheat bread enriched with bioprocessed rye bran in individuals with mild gastrointestinal symptoms. *Nutr. J.* 13, 1–9. doi: 10.1186/1475-2891-13-104/FIGURES/4

Lappi, J., Selinheimo, E., Schwab, U., Katina, K., Lehtinen, P., Mykkänen, H., et al. (2010). Sourdough fermentation of wholemeal wheat bread increases solubility of arabinoxylan and protein and decreases postprandial glucose and insulin responses. *J. Cereal Sci.* 51, 152–158. doi: 10.1016/J.JCS.2009.11.006

Limbad, M., Maddox, N. G., Hamid, N., and Kantono, K. (2020). Sensory and physicochemical characterization of sourdough bread prepared with a coconut water kefir starter. *Foods* 9:1165. doi: 10.3390/FOODS9091165

Lynch, K. M., Coffey, A., and Arendt, E. K. (2018). Exopolysaccharide producing lactic acid bacteria: their techno-functional role and potential application in gluten-free bread products. *Food Res. Int.* 110, 52–61. doi: 10.1016/J.FOODRES.2017.03.012

MacKay, K. A., Tucker, A. J., Duncan, A. M., Graham, T. E., and Robinson, L. E. (2012). Whole grain wheat sourdough bread does not affect plasminogen activator inhibitor-1 in adults with normal or impaired carbohydrate metabolism. *Nutr. Metab. Cardiovasc. Dis.* 22, 704–711. doi: 10.1016/J.NUMECD.2010.10.018

Michel, E., Masson, E., Bubbendorf, S., Lapicque, L., Nidelet, T., Segond, D., et al. (2019). Artisanal and farmers bread making practices differently shape fungal species diversity in French sourdoughs. *BioRxiv* 679472. doi: 10.1101/679472

Nachtigall, C., Rohm, H., and Jaros, D. (2021). Degradation of exopolysaccharides from lactic acid bacteria by thermal, chemical, enzymatic and ultrasound stresses. *Foods* 10:396. doi: 10.3390/FOODS10020396

Najjar, A. M., Parsons, P. M., Duncan, A. M., Robinson, L. E., Yada, R. Y., and Graham, T. E. (2008). The acute impact of ingestion of breads of varying composition on blood glucose, insulin and incretins following first and second meals. *Br. J. Nutr.* 101, 391–398. doi: 10.1017/S0007114508003085

Nataraj, B. H., Ali, S. A., Behare, P. V., and Yadav, H. (2020). Postbiotics-parabiotics: the new horizons in microbial biotherapy and functional foods. *Microb. Cell Factories* 19, 1–22. doi: 10.1186/S12934-020-01426-W/TABLES/2

Păcularu-Burada, B., Georgescu, L. A., and Bahrim, G. E. (2020a). Current approaches in sourdough production with valuable characteristics for technological and functional applications. *The annals of the university Dunarea de Jos of Galati. Fascicle VI Food Technol.* 44, 132–148. doi: 10.35219/FOODTECHNOLOGY.2020.1.08

Păcularu-Burada, B., Georgescu, L. A., Vasile, M. A., Rocha, J. M., and Bahrim, G. E. (2020b). Selection of wild lactic acid bacteria strains as promoters of postbiotics in gluten-free sourdoughs. *Microorganisms* 8:643. doi: 10.3390/MICROORGANISMS8050643

Palla, M., Blandino, M., Grassi, A., Giordano, D., Sgherri, C., Quartacci, M. F., et al. (2020). Characterization and selection of functional yeast strains during sourdough fermentation of different cereal wholegrain flours. *Sci. Rep.* 10, 12856–12815. doi: 10.1038/s41598-020-69774-6

Papadimitriou, K., Zoumpopoulou, G., Georgalaki, M., Alexandraki, V., Kazou, M., Anastasiou, R., et al. (2019). Sourdough Bread. *Innovations in Traditional Foods*, 127–158. doi: 10.1016/B978-0-12-814887-7.00006-X

Petrova, P., and Petrov, K. (2020). Lactic acid fermentation of cereals and Pseudocereals: ancient nutritional biotechnologies with modern applications. *Nutrients* 12:1118. doi: 10.3390/NU12041118

Pico, J., Bernal, J., and Gómez, M. (2015). Wheat bread aroma compounds in crumb and crust: a review. *Food Res. Int.* 75, 200–215. doi: 10.1016/J.FOODRES.2015.05.051

Plessas, S., Mantzourani, I., and Bekatorou, A. (2020). Evaluation of pediococcus pentosaceus SP2 as starter culture on sourdough bread making. *Foods* 9:77. doi: 10.3390/FOODS9010077

Pontonio, E., Arora, K., Dingeo, C., Carafa, I., Celano, G., Scarpino, V., et al. (2021). Commercial organic versus conventional whole rye and wheat flours for making sourdough bread: safety, nutritional, and sensory implications. *Front. Microbiol.* 12:674413. doi: 10.3389/fmicb.2021.674413

Poutanen, K., Flander, L., and Katina, K. (2009). Sourdough and cereal fermentation in a nutritional perspective. *Food Microbiol.* 26, 693–699. doi: 10.1016/J.FM.2009.07.011

Preedy, V. R., and Watson, R. R. (2019). Flour and breads and their fortification in health and disease prevention. *Academic Press.* doi: 10.1016/C2017-0-01593-8

Reese, A. T., Madden, A. A., Joossens, M., Lacaze, G., and Dunn, R. R. (2020). Influences of ingredients and bakers on the bacteria and fungi in sourdough starters and bread. *MSphere* 5. doi: 10.1128/MSPHERE.00950-19

Rezaei, M. N., Aslankoohi, E., Verstrepen, K. J., and Courtin, C. M. (2015). Contribution of the tricarboxylic acid (TCA) cycle and the glyoxylate shunt in Saccharomyces cerevisiae to succinic acid production during dough fermentation. *Int. J. Food Microbiol.* 204, 24–32. doi: 10.1016/J.IJFOODMICRO.2015.03.004

Rizzello, C. G., Portincasa, P., Montemurro, M., di Palo, D. M., Lorusso, M. P., de Angelis, M., et al. (2019). Sourdough fermented breads are more digestible than Those started with Baker's yeast alone: an *in vivo* challenge dissecting distinct gastrointestinal responses. *Nutrients* 11:2954. doi: 10.3390/NU11122954

Sadeghi, A., Ebrahimi, M., Mortazavi, S. A., and Abedfar, A. (2019). Application of the selected antifungal LAB isolate as a protective starter culture in pan whole-wheat sourdough bread. *Food Control* 95, 298–307. doi: 10.1016/J.FOODCONT.2018.08.013

Salminen, S., Collado, M. C., Endo, A., Hill, C., Lebeer, S., Quigley, E. M. M., et al. (2021). The International Scientific Association of Probiotics and Prebiotics (ISAPP) consensus statement on the definition and scope of postbiotics. *Nature Reviews Gastroenterology & Hepatology* 18, 649–667. doi: 10.1038/s41575-021-00440-6

Scazzina, F., Del Rio, D., Pellegrini, N., and Brighenti, F. (2009). Sourdough bread: starch digestibility and postprandial glycemic response. *J. Cereal Sci.* 49, 419–421. doi: 10.1016/J.JCS.2008.12.008

Seitter, M., Fleig, M., Schmidt, H., and Hertel, C. (2019). Effect of exopolysaccharides produced by lactobacillus sanfranciscensis on the processing properties of wheat doughs. *Eur. Food Res. Technol.* 246, 461–469. doi: 10.1007/S00217-019-03413-X

Shigwedha, N., Zhang, L., Sichel, L., Jia, L., Gong, P., Liu, W., et al. (2014). More than a few LAB alleviate common allergies: impact of paraprobiotics in comparison to probiotical live cells. *J. Biosci. Med.* 2, 56–64. doi: 10.4236/JBM.2014.23008

Spaggiari, L., Sala, A., Ardizzoni, A., De Seta, F., Singh, D. K., Gacser, A., et al. (2022). *Lactobacillus acidophilus*, *L. plantarum*, *L. rhamnosus*, and *L. reuteri* cell-free supernatants inhibit candida parapsilosis pathogenic potential upon infection of vaginal epithelial cells monolayer and in a transwell coculture system *in vitro*. *Microbiol. Spectr.* 10:e0269621.

Urien, C., Legrand, J., Montalent, P., Casaregola, S., and Sicard, D. (2019). Fungal species diversity in French bread sourdoughs made of organic wheat flour. *Front. Microbiol.* 10:201. doi: 10.3389/fmicb.2019.00201

Varsha, K. K., Priya, S., Devendra, L., and Nampoothiri, K. M. (2014). Control of spoilage fungi by protective lactic acid bacteria displaying probiotic properties. *Appl. Biochem. Biotechnol.* 172, 3402–3413. doi: 10.1007/S12010-014-0779-4

Wang, T., He, F., and Chen, G. (2014). Improving bioaccessibility and bioavailability of phenolic compounds in cereal grains through processing technologies: a concise review. *J. Funct. Foods* 7, 101–111. doi: 10.1016/J.JFF.2014.01.033

Zamaratskaia, G., Johansson, D. P., Junqueira, M. A., Deissler, L., Langton, M., Hellström, P. M., et al. (2017). Impact of sourdough fermentation on appetite and postprandial metabolic responses – a randomised cross-over trial with whole grain rye crispbread. *Br. J. Nutr.* 118, 686–697. doi: 10.1017/S000711451700263X

Zhang, L., Taal, M., Boom, R. M., Chen, X. D., and Schutyser, M. A. I. (2016). Viability of lactobacillus plantarum P8 in bread during baking and storage. 7–10.

Zhang, L., Taal, M. A., Boom, R. M., Chen, X. D., and Schutyser, M. A. I. (2018). Effect of baking conditions and storage on the viability of lactobacillus plantarum supplemented to bread. *LWT* 87, 318–325. doi: 10.1016/J.LWT.2017.09.005

frontiers | Frontiers in Microbiology

TYPE Original Research
PUBLISHED 23 September 2022
DOI 10.3389/fmicb.2022.1000683

OPEN ACCESS

EDITED BY
Paloma López,
Margarita Salas Center for Biological Research (CSIC), Spain

REVIEWED BY
Teresa Requena,
Spanish National Research Council (CSIC), Spain
Tomás García-Cayuela,
Tecnologico de Monterrey, Mexico
Analia Graciela Abraham,
National University of La Plata, Argentina

*CORRESPONDENCE
Baltasar Mayo
baltasar.mayo@ipla.csic.es

SPECIALTY SECTION
This article was submitted to Food Microbiology, a section of the journal Frontiers in Microbiology

RECEIVED 22 July 2022
ACCEPTED 06 September 2022
PUBLISHED 23 September 2022

CITATION
Rodríguez J, Vázquez L, Flórez AB and Mayo B (2022) Phenotype testing, genome analysis, and metabolic interactions of three lactic acid bacteria strains existing as a consortium in a naturally fermented milk. *Front. Microbiol.* 13:1000683. doi: 10.3389/fmicb.2022.1000683

Phenotype testing, genome analysis, and metabolic interactions of three lactic acid bacteria strains existing as a consortium in a naturally fermented milk

Javier Rodríguez[1,2], Lucía Vázquez[1,2], Ana Belén Flórez[1,2] and Baltasar Mayo[1,2]*

[1]Departamento de Microbiología y Bioquímica, Instituto de Productos Lácteos de Asturias (IPLA), Consejo Superior de Investigaciones Científicas (CSIC), Villaviciosa, Spain, [2]Instituto de Investigación Sanitaria del Principado de Asturias (ISPA), Oviedo, Spain

This work reports the characterization of three lactic acid bacteria (LAB) strains –*Lactococcus lactis* LA1, *Lactococcus cremoris* LA10, and *Lactiplantibacillus plantarum* LA30– existing as a stable consortium in a backslopping-inoculated, naturally fermented milk (NFM). This study aimed at uncovering the biochemical and genetic basis of the stability of the consortium and the cooperativity among the strains during milk fermentation. All three strains were subjected to phenotyping, covering the utilization of carbohydrates, enzyme activity, and antibiotic resistance. The strains were grown in milk individually, as well as in all possible combinations, and the resulting fermented product was analyzed for sugars, organic acids, and volatile compounds. Finally, the genomes of the three strains were sequenced and analyzed for genes associated with technological and safety properties. As expected, wide phenotypic diversity was seen between the strains. *Lactococcus cremoris* LA10 was the only strain to reach high cell densities and coagulate milk alone after incubation at 22°C for 24h; congruently, it possessed a gene coding for a PrtP type II caseinolytic protease. Compared to any other fermentation, acetaldehyde concentrations were greater by a factor of six when all three strains grew together in milk, suggesting that its production might be the result of an interaction between them. *Lactococcus lactis* LA1, which carried a plasmid-encoded *citQRP* operon, was able to utilize milk citrate producing diacetyl and acetoin. No genes encoding virulence traits or pathogenicity factors were identified in any of the strains, and none produced biogenic amines from amino acid precursors, suggesting them to be safe. *Lactiplantibacillus plantarum* LA30 was susceptible to tetracycline, although it harbors a disrupted antibiotic resistance gene belonging to the *tetM/tetW/tetO/tetS* family. All three strains contained large numbers of pseudogenes, suggesting that they are well adapted ("domesticated") to the milk environment. The consortium as a whole or its individual strains might have a use as a starter or as starter components for dairy fermentations. The study of simple consortia, such as that existing in this NFM, can help reveal how microorganisms interact with one another,

and what influence they may have on the sensorial properties of fermented products.

KEYWORDS

lactic acid bacteria, *Lactococcus lactis*, *Lactococcus cremoris*, *Lactiplantibacillus plantarum*, starters, naturally fermented milk, consortium, genomics

Introduction

Fermentation is perhaps the oldest milk preservation technique. Lactic acid bacteria (LAB) lie behind the spontaneous fermentation of milk; these promote its acidification, inhibiting the growth of spoilage and pathogenic microorganisms, and causing coagulation when the pH approaches the isoelectric point of casein (≈pH 4.6; Sharma et al., 2021). The enzymes of LAB also partially digest lactose and milk proteins, contributing to the bioavailability of sugars and amino acids and the formation of taste and aroma compounds (Bintsis, 2018). Two subclasses of naturally fermented milks (NFMs) can be distinguished: non-inoculated and inoculated (Robinson and Tamime, 2006). The former NFMs are made by leaving milk at room temperature until acidification causes the coagulum to appear, while the latter are manufactured by adding a portion of a previous batch to a new one –a process known as backslopping (Garofalo et al., 2020). In every transfer each LAB strain must compete with all other bacteria present and is therefore under pressure to grow quickly.

In nature, microorganisms do not live alone but in complex communities where positive and negative interactions occur (Weiland-Bräuer, 2021). Microbial interplay is mediated *via* a variety of molecular and physiological mechanisms, among which the exchange of metabolites (cross-feeding) is among the most typical (Pierce and Dutton, 2022). Trophic chains in foods enable multiple groups of organisms to survive on limited resources and under stressful conditions (Shanafelt and Loreau, 2018), such as those that reign in the acidic environments of fermented dairy foods (Oshiro et al., 2019; Sun and D'Amico, 2021). Some microbes, however, produce substances that inhibit or kill other microorganisms, impeding the development of their competitors (Barua et al., 2021). Although a plethora of microbial interactions exists, four main types are generally contemplated: competition, amensalism, commensalism and mutualism (Mayo et al., 2021; Pierce and Dutton, 2022). These interactions are not mutually exclusive, and over the manufacture and ripening of dairy products, many may occur at the same time among the different components of the microbial community (Smid and Lacroix, 2013; Mayo et al., 2021). Indeed, some communities have properties that could not be predicted from examining those of their individual members (Minty et al., 2013). They also contain genetic and functional redundancy, which contributes to their robustness (Shapiro and Polz, 2014).

Some years ago, our laboratory reported on an inoculated NFM of unknown (although Eastern) origin, to contain a bacterial consortium of just three strains (Alegría et al., 2010), one of *Lactococcus lactis* subsp. *lactis*, one of *Lactococcus cremoris* subsp. *cremoris* (formerly *Lactococcus lactis* subsp. *cremoris*), and one of *Lactiplantibacillus plantarum* (formerly *Lactobacillus plantarum*). All three strains were found present in fixed numbers (10^8–10^9 cfu ml^{-1} lactococci; 10^6–10^7 cfu ml^{-1} *L. plantarum*) in batches sampled some 18 months apart, indicating the partnership to be very stable. The main goals of the current work were to reveal the biochemical and genetic basis of the consortium stability and the interplay of the strains during milk fermentation. This knowledge could help in the rational use of the consortium as a starter in dairy and may provide fundamental knowledge for the design of more complex, multi-strain cultures. In summary, the study reports on the phenotypic properties of the individual strains, the sequencing and analysis of their genomes, and some strain–strain interactions seen to occur during their growth in milk.

Materials and methods

Strains and culture conditions

Lactococcus lactis subsp. *lactis* LA1 (*L. lactis*), *Lactococcus cremoris* subsp. *cremoris* (*L. cremoris*) LA10, and *Lactiplantibacillus plantarum* (*L. plantarum*) LA30 had been isolated from an NFM in a previous work (Alegría et al., 2010); they were the only bacteria present in that fermented milk. Unless otherwise stated, strains were cultured in M17 broth (Oxoid, Basingstoke, United Kingdom) supplemented with 0.5% glucose (GM17; lactococci) or MRS (Oxoid; *L. plantarum*) in aerobiosis at 32°C (the routine testing temperature for mesophilic LAB) for 24–48 h. When required for plates, media were solidified by adding 2% agar to the liquid version; culturing was performed under the same conditions.

Strain identification by 16S rRNA gene sequencing

The previous identification of the strains was confirmed by PCR amplification of a major part of the 16S rRNA gene, using the universal primers 27F (5′-AGAGTTTGATCCTGGCTCAG-3′)

and 1492R (5′-GGTTACCTTGTTACGACTT-3′), sequencing the amplicons, and comparing them with those in databases, as reported elsewhere (Rodríguez et al., 2022).

Phenotyping of strains

The phenotypic profiles of the individual strains were determined *via* a battery of biochemical tests, as described below.

Fermentation of carbohydrates

The carbohydrate fermentation profile was assessed using the API50 CHL system (bioMérieux, Montalieu-Vercieu, France) following the supplier's recommendations. Briefly, a single colony of each strain grown on either GM17 or MRS agar plates was suspended in 2 ml of sterile saline (0.9% NaCl) to reach a density corresponding to McFarland standard 2 (spectrophotometric equivalent of $\approx 6 \times 10^8$ cfu ml^{-1}). This suspension was then used to inoculate the CHL medium at 1% (v/v). A 180 ml aliquot of the inoculated medium were dispensed into the API50 strip wells; these were then covered with oil and the strips incubated at 32°C for 48 h.

Enzyme activities

Enzyme activities were measured using the commercial, semi-quantitative API-ZYM system (bioMérieux) according to the manufacturer's instructions. Sixty-five µl of cell suspensions of isolated colonies from agar plates, corresponding to McFarland standard 5 ($\approx 1 \times 10^9$ cfu ml^{-1}), were inoculated into each well of an API-ZYM strip. This was incubated for 4 h at 32°C and developed as recommended. Following the bioMérieux scale, the activity of each enzyme was expressed as 0 to ≥40 nmol of substrate hydrolyzed.

Antimicrobial resistance–susceptibility

The minimum inhibitory concentration (MIC) of 16 antibiotics was determined for each strain by broth microdilution using VetMIC™ plates for LAB (National Veterinary Institute of Sweden, Uppsala, Sweden). The wells were inoculated with 150 µl of a cell suspension corresponding to McFarland standard 1 diluted 1:1,000 in liquid IsoSensitest (Oxoid) for lactococci, or LSM (Klare et al., 2005) for lactobacilli ($\approx 3 \times 10^6$ cfu ml^{-1}). The resistance-susceptibility of the strains was defined following the European Food Safety Authority's (EFSA) microbiological cut-offs for *L. lactis* and *L. plantarum*/*L. pentosus* (EFSA FEEDAP Panel (EFSA Panel on Additives and Products or Substances used in Animal Feed), 2018).

Production of GABA and biogenic amines

The three strains were tested for the production (in culture supernatants) of γ-aminobutyric acid (GABA) from monosodium glutamate, and the biogenic amines histamine, tyramine and putrescine from tyrosine, histidine, and arginine/lysine, respectively. Strains were grown in either GM17 (lactococci) or MRS (*L. plantarum*) supplemented with 2 mM of one of the precursors. After incubation, amino acids and derivatives in supernatants were derivatised with diethyl ethoxymethylenemalonate (DEEMM) and identified and quantified by ultra-HPLCI, according to a standardized protocol (Redruello et al., 2013). *Enterococcus faecalis* V583 was used as a positive control for tyramine production.

Growth and metabolites production in milk

UHT-treated, semi-skimmed milk (CAPSA, Siero, Spain) was inoculated with each strain singly, two by two, and all three strains together, giving rise to seven different fermentations: LA1, LA10, LA30, LA1 + LA10, LA1 + LA30, LA10 + LA30, and LA1 + LA10 + LA30. An inoculum size of $\approx 3 \times 10^5$ cfu ml^{-1} was always used, and the incubations proceed at 22°C (which mirrors the room fermentation temperature of the NFM) for 48 h. The growth of the strains, the pH reached, and the production of organic acids and volatile compounds, were determined as described below. Unless otherwise stated, analyses were performed in triplicate.

Growth of the strains in milk

Bacterial counts were recorded by dissolving the inoculated milk samples in a warm 2% citrate solution and making 10-fold dilutions in saline. These dilutions were then plated onto GM17 for counting lactococci, and MRS for counting *L. plantarum*. The pH of the milk was measured using a pH-meter (Crison, Barcelona, Spain).

Production of organic acids

The organic acids and sugars produced or consumed during growth in milk (by both individual strains and their mixtures) were determined by Ultra High Performance Liquid Chromatography (UHPLC) following the method of Alegría et al. (2016). Briefly, compounds were separated in an ICSep ICE-ION-300 ion-exchange column (Waters, Waltham, MASS, United States), with 8.5 mN H_2SO_4 as the mobile phase (operating temperature 65°C, flow rate of 0.4 ml min^{-1}). Sugars were identified using a Waters model 410 differential refractometer at 280 nm, and organic acids using a Waters model 996 photodiode array detector at 210 nm. The concentration of individual metabolites was obtained using calibration curves prepared with commercial standards.

Production of volatile compounds

Volatile compounds in the fermented milks were quantified by headspace/gas chromatography/mass spectrometry (HS/GC/MS) using an Agilent apparatus with G 1888 HS, 6890 GC and 5975B inert MSD components (Agilent Technologies, Wilmington, DE, United States), equipped with an HP-Innowax column (length 60 m, internal diameter 0.25 mm, 0 film.25 µm; Agilent). Sample preparation and gas chromatographic analysis

were performed as described by Fernández et al. (2011). After incubation, 100 µl of internal standard (cyclohexanone, 0.36 mg ml^{-1}) were added and these mixtures stored at −80°C until analysis. Peaks were quantified as the relative total ionic count with respect to the internal standard.

Genome sequencing and analysis

For genome sequencing, total DNA from the three trains was extracted using the QIAmp DNA Mini Kit (Qiagen, Hilden, Germany). Sequencing libraries were prepared using the TruSeq DNA PCR-free Sample Preparation Kit (Illumina, San Diego, CA, United States), and paired-end sequenced using a HiSeq 1500 System. Reads were checked for quality with FastQC,[1] and trimmed for quality optimization with TrimGalore.[2] Contigs were assembled using Velvet software v.1.2.10.[3] Genomes were annotated and analyzed using PATRIC services.[4] Antibiotic resistance and virulence genes were further investigated by genome comparison against sequences in the Resfinder,[5] CARD,[6] VFDB (Virulence Factor Database; http://www.mgc.ac.cn/VFs/), and Victors[7] databases. Whole-genome sequence data were used to ascertain the phylogenetic relationships between the sequenced strains and the type strains of *Lactococcus* and lactobacilli species by means of digital DNA–DNA hybridization (dDDH) and orthologous average nucleotide identity (orthoANI) analysis, as reported by Meier-Kolthoff and Göker (2019) and Yoon et al. (2017), respectively.

The genome sequences of all three examined strains were deposited in the GenBank database under Bioproject PRJNA876833 and BioSample accession numbers SAMN30673470 (*L. lactis* LA1), SAMN30673504 (*L. cremoris* LA10), and SAMN30673505 (*L. plantarum* LA30).

Results and discussion

This work reports on the phenotypic and genomic characterization of three strains of different species that together form a highly stable bacterial consortium capable of producing an appealing NFM, widely-spread and consumed in households across Europe. Complex, undefined microbial communities are widely used as starters in food biotechnology, including the manufacture of cheese, and other fermented food commodities based on meat, vegetables, cereals and fish (Oshiro et al., 2019; Sun and D'Amico, 2021). Identifying their components and characterizing at phenotypic and genetic levels their stability and cooperativity properties during milk fermentation could help the rational design of multi-strain starters from a pool of genome-sequenced LAB of different origins (Minty et al., 2013; Shapiro and Polz, 2014).

Biochemical phenotyping

After confirming the previous identification of the strains, they were subjected to a battery of phenotypic tests, including, among others, carbohydrate utilization, enzyme profiling, and antibiotic resistance. Table 1 shows the carbohydrate fermentation profiles of the three LAB strains. Wide variation was noted: among the 49 carbohydrates tested by the API-50 strips, *L. lactis* LA1 fermented 13, *L. cremoris* LA10 used only 6, and *L. plantarum* LA30 fermented 18. The enzyme activities of the strains, as determined using the API-ZYM system are summarized in Table 2. The two *Lactococcus* strains showed a reduced and weak profile, but strong acid and alkaline phosphatase activity. In contrast, *L. plantarum* LA30 showed vigorous leucine arylamidase (aminopeptidase), valine arylamidase (aminopeptidase), and β-galactosidase activity, and moderate β-glucosidase and N-acetyl-β-glucosidase activity. In agreement with the present results, wide phenotypic variations have been repeatedly reported across LAB species and strains (Siezen et al., 2010; Bayjanov et al., 2013; Moraes et al., 2013). A reduced carbohydrate fermentation profile has been reported for dairy lactococci compared to those of plant origin (Kelly et al., 2010; Laroute et al., 2017; Wels et al., 2019), but the small number of carbohydrates (only six) utilized by *L. cremoris* LA10 was surprising, suggesting it to be a "domesticated" dairy strain (Cavanagh et al., 2015). Similar enzyme profiles to those noted for all three strains of this study have been reported by other authors (Medina et al., 2001; Câmara et al., 2019).

Safety assessment of the strains

Table 3 shows the results of the resistance-susceptibility analysis for the 16 antibiotics tested. The MICs recorded ranged from <0.03 µg ml^{-1} to >128 µg ml^{-1}. *Lactiplantibacillus plantarum* LA30 showed moderate resistance to tetracycline (32 µg ml^{-1}), which matches EFSA's cut-off value for this antibiotic, and strong resistance to vancomycin (>128 µg ml^{-1}), while *L. lactis* LA1 proved to be strongly resistant to rifampicin (>64 µg ml^{-1}). Vancomycin resistance in lactobacilli is considered intrinsic (Campedelli et al., 2018), and rifampicin resistance in lactococci as usually being caused by either non-specific mechanisms or mutations in the *rpoB* gene (van Pijkeren and Britton, 2012; Goldstein, 2014).

Lactococcus lactis LA1 proved to be a GABA producer (6.29 mM), while the other two strains were considered non-producers (<0.64 mM; Redruello et al., 2021). None of the strains produced biogenic amines from the precursor amino acids

1 https://www.bioinformatics.babraham.ac.uk/projects/fastqc/
2 https://www.bioinformatics.babraham.ac.uk/projects/trim_galore
3 https://www.ebi.ac.uk/~zerbino/velvet/
4 https://www.patricbrc.org/
5 https://cge.cbs.dtu.dk/services/ResFinder/
6 https://card.mcmaster.ca/
7 http://www.phidias.us/victors/

10.3389/fmicb.2022.1000683

TABLE 1 Carbohydrate fermentation profile of *Lactococcus lactis* subsp. *lactis* LA1, *Lactococcus cremoris* subsp. *cremoris* LA10, and *Lactiplantibacillus plantarum* LA30.

Strain	Carbohydrate[a]																		
	GLU	FRU	MAN	LAC	NAG	ESC	GAL	RIB	AMY	ARB	SAL	CEL	MAL	MEL	MNN	SUC	TRE	MLZ	GEN	GNT
LA1	+	+	+	+	+	+	+	+	−	+	+	+	−	−	−	−	+	−	+	−
LA10	+	+	+	+	+	+	−	−	−	−	−	−	−	−	−	−	−	−	−	−
LA30	+	+	+	+	+	+	+	−	+	+	+	+	+	+	+	+	−	+	+	+

Carbohydrates from the API-50 CHL utilized by none of the strains: D-adonitol, D-arabinose, L-arabinose, D-arabitol, L-arabitol, dulcitol, erythritol, glycerol, glycogen, D-fucose, L-fucose, inositol, inuline, 2-ketogluconate, 5-ketogluconate, D-lyxose, methyl-αD-glucopyranoside, methyl-αD-mannopyranoside, methyl-βD-xylopyranoside, D-raffinose, L-rhamnose, D-sorbitol, L-sorbose, starch, D-tagatose, D-turanose, xylitol, D-xylose, and L-xylose.

[a]Carbohydrate: GLU, D-glucose; FRU, D-fructose; MAN, D-mannose; LAC, lactose; NAG, N-acetylglucosamine; ESC, esculine; GAL, D-galactose; RIB, D-ribose; AMY, amygdaline; ARB, arbutine; SAL, salicine; CEL, D-cellobiose; MAL, D-maltose; MEL, mellibiose; MNN, D-mannitol; SUC, D-sucrose; TRE, D-threhalose; MLZ, D-melezitose; GEN, gentiobiose; GNT, gluconate.

tested; acting as a control, *E. faecalis* V583 produced 5.20 mM tyramine from tyrosine. Production of GABA and formation of biogenic amines require amino acid-specific decarboxylases and are well-known, strain-specific characters (Ladero et al., 2015).

Growth and metabolite production

After 48 h incubation at 22°C, only *L. cremoris* LA10, and the combinations containing this strain, coagulated the milk, with the final pH either close to or below 4.6 (4.52 ± 0.33; Figure 1). Under the same incubation conditions, neither *L. lactis* LA1 nor *L. plantarum* LA30, either alone or combined, could coagulate the milk (final pH always >6.0). The fermented milks were stored for up to 1 month at 4°C, during which time a small amount of postacidification was observed (0.21 ± 0.04 pH units).

Figure 2 summarizes the microbial counts recorded during growth in milk. When grown alone, *L. cremoris* LA10 reached a cell numbers in milk of over 9 $\log_{10}$ cfu ml^{-1} (9.14 ± 0.03), while *L. lactis* LA1 and *L. plantarum* LA30 reached cell numbers of 0.5 and 2 $\log_{10}$ units lower, respectively (Figure 2). Although not confirmed in this study, as previously determined (Alegría et al., 2010), in the fermented milks made by *L. lactis* LA1 and *L. plantarum* LA30 in combination, equal numbers were assumed for both strains. Alone or combined, counts of *L. plantarum* LA30 were very similar, suggesting the growth of this strain to not be truly stimulated by any companion *Lactococcus*. Similar results were also obtained by real time quantitative PCR, using strain-specific oligonucleotide primers (data not shown).

The individual and combined strains showed various patterns of production/consumption of organic acids and sugars (Table 4). All strains and combinations utilized most of the glucose in milk and part of the lactose. Moreover, *L. cremoris* LA10, and all mixtures including this strain released some galactose to the milk (mean 8.6 ± 2.7 mg 100 ml^{-1}). However, this amount was within the range found in cheese and other foods, and low enough to be acceptable even for diets to tackle with classic galactosaemia (Van Calcar et al., 2014). Lactic acid was produced by all three strains, but strongly by *L. cremoris* LA10 and its combinations. Moderate amounts of acetic acid were produced in all milks fermented with *L. lactis* LA1. All –but only– the fermentations involving this latter strain showed citric acid to be readily consumed. Small variations in the fate of other organic acids in the different fermentations were also scored (Table 4).

Among the 12 volatile compounds detected in the fermented milks, only six were quantified by HS/GC/MS (Table 5). In agreement with the utilization of citrate, diacetyl and acetoin were detected mostly in milks fermented by *L. lactis* LA1. Confirming the previous HPLC analysis, the presence of acetic acid was also associated with fermentations involving this strain. Surprisingly, and compared to any other fermented milk, the sample inoculated with all three strains showed 6 times the amount of acetaldehyde, suggesting it may be the result of an interaction between the consortium strains. In

TABLE 2 Enzyme activities measured with the API-ZYM system of *L. lactis* subsp. *lactis* LA1, *L. cremoris* subsp. *cremoris* LA10, and *L. plantarum* LA30.

Strain	Enzyme activity[a] (nmol)									
	Esterase	Esterase lipase	Lipase	Leu-aryl	Val-aryl	Acid-phos	N-nph	β-gal	β-glu	N-acetyl-β-glu
LA1	5	5	5	0	0	≥40	≥40	5	0	0
LA10	5	5	0	5	0	≥40	≥40	5	0	0
LA30	0	0	0	≥40	≥40	5	20	≥40	20	20

Trypsin, α-chymotrypsin, alkaline phosphatase, cystine arylamidase, α-galactosidase, α-glucuronidase, α-glucosidase, α-mannosidase, and α-fucosidase activities were not detected in any of the strains.
[a]Activity: Esterase, esterase C4; Esterase lipase, esterase C8; Lipase, lipase C14; Leu-aryl, leucine arylamidase; Val-aryl, valine arylamidase; Acid-phos, acid phosphatase; N-nph, naftol-AS-BI-phosphohydrolase; β-gal, β-galactosidase; β-glu, β-glucosidase; N-acetyl-β-glu, N-acetyl-β-glucosaminidase.

TABLE 3 Minimum inhibitory concentration of 16 antibiotics to *L. lactis* subsp. *lactis* LA1, *L. cremoris* subsp. *cremoris* LA10, and *L. plantarum* LA30.

Strain	Minimum inhibitory concentration (MIC)															
	Gm	Km	Sm	Nm	Tc	Em	Cl	Cm	Am	Pc	Va	Q-da	Lz	Tm	Ci	Rif
LA1	<0.5[a]	8	16	1	1	0.12	0.06	4	0.25	0.25	0.5	2	2	>64	2	>64
LA10	<0.5	<2	4	<0.5	0.5	0.03	<0.06	2	<0.03	<0.03	<0.25	2	0.5	>64	1	8
LA30	<0.5	8	2	<0.5	32	0.12	2	8	1	4	>128	2	4	0.25	16	4
Cut-offs for *lactococci*[b]	**32**	**64**	**32**	–	**4**	**1**	**1**	**8**	**2**	–	**4**	–	–	–	–	–
Cut-offs for *L. plantarum*[a]	**16**	**64**	**nr**	–	**32**	**1**	**4**	**8**	**2**	**2**	**nr**	–	–	–	–	–

Key of antibiotics: Gm, gentamicin; Km, kanamycin; Sm, streptomycin; Nm, neomycin; Tc, tetracycline; Em, erythromycin; Cl, clindamycin; Cm, chloramphenicol; Am, ampicillin; Pc, penicillin G; Va, vancomycin; Q-da, quinupristin-dalfopristin; Lz, linezolid; Tm, trimethoprim; Ci, ciprofloxacin; Rif, rifampicin.
[a]MIC values are in μg ml^{-1}.
[b]The cut-offs applied were those of EFSA FEEDAP Panel (EFSA Panel on Additives and Products or Substances used in Animal Feed) (2018); nr, not required; –, cut-off not established.

bacteria, acetaldehyde can be derived from the metabolism of amino acids, nucleotides or pyruvate (Bongers et al., 2005). However, despite the several biochemical pathways thus available, acetaldehyde is hardly ever detected as a fermentation end-product of LAB species other than those in yoghurt cultures composed of *Lactobacillus delbrueckii* subsp. *bulgaricus* and *Streptococcus thermophilus* (Chen et al., 2017). Although the nature of the interaction between the three components of the consortium leading to increased acetaldehyde production deserves further investigation, this result reinforces the view that some communities can display properties not shown by their individual members (Minty et al., 2013).

The flavor components of fermented milks include volatile and non-volatile compounds; some are already present in the starting milk, but most are produced during fermentation (Settachaimongkon et al., 2014; Beltrán-Barrientos et al., 2019). The major volatile compounds commonly include lactic and acetic acids, acetaldehyde, diacetyl, acetoin, 2,3-butanediol, and 2-butanone (Chen et al., 2017). These compounds are mostly generated through glycolysis or *via* the metabolism of citrate. In the presence of a fermentable carbohydrate (e.g., lactose), citrate is utilized by *L. lactis* subsp. *lactis* biovar *diacetylactis* as a secondary means of generating proton motive force (PMF; Drider et al., 2004). By increasing the intracellular redox potential of the cell, enhancing disulfide bond formation and reducing cofactor reoxidation (Waché et al., 2002), enhanced PMF promotes cell growth.

Genome analysis

Whole-genome sequencing (WGS) and analysis is currently considered as the gold standard of genetic characterization of microorganisms, including LAB (Liu et al., 2005). The general features of the genome sequences of the three strains of this study are summarized in Table 6. These proved to be similar to those on the literature for strains of the corresponding LAB species. A large number of corrupted genes was found in the genome of all three (59, 105, and 15 for *L. lactis* LA1, *L. cremoris* LA10, and *L. plantarum* LA30, respectively). Conventional PCR amplification, sequencing and sequence comparison around the corrupted positions in seven single-copy genes (three from *L. lactis* LA1 and four from *L. plantarum* LA30) confirmed all mutations identified by genome sequencing. Even though LAB are well known to show gene decay as part of their adaptation (domestication) to the milk environment (Callanan et al., 2008; Cavanagh et al., 2015), one of the most striking features of the sequenced strains was the large number of corrupted genes possessed by all three. In particular, the genome of *L. cremoris* LA10 was so eroded that, as suggested for other *L. cremoris* strains (Wels et al., 2019), it would seem to now be restricted to the dairy environment.

Identification by genome data

The taxonomic identification of the strains by *in silico* dDDH and OrthoANIu analyses of the genomic data against the type

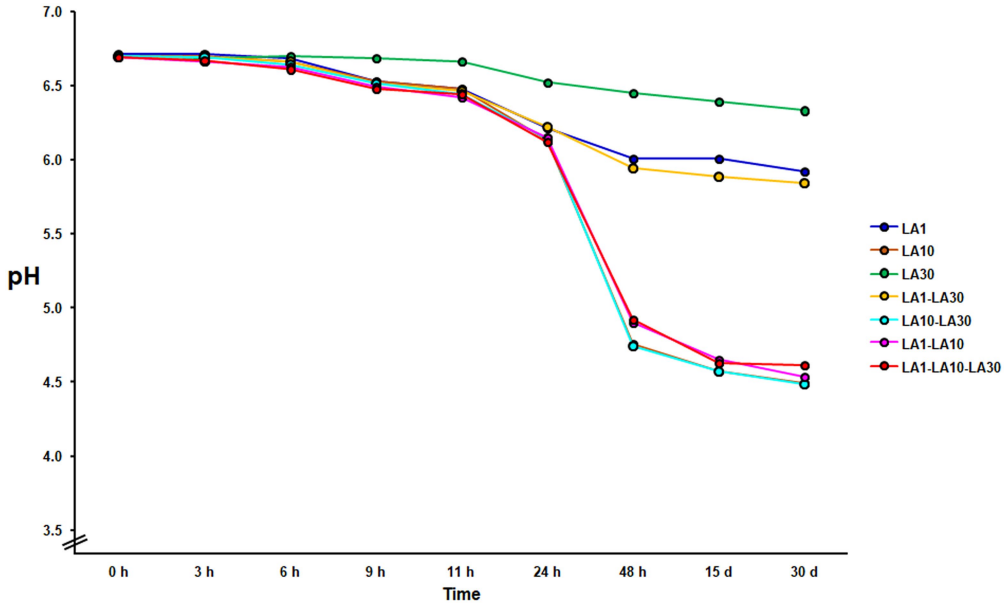

FIGURE 1
Evolution of the pH during milk fermentation with the individual strains of the consortium and all their mixture combinations. Curves with highly similar slopes were seen in replicate experiments. For the sake of clarity, only one is depicted.

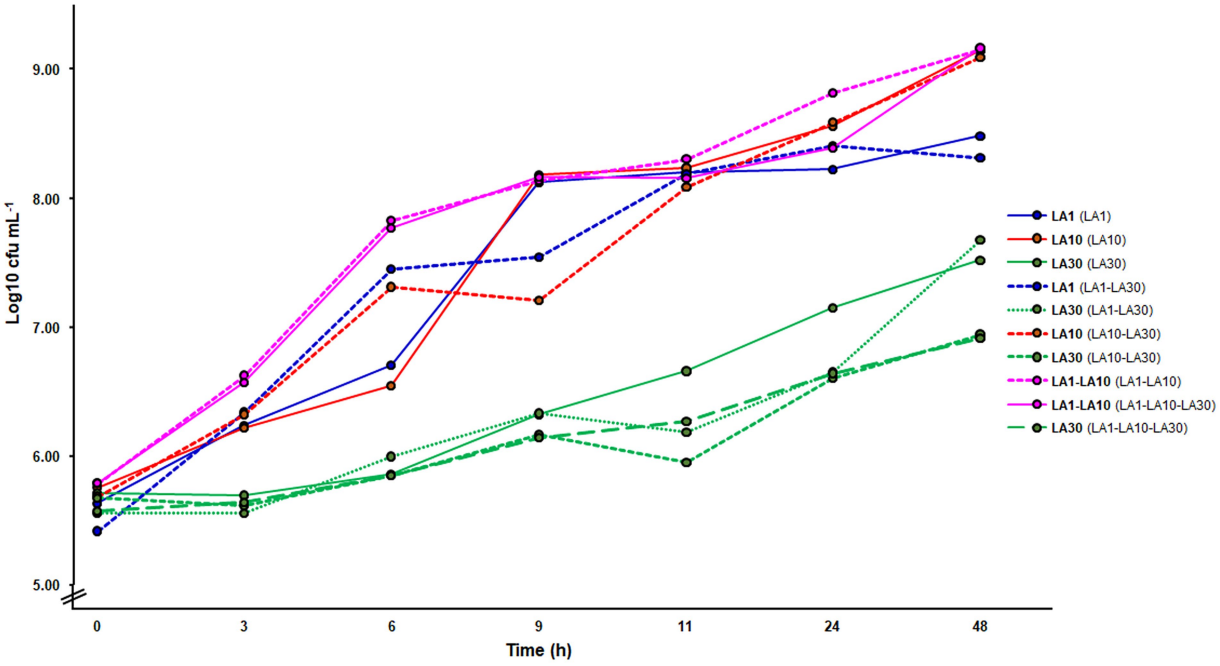

FIGURE 2
Microbial counts in GM17 (lactococci) and MRS (*Lactiplantibacillus plantarum*) along the fermentation of milk with the individual strains and their mixtures. In bold, the strain(s) counted on each of the curves; in parenthesis, the fermentation from which the counting was made.

strains of *Lactococcus* spp. and *Lactiplantibacillus* spp. confirmed the strains as belonging to *L. lactis* subp. *Lactis* (LA1), *L. cremoris* subsp. *cremoris* (LA10), and *L. plantarum* (LA30), respectively. LA1 showed the highest dDDH and OrthoANIu values to *L. lactis* subsp. *lactis* biovar *diacetylactis* GL2^T (Supplementary Table S1); thus, LA1 was considered to belong to the *diacetylactis* biovar; phenotypic data were then supported by genome analysis (see below).

10.3389/fmicb.2022.1000683

TABLE 4 Production and consumption of organic acids and sugars during growth in milk at 32°C for 48h alone or in several combinations of *L. lactis* subsp. *lactis* LA1, *L. cremoris* subsp. *cremoris* LA10, and *L. plantarum* LA30.

Strain–strain mixtures	Organic acid/sugar[a]									
	Orotic	Citric	Pyruvic	Succinic	Lactic	Formic	Acetic	Uric	Hippuric	Lactose[b]	Glucose	Galactose
Uninoculated milk	1.30 ± 0.04	25.6 ± 0.8	0.02 ± 0.01	–	0.20 ± 0.1	–	–	0.40 ± 0.02	0.36 ± 0.01	812.40 ± 28	1.70 ± 0.04	2.40 ± 0.1
LA1	0.90 ± 0.30	1.9 ± 0.6	0.80 ± 0.30	–	25.80 ± 7.7	–	6.70 ± 1.9	0.30 ± 0.10	0.20 ± 0.10	782.60 ± 34	0.10 ± 0.04	2.00 ± 0.7
LA10	0.90 ± 0.02	21.7 ± 5.9	0.10 ± 0.01	0.60 ± 0.02	104.80 ± 2	0.10 ± 0.01	0.80 ± 0.1	0.30 ± 0.01	–	695.60 ± 18	0.10 ± 0.01	9.00 ± 0.1
LA30	1.05 ± 0.30	20.6 ± 6.2	0.05 ± 0.02	–	5.60 ± 1.9	–	0.30 ± 0.1	0.30 ± 0.10	0.20 ± 0.08	777.30 ± 15	0.10 ± 0.01	2.25 ± 0.7
LA1-LA10	1.15 ± 0.02	–	0.50 ± 0.01	0.30 ± 0.02	134.40 ± 2	0.15 ± 0.01	10.60 ± 0.1	0.45 ± 0.01	–	725.00 ± 18	0.10 ± 0.01	6.50 ± 0.1
LA1-LA30	1.30 ± 0.02	3.4 ± 0.4	1.30 ± 0.07	–	38.70 ± 0.5	–	9.80 ± 0.5	0.40 ± 0.01	0.35 ± 0.03	798.70 ± 20	0.10 ± 0.01	3.10 ± 0.1
LA10-LA30	1.10 ± 0.02	26.3 ± 0.2	0.40 ± 0.10	0.80 ± 0.10	129.20 ± 2	–	1.30 ± 0.1	0.40 ± 0.01	–	710.20 ± 90	0.10 ± 0.01	12.20 ± 0.1
LA1-LA10-LA30	1.15 ± 0.06	–	0.70 ± 0.03	0.50 ± 0.10	137.30 ± 5	0.10 ± 0.01	10.50 ± 0.5	0.45 ± 0.02	–	712.80 ± 41	0.10 ± 0.02	6.60 ± 0.3

–, not detected. [a]Average results of three independent assays are reported in mg 100 ml^{-1}.
[b]Experimental results are being reported (the system is overloaded with the actual content).

Proteolytic system and amino acid catabolism

The efficient growth of LAB in milk requires the presence of an extracellular, cell envelope-associated, caseinolytic proteinase (PrtP, PrtB, PrtH, or equivalent) to meet the strong demand for nitrogen (Liu et al., 2010). A gene encoding a 1960 amino acids long PrtP type II pre-pro-proteinase showing 99% identity to that of *L. cremoris* subsp. *cremoris* SK11 (De Vos et al., 1989) was identified in the genome of *L. cremoris* LA10. As expected, downstream of the proteinase gene, oppositely orientated and 320 bp away, an ORF encoding a peptidylprolyl isomerase-like lipoprotein of 299 amino acids was detected, known as PrtM (Haandrikman et al., 1989). This acts as a chaperone that converts the pro-proteinase into the active protease. The ORF and its encoded protein were identical to those reported in other strains of this species (Haandrikman et al., 1989). The two genes, *prtP* and *prtM*, were found in a 19,727-bp-long contig associated with sequences involved in plasmid replication. With minor rearrangements, the whole contig sequence showed extensive homology to lactococcal proteinase plasmids, particularly to segments of the long plasmids pDRC3A (103.88 kbp) from *L. lactis* subsp. *lactis* DRC3 (NZ_CP064836.1) and pJM3A (75.81 kbp) from *L. cremoris* subsp. *cremoris* JM3 (NZ_CP016737.1). Although a plasmid location of the proteinase genes in *L. cremoris* LA10 is strongly suggested, the proteinase activity proved to be stable and proteinase-negative variants never observed.

No genes encoding an equivalent proteinase and its maturation protein were identified in the genome of *L. lactis* LA1 or *L. plantarum* LA30. Consequently, these strains grew more slowly in milk that did *L. cremoris* LA10. *Via* the action of the proteinase, *L. cremoris* LA10 could provide casein nitrogen to its partners in mixed fermentations; certainly it has long been recognized that the proteolytic activity of proteinase-positive strains enables non-proteolytic variants to reach high cell densities in milk (Juillard et al., 1996). However, great differences in proteolytic activity have been reported among proteinase-positive strains (Kieliszek et al., 2021), and the stimulation of the growth of proteinase-negative strains by their proteinase-positive counterparts has recently been shown to be strain-specific (Canon et al., 2021). Indeed, the growth of *L. plantarum* LA30 in the present work did not seem to be stimulated by *L. cremoris* LA10. Despite this, *L. plantarum* might be stimulated by other amino acid-derived compounds, such as the GABA produced from glutamate by *L. lactis* LA1, as has been reported for *Leuconostoc mesenteroides* in a traditional cheese starter system (Erkus et al., 2013).

Complex repertoires of genes involved in protein and peptide degradation and subsequent amino acid catabolism and flavor formation were detected in all three strains. Indeed, all strains possessed complex repertoires of genes coding for proteases (14–17 per strain), peptidases (including amino-, carboxy-, and endo-peptidases; 26–31), different amino acid/di–/tri–/oligo-peptide transporters (15–29), aminotrasferases and transaminases (14–21). This genetic repertoire suggests that these strains might be used in starter cultures for other dairy products. Most amino

TABLE 5 Relative abundance of the volatile compounds produced and quantified during growth in milk at 32°C for 48h of *L. lactis* subsp. *lactis* LA1, *L. cremoris* subsp. *cremoris* LA10, and *L. plantarum* LA30, each incubated alone or in combination.

Strain–strain mixtures	Volatile compound[a,b]					
	Acetaldehyde	2-Propanone	Ethanol	Diacetyl	Acetoin	Acetic acid
Uninoculated milk	–	–	–	–	–	–
LA1	67 ± 19	4 ± 2	19 ± 5	5 ± 1	62 ± 10	23 ± 6
LA10	71 ± 4	27 ± 4	122 ± 6	–	7 ± 5	–
LA30	50 ± 32	16 ± 12	33 ± 5	–	4 ± 2	–
LA1-LA10	152 ± 43	11 ± 2	23 ± 5	30 ± 7	123 ± 37	51 ± 20
LA1-LA30	63 ± 29	14 ± 5	11 ± 2	13 ± 6	66 ± 25	25 ± 19
LA10-LA30	100 ± 19	28 ± 9	115 ± 25	–	14 ± 7	–
LA1-LA10-LA30	602 ± 37	11 ± 3	23 ± 4	31 ± 17	144 ± 34	51 ± 20

–, not detected.
[a]Carbon disulfide, 2-methyl propanal, 2-propanone, 3-methyl butanal, 2-methyl-1-propanol, and 3-methyl-1-butanol were detected in most fermentations but not quantified.
[b]Results are average of three independent assays.

acid-derived volatile compounds, however, may only have a significant impact on the sensory profile of long-ripened fermented dairy products, such as cheese (Smid and Kleerebezem, 2014).

Lactose utilization

To grow efficiently in milk, LAB also require a proficient lactose utilization system (this sugar is the main carbon source in this medium). The genetics of lactose utilization by LAB species and strains is complex but rather well known (for a recent review see Iskandar et al., 2019). Lactose is metabolized by LAB either *via* the Leloir or tagatose-6-phosphate pathways. Lactose catabolism in LAB normally proceeds by the Leloir pathway, whereas the tagatose-6-phosphate pathway is mostly restricted to strains of *Lactococcus* spp., *Lacticaseibacillus casei* and *Lacticaseibacillus paracasei* species (Iskandar et al., 2019). However, gene content variation in terms of the components of these lactose pathways in LAB strains of different origin has been repeatedly reported (Passerini et al., 2013). Gene clusters encoding proteins involved in the two pathways were identified in the genome of *L. lactis* LA1 and *L. cremoris* LA10, while in *L. plantarum* LA30 only genes of the Leloir pathway were found (Supplementary Table S2).

In the Leloir pathway, lactose is internalized by the product of *galP*, and then hydrolysed by a β-galactosidase (encoded by *lacZ*; Iskandar et al., 2019). The genome of *L. plantarum* LA30 showed three genes encoding lactose/galactose permeases, of which one was associated with a β-galactosidase-encoding gene (*lacZ*). Three other β-galactosidase genes were found scattered throughout the *L. plantarum* genome, one of which was heterodimeric (*lacLM*). The genome of *L. lactis* LA1 and *L. cremoris* LA10 showed a single locus harboring canonical genes of the Leloir pathway for lactose and galactose (*galPMKTE*; Figure 3). A β-galactosidase-encoding gene was located close to the Leloir pathway genes in the *L. lactis* LA1 genome. No *lacZ* gene was found in the genome of *L. cremoris* LA10. In this latter strain, the sequence encoding the galactokinase gene (*galK*) contained a mutation splitting the ORF into two halves. This would explain the inability of *L. cremoris* LA10 to utilize intracellular galactose in the API-50 test, and the presence of galactose in the supernatant of all milk samples fermented with this strain. Although a galactose permease and several low-affinity galactose PTS systems have been shown to be active in *L. lactis* and *L. cremoris* (and probably in other LAB species; Solopova et al., 2018), the internalization of galactose from milk by LA1 and LA30 strains in the presence of an extremely high amount of lactose might be repressed.

A single locus containing all required genes for the tagatose-6-phosphate pathway was identified in the genome of both lactococcal strains. Not surprisingly, each was associated with plasmid-encoded traits. Within this locus, an operon-like structure harboring genes coding for galactose-6-phosphate isomerase (*lacAB*), tagatose-6-phosphate kinase (*lacC*), tagatose 1,6-bisphosphate aldolase (*lacD*), the lactose-specific components of the PTS system (*lacFE*), 6-phospho-beta-galactosidase (*lacG*), and LacX (*lacX*), were identified, plus the oppositely transcribed gene encoding the pathway regulator (*lacR*; Figure 3).

In *L. cremoris* LA10, lactose must be utilized *via* the tagatose-6-phosphate pathway since it lacks the *lacZ* gene and has a mutation in *galK*. However, in *L. lactis* LA1 the gene collections required for both pathways appear to be complete, suggesting them to be functional.

Citrate metabolism

Diacetyl (2,3-butanedione) and acetoin (3-hydroxy-2-butanone) are creamy and buttery flavor compounds formed from pyruvate, which are pivotal in many dairy products (Afshari et al., 2020).

In agreement with the citrate-utilizing phenotype of *L. lactis* subsp. *lactis* biovar *diacetylactis* LA1, two gene clusters (one plasmid-located and one in the chromosome) involved in citrate fermentation were identified in its genome. The plasmid-borne *citQRP* operon encodes the only citrate transporter system identified to date in lactococci of the *diacetylactis* biovar., CitP (García-Quintáns et al., 2008), as well as the transcriptional regulator CitR, and a putative protein

TABLE 6 General features of the genome sequences of *L. lactis* subsp. *lactis* LA1, *L. cremoris* subsp. *cremoris* LA10, and *L. plantarum* LA30 strains from the fermented milk consortium.

Property/ encoding genes[a]	*L. lactis* subsp. *lactis* LA1	*L. cremoris* subsp. *cremoris* LA10	*L. plantarum* LA30
Genome size (bp)	2,433,628	2,387,995	3,225,998
G + C content	34.99	35.52	44.39
No. of contigs	104	202	253
Contig N50	61,997	27,520	8,2,412
No. of coding sequences	2,558	2,629	3,271
Proteins with functional assignments	1,986	2,007	1,802
Hypothetical CDS	571	621	1,469
No. of PATRIC subsystems	204	204	169
Antibiotic Resistance (PATRIC/CARD)	26/2	27/2	25/0
Acquired resistance to antibiotics	–	–	–
Virulence Factors (VFDB/Victors)	1/7	1/7	0/0
Penicillin binding proteins	2	1	4
Efflux-related proteins	27	25	28
Resistance to heavy metals	7	6	6
Distinct rRNA operons (23S + 16S + 5.8S)	4 (1 + 1 + 2)	4 (1 + 1 + 2)	3 (1 + 1 + 1)
tRNA molecules	51	50	57
Transporter (TCDB)	73	77	14
Proteases	15	17	18
Caseinolitic proteases (PtrP-like)	–	1	–
Peptidases	26	26	33
Transposases/mobile elements	26	23	39
Glycosil hydrolases	35	12	24
Phage-derived proteins	164	123	25
Tentative functional integrated phages	1	1	2
Plasmid replication proteins	6	11	1
CRISPR loci	–	–	-
Bacteriocins	Lactococcin A	–	Plantaricin F
Toxin-antitoxin systems	Exfoliative toxin A	Exfoliative toxin A	YdcE, HigB-HigA, YefM

[a]Only complete, non-corrupted genes were included.

CitQ (López de Felipe et al., 1995). *citP* and its accompanying genes were identified as associated with genes coding for plasmid replication functions in a contig of 7,270 bp, suggesting a plasmid location (Figure 4). The whole sequence was identical to a major part of the citrate plasmids from *L. lactis* subsp. *lactis* biovar *diacetylactis*, i.e., pSD96_04 (CP043528.1), pAH1-6 (CP093419.1) and pCRL1127 (AF409136.1). Compared to these plasmids, the contig in *L. lactis* LA1 lacked the complete nucleotide sequence of a 999 bp-long IS982-like element. This was found in a larger contig, and might have prevented the assembly software allocating a copy to the citrate plasmid. No such an equivalent cluster was identified in either *L. cremoris* LA10 or *L. plantarum* LA30 genomes.

The formation of pyruvate from citrate involves the chromosomally clustered genes *citM-citI-citCDEFXG*, which encode the α-, β-, and γ-citrate lyase subunits (CitF, CitE, and CitD, respectively), the CitC, CitX and CitG auxiliary proteins, and the oxaloacetate decarboxylase CitM (Passerini et al., 2013). Upstream of *citC* is a divergent open reading frame coding CitI, which may regulate the expression of CitP and the assembly of the citrate lyase complex (Martín et al., 2005). All these genes and others encoding key enzymes involved in diacetyl formation (α-acetolactate synthase, lactate dehydrogenase and α-acetolactate decarboxylase) were identified in the genome of *L. lactis* LA1 (Figure 4). These genes support genetically the diacetyl- and acetoin-producing phenotype of this strain. Again, no genes involved in citrate metabolism were identified in *L. cremoris* LA10, and only genes coding for the citrate lyase complex were detected in *L. plantarum* LA30 (Figure 4).

Safety assessment

Beyond genes encoding multidrug efflux pumps (Table 6) and proteins involved in heavy metal homeostasis (around seven in each strain), no genes associated with virulence or pathogenicity factors were detected in any of the strains. Two consecutive ORFs, the products of which were identical to the N- and C-terminal parts of a ribosomal protection protein of the TetM/TetW/TetO/TetS family involved in tetracycline resistance, were observed in the genome of *L. plantarum* LA30. These ORFs resulted from an internal mutation of the tetracycline resistance gene, which gave rise to two non-functional protein halves. This gene was located on a 90,000 bp-long contig, suggesting it to be chromosomally encoded. Gene context analysis showed it to have no relationship with sequences involved in mobilization.

Mutations in the *rpoB* gene, which encodes the β subunit of the bacterial RNA polymerase, are known to be related to resistance to rifampicin in *L. lactis* (Goldstein, 2014). Analysis of the *L. lactis* LA1 *rpoB* gene proved to contain mutations leading to two amino acid changes (D489V and H499N). However, the same amino acid replacements were found in the deduced RpoB sequence from the highly susceptible *L. cremoris* LA10 strain. Thus, the cause of this resistance in the LA1 strain remains to be determined. Certain multidrug resistance (MDR)

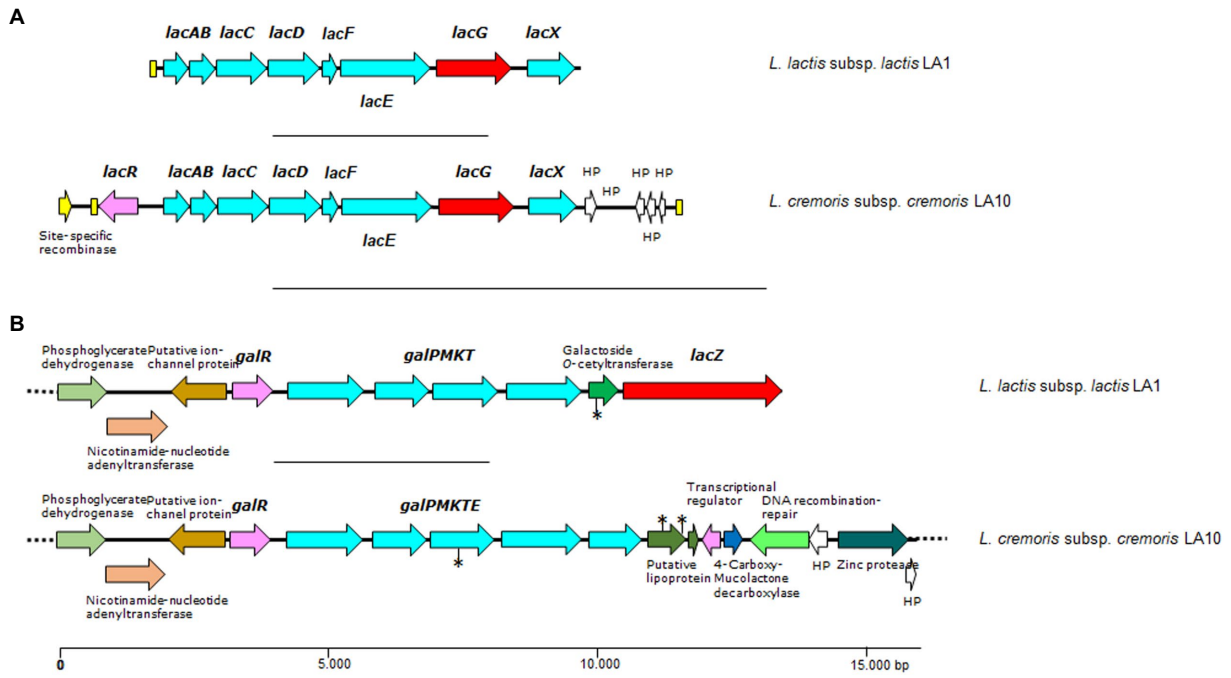

FIGURE 3
Genetic organization of lactose/galactose gene clusters (A and B) found in the genome of *L. lactis* LA1 and *L. cremoris* LA10 isolated from a naturally fermented milk. Color code: in red, genes coding for β-galactosidases, *lacZ*, or phospho-β-galactosidase, *lacG*; in pale blue, genes and components of carbohydrate transporter and metabolism; in yellow, open reading frames (ORFs) encoding transposases or mobilization proteins; in purple, genes coding for regulatory proteins. Yellow boxes indicate DNA repeats, and the asterisks denote ORFs containing mutations disrupting the gene. Dotted lines indicate that the contig extends beyond the depicted area.

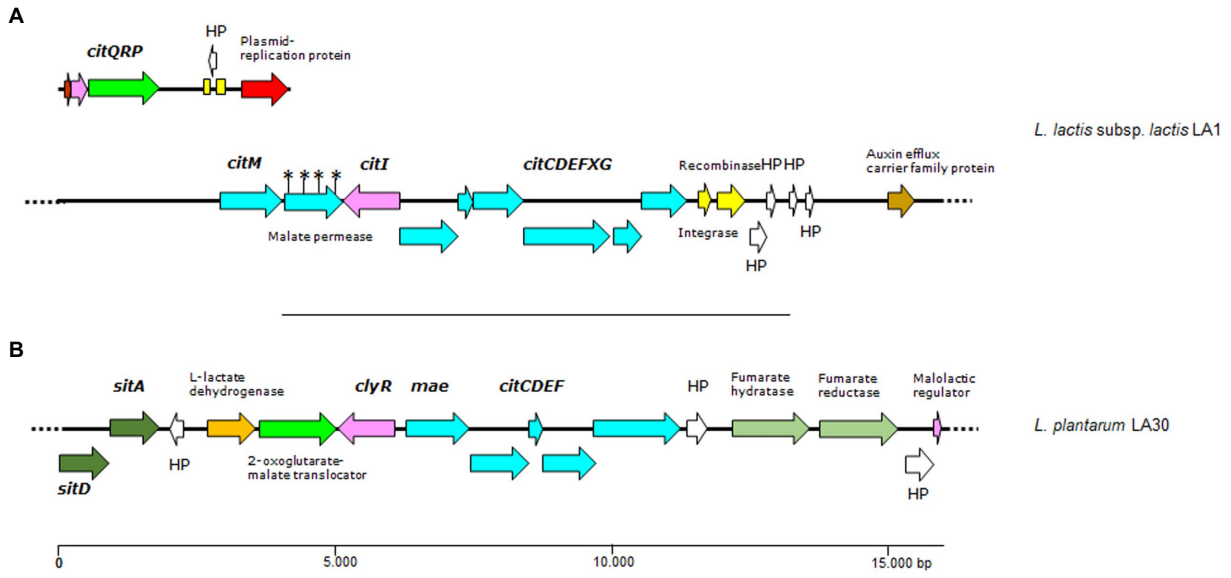

FIGURE 4
Genetic organization of citrate gene clusters (A and B) found in contigs of the genome of *L. lactis* LA1 and *L. plantarum* LA30. Color code: in pale blue, genes of the citrate operons (*citM-citCDEFXG*) and (*mae-citCDEF*); in green, genes involved in transport, including a plasmid-borne citrate permease (*citP*); in pink, genes encoding regulatory proteins; in yellow, genes encoding mobilization proteins; in white, genes encoding hypothetical proteins; any other color, other genes. Yellow boxes indicate DNA repeats, and the asterisks denote ORFs dirupted due to mutations disrupting a gene. Dotted lines as in Figure 3.

transporters devoted to cell detoxification have also been implicated in rifampicin resistance in lactococci (Filipic et al., 2013).

Apart from a glutamic acid decarboxylase gene present in all three strains, and in agreement with the strains having a negative phenotype for the production of biogenic amines, virtually no genes coding for decarboxylases that might act on amino acids were detected. The exception was a gene in *L. plantarum* LA30 coding for a lysine decarboxylase-family protein. This gene was detected in the vicinity of that coding for L-*O*-lysylphosphatidylglycerol synthase, an enzyme involved in the synthesis of the major bacterial membrane phospholipid (Carey et al., 2022). Lysine carboxylases convert lysine to 1,5-pentanediamine (cadaverine), another well-known cell wall component contributing to maintaining normal bacterial growth (Takatsuka and Kamio, 2004).

Conclusion

In summary, this work reports the phenotypic and genomic characterization of three strains of different species found as the components of a stable LAB consortium of a NFM. All three strains were susceptible to all important antibiotics, and the inactive TetM/TetW/TetO/TetS-encoding gene does not seem to be associated to any spreading feature, such as plasmids, insertion sequence (IS) elements or transposons, which, according to EFSA's recommendations (EFSA FEEDAP Panel (EFSA Panel on Additives and Products or Substances used in Animal Feed), 2018) is considered of no concern. Further, genome analysis detected no gene coding for virulence or pathogenicity factors, and none of the strains produced biogenic amines from precursor amino acids. The stability of the consortium must certainly have an underlying biochemical (and thus genetic) basis, though what this might be has yet to be revealed. The *L. cremoris* LA10 strain was the only one of those examined to have a PrtP type II proteinase capable of digesting milk caseins, which may produce the peptides required to feed its nitrogen demands –and perhaps those of its consortium partners. *Lactococcus lactis* LA1 was found to belong to subsp. *lactis* biovar *diacetylactis*, and to utilize milk citrate to produce secondary C-4 metabolite aroma compounds, such as diacetyl and acetoin –the main contributors to the flavor pattern of this NFM. The role of *L. plantarum* LA30 in the consortium, and its interactions with its lactococcal companions, remains to be determined. The consortium as a whole or its individual strains might have a use as a starter or as starter components for dairy fermentations.

Data availability statement

The data presented in the study are deposited in GenBank database under under Bioproject PRJNA876833 and BioSample accession numbers SAMN30673470 (L. lactis LA1), SAMN30673504 (L. cremoris LA10), and SAMN30673505 (L. plantarum LA30).

Author contributions

JR and LV: experimental work, analysis of results, and draft editing. AF: conceptualization of research, analysis of results, and manuscript revision and editing. BM: conceptualization of research, analysis of results, revision and editing of the manuscript, funding acquisition, and material resources. All authors contributed to the article and approved the submitted version.

Funding

This research was supported by projects from the Spanish Ministry of Science and Innovation (PID2019-110549RB-I00/AEI/10.13039/501100011033) and the Principality of Asturias (AYUD/2021/57336). A Ph.D. grant from the Severo Ochoa Program of the Principality of Asturias was awarded to JR (BP19-098).

Acknowledgments

Thanks are owed to Paula Fernández Bayón and Eva Armindo Rivero for their skilful technical contributions to this work.

Conflict of interest

The authors declare that the research was conducted in the absence of any commercial or financial relationships that could be construed as a potential conflict of interest.

Publisher's note

Supplementary material

The Supplementary material for this article can be found online at: https://www.frontiersin.org/articles/10.3389/fmicb.2022.1000683/full#supplementary-material

References

Afshari, R., Pillidge, C. J., Dias, D. A., Osborn, A. M., and Gill, H. (2020). Cheesomics: the future pathway to understanding cheese flavour and quality. *Crit. Rev. Food Sci. Nutr.* 60, 33–47. doi: 10.1080/10408398.2018.1512471

Alegría, A., Fernández, M. E., Delgado, S., and Mayo, B. (2010). Microbial characterization and stability of a farmhouse natural fermented milk from Spain. *Int. J. Dairy Technol.* 63, 423–430. doi: 10.1111/j.1471-0307.2010.00601.x

Alegría, A., González, P., Delgado, S., Flórez, A. B., Hernández-Barranco, A. M., Rodríguez, A., et al. (2016). Characterisation of the technological behaviour of mixtures of mesophilic lactic acid bacteria isolated from traditional cheeses made of raw milk without added starters. *Int. J. Dairy Technol.* 69, 507–519. doi: 10.1111/1471-0307.12253

Barua, N., Herken, A. M., Stern, K. R., Reese, S., Powers, R. L., Morrell-Falvey, J. L., et al. (2021). Simultaneous discovery of positive and negative interactions among rhizosphere bacteria using microwell recovery arrays. *Front. Microbiol.* 11:601788. doi: 10.3389/fmicb.2020.601788

Bayjanov, J. R., Starrenburg, M. J., van der Sijde, M. R., Siezen, R. J., and van Hijum, S. A. (2013). Genotype-phenotype matching analysis of 38 *Lactococcus lactis* strains using random forest methods. *BMC Microbiol.* 13:68. doi: 10.1186/1471-2180-13-68

Beltrán-Barrientos, L. M., Garcia, H. S., Reyes-Díaz, R., Estrada-Montoya, M. C., Torres-Llanez, M. J., Hernández-Mendoza, A., et al. (2019). Cooperation between *Lactococcus lactis* NRRL B-50571 and NRRL B-50572 for aroma formation in fermented milk. *Foods* 8:645. doi: 10.3390/foods8120645

Bintsis, T. (2018). Lactic acid bacteria as starter cultures: an update in their metabolism and genetics. *AIMS Microbiol.* 4, 665–684. doi: 10.3934/microbiol.2018.4.665

Bongers, R. S., Hoefnagel, M. H. N., and Kleerebezem, M. (2005). High-level acetaldehyde production in *Lactococcus lactis* by metabolic engineering. *Appl. Environ. Microbiol.* 71, 1109–1113. doi: 10.1128/AEM.71.2.1109-1113.2005

Callanan, M., Kaleta, P., O'Callaghan, J., O'Sullivan, O., Jordan, K., McAuliffe, O., et al. (2008). Genome sequence of *lactobacillus helveticus*, an organism distinguished by selective gene loss and insertion sequence element expansion. *J. Bacteriol.* 190, 727–735. doi: 10.1128/JB.01295-07

Câmara, S. P., Dapkevicius, A., Riquelme, C., Elias, R. B., Silva, C., Malcata, F. X., et al. (2019). Potential of lactic acid bacteria from Pico cheese for starter culture development. *Food Sci. Technol. Int.* 25, 303–317. doi: 10.1177/1082013218823129

Campedelli, I., Mathur, H., Salvetti, E., Clarke, S., Rea, M. C., Torriani, S., et al. (2018). Genus-wide assessment of antibiotic resistance in *lactobacillus* spp. *Appl. Environ. Microbiol.* 85, e01738–e01718. doi: 10.1128/AEM.01738-18

Canon, F., Maillard, M. B., Henry, G., Thierry, A., and Gagnaire, V. (2021). Positive interactions between lactic acid bacteria promoted by nitrogen-based nutritional dependencies. *Appl. Environ. Microbiol.* 87:e0105521. doi: 10.1128/AEM.01055-21

Carey, A. B., Ashenden, A., and Köper, I. (2022). Model architectures for bacterial membranes. *Biophys. Rev.* 14, 111–143. doi: 10.1007/s12551-021-00913-7

Cavanagh, D., Fitzgerald, G. F., and McAuliffe, O. (2015). From field to fermentation: the origins of *Lactococcus lactis* and its domestication to the dairy environment. *Food Microbiol.* 47, 45–61. doi: 10.1016/j.fm.2014.11.001

Chen, C., Zhao, S., Hao, G., Yu, H., Tian, H., and Zhao, G. (2017). Role of lactic acid bacteria on the yogurt flavour: a review. *Int. J. Food Prop.* 20, S316–S330. doi: 10.1080/10942912.2017.1295988

De Vos, W. M., Vos, P., de Haard, H., and Boerrigter, I. (1989). Cloning and expression of the *Lactococcus lactis* subsp. *cremoris* SK11 gene encoding an extracellular serine proteinase. *Gene* 85:169. doi: 10.1016/0378-1119(89)90477-0

Drider, D., Bekal, S., and Prévost, H. (2004). Genetic organization and expression of citrate permease in lactic acid bacteria. *Genet. Mol. Res.* 3, 273–281.

EFSA FEEDAP Panel (EFSA Panel on Additives and Products or Substances used in Animal Feed) (2018). Guidance on the characterisation of microorganisms used as feed additives or as production organisms. *EFSA J.* 16:e05206. doi: 10.2903/j.efsa.2018.5206

Erkus, O., de Jager, V. C., Spus, M., van Alen-Boerrigter, I. J., van Rijswijck, I. M., Hazelwood, L., et al. (2013). Multifactorial diversity sustains microbial community stability. *ISME J.* 7, 2126–2136. doi: 10.1038/ismej.2013.108

Fernández, E., Alegría, A., Delgado, S., Martín, M. C., and Mayo, B. (2011). Comparative phenotypic and molecular genetic profiling of wild *Lactococcus lactis* subsp. *lactis* strains of the *L. lactis* subsp. *lactis* and *L. lactis* subsp. *cremoris* genotypes, isolated from starter-free cheeses made of raw milk. *Appl. Environ. Microbiol.* 77, 5324–5335. doi: 10.1128/AEM.02991-10

Filipic, B., Golic, N., Jovcic, B., Tolinacki, M., Bay, D. C., Turner, R. J., et al. (2013). The *cmbT* gene encodes a novel major facilitator multidrug resistance transporter in *Lactococcus lactis*. *Res. Microbiol.* 164, 46–54. doi: 10.1016/j.resmic.2012.09.003

García-Quintáns, N., Repizo, G., Martín, M., Magni, C., and López, P. (2008). Activation of the diacetyl/acetoin pathway in *Lactococcus lactis* subsp. *lactis* bv. *Diacetylactis* CRL264 by acidic growth. *Appl. Environ. Microbiol.* 74:1988. doi: 10.1128/AEM.01851-07

Garofalo, C., Ferrocino, I., Reale, A., Sabbatini, R., Milanović, V., Alkić-Subašić, M., et al. (2020). Study of kefir drinks produced by backslopping method using kefir grains from Bosnia and Herzegovina: microbial dynamics and volatilome profile. *Food Res. Int.* 137:109369. doi: 10.1016/j.foodres.2020.109369

Goldstein, B. P. (2014). Resistance to rifampicin: a review. *J. Antibiot. (Tokyo)* 67, 625–630. doi: 10.1038/ja.2014.107

Haandrikman, A. J., Kok, J., Laan, H., Soemitro, S., Ledeboer, A. M., Konings, W. N., et al. (1989). Identification of a gene required for maturation of an extracellular lactococcal serine proteinase. *J. Bacteriol.* 171, 2789–2794. doi: 10.1128/jb.171.5.2789-2794.1989

Iskandar, C. F., Cailliez-Grimal, C., Borges, F., and Revoll-Junelles, A. M. (2019). Review of lactose and galactose metabolism in lactic acid bacteria dedicated to expert genomic annotation. *Trends Food Sci. Technol.* 88, 121–132. doi: 10.1016/j.tifs.2019.03.020

Juillard, V., Furlan, S., Foucaud, C., and Richard, J. (1996). Mixed cultures of proteinase-positive and proteinase-negative strains of *Lactococcus lactis* in milk. *J. Dairy Sci.* 79, 964–970. doi: 10.3168/jds.S0022-0302(96)76447-0

Kelly, W. J., Ward, L. J., and Leahy, S. C. (2010). Chromosomal diversity in *Lactococcus lactis* and the origin of dairy starter cultures. *Genome Biol. Evol.* 2, 729–744. doi: 10.1093/gbe/evq056

Kieliszek, M., Pobiega, K., Piwowarek, K., and Kot, A. M. (2021). Characteristics of the proteolytic enzymes produced by lactic acid bacteria. *Molecules* 26:1858. doi: 10.3390/molecules26071858

Klare, I., Konstabel, C., Müller-Bertling, S., Reissbrodt, R., Huys, G., Vancanneyt, M., et al. (2005). Evaluation of new broth media for microdilution antibiotic susceptibility testing of lactobacilli, pediococci, lactococci, and bifidobacteria. *Appl. Environ. Microbiol.* 71, 8982–8986. doi: 10.1128/AEM.71.12.8982-8986.2005

Ladero, V., Martín, M. C., Mayo, B., Flórez, A. B., Fernández, M., and Álvarez, M. A. (2015). Genetic and functional analysis of the amine production capacity among starter and non-starter lactic acid bacteria isolated from artisanal cheeses. *Eur. Food Res. Technol.* 241, 377–383. doi: 10.1007/s00217-015-2469-z

Laroute, V., Tormo, H., Couderc, C., Mercier-Bonin, M., Le Bourgeois, P., Cocaign-Bousquet, M., et al. (2017). From genome to phenotype: an integrative spproach to evaluate the biodiversity of *Lactococcus lactis*. *Microorganisms* 5:27. doi: 10.3390/microorganisms5020027

Liu, M., Bayjanov, J. R., Renckens, B., Nauta, A., and Siezen, R. J. (2010). The proteolytic system of lactic acid bacteria revisited: a genomic comparison. *BMC Genomics* 11:36. doi: 10.1186/1471-2164-11-36

Liu, M., van Enckevort, F. H. J., and Siezen, R. J. (2005). Genome update: lactic acid bacteria genome sequencing is booming. *Microbiology (Reading)* 151, 3811–3814. doi: 10.1099/mic.0.28557-0

López de Felipe, F., Magni, C., de Mendoza, D., and López, P. (1995). Citrate utilization gene cluster of the *Lactococcus lactis* biovar *diacetylactis*: organization and regulation of expression. *Mol. Gen. Genet.* 246, 590–599. doi: 10.1007/bf00298965

Martín, M. G., Magni, C., De Mendoza, D., and López, P. (2005). CitI, a transcription factor involved in regulation of citrate metabolism in lactic acid bacteria. *J. Bacteriol.* 187, 5146–5155. doi: 10.1128/JB.187.15.5146-5155.2005

Mayo, B., Rodríguez, J., Vázquez, L., and Flórez, A. B. (2021). Microbial interactions within the cheese ecosystem and their application to improve quality and safety. *Foods* 10:602. doi: 10.3390/foods10030602

Medina, R., Katz, M., Gonzalez, S., and Oliver, G. (2001). Characterization of the lactic acid bacteria in ewe's milk and cheese from Northwest Argentina. *J. Food Prot.* 64, 559–563. doi: 10.4315/0362-028x-64.4.559

Meier-Kolthoff, J. P., and Göker, M. (2019). TYGS is an automated high-throughput platform for state-of-the-art genome-based taxonomy. *Nat. Commun.* 10:2182. doi: 10.1038/s41467-019-10210-3

Minty, J. J., Singer, M. E., Scholz, S. A., Bae, C. H., Ahn, J. H., Foster, C. E., et al. (2013). Design and characterization of synthetic fungal-bacterial consortia for direct production of isobutanol from cellulosic biomass. *Proc. Natl. Acad. Sci. U. S. A.* 110, 14592–14597. doi: 10.1073/pnas.1218447110

Moraes, P. M., Perin, L. M., Júnior, A. S., and Nero, L. A. (2013). Comparison of phenotypic and molecular tests to identify lactic acid bacteria. *Braz. J. Microbiol.* 44, 109–112. doi: 10.1590/S1517-83822013000100015

Oshiro, M., Momoda, R., Tanaka, M., Zendo, T., and Nakayama, J. (2019). Dense tracking of the dynamics of the microbial community and chemicals constituents in spontaneous wheat sourdough during two months of backslopping. *J. Biosci. Bioeng.* 128, 170–176. doi: 10.1016/j.jbiosc.2019.02.006

Passerini, D., Laroute, V., Coddeville, M., Le Bourgeois, P., Loubière, P., Ritzenthaler, P., et al. (2013). New insights into *Lactococcus lactis* diacetyl- and acetoin-producing strains isolated from diverse origins. *Int. J. Food Microbiol.* 160, 329–336. doi: 10.1016/j.ijfoodmicro.2012.10.023

Pierce, E. C., and Dutton, R. J. (2022). Putting microbial interactions back into community contexts. *Curr. Opin. Microbiol.* 65, 56–63. doi: 10.1016/j.mib.2021.10.008

Redruello, B., Ladero, V., Cuesta, I., Álvarez-Buylla, J. R., Martín, M. C., Fernández, M., et al. (2013). A fast, reliable, ultra high performance liquid chromatography method for the simultaneous determination of amino acids, biogenic amines and ammonium ions in cheese, using diethyl ethoxymethylenemalonate as a derivatising agent. *Food Chem.* 139, 1029–1035. doi: 10.1016/j.foodchem.2013.01.071

Redruello, B., Saidi, Y., Sampedro, L., Ladero, V., Del Rio, B., and Alvarez, M. A. (2021). GABA-producing *Lactococcus lactis* strains isolated from camel's milk as starters for the production of GABA-enriched cheese. *Foods* 10:633. doi: 10.3390/foods10030633

Robinson, R. K., and Tamime, A. Y. (2006). "Types of fermented milks" in *Fermented Milks*. ed. A. Y. Tamime (Hoboken: Wiley), 1–10.

Rodríguez, J., González-Guerra, A., Vázquez, L., Fernández-López, R., Flórez, A. B., de la Cruz, F., et al. (2022). Isolation and phenotypic and genomic characterization of *Tetragenococcus* spp. from two Spanish traditional blue-veined cheeses made of raw milk. *Int. J. Food Microbiol.* 371:109670. doi: 10.1016/j.ijfoodmicro.2022.109670

Settachaimongkon, S., Nout, M. J., Antunes Fernandes, E. C., Hettinga, K. A., Vervoort, J. M., van Hooijdonk, T. C., et al. (2014). Influence of different proteolytic strains of *Streptococcus thermophilus* in co-culture with *lactobacillus delbrueckii* subsp. *bulgaricus* on the metabolite profile of set-yoghurt. *Int. J. Food Microbiol.* 177:29. doi: 10.1016/j.ijfoodmicro.2014.02.008

Shanafelt, D. W., and Loreau, M. (2018). Stability trophic cascades in food chains. *R. Soc. Open Sci.* 5:180995. doi: 10.1098/rsos.180995

Shapiro, B. J., and Polz, M. F. (2014). Ordering microbial diversity into ecologically and genetically cohesive units. *Trends Microbiol.* 22, 235–247. doi: 10.1016/j.tim.2014.02.006

Sharma, H., Ozogul, F., Bartkiene, E., and Rocha, J. M. (2021). Impact of lactic acid bacteria and their metabolites on the techno-functional properties and health benefits of fermented dairy products. *Crit. Rev. Food Sci. Nutr.* 30, 1–23. doi: 10.1080/10408398.2021.2007844

Siezen, R. J., Tzeneva, V. A., Castioni, A., Wels, M., Phan, H. T., Rademaker, J. L., et al. (2010). Phenotypic and genomic diversity of *lactobacillus plantarum* strains isolated from various environmental niches. *Environ. Microbiol.* 12, 758–773. doi: 10.1111/j.1462-2920.2009.02119.x

Smid, E. J., and Kleerebezem, M. (2014). Production of aroma compounds in lactic fermentations. *Annu. Rev. Food Sci. Technol.* 5, 313–326. doi: 10.1146/annurev-food-030713-092339

Smid, E. J., and Lacroix, C. (2013). Microbe-microbe interactions in mixed culture food fermentations. *Curr. Opin. Biotechnol.* 24, 148–154. doi: 10.1016/j.copbio.2012.11.007

Solopova, A., Bachmann, H., Teusink, B., Kok, J., and Kuipers, O. P. (2018). Further elucidation of galactose utilization in *Lactococcus lactis* MG1363. *Front. Microbiol.* 9:1803. doi: 10.3389/fmicb.2018.01803

Sun, L., and D'Amico, D. J. (2021). Composition, succession, and source tracking of microbial communities throughout the traditional production of a farmstead cheese. *mSystems* 6:e0083021. doi: 10.1128/mSystems.00830-21

Takatsuka, Y., and Kamio, Y. (2004). Molecular dissection of the *Selenomonas ruminantium* cell envelope and lysine decarboxylase involved in the biosynthesis of a polyamine covalently linked to the cell wall peptidoglycan layer. *Biosci. Biotechnol. Biochem.* 68, 1–19. doi: 10.1271/bbb.68.1

Van Calcar, S. C., Bernstein, L. E., Rohr, F. J., Yannicelli, S., Berry, G. T., and Scaman, C. H. (2014). Galactose content of legumes, caseinates, and some hard cheeses: implications for diet treatment of classic galactosemia. *J. Agric. Food Chem.* 62, 1397–1402. doi: 10.1021/jf404995a

van Pijkeren, J. P., and Britton, R. A. (2012). High efficiency recombineering in lactic acid bacteria. *Nucleic Acids Res.* 40:e76. doi: 10.1093/nar/gks147

Waché, Y., Riondet, C., Diviès, C., and Cachon, R. (2002). Effect of reducing agents on the acidification capacity and the proton motive force of *Lactococcus lactis* ssp. *cremoris* resting cells. *Bioelectrochemistry* 57:113. doi: 10.1016/s1567-5394(02)00051-8

Weiland-Bräuer, N. (2021). Friends or foes-microbial interactions in nature. *Biology* 10:496. doi: 10.3390/biology10060496

Wels, M., Siezen, R., van Hijum, S., Kelly, W. J., and Bachmann, H. (2019). Comparative genome analysis of *Lactococcus lactis* indicates niche adaptation and resolves fenotype/phenotype disparity. *Front. Microbiol.* 10:4. doi: 10.3389/fmicb.2019.00004

Yoon, S. H., Ha, S. M., Lim, J. M., Kwon, S. J., and Chun, J. (2017). A large-scale evaluation of algorithms to calculate average nucleotide identity. *Antonie Van Leeuwenhoek* 110, 1281–1286. doi: 10.1007/s10482-017-0844-4

frontiers | Frontiers in Microbiology

TYPE Original Research
PUBLISHED 16 December 2022
DOI 10.3389/fmicb.2022.1052675

OPEN ACCESS

EDITED BY
Giuseppe Spano,
University of Foggia,
Italy

REVIEWED BY
Pasquale Russo,
University of Milan,
Italy
Jorge Reinheimer,
National University of Littoral, Argentina
Jordi Espadaler Mazo,
AB-Biotics SA, Spain

*CORRESPONDENCE
Juan Miguel Rodríguez
jmrodrig@ucm.es
Claudio Alba
c.alba@ucm.es

SPECIALTY SECTION
This article was submitted to Food Microbiology, a section of the journal Frontiers in Microbiology

RECEIVED 24 September 2022
ACCEPTED 30 November 2022
PUBLISHED 16 December 2022

CITATION
Mozota M, Castro I, Gómez-Torres N, Arroyo R, Gutiérrez-Díaz I, Delgado S, Rodríguez JM and Alba C (2022) Administration of *Ligilactobacillus salivarius* CECT 30632 to elderly during the COVID-19 pandemic: Nasal and fecal metataxonomic analysis and fatty acid profiling.
Front. Microbiol. 13:1052675.
doi: 10.3389/fmicb.2022.1052675

Administration of *Ligilactobacillus salivarius* CECT 30632 to elderly during the COVID-19 pandemic: Nasal and fecal metataxonomic analysis and fatty acid profiling

Marta Mozota[1], Irma Castro[1], Natalia Gómez-Torres[1], Rebeca Arroyo[1], Isabel Gutiérrez-Díaz[2], Susana Delgado[2], Juan Miguel Rodríguez[1]* and Claudio Alba[1]*

[1]Department of Nutrition and Food Science, Complutense University of Madrid, Madrid, Spain, [2]Department of Microbiology and Biochemistry, Dairy Research Institute of Asturias (IPLA-CSIC), Villaviciosa, Spain

Elderly was the most affected population during the first COVID-19 and those living in nursing homes represented the most vulnerable group, with high mortality rates, until vaccines became available. In a previous article, we presented an open-label trial showing the beneficial effect of the strain *Ligilactobacillus salivarius* CECT 30632 (previously known as *L. salivarius* MP101) on the functional and nutritional status, and on the nasal and fecal inflammatory profiles of elderly residing in a nursing home highly affected by the pandemic. The objective of this *post-hoc* analysis was to elucidate if there were changes in the nasal and fecal bacteriomes of a subset of these patients as a result of the administration of the strain for 4 months and, also, its impact on their fecal fatty acids profiles. Culture-based methods showed that, while *L. salivarius* (species level) could not be detected in any of the fecal samples at day 0, *L. salivarius* CECT 30632 (strain level) was present in all the recruited people at day 120. Paradoxically, the increase in the *L. salivarius* counts was not reflected in changes in the metataxonomic analysis of the nasal and fecal samples or in changes in the fatty acid profiles in the fecal samples of the recruited people. Overall, our results indicate that *L. salivarius* CECT 30632 colonized, at least temporarily, the intestinal tract of the recruited elderly and may have contributed to improvements in their functional, nutritional, and immunological status, without changing the general structure of their nasal and fecal bacteriomes when assessed at the genus level. They also suggest the ability of low abundance bacteria to train immunity.

KEYWORDS

probiotics, *Ligilactobacillus salivarius*, elderly, metataxonomics, fatty acid, nursing home, COVID-19

Introduction

The coronavirus disease-2019 (COVID-19), caused by the Severe Acute Respiratory Syndrome Coronavirus 2 (SARS-CoV-2), has been the responsible for several millions of deaths around the world, being recognized by the WHO as a pandemic on 11 March 2020. Elderly was the most affected population during the first COVID-19 waves. In fact, the risk of a severe course, functional and nutritional complications, and mortality from COVID-19 was much higher among older people (≥65 years) than among younger people (Boccardi et al., 2020; Liu et al., 2020; Silva et al., 2020; Pizarro-Pennarolli et al., 2021; Palavras et al., 2022). Such a strong impact on elderly has been explained on the basis of an accumulation of risk factors, including multiple key comorbidities, such as, among others, weakened immune systems, hypertension, diabetes, cardiovascular disease, chronic kidney disease, and chronic respiratory disease (Araújo et al., 2021). Among the elderly, those living in nursing homes represented the most vulnerable group until vaccines became available (Aguilar-Palacio et al., 2022). The huge impact of the initial pandemic waves on this group has been linked to the pre-COVID-19 living conditions in long-term care facilities, which facilitated the spread of the virus among highly vulnerable people (Lai et al., 2020; Araújo et al., 2021).

Some studies have indicated an implication of the host microbiota in the individual susceptibility to COVID-19 and in the severity of the disease (Gu et al., 2020: Zuo et al., 2020; Albrich et al., 2022). People with an altered respiratory or gut microbiota would be at a higher risk of suffering a more severe infection, complications, and sequela because of their inability to develop correct immune responses (He et al., 2020a,b). Interestingly, aging has a negative impact on the composition of the gut microbiota (Claesson et al., 2011) and this aging-driven altered microbiota usually promotes inflammation (Guigoz et al., 2008).

In this context, the modulation of the respiratory tract and gut microbiotas and their associated immune responses may be a strategy to minimize the impact of COVID-19 and to foster a full recovery in vulnerable populations. In a previous article, we described the beneficial effect of a probiotic strain (*Ligilactobacillus salivarius* CECT 30632) on the functional and nutritional status, and on the nasal and fecal inflammatory profiles of elderly residing in nursing homes highly affected by the pandemic (Mozota et al., 2021). In this work, we present the results of the metataxonomic analysis performed with the nasal and fecal samples of a subset of these patients, before and after the administration of the strain for 4 months and, also, its impact on their fecal fatty acids profiles.

Materials and methods

Study design and participants

The general design of the trial (an open-label trial without a control arm) has already been published (Mozota et al., 2021). Briefly, the study was carried out in an elderly nursing home located in Moralzarzal (Madrid, Spain), and was designed to include all the residents as long as (a) informed consent was obtained from the participants or their legal representatives, (b) they were not fed by parenteral nutrition exclusively, and/or (c) they were not allergic to cow's milk proteins (because the probiotic was delivered in a dairy food matrix). A total of 25 residents, aged 74–98, met these criteria and started the trial. Starting at day 0, the residents consumed daily a fermented dairy product (125 g; ~9.3 log10 CFU of *L. salivarius* CECT 30632 per product) for 4 months. Two samples (nasal wash and feces) were collected from each patient at recruitment (day 0) and at the end of the study (day 120). The nasal wash was obtained using a standardized protocol (Stewart et al., 2017). Aliquots of the samples were stored at −80°C until the analyzes were performed. This study was conducted according to the guidelines laid down in the Declaration of Helsinki and was approved by the Ethics Committee of the Hospital Clínico San Carlos (Madrid, Spain) (protocol: CEIC 20/263-E_COVID; date of approval: 01/04/2020, act 4.1/20).

In a previous work, the functional, cognitive and nutritional status of the patients was evaluated, according to standard procedures, before and after the administration of the probiotic strain, and their nasal and fecal inflammatory profiles were also measured (Mozota et al., 2021). A total of 22 out of the 25 recruited participants finished the trial. After the immunological analysis of their samples, and due to the low amount available of some them, we only kept aliquots of the nasal and fecal samples from a subset of 15 residents, which are the ones that have been analyzed in this study. The demographic and health-related data (age, gender, body mass index, SARS-CoV-2 status, comorbidities, and medication) that were recorded at recruitment and at the end of the study for this subset of residents are shown in Table 1; Supplementary Table S1, respectively. Their samples were submitted to culture-based and culture-independent analyzes and, additionally (in the case of the fecal samples), to the analysis of their fatty acids' profiles, following the procedures described below.

TABLE 1 Demographic characteristics of the elderly population (*n*=15).

	Mean (95% and CI) or *n* (%)
Age (years)	84.73 (75.87–93.60)
Gender	
Male	7 (46.67%)
Female	8 (53.33%)
BMI (kg/m2)	
Day 0	24.61 (20.64–28.57)
Day 120	24.47 (21.56–27.39)
SARS-CoV-2 (positive PCR)	
Day 0	11 (73%)
Day 120	0 (0%)

Detection and quantification of *Ligilactobacillus salivarius* in the fecal samples by culture-dependent methods

Fecal samples collected during the trial were serially diluted and plated onto agar plates of MRS (Oxoid, Basingstoke, UK) supplemented with L-cysteine (2.5 g/l; MRS-Cys) for isolation of lactobacilli. MRS-Cys plates were incubated anaerobically (85% nitrogen, 10% hydrogen, 5% carbon dioxide) in an anaerobic workstation (DW Scientific, Shipley, UK) for up to 72 h at 37°C. After incubation, colonies were enumerated and at least one representative of each colony morphology was selected from the agar plates in order to calculate the *L. salivarius* count and the total *Lactobacillus* count. The latter parameter included all the new genera in which this genus was reclassified recently (Zheng et al., 2020). The isolates were identified by Matrix Assisted Laser Desorption Ionization-Time of Flight (MALDI-TOF) mass spectrometry (Bruker GmbH, Bremen, Germany) and 16S rDNA sequencing (Mediano et al., 2017). The isolates identified as *L. salivarius* were genotyped by RAPD profiling as described (Ruiz-Barba et al., 2005) to assess if they shared the same profile that *L. salivarius* CECT 30632.

DNA extraction from the nasal and fecal samples

Two different protocols were performed depending on the type of biological sample. For nasal samples (1 g), DNA was extracted following the protocol described by Pérez et al. (2019). This protocol includes a first centrifugation at 13,000 rpm for 10 min at 4°C, an incubation with lysozyme (5 mg/ml), mutanolysin (25,000 U/ml), and lysostaphin (4,000 U/ml), a mechanical lysis using the FastPrep BIO 101 instrument (Thermo Scientific, Waltham, MA) and an incubation with proteinase K (250 μg/ml) at 56°C for 30 min. Then, the DNA was extracted using the QIAamp DNA Stool Kit (Qiagen, Hilden, Germany), following the instructions of the manufacturer. The protocol described by Lackey et al. (2019) was used for the fecal samples (1 g). In all cases, DNA was eluted in 20 μl of nuclease-free water and its concentration was estimated with a ND-1000 UV spectrophotometer (Nano Drop Technologies, Wilmington, DE, USA).

Detection and quantification of *Ligilactobacillus salivarius* in the fecal samples by real-time quantitative PCR (qPCR) assays

Quantification of *L. salivarius* DNA in the fecal samples of the residents was carried out using the procedure described by Harrow et al. (2007). The DNA concentration of all samples was adjusted to 5 ng/μL. A commercial real-time PCR thermocycler (CFX96™, Bio-Rad Laboratories, Hercules, CA, USA) was used for all experiments. Standard curves using 1 : 10 DNA dilutions (ranging from 2 ng to 0.2 pg) from *L. salivarius* CECT5713 were used to calculate the concentrations of the unknown bacterial genomic targets. Threshold cycle (Ct) values between 14.92 and 21.15 were obtained for this range of bacterial DNA ($R^2 \geq 0.991$). The Ct values measured for DNA extracted from two strains belonging to two non-target species (*Lactiplantibacillus plantarum* MP02 and *L. reuteri* MP07; our own collection) were $\geq 39.36 \pm 0.57$. These control strains were selected because they are closely related, from a taxonomical point of view, to *L. salivarius* (Salvetti et al., 2018). All samples and standards were run in triplicate.

Metataxonomic analysis

The 16S rRNA gene amplification and sequencing, targeting the V3-V4 hypervariable regions of the 16S rRNA gene, was performed in the MiSeq 300PE system of Illumina (Illumina Inc., San Diego, CA, United States) at the facilities of Parque Científico de Madrid (Tres Cantos, Spain) with the universal primers S-D-Bact-0341-b-S-17 (ACACTGACGACATGGTTCTACACC TACGGGNGGCWGCAG) and S-D-Bact-0785-a-A-21 (TACGG TAGCAGAGACTTGGTCTGACTACHVGGGTATCTAATCC), as previously described (Klindworth et al., 2013; Aparicio et al., 2020). The pooled, purified, and barcoded DNA amplicons were sequenced using the Illumina MiSeq pair-end protocol (Illumina Inc.).

Demultiplexing preprocessing analysis of the V3-V4 amplicons was conducted using MiSeq Reporter analysis software (version 2.6.2.3), according to the manufacturer's guidelines. After the demultiplexing step, the metataxonomic analyzes were conducted with QIIME 2 2022.2 (Bolyen et al., 2019). Denoising and ASVs (Amplicon sequence variants) selection were performed with DADA2 (Callahan et al., 2016). The forward reads were truncated at position 290 by trimming the last 10 nucleotides, while the reverse ones were truncated at the 249 nucleotides by trimming the last 8 nucleotides, in order to discard nucleotides in positions for which median quality was Q20 or below.

Taxonomy was assigned to ASVs with the q2-feature-classifier (Bokulich et al., 2018) by using a classify-sklearn naïve Bayes taxonomy classifier against the SILVA 138.1 reference database (Quast et al., 2013). Subsequent bioinformatic analysis was conducted using R version 3.5.1 (R Core Team, 2021).[1] The decontam package version 1.2.1 (Davis et al., 2018) was used to identify, visualize, and remove contaminating DNA with one negative extraction control. A table of amplicon sequence variants (ASVs) counts per sample was generated, and bacterial taxa abundances were normalized with the total sum scaling normalization method, dividing each ASV count by the total library size in order to yield their relative proportion of counts for each sample (Paulson et al., 2013).

1 https://www.R-project.org

TABLE 2 Microbiological parameters, expressed as mean (95% CI), in the feces of the participants before (T1) and after 120days of supplementation with *Ligilactobacillus salivarius* CECT 30632 (T2).

Parameter	T1	T2	*p*-value
Colony-forming units (log_{10} CFU/g)			
Total *Lactobacillus*	6.84 (6.53–7.15)	7.29 (6.97–7.62)	<0.001
L. salivarius	nd	5.82 (5.38–6.26)	-
qPCR (DNA copies/g)			
L. salivarius	nd	6.42 (6.05–6.79)	-

nd, No detected in any sample.

Alpha diversity was studied with the R vegan package (Version: 2.5.6) using the Shannon and Simpson diversity indices. Differences between groups were assessed using Wilcoxon rank-sum tests or the exact Friedman rank sum with FDR correction in order to perform paired comparisons. Beta diversity was assessed through two distance matrices: (a) relative abundance with the Bray-Curtis index; and (b) presence/absence distance matrix using the binary Jaccard. Principal coordinate analysis (PCoA) was used to plot patterns of bacterial community diversity. The PERMANOVA analysis with 999 permutations was performed to reveal statistical differences.

Analyzes of fatty acids (FAs) in the fecal samples

One hundred µl of a 1:10 dilution of feces (w/v) in phosphate buffer saline solution (PBS; pH 7.4) was supplemented with 100 µl of 2-ethyl butyric acid (Sigma-Aldrich, St. Louis, MO, USA) as an internal standard (1 mg/ml in methanol), and acidified with 100 µl of 20% formic acid (v/v). The acidic solution was then extracted with 1 ml of methanol and centrifuged for 10 min at 15,800 × *g*. Supernatants were kept at −20°C until analysis in a gas chromatography (GC) apparatus. The system used is composed of a 6,890 GC injection module (Agilent Technologies, CA, USA) with a HP-FFAP (30 m × 0.250 mm × 0.25 µm) column (Agilent Technologies) using a split/splitless injector in the split mode with a split ratio of 1:20. The injection volume of the samples was 1 µl. The injector and detector temperatures were kept at 240 °C and 250°C, respectively. The temperature of the column oven was set at 110°C, increased at 6°C/min to 170°C then increased at 25°C/min to 240°C, yielding a total GC run time of 18 min. Helium was used as carrier gas, at a constant flow rate of 1.3 ml/min. The chromatographic system was equipped with a flame ionization detector (FID). Data acquisition and processing were performed using ChemStation Agilent software (Agilent Technologies).

Statistical analyzes were performed using IBM SPSS Statistics v. 27.0.1 (IBM, Armonk, NY, USA). To examine the changes of the paired samples between the two time periods, we used the non-parametric Wilcoxon signed-rank test, and two-tailed probability values of $p \leq 0.05$ were considered significant. In turn, medians, means, and interquartile ranges (IQR; Q1 and Q3) were represented in box and whisker graphics using Origin Pro-2021 software (OriginLab, Northampton, Massachusetts, USA).

Results

Evolution of the COVID-19 status of the participants

The mean age of the participants was, approximately, 85 years (Table 1). The recruited residents included 8 females and 7 males and all of them had several comorbidities and were polymedicated (Supplementary Table S1). A high percentage of them ($n = 11$; 73%) were SARS-CoV-2-positive at day 0 but, in contrast, all of them were negative at day 120. None of them became infected or re-infected with SARS-CoV-2 during the assay.

Specific detection and quantification of *Ligilactobacillus salivarius* colonies and DNA in the fecal samples

The total *Lactobacillus* count oscillated between 5.7 and 7.7 log10 CFU/g at the beginning of the trial and increased slightly after the probiotic treatment (6.0–8.7 log10 CFU/g) (Table 2). In contrast, at the beginning of the trial, *L. salivarius* could not be detected in the feces of the participants. However, *L. salivarius* colonies were present in the samples of all the residents after the administration of the probiotic strain and its concentrations ranged between 4.4 and 7.1 log10 CFU/g (Table 2).

Only those samples from which *L. salivarius* was cultured provided a positive result using the *L. salivarius*-specific qPCR assay (Table 2). Therefore, there was a complete qualitative agreement between both techniques (Table 2).

Finally, the *L. salivarius* isolates were genetically typified by the RAPD technique. Their profiles were identical to that of *L. salivarius* CECT 30632 (data not shown).

Metataxonomic analysis of the nasal samples

The 16S rRNA gene sequencing analysis of the nasal samples yielded 653,484 high-quality filtered sequences, ranging from 17,098 to 44,506 per sample [median (IQR) = 29,686.5 (26,041.25–33,718.5) sequences per sample].

Alpha diversity, as measured using the Shannon and Simpson diversity indices, was not significantly different when the nasal samples collected at day 0 [Shannon index = 3.90 (3.4–4.6); Simpson index = 0.92 (0.90–0.97)] were compared with those obtained at day 120 [Shannon index = 3.60 (1.82–4.48); Simpson index = 0.89 (0.69–0.97)] ($p = 0.76$ and $p = 0.37$, respectively) (Figure 1).

Beta diversity analysis at the ASV level revealed that nasal samples did not cluster according to the sampling times. When the nasal samples collected at day 0 were compared with those obtained at day 120, there were no statistical differences in relation to the relative abundance (Bray–Curtis distance matrix; $p = 0.85$) or to the presence/absence of different ASV sequences (binary Jaccard distance matrix; $p = 0.70$, respectively) (Figure 2).

Taxonomic analysis of the nasal sequences indicated that the bacterial profile was dominated by the phylum Firmicutes, followed by the phyla Proteobacteria, Bacteroidota, and Actinobacteriota. At the genera level, the 19 most abundant ones at both sampling times are shown in Table 3 and Supplementary Figure S1. However, no statistical changes were detected in the relative abundance of any of the main bacterial genera as a consequence of the administration of the probiotic strain.

Metataxonomic analysis of the fecal samples

The 16S rRNA gene sequencing analysis of the fecal samples yielded 844,567 high-quality filtered sequences, ranging from 21,950 to 35,737 per sample [median (IQR) = 28,144.5 (25,669.5 – 30,502.5) sequences per sample].

Again, alpha diversity was not significantly different between the samples collected at day 0 [Shannon index = 4.14 (3.90–4.46); Simpson index = 0.97 (0.95–0.98)] and those obtained at day 120 [Shannon index = 4.40 (4.23–4.55); Simpson index = 0.98 (0.97–0.98)] ($p = 0.76$ and $p = 0.37$, respectively) (Figure 3). Similarly, beta diversity analysis at the ASV level revealed that fecal samples did not cluster according to the sampling times ($p = 0.51$ in the case of the Bray–Curtis distance matrix and $p = 0.82$ in that of the binary Jaccard distance matrix) (Figure 4).

Taxonomic analysis of the fecal sequences indicated that the fecal bacterial profile was dominated by the phylum Firmicutes, followed by the phyla Bacteroidota, Proteobacteria, Actinobacteriota, and Verrucomicrobiota. At the genera level, the 19 most abundant ones at both sampling times are shown in Table 4; Supplementary Figure S2. Similarly to the nasal samples, no statistical changes were detected in the relative abundance of any of the main bacterial genera as a consequence of the administration of the probiotic strain.

Profiles of fatty acids in the fecal samples

There were no statistically significant differences in the levels of total fatty acids (FAs) between the two sampling times ($p = 0.925$). Similarly, there were no statistically significant differences in the fecal concentration of the three main short chain fatty acids (SFCAs) between the two sampling times (acetic: $p = 0.551$; propionic: $p = 0.972$; butyric: $p = 0.646$) (Table 5). In addition, the sum of the concentrations of these three main SCFAs was similar at both time points ($p = 0.875$) (Table 5) and, also, the acetic/propionic ratio ($p = 0.382$).

In relation to branched chain fatty acids (BCFAs), formed by isobutyric and isovaleric acids, their concentrations were similar in the two sampling times evaluated in this study ($p = 0.173$ and $p = 0.388$ for isobutyric and isovaleric acid, respectively) (Table 5).

The number of samples in which caproic acid, a medium-chain fatty acid (MFCA), was detectable was particularly low ($n \leq 5$ in each sampling point), and although its concentration tended to decrease after the administration of the probiotic strain (Table 5), the difference did not reach a statistically significant value ($p = 0.593$).

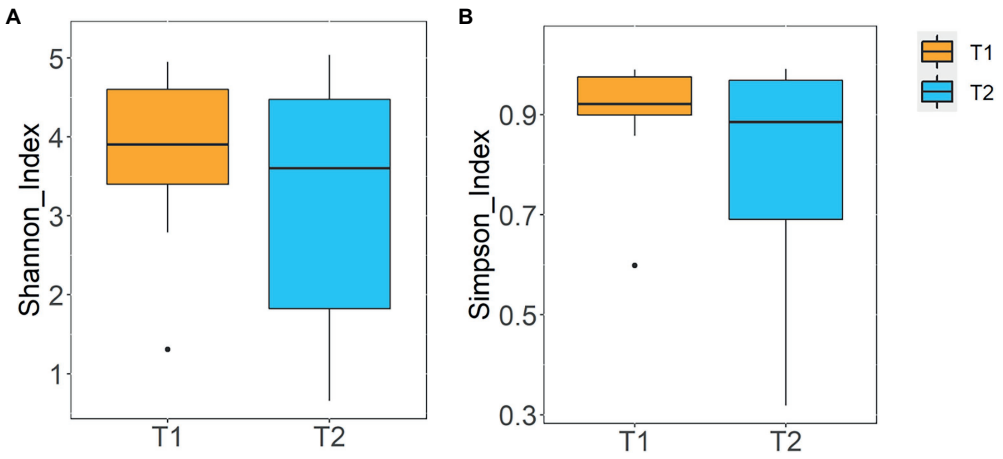

FIGURE 1
Alpha diversity at the ASV level of the nasal samples obtained at day 0 (T1) and at day 120 (T2). **(A)** Shannon diversity index; **(B)** Simpson diversity index.

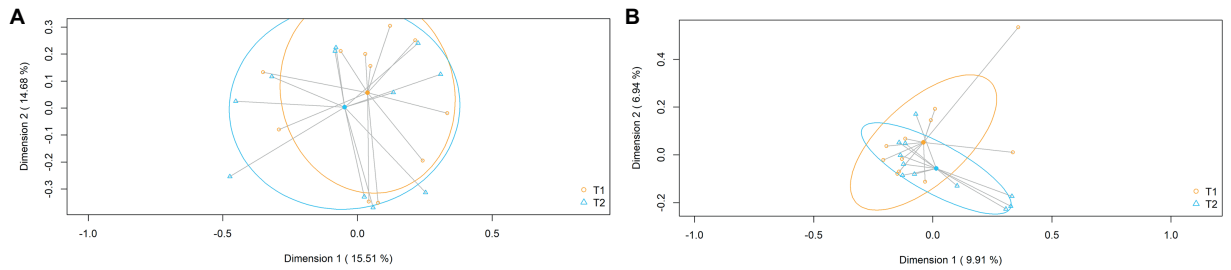

FIGURE 2
Beta diversity at the ASV level of the nasal samples obtained at day 0 (T1) and at day 120 (T2). **(A)** PCoA plots based on the Bray–Curtis dissimilarity index (relative abundance); **(B)** PCoA plots based on the Jaccard's coefficient for binary data (presence of absence).

Discussion

The elderly was the most affected population during the first months of the COVID-19 pandemic. Within this population, those living in nursing homes constituted a particularly vulnerable group, characterized by high rates of infection and death (Lai et al., 2020; Araújo et al., 2021). These high mortality rates have been linked to the accumulation of risk factors or comorbidities that are typically associated with aging (Trecarichi et al., 2020; Heras et al., 2021; Suñer et al., 2021), together with high levels of community and intra-home transmission and the lack of proper policy responses in relation to the situation in nursing homes (Sepulveda et al., 2020). The situation was particularly worrying in Spain since this country has one of the world's highest aging index while the percentage of elderly living in nursing homes is also high (Aguilar-Palacio et al., 2022).

The nursing home that we selected for the trial was severely affected by COVID-19. Immediately before the pandemic, there were 47 older people living in this care center but it has a devastating impact on the residents when it reached the village. In a few weeks, approximately 40% ($n = 18$) of them died (10 with acute COVID-19-related symptoms) although none was tested for SARS-CoV-2. Later, the 29 surviving residents and the workers were PCR tested and most of them (> 80% of the residents and all the workers except one) were PCR-positive.

Initially, we investigated the effect of *L. salivarius* CECT 30632 on the functional (Barthel index), cognitive (GDS/FAST) and nutritional (MNA) status, and on the nasal and fecal inflammatory profiles of the 25 recruited participants that fulfilled the inclusion criteria (Mozota et al., 2021). After the trial, no changes in the cognitive score were detected but the cognitive and nutritional status improved significantly. In addition, the concentrations of some immune factors changed significantly after the consumption of the probiotic strain. Among them, it must be highlighted that the concentrations of some immune factors used as biomarkers of acute viral respiratory infections, such as BAFF/TNFSF13B, APRIL/TNFSF13, or IL-8 (Alba et al., 2021), decreased significantly (Mozota et al., 2021). Since we kept aliquots of the samples obtained at both sampling times from a subset of 15 residents, in this subsequent study we evaluated the effect of the administration of the strain on the nasal and fecal microbiota and in the fecal fatty acid profile of the recruited people.

Culture-based methods showed that *L. salivarius* (species level) could not be detected in any of the fecal samples at day 0. It has already been described that aging is associated with the absence of *L. salivarius* from the gut microbiome (Le Roy et al., 2015). In contrast, *L. salivarius* CECT 30632 (strain level) was present in all the recruited people at day 120 at concentrations ranging from 4.4 to 7.1 log10 CFU/g. Since we did not identify and genotype all the colonies growing on MRS-Cys plates, we cannot completely discard that other *L. salivarius* strains may be also present in the fecal samples of the participants. However, the lack of isolation and PCR detection of *L. salivarius* at baseline makes likely the possibility that all the *L. salivarius*-like colonies belonged to the administered strain. These values indicates that the strain was able to survive the transit through the digestive tract and to reach the gut in relatively high concentrations. It must be taken into account that the actual gut concentrations might be substantially higher since we only tested fecal samples and, therefore, the concentration of the strain attached to the gut mucosa remains unknown. The gut microbiota is an ecological succession (Falony et al., 2018), where the abundance of bacteria changes across the intestine, meaning that a particular strain could be highly abundant in a proximal segment of the intestine and less abundant in a distal segment, hence leading to lower counts in stools. Culture-based methods and *L. salivarius*-specific qPCR evidenced that, at least, there was a change affecting to one species (*L. salivarius*) and one strain (*L. salivarius* CECT 30632) in the microbiota of the recruited individuals.

Paradoxically, the increase in the *L. salivarius* counts was not reflected in changes in the metataxonomic analysis of the fecal samples. This fact may be due to the fact that the metataxonomic approach used in this study (targeting the V3-V4 hypervariable regions of the 16S rRNA gene) does not allow a proper discrimination at the species level and, as a consequence, we could not assess the change in the relative abundance of the sequences corresponding to the *L. salivarius* species. So far, most of the metataxonomic analysis performed to study the human bacteriome have relied in methods which only allow a proper discrimination at the taxonomic level of genus or higher. In order

TABLE 3 Relative frequencies, medians and interquartile range (IQR) of the relative abundance (%) of the most abundant bacterial phyla (in bold) and genera (in italics) detected in the nasal samples collected at day 0 (T1) and 120 (T2).

Phylum	**T1**		**T2**		***p*-value[2]**
Genus	***n* (%)[1]**	**Median (IQR)**	***n* (%)[1]**	**Median (IQR)**	
Firmicutes	15 (100%)	61.43 (46.45–76.46)	15 (100%)	52.37 (42.61–67.50)	0.61
Blautia	15 (100%)	3.36 (1.13–5.26)	14 (93.33%)	1.27 (0.83–1.78)	0.12
Subdoligranulum	11 (73.33%)	3.06 (0.32–5.27)	12 (80%)	0.94 (0.12–3.73)	0.12
[Eubacterium]_hallii_group	14 (93.33%)	2.20 (0.98–6.13)	11 (73.33%)	0.68 (0.13–1.24)	0.01
Christensenellaceae_R.7	14 (93.33%)	1.10 (0.08–2.94)	13 (86.67%)	0.87 (0.09–4.64)	0.12
Anaerostipes	13 (86.67%)	2.00 (0.28–4.40)	13 (86.67%)	0.45 (0.16–1.42)	0.12
Streptococcus	15 (100%)	0.93 (0.4–1.95)	14 (93.33%)	0.54 (0.19–1.62)	0.30
[Eubacterium]_coprostanoligenes_group	14 (93.33%)	1.43 (1.09–2.16)	14 (93.33%)	1.66 (0.73–2.12)	1.00
Clostridia_UCG.014	9 (60.00%)	0.81 (<0.01–2.33)	10 (66.67%)	0.50 (<0.01–3.9)	0.30
Oscillospiraceae-UCG.002	13 (86.67%)	0.38 (0.18–1.81)	14 (93.33%)	1.46 (0.41–2.87)	0.30
Faecalibacterium	13 (86.67%)	0.60 (0.48–1.62)	15 (100%)	1.54 (1.02–2.73)	0.30
Incertae_Sedis	14 (93.33%)	0.60 (0.42–0.76)	14 (93.33%)	0.96 (0.27–1.42)	0.61
Ruminococcus	11 (73.33%)	0.57 (0.03–1.32)	12 (80%)	0.48 (0.17–2.70)	0.12
Bacteroidota	15 (100%)	13.64 (6.46–35.42)	15 (100%)	31.83 (20.72–38.89)	0.12
Bacteroides	15 (100%)	6.70 (1.41–24.92)	14 (93.33%)	14.67 (8.23–27.20)	0.12
Alistipes	15 (100%)	2.38 (0.48–3.36)	14 (93.33%)	2.48 (1.24–4.51)	0.61
Parabacteroides	15 (100%)	0.52 (0.21–2.66)	14 (93.33%)	3.34 (1.74–4.81)	0.12
Proteobacteria	15 (100%)	4.23 (1.26–7.44)	15 (100%)	5.61 (3.57–9.31)	0.61
Escherichia/Shigella	10 (66.67%)	0.06 (<0.01–3.47)	12 (80%)	1.45 (0.31–4.58)	0.12
Actinobacteriota	15 (100%)	4.01 (2.34–7.41)	15 (100%)	2.33 (0.80–2.86)	0.01
Bifidobacterium	14 (93.33%)	1.03 (0.80–5.43)	14 (93.33%)	0.36 (0.23–1.84)	0.30
Verrucomicrobiota	13 (86.67%)	2.81 (0.14–6.06)	14 (93.33%)	1.31 (0.36–3.47)	0.61
Akkermansia	11 (73.33%)	2.72 (0.11–5.80)	12 (80%)	1.18 (0.06–3.44)	0.61
Minor_phyla	15 (100%)	2.06 (0.69–4.45)	15 (100%)	2.66 (2.40–3.31)	0.30
Minor_genera	15 (100%)	30.26 (25.59–33.38)	15 (100%)	31.76 (25.06–41.04)	0.30
Unclassified_genera	15 (100%)	9.19 (7.77–20.95)	15 (100%)	9.95 (8.04–15.69)	0.61

[1]*n* (%): Number of samples in which the phylum/genus was detected (relative frequency of detection).
[2]Exact *p*-values for pairwise comparison of Friedman rank sum with FDR correction.

to achieve species or strain level discrimination, it will be necessary to apply developing procedures, including full-length 16S rRNA gene sequencing (Yang et al., 2020; Zhang et al., 2021) and metagenome-assembled genomes (Arikawa et al., 2021; Holman et al., 2022), and/or the combination of culture-dependent and independent techniques.

The metataxomonic analysis did not find differences between both sampling times in relation to the relative abundance of the genus *Lactobacillus* (*sensu* lato). This is not surprising since the probiotic treatment led to a very moderate increase in the total *Lactobacillus* counts. Although studies addressing the impact of aging on the fecal levels of *Lactobacillus* have provided contradictory results (Salazar et al., 2020), this genus is not among the most abundant ones in feces of elderly people (Claesson et al., 2011, 2012; Albrich et al., 2022; Yan et al., 2022). In addition, hypertension, which is a very common comorbidity among the elderly and a risk factor for COVID-19, has been linked to a depletion in *Lactobacillus* levels (Ghosh et al., 2020). In this study, most of the recruited elderly presented this comorbidity (Supplementary Table S1). Therefore, it is highly probable that small increases in the percentage of sequences of a low abundance genus may remain undetected using a metataxonomic approach based on partial 16S rRNA gene sequences. The number of sequences per sample obtained in this work (from 21,950 to 35,737) allows the detection of shifts related to the most abundant genera but it may be not enough to detect shifts in the populations of the rarest genera, which relative abundance may be 10,000 to 100,000 times lower. This highlights the importance of a suitable sequencing depth for being able to detect changes affecting low abundance genera or species. The discrepancy between culture-based methods, qPCR and 16S rRNA sequencing observed in this study reveals that metataxonomic approaches may be unsuited to detect changes readily measurable by culture-based methods or qPCR. This fact is in agreement with a recent study which demonstrated that low abundance bacteria can train immunity (Han et al., 2022).

The administration of the probiotic strain did not change the fatty acid profiles in the fecal samples of the recruited people, a finding that is in agreement with the lack of metataxomic changes observed in this study. Interestingly, it has been reported that there

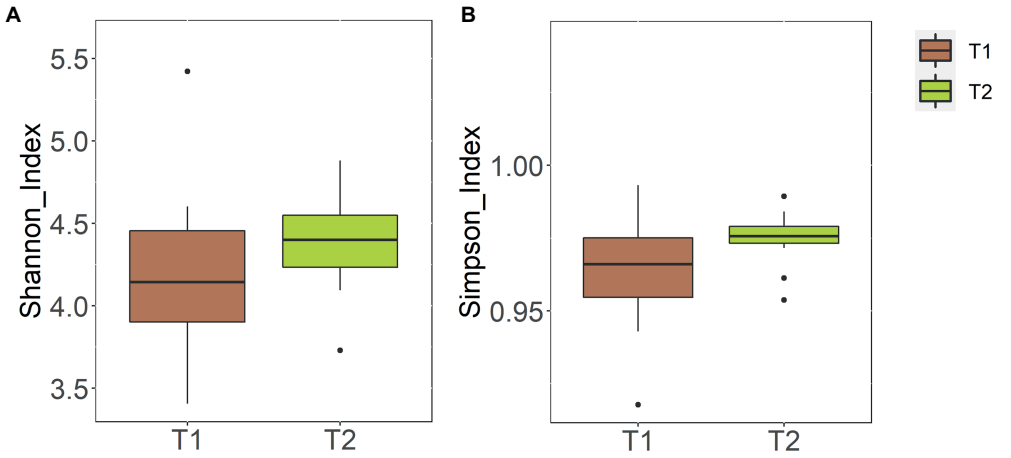

FIGURE 3
Alpha diversity at the ASV level of the fecal samples obtained at day 0 (T1) and at day 120 (T2). **(A)** Shannon diversity index; **(B)** Simpson diversity index.

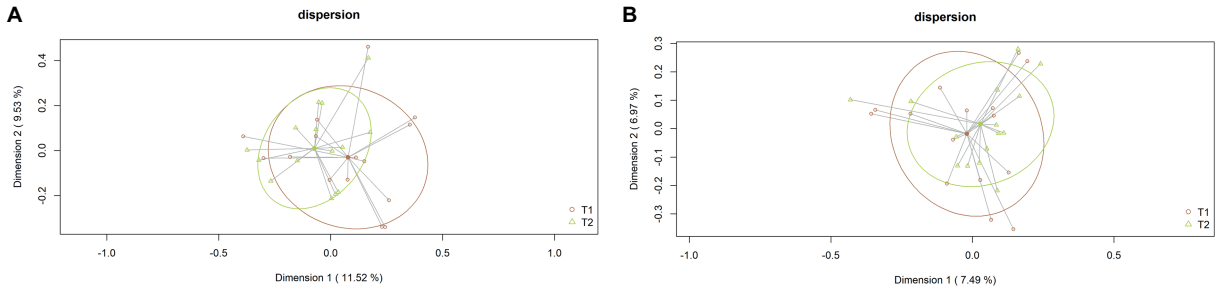

FIGURE 4
Beta diversity at the ASV level of the fecal samples obtained at day 0 (T1) and at day 120 (T2). **(A)** PCoA plots based on the Bray–Curtis dissimilarity index (relative abundance); **(B)** PCoA plots based on the Jaccard's coefficient for binary data (presence of absence).

were no differences in fecal SCFA concentrations among people with different *Lactobacillus* counts (Le Roy et al., 2015). Since *Lactobacillus* sp. are not the main SCFAs producers and many other bacterial groups are able to produce higher SCFAs amounts as a result of gut fermentation processes, the moderate increase in total *Lactobacillus* observed in the recruited elderly may have not been enough to increase the fecal SCFAs values in their fecal waters, either by the probiotic strain itself or by fostering metabolic cross-feeding interactions with other SCFAs-producing bacteria.

SCFAs are a result of the metabolism of the gut microbiota and play several beneficial roles for the host health (Puertollano et al., 2014; Morrison and Preston, 2016; van der Beek et al., 2017). Aging-related disturbances in the composition of the gut microbiota are typically associated with lower levels of SCFAs and an enrichment in the pathways responsible for the degradation of SCFAs (Yan et al., 2022). Although it has been observed that patients with COVID-19 had an impaired production of SCFAs by their gut microbiomes (Zhang et al., 2022), these metabolites seem unable to prevent the entry and replication of SARS-CoV-2 in gut cells (Pascoal et al., 2021).

Overall, the results of this work and those obtained in a previous study with the same cohort indicate that the strain was able to reach the gut in all the recruited elderly, and suggest that it was able induce beneficial immune responses both at the respiratory and gut level, contributing to an improvement in functional and nutritional scores (Mozota et al., 2021). COVID-19 is associated with the overproduction of proinflammatory cytokines (Zazzara et al., 2022); in this pandemic context, immune enhancement functions are particularly relevant for the elderly, because of the immunosenescence associated with aging (Aw et al., 2007; Wang et al., 2022), but, most especially, for those residing in nursing homes. A study assessing microbiota–health correlations among elderly found that the serum levels of several markers of inflammation (TNF-α, IL-6 and IL-8, and C-reactive protein) were significantly higher among subjects living in long-stay nursing homes than among community dwellers (Claesson et al., 2012). Long-stay elderly also obtained poorer scores for comorbidity, functionality, nutritional state, muscle mass, and mental activity (Claesson et al., 2012).

TABLE 4 Relative frequencies, medians and interquartile range (IQR) of the relative abundance (%) of the most abundant bacterial phyla (in bold) and genera (in italics) detected in the fecal samples collected at day 0 (T1) and 120 (T2).

Phylum	T1		T2		*p*-value[2]
Genus	*n* (%)[1]	Median (IQR)	*n* (%)[1]	Median (IQR)	
Firmicutes	11 (100%)	48.83 (32.91–54.71)	11 (100%)	49.29 (13.33–64.27)	1.00
Staphylococcus	11 (100%)	15.37 (4.08–36.40)	11 (100%)	5.05 (0.48–35.83)	0.55
Streptococcus	11 (100%)	1.16 (0.74–4.60)	9 (81.82%)	0.32 (0.08–1.10)	0.07
Anaerococcus	8 (72.73%)	0.94 (0.13–4.30)	7 (63.64%)	0.18 (<0.01–3.37)	0.55
Peptoniphilus	8 (72.73%)	0.64 (0.05–2.56)	6 (54.55%)	0.19 (<0.01–5.60)	1.00
Dolosigranulum	6 (54.55%)	0.03 (<0.01–1.70)	6 (54.55%)	0.04 (<0.01–0.53)	1.00
Anoxybacillus	10 (90.91%)	1.77 (0.65–3.05)	10 (90.91%)	1.67 (0.28–2.58)	0.23
Finegoldia	7 (63.64%)	0.29 (<0.01–1.58)	4 (36.36%)	<0.01 (<0.01–1.46)	1.00
Proteobacteria	11 (100%)	20.28 (10.92–27.91)	11 (100%)	20.78 (15.74–41.52)	0.55
Pseudomonas	5 (45.45%)	<0.01 (<0.01–0.12)	4 (36.36%)	<0.01 (<0.01–0.13)	1.00
Serratia	2 (18.18%)	<0.01 (<0.01–<0.01)	3 (27.27%)	<0.01 (<0.01–0.10)	1.00
Moraxella	1 (9.09%)	<0.01 (<0.01–<0.01)	1 (9.09%)	<0.01 (<0.01–0.13)	1.00
Colwellia	10 (90.91%)	2.06 (1.05–4.10)	11 (100%)	1.90 (0.14–3.04)	0.55
Sulfitobacter	9 (81.82%)	0.65 (0.32–1.6)	8 (72.73%)	0.41 (0.02–1.50)	1.00
Litoreibacter	9 (81.82%)	0.94 (0.51–1.05)	7 (63.64%)	0.35 (<0.01–0.75)	0.23
Sphingorhabdus	9 (81.82%)	0.78 (0.25–1.47)	10 (90.91%)	0.35 (0.09–0.76)	0.23
Bacteroidota	11 (100%)	10.89 (5.06–14.28)	11 (100%)	9.17 (1.00–13.13)	1.00
Maribacter	10 (90.91%)	1.56 (0.68–2.46)	11 (100%)	1.95 (0.35–2.46)	1.00
Prevotella	7 (63.64%)	0.06 (<0.01–0.54)	5 (45.45%)	<0.01 (<0.01–0.23)	1.00
Actinobacteriota	11 (100%)	7.18 (4.17–19.46)	11 (100%)	4.27 (2.27–7.20)	0.23
Corynebacterium	10 (90.91%)	4.50 (0.31–11.91)	10 (90.91%)	1.57 (0.43–2.01)	0.23
Cyanobacteria	10 (90.91%)	0.46 (0.29–0.68)	10 (90.91%)	0.51 (0.16–1.01)	1.00
Chloroplast	10 (90.91%)	0.46 (0.29–0.68)	9 (81.82%)	0.48 (0.16–0.98)	1.00
Minor_phyla	11 (100%)	6.81 (4.67–8.18)	11 (100%)	5.44 (0.49–8.47)	0.23
Minor_genera	11 (100%)	21.17 (12.70–27.54)	11 (100%)	12.69 (1.56–29.85)	0.55
Unclassified_genera	11 (100%)	10.7 (5.33–17.43)	11 (100%)	7.96 (0.90–13.82)	0.55

[1]*n* (%): Number of samples in which the phylum/genus was detected (relative frequency of detection).
[2]Exact *p*-values for pairwise comparison of Friedman rank sum with FDR correction.

TABLE 5 Concentration (μg/g) and frequency of detection (% samples) of fecal fatty acids (FAs) at day 0 (T1) and 120 (T2). The *p*-values are related to the concentration de the FAs at both sampling times.

Fatty acid	T1		T2		*p*-values
	Concentration	% samples	Concentration	% samples	
SCFAs					
Acetic	3272.01 ± 2760.79	100	3100.50 ± 1848.35	100	0.551
Propionic	1146.10 ± 926.92	93	946.31 ± 669.98	100	0.972
Isobutyric	249.60 ± 148.62	57	173.06 ± 160.12	57	
Butyric	851.30 ± 1169.79	93	576.03 ± 733.90	71	0.646
Acetic/propionic ratio	3.19 ± 1.04		3.96 ± 1.57		0.382
Total	5126.74 ± 4715.54	100	4458.26 ± 3043.43	100	0.875
BCFAs	647.80 ± 525.95	93	459.92 ± 478.57	100	
Isovaleric	494.20 ± 360.17	93	388.80 ± 329.07	93	0.388
Isobutyric	249.60 ± 148.62	57	173.06 ± 160.12	57	0.173
MCFAs	283.67 ± 313.72		111.02 ± 121.66		
Caproic	283.67 ± 313.72	21	111.02 ± 121.66	36	0.593
Total FAs	6022.21 ± 5462.42	100	5101.11 ± 3705.72	100	0.925

The association of elderly with inflammation argues in favor of approaches enabling immunomodulation (Guigoz et al., 2008), such as the use of probiotics. This was particularly challenging in the frame of the COVID-19 pandemic. The first published studies about the use of probiotics in hospitalized COVID-19 patients described a positive effect, including a reduction in the duration of diarrheal episodes, in the risk of respiratory failure and/or in the risk of death (d'Ettorre et al., 2020; Ceccarelli et al., 2021). However, such studies did not address the potential mechanisms responsible for the observed benefits. More recently, it was reported that a *Lactiplantibacillus plantarum* strain was able to induce innate cytokine responses with the potential for providing a protection against the more severe courses of this disease (Kageyama et al., 2022). Similarly to our results, other studies involving the oral administration of a probiotic formula to COVID-19 outpatients did not find significant changes in the composition of the fecal bacteriome as a result of the probiotic intake (Gutiérrez-Castrellón et al., 2022). The authors suggested that the probiotic product primarily acted by interacting with the host immune system since they observed increased titers of anti-SARS-CoV2 specific antibodies compared to placebo.

This study faces some limitations. Because of the low number of participants, the lack of randomization, and the lack of a placebo group, the observed beneficial effects must be confirmed in future well-designed placebo-controlled trials involving a high number of elderly. However, our results indicate that *L. salivarius* CECT 30632 colonized, at least temporarily, the intestinal tract of the recruited elderly and may have contributed to improvements in their functional, nutritional, and immunological status, without changing the general structure of their nasal and fecal bacteriomes when assessed at the genus level.

Data availability statement

The datasets presented in this study can be found in online repositories. The names of the repository/repositories and accession number(s) can be found at: https://www.ncbi.nlm.nih.gov/bioproject/PRJNA880542/.

Ethics statement

The studies involving human participants were reviewed and approved by Ethics Committee of the Hospital Clínico San Carlos (Madrid, Spain; protocol: CEIC 20/263-E_COVID; date of approval: 01/04/2020, act 4.1/20). The patients/participants provided their written informed consent to participate in this study.

Author contributions

JR: conceptualization. MM, IC, NG-T, RA, SD, and IG-D: methodology. CA: software. JR and SD: resources and writing—review and editing, funding acquisition. NG-T, CA, SD, and JR: data curation. JR, CA, and SD: writing—original draft preparation. All authors have read and agreed to the published version of the manuscript.

Acknowledgments

We acknowledge the recruited elderly and the staff of the nursing home for their effort, support, and implication in this trial. We are grateful to Villa Villera for developing, producing, and shipping the dairy product used as the test product in the trial, and to Leonides Fernández (UCM) for critical reading of the manuscript.

Conflict of interest

The authors declare that the research was conducted in the absence of any commercial or financial relationships that could be construed as a potential conflict of interest.

Publisher's note

Supplementary material

The Supplementary material for this article can be found online at: https://www.frontiersin.org/articles/10.3389/fmicb.2022.1052675/full#supplementary-material

References

Aguilar-Palacio, I., Maldonado, L., Marcos-Campos, I., Castel-Feced, S., Malo, S., Aibar, C., et al. (2022). Understanding the COVID-19 pandemic in nursing homes (Aragón, Spain): sociodemographic and clinical factors associated with hospitalization and mortality. *Front. Public Health* 10:928174. doi: 10.3389/fpubh.2022.928174

Alba, C., Aparicio, M., González-Martínez, F., González-Sánchez, M. I., Pérez-Moreno, J., del Castillo, B. T., et al. (2021). Nasal and fecal microbiota and immunoprofiling of infants with and without RSV bronchiolitis. *Front. Microbiol.* 12:667832. doi: 10.3389/fmicb.2021.667832

Albrich, W. C., Ghosh, T. S., Ahearn-Ford, S., Mikaeloff, F., Lunjani, N., Forde, B., et al. (2022). A high-risk gut microbiota configuration associates with fatal hyperinflammatory immune and metabolic responses to SARS-CoV-2. *Gut Microbes* 14:2073131. doi: 10.1080/19490976.2022.2073131

Aparicio, M., Alba, C., CAM Public Health Area 6 PSGORodríguez, J. M., and Fernández, L. (2020). Microbiological and immunological markers in milk and infant feces for common gastrointestinal disorders: a pilot study. *Nutrients* 12:634. doi: 10.3390/nu12030634

Araújo, M., Nunes, V., Costa, L. A., Souza, T. A., Torres, G. V., and Nobre, T. (2021). Health conditions of potential risk for severe Covid-19 in institutionalized elderly people. *PLoS One* 16:e0245432. doi: 10.1371/journal.pone.0245432

Arikawa, K., Ide, K., Kogawa, M., Saeki, T., Yoda, T., Endoh, T., et al. (2021). Recovery of strain-resolved genomes from human microbiome through an integration framework of single-cell genomics and metagenomics. *Microbiome* 9:202. doi: 10.1186/s40168-021-01152-4

Aw, D., Silva, A. B., and Palmer, D. B. (2007). Immunosenescence: emerging challenges for an ageing population. *Immunology* 120, 435–446. doi: 10.1111/j.1365-2567.2007.02555.x

Boccardi, V., Ruggiero, C., and Mecocci, P. (2020). COVID-19: a geriatric emergency. *Geriatrics* 5:24. doi: 10.3390/geriatrics5020024

Bokulich, N. A., Kaehler, B. D., Rideout, J. R., Dillon, M., Bolyen, E., Knight, R., et al. (2018). Optimizing taxonomic classification of marker-gene amplicon sequences with QIIME 2's q2-feature-classifier plugin. *Microbiome* 6:90. doi: 10.1186/s40168-018-0470-z

Bolyen, E., Rideout, J. R., Dillon, M. R., Bokulich, N. A., Abnet, C. C., Al-Ghalith, G. A., et al. (2019). Reproducible, interactive, scalable and extensible microbiome data science using QIIME 2. *Nat. Biotechnol.* 37, 852–857. doi: 10.1038/s41587-019-0209-9

Callahan, B. J., McMurdie, P. J., Rosen, M. J., Han, A. W., Johnson, A. J., and Holmes, S. P. (2016). DADA2: high-resolution sample inference from Illumina amplicon data. *Nat. Methods* 13, 581–583. doi: 10.1038/nmeth.3869

Ceccarelli, G., Borrazzo, C., Pinacchio, C., Santinelli, L., Innocenti, G. P., Cavallari, E. N., et al. (2021). Oral bacteriotherapy in patients with COVID-19: a retrospective cohort study. *Front. Nutr.* 7:613928. doi: 10.3389/fnut.2020.613928

Claesson, M. J., Cusack, S., O'Sullivan, O., Greene-Diniz, R., de Weerd, H., Flannery, E., et al. (2011). Composition, variability, and temporal stability of the intestinal microbiota of the elderly. *Proc. Natl. Acad. Sci. U. S. A.* 108, 4586–4591. doi: 10.1073/pnas.1000097107

Claesson, M. J., Jeffery, I. B., Conde, S., Power, S. E., O'Connor, E. M., Cusack, S., et al. (2012). Gut microbiota composition correlates with diet and health in the elderly. *Nature* 488, 178–184. doi: 10.1038/nature11319

Davis, N. M., Proctor, D. M., Holmes, S. P., Relman, D. A., and Callahan, B. J. (2018). Simple statistical identification and removal of contaminant sequences in marker-gene and metagenomics data. *Microbiome* 6:226. doi: 10.1186/s40168-018-0605-2

d'Ettorre, G., Ceccarelli, G., Marazzato, M., Campagna, G., Pinacchio, C., Alessandri, F., et al. (2020). Challenges in the management of SARS-CoV2 infection: the role of oral bacteriotherapy as complementary therapeutic strategy to avoid the progression of COVID-19. *Front. Med.* 7:389. doi: 10.3389/fmed.2020.00389

Falony, G., Vieira-Silva, S., and Raes, J. (2018). Richness and ecosystem development across faecal snapshots of the gut microbiota. *Nat. Microbiol.* 3, 526–528. doi: 10.1038/s41564-018-0143-5

Ghosh, T. S., Arnoux, J., and O'Toole, P. W. (2020). Metagenomic analysis reveals distinct patterns of gut *Lactobacillus* prevalence, abundance, and geographical variation in health and disease. *Gut Microbes* 12, 1822729–1822719. doi: 10.1080/19490976.2020.1822729

Gu, S., Chen, Y., Wu, Z., Chen, Y., Gao, H., Lv, L., et al. Alterations of the gut microbiota in patients with COVID-19 or H1N1 influenza. *Clin. Infect. Dis.* 71, 2669–2678. doi: 10.1093/cid/ciaa709

Guigoz, Y., Doré, J., and Schiffrin, E. J. (2008). The inflammatory status of old age can be nurtured from the intestinal environment. *Curr. Opin. Clin. Nutr. Metab. Care* 11, 13–20. doi: 10.1097/MCO.0b013e3282f2bfdf

Gutiérrez-Castrellón, P., Gandara-Martí, T., Abreu-Y Abreu, A. T., Nieto-Rufino, C. D., López-Orduña, E., Jiménez-Escobar, I., et al. (2022). Probiotic improves symptomatic and viral clearance in Covid 19 outpatients: a randomized, quadruple-blinded, placebo-controlled trial. *Gut Microbes* 14:2018899. doi: 10.1080/19490976.2021.2018899

Han, G., Luong, H., and Vaishnava, S. (2022). Low abundance members of the gut microbiome exhibit high immunogenicity. *Gut Microbes* 14:2104086. doi: 10.1080/19490976.2022.2104086

Harrow, S. A., Ravindran, V., Butler, R. C., Marshall, J. W., and Tannock, G. W. (2007). Real-time quantitative PCR measurement of ileal *Lactobacillus salivarius* populations from broiler chickens to determine the influence of farming practices. *Appl. Environ. Microbiol.* 73, 7123–7127. doi: 10.1128/AEM.01289-07

He, L. H., Ren, L. F., Li, J. F., Wu, Y. N., Li, X., and Zhang, L. (2020a). Intestinal flora as a potential strategy to fight SARS-CoV-2 infection. *Front. Microbiol.* 11:1388. doi: 10.3389/fmicb.2020.01388

He, Y., Wang, J., Li, F., and Shi, Y. (2020b). Main clinical features of COVID-19 and potential prognostic and therapeutic value of the microbiota in SARS-CoV-2 infections. *Front. Microbiol.* 11:1302. doi: 10.3389/fmicb.2020.01302

Heras, E., Garibaldi, P., Boix, M., Valero, O., Castillo, J., Curbelo, Y., et al. (2021). COVID-19 mortality risk factors in older people in a long-term care center. *Eur. Geriatr. Med.* 12, 601–607. doi: 10.1007/s41999-020-00432-w

Holman, D. B., Kommadath, A., Tingley, J. P., and Abbott, D. W. (2022). Novel insights into the pig gut microbiome using metagenome-assembled genomes. *Microbiol. Spectr.* 10:e0238022. doi: 10.1128/spectrum.02380-22

Kageyama, Y., Nishizaki, Y., Aida, K., Yayama, K., Ebisui, T., Akiyama, T., et al. (2022). *Lactobacillus plantarum* induces innate cytokine responses that potentially provide a protective benefit against COVID-19: a single-arm, double-blind, prospective trial combined with an in vitro cytokine response assay. *Exp. Ther. Med.* 23:20. doi: 10.3892/etm.2021.10942

Klindworth, A., Pruesse, E., Schweer, T., Peplies, J., Quast, C., Horn, M., et al. (2013). Evaluation of general 16S ribosomal RNA gene PCR primers for classical and next-generation sequencing-based diversity studies. *Nucleic Acids Res.* 41:e1. doi: 10.1093/nar/gks808

Lackey, K. A., Williams, J. E., Meehan, C. L., Zachek, J. A., Benda, E. D., Price, W. J., et al. (2019). What's normal? Microbiomes in human milk and infant feces are related to each other but vary geographically: the INSPIRE study. *Front. Nutr.* 6:45. doi: 10.3389/fnut.2019.00045

Lai, C. C., Wang, J. H., Ko, W. C., Yen, M. Y., Lu, M. C., Lee, C. M., et al. (2020). COVID-19 in long-term care facilities: an upcoming threat that cannot be ignored. *J. Microbiol. Immunol. Infect.* 53, 444–446. doi: 10.1016/j.jmii.2020.04.008

Le Roy, C. I., Štšepetova, J., Sepp, E., Songisepp, E., Claus, S. P., and Mikelsaar, M. (2015). New insights into the impact of *Lactobacillus* population on host-bacteria metabolic interplay. *Oncotarget* 6, 30545–30556. doi: 10.18632/oncotarget.5906

Liu, K., Chen, Y., Lin, R., and Han, K. (2020). Clinical features of COVID-19 in elderly patients: a comparison with young and middle-aged patients. *J. Infect.* 80, e14–e18. doi: 10.1016/j.jinf.2020.03.005

Mediano, P., Fernández, L., Jiménez, E., Arroyo, R., Espinosa-Martos, I., Rodríguez, J. M., et al. (2017). Microbial diversity in milk of women with mastitis: potential role of coagulase-negative staphylococci, viridans group streptococci, and corynebacteria. *J. Hum. Lact.* 33, 309–318. doi: 10.1177/0890334417692968

Morrison, D. J., and Preston, T. (2016). Formation of short chain fatty acids by the gut microbiota and their impact on human metabolism. *Gut Microbes* 7, 189–200. doi: 10.1080/19490976.2015.1134082

Mozota, M., Castro, I., Gómez-Torres, N., Arroyo, R., Lailla, Y., Somada, M., et al. (2021). Administration of *Ligilactobacillus salivarius* MP101 in an elderly nursing home during the COVID-19 pandemic: immunological and nutritional impact. *Foods* 10:2149. doi: 10.3390/foods10092149

Palavras, M. J., Faria, C., Fernandes, P., Lagarto, A., Ponciano, A., Alçada, F., et al. (2022). The impact of the third wave of the COVID-19 pandemic on the elderly and very elderly population in a tertiary care hospital in Portugal. *Cureus* 14:e22653. doi: 10.7759/cureus.22653

Pascoal, L. B., Rodrigues, P. B., Genaro, L. M., Gomes, A., Toledo-Teixeira, D. A., Parise, P. L., et al. (2021). Microbiota-derived short-chain fatty acids do not interfere with SARS-CoV-2 infection of human colonic samples. *Gut Microbes* 13, 1–9. doi: 10.1080/19490976.2021.1874740

Paulson, J. N., Stine, O. C., Bravo, H. C., and Pop, M. (2013). Differential abundance analysis for microbial marker-gene surveys. *Nat. Methods* 10, 1200–1202. doi: 10.1038/nmeth.2658

Pérez, T., Alba, C., Aparicio, M., de Andrés, J., Ruiz Santa Quiteria, J. A., Rodríguez, J. M., et al. (2019). Abundant bacteria in the proximal and distal intestine of healthy Siberian sturgeons (*Acipenser baerii*). *Aquaculture* 506, 325–336. doi: 10.1016/j.aquaculture.2019.03.055

Pizarro-Pennarolli, C., Sánchez-Rojas, C., Torres-Castro, R., Vera-Uribe, R., Sanchez-Ramirez, D. C., Vasconcello-Castillo, L., et al. (2021). Assessment of activities of daily living in patients post COVID-19: a systematic review. *Peer J.* 9:e11026. doi: 10.7717/peerj.11026.eCollection

Puertollano, E., Kolida, S., and Yaqoob, P. (2014). Biological significance of short-chain fatty acid metabolism by the intestinal microbiome. *Curr. Opin. Clin. Nutr. Metab. Care* 17, 139–144. doi: 10.1097/MCO.0000000000000025

Quast, C., Pruesse, E., Yilmaz, P., Gerken, J., Schweer, T., Yarza, P., et al. (2013). The SILVA ribosomal RNA gene database project: improved data processing and web-based tools. *Nucleic Acids Res.* 41, D590–D596. doi: 10.1093/nar/gks1219

R Core Team (2021). R: A language and environment for statistical computing. R Foundation for Statistical Computing, Vienna, Austria.. URL https://www.R-project.org/.

Ruiz-Barba, J. L., Maldonado, A., and Jiménez-Díaz, R. (2005). Small-scale total DNA extraction from bacteria and yeast for PCR applications. *Anal. Biochem.* 347, 333–335. doi: 10.1016/j.ab.2005.09.028

Salazar, N., González, S., Nogacka, A. M., Rios-Covián, D., Arboleya, S., Gueimonde, M., et al. (2020). Microbiome: effects of ageing and diet. *Curr. Issues Mol. Biol.* 36, 33–62. doi: 10.21775/cimb.036.033

Salvetti, E., Harris, H. M. B., Felis, G. E., and O'Toole, P. W. (2018). Comparative genomics of the genus *Lactobacillus* reveals robust phylogroups that provide the basis for reclassification. *Appl. Environ. Microbiol.* 84, e00993–e00918. doi: 10.1128/AEM.00993-18

Sepulveda, E. R., Stall, N. M., and Sinha, S. K. (2020). A comparison of COVID-19 mortality rates among long-term care residents in 12 OECD countries. *J. Am. Med. Dir. Assoc.* 21, 1572–1574.e3. doi: 10.1016/j.jamda.2020.08.039

Silva, D. F. O., Lima, S. C. V. C., Sena-Evangelista, K. C. M., Marchioni, D. M., Cobucci, R. N., and Andrade, F. B. (2020). Nutritional risk screening tools for older adults with COVID-19: a systematic review. *Nutrients* 12:2956. doi: 10.3390/nu12102956

Stewart, C. J., Mansbach, J. M., Wong, M. C., Ajami, N. J., Petrosino, J. F., Camargo, C. A., et al. (2017). Associations of nasopharyngeal metabolome and microbiome with severity among infants with bronchiolitis. A multiomic analysis. *Am. J. Respir. Crit. Care Med.* 196, 882–891. doi: 10.1164/rccm.201701-0071OC

Suñer, C., Ouchi, D., Mas, M. À., Lopez Alarcon, R., Massot Mesquida, M., Prat, N., et al. (2021). A retrospective cohort study of risk factors for mortality among nursing homes exposed to COVID-19 in Spain. *Nat. Aging* 1, 579–584. doi: 10.1038/s43587-021-00079-7

Trecarichi, E. M., Mazzitelli, M., Serapide, F., Pelle, M. C., Tassone, B., Arrighi, E., et al. (2020). Clinical characteristics and predictors of mortality associated with COVID-19 in elderly patients from a long-term care facility. *Sci. Rep.* 10, 20834–20837. doi: 10.1038/s41598-020-77641-7

van der Beek, C. M., Dejong, C. H. C., Troost, F. J., Masclee, A. A. M., and Lenaerts, K. (2017). Role of short-chain fatty acids in colonic inflammation, carcinogenesis, and mucosal protection and healing. *Nutr. Rev.* 75, 286–305. doi: 10.1093/nutrit/nuw067

Wang, Y., Dong, C., Han, Y., Gu, Z., and Sun, C. (2022). Immunosenescence, aging and successful aging. *Front. Immunol.* 13:942796. doi: 10.3389/fimmu.2022.942796

Yan, H., Qin, Q., Yan, S., Chen, J., Yang, Y., Li, T., et al. (2022). Comparison of the gut microbiota in different age groups in China. *Front. Cell. Infect. Microbiol.* 12:877914. doi: 10.3389/fcimb.2022.877914

Yang, J., Pu, J., Lu, S., Bai, X., Wu, Y., Jin, D., et al. (2020). Species-level analysis of human gut microbiota with metataxonomics. *Front. Microbiol.* 11:2029. doi: 10.3389/fmicb.2020.02029

Zazzara, M. B., Bellieni, A., Calvani, R., Coelho-Junior, H. J., Picca, A., and Marzetti, E. (2022). Inflammaging at the time of COVID-19. *Clin. Geriatr. Med.* 38, 473–481. doi: 10.1016/j.cger.2022.03.003

Zhang, B., Brock, M., Arana, C., Dende, C., van Oers, N. S., Hooper, L. V., et al. (2021). Impact of bead-beating intensity on the genus- and species-level characterization of the gut microbiome using amplicon and complete 16S rRNA gene sequencing. *Front. Cell. Infect. Microbiol.* 11:678522. doi: 10.3389/fcimb.2021.678522

Zhang, F., Wan, Y., Zuo, T., Yeoh, Y. K., Liu, Q., Zhang, L., et al. (2022). Prolonged impairment of short-chain fatty acid and L-isoleucine biosynthesis in gut microbiome in patients with COVID-19. *Gastroenterology* 162, 548–561.e4. doi: 10.1053/j.gastro.2021.10.013

Zheng, J., Wittouck, S., Salvetti, E., Franz, C., Harris, H., Mattarelli, P., et al. (2020). A taxonomic note on the genus *Lactobacillus*: description of 23 novel genera, emended description of the genus *Lactobacillus* Beijerinck 1901, and union of *Lactobacillaceae* and *Leuconostocaceae*. *Int. J. Syst. Evol. Microbiol.* 70, 2782–2858. doi: 10.1099/ijsem.0.004107

Zuo, T., Zhang, F., Lui, G., Yeoh, Y. K., Li, A., Zhan, H., et al. (2020). Alterations in gut microbiota of patients with COVID-19 during time of hospitalization. *Gastroenterology* 159, 944–955.e8. doi: 10.1053/j.gastro.2020.05.048

frontiers | Frontiers in Microbiology

TYPE Review
PUBLISHED 23 December 2022
DOI 10.3389/fmicb.2022.1092248

OPEN ACCESS

EDITED BY
Giuseppe Spano,
University of Foggia, Italy

REVIEWED BY
Marwa Moumni,
Marche Polytechnic University, Italy
Nariman El Abed,
National Institute of Applied Science and Technology, Tunisia

*CORRESPONDENCE
João Miguel Rocha
jmfrocha@fe.up.pt

SPECIALTY SECTION
This article was submitted to Food Microbiology, a section of the journal Frontiers in Microbiology

RECEIVED 07 November 2022
ACCEPTED 29 November 2022
PUBLISHED 23 December 2022

CITATION
Sharma H, Fidan H, Özogul F and Rocha JM (2022) Recent development in the preservation effect of lactic acid bacteria and essential oils on chicken and seafood products. *Front. Microbiol.* 13:1092248. doi: 10.3389/fmicb.2022.1092248

Recent development in the preservation effect of lactic acid bacteria and essential oils on chicken and seafood products

Heena Sharma[1], Hafize Fidan[2], Fatih Özogul[3] and João Miguel Rocha[4,5]*

[1]Food Technology Lab, Dairy Technology Division, ICAR-National Dairy Research Institute, Karnal, India, [2]Department of Tourism and Culinary Management, University of Food Technologies, Plovdiv, Bulgaria, [3]Department of Seafood Processing Technology, Faculty of Fisheries, Çukurova University, Adana, Türkiye, [4]LEPABE – Laboratory for Process Engineering, Environment, Biotechnology and Energy, Faculty of Engineering, University of Porto, Porto, Portugal, [5]ALiCE – Associate Laboratory in Chemical Engineering, Faculty of Engineering, University of Porto, Porto, Portugal

Chicken and seafood are highly perishable owing to the higher moisture and unsaturated fatty acids content which make them more prone to oxidation and microbial growth. In order to preserve the nutritional quality and extend the shelf-life of such products, consumers now prefer chemical-free alternatives, such as lactic acid bacteria (LAB) and essential oils (EOs), which exert a bio-preservative effect as antimicrobial and antioxidant compounds. This review will provide in-depth information about the properties and main mechanisms of oxidation and microbial spoilage in chicken and seafood. Furthermore, the basic chemistry and mode of action of LAB and EOs will be discussed to shed light on their successful application in chicken and seafood products. Metabolites of LAB and EOs, either alone or in combination, inhibit or retard lipid oxidation and microbial growth by virtue of their principal constituents and bioactive compounds including phenolic compounds and organic acids (lactic acid, propionic acid, and acetic acid) and others. Therefore, the application of LAB and EOs is widely recognized to extend the shelf-life of chicken and seafood products naturally without altering their functional and physicochemical properties. However, the incorporation of any of these agents requires the optimization steps necessary to avoid undesirable sensory changes. In addition, toxicity risks associated with EOs also demand the regularization of an optimum dose for their inclusion in the products.

KEYWORDS

chicken products, seafood, bioactive compounds, essential oils, lactic acid bacteria, action mechanisms, preservation, biological activity

1 Introduction

Chicken meat and seafood are recognized as nutritionally superior foods with lower fat content and more unsaturated fatty acid content than meat from other species (Kumar et al., 2015b). Apart from containing proteins and amino acids with high biological value, vitamins, and other essential nutrients, these are economically affordable and not associated with any cultural or religious taboos owing to which chicken meat and seafood are consumed at a leading rate across the globe. However, the quality and nutritional value of the chicken and fish meat and the resultant products are of paramount importance which can influence its acceptability significantly. Furthermore, chicken and seafood also act as major potential sources of foodborne illness as they harbor various foodborne pathogens including *Salmonella* spp., *Escherichia coli*, *Listeria monocytogenes,* and *Campylobacter* sp. *Salmonella* infection has reported almost 94 million illnesses and 1.5 lakhs deaths worldwide (Heredia and García, 2018). Therefore, all the factors beginning from farm management to the table of the consumers should be emphasized and given due consideration in order to ensure desirable and optimum meat quality. The importance of ensuring food safety is increasing day-by-day. In this direction, various measures have been taken, such as the widespread use of chemical preservatives in food, to prevent the spread of pathogenic microorganisms in the food industry, extend the shelf-life of food, and prevent economic losses (Françoise, 2010). The association of these chemical preservatives with cancer and other health-related risks has necessitated researchers to explore safer alternatives including bio-preservation and the use of protective cultures. In this regard, a group of lactic acid bacteria (LAB) and their antimicrobials and essential oils (EOs) have been successfully explored for their multipurpose use in chicken meat and seafood. Generally, homofermentative LAB is considered for its meat preservation action owing to the production of only lactic acid from various sources of carbohydrates. LAB antimicrobials, such as bacteriocins (bioactive cationic peptides or proteins) and other organic acids, help in inhibiting spoilage and maintaining the quality of chicken meat and seafood (Ibrahim et al., 2021), while EOs are the secondary metabolites of plant origin that not only inhibit the pathogenic microorganisms but also pose several health benefits including antimicrobial and antioxidant activity (Sharma et al., 2020). However, owing to the unique composition of meat and seafood and the different nature of EOs and LAB, interaction among these results in several complex mechanisms leading to either synergistic or antagonistic actions. Looking at the potential of the use of LAB and EOs in the meat industry especially, chicken meat and seafood, the present review summarizes the basic principles and mechanisms of action of different EOs and LAB metabolites in meat and seafood preservation. Furthermore, this review is aimed at updating the knowledge regarding various active components of EOs and different LAB strains used in the chicken meat and seafood industry. The detailed discussion has also been focused on the significance and health benefits of EOs.

2 The essential parameters of chicken and seafood products for human consumption

2.1 Nutritive value of chicken meat and seafood

Chicken meat and meat products have an edge over other types of meat in terms of nutritional value offered to consumers. Scientific studies validate the presence of higher protein and lower fat content in chicken meat than in red meat, thereby giving a feeling of satiety to consumers. Noteworthy, it is recommended to consume it without skin as the latter contains almost 3 times more fat than chicken meat without skin. Furthermore, the lower content of saturated fatty acids in chicken meat results in lower calorific value, thus making it suitable for people suffering from cardiovascular diseases. The risk of such diseases could be reduced by 19% upon replacing red meat with chicken meat in diets (Bernstein et al., 2010). Reports also suggest a positive correlation between dietary saturated fatty acid content and insulin resistance, thereby the occurrence of diabetes (Pan et al., 2011). Therefore, chicken meat can be considered a boon for people afflicted with diabetes as compared with red meat. However, cholesterol content does not contribute to any striking feature of the nutritional value of chicken meat as it is present in almost the same content as in other types of meat. The availability of easily degradable and high-quality proteins in chicken meat makes it a valuable and healthy source of animal protein not only for people with no specific requirement (average daily requirement is 0.66 g kg^{-1} bodyweight) but also for pregnant women (23 g day^{-1} more protein required during late gestation period), athletes, and young children (1.2–1.3 g kg^{-1} body weight) as their requirement is at par with other people. Moreover, the lower level of collagen further adds to the easier digestible characteristic of chicken meat. Among vitamins and minerals, chicken meat contains higher amounts of calcium, sodium, phosphorous, and vitamins B_3 (niacin), A, and B_6 than other meats (Talukder et al., 2013). These minerals and vitamins play vital roles in various physiological activities such as protein synthesis, energy metabolism, maintaining lower lipids, cholesterol levels, and normal gut functions. Though the mechanism is still unclear, the production of aromatic amines, N-nitrous compounds, and others are directly involved in inducing cancers in humans with the consumption of red meat while, white meat is often associated with a lower incidence of cancer (Zhu et al., 2014). Thus, it can be inferred that

the availability of all the essential nutrients confers nutritional benefits to chicken meat; however, research based on the impact of chicken consumption on health effects should be interpreted cautiously as human physiology is a complex process involving various significant factors influencing the occurrence of certain diseases.

As compared to red and white meat, meat obtained from fish and seafood is considered to be more nutritious and healthier for malnutrition and obese people (Cena and Calder, 2020; Maulu et al., 2021). Globally, fish contributes to the third most important source of animal proteins after cereals and milk and contains higher protein content and lesser energy as compared to red meat. The health benefits associated with the consumption of fish and seafood also provide them an edge because they are nutritious and healthy foods for human consumption (Tacon et al., 2020). Omega-3 polyunsaturated fatty acids present in seafood make them suitable for persons more prone to cardiovascular diseases. Furthermore, the trace minerals, such as iodine, chromium, and selenium, required for maintenance and daily activities are also present in abundance in seafood.

2.2 Quality parameters to assess chicken meat quality and seafood

Though it is widely accepted that chicken meat and meat products are among the top-most commodities consumed throughout the world, there are various technological and quality parameters that influence their acceptability and purchasing (Kumar et al., 2015a). The pH, water holding capacity, drip loss, and color of the meat significantly impact the meat quality and its subsequent shelf-life owing to various factors including stress before slaughter, the genotype of the animal, and meat handling and processing conditions. Animals subjected to chronic stress before slaughter often produce meat that has higher ultimate pH (6.5–6.8). Though higher pH inhibits drip loss and presents a dry appearance on the meat surface, such type of meat, also known as dark, firm, and dry, is more prone to microbial spoilage and thus, ultimately has a shorter shelf-life (Gonzalez-Rivas et al., 2020). On the other hand, higher temperatures and lower ultimate pH of meat cause protein denaturation, thereby decreasing the water-holding capacity. Exposure to heat stress brought a significant increase in creatine kinase and glutamic-pyruvic transaminase of chicken plasma associated with higher cooking loss and lower water holding capacity. Furthermore, lower pH is also associated with the oxidation of myoglobin (meat pigment; purple color) to met-myoglobin (brown meat color) which is aesthetically unappealing (Pardo et al., 2021).

Due to their highly perishable nature, the majority of the seafood is transported in ice across various parts of the country. Higher moisture content and neutral pH of seafood also make them more prone to microbial spoilage (Yavuzer and Köse, 2022). Microbial growth generally leads to the production of alkaline compounds in fish, including ammonia, which results in a higher pH value (9.2) of seafood, thereby indicating incipient spoilage conditions. Furthermore, the degradation of proteins also results in the development of amino acids and other amines, as a result of which the total volatile base nitrogen of seafood increases. It has been considered that a level of 30–35 mg TVBN per 100 g is acceptable as the average quality of fish. Furthermore, the production of histamine, cadaverine, and putrescine, as detected by analytical techniques, suggests possible signs of spoilage in fish (Yavuzer, 2021). Therefore, careful handling and storage of seafood is a must for its improved shelf-life and better sensory acceptability.

3 The significance of lactic acid bacteria and their preservative effects on chicken and seafood products

3.1 Bio-preservative properties

Foodborne infections and intoxications are significant problems due to their harmful effects on human health and the economy. Despite advances in food technology, the number of illnesses caused by unsafe food is increasing rapidly. The past several decades have witnessed the wide-scale utilization of chemical preservatives in the food industries. However, several studies have shown that these chemical food preservatives are associated with toxicological problems and diseases (allergic reactions, heart disease, neurological problems, and cancer). Therefore, interest in replacing chemical preservatives with natural alternatives that are safer for consumers and the environment has increased over the past decade. Additionally, today's consumers worldwide are more health conscious and consume foods that do not contain artificial preservatives and use bio-preservatives (Alipin and Safitri, 2016).

Biopreservation is defined as the preservation of foods using biological agents or extending the shelf-life of foods and improving food safety by using microorganisms and their metabolites. It refers to the inhibition of unwanted or pathogenic microorganisms due to antagonistic microbial interference for nutrient competition and the production of antimicrobial metabolites, such as organic acids, hydrogen peroxide, diacetyl, reuterin, bacteriocins, and other low-molecular-weight metabolites (Sakaridis et al., 2014). Over the past few decades, LAB has been widely used for the preservation of fermented and cooked meat products, and a variety of strains have been found to be effective against pathogens and spoilage microorganisms (Bartkiene et al., 2020, 2022;

Küley et al., 2020; Zokaityte et al., 2020; Ağagündüz et al., 2021, 2022; Sharma et al., 2021; Petkova et al., 2022; Rathod et al., 2022; Trakselyte-Rupsiene et al., 2022; Yilmaz et al., 2022a,b). However, research on the biopreservation of fresh poultry meat is quite limited and is even scarcer for fresh fish products. In food production, applying a minimum level of processing and preferring natural additives to ensure food safety is essential. For this purpose, antagonistic microorganisms and their antimicrobial metabolites and the use of biological control systems that induce the inhibition of spoilage bacteria are recommended. Antimicrobial compounds are used in food because of their ability to slow down the development of undesirable microorganisms in food products (Kupryś-Caruk et al., 2019).

Nevertheless, bioprotective culture is defined as microorganisms that prevent the proliferation of pathogens that cause food spoilage and reduce the shelf-life of foods, and this process is carried out without changing the organoleptic properties of foods. The best-known of these microorganisms are LAB and Gram-positive bacteria (Djenane et al., 2006; Guluwa et al., 2021). Several researchers investigated the lactic acid bacteria and their preservation properties on poultry and fish products (Erol et al., 2021; Dissasa et al., 2022). For example, a potential natural food additive using LAB from fermented *Tilapia niloticus* combined with different spices (9% turmeric, 6% chili, and 9% black pepper) on foodborne pathogens was studied. The greatest antimicrobial activity by LAB on *Bacillus cereus* was observed in fermented tilapia combined with black pepper. In contrast, fermented fish combined with chili demonstrated the greatest antimicrobial activity on *Staphylococcus aureus, Escherichia coli,* and *Salmonella enterica* Serovar Typhimurium (Erol et al., 2021). In another study, Dissasa et al. (2022) reported the antimicrobial activity of the antimicrobial peptides from LAB on the growth of pathogenic bacteria from fish in Ethiopia. With the well diffusion assay, *Lactiplantibacillus plantarum*, *Lacticaseibacillus casei* LC2W, and *Lacticaseibacillus paracasei* sub *paracasei* demonstrated strong antibacterial activity on *Edwardsiella tarda* (19 mm), *Aeromonas hydrophila* (18 mm), and *Pseudomonas fluorescens* (18 mm), respectively. The research demonstrates the antimicrobial activity of four strains of LABs on bacterial fish pathogens and states the application opportunities as a biopreservative of fish products.

Poultry meat is thought of as one of the most common foods that result in foodborne infection and intoxication. Alipin and Safitri (2016) reported the potential of LAB from a healthy broiler intestine to prevent the growth of *Salmonella* spp. (*Lactobacillus* spp., *Streptococcus* spp., and *Bifidobacterium bifidum*). Sakaridis et al. (2014) studied the possibility of *Ligilactobacillus salivarius* being used as a protective culture to enhance the safety and prolong the shelf-life of chicken products. They found the antagonistic activity of LAB from poultry carcasses against the pathogenic bacteria (*Salmonella* spp. and *L. monocytogenes*). They reported a decrease in the *Salmonella* population on the fifth day. Wyszyńska and Godlewska (2021) studied strategies to prevent the development of *Campylobacter* in the microbiome of chickens using LAB, which appears to represent a major barrier against pathogen invasion in the gastrointestinal tract.

Lactic acid bacteria have many benefits for the food industry and find application in the preservation of food raw materials by participating in the optimization of the metabolic activity of the microbial environment and reducing the viability of the unwanted microbial population (Abiola et al., 2022). Masoumi et al. (2022) studied the microbial and physicochemical properties of raw chicken filets immersed in yogurt containing *L. casei* stored at 4°C for 9 days. They revealed that the amount of *S. aureus*, fecal coliforms, yeast, and mold (filamentous fungi) counts decreased in chicken filets preserved with the probiotic yogurt. Petkova et al. (2022) reported that LAB, a major component of fermented foods, is a major biological tool for a wide variety of food toxins, including bacterial toxins (Shiga toxin, listeriolysin, and botulinum toxin), mycotoxins (aflatoxin, ochratoxin, zearalenone, and fumonisin), pesticides (organochlorines, organophosphates, and synthetic pyrethroids), and heavy metals and natural anti-nutrients including phytates, oxalates, and cyanide-generating glycosides.

3.2 Preservation mechanism by using LAB antimicrobials

Although many microorganisms have a bioprotective effect, almost all are LAB. The most commonly used lactic acid bacteria are the bioprotective cultures *Aerococcus, Carnobacterium, Lactobacillus, Bifidobacterium, Lactococcus, Enterococcus, Leuconostoc, Oenococcus, Pediococcus, Melissococcus, Tetragenococcus, Vagococcus, Streptococcus,* and *Weissella*. LAB has effective bioprotective potential and inhibitory effects, and this is because it naturally dominates the microbiota of many foods during storage. In addition, it has competitive properties against pathogenic microorganisms when consuming food and can produce compounds, such as bacteriocin, organic acid, hydrogen peroxide, and enzymes. In addition, antimicrobial peptides produced by LAB are easily degraded by digestive proteases and therefore do not cause disturbances in the gut microbiota (Khorshidian et al., 2016).

The use of antimicrobial substances produced by LAB leads to a modification of the environment to win the competition against microorganisms. The antimicrobial activity of LAB is performed by the compounds produced by them, which could be grouped as organic acids (mainly, lactic acid, and acetic acid), diacetyl, hydrogen peroxide, reuterin, and bacteriocins, which also show antimicrobial activity in microorganisms that affect food safety and shorten their shelf-life. The mechanism of the action of lactic acid bacteria is presented in **Figure 1**.

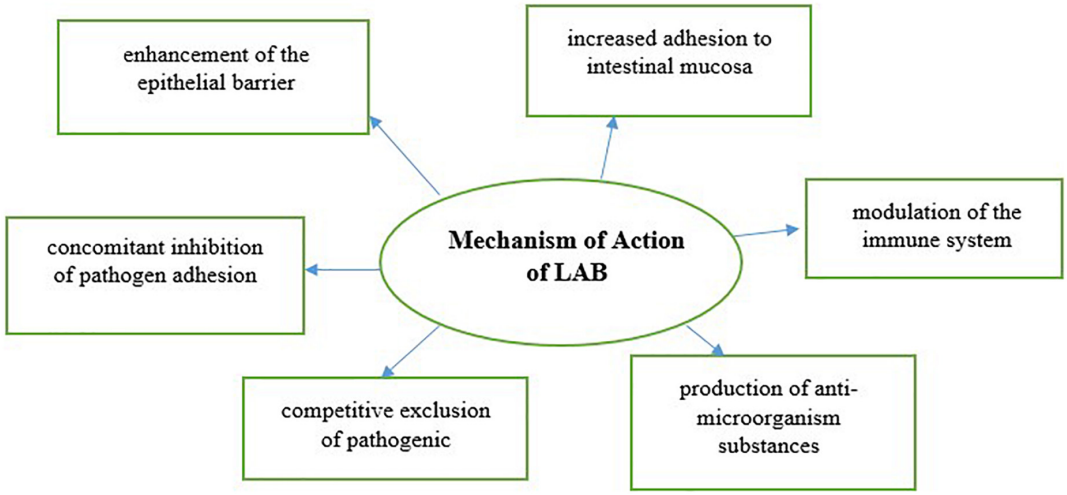

FIGURE 1
Mechanism of action of lactic acid bacteria.

For example, lactic acid lowers the medium's pH and increases the cell membrane's permeability. In this way, it enhances the action of other antimicrobial substances. In addition, due to its hydrophobic characteristic, the undissolved form of lactic and acetic acid enters the cell by passing through the cell membrane. Cell death occurs due to its solubilization in the cell and a decrease in cytoplasmic pH. LAB forms hydrogen peroxide (H_2O_2) with the enzyme flavoprotein oxidase in the presence of oxygen. Since there is no catalase enzyme in LAB, the H_2O_2 molecule gets accumulated in the environment and oxidizes the lipid membrane and cellular proteins of the target cell. Thus, it produces an antagonistic effect against bacteria, yeasts, molds, and viruses. The antimicrobial effect of the H_2O_2 molecule in non-lethal doses occurs as a result of its reaction with the thiocyanate compound in the presence of the lactoperoxidase enzyme found in milk.

Lactic acid bacteria produce antibacterial peptides or proteins, known as bacteriocins, composed of amino acids synthesized in the ribosomes of some LAB, that are released extracellularly to inhibit the growth of pathogenic microorganisms resistant to conventional antimicrobials. In addition, bacteriocins are versatile antimicrobial agents that can be used as biopreservative and can benefit the digestive system and health. Nisin and natamycin (pimaricin) are generally recognized as safe (GRAS) bacteriocins. Nisin is the most studied of the bacteriocins used in the food industry in terms of biochemistry and genetics. Nisin, an antimicrobial substance, is a polypeptide bacteriocin formed during the fermentation of modified milk that shows acidic properties. It shows greater temperature resistance between pH 3 and 7. Although it is effective against some Gram-positive bacteria and some spore-producing bacteria, it is not effective against molds, yeasts, and Gram-negative bacteria (Raman et al., 2022). Bacteriocins have different mechanisms of action. Some of them have the ability to increase the permeability of the cell membrane of the target microorganism by forming pores and can also inhibit the synthesis of the cell wall. Some manage to penetrate the cytoplasm of the bacterium and secrete DNA or RNA. Bacteriocins have a narrow range of inhibitory activity and can inhibit only strains closely related to the producing organism or inhibit a wide range of Gram-positive microorganisms. Bacteriocins used for biodefense can be incorporated into food in three ways: (i) inoculation of bacteria into the food, (ii) addition of purified or partially purified bacteriocins to the food, and (iii) the addition of a component fermented by bacteriocin-producing strains (Betancur-Hurtado et al., 2022).

3.3 Applications of LAB antimicrobials on chicken products

Lactic acid bacteria are considered natural microbiota of fermented meat products and exert their beneficial and preservative effect on meat and meat products owing to the production of bacteriocins. Bacteriocins are biologically active substances that are synthesized by ribosomal proteins and possess similar peptide structures (Silva et al., 2018). Among different classes of bacteriocins, class I belongs to the group involved in food preservation and is considered to tolerate high temperatures (Bolívar-Monsalve et al., 2019), while a purified class II bacteriocins, leucocin A, is recognized as a promising candidate with the potential to inhibit listerial activity and tolerate extreme conditions during the fermentation process in meat products (Barcenilla et al., 2022). For example, nisin produced from *Lactococcus lactis* is a class I bacteriocin that is used commercially by the food industry. On the other hand,

lantibiotics (consisting of B α-peptide and type A1 β-peptide) exhibit biopreservation activity as they form pores in the cell membrane of the bacteria. Though a few of the bacteriocins are recognized as inhibitors of both spoilage and pathogenic organisms, the majority of these exert an inhibitory effect on Gram-positive bacteria (Yildirim et al., 2016; Caulier et al., 2019). Since bacteriocins need to cross the cell wall for exerting their effect on Gram-negative bacteria, certain physical and chemical treatments are required for the synergistic approach. However, the presence of bacteriocin-specific receptors on cell membrane protein might make the bacteriocins execute their mode of action (Acuña et al., 2012). Other compounds that are generated during the fermentation process of meat and seafood products by LAB comprise aldehydes, ketones, organic acids, acetoin, and hydrogen peroxide, which possess immense antimicrobial and antifungal properties (Egan et al., 2016). Various pathogenic organisms, such as *L. monocytogenes*, *Salmonella* spp., and *E. coli*, in chicken and seafood, have been targeted by the application of LAB. The bio-preservative effect of LAB bacteria has been elucidated in chicken products by decreasing the growth of *L. monocytogenes* and *Salmonella* by 85 and 92%, respectively, during the refrigerated storage of 6 days (Sakaridis et al., 2012). Since the incorporation of LAB might alter the sensory properties of chicken products owing to the reduction in pH, studies demonstrate no decrease in the overall acceptability of chicken and seafood (Balay et al., 2017). In another study, *Leuconostoc pseudomesenteroides* decreased pathogen counts to 0.9 log CFU/g under MAP-packaged fresh chicken meat burger (Melero et al., 2012). Though research on the bio-preservative effect of LAB suggests that metabolites produced by LAB certainly possess antimicrobial characteristics and have the potential to improve the shelf-life of chicken products without alteration of sensory properties, considering the fact that meat matrix is a complex food system as a result of which reproducible results cannot be expected.

3.4 Synergistic effect of LAB antimicrobials with other compounds

Due to synergistic effects, some authors demonstrated that combined treatments of lactic acid bacteria and other compounds could have better antimicrobial activity than either treatment (Ruíz et al., 2012). According to the literature, the lactic acid bacteria could be combined and can demonstrate their synergistic potential with various compounds (Zhou et al., 2016). For example, Ruíz et al. (2012) reported the extensive inhibitory potential of a bacteriocin-like substance from *Lacticaseibacillus rhamnosus* L60 and *Limosilactobacillus fermentum* L23 on pathogenic bacteria. In contrast, Aminnezhad et al. (2015) revealed the synergistic ability of the cell-free substances of *L. rhamnosus* and *L. casei* against the growth of *Pseudomonas aeruginosa* PTCC 1430.

The antimicrobial activity of EOs is largely examined. Hashem et al. (2019) showed that the combination of lactic acid bacteria with EOs led to a synergistic activity against *S. aureus*. Almost all studied cell-free supernatant–medicinal oil combinations showed marked synergistic activity against *S. aureus, E. coli,* and *Klebsiella pneumoniae*. In another study, Kim et al. (2022) reported the synergistic antibacterial potential of lactic acid bacteria combined with *Curcuma longa* rhizome extract against *Cutibacterium acnes*.

Lactic acid bacteria could be used in synergism with other compounds in order to reduce pathogenic bacteria in plants, too. In the study of Lin et al. (2020), it was reported that the ability of *Lactiplantibacillus pentosus* and *Leuconostoc fallax* to suppress plant diseases is highly dependent on chitosan. *L. pentosus* and *L. fallax* together with chitosan expressed strong inhibitory effects against plant pathogens. LAB strains are in a desirable synergism with the mixture of glycerol, sucrose, and chitosan after being cultured in fish surimi due to their ability to inhibit the growth of *Alternaria brassicicola* and black rot caused by *Xanthomonas campestris* pv. *campestris*, known to cause vegetable diseases including cabbage black spot and black rot.

However, antibiotic-resistant microorganisms are a common health concern that reported the positive synergistic potential of bacteriocins from lactic acid bacteria isolated from traditionally fermented products of India with antibiotics, including cefotaxime, polymyxin B, imipenem, and tigecycline, against pathogens, such as *Streptococcus pyogenes, Enterococcus faecalis, Escherichia coli, Klebsiella pneumoniae,* and *Bacillus cereus*.

Lactic acid bacteria find applications in a combination with organic salts. According to Bolivar et al. (2018), the organic salts namely butyrate, propionate, succinate, citrate, formate, fumarate, glutamate, and acetate could be used in combination with probiotics in order to inhibit the growth of *Vibrio alginolyticus, A. hydrophila, E. coli, P. aeruginosa,* and *Streptococcus agalactiae*. The lactic acid strains show their antibacterial capacity combined with mineral elements. Gyawali and Ibrahim (2012) reported that copper in combination with lactic acid has been shown to eliminate the presence of foodborne pathogens, such as *Salmonella* and *E. coli* O157:H7.

4 The preservative effects of EOs on chicken and seafood product

Interest in spices and aromatic and other plants, which are natural sources of antioxidants, has increased in recent years (Aboukhalaf et al., 2020, 2022; Neves et al., 2021; Mechqoq et al., 2022; Melo et al., 2022; Munekata et al., 2022; Özogul et al., 2022). Natural plant extracts are used in the food industry as alternative preservatives. It is possible to prevent or delay some chemical spoilage that occurs during food storage with the use of

small amounts of EOs that are potential antioxidants due to their radical scavenging activities (Dupuis et al., 2022). Mariotti et al. (2022) confirmed the importance of evaluating natural products to consolidate the idea of safe EO applications in reducing and preventing intensive livestock infections.

Essential oils could be produced by different parts of plants. They consist of naturally occurring antimicrobial and antioxidant agents, which are extracted from different plant materials, such as leaves, bark, stems, roots, flowers, and fruits. Although more than 3,000 types of EOs are known, only some of them are of commercial interest for applications in the food industry.

4.1 Antimicrobial activity

Essential oils are important agents with anti-inflammatory, antibacterial, and antioxidant properties (Nehme et al., 2021) due to their potential to be an alternative to chemical preservatives and antibiotics, especially as a preservative against foodborne pathogens (Evren and Tekgüler, 2011). Bacteria, such as *L. monocytogenes, E. faecalis, Staphylococcus* spp., *Micrococcus* spp., *Bacillus* spp., *Campylobacter jejuni, Vibrio parahaemolyticus, Pseudomonas fluorescens, Shigella coli,* and *Escherichia* spp., and yeasts that cause food spoilage and poisoning can be destroyed with EOs. Gram-negative bacteria are said to be more resistant to the influence of EOs than Gram-positive bacteria, and this resistance of Gram-negative bacteria may arise from the cell wall. The antimicrobial properties of plant EOs are related to the main bioactive components in the composition of the plant sample, such as phenolic acids, terpenes, aldehydes, and flavonoids. The cell permeability and sensitivity could be affected by several mechanisms, such as changing the fatty acid profile, influencing the structure of cell membranes, and destroying membrane proteins. The aromatic and phenolic compounds manifest their antimicrobial ability due to the structural and functional transformation that are provoked in the bacterial cytoplasmic membrane (Yousefi et al., 2020).

Several studies have proved the influence of EOs on the quality and shelf-life of chicken and fish products. For example, Sharma et al. (2017) revealed that the fresh chicken sausages vacuumed and stored for 45 days in combination with clove, basil, cassia, and thyme oils showed a slower rate of increase in microbial count than the control sample. In another study, Sharma et al. (2020) revealed that chicken samples treated with EOs were characterized by a lower microbial count and, therefore, enhanced the shelf-life of chicken sausages. Alhijazeen (2021) reported the positive antimicrobial effect of the oregano essential oil and rosemary extract on the survival and growth of *S. aureus* and the total aerobic bacteria in cooked ground chicken meat stored at different temperatures. Wei et al. (2022) stated that cassia bark EO, cinnamon EO, tea tree EO, and angelica EO had the best antibacterial effect treated on marinated chicken. According to the results of Zubair et al. (2022), clove and cinnamon EOs extended the shelf-life of the studied products as they showed significant antimicrobial properties for total plate count and *Salmonella* during storage for 45 days of ready-to-eat chicken sausages.

The effect of EOs is investigated also in a combination with other current culinary treatments. For example, "sous vide" is considered a cooking method for vacuumed products placed in a water bath or steam oven at controllable low temperatures and is used for the treatment of various types of meat and vegetables. In ordinary boiling water, nutrient-rich food loses a great deal of them as they are passed into the fluid. Unlike the traditional cooking methods, foods could be prepared through the method of "sous vide," where they retain almost all their nutritive value. Kacaniova et al. (2021) studied the sous vide thermal treatment on the microbiological quality of fresh turkey breast meat after the products were processed with thyme and rosemary Eos. The study showed that the sous vide method with the combination of EOs is an effective method and it can be used to protect the microbiota of turkey meat and *L. monocytogenes* survival. According to Hien and Dao (2021), while EOs are used and added to food products, they are not very effective in their pure form. They attributed the reason for the lower effectiveness of the pure oils to the lipophilic nature of the oils and the difficulties caused by this when used in food products. Therefore, they utilized nanoemulsions obtained from black pepper essential oil characterized by good dispersion, long-term stability, and transparency. Their study showed that *E. coli* and *S. enterica* were more sensitive to black pepper essential oil nanoemulsion than free essential oil.

Essential oils find application in different forms of edible coatings used widely in the food industry in order to extend the shelf-life of food products. In a study, it was shown the antimicrobial ability of the milk-protein-based edible films containing oregano, pimento, or a mix of oregano–pimento EOs on muscle slices against *E. coli* O157:H7 or *Pseudomonas* spp. (Oussalah et al., 2007).

Essential oils are also used as growth promoters of livestock, due to the fact that they find application as feed additives to improve feed intake, and to improve animal health status (Mucha and Witkowska, 2021). Oblakova et al. (2021) observed that the addition of *Matricaria chamomilla, Rosmarinus officinalis, Lavandula angustifolia, Origanum vulgare, Thymus vulgaris,* and *Hypericum perforatum* EOs to the feed of turkey broilers had a positive influence on the microbial quality of breast and thigh meat.

However, fish meat is one of the food products that is highly perishable due to its composition (Hassoun and Çoban, 2017). In the study of Kunova et al. (2021), the EOs from *Citrus lemon* and *Cinnamomum camphora* were used to treat the rainbow trout meat for evaluating the microbiological quality (viable counts of bacteria and identification of present microbiota). Their results showed that lemon and *C. camphora* EOs had a definite effect on the microbiological quality of fish meat,

maintaining a high microbial quality of the fish filets during 7 days of cold storage. Al-Hajj et al. (2017) revealed that the *Pulicaria inuloides* EO inhibited all tested microorganisms, *viz. L. monocytogenes, E. coli,* and *S. aureus*. They also reported that *Pulicaria inuloides* and *Pulicaria crispa* EOs are able to eliminate *L. monocytogenes, E. coli,* and *S. aureus* inoculated in fish filets. According to Austin and Mcintosh (2006), the natural oregano essential oil had the ability to extend the shelf-life of rainbow trout containment showing good microbial load results. The results reported by Maghami et al. (2019) showed that coating fish filets with fennel EO significantly increased the microbiological safety of the product as they showed a lower number of mesophilic, psychotropic, pseudomonas, and lactic acid bacteria in coated fillets compared with control samples.

4.2 Antioxidant activity

A large proportion of plant EOs is classified by the US Food and Drug Administration (FDA) as GRAS (generally safe and harmless) additives that are applied to improve the organoleptic properties of foods or are used as food additives. Studies have been done that define their antibacterial, antiviral, antifungal, anti-inflammatory, antiseptic, antioxidant, anti-toxinogenic, and insecticidal properties. Studies have focused on the utility of these compounds in eliminating microorganisms that have become resistant to antibiotics. EOs are also potentially effective in food preservation.

Antioxidants are important substances in terms of nutrition as they reduce physiological stress in organs and cells. Disease resistance and immune competence in animals and humans are linked to the antioxidant mechanism. The compounds with the highest risk of oxidation are lipids. Oxidation of lipids occurs during the storage of raw materials, processing, heat treatment, and storage of finished products. Adding antioxidants, especially to oils and foods containing fat, is a method of extending shelf-life. Due to the suspicion that synthetic antioxidants may be carcinogenic, the use of antioxidants such as BHA (Beta Hydroxy acids) and BHT (Butylated hydroxytoluene) in foods has been restricted. In addition, due to the undesirable effects of oxidized lipids on the human body, the formation of these products in foods should be prevented as much as possible. Synthetic antioxidants are often used in food processing to extend the shelf-life of foods.

For this reason, research into using EOs as alternative antioxidants has accelerated in recent years. The antioxidant properties of EOs are due to the phenolic hydroxyl groups in the components' structure. The antioxidant effect of these oils varies depending on the number of active ingredients, the type of solvent used in the extraction, and the extraction method.

In their study, Sharma et al. (2020) observed significantly better oxidative stability due to the higher values for DPPH (2,2-diphenyl-1-picrylhydrazyl) activity and total phenolic content for chicken products treated with four different blends of EOs. In their study, Albarracín et al. (2012) showed that the use of the thyme and rosemary EOs reduced the oxidative processes of tilapia filets from the ninth day of storage. According to Sharma et al. (2017), the treatment of chicken sausages with plat EOs showed the least rate of increase in oxidation.

The availability of phenolic compounds from EOs was evaluated by the determination of total phenolic compounds present in the films during storage (Oussalah et al., 2007). They evaluated the antioxidant properties of edible films treated with EOs during storage and demonstrated that oregano-based films had the ability to stabilize lipid oxidation in beef muscle samples, whereas pimento-based films presented the highest antioxidant activity. The results reported by Zubair et al. (2022) also showed the positive effect of essential oil, clove oil, on the polyphenol content and DPPH at a storage period of 45 days.

5 Combined impact of LAB and EOs on chicken and seafood

The group of lactic acid bacteria has been used widely in the meat industry to achieve the desired techno-functional properties and storage stability of chicken and seafood products. In addition to technological properties, these also impart characteristic sensory attributes to the meat products, as a result of which the consumer acceptability of the meat products is enhanced. The main function of LAB is to lower the pH of the meat product; however, various factors influence the final pH of the product, thus determining the safety and storage stability of the finished product. Being probiotic in nature, LAB also confers potential health virtues to meat products in addition to improving the techno-functional properties of meat products (**Table 1**). However, along with LAB, other microorganisms may also survive and grow under a conducible environment produced during the fermentation of meat products, which in turn, may pose a risk to human health. Therefore, a complete, safe, and wholesome meat for humans may include antimicrobials, which could selectively inhibit the growth of pathogenic or undesirable microorganisms.

5.1 The preservative effect of LAB and EOs on chicken products

Chicken products have a shorter shelf-life as compared to red meat owing to their high polyunsaturated fatty acid content (Sharma et al., 2018). Therefore, it is suggested that the fermentation process can be used to enhance the shelf-life of chicken meat products with desired techno-functional and sensory properties. The majority of the fermentation processes are caused by the group of LAB, and it is considered that these have a higher chance of bacterial survival in the meat matrix

TABLE 1 Application of LAB-produced bacteriocins and organic acids in chicken and seafood.

S. no.	Lab species	Metabolite	Preservative action	Food	References
1	*Lactococcus lactis*	Nisin	Bacteriocin	Trout	Wang et al., 2020
2	*Lactobacillus delbrueckii* subsp. *bulgaricus*	Lactic acid	Organic acid	Salmon	Ayivi et al., 2020; Jadhav and Annapure, 2021
3	*Lactococcus lactis* subsp. *cremoris*	Formic acid	Organic acid	Poultry	Gómez-García et al., 2019; Ricke et al., 2020
4	*Lactococcus lactis* subsp. *lactis*	Succinic acid	Organic acid	Chicken meat	Radkowski et al., 2018
5	*Limosilactobacillus reuteri*	Malic acid	Organic acid	Meat products	Ghoul and Mitri, 2016
6	*Lactococcus lactis* subsp. *lactis*	Propionic acid	Organic acid	Poultry products	Gonzalez-Fandos et al., 2020
7	*Lactobacillus acidophilus*	Acetic acid	Organic acid	Salmon	Gómez-García et al., 2019
8	*Lactobacillus acidophilus*	Butyric acid	Organic acid	Poultry	Reuben et al., 2021
9	*Limosilactobacillus reuteri*	Hydrogen peroxide	Antimicrobial	Chicken meat	Asare et al., 2020
10	*Streptococcus diacetyl lactis*	Diacetyl	Antimicrobial	Chicken meat	Yu et al., 2021

than all other microorganisms. In this regard, the beneficial effect of EOs has been observed along with LAB in chicken meat products, wherein no inhibition effect was observed in the growth of LAB (Leite de Souza, 2021). The Italian-type sausage was incorporated with basil essential oil (0.75 mg g^{-1}), and no change in the growth and survival of LAB was observed during 60 days of cold storage (Gaio et al., 2015). Similarly, no changes in viable counts were recorded in Tunisian dry fermented chicken sausage incorporated with a blend of oregano and thyme essential oil (0.25%) (El Adab and Hassouna, 2016), indicating that the combination of EOs and LAB has proven to be synergistic for extending the shelf-life of chicken products and inhibiting the growth of undesirable and spoilage bacteria. In another study conducted by Chaves-López et al. (2012), it was interesting to note that the incorporation of oregano essential oil (0.01%) in Spanish-fermented sausage enhanced the viable count of LAB over time. The increase in LAB count was attributed mainly to the diffusion of essential oil across the casing into the sausage matrix which could additionally exert stimulatory growth on LAB. EOs are known to exert a stimulatory effect due to the utilization of carbon and other energy sources (Badia et al., 2020). Furthermore, osmotic stressed conditions and potassium efflux contributed by EOs are well tolerated by LAB along with the generation of adenosine triphosphate, thus ensuring their survival even in the presence of EOs (Holley and Patel, 2005; El Adab and Hassouna, 2016). Therefore, these studies establish that LAB adapt well to the environment brought by the incorporation of EOs in the meat matrix, thus enabling this group of bacteria to outgrow other microorganisms.

Though several studies suggest that EOs have a stimulatory effect on the growth of LAB which, in turn, results in higher storage stability and shelf-life of chicken meat products, there are a few studies reporting that EOs alone could also improve and maintain the quality of chicken meat for a longer period of time. These findings have been observed in fermented chicken products, wherein no effect was observed on LAB viable count, while other pathogenic microorganisms including *S. aureus* and *L. monocytogenes* have been inhibited (Lu et al., 2015). In fact, fewer studies have reported the inhibitory effect of EOs on the growth of LAB bacteria in bologna sausage, dry sausage, and some ready-to-cook chicken products (Badia et al., 2020; Tomović et al., 2020).

5.2 The preservative effect of LAB and EOs on seafood products

Similar to chicken meat and meat products, seafood is also prone to microbial spoilage owing to its perishable nature due to higher moisture content. Generally, end products of enzymatic and microbial reactions in seafood often lead to the development of potential health-hazardous metabolic products which, in turn, deteriorate the physicochemical, sensory, and nutritional properties (Olatunde and Benjakul, 2018; Hussain et al., 2021). Therefore, suitable preservation techniques in terms of natural preservatives are required for keeping up the quality and storage stability, subsequently improving the shelf-life of seafood. In this regard, microorganisms, mainly LAB, and EOs have been used widely to preserve the natural aroma and quality of seafood such as bream filets *Megalobrama amblycephala* (Nisar et al., 2019), cobia steak *Rachycentron canadum* (Remya et al., 2017), shrimp *Parapenaeus longirostris* (Alparslan et al., 2016), and fish carp burger *Cyprinus carpio* (Ehsani et al., 2020). Though

extensive literature is available regarding the beneficial effect of EOs on the microbial safety of seafood, the majority of the studies reported that the incorporation of EOs in fresh seafood including common carp filet (Zhang et al., 2017), red drum filet (Cai et al., 2015), and crayfish (Duman et al., 2015) inhibited the growth and decreased the viable count of LAB along with other microorganisms. However, sensory scores and shelf-life were enhanced by an average of 5–7 days for seafood. There are very few studies available on the effect of EOs on fermented seafood. Improvement in the production of fish-fermented flour was observed by the addition of *Pimenta racemosa* essential oil (0.5–2 $\mu L\ g^{-1}$) in which the inhibitory effect was observed on the growth of pathogenic microorganisms; however, this study lacks the effect on the viable count of LAB bacteria (Adjou et al., 2021). In another study conducted by Boulares et al. (2018), sea bass filets were observed with lower total volatile base nitrogen content (1.12 vs. 30.47 mg $100\ g^{-1}$) in the sample treated with lactic acid bacteria and citrus essential oil as compared with the control. In addition, biogenic amines including agmatine, putrescine, and cadaverine, were also decreased upon the combined application of LAB and essential oil, indicating the synergistic effect of these on the preservation of seafood.

6 Therapeutic benefits of LAB and EOs on chicken and seafood products

High moisture content, nutritive value, and neutral pH are considered to be significant factors playing a role in the quality and shelf-life of chicken meat and seafood products. Therefore, several preservative methods and techniques have been developed to maintain and improve their storage stability. However, owing to the carcinogenic and other harmful health effects associated with chemicals, suitable bio-preservative technologies have been investigated. Among these, the use of LAB and EOs have been proven successful owing to their contributions to the enhancement of the shelf-life and nutritive value of meat products without altering the sensory properties of the food (Kumar et al., 2018).

Lactic acid bacteria are the most important microbiota of fermented chicken and seafood products. Furthermore, natural microbiota, such as LAB, have also been used as a natural bio-preservative, an alternative to chemical preservatives. The incorporation of LAB in chicken meat products ensures that the meat products are safe, healthy, and wholesome for consumption without posing any health risks to the consumers. This group of bacteria outgrows the pathogenic organisms owing to their ability to adapt to harsh acidic environments, thereby resulting in the elimination of closely related microbial strains. LAB mainly exert their preservative actions by generating and producing bacteriocins and organic acids. The antimicrobial activity of LAB has been demonstrated in salmon, wherein antimicrobial compounds have been synthesized by LAB, resulting in the modulation of microbiota (Ibrahim et al., 2021). Furthermore, the inhibition of fungal growth and fungicidal activity of LAB against *Aspergillus fumigatus*, *Penicillium expansum*, *Fusarium culmorum*, *Aspergillus niger* has been well investigated in fishery products (Cizeikiene et al., 2013). Therefore, the application of LAB in chicken meat and seafood products allows the elimination of foodborne pathogens and contaminants by producing certain antimicrobial compounds, thus enhancing the shelf-life and storage stability of such products.

Essential oils have been used for the treatment of various diseases and are well-recognized for their potential medicinal value and health benefits since the time memorial. Furthermore, with the increase in the incidence of chronic diseases and metabolic disorders, several investigations have been carried out for the identification of bioactive compounds present in EOs, which are responsible for their biological activity. With progression in time, advances in the extraction techniques of EOs (hydro-distillation, aqueous extraction, solvent extraction, cold and hot pressing, and supercritical fluid extraction process) were investigated for improvement in efficiency and yield. Therefore, the composition and bioavailability of EOs may differ according to the extraction procedure and the method of application in meat products and seafood (Sharma et al., 2019). The bioavailability of EOs depends on many factors including physiological conditions, environmental factors, individual dietary regimens, and others. The majority of the EOs are absorbed from the meat matrix and cross the blood–brain barrier efficiently owing to the hydrophobic nature and smaller size of volatile compounds. Beneficial health effects of EOs and their active compounds are possible through ingestion, inhalation, and absorption through the skin. It has been recognized that EOs containing hydrocarbons (limonene, azulene, cadinene, and myrcene) are associated with antiviral, antibacterial, and hepatoprotective activities, while oxides and esters are related to anti-inflammatory properties (**Table 2**).

Phenols and aldehydes present in EOs contribute to antiviral, antipyretic, antimicrobial, vasodilator, and spasmolytic activity. Several EOs, for instance, cinnamon oil, thyme oil, oregano oil, clove oil, and holy basil oil have been used in chicken and seafood products. Polyphenol compounds present in the extract of cinnamon essential oil drastically declined the secretion of TNF-α when given to mice orally for 6 days (Hong et al., 2012), thus indicating the anti-inflammatory property of cinnamon oil. Moreover, cinnamon oil has shown anti-diabetic, anti-cancer, and anti-hypertriglyceridemia potential owing to its biologically active component, cinnamaldehyde. Polyphenols present in EOs are also known to regulate the metabolism of glucose and repair pancreatic β-cells, thus enhancing the islets' function (Li et al., 2013). Oregano essentials are considered to exert higher antibacterial activity than cinnamon essential oil; however, the major advantage of using the latter in meat and

TABLE 2 Therapeutic benefits of using essential oils in chicken and seafood.

S. no.	Essential oil	Active component	Properties	Food product	References
1	Chamomile essential oil (*Matricaria recutita*)	Bisabolol, chamazulene	Anti-inflammatory, anti-allergic, decongestant, and antispasmodic	Chicken	Anastasiou et al., 2019
2	Anise essential oil (*Pimpinella anisum*)	Anethole	Antispasmodic, carminative, and diuretic	Chicken filets	Fathi-Achachlouei et al., 2021
3	Nutmeg essential oil (*Myristica Fragrans* Houtt.)	Sabinene, 4-terpineol, myristicin	Anti-microbial, antiparasitic, and analgesic	Ready-to-cook barbecued chicken	Shekarforoush et al., 2014
4	Cedar essential oil (*Juniperus virginiana*)	Limonene	Larvicidal, antifungal, astringent, and decongestant	Chicken breast filet	Kamkar et al., 2021
5	Dill essential oil (*Anethum graveolens L.*)	Carvone	Antispasmodic	Chicken	Vispute et al., 2019
6	Garlic essential oil (*Allium Sativum*)	Diallyl disulfide	Hypoglycemic, antiviral, antifungal, antispasmodic, and antioxidant	Chicken nuggets	Raeisi et al., 2021
7	Clove essential oil (*Syzygium aromaticum* L)	Eugenol	Antiviral, antimicrobial, and carminative	Ready-to-eat chicken sausages	Zubair et al., 2022
8	Cinnamon essential oil (*Cinnamomum zeylanicum*)	Cinnamaldehyde	Antibacterial, antiviral, antifungal, and parasiticide	common carp (*Cyprinus carpio*)	Zhang et al., 2017
9	Sweet orange essential oil (*Citrus sinensis*)	Limonene	Antiseptic, carminative, and tonic	Shrimps	Alparslan et al., 2016
10	Eucalyptus essential oil (*Eucalyptus globulus*)	1,8- cineole	Antimicrobial and antiviral	Fresh chicken meat	Sharafati Chaleshtori et al., 2016
11	Peppermint essential oil (*Menthae piperitae aetheroleum*)	Methanol and menthone	Decongestant, expectorant, antimicrobial, and anesthetic	Fish skin gelatin film	Yanwong and Threepopnatkul, 2015
12	Lavender essential oil (*Lavandula angustifolia*)	Linalool and linalyl acetate	Spasmodic, anti-inflammatory, and antimicrobial	Fish gelatin based composite films	Sun et al., 2021
13	Tea tree essential oil (*Melaleuca alternifolia*)	Terpinene-1-ol-4	Antimicrobial, antiviral, and antispasmodic	Marinated chicken	Wei et al., 2022
14	Lemon essential oil (*Citrus limon*)	Limonene	Digestive tonic carminative, purgative, and metabolism regulator	Rainbow trout meat	Kunova et al., 2021

seafood products include the prevention of the development of antimicrobial resistance and their higher efficacy for a longer duration (Almasaudi et al., 2022). The other physical and physiological health benefits of EOs are pain alleviation and memory and mood improvement by rosemary essential oil. Peppermint oil is demonstrated to relive nausea, clear skin conditions, and improve the digestive system, while lavender oil reduces the soreness of muscles and relieves pain. Fast wound healing, mood enhancer, and stress reduction have been documented in one of the earliest known EOs, Frankincense oil (Pirnia et al., 2022).

Apart from antimicrobial activity, the antioxidant activity of chicken meat products was also enhanced, thereby adding to the nutritional value of chicken products (Sharma et al., 2020). The major problem of the chicken meat industry related to oxidative rancidity and subsequent spoilage and deterioration of chicken products has been addressed by the incorporation of blends of EOs (thyme, clove, holy basil, and oregano) in emulsion-based chicken sausage, wherein the antioxidant activity of blend incorporated products was significantly higher ($p < 0.05$) than the control products along with higher total phenolic content (Sharma et al., 2017, 2018). The inclusion of dietary antioxidants reduced the occurrence of certain diseases as these are inversely related to cardiovascular diseases. These mobilize the oxidized low-density lipoproteins in macrophages as of result of which, coronary heart disease incidence is drastically reduced. Furthermore, the antioxidants consumed through meat and meat products also help in declining the pathological changes occurring in the body owing to oxidative stress caused by free radical formation (Wilson et al., 2017). Recent

researchers have also demonstrated that the incorporation of EOs in edible packaging film also serves as an antioxidant and antimicrobial preservative for chicken and seafood. In one of the studies, the shelf-life of chicken patties wrapped in an edible film containing a blend of oregano and thyme EOs was enhanced by up to 30 days with no signs of incipient spoilage (Kumar et al., 2018). Though it is argued from time to time that the use of EOs in meat products is an expensive process, and taking into consideration the extraction procedure of essential oil from parts of the plant, the health benefits accrued by the application of EOs in meat products outweigh the disadvantage of cost (Kumar et al., 2017).

7 Facts and gaps for the application of LAB and EOs in the meat industry

Essential oils are considered to be comprised of 60–80 components in different proportions, and the components present in higher proportions are responsible for their biological activity and preservative effect on meat products. Studies suggest that EOs containing more aldehydes and phenols exert the most potent effect followed by terpene and ketones containing oils. Therefore, the composition of EOs varies, which mainly contributes to their variation in their mode of action. Furthermore, all the EOs are recognized as hydrophobic in nature, thereby indicating their ability to penetrate cells easily, which, in turn, leads to permeabilization and subsequent death of the cell owing to the depolarization of membranes (Perricone et al., 2015). However, owing to the variety of compounds present in a meat matrix, the major drawback is their interaction with the food matrix. Though the presence of high fat and proteins in meat will interfere with the antibacterial action of EOs in an aqueous phase owing to the protective effect brought by the meat components and their ability to absorb oils, high water and salt concentration in chicken meat products might facilitate the action of EOs. In addition, meat products containing high amount of complex sugar often decreases the efficacy of EOs, which indicates that novel meat products incorporated with EOs should contain a higher amount of simple sugars such as glucose.

The physical state and structure of the food may also affect the efficacy of EOs significantly. For instance, the activity of EOs would always be higher in the product containing more water and liquid as compared to the solid or intact meat piece. This might be due to the diffusion and uniform distribution of EOs in the product. In addition to this, the use of EOs in the packaging films of meat products has also been proven efficacious for their mode of action (Zubair et al., 2021). The major limitation of the application of essential oils in meat products is the perception of a strong aroma, even after cooking, which might decrease their palatability. In this regard, it was proposed to prepare nanoemulsions so that alterations in the organoleptic qualities can be minimized (Xia et al., 2022).

Lactic acid bacteria has played a critical role in the preservation and improvement of the shelf-life of meat and meat products by the production of bacteriocins and organic acids. Several investigations regarding the application of LAB in meat products have been carried out at the lab level; however, reproducing these results at the industrial scale may pose some problems.

8 Future perspective

Essential oils contain a variety of compounds that are of biological importance. However, the exact component interacting with meat products still remains uninvestigated in the majority of the products. These studies would further provide insights into the synergistic and antagonistic effect of EOs with particular meat products. Moreover, excessive use of EOs in meat and meat products would not only alter the sensory properties but might cause certain health issues, such as irritation of mucous membranes, respiratory problems, and others. Therefore, the levels and safe doses of essential oils should be optimized and validated using *in vitro* and *in vivo* techniques (Macwan et al., 2016). Finally, more suitable approaches should be devised in order to mask the effect of EOs in meat and seafood products so that the consumer acceptability of these products is not affected. Novel and cost-effective methods and techniques for the targeted delivery or controlled release of EOs should be investigated to protect them from degradation in the gut system and decrease the chance of declined sensory acceptability of the product (Mucha and Witkowska, 2021).

9 Conclusion

Chicken meat and seafood are prone to microbial spoilage owing to their neutral pH and higher moisture and fat content. Being highly nutritious, these both require certain preservation methods for their extended shelf-life and maintenance of textural attributes. For long, chemical preservatives have been used; however, these are also associated with toxicological and cancerous problems in consumers; thus natural preservatives, such as LAB and EOs, were explored for their critical role in meat and seafood preservation. Though several investigations and demonstrations have been conducted regarding the application of EOs and LAB in the preservation of chicken meat and seafood products, there are a few limitations that need to be addressed for the utilization of their full potential as a bio-preservative in the area of meat science. Bacteriocins produced by LAB offer major limitations owing to their dependency on the time and temperature of meat products storage, pH of the meat

product, and their interaction with the associated microbiota of the food. Another major limitation is the lack of regulations on the use of novel bacteriocins as food additives in meat and meat products.

Author contributions

HS, HF, and FÖ: conceptualization. HS and HF: methodology, validation, formal analysis, investigation, and writing – original draft preparation. JR: resources. FÖ and JR: data curation, writing – review and editing, and supervision. HS, HF, FÖ, and JR: visualization. All authors have read and agreed to the published version of the manuscript.

Funding

This work was based upon the work from COST Action 18101 SOURDOMICS – Sourdough biotechnology network towards novel, healthier and sustainable food and bioprocesses (https://sourdomics.com/ and https://www.cost.eu/actions/CA18101/, accessed July 11, 2022), where the author FÖ is the leader of the working group "Food safety, health promoting, sensorial perception and consumers' behavior," and the author JR is the Chair and Grant Holder Scientific Representative, and is supported by COST (European Cooperation in Science and Technology) (https://www.cost.eu/, accessed July 11, 2022). COST is a funding agency for research and innovation networks. Regarding to the author JR, this work was also financially supported by LA/P/0045/2020 (ALiCE) and UIDB/00511/2020 – UIDP/00511/2020 (LEPABE) funded by national funds through FCT/MCTES (PIDDAC).

Conflict of interest

The authors declare that the research was conducted in the absence of any commercial or financial relationships that could be construed as a potential conflict of interest.

Publisher's note

References

Abiola, R. R., Okoro, E. K., and Sokunbi, O. (2022). Lactic acid bacteria and the food industry – A comprehensive review. *Int. J. Health Sci. Res.* 12.

Aboukhalaf, A., El Amraoui, B., Tabatou, M., Rocha, J. M., and Belahsen, R. (2020). Screening of the antimicrobial activity of some extracts of edible wild plants in Morocco. *J. Funct. Food Health Dis.* 6, 265–273. doi: 10.31989/ffhd.v10i6.718

Aboukhalaf, A., Tbatou, M., Kalili, A., Naciri, K., Moujabbir, S., Sahel, K., et al. (2022). Traditional knowledge and use of wild edible plants in Sidi Bennour region (Central Morocco). *Ethnobotany Res. Appl.* 23, 1–18.

Acuña, L., Picariello, G., Sesma, F., Morero, R. D., and Bellomio, A. (2012). A new hybrid bacteriocin, Ent35–MccV, displays antimicrobial activity against pathogenic Gram-positive and Gram-negative bacteria. *FEBS Open Bio.* 2:12. doi: 10.1016/J.FOB.2012.01.002

Adjou, E. S., Makosso, T. U., Allavo, A., Akotowanou, O., Kogbeto, J. A., Vodounou, A., et al. (2021). Effect of essential oil of pimenta racemosa on microflora affecting quality of african mustard obtained from fermented seeds of parkia biglobosa jack. P. BR. *Food Environ. Saf. J.* 20, 165–171. doi: 10.4316/fens.2021.018

Ağagündüz, D., Yılmaz, B., Koçak, T., Başar, H. B., Rocha, J. M., and Özoğul, F. (2022). Novel candidate microorganisms for fermentation technology: From potential benefits to safety issues. *Foods* 11:3074. doi: 10.3390/foods11193074

Ağagündüz, D., Yılmaz, B., Şahin, T. O., Güneşliol, B. E., Ayten, S., Russo, P., et al. (2021). Dairy lactic acid bacteria and their potential function in dietetics: The food–gut-health axis. *Foods* 10:3099. doi: 10.3390/foods10123099

Albarracín, W., Alfonso, C., and Sancez, I. (2012). Application of essential oils as a preservative to improve the shelf life of *Nile tilapia* (*Oreochoromisniloticus*). *Vitae* 19, 34–40.

Al-Hajj, N. Q. M., Algabr, M. N., Raza, H., Thabi, R., Ammar, A. F., Aboshora, W., et al. (2017). Antibacterial activities of the essential oils of some aromatic medicinal plants to control pathogenic bacteria and extend the shelf-life of seafood. *Turkish J. Fish. Aquat. Sci.* 17, 181–191. doi: 10.4194/1303-2712-v17_1_20

Alhijazeen, M. (2021). The combination effect of adding rosemary extract and oregano essential oil on ground chicken meat quality. *Food Sci. Tech.* 42. doi: 10.1590/fst.57120

Alipin, K., and Safitri, R. (2016). The potential of indigenous Lactic Acid Bacteria against *Salmonella* sp. *AIP Conf. Proc.* 1744:020031.

Almasaudi, N. M., Al-Qurashi, A. D., Elsayed, M. I., and Abo-Elyousr, K. A. M. (2022). EOs of oregano and cinnamon as an alternative method for control of gray mold disease of table grapes caused by Botrytis cinerea. *J. Plant Pathol.* 104, 317–328. doi: 10.1007/S42161-021-01008-8

Alparslan, Y., Yapici, H. H., Metin, C., Baygar, T., Günlü, A., and Baygar, T. (2016). Quality assessment of shrimps preserved with orange leaf essential oil incorporated gelatin. *LWT - Food Sci. Technol.* 72, 457–466. doi: 10.1016/J.LWT.2016.04.066

Aminnezhad, S., Kermanshahi, R. K., and Ranjbar, R. (2015). Evaluation of synergistic interactions between cell-free supernatant of Lactobacillus strains and amikacin and genetamicin against Pseudomonas aeruginosa. *Jundishapur. J. Microbiol.* 8:16592. doi: 10.5812/jjm.8(4)2015.16592

Anastasiou, T. I., Mandalakis, M., Krigas, N., Vézignol, T., Lazari, D., Katharios, P., et al. (2019). Comparative evaluation of essential oils from medicinal-aromatic plants of Greece: Chemical composition, antioxidant capacity and antimicrobial activity against bacterial fish pathogens. *Molecules* 25:148. doi: 10.3390/molecules25010148

Asare, P. T., Zurfluh, K., Greppi, A., Lynch, D., Schwab, C., Stephan, R., et al. (2020). Reuterin demonstrates potent antimicrobial activity against a broad panel of human and poultry meat Campylobacter spp. isolates. *Microorganism* 8:78. doi: 10.3390/MICROORGANISMS8010078

Austin, B., and Mcintosh, D. (2006). Natural antibacterial compounds on the surface of rainbow trout, *Salmo gairdneri* Richardson. *J. Fish Dis.* 11, 275–277. doi: 10.1111/j.1365-2761.1988.tb00550.x

Ayivi, R. D., Gyawali, R., Krastanov, A., Aljaloud, S. O., Worku, M., Tahergorabi, R., et al. (2020). Lactic acid bacteria: Food safety and human health applications. *Dairy* 1, 202–232. doi: 10.3390/DAIRY1030015

Badia, V., de Oliveira, M. S. R., Polmann, G., Milkievicz, T., Galvão, A. C., da Silva, et al. (2020). Effect of the addition of antimicrobial oregano (*Origanum vulgare*) and rosemary (*Rosmarinus officinalis*) EOs on lactic acid bacteria growth in refrigerated vacuum-packed *Tuscan sausage*. *Braz. J. Microbiol.* 51, 289–301. doi: 10.1007/S42770-019-00146-7

Balay, D. R., Dangeti, R. V., Kaur, K., and McMullen, L. M. (2017). Purification of leucocin a for use on wieners to inhibit Listeria monocytogenes in the presence of spoilage organisms. *Int. J. Food Microbiol.* 255, 25–31. doi: 10.1016/J.IJFOODMICRO.2017.05.016

Barcenilla, C., Ducic, M., López, M., Prieto, M., and Álvarez-Ordóñez, A. (2022). Application of lactic acid bacteria for the biopreservation of meat products: A systematic review. *Meat Sci.* 183:108661. doi: 10.1016/j.meatsci.2021.108661

Bartkiene, E., Lele, V., Ruzauskas, M., Mayrhofer, S., Domig, K., Starkute, V., et al. (2020). Lactic acid bacteria isolation from spontaneous sourdough and their characterization including antimicrobial and antifungal properties evaluation. *Microorganisms* 8:64. doi: 10.3390/microorganisms8010064

Bartkiene, E., Özogul, F., and Rocha, J. M. (2022). Bread sourdough lactic acid bacteria – technological, antimicrobial, toxin-degrading, immune system- and faecal microbiota-modelling biological agents for the preparation of food, nutraceuticals and feed. *Foods* 11, 452. doi: 10.3390/foods11030452

Bernstein, A. M., Sun, Q., Hu, F. B., Stampfer, M. J., Manson, J. E., and Willett, W. C. (2010). Major dietary protein sources and risk of coronary heart disease in women. *Circulation* 122, 876–883. doi: 10.1161/CIRCULATIONAHA.109.915165

Betancur-Hurtado, C. A., Barreto Lopez, L. M., Rondon Castillo, A. J., Trujillo-Peralta, M. C., Hernandez-Velasco, X., Tellez-Isaias, G., et al. (2022). An *In vivo* pilot study on probiotic potential of lactic acid bacteria isolated from the gastrointestinal tract of creole hens (*Gallus gallus* domesticus) native to Montería, Córdoba, Colombia in broiler chickens. *Poultry* 1, 157–168. doi: 10.3390/poultry1030014

Bolívar-Monsalve, J., Ramírez-Toro, C., Bolívar, G., and Ceballos-González, C. (2019). Mechanisms of action of novel ingredients used in edible films to preserve microbial quality and oxidative stability in sausages - a review. *Trends Food Sci. Technol.* 89, 100–109. doi: 10.1016/J.TIFS.2019.05.011

Bolivar, N. C., Legarda, E. C., Seiffert, W. Q., Andreatta, E. R., and do Nascimento Vieira, F. (2018). Combining a probiotic with organic salts presents synergistic *in vitro* inhibition against aquaculture bacterial pathogens. *Braz. Arch. Biol. Technol* 61:e18160694. doi: 10.1590/1678-4324-2018160694

Boulares, M., Ben Moussa, O., Mankai, M., Sadok, S., and Hassouna, M. (2018). Effects of lactic acid bacteria and citrus essential oil on the quality of vacuum-packed sea bass (*Dicentrarchus labrax*) fillets during refrigerated storage. *J. Aquat. Food Prod. Technol.* 27, 698–711. doi: 10.1080/10498850.2018.1484544

Cai, L., Cao, A., Li, Y., Song, Z., Leng, L., and Li, J. (2015). The effects of essential oil treatment on the biogenic amines inhibition and quality preservation of red drum (*Sciaenops ocellatus*) fillets. *Food Control* 56, 1–8. doi: 10.1016/J.FOODCONT.2015.03.009

Caulier, S., Nannan, C., Gillis, A., Licciardi, F., Bragard, C., and Mahillon, J. (2019). Overview of the antimicrobial compounds produced by members of the *Bacillus subtilis* group. *Front. Microbiol.* 10:302. doi: 10.3389/FMICB.2019.00302

Cena, H., and Calder, P. C. (2020). Defining a healthy diet: Evidence for the role of contemporary dietary patterns in health and disease. *Nutrients* 12:334. doi: 10.3390/nu12020334

Chaves-López, C., Martin-Sánchez, M., Fuentes-Zaragoza, E., Viuda-Martos, M., Fernández-López, J., Sendra, E., et al. (2012). Role of Oregano (*Origanum vulgare*) essential oil as a surface fungus inhibitor on fermented sausages: Evaluation of its effect on microbial and physicochemical characteristics. *J. Food Prot.* 75, 104–111. doi: 10.4315/0362-028X.JFP-11-184

Cizeikiene, D., Juodeikiene, G., Paskevicius, A., and Bartkiene, E. (2013). Antimicrobial activity of lactic acid bacteria against pathogenic and spoilage microorganism isolated from food and their control in wheat bread. *Food Control.* 31, 539–545. doi: 10.1016/J.FOODCONT.2012.12.004

Djenane, D., Martinez, L., Sanchez-Escalante, A., Montañés, L., Parmo, D., Yangüela, J., et al. (2006). Effect of lactic acid bacteria on beef steak microbial flora stored under modified atmosphere and on listeria monocytogenes in broth cultures. *Food Sci. Technol. Int.* 12, 287–295. doi: 10.1177/1082013206067788

Dissasa, G., Lemma, B., and Mamo, H. (2022). Antimicrobial activity of lactic acid bacteria (Lab) isolated from yoghurt and fish against pathogenic bacteria isolated from fish in ethiopia. *J. Microbiol. Biotechnol.* 7:00234.

Duman, M., Çoban, Ö, and Özpolat, E. (2015). Effects of rosemary and thyme oils on shelf lÝfe of marinated sauce crayfish. *J. Anim. Plant Sci.* 25, 1771–1778.

Dupuis, V., Cerbu, C., Witkowski, L., Potarniche, A.-V., Timar, M. C., Żychska, M., et al. (2022). Nanodelivery of essential oils as efficient tools against antimicrobial resistance: A review of the type and physicalchemical properties of the delivery systems and applications. *Drug Delivery* 29, 1007–1024. doi: 10.1080/10717544.2022.2056663

Egan, K., Field, D., Rea, M. C., Ross, R. P., Hill, C., and Cotter, P. D. (2016). Bacteriocins: Novel solutions to age old spore-related problems? *Front. Microbiol.* 7:461. doi: 10.3389/FMICB.2016.00461

Ehsani, A., Hashemi, M., Afshari, A., Aminzare, M., Raeisi, M., and Zeinali, T. (2020). Effect of different types of active biodegradable films containing lactoperoxidase system or sage essential oil on the shelf life of fish burger during refrigerated storage. *LWT* 117:108633. doi: 10.1016/J.LWT.2019.108633

El Adab, S., and Hassouna, M. (2016). Proteolysis, lipolysis and sensory characteristics of a tunisian dry fermented poultry meat sausage with oregano and thyme EOs. *J. Food Saf.* 36, 19–32. doi: 10.1111/JFS.12209

Erol, I., Kotil, S., Fidan, O., Yetiman, A., Durdagi, S., and Ortakci, F. (2021). Silico analysis of bacteriocins from lactic acid bacteria against SARS-CoV-2. *Probiotics Antimicrob. Proteins*. doi: 10.1007/s12602-021-09879-0

Evren, M., and Tekgüler, B. (2011). Antimicrobial acticity of essential oils. *Elektronik Mikrobiyoloji Dergisi* 9, 28–40.

Fathi-Achachlouei, B., Babolanimogadam, N., and Zahedi, Y. (2021). Influence of anise (*Pimpinella anisum* L.) essential oil on the microbial, chemical, and sensory properties of chicken fillets wrapped with gelatin film. *Food Sci. Technol. Int.* 27, 123–134. doi: 10.1177/1082013220935224

Françoise, L. (2010). Occurrence and role of lactic acid bacteria in seafood products. *Food Microbiol.* 27, 698–709. doi: 10.1016/j.fm.2010.05.016

Gaio, I., Saggiorato, A. G., Treichel, H., Cichoski, A. J., Astolfi, V., Cardoso, R. I., et al. (2015). Antibacterial activity of basil essential oil (*Ocimum basilicum* L.) in Italian-type sausage. *J. Verbraucherschutz Leb.* 10, 323–329. doi: 10.1007/S00003-015-0936-X

Ghoul, M., and Mitri, S. (2016). The ecology and evolution of microbial competition. *Trends Microbiol.* 24, 833–845. doi: 10.1016/J.TIM.2016.06.011

Gómez-García, M., Sol, C., De Nova, P. J. G., Puyalto, M., Mesas, L., Puente, H., et al. (2019). Antimicrobial activity of a selection of organic acids, their salts and EOs against swine enteropathogenic bacteria. *Porc. Heal. Manag.* 5:92. doi: 10.1186/S40813-019-0139-4/TABLES/7

Gonzalez-Fandos, E., Martinez-Laorden, A., and Perez-Arnedo, I. (2020). Combined effect of organic acids and modified atmosphere packaging on *Listeria monocytogenes* in chicken legs. *Animals* 10:1818. doi: 10.3390/ANI10101818

Gonzalez-Rivas, P. A., Chauhan, S. S., Ha, M., Fegan, N., Dunshea, F. R., and Warner, R. D. (2020). Effects of heat stress on animal physiology, metabolism, and meat quality: A review. *Meat Sci.* 162:108025. doi: 10.1016/J.MEATSCI.2019.108025

Guluwa, L. Y., Ari, M. M., Ogara, I. M., and Adua, M. M. (2021). Effect of lactic acid bacteria probiotics on growth performance and nutrient digestibilityof ross 308 broiler chicks. *J. Anim. Sci. Livest. Prod.* 5:004.

Gyawali, R., and Ibrahim, S. A. (2012). Impact of plant derivatives on the growth of foodborne pathogens and the functionality of probiotics. *Appl. Microbiol. Biotechnol.* 95, 29–45. doi: 10.1007/s00253-012-4117-x

Hashem, A., Tabassum, B., and Abd Allah, E. F. (2019). Bacillus subtilis: A plant-growth promoting rhizobacterium that also impacts biotic stress. *Saudi J. Biol. Sci.* 26, 1291–1297. doi: 10.1016/j.sjbs.2019.05.004

Hassoun, A., and Çoban, O. E. (2017). Essential oils for antimicrobial and antioxidant applications in fish and other seafood products. *Trends Food Sci. Tech.* 68, 26–36. doi: 10.1016/j.tifs.2017.07.016

Heredia, N., and García, S. (2018). Animals as sources of food-borne pathogens: A review. *Anim. Nutr.* 4, 250–255. doi: 10.1016/j.aninu.2018.04.006

Hien, L. T. M., and Dao, D. T. A. (2021). Black pepper essential oil nanoemulsions formulation using EPI and PIT methods. *J. Food Process. Preserv.* 45:e15216. doi: 10.1111/jfpp.15216

Holley, R. A., and Patel, D. (2005). Improvement in shelf-life and safety of perishable foods by plant EOs and smoke antimicrobials. *Food Microbiol.* 22, 273–292. doi: 10.1016/J.FM.2004.08.006

Hong, J. W., Yang, G. E., Kim, Y. B., Eom, S. H., Lew, J. H., and Kang, H. (2012). Anti-inflammatory activity of cinnamon water extract in vivo and in vitro LPS-induced models. *BMC Complement. Altern. Med.* 12:237. doi: 10.1186/1472-6882-12-237

Hussain, M. A., Sumon, T. A., Mazumder, S. K., Ali, M. M., Jang, W. J., Abualreesh, M. H., et al. (2021). EOs and chitosan as alternatives to chemical preservatives for fish and fisheries products: A review. *Food Control.* 129:108244. doi: 10.1016/j.foodcont.2021.108244

Ibrahim, S. A., Ayivi, R. D., Zimmerman, T., Siddiqui, S. A., Altemimi, A. B., Fidan, H., et al. (2021). Lactic acid bacteria as antimicrobial agents: Food safety and microbial food spoilage prevention. *Foods* 10:3131. doi: 10.3390/foods10123131

Jadhav, H. B., and Annapure, U. (2021). Consequences of non-thermal cold plasma treatment on meat and dairy lipids – a review. *Futur. Foods* 4:100095. doi: 10.1016/J.FUFO.2021.100095

Kacaniova, M., Galovičová, L., Šimora, V., Ďúranová, H., Borotová, P., Štefániková, J., et al. (2021). Chemical composition and biological activity of Salvia officinalis essential oil. *Acta Hortic. Regiotecturae* 24, 81–88. doi: 10.2478/ahr-2021-0028

Kamkar, A., Molaee-aghaee, E., Khanjari, A., Akhondzadeh-basti, A., Noudoost, B., Sariatifar, N., et al. (2021). Nanocomposite active packaging based on chitosan biopolymer loaded with nano-liposomal essential oil: Its characterizations and effects on microbial, and chemical properties of refrigerated chicken breast fillet. *Int. J. Food Micro.* 342:109071. doi: 10.1016/j.ijfoodmicro.2021.109071

Khorshidian, N., Yousefi Asli, M., Hosseini, H., Shadnoush, M., and Mortazavian, A. M. (2016). Potential anticarcinogenic effects of lactic acid bacteria and probiotics in detoxification of process-induced food toxicants. *Int. J. Cancer Manage.* 9:7920. doi: 10.17795/ijcp-7920

Kim, S., Song, H., Jin, J. S., Lee, W. J., and Kim, J. (2022). Genomic and phenotypic characterization of cutibacterium acnes bacteriophages isolated from acne patients. *Antibiotics* 11:1041. doi: 10.3390/antibiotics11081041

Küley, E., Özyurt, G., Özogul, I., Boga, M., Akyol, I., Rocha, J. M., et al. (2020). The role of selected lactic acid bacteria on organic acid accumulation during wet and spray-dried fish-based silages. contributions to the winning combination of microbial food safety and environmental sustainability. *Microorganisms* 8:172. doi: 10.3390/microorganisms8020172

Kumar, A., Mendiratta, S. K., and Sen, A. R. (2015a). Steam cooked meat spread: A new dimension to spent hen meat utilisation. *Ind. J. Poultry Sci.* 50, 315–318.

Kumar, A., Mendiratta, S. K., Sen, A. R., Kandeepan, G., Talukder, S., Sharma, H., et al. (2015b). Preparation and storage stability of meat spread developed from spent hens. *Vet. World* 8, 651–655. doi: 10.14202/vetworld.2015.651-655

Kumar, S., Mendiratta, S. K., Agrawal, R. K., Sharma, H., and Singh, B. P. (2018). Anti-oxidant and anti-microbial properties of mutton nuggets incorporated with blends of EOs. *J. Food Sci. Technol.* 55, 821–832. doi: 10.1007/s13197-017-3009-6

Kumar, S., Mendiratta, S. K., Sharma, H., Agarwal, R. K., Kandeepan, G., and Singh, B. P. (2017). Production cost of mutton nuggets developed by incorporating flaxseed flour, blend of EOs and their selected combinations. *J. Anim. Res.* 7:613. doi: 10.5958/2277-940x.2017.00093.6

Kunova, S., Sendra, E., Haščík, P., Vukovic, N., Vukić, M., and Kacaniova, M. (2021). Influence of essential oils on the microbiological quality of fish meat during storage. *Animals* 11:3145. doi: 10.3390/ani11113145

Kupryś-Caruk, M., Michalczuk, M., Chabłowska, B., and Stefańska, I. (2019). Comparison of the effect of lactic acid bacteria added to feed or water on growth performance, health status and gut microbiota of chickens broilers. *Ann. Warsaw Univ. Life Sci. SGGW Anim. Sci.* 58, 55–67. doi: 10.22630/AAS.2019.58.1.7

Leite, and de Souza, E. (2021). Insights into the current evidence on the effects of EOs toward beneficial microorganisms in foods with a special emphasis to lactic acid bacteria – a review. *Trends Food Sci. Technol.* 114, 333–341. doi: 10.1016/j.tifs.2021.06.011

Li, R., Liang, T., Xu, L., Li, Y., Zhang, S., and Duan, X. (2013). Protective effect of cinnamon polyphenols against STZ-diabetic mice fed high-sugar, high-fat diet and its underlying mechanism. *Food Chem. Toxicol.* 51, 419–425. doi: 10.1016/J.FCT.2012.10.024

Lin, Y.-C., Chung, K.-R., and Huang, J. W. (2020). A synergistic effect of chitosan and lactic acid bacteria on the control of cruciferous vegetable diseases. *Plant Path. J.* 36, 157–169. doi: 10.5423/PPJ.OA.01.2020.0004

Lu, S., Ji, H., Wang, Q., Li, B., Li, K., Xu, C., et al. (2015). The effects of starter cultures and plant extracts on the biogenic amine accumulation in traditional Chinese smoked horsemeat sausages. *Food Control.* 50, 869–875. doi: 10.1016/J.FOODCONT.2014.08.015

Macwan, S. R., Dabhi, B. K., Aparnathi, K. D., and Prajapati, J. B. (2016). EOs of herbs and spices: Their antimicrobial activity and application in preservation of food. *Int. J. Curr. Microbiol. Appl. Sci.* 5, 885–901. doi: 10.20546/ijcmas.2016.505.092

Maghami, M., Motalebi, A. A., and Anvar, S. A. A. (2019). Influence of chitosan nanoparticles and fennel essential oils (*Foeniculum vulgare*) on the shelf life of Huso huso fish fillets during the storage. *Food Sci. Nutr.* 7, 3030–3041. doi: 10.1002/fsn3.1161

Mariotti, M., Lombardini, G., Rizzo, S., Scarafile, D., Modesto, M., Truzzi, E., et al. (2022). Potential applications of essential oils for environmental sanitization and antimicrobial treatment of intensive livestock infections. *Microorganisms* 10:822. doi: 10.3390/microorganisms10040822

Masoumi, B., Abbasi, A., Mazloomi, S., and Shaghaghian, S. (2022). Investigating the effect of probiotics as natural preservatives on the microbial and physicochemical properties of yogurt-marinated chicken fillets. *J. Food Qual.* 2022:5625114. doi: 10.1155/2022/5625114

Maulu, S., Nawanzi, K., Abdel-Tawwab, M., and Khalil, H. S. (2021). Fish nutritional value as an approach to children's nutrition. *Front. Nutr.* 8:780844. doi: 10.3389/fnut.2021.780844

Mechqoq, H., Hourfane, S., El Yaagoubi, M., El Hamdaoui, A., Msanda, F., Almeida, J. R. F. S., et al. (2022). Phytochemical screening, in-vitro evaluation of the antioxidant and dermocosmetic activities of four moroccan plants: *Halimium antiatlanticum*, *Adenocarpus artemisiifolius*, *Pistacia lentiscus* and *Leonotis nepetifolia*. *Cosmetics* 9:94. doi: 10.3390/cosmetics9050094

Melero, B., Diez, A. M., Rajkovic, A., Jaime, I., and Rovira, J. (2012). Behaviour of non-stressed and stressed *Listeria monocytogenes* and *Campylobacter jejuni* cells on fresh chicken burger meat packaged under modified atmosphere and inoculated with protective culture. *Int. J. Food Microbiol.* 158, 107–112. doi: 10.1016/J.IJFOODMICRO.2012.07.003

Melo, R. S., Reis, S. A. G. B., Guimarães, A. L., Silva, N. D. S., Rocha, J. M., Aouad, N. E., et al. (2022). Phytocosmetic emulsion containing extract of *Morus nigra* L. (Moraceae): Development, stability study, antioxidant and antibacterial activities. *Cosmetics* 9:39. doi: 10.3390/cosmetics9020039

Mucha, W., and Witkowska, D. (2021). The applicability of EOs in different stages of production of animal-based foods. *Molecules* 26:3798. doi: 10.3390/molecules26133798

Munekata, P. E., Pateiro, M., Rocchetti, G., Rocha, J. M., and Lorenzo, J. M. (2022). Application of metabolomics to decipher the role of bioactive compounds in plant and animal foods. *Curr. Opin. Food Sci.* 46:100851. doi: 10.1016/j.cofs.2022.100851

Nehme, R., Andrés, S., Pereira, R. B., Ben Jemaa, M., Bouhallab, S., Ceciliani, F., et al. (2021). Essential oils in livestock: From health to food quality. *Antioxidants* 10:330. doi: 10.3390/antiox10020330

Neves, M., Antunes, M., Fernandes, W., Campos, M. J., Azevedo, Z. M., Freitas, V., et al. (2021). Physicochemical and nutritional profile of leaves, flowers, and fruits of the edible halophyte chorão-da-praia (*Carpobrotus edulis*) on Portuguese west shores. *Food Biosci.* 43:101288. doi: 10.1016/j.fbio.2021.101288

Nisar, T., Yang, X., Alim, A., Iqbal, M., Wang, Z. C., and Guo, Y. (2019). Physicochemical responses and microbiological changes of bream (*Megalobrama ambycephala*) to pectin based coatings enriched with clove essential oil during refrigeration. *Int. J. Biol. Macromol.* 124, 1156–1166. doi: 10.1016/J.IJBIOMAC.2018.12.005

Oblakova, M., Hristakieva, P., Mincheva, N., Ivanova, I., Lalev, M., Ivanov, N. et al. (2021). Effect of Dietary Herbal Essential Oils on the Performance and Meat Quality of Female Turkeys Broilers. *Trakia J. Sci.* 2, 130–138. doi: 10.15547/tjs.2021.02.003

Olatunde, O. O., and Benjakul, S. (2018). Natural preservatives for extending the shelf-life of seafood: A revisit. *Compr. Rev. Food Sci. Food Saf.* 17, 1595–1612. doi: 10.1111/1541-4337.12390

Oussalah, M., Caillet, S., Saucier, L., and Lacroix, M. (2007). Inhibitory effects of selected plant essential oils on the growth of four pathogenic bacteria: *E. coli* O157:H7 *Salmonella Typhimurium*, *Staphylococcus aureus* and *Listeria monocytogenes*. *Food Control* 18, 414–420.

Özogul, F., Küley, E., Küley, F., Kulawik, P., and Rocha, J. M. (2022). Impact of sumac, cumin, black pepper and red pepper extracts in the development of foodborne pathogens and formation of biogenic amines. *Eur. Food Res. Technol.* 248:3.

Pan, A., Sun, Q., Bernstein, A. M., Schulze, M. B., Manson, J. A. E., Willett, W. C., et al. (2011). Red meat consumption and risk of type 2 diabetes: 3 cohorts of US adults and an updated meta-analysis. *Am. J. Clin. Nutr.* 94, 1088–1096. doi: 10.3945/AJCN.111.018978

Pardo, Z., Fernández-Fígares, I., Lachica, M., Lara, L., Nieto, R., and Seiquer, I. (2021). Impact of heat stress on meat quality and antioxidant markers in iberian pigs. *Antioxidants* 10:1911. doi: 10.3390/ANTIOX10121911/S1

Perricone, M., Arace, E., Corbo, M. R., Sinigaglia, M., and Bevilacqua, A. (2015). Bioactivity of EOs: A review on their interaction with food components. *Front. Microbiol.* 6:76. doi: 10.3389/fmicb.2015.00076

Petkova, M., Gotcheva, V., Dimova, M., Bartkiene, E., Rocha, J. M., and Angelov, A. (2022). Screening of Lactiplantibacillus plantarum strains from sourdoughs for biosuppression of Pseudomonas syringae pv. syringae and *Botrytis cinerea* in table grapes. *Microorganisms* 10:2094. doi: 10.3390/microorganisms10112094

Pirnia, M., Shirani, K., Tabatabaee Yazdi, F., Moratazavi, S. A., and Mohebbi, M. (2022). Characterization of antioxidant active biopolymer bilayer film based

on gelatin-frankincense incorporated with ascorbic acid and *Hyssopus officinalis* essential oil. *Food Chem: X* 14:100300. doi: 10.1016/J.FOCHX.2022.100300

Radkowski, M., Zdrodowska, B., and Gomółka-Pawlicka, M. (2018). Effect of succinic acid on elimination of *Salmonella* in Chicken meat. *J. Food Prot.* 81, 1491–1495. doi: 10.4315/0362-028X.JFP-17-446

Raeisi, S., Ojagh, S. M., Pourashouri, P., Salaün, F., and Quek, S. Y. (2021). Shelf-life and quality of chicken nuggets fortified with encapsulated fish oil and garlic essential oil during refrigerated storage. *J. Food Sci. Technol.* 58, 121–128. doi: 10.1007/s13197-020-04521-3

Raman, J., Kim, J.-S., Choi, K. R., Eun, H., Yang, D., Ko, Y.-J., et al. (2022). Application of lactic acid bacteria (LAB) in sustainable agriculture: Advantages and limitations. *Int. J. Mol. Sci.* 23:7784. doi: 10.3390/ijms23147784

Rathod, N. B., Nirmal, N. P., Pagarkar, A., Özogul, F., and Rocha, J. M. (2022). Antimicrobial impacts of microbial metabolites on the preservation of fish and fishery products: A review with current knowledge. *Microorganisms* 10:773. doi: 10.3390/microorganisms10040773

Remya, S., Mohan, C. O., Venkateshwarlu, G., Sivaraman, G. K., and Ravishankar, C. N. (2017). Combined effect of O2 scavenger and antimicrobial film on shelf life of fresh cobia (*Rachycentron canadum*) fish steaks stored at 2 °C. *Food Control* 71, 71–78. doi: 10.1016/J.FOODCONT.2016.05.038

Reuben, R. C., Sarkar, S. L., Roy, P. C., Anwar, A., Hossain, M. A., and Jahid, I. K. (2021). Prebiotics, probiotics and postbiotics for sustainable poultry production. Worlds. *Poult. Sci. J.* 77, 825–882. doi: 10.1080/00439339.2021.1960234

Ricke, S. C., Dittoe, D. K., and Richardson, K. E. (2020). Formic acid as an antimicrobial for poultry production: A review. *Front. Vet. Sci.* 7:563. doi: 10.3389/FVETS.2020.00563

Ruíz, F. O., Gerbaldo, G., García, M. J., Giordano, W., Pascual, L., and Barberis, I. L. (2012). Synergistic effect between two bacteriocin-like inhibitory substances produced by *Lactobacilli strains* with inhibitory activity for *Streptococcus agalactiae*. *Curr. Microbiol.* 64, 349–356. doi: 10.1007/s00284-011-0077-0

Sakaridis, I., Soultos, N., Batzios, C., Ambrosiadis, I., and Koidis, P. (2014). Lactic acid bacteria isolated from chicken carcasses with inhibitory activity against *Salmonella* spp. and *Listeria monocytogenes*. *Czech J. Food Sci.* 32, 61–68.

Sakaridis, I., Soultos, N., Dovas, C. I., Papavergou, E., Ambrosiadis, I., and Koidis, P. (2012). Lactic acid bacteria from chicken carcasses with inhibitory activity against *Salmonella spp*. and *Listeria monocytogenes*. *Anaerobe* 18, 62–66. doi: 10.1016/J.ANAEROBE.2011.09.009

Sharafati Chaleshtori, F., Taghizadeh, M., Rafieian-kopaei, M., and Sharafati-chaleshtori, R. (2016). Effect of chitosan incorporated with cumin and eucalyptus essential oils as antimicrobial agents on fresh chicken meat. *J. Food Process Preser.* 40, 396–404. doi: 10.1111/jfpp.12616

Sharma, H., Mendiratta, S. K., Agarwal, R., and Goswami, M. (2019). Optimization of various EOs and their effect on the microbial and sensory attributes of chicken sausages. *Agric. Res.* 8, 374–382. doi: 10.1007/s40003-018-0367-x

Sharma, H., Mendiratta, S. K., Agarwal, R. K., and Gurunathan, K. (2020). Bio-preservative effect of blends of EOs: Natural anti-oxidant and anti-microbial agents for the shelf life enhancement of emulsion based chicken sausages. *J. Food Sci. Technol.* 57, 3040–3050. doi: 10.1007/s13197-020-04337-1

Sharma, H., Mendiratta, S. K., Agarwal, R. K., Kumar, S., and Soni, A. (2017). Evaluation of anti-oxidant and anti-microbial activity of various EOs in fresh chicken sausages. *J. Food Sci. Technol.* 54, 279–292. doi: 10.1007/s13197-016-2461-z

Sharma, H., Mendiratta, S. K., Agrawal, R. K., Talukder, S., and Kumar, S. (2018). Studies on the potential application of various blends of EOs as antioxidant and antimicrobial preservatives in emulsion based chicken sausages. *Br. Food J.* 120, 1398–1411. doi: 10.1108/BFJ-03-2018-0185

Sharma, H., Özogul, F., Bartkiéne, E., and Rocha, J. M. (2021). Impact of lactic acid bacteria and their metabolites on the techno-functional properties and health benefits of fermented dairy products. *Crit. Rev. Food Sci. Nutrition*. Online ahead of print. doi: 10.1080/10408398.2021.2007844

Shekarforoush, S., Firouzi, R., and Kafshdozan, K. (2014). Antimicrobial activities of oregano and nutmeg essential oils combined with emulsifier/stabilizer compound in ready-to-cook barbecued chicken. *Iranian J. Vety. Res.* 15, 159–163.

Silva, H. L. A., Balthazar, C. F., Silva, R., Vieira, A. H., Costa, R. G. B., Esmerino, E. A., et al. (2018). Sodium reduction and flavor enhancer addition in probiotic prato cheese: Contributions of quantitative descriptive analysis and temporal dominance of sensations for sensory profiling. *J. Dairy Sci.* 101, 8837–8846. doi: 10.3168/jds.2018-14819

Sun, X., Wang, J., Zhang, H., Dong, M., Li, L., Jia, P., et al. (2021). Development of functional gelatin-based composite films incorporating oil-in-water lavender essential oil nano-emulsions: Effects on physicochemical properties and cherry tomatoes preservation. *LWT* 142:110987. doi: 10.1016/j.lwt.2021.110987

Tacon, A. G. J., Lemos, D., and Metian, M. (2020). Fish for health: Improved nutritional quality of cultured fish for human consumption. *Rev. Fish. Sci. Aquac.* 28, 449–458. doi: 10.1080/23308249.2020.1762163

Talukder, S., Sharma, B. D., Mendiratta, S. K., Malav, O. P., Sharma, H., and Gokulakrishnan, P. (2013). Development and evaluation of extended restructured chicken meat block incorporated with colocasia (*Colocasia esculenta*) flour. *J. Food Proc. Technol.* 4:207.

Tomović, V., Šojić, B., Savanović, J., Kocić-Tanackov, S., Pavlić, B., Jokanović, M., et al. (2020). New formulation towards healthier meat products: *Juniperus communis* L. essential oil as alternative for sodium nitrite in dry fermented sausages. *Foods* 9:1066. doi: 10.3390/FOODS9081066

Trakselyte-Rupsiene, K., Juodeikiene, G., Alzbergaite, G., Zadeike, D., Bartkiene, E., Özogul, F., et al. (2022). Bio-refinery of plant drinks press cake permeate using ultrafiltration and lactobacillus fermentation into antimicrobials and its effect on the growth of wheatgrass in vivo. *Food Biosci.* 46:101427. doi: 10.1016/j.fbio.2021.101427

Vispute, M. M., Sharma, D., Manda, A. B., Rokade, J. J., Tyagi, P. K., and Yadav, A. S. (2019). Effect of dietary supplementation of hemp (*Cannabis sativa*) and dill seed (*Anethum graveolens*) on performance, serum biochemicals and gut health of broiler chickens. *J. Anim. Physio. Ani. Nutri.* 103, 525–533. doi: 10.1111/jpn.13052

Wang, Y., Wang, J., Bai, D., Wei, Y., Sun, J., Luo, Y., et al. (2020). Synergistic inhibition mechanism of pediocin PA-1 and L-lactic acid against *Aeromonas hydrophila*. *Biochim. Biophys. Acta - Biomembr.* 1862:183346. doi: 10.1016/J.BBAMEM.2020.183346

Wei, Q., Liu, X., Zhao, S., Li, S., and Zhang, J. (2022). Preservative effect of compound spices extracts on marinated chicken. *Poult. Sci.* 101:101778. doi: 10.1016/j.psj.2022.101778

Wilson, D. W., Nash, P., Singh, H., Griffiths, K., Singh, R., De Meester, F., et al. (2017). The role of food antioxidants, benefits of functional foods, and influence of feeding habits on the health of the older person: An overview. *Antioxidants* 6, 1–20. doi: 10.3390/antiox6040081

Wyszyńska, A. K., and Godlewska, R. (2021). Lactic acid bacteria – A promising tool for controlling chicken campylobacter infection. *Front. Microbiol.* 12:703441. doi: 10.3389/fmicb.2021.703441

Xia, Y., Wang, Y., Lou, S., Wen, M., and Ni, X. (2022). Fabrication and characterization of zein-encapsulated Litsea cubeba oil nanoparticles and its effect on the quality of fresh pork. *Food Biosci.* 49:101834. doi: 10.1016/J.FBIO.2022.101834

Yanwong, S., and Threepopnatkul, P. (2015). Effect of peppermint and citronella essential oils on properties of fish skin gelatin edible films. *IOP Conf. Ser: Mater. Sci. Eng.* 87:012064. doi: 10.1088/1757-899X/87/1/012064

Yavuzer, E. (2021). Determination of fish quality parameters with low cost electronic nose. *Food Biosci.* 41:100948. doi: 10.1016/J.FBIO.2021.100948

Yavuzer, E., and Köse, M. (2022). Prediction of fish quality level with machine learning. *Int. J. Food Sci. Technol.* 57, 5250–5255. doi: 10.1111/IJFS.15853

Yildirim, Z., Yerlikaya, S., Öncül, N., and Sakin, T. (2016). Inhibitory effect of lactococcin BZ against *Listeria innocua* and indigenous microbiota of fresh beef. *Food Technol. Biotechnol.* 54:317. doi: 10.17113/FTB.54.03.16.4373

Yilmaz, B., Bangara, S. P., Echegaray, N., Surib, S., Tomasevic, I., Lorenzo, J. M., et al. (2022a). The impacts of *Lactiplantibacillus plantarum* on the functional properties of fermented foods: A review of current knowledge. *Microorganisms* 10:826. doi: 10.3390/microorganisms10040826

Yilmaz, N., Özogul, F., Fadiloglu, E. E., Moradi, M., Simat, V., and Rocha, J. M. (2022b). Reduction of biogenic amine formation by foodborne pathogens using postbiotics in lysine-decarboxylase broth. *J. Biotechnol.* 358, 118–127. doi: 10.1016/j.jbiotec.2022.09.003

Yousefi, M., Khorshidian, N., and Hosseini, H. (2020). Potential application of essential oils for mitigation of *Listeria monocytogenes* in meat and poultry products. *Front. Nutr.* 7:577287. doi: 10.3389/fnut.2020.577287

Yu, H. H., Chin, Y. W., and Paik, H. D. (2021). Application of natural preservatives for meat and meat products against food-borne pathogens and spoilage bacteria: A review. *Foods* 10:2418. doi: 10.3390/FOODS10102418

Zhang, Y., Li, D., Lv, J., Li, Q., Kong, C., and Luo, Y. (2017). Effect of cinnamon essential oil on bacterial diversity and shelf-life in vacuum-packaged common carp (*Cyprinus carpio*) during refrigerated storage. *Int. J. Food Microbiol.* 249, 1–8. doi: 10.1016/j.ijfoodmicro.2016.10.008

Zhou, Y., Drouin, P., and Lafrenière, C. (2016). Effect of temperature (5–25°C) on epiphytic lactic acid bacteria populations and fermentation of whole-plant corn silage. *J. Appl. Microbiol.* 121, 657–671. doi: 10.1111/jam.13198

Zhu, H. C., Yang, X., Xu, L. P., Zhao, L. J., Tao, G. Z., Zhang, C., et al. (2014). Meat consumption is associated with esophageal cancer risk in a meat- and cancer-histological-type dependent manner. *Dig. Dis. Sci.* 59, 664–673. doi: 10.1007/S10620-013-2928-Y

Zokaityte, E., Cernauskas, D., Klupsaite, D., Lele, V., Starkute, V., Zavistanaviciute, P., et al. (2020). Bioconversion of milk permeate with selected lactic acid bacteria strains and apple by-products into beverages with antimicrobial properties and enriched with galactooligosaccharides. *Microorganisms* 8:1182. doi: 10.3390/microorganisms8081182

Zubair, M., Pradhan, R. A., Arshad, M., and Ullah, A. (2021). Recent advances in lipid derived bio-based materials for food packaging applications. *Macromol. Mater. Eng.* 306:2000799. doi: 10.1002/MAME.202000799

Zubair, M., Shahzad, S., Hussain, A., Pradhan, R. A., Arshad, M., and Ullah, A. (2022). Current trends in the utilization of essential oils for polysaccharide- and protein-derived food packaging materials. *Polymers* 14:1146. doi: 10.3390/polym14061146

frontiers | Frontiers in Microbiology

TYPE Original Research
PUBLISHED 11 January 2023
DOI 10.3389/fmicb.2022.1077375

OPEN ACCESS

EDITED BY
Michael Gänzle,
University of Alberta, Canada

REVIEWED BY
Julia Bechtner,
Aarhus University, Denmark
Per Johansson,
University of Helsinki, Finland

*CORRESPONDENCE
Paloma López
✉ plg@cib.csic.es
Hadda-Imene Ouzari
✉ ouzari.imene@gmail.com

SPECIALTY SECTION
This article was submitted to Food Microbiology, a section of the journal Frontiers in Microbiology

RECEIVED 22 October 2022
ACCEPTED 16 December 2022
PUBLISHED 11 January 2023

CITATION
Besrour-Aouam N, de Los Rios V, Hernández-Alcántara AM, Mohedano ML, Najjari A, López P and Ouzari H-I (2023) Proteomic and *in silico* analyses of dextran synthesis influence on *Leuconostoc lactis* AV1n adaptation to temperature change.
Front. Microbiol. 13:1077375.
doi: 10.3389/fmicb.2022.1077375

Proteomic and *in silico* analyses of dextran synthesis influence on *Leuconostoc lactis* AV1n adaptation to temperature change

Norhane Besrour-Aouam[1,2], Vivian de Los Rios[1], Annel M. Hernández-Alcántara[1], Mª Luz Mohedano[1], Afef Najjari[2], Paloma López[1]* and Hadda-Imene Ouzari[2]*

[1]Centro de Investigaciones Biológicas Margarita Salas, CIB-CSIC, Madrid, Spain, [2]Laboratoire Microorganismes et Biomolécules Actives (LR03ES03), Faculté des Sciences de Tunis, Université Tunis El Manar, Tunis, Tunisia

Leuconostoc lactis is found in vegetables, fruits, and meat and is used by the food industry in the preparation of dairy products, wines, and sugars. We have previously demonstrated that the dextransucrase of *Lc. lactis* (DsrLL) AV1n produces a high-molecular-weight dextran from sucrose, indicating its potential use as a dextran-forming starter culture. We have also shown that this bacterium was able to produce 10-fold higher levels of dextran at 20°C than at 37°C, at the former temperature accompanied by an increase in *dsrLL* gene expression. However, the general physiological response of *Lc. lactis* AV1n to cold temperature in the presence of sucrose, leading to increased production of dextran, has not been yet investigated. Therefore, we have used a quantitative proteomics approach to investigate the cold temperature-induced changes in the proteomic profile of this strain in comparison to its proteomic response at 37°C. In total, 337 proteins were found to be differentially expressed at the applied significance criteria (adjusted p-value $\leq$ 0.05, FDR 5%, and with a fold-change $\geq$ 1.5 or $\leq$ 0.67) with 204 proteins overexpressed, among which 13% were involved in protein as well as cell wall, and envelope component biosynthesis including DsrLL. Proteins implicated in cold stress were expressed at a high level at 20°C and possibly play a role in the upregulation of DsrLL, allowing the efficient synthesis of the protein essential for its adaptation to cold. Post-transcriptional regulation of DsrLL expression also seems to take place through the interplay of exonucleases and endonucleases overexpressed at 20°C, which would influence the half-life of the *dsrLL* transcript. Furthermore, the mechanism of cold resistance of *Lc. lactis* AV1n seems to be also based on energy saving through a decrease in growth rate mediated by a decrease in

carbohydrate metabolism and its orientation toward the production pathways for storage molecules. Thus, this better understanding of the responses to low temperature and mechanisms for environmental adaptation of *Lc. lactis* could be exploited for industrial use of strains belonging to this species.

KEYWORDS

***Leuconostoc*, dextran, exopolysaccharides, lactic acid bacteria, proteomic**

1. Introduction

Lactic acid bacteria (LAB) are a heterogeneous group of strains from different genera defined as Gram positive with a low G + C content in its genome, microaerophilic, and synthesize lactic acid as the main or only end product of their carbohydrate metabolisms. LAB are non-spore forming, and many of them are generally recognized as safe (GRAS) by the U.S. Food and Drug Administration (Makarova et al., 2006). They have been traditionally used to produce various fermented foods from animal products (e.g., milk, meat, and fish) or plants (e.g., vegetables, wine, and olives) (Zarour et al., 2017b). In fact, these so-called "starter strains" have the capacity to contribute to food safety and/or to offer one or more organoleptic, technological, nutritional, or health benefits through the synthesis of various products such as vitamins (e.g., folate and riboflavin) (Mosso et al., 2018; Mohedano et al., 2019), enzymes (e.g., phytase and lipases) (Anastasio et al., 2010; Zarour et al., 2018), antimicrobial peptides (e.g., bacteriocins) (Maldonado-Barragan and West, 2020) and exopolysaccharides (EPS) (Oleksy and Klewicka, 2016). The latter are polymers synthesized by LAB that differ in their chemical composition, type of linkage, degree and type of branching, and molecular mass. They are classified, according to their chemical composition, as follows: (1) hetepolysaccharide (HePS), which contain repeating units of several different types of monosaccharides, and (2) homopolysaccharides (HoPS), made of only glucose, fructose, or galactose residues (Pérez-Ramos et al., 2015). The use of the food-grade LAB EPS is currently of growing attention and commercial interest, particularly regarding dextran-type HoPS. Dextrans are α-glucan polymers, with major chains formed by glucoses joined by α-(1-6) linkages and with branches that arise from α-(1-2), α-(1-3), and α-(1-4) bonds (Monsan et al., 2001). These molecules are synthesized by several species of the genera *Leuconostoc* (Zarour et al., 2017a), *Lactobacillus* (Nácher-Vázquez et al., 2017), *Streptococcus* (Germaine and Schachtele, 1976), and *Weissella* (Malang et al., 2015; Llamas-Arriba et al., 2021) due to the catalytic activity of a single extracellular enzyme: the dextransucrase (Dsr). The Dsr enzymes are encoded by the *dsr* genes and are responsible for the synthesis of dextran catalyzing the hydrolysis of sucrose coupled to the transfer of glucose to the nascent α-glucan polymer and generating also free fructose (Werning et al., 2012). The molecular weight of dextrans varies from one polymer to another. There are high-molecular-weight dextrans that can reach up to 10^8 Da (Besrour-Aouam et al., 2021) and others of low-molecular-weight not exceeding around 3×10^4 Da (Claverie et al., 2017). Dextran application largely depends on their size. Low-molecular-weight dextrans are generally used for clinical application (Patel and Goyal, 2011), whereas high-molecular-weight ones have been the subject of several research studies aimed at stabilizing their potential as biothickeners, which could be synthesized *in situ* by bacteria, particularly from *Leuconostoc* and *Weissella* genus, during the fermentation of food matrices (Katina et al., 2009; Galle et al., 2012; Kothari et al., 2014). Moreover, according to recent studies, dextrans are postbiotics and could bring health benefits due to their antiviral and immunomodulatory properties (Nácher-Vázquez et al., 2015; Zarour et al., 2017a) and, thus, contribute to the clean label formulation of industrial food. Therefore, dextran-producing LAB have been tested in fermented dairy products in order to increase viscosity and reduce syneresis and, in low-fat cheese, to enhance creaminess (Kothari et al., 2014). Dextran-producing *Leuconostoc lactis* and *Weissella confusa* strains have been used as starters in pureed carrots to replace hydrocolloid additive and confer a suitable thick texture (Juvonen et al., 2015). These bacteria have also shown a special interest in the bakery industry since they contributed to the nutritional enrichment, shelf life and volume improvement of bread (Katina et al., 2009; Hu and Ganzle, 2018), and gluten-free bread (Galle et al., 2012; Rühmkorf et al., 2012).

The ecological role of dextrans for bacteria is not clearly understood. However, it has been suggested that they could play the role of carbon source as has been studied for *Streptococcus mutans*. In addition, to produce Dsr, this bacterium can produce an extracellular dextranase, which would produce isomaltooligosaccharides from dextran hydrolysis and these are ingested by bacteria and then converted into glucose by an intracellular glucan α-1,6-glucosidase (Klahan et al., 2018). Dextran could also be synthesized in response to environmental stress undergone by the bacteria. Thus, exposure to cold temperature (0–6°C) for a few weeks resulted in increased production of dextran by *Leuconostoc gelidum* and

Leuconostoc gasicomitatum (Lyhs et al., 2004). Furthermore, upon cold shift during sourdough fermentation, *Weissella cibaria* 10 M was able to produce high dextran yield (Hu and Ganzle, 2018). This dextran production in response to cold temperature could be interpreted as a potential protective barrier for the bacteria, which would be an interesting property for a strain, given that recently studies have increasingly focused on the search for starters strains of interest not only of functional properties but also in terms of robustness and industrial performance with optimal survival during frozen storage, low-temperature fermentation during cheese ripening, or refrigerated storage of fermented products.

We have previously demonstrated that *Lc. lactis* AV1n isolated from a Tunisian avocado synthesizes a dextran-type HoPS with a main chain of glucopyranose units with α-(1-6) linkages and 9% substitution, at positions *O*-3, by side chains composed of a single residue of glucose and with a molecular mass of 2.61×10^8 Da (Besrour-Aouam et al., 2019). This dextran is synthesized by a Dsr (named DsrLL), and the enzyme was visualized *in situ* by a zymogram (Besrour-Aouam et al., 2021). Moreover, the *dsrLL* gene of *Lc. lactis* AV1n has been previously sequenced and its homologous and heterologous overexpression confirmed that, indeed, the DsrLL enzyme synthesizes *in vivo* dextran (Besrour-Aouam et al., 2019). Furthermore, we have shown that expression of the *dsrLL* gene is induced in the presence of sucrose at low temperatures (Besrour-Aouam et al., 2019).

A better understanding of the responses to low temperatures may contribute to the optimization of fermented processes, storage of the products, and conservation conditions. Therefore, to further analyze DsrLL expression in response to low temperature and better understand the resistance mechanisms induced by the bacterium, a proteomic study of *Lc. lactis* AV1n in the presence of sucrose at 20°C and 37°C was carried out in this study. The obtained results, coupled with an analysis of the bacteria draft genome (Besrour-Aouam et al., 2021) and a predictive study of the folding of its *dsrLL* mRNA, have allowed us to present a road map of some of the regulatory mechanisms involved in the adaptation of this bacterium to cold temperatures.

2. Materials and methods

2.1. Bacterial strain and growth medium

The bacteria used in this study were *Lc. lactis* AV1n isolated from a Tunisian avocado and the recombinant *Lc. lactis* AV1n[pRCR21] strain (Besrour-Aouam et al., 2019). The latter harbors the pRCR21 plasmid, which carries the $P_{dsrLL-mrfp}$ transcriptional fusion encoding the mCherry protein under the control of the promoter of the *dsrLL* gene of *Lc. lactis* AV1n. Also, pRCR21 carries the *cat* gene encoding the chloramphenicol acetyl transferase, which confers Cm^R to the bacterium. The bacteria were grown in MRS broth (Condalab, Torrejon de Ardoz, Madrid, Spain) supplemented with 2% glucose (MRSG) or with 2% sucrose (MRSS). In addition, the MRSS was supplemented with chloramphenicol (Cm) at 10 μg/ml, when *Lc. lactis* AV1n[pRCR21] was grown.

2.2. Analysis of bacterial growth and EPS production

Precultures of AV1n and AV1n[pRCR21] were generated by growth of the strains up to an optical density at 600 nm ($OD_{600\ nm}$) of 1.0 at 20°C, 30°C, or 37°C in MRSS. Then, cells from each culture were sedimented by centrifugation (9,300 × *g*, 10 min, 4°C), resuspended independently in fresh MRSS, and diluted 1:10 in MRSS. The cultures were then grown at 20°C, 30°C, or 37°C, respectively, as their corresponding precultures. The growth rate (μ) of the bacteria during the exponential phase was determined as previously described (Llamas-Arriba et al., 2021).

To determine the EPS concentration, samples were taken, when the cultures reached an $OD_{600\ nm}$ of 1.0 for the proteomic analysis experiments, or as indicated in the "2.9 Cold shock experiment" section and subjected to centrifugation (9,300 × g, 10 min, 4°C). Then, the dextran present in the culture supernatants was recovered by precipitation with three volumes of absolute ethanol and two washes with 80% (v/v) ethanol. Afterward, the polymer concentration was measured as neutral carbohydrate content as determined by the phenol–sulfuric acid method using a glucose calibration curve (Dubois et al., 1956). Experiments were performed in triplicate.

2.3. Cultures for preparation of total protein extracts

For the proteomic analysis of *Lc. lactis* cold response, the AV1n[pRCR21] strain was grown in MRSS medium at 20°C or 37°C. Precultures and cultures were generated as described in the "2.1 Bacterial strain and growth medium" section. The cultures were grown until they reached the point of transition between the end of the exponential phase and the beginning of the stationary phase. Then, a volume of bacterial culture containing 4.5×10^9 colony-forming units (cfu) was harvested by centrifugation (11,269 × g, 10 min, 4°C), washed with cold PBS (pH 7.4), and stored at −80°C prior to protein extraction. Three cultures grown in either condition were prepared and stored.

2.4. Proteins extraction and quantification

For the protein extraction from the 6 cultures, the bacterial pellets stored at −80°C were thawed at 4°C and each was resuspended in 291 µl of cold PBS (137 mM NaCl, 2.7 mM KCl, 8 mM Na_2HPO_4, and 2 mM KH_2PO_4) pH 7.0 and 9 µl of 10% SDS. Then, each suspension was transferred into a Lysing Matrix B cryotube containing glass beads (MP Bio Germany GmbH) previously cooled to 0°C and subjected to two cycles of 45 s at a speed of 6, to break the bacterial cells in Ribolyser® equipment (Hybaid). The tubes were then centrifuged (11,269 × g, 20 min, 4°C), and the upper suspensions containing the total protein extracts were collected and stored at −80°C. Protein quantification was performed using the Qubit® Protein Assay Kit and the Qubit® 1.0 fluorometer.

2.5. Sample preparation for proteomic analysis

For the analysis of the proteomic profile at 20°C or 37°C, protein extracts were fractionated by SDS-PAGE (in a 10% SDS-polyacrylamide gel) till the whole proteome had penetrated in the resolving gel (about 1 cm of total migration). Gels were stained with Colloidal Blue Staining Kit (Invitrogen). Each proteome was excised and cut into small pieces prior to manual in-gel digestion with trypsin. Excised bands were separately detained with 50 mM ammonium bicarbonate (ABC) (Sigma-Aldrich) and 50% acetonitrile (ACN) (Fisher Chemical). Samples were then reduced with 10 mM dithiothreitol (Bio-Rad) in 50 mM ABC and alkylated with 55 mM iodoacetamide (GE Healthcare Life Sciences) in 50 mM ABC. Then, gel pieces were digested with porcine trypsin (Thermo Fisher Scientific), at a final concentration 12.5 ng/ml in 50 mM ABC, overnight at 37°C. Peptides were extracted using 100% ACN and 0.5% trifluoroacetic acid (Sigma-Aldrich), purified using a Zip Tip (Millipore, Sigma-Aldrich), and dried. Finally, samples were reconstituted in 12 µl of 0.1% formic acid in water (Fisher Chemical) and the peptides were quantified using the Qubit® Protein Assay Kit and the Qubit® 1.0 fluorometer.

2.6. Mass spectrometry

Peptide separations were carried out on an Easy-nLC 1000 nano system (Thermo Fisher Scientific). For each analysis, the sample was loaded into an Acclaim PepMap 100 precolumn (Thermo Fisher Scientific) and eluted through rapid-separation liquid chromatography (RSLC) PepMap C18 column (Thermo Scientific) (50 cm long, 75 µm inner diameter, 2 µm particle size). The mobile phase flow rate was 300 nl/min using 0.1% formic acid in water (solvent A) and 0.1% formic acid and 100% acetonitrile (solvent B). The gradient profile was set as follows: 5–35% solvent B for 100 min, 35–45% solvent B for 20 min, 45–100% solvent B for 5 min, and 100% solvent B for 15 min. Four microliters of sample were injected. MS analysis was performed using a Q-Exactive mass spectrometer (Thermo Scientific). For ionization, 1,900 V of liquid junction voltage and 300°C capillary temperature were used. The full-scan method employed an m/z 400–1,500 mass selection, an Orbitrap resolution of 70,000 (at m/z 200), a target automatic gain control (AGC) value of 3e6, and maximum injection times of 100 ms. After the survey scan, the 15 most intense precursor ions were selected for MS/MS fragmentation. Fragmentation was performed with a normalized collision energy of 27 eV, and MS/MS scans were acquired with a starting mass of m/z 200, AGC target was 2e5, resolution of 17,500 (at m/z 200), intensity threshold of 8e4, isolation window of 2.0 m/z units, and maximum IT was 100 ms. Charge state screening was enabled to reject unassigned, singly charged, and equal or more than seven protonated ions. A dynamic exclusion time of 20 s was used to discriminate against previously selected ions.

2.7. Proteomic data analysis and accessibility

Raw files were processed with MaxQuant software, version 1.6.5.0 (Cox and Mann, 2008) using standardized protocols (Tyanova et al., 2016). Mass spectra *.raw files were searched against the *Lc. lactis* (UniProtKB/Swiss—Prot/TrEMBL, July 2019, 6,259 sequences) protein database, supplemented with the mCherry protein sequence. In the search parameters, the methionine oxidation was established as variable modification and carbamidomethylation of cysteines as a fixed modification. The minimal peptide length was set to 7 amino acids and a maximum of two tryptic missed cleavages were allowed. The results were filtered at 0.01 false discovery rate (FDR; peptide and protein level) and subsequently the MaxQuant output file (proteinGroup.txt) was loaded in the Perseus software, version 1.6.5.0 (Tyanova et al., 2016) for further statistical analysis. A minimum of 66% label-free quantification valid values per group was required for quantification. Missing values were imputed from the observed normal distribution of intensities for proteins expressed differentially. Then, a two-sample Student's *t*-test with a permutation-based FDR was performed. Only proteins with an adjusted p-value ≤ 0.05, FDR 5%, and log2 ratio of ≥ 1.5 or ≤ 0.67 were considered as deregulated following the same criteria as in other proteomic analyses (Peláez-García et al., 2015; Liu et al., 2017; Romero-Gavilán et al., 2022; Solis-Fernández et al., 2022). The protein identification by nLC-MS/MS was carried out in the Proteomics and Genomics Facility at the Biological Research Center Margarita Salas (CIB-CSIC).

Data sets have been submitted to the PRIDE proteomics identification database (Pérez-Riverol et al., 2019, 2022; Deutsch et al., 2020) and are accessible under accession no. (AC) PXD037250.

Functional classification of detected proteins was performed using the Uniprot database[1] and the Kyoto encyclopedia genes and genomes (KEGG) pathways database.[2]

2.8. Informatic analysis of predicted mRNA nucleotide sequence

Secondary structure predictions of the *dsrLL* and the *mrfp* transcripts were obtained by using the RNAfold web server (The ViennaRNA Web Services, version 2.4.18).

2.9. Cold shock experiment

For the analysis of the cold shock effect on strain survival in the presence or absence of dextran synthesis, *Lc. lactis* AV1n[pRCR21] was grown in MRSS or MRSG up to an $OD_{600\ nm}$ of 1.0 at 37°C. Then, the cells were sedimented by centrifugation (9,300 × g, 10 min, 4°C), resuspended in fresh MRSS or MRSG, diluted 1:10 in MRSS or MRSG, respectively, and grown at 37°C till the end of the exponential phase. The cells were then harvested by centrifugation at room temperature (9,300 × g, 3 min at 21°C), resuspended at 37°C in prewarmed MRSS or MRSG medium, respectively, and immediately chilled to 10°C (cold shocked) and maintained at this temperature for 18 h. Afterward, 1 ml of each culture was frozen at −80°C without any cryoprotective agent and maintained frozen for 3 days prior to the evaluation of cell survival after thawing.

The fluorescence of the mCherry protein in the bacterial cultures, before and after the exposure to 10°C, was measured by excitation at a wavelength of 587 nm and detection of emission at 610 nm using a Varioskan Flask System (Thermo Fisher Scientific), as previously described (Besrour-Aouam et al., 2019). Colony-forming units/ml were determined prior to and after the cold shock at 10°C and after thawing, frozen-cold pretreated cultures by serially diluting in saline solution (NaCl 0.85%), spread plating, and incubation overnight.

EPS concentration in supernatants of cultures subjected to the 10°C cold shocks was determined as described in the "2.1 Bacterial strain and growth medium" section. The experiments were performed in triplicate and mean values, with standard deviations, are presented.

2.10. Statistical analysis

All experiments were performed in triplicate. The results are expressed as means, with the corresponding standard deviations. For the analysis of mCherry fluorescence and survival of *Lc. lactis* AV1n[pRCR21] under cold shock, differences before and after treatment as well as between influence of carbon source were analyzed. The results were subjected to a one-way analysis of variance (ANOVA). A two factorial randomized complete block design with interactions was performed, with experiments on different days treated as random blocks. A p-value of ≤ 0.05 was considered significant. For the analysis of survival of strains under cold shock, a mean pairwise comparison of all conditions tested by a Tukey's test ($\alpha = 0.05$) was performed. All analyses were done with the R software, version 4.2.1 (R Core Team, 2022).

3. Results and discussion

3.1. Selection and generation of cultures for protein analysis

Our previous results indicated that *Lc. lactis* AV1n DsrLL, which synthetized dextran using sucrose as substrate, was involved in the response of the strain to low-temperature stress since this bacterium was able to produce higher levels of dextran at low temperature (Besrour-Aouam et al., 2019). Furthermore, we have shown that a transcriptional activation of the *dsrLL* gene expression in *Lc. lactis* takes place when the temperature decreases (Besrour-Aouam et al., 2019). This conclusion was inferred from the analysis of expression of the $P_{dsrLL-mrfp}$ transcriptional fusion in *Lc. lactis* AV1n[pRCR21] by measuring the fluorescence of the mCherry protein, the product of the *mrfp* gene at different temperatures.

Therefore, a proteomic analysis of the *Lc. lactis* AV1n[pRCR21] at different temperatures could provide information on alterations of the DsrLL levels encoded by the *dsrLL* gene present in the chromosome and, in addition, could estimate transcriptional activation of *dsrLL* gene expression by measurement of the mCherry levels encoded by the $P_{dsrLL-mrfp}$ carried by the pRCR21 plasmid. However, prior to performing the proteomic study, it was assessed a comparative analysis of growth and EPS production in the presence of sucrose by the parental AV1n and the recombinant AV1n[pRCR21] strains at 20°C, 30°C, and 37°C (**Figure 1**). Concerning the EPS production (measured when the cultures reached an $OD_{600\ nm} = 1.0$), almost the same levels were produced by the two strains at each of the three temperatures tested (4.1–4.5 g/L at 20°C, 3 g/L at 30°C, and 0.4 g/L at 37°C). Moreover, as previously observed (Besrour-Aouam et al., 2019), both strains were able to produce 10-fold higher levels of dextran at 20°C than at 37°C (Besrour-Aouam et al., 2019). Concerning to the growth, both bacteria showed the same pattern at the three temperatures tested. At 20°C, an optimal growth with the lowest μ was observed [$\mu = 0.27\ h^{-1}$ or $0.22\ h^{-1}$ for AV1n or AV1n(pRCR21) strains, respectively], which seems to stimulate

1 http://www.uniprot.org/

2 https://www.genome.jp/kegg/pathway.html

a self-adjustment for the bacteria to develop cold resistance mechanisms. Moreover, at 30°C and 37°C, for each strain, the growth rate was similar at both temperatures, but it was lower for the recombinant strain than for the parental strain (0.7 and 0.8 h^{-1} vs. 1.0 and 1.1 h^{-1}). However, a marked decrease in growth was not observed for *Lc. lactis* AV1n[pRCR21].

To gain insight into the response of *Lc. lactis* to low temperature, the analysis of the protein profile of *Lc. lactis* AV1n[pRCR21] was carried out in the presence of sucrose at 20°C and 37°C. Moreover, taking in consideration growth differences at these two temperatures, samples for preparations of total protein extracts were withdrawn when the cultures were in the same growth state, the transition from exponential to stationary phase (at $OD_{600\ nm} = 2.6$ or $OD_{600\ nm} = 2.8$, after 4 or 9 h of growth at 37°C or 20°C, respectively; **Figure 1**).

3.2. Functional analysis of the differentially expressed proteins

Previous analysis of the amino acid sequence of the DsrLL supported its extracellular location and revealed that the protein contains an LPXTG cell wall anchor domain at its carboxyl-terminal region. Thus, the overall analysis predicted that the *dsrLL* gene encodes an active DsrLL enzyme bound to the cell wall (Besrour-Aouam et al., 2019). Thus, the proteomic study was carried out by nanoHPLC-MS-MS analysis of cellular protein extracts after tryptic digestion. Comparison with the *Lc. lactis* database (Uniprot-TrEMBL) identified 1,385 proteins, of which 337 were differentially expressed. Two hundred and four were overproduced at 20°C and 133 were downregulated in comparison with the levels detected at 37°C. Only proteins with an adjusted p-value ≤ 0.05, FDR 5%, and log2 ratio of ≥ 1.5 or ≤ 0.67 were considered differentially expressed (**Supplementary Table 1**). Moreover, the increase in proteins levels varied as follows: (1) at 20°C, from 53-fold for the phosphonate ABC transporter substrate-binding protein to 1.5-fold for the UDP-galactopyranose mutase, and (2) at 37°C, from 17-fold for an uncharacterized protein (Ac: A0A1B1ZZ24) to 1.4-fold for the type I restriction enzyme R Protein.

In addition, 19 proteins were only detected at 20°C (**Supplementary Table 2**) and 9 proteins were only identified at 37°C (**Supplementary Table 3**). The first group included the DsrLL (Ac: A0A411G111) and a CspA cold shock protein (Ac: A0A1B2A2G5), and the second group included the ClpE protease and the DNA repair protein Rec O.

Figure 2 depicts a volcano plot of the distribution of the total proteins quantified with the upregulated at 20°C in green and the downregulated at 20°C in red. Among the upregulated proteins, only 28 showed a log2 ratio > 2, including the mCherry, and of the downregulated proteins, only 33 had a log2 ratio < -2, including the universal stress protein UspA, indicating that both 20°C and 37°C have a stressful effect on *Lc. lactis* AV1n.

In addition, a functional classification of differentially expressed proteins and determination of the biological pathway to which they belong were performed using the Uniprot database and the KEGG pathway database, respectively. The proteins were included in 14 categories, and the proportion of each one is shown in **Figure 3**. Proteins overexpressed at 20°C were mainly involved in genetic information processing (15%), protein biosynthesis (translation 14%), components of transport (14%), and cell division, cell wall, EPS, and fatty acids metabolism (13%), with DsrLL being included in this last category, as expected from our previous results (**Supplementary Tables 1, 2**). Proteins underexpressed at 20°C, apart from hypothetical proteins, were mainly involved in nucleotide (12%), carbohydrate (7%), and amino acid (11%) metabolism (**Supplementary Tables 1, 3**). The 19 proteins only detected at 20°C belonged to 8 categories (EPS biosynthesis, stress response, processing of genetic information, membrane transport, transcriptional regulators, general functions, protein biosynthesis, or uncharacterized) (**Supplementary Table 2**). Furthermore, the 9 proteins, only detected at 37°C, belonged to eight different categories (stress response, processing of genetic information, amino acid, carbohydrate or fatty acid metabolisms, cofactors of metabolism, electron transport chain, or uncharacterized) (**Supplementary Table 3**).

3.3. Analysis of key proteins involved in the regulation of the *dsrLL* expression transcript

In response to a temperature decrease, microorganisms adapt by triggering a physiological response, which includes the synthesis of cold shock proteins (Csps). 4 Csps encoding genes have been detected after the analysis of the *Lc. lactis* AV1n draft genome (Besrour-Aouam et al., 2021). Also, in this genome, we have detected 3 DEAD box RNA helicases (DBRH) coding genes, showing that this bacterium is genetically prepared to counteract cold stress. Consistent with this observation, one CspA was only detected at 20°C (Ac: A0A1B2A2G5), and a 40-fold upregulation of other CspA (A0A0N8VZ44), as well as a moderate upregulation of 3 DBRH (3. 7-, 1. 8-, and 1.5-fold upregulation of CshA, CshB, and YfmL, respectively), was observed at this temperature (**Supplementary Table 1**).

Furthermore, higher levels of GrpE (1.6-fold upregulation), DnaK chaperone (3.4-fold upregulation), and UspA universal stress protein (3.8-fold upregulation) were observed at 37°C (**Supplementary Table 1**). These proteins are implicated in heat shock response and their induction suggested that this temperature may impose a moderate heat stress for this bacterium (Champomier-Vergès et al., 2010; Rossi et al., 2016).

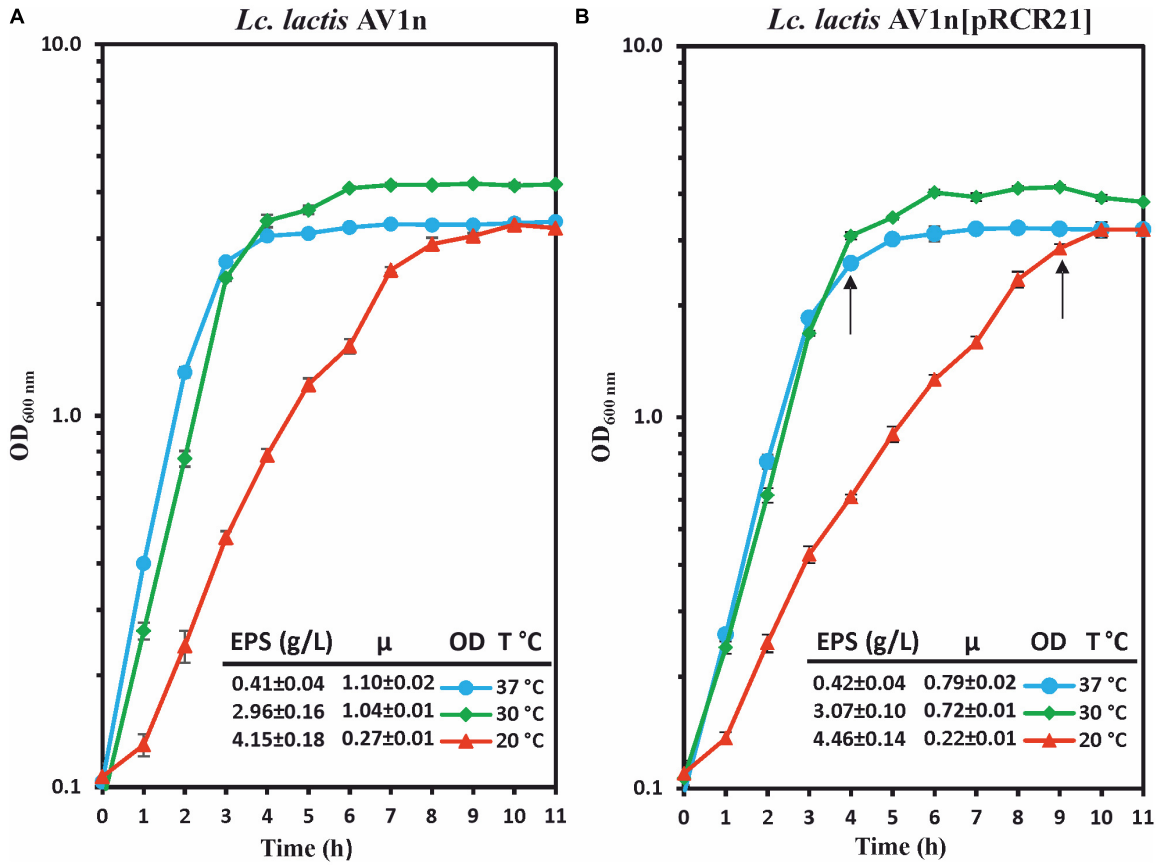

FIGURE 1
Analysis of growth and dextran production by *Lc. lactis* AV1n **(A)** and *Lc. lactis* AV1n[pRCR21] **(B)**. Bacteria were grown in MRSS at 20°C, 30°C, and 37°C. Levels of dextran produced by the LAB at $OD_{600\ nm} = 1.0$ are also depicted. The mean values and the standard deviation of three independent experiments are depicted. Arrows indicated the time at which samples for the proteomic analysis were taken.

DsrLL was only detected at 20°C, showing that low levels of Dsr catalyzing the synthesis of 0.4 g/L of dextran at 37°C were undetectable by the proteomic analysis performed here (**Supplementary Table 2**). Furthermore, these results confirmed, as expected, that a substantial upregulation of DsrLL levels takes place at 20°C, indicating that this enzyme plays a prominent role in the adaptation of *Lc. lactis* AV1n to low temperature.

The high levels of DsrLL detected at 20°C also correlate with our previous observation of a significant activation of transcription from P_{dsrLL} at low temperature (Besrour-Aouam et al., 2019). In addition, the proteomic analysis revealed a 6.2-fold increase of the mCherry protein at 20°C vs. 37°C, confirming the induction of DsrLL production at the transcriptional level from the P_{dsrLL} promoter. However, the increase in the mCherry levels at 20°C was lower than that of DsrLL (>50-fold), indicating that probably a more complex regulation of the *dsrLL* gene expression was taking place.

Cold-inducible promoters regulate the expression of genes coding for specific proteins that will ensure the survival of the bacterium. This is the case, for example, of the Csps proteins (Barria et al., 2013), which are found in LAB (Kim et al., 1998; Wouters et al., 1999). In addition to the regulation of the expression of genes encoding Csps, other cold-inducible genes seem to be controlled at several levels. It is thought to take place at the level of transcription, translation, and mRNA stability and to involve several characteristic genetic elements. The cold shock promoters generally include sequences rich in AT nucleotides (UP-element), located in the −65 region upstream of the transcription start site, which would stimulate gene transcription by interacting with the α subunit of the RNA polymerase at low temperature (Wouters et al., 2000; Singh et al., 2014). These promoters also possess an untranslated region (UTR) of approximately 100 nt between the promoter sequence and the ribosomal binding site (SD sequence) capable of modulating translation through the formation of secondary structures and mRNA–protein interactions (Singh et al., 2014).

We have previously detected the location of the start site of the *Lc. lactis* AV1n *dsrLL* transcript by primer extension (Besrour-Aouam et al., 2019). This allowed us to predict the

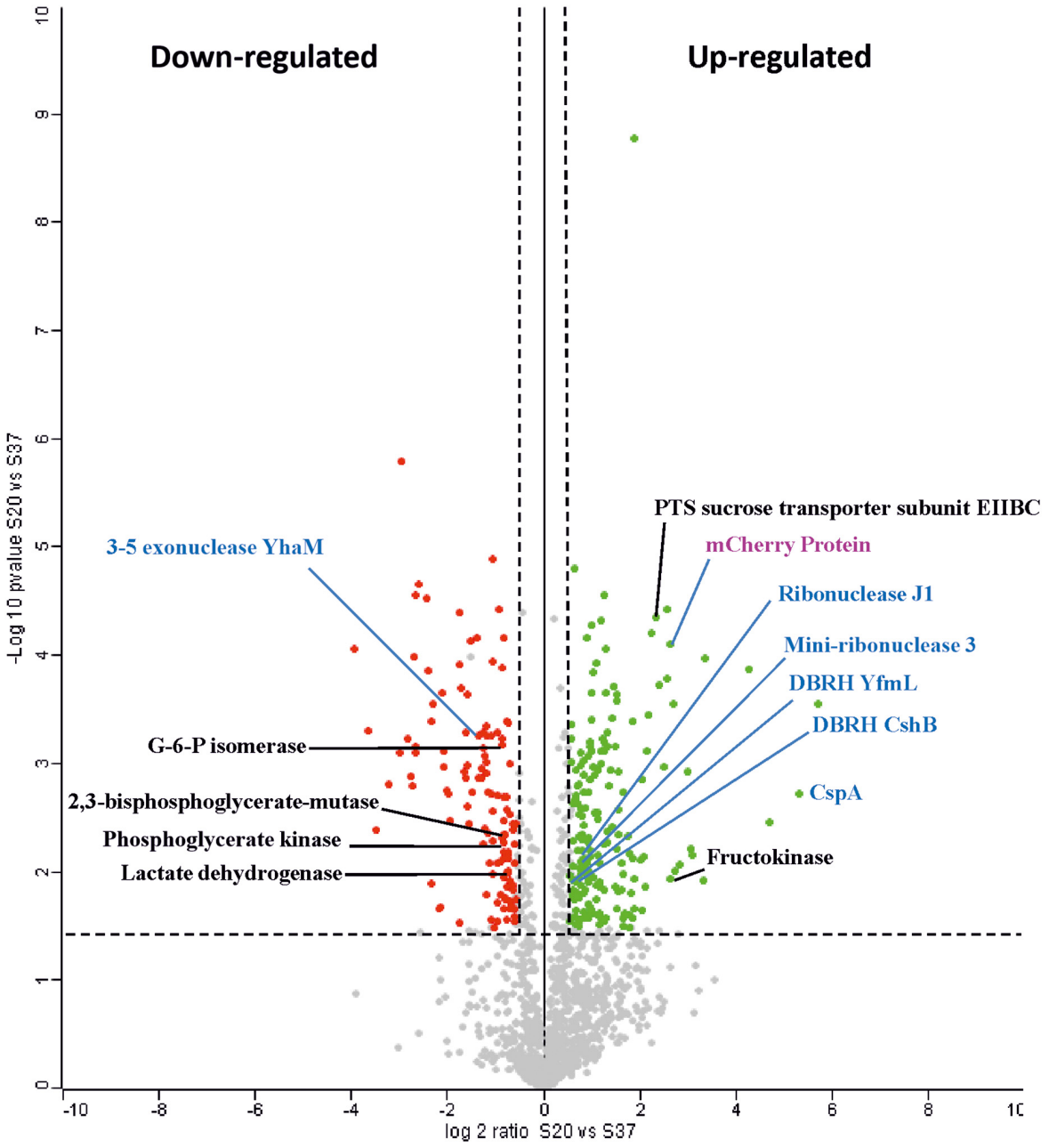

FIGURE 2
Volcano plot of upregulated and downregulated proteins in *Lc. lactis* AV1n[pRCR21] cultures grown to 20°C vs. 37°C. A test comparison of 1,385 quantified proteins was performed. Only proteins with a differential expression level in the range ± 10 are shown (**Supplementary Table 1**). The *x*-axis is log2 ratio of protein expression differences between two groups (S20°C vs. S37°C), and the *y*-axis is the *p*-value based on −log10. Red circles indicate differentially expressed proteins (downregulated), and green circles indicate differentially expressed (upregulated). Gray dots indicate non-differentially expressed proteins. The dashed horizontal line indicates the threshold of the adjusted *p*-value ≤ 0.05, FDR 5%, whereas dashed vertical lines enclose an area with a log2 ratio ± 0.58 (i.e., ratio ≥ 1.5 or ≤ 0.67). Blue color is used to group proteins involved in cold shock response, whereas black color is for those involved in carbohydrate metabolism. The mCherry protein is denoted in purple color.

−10 region of the P_{dsrLL} promoter and to determine the extent of its UTR in the bacterial chromosome (Besrour-Aouam et al., 2019; **Figure 4**). In the case of *Lc. lactis* AV1n[pRCR21], the P_{dsrLL} is present in two copies, one in the chromosome (**Figure 4A**) and the other in the pRCR21 plasmid (**Figure 4B**). Both promoters contain the same AT-rich sequence "TAaTGCTaaAttcg" similar to the consensus sequence of the "UP-element" (TACTNCTGGAAAGT) located upstream of the −10 region (**Figures 4A, B**). A UTR is also present, which will not be translated, of 141 nucleotides in the chromosome

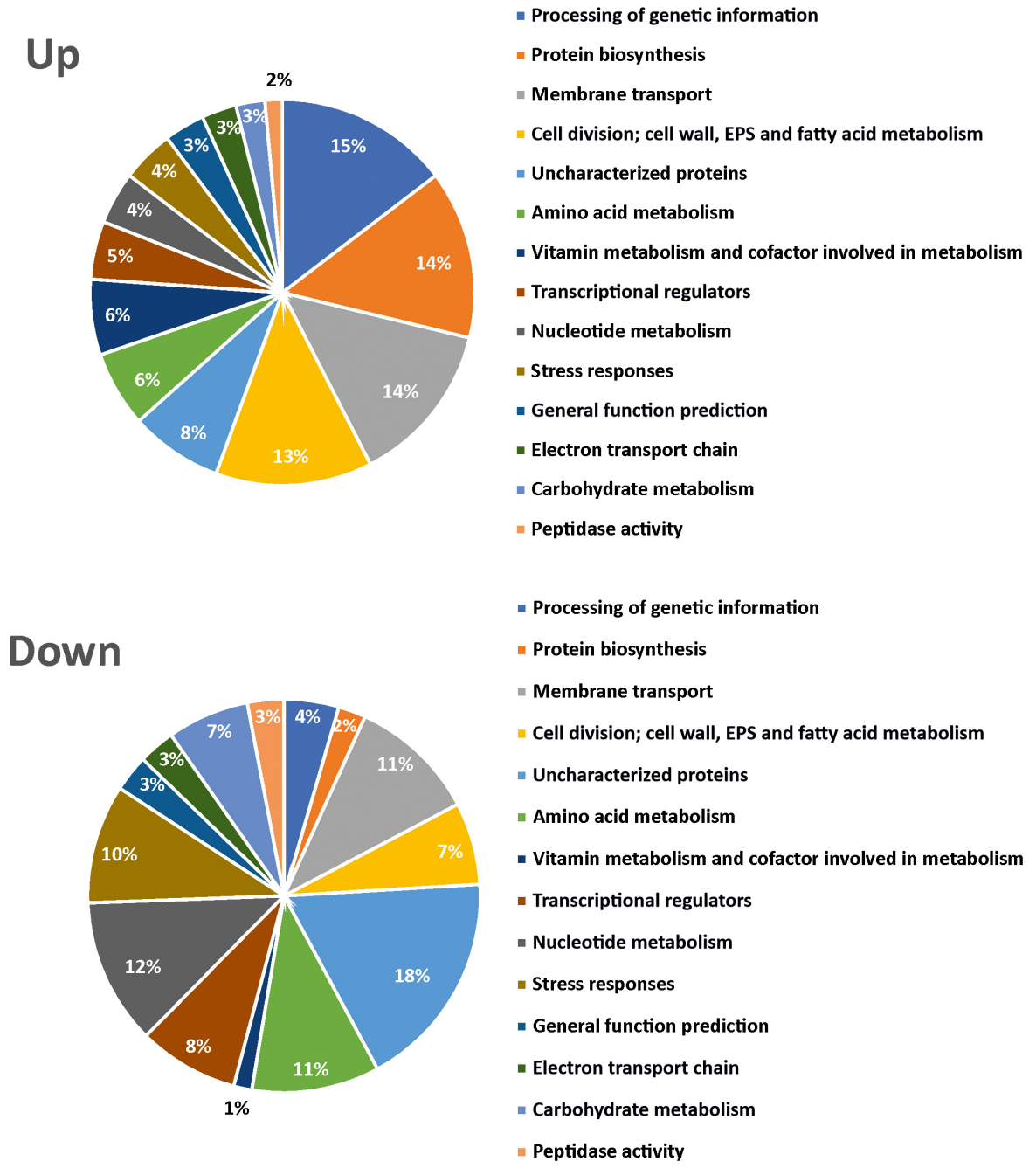

FIGURE 3
Pie chart representation in *Lc. lactis* AV1n[pRCR21] of upregulated and downregulated proteins at 20°C vs. 37°C. Fourteen different categories and their relative percentage are depicted.

and of 173 nucleotides in the plasmid, which both contain potential low-temperature regulation-related sequences, such as the cold box "TtAACAttTaC" close to the consensus sequence (TGAACAACTGC) and DEAD box "AtCgtTtGTA" very similar to the consensus sequence (AACAGTGGTA) (**Figure 4**), which could act as a binding site for the regulatory proteins Csp and DBRH (Singh et al., 2014).

These proteins act as RNA chaperones and are essential for efficient protein synthesis and cell survival at low temperatures. Moreover, both types of proteins are known to be overproduced at low temperatures in many Gram-positive and Gram-negative bacteria (Iost et al., 2013) and may play a role in the upregulation of DsrLL expression at the post-transcriptional level. In fact, as stated earlier, the overproduction of the 2

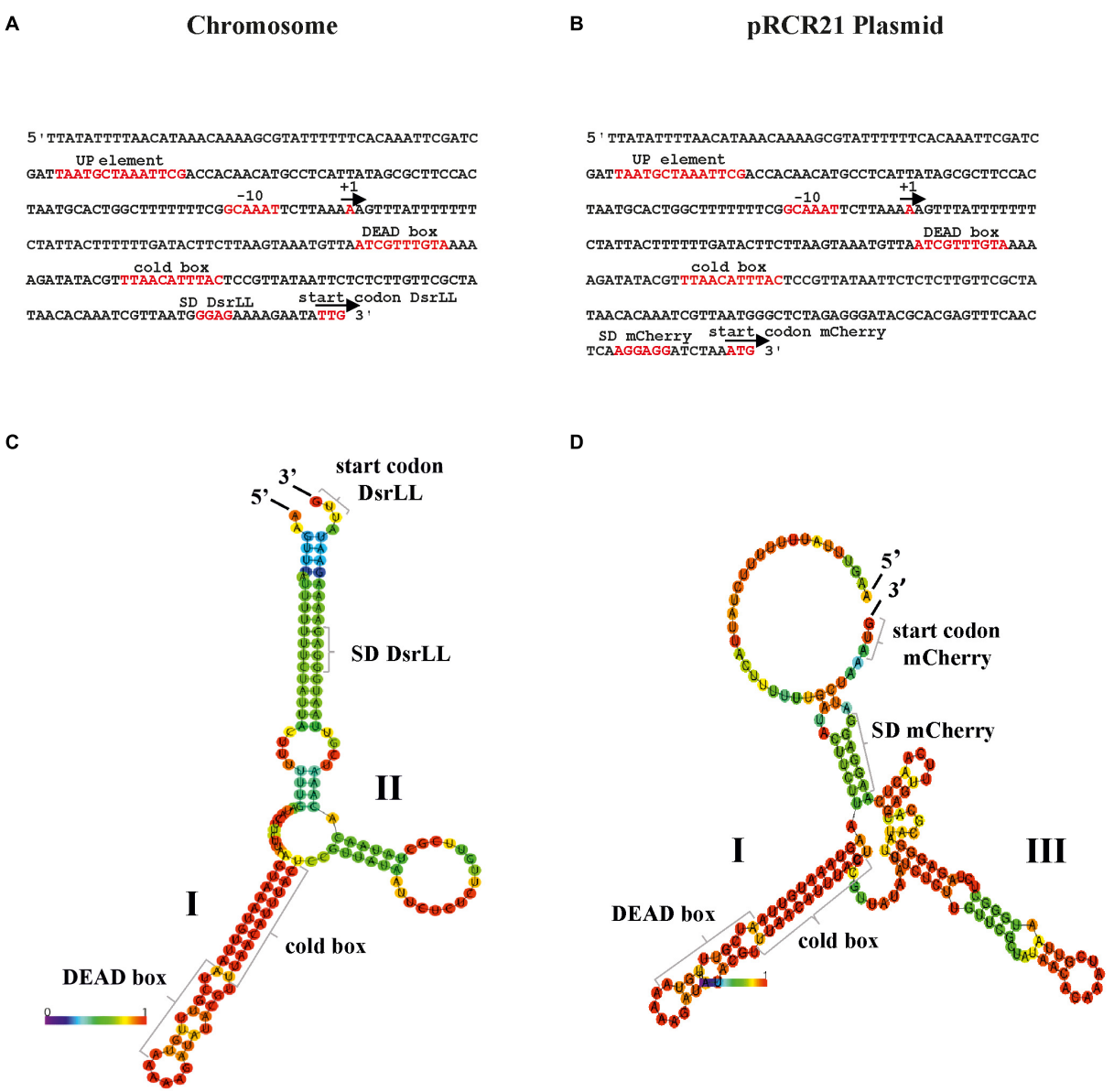

FIGURE 4
Regulatory signals for expression from P_{dsrLL} in *Lc. lactis* AV1n[pRCR21]. The P_{dsrLL} promoters of *Lc. lactis* AV1n and putative regulatory elements involved in their strength when present in the bacterial chromosome **(A)** or the pRCR21 plasmid **(B)** are shown. Also, the predictive folding of the UTR of the *dsrLL* **(C)** and *mrfp* **(D)** transcripts is depicted. In **(A,B)**, the + 1 transcription initiation site, −10 region, UP-element, cold box, DEAD box, as well as the Shine–Dalgarno (SD) sequences and the translation initiation sites of *dsrLL* **(C)** and *mrfp* **(D)** genes are framed in red. **(C,D)** Indicate the location and sequence of the 5′- and 3′-ends, secondary structures I and II in **(C)** and structures I and III in **(D)**, DEAD box, cold box, ribosomal binding sites, and translation initiation codon (start codon) of the d*srLL* **(C)** or *mrfp* **(D)** genes. The folding of the UTR from the chromosome and pRCR21 plasmid has a ΔG of −29.78 and −39.99 kcal/mol, respectively.

CspA designated as the major cold shock proteins (Beales, 2004), with a high induction level, as well as 3 DBRH (CshA, CshB, and YfmL) (**Supplementary Table 1**) was detected at 20°C.

The mRNAs, being single-stranded nucleic acids, would tend to fold and form secondary structures that prevent the efficient initiation of translation. Predictive folding of the UTR of the *dsrLL* (**Figure 4C**) and *mrfp* (**Figure 4D**) mRNAs with the RNAfold program revealed in both regions the presence of a complex secondary structure I, which contains the cold and DEAD boxes, followed by a small secondary structure II in the former transcript and a more complex secondary structure III in the latter, accompanied by differential ribosomal binding sites blockings in a double-stranded region. Moreover, the total ΔG of the chromosomal and plasmidic UTR folding was different (−29.78 kcal/mol vs. −39.99 kcal/mol).

Furthermore, the prediction of the folding of the entire transcripts (**Figure 5**) revealed that structure I was still present in both the *dsrLL* (**Figure 5A**) and the *mrfp* (**Figure 5B**), whereas instead of structures II and III, there were now predicted structures IV and V. Therefore, due to these differences, and as expected for the nature of the transcriptional (non-translational) $P_{dsrLL-mrfp}$ fusion, its expression was predominantly valid only to assess the strength of the promoter at different temperatures and not for the analysis of post-transcriptional regulations.

Concerning the potential post-transcriptional regulation of *dsrLL* gene expression in *Lc. lactis* AV1n, a detailed analysis of the 5′ and 3′ regions (enlarged in **Figure 6**) of the total transcript indicates that the complex structures I (carrying the CspA and DBRH proteins-binding boxes) and IV (carrying the ribosomal binding *SD* sequence and the DsrLL translational start codon) could be the target for endonucleases. Also, the existence of a transcriptional ρ independent terminator at the 3′-end of the *dsrLL* mRNA, which will not only be involved in the dissociation of RNA polymerase during transcription but could also partially prevent mRNA degradation by 3′–5′ exonucleases. In fact, among these exonucleases, the enzyme YhaM was detected as negatively expressed (2.3-fold downregulated) in *Lc lactis* AV1n at 20°C and has been previously studied in *Streptococcus pyogenes* (Broglia et al., 2020).

On these bases, the stabilization of the secondary structures at low temperatures can occur and folding of the UTR of the *dsrLL* mRNA could slow down the transcription performed by the RNA polymerase at the complex secondary structure. However, the binding to the DEAD and cold boxes of the abundant DBRH and CspA proteins at 20°C should prevent the formation of the secondary structure I. In fact, these 2 types of proteins may have a cooperative activity during cold stress response as reported previously in *Bacillus subtilis* (Hunger et al., 2005). The CshA exhibited the highest fold-change among the 3 DBRH overexpressed at 20°C (**Supplementary Table 1**), and recent studies revealed that this protein was able to auto-regulate its own expression by binding to the UTR of its mRNA (Salze et al., 2020). In addition, proteins CshA and CshB could destabilize the unfavorable secondary structure I by unwinding them in an ATP-dependent manner, then the single-stranded mRNA can successively be bound by Csps to prevent refolding until translation is initiated at the ribosome. Furthermore, DBRH CshA seems to play a more important role in RNA processing since *Enterococcus faecalis* Δ*CshA* gene mutant was the most stress impacted strain (Salze et al., 2020).

The control of mRNA turnover is essential in bacteria to allow rapid adaptation to stress environments. It directly affects protein synthesis by modulating the amount of mRNA available for translation. The decay of the transcripts is usually initiated by endoribonucleases, which produce intermediate fragments that are subsequently degraded by exoribonucleases. Structures I and IV could be stabilized in the total mRNA folding and they could be the target of an endonuclease. The proteomic analysis revealed increased levels of two endonucleases at 20°C: the ribonuclease J1 (1.9-fold upregulated) and the mini-ribonuclease III (2.8-fold upregulated). Ribonuclease J1 was the first ribonuclease identified in Gram-positive bacteria to be able to perform both types of activity, endonucleolytic and 5′ exonucleolytic, using a single catalytic site (Laalami and Putzer, 2011), and it could be involved in mRNA decay. Mini-ribonuclease III belongs to the class of ribonucleases that bind to and cleave double-stranded RNAs. It was identified as an enzyme involved in the maturation of 23S ribosomal RNA in *B. subtilis* (Redko et al., 2008). In addition, mini-ribonuclease III from different bacterial species can cleave long double-stranded RNAs, such as mRNA complex secondary structure, with a certain degree of sequence specificity (Glow et al., 2015).

In summary, it appears that Csps, DBRH, and ribonuclease(s), commonly known as cold shock response gene families in bacteria, tightly regulate RNA metabolism to adapt to a changing environment and to optimally activate *dsrLL* gene translation.

Thus, based on the current knowledge, and the study performed here, a regulatory model for the expression of DsrLL at 20°C and 37°C is proposed (**Figure 7**). At the transcriptional level, it seems that temperature-dependent alterations of the DNA negative supercoiling (Wouters et al., 2000) and DNA bending (Prosseda et al., 2010) result in a more efficient binding of the α subunit of the RNA polymerase to the UP element and as a consequence of higher synthesis of the *dsrLL* mRNA at 20°C. Then, at both temperatures, only transcripts that interact with Csps and DBRH will not contain structure I and will be correctly processed at structure IV by an endoribonuclease (presumably by mini-RNase III enzyme and/or ribonuclease J1). If J1 will be involved in the processing of structure IV, after its endonucleolytic incision at the structure, its 5′ exonucleolytic activity could generate an RNA species, in which the SD sequence could be exposed for ribosomal binding and subsequent translation of DsrLL, contributing to mRNA turnover, a role previously proposed for this ribonuclease (Condon, 2010). According to the proteomic results obtained for the various proteins involved in stability, processing, and degradation of these molecules will be substantially more abundant at 20°C than at 37°C. Consequently, translation of this mRNA species will be most efficient at low temperature. In addition, mRNA molecules containing the secondary structure I will be more abundant at 37°C, due to the lower levels of Csps and DBRH proteins. Also, they could be processing by endoribonucleases and degraded by exonucleases. In this context, the higher abundance of the 3′–5′ exonuclease YhaM at 37°C should potentiate degradation of untranslated mRNA molecules.

Finally, another post-translational factor seems to influence the coupling of the Dsr with a cold response. This enzyme acts extracellularly, and after being synthesized in the bacterial cytosol, it is translocated through the cell membrane due to

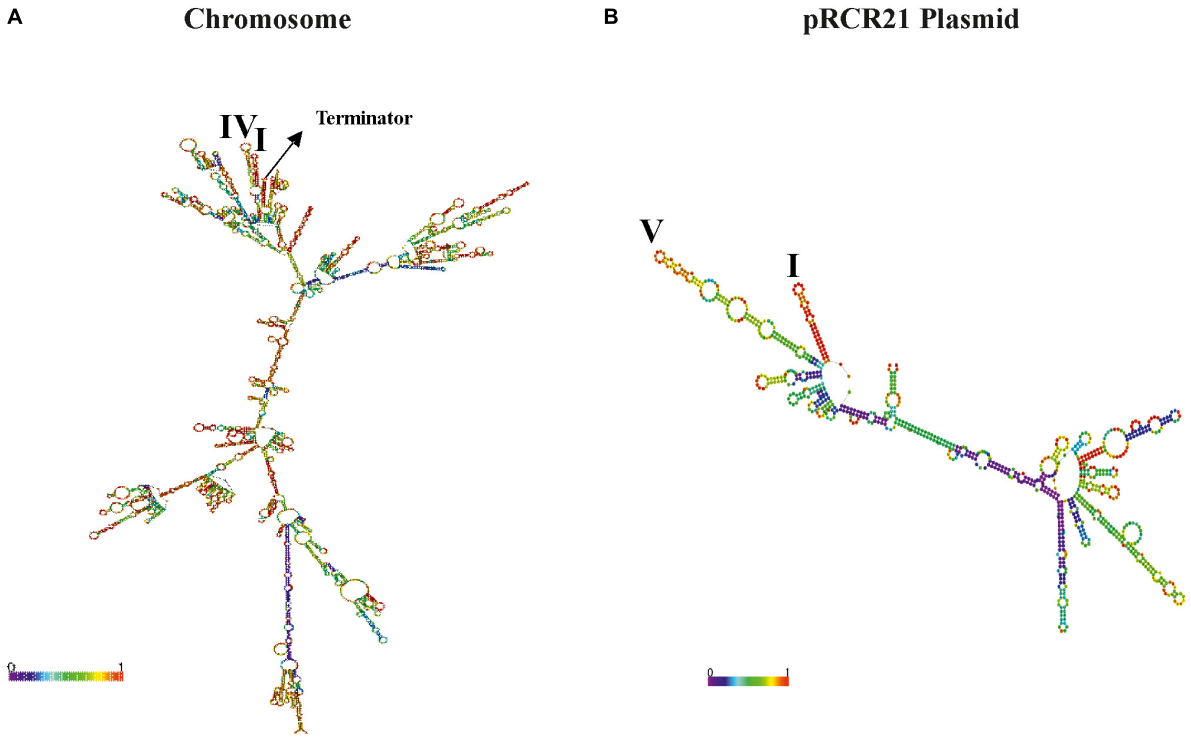

FIGURE 5
Predicted folding of the transcripts driven from P_{dsrLL} promoter in *Lc. lactis* AV1n[pRCR21]. **(A)** The chromosomal *drLL* mRNA is depicted, along with the location of complex secondary structures I and IV as well as the Rho-independent terminator. **(B)** The *mrfp* transcript encoded by pRCR21 is depicted, along with the location of complex secondary structures I and V.

a signal peptide sequence in the N-terminal region of the protein (Besrour-Aouam et al., 2019), which is cleaved off post-translationally to lead the protein to the secretory pathway, by a signal peptidase (Nielsen et al., 1997; van Roosmalen et al., 2004). Therefore, it is probable that the high levels of DsrLL synthesized at 20°C will be efficiently secreted because it was detected at this temperature a 2.9-fold increase of the peptidase I, accompanied by a 1.7-fold upregulation of the protein translocase subunits SecA and SecY, members of the secretory pathway (**Supplementary Table 1**).

3.4. Effect of cold temperature in *L. lactis* AV1n carbohydrates metabolism and cell wall development

In addition to the increase in DsrLL production in response to the drop in temperature, the bacterium possesses other cold resistance mechanisms, including the activation of metabolic pathways. Indeed, membrane transporters (for active transport and secretion of molecules) are among the group of proteins most overexpressed at 20°C (**Supplementary Tables 1, 2** and **Figure 2**) and include the PTS sucrose transporter subunit EIIBCA with a 5.9-fold increase at this temperature. This transporter ensures the internalization of sucrose, which was the only carbon source available in the medium in the proteomic study performed here.

Moreover, the machinery for the transport and/or metabolism of other disaccharides or unrelated monosaccharides seems to be downregulated in the absence of the substrates (**Supplementary Table 1**). Thus, at 20°C, a 2.3-fold decrease in the maltose phosphorylase was detected. Moreover, the PTS mannose transporter subunits IID (Ac: A0A1B2A3C0) and EIIAB (A0A1B2A1F3) were 1.7- and 1.8-fold downregulated, respectively, as well as the mannose-6-phosphate isomerase, whose levels were decreased by 6.4-fold. Therefore, it seems that in *Lc. lactis* AV1n, at low temperature, certain metabolic pathways, rather than others, are favored to ensure its survival (**Figure 8**).

Thus, in addition to the hydrolysis of some sucrose molecules by DsrLL, at 20°C, other molecules of this disaccharide pool could be internalized and then hydrolyzed by a sucrose-6-P hydrolase into glucose-6-P and fructose, monosaccharides that will be directed toward different pathways. Among the transcriptional regulators, downregulated at 20°C, a 2.4-fold decrease in the sucrose operon repressor ScrR (Ac: A0A1B1ZZZ0) was detected, which precedes the mannitol dehydrogenase and the fructokinase genes in the *Lc.*

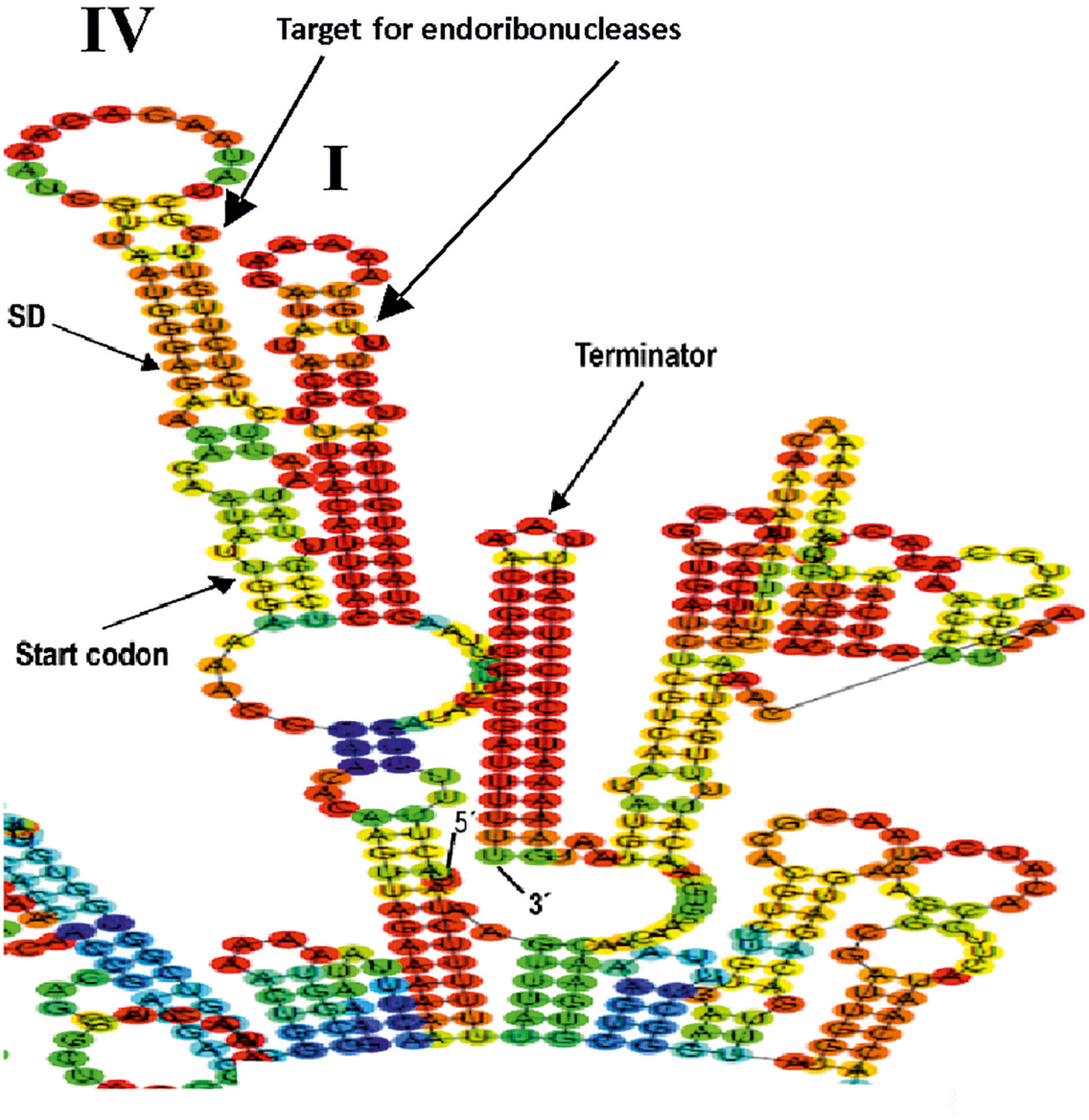

FIGURE 6
Details of predictive folding of the *dsrLL* transcript driven from P_{dsrLL} promoter encoded by in *Lc. lactis* AV1n[pRCR21] chromosome. The 5′- and 3′-ends of the mRNA are indicated. The sequences of the secondary structures I and IV, ribosomal binding site (SD), *dsrLL* translation initiation codon (start codon), and Rho-independent terminator are shown in detail.

lactis AV1n genome (Besrour-Aouam et al., 2021) and which seems to co-regulate them. It can be assumed that the decrease in the expression of this repressor would lead to a slight increase in the expression of mannitol dehydrogenase (not detected in the proteomic analysis) and thus in the production of mannitol, previously observed, when the bacterium was grown in the presence of sucrose (Besrour-Aouam et al., 2021). This implies that some of the fructose released during dextran synthesis and hydrolysis of internalized sucrose will be metabolized by this biosynthetic pathway (**Figure 8**). This probable increase in mannitol production triggered by the bacterium may be necessary for two reasons: (1) as an alternative pathway to regenerate NAD+ and (2) to stabilize lipid and protein structures of the cell membrane (Wisselink et al., 2002), a role that is consistent with the bacterial membrane integrity protection under environmental stress. Furthermore, the 1.8-fold decrease in glucose-6-P isomerase, detected at 20°C, implies that the fructose-6-P generated by fructose phosphorylation by the 6.2-fold upregulated fructokinase will be preferentially directed toward other pathways, in particular that of peptidoglycan synthesis (refer to details mentioned later), rather than glycolysis (**Figure 8**).

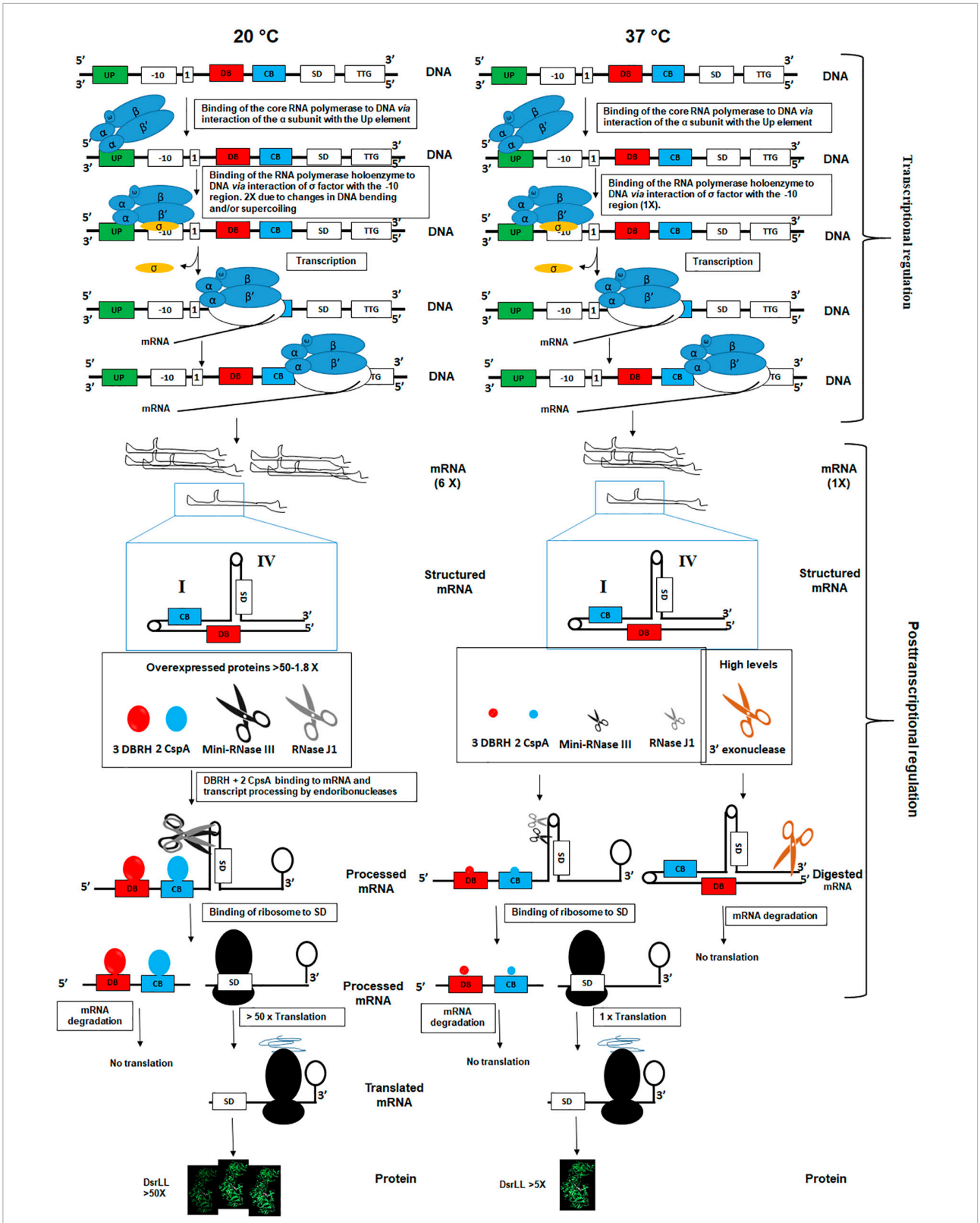

FIGURE 7
Model of transcriptional and post-transcriptional regulation of *dsrLL* gene expression in *Lc. lactis* at 20°C and 37°C. The influence of DNA bending and supercoiling at the two temperatures on the efficient utilization of promoter by RNA polymerase are indicated. Also, influence of mRNA folding vs. 3 DBRH and 2 CspA binding as well as ribonucleases binding and catalysis in the fate and turnover of the transcript at 20°C and 37°C are proposed.

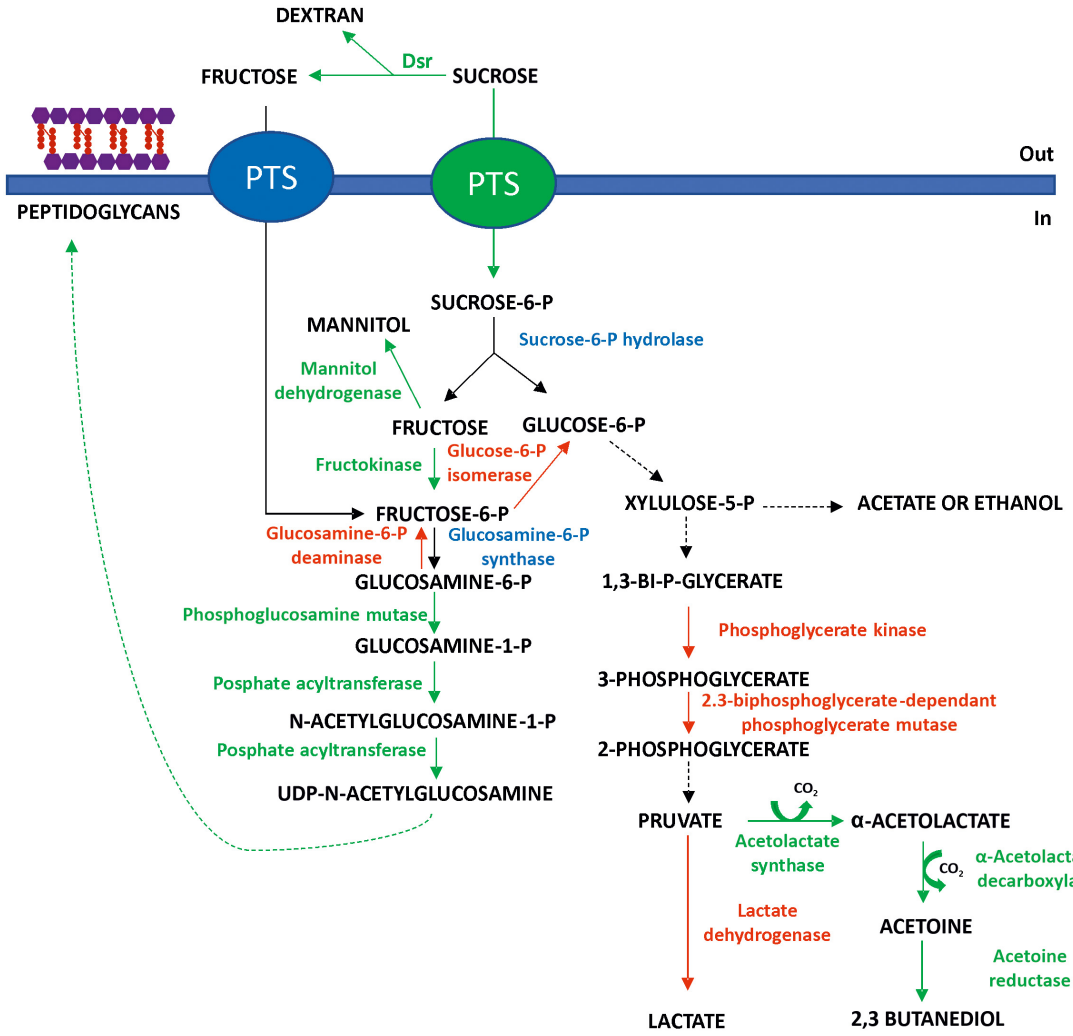

FIGURE 8
Prediction of major carbohydrate utilization pathways in *Lc. lactis* AV1n at 20°C in the presence of sucrose as the sole carbon source, suggested by proteomic analysis. Red indicates the downregulated enzymes, green indicates the upregulated ones, and blue indicates non-differentially expressed enzymes.

Moreover, the glucose-6-P glycolysis pathway should have been slowed down since a 1.5-fold under-regulation of the 2,3-biphosphoglycerate-dependant phosphoglycerate mutase was observed, which is present in two copies in the proteome (Ac: A0A0Q0U9Y5 and A0A1 × 0V3P9), as well as the 1.8-fold decrease in the phosphoglycerate kinase and the 1.5-fold downregulation of lactate dehydrogenase levels (**Supplementary Table 1**). These 3 enzymes are involved in the heterolactic fermentation pathway of the bacterium (**Figure 8**), and the detected reduction of the level of the enzymes, which should result in their lower catalysis, could contribute to the decrease in the bacterium growth rate observed at 20°C (**Figure 1**).

Furthermore, it seems that at 20°C, the pyruvate generated from glycolysis will be preferentially directed to the acetoin and 2,3-butanediol biosynthetic pathway (Xiao and Xu, 2007) since a 2.4-fold increase in the acetolactate synthase and the α-acetolactate decarboxylase levels was observed, as well as a 2.0-fold upregulation of acetoin reductase (**Figure 8**). This upregulation of the pathway will not only reduce acid production in the medium and thus limit acid stress but it will be also a mechanism that the bacterium has evolved to store energy. Furthermore, due to the reversible transformation between acetoin and 2,3-butanediol coupled with NAD^+/NADH conversion, this pathway has been considered to participate in the regulation of the NAD^+/NADH ratio in bacteria (Xiao and Xu, 2007).

In addition, despite the decrease in the growth rate of *Lc. lactis* AV1n[pRCR21], enzymes involved in the synthesis of peptidoglycans (**Figure 8**), a major component of the

cell wall of Gram-negative and Gram-positive bacteria, were up-regulated at 20°C. In particular, a 1.7- and 19.5-fold increase in phosphoglucosamine mutase and phosphate acyltransferase, 2 enzymes involved in the synthesis of UDP-*N*-acetylglucosamine, which is one of the key elements in peptidoglycan biosynthesis. By contrast, enzymes associated with the recycling of these molecules to the glycolysis pathway such as *N*-acetylglucosamine-6-phosphate deacetylase and glucosamine-6-phosphate deaminase were downregulated (4.3- and 3.4-fold decrease, respectively), probably to favor the cell wall biosynthetic pathway (**Figure 8**). This behavior has been previously observed for *Lactiplantibacillus plantarum* K25, in which the biosynthesis of its cell wall components was increased following exposure to cold (Liu et al., 2020).

In addition to the increase in proteins involved in cell wall synthesis, in *Lc. lactis* AV1n at 20°C a 1.6-fold increase in DNDP-4-keto-6-deoxy-glucose 2,3 dehydratase levels was observed (**Supplementary Table 1**), an enzyme involved in the heteropolysaccharide formation pathway of the bacterial capsule. This can be explained by the fact that the cell wall is the first line of defense against external stresses, and this mechanism took place in *Lc. lactis* AV1n synchronically with an increase in DsrLL expression.

The production of dextran in *Lc. lactis* included in the response to cold exposure could contribute to the decrease in bacterial growth detected at 20°C (**Figure 1**). This behavior has also been reported for *W. cibaria* 10 M, which showed a higher growth rate at 30°C; while Dsr expression was higher at 15°C (Hu and Ganzle, 2018). Moreover, proteomic analysis of *Sphingopyxis alaskensis* showed that several proteins related to the cell wall, membrane, EPS biosynthesis, and envelope biogenesis had a higher abundance at 10°C (Ting et al., 2010). Therefore, the generation of a biofilm matrix composed of dextran and the reinforcement of the cell wall could constitute a physical barrier protecting the integrity of the cell membrane at low temperatures.

Other resistance mechanisms developed by the bacterium have also been observed in this study, and involve effects in nucleotide catabolism from nucleic acids and recycling pathways, being energetically less costly than their *de novo* synthesis, are probably favored in the bacterium in periods of stress. Also, there were negatively regulated at 20°C, the enzymes encoded by the operon involved in the *de novo* biosynthesis of pyrimidine nucleotides (a 2. 2-, 1. 8-, 1. 6-, and 1.8 decrease, respectively, for the aspartate carbamoyltransferase, the dihydroorotase, the carbamoyl-phosphate synthase large chain, and the dihydroorotate dehydrogenase) as well those enzymes responsible for purine nucleotides biosynthesis (1.7-fold downregulation for both the glutamine amidotransferase and the adenylosuccinate lyase) (**Supplementary Table 1**). By contrast, the adenine phosphoribosyltransferase involved in the salvage pathways of these nitrogenous bases was 2.5-fold positively regulated (**Supplementary Table 1**).

Finally, the increase in the machinery involved in protein translation represents one of the most upregulated proteins (14%) at 20°C (**Figure 3**), correlating with a need for newly synthesized proteins (membrane transporters, cell wall components), which are the critical biological process for cell viability.

3.5. Oxidative stress-related protein

Oxygen is considered one of the critical factors affecting the survival of anaerobic aerotolerant LAB. It is known that under cold stress conditions, oxygen solubility increases, generating an increase in reactive oxygen species (ROS), leading to oxidative stress (Tribelli and Lopez, 2018). When accumulated, ROS can lead to damage in proteins, DNA, and lipids and thus trigger the expression of specific proteins to protect cell machinery. In this context, a range of antioxidant enzymes was detected as overexpressed at 20°C (**Supplementary Table 1**), such as NADH oxidase (5.0-fold upregulation), glutathione peroxidase (3.4-fold upregulation), and a thiol peroxidase (1.7-fold upregulation). In addition, the glutathione reductase and other thiol peroxidase were only detected at 20°C (**Supplementary Table 2**), indicating that *Lc. lactis* AV1n is undergoing real oxidative stress at low temperatures. NADH oxidase is an O_2-consuming enzyme, generally involved in the aerobic metabolism of microaerophilic bacteria, responsible for the rapid removal of O_2, and plays a crucial role in maintaining the intracellular redox balance (Feng and Wang, 2020). Interestingly, another NADH oxidase that is involved in the electron transfer chain was only detected at 37°C, indicating that oxidative stress also takes place at this temperature.

In addition, the glutathione redox cycle allows the protection of the cells against oxidative stress as previously described for *Lactobacillus fermentum* ME-3 (Kullisaar et al., 2010). In this cycle, glutathione is oxidized by glutathione peroxidase to a disulfide, which can be reduced back to glutathione by glutathione reductase (Feng and Wang, 2020). In this context, *Lc. lactis* AV1n overproduces the two enzymes involved in the glutathione redox cycle at 20°C, a result supporting that the bacterium is subjected to oxidative stress at this temperature.

Moreover, the upregulation of the 3 DBRH at 20°C can be assigned to the presence of oxidative stress in addition to the cold response (Salze et al., 2020).

Furthermore, at 20°C, a 2.3-fold increase was observed in the demethylmenaquinone methyltransferase (Ac: A0A0Q0U6R9), an enzyme that catalyzes the final step of menaquinone (vitamin K_2) biosynthesis. Also, at this low temperature, a 3.1-fold increase in cytochrome O ubiquinol oxidase (Ac: A0A1 × 0V2Y4) was observed, an enzyme

involved in the synthesis of ubiquinone (coenzyme Q). Both vitamin K_2 and coenzyme Q are part of the electron transport chain of aerobic respiratory metabolism, and although LAB has historically been classified as anaerobic, aerotolerant, and unable to obtain energy through respiration, a variety of them contain rudimentary electron transport chains that can be reconstituted by the addition of either heme alone or combined heme and menaquinone to the growth medium. Therefore, these activated electron transport chains at 20°C could lead to higher biomass production, provide a contribution to make the bacteria more resistant to oxidative and acidic stresses, and support prolonged survival at low temperatures through respiration (Brooijmans et al., 2009). It can, thus, be assumed that the upregulation of the synthesis of these molecules is clearly an additional defense against oxidative stress for *Lc. lactis* AV1n (Papadimitriou et al., 2016).

3.6. Behavior and survival of *Lc. lactis* AV1n[pRCR21] under cold shock

Previous studies have shown that, at extreme temperatures (e.g., −20°C), cell viability was significantly improved, when bacteria were previously cold shocked, allowing resistance mechanisms to be developed for cell adaptation to the new conditions (Kim and Dunn, 1997). Among these mechanisms, the results reported here indicated that the dextran produced by *Lc. lactis* could provide the bacterium protection of its cellular integrity against cold shock stress by constituting a physical barrier. To test this hypothesis, *Lc. lactis* AV1n[pRCR21] was subjected to a two-stage cold shock by: (1) an abrupt shift of exponentially growing cultures from 37°C to 10°C and incubation of the bacterium at this latter temperature for 18 h and (2) a subsequent transfer of the cultures at −80°C and their maintenance frozen during 3 days. These bacterial cold shocks were performed in the presence or absence of dextran production (bacterial cultures in MRSS or MRSG medium). Then, cell survival was assayed by plate counting prior to transfer of the cultures at 10°C, after the cold shock at 10°C, and after thawing the frozen cultures (**Figure 9**). Moreover, before and after the exposure to 10°C, the transcription of the *dsrLL* gene was estimated by measurement of the mCherry fluorescence emitted by the bacteria and expressed from the *mrfp* gene fussed to the P_{dsrLL} promoter (**Table 1**). In addition, the levels of dextran produced during the 10°C cold shocks were determined.

Comparison of the mCherry fluorescence from cultures grown in MRSS and MRSG revealed that before and after the cold shock, the presence in the medium of sucrose, instead of glucose, resulted in a 2.7- and 2.6-fold increase in transcription from the P_{dsrLL} promoter, supporting previous results obtained when testing the influence of carbon source in cultures grown at 37°C or 20°C (Besrour-Aouam et al., 2019). In addition, a low and not significant ($p = 0.09$) increase in fluorescence was observed corrected for the biomass after the temperature downshifts in both growth media (in MRSS, 0.60 ± 0.03 after vs. 0.54 ± 0.05 before the cold shock, as well as in MRSG 0.22 ± 0.01 after vs. 0.21 ± 0.14 before cold shock), showing that the bacterium exposure to 10°C for 18 h did not result in high activation of transcription from P_{dsrLL}. The interaction between "Before cold and After cold" in either MRSS or MRSG was not significant ($p = 0.09$). However, the production of dextran was detected (0.33 ± 0.06 g/L) during the 18 h incubation at 10°C in MRSS, showing that the DsrLL was, in fact, active in this condition since the dextran previously produced by the bacterium at 37°C was removed by sedimentation and resuspension of the cells in fresh MRSS medium prior to the cold shock treatment.

In general, upon temperature downshift, there is a transient arrest of bacterial cell growth for a few hours called the acclimation phase when the bacteria adapt to the new environment by producing cold-inducible proteins. After this phase, cells become adapted to low temperatures and resume growth but at a slower rate (Barria et al., 2013). Analysis of cell survival of *Lc. lactis* AV1n[pRCR21] revealed better adaptation of the bacterium to the cold shock in MRSS than in MRSG (**Figure 9**). In fact, in the presence of glucose cells, growth did not take place during the 18 h incubation period at 10°C since the number of viable cells did not increase ($6.67 \times 10^8 \pm 0.29 \times 10^8$ cfu/ml before vs. $6.78 \times 10^8 \pm 0.25 \times 10^8$ cfu/ml after cold shock) (**Figure 9**). However, in the presence of sucrose, the bacterium grew during the 10°C cold shocks, and the number of viable cells increased 2-fold, with statistical significance ($p = 2e^{-5}$), from $6.38 \times 10^8 \pm 0.81 \times 10^8$ to $1.25 \times 10^9 \pm 0.90 \times 10^8$ cfu/ml (**Figure 9**). According to the results presented here, it seems that the acclimation phase for *Lc. lactis* AV1n took place during the 18 h at 10°C in the presence of sucrose and not of glucose, and this difference could be partially attributed to the production of dextran by the strain during growth at 10°C in MRSS, which should support better adaptation to the cold temperature.

We also observed that cell viability after 3 days of freezing at −80°C was better for cold-pretreated cultures in MRSS (93.6% survival) than those in MRSG (65.2% survival) (**Figure 9**), supporting also the potential cryoprotective role of the dextran produced by the bacterium. In fact, this activity has already been demonstrated for HePS produced by other bacteria, e.g., the polymer synthesized by *Pseudomonas* sp. ID1, which was able to preserve bacterial cell structure and contribute to the maintenance of bacterial viability after exposure to freezing temperature (Carrión et al., 2015). Also, the HePS from *Colwellia psychrerythraea* 34H showed a cryoprotection effect by having a significant inhibitory effect on ice recrystallization (Casillo et al., 2017). However, it should be stated that dextran formation is a multifactorial extracellular process and the amount of dextran may also

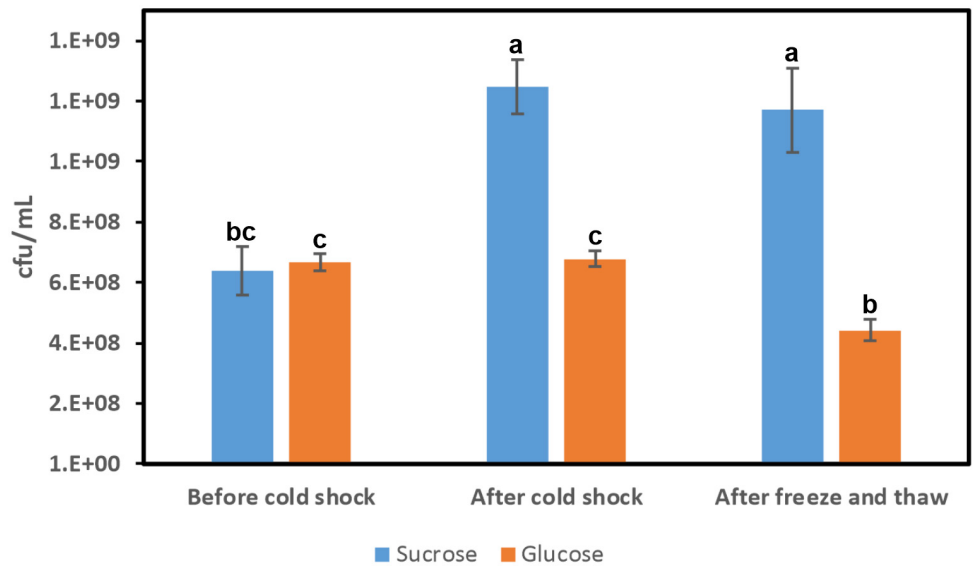

FIGURE 9
Influence of cold shock in *Lc. lactis* AV1n[pRCR21] cell viability. Cultures were grown in MRSS or MRSG at 37°C (before cold shock), after exposure at 10°C for 18 h (after cold shock), and during 3 days frozen period at −80°C, thawed (freeze and thaw). Cell survival was determined by plate counting at the states indicated. The means of three determinations and the standard deviations are indicated. Different superscript letters indicate that the levels differed significantly ($p = 2e^{-5}$).

TABLE 1 Analysis of fluorescence and growth of *Lc. lactis* AV1n[pRCR21] before and after 10°C cold shock.

Condition	Growth medium	Fluorescence (a.u.)	$OD_{600\ nm}$	[1]Ratio Fl/OD	[2]Ratio Fl/OD in MRSS Fl/OD in MRSG
After cold shock	MRSS	4.96 ± 0.20	8.35 ± 0.58	0.60 ± 0.03^{A}	2.62^{a}
Before cold shock	MRSS	3.43 ± 0.34	6.63 ± 0.25	0.54 ± 0.05^{A}	2.73^{a}
After cold shock	MRSG	1.61 ± 0.31	7.40 ± 0.75	0.22 ± 0.01^{B}	
Before cold shock	MRSG	0.93 ± 0.60	4.43 ± 0.30	0.21 ± 0.14^{B}	

The bacterium was grown at 37°C in either MRSS or MRSG and then subjected to 10°C cold shocks for 18 h. The means of three determinations and the standard deviations are indicated. [1]The fluorescence (Fl) of the cultures was corrected taking in account the biomasses of the cultures estimated by the $OD_{600\ nm}$ (OD) and calculated as the ratio Fl/OD. Different superscript letters indicate that the levels differed significantly ($p \leq 2e^{-3}$). Differences between "before cold" in MRSS and MRSG ($p = 2e^{-3}$) and between "after cold" in MRSS and MRSG ($p = 8e^{-6}$) were significant. [2]The Influence of growth medium in levels of fluorescence was estimated by calculating the ratio of Fl/OD.

arise from other factors and not necessarily from higher enzyme concentration, e.g., slower extracellular acidification during growth at low temperature. Therefore, further studies are needed to clarify the cryoprotectant potential effect of the dextran.

4. Conclusion

From the proteomic analysis performed here, it can be inferred that the cold adaptation mechanism used by *Lc. lactis* AV1n is mainly based on an improvement of its protein synthesis capacity, an increase in dextran production, and peptidoglycan biosynthesis in order to protect the cells from external aggression. It also consists of an energy saving by the decrease in the growth rate mediated not only by the decrease in the carbohydrate metabolism and its orientation toward the production of storage molecules but also by the preferential use of molecule recycling pathways, rather than their *de novo* synthesis.

The adaptation of LAB to low temperatures contributes to the industrial performance of the strains. Thus, a better understanding of reactions at low temperatures can contribute to the optimization of fermentation processes at cold temperatures, refrigerated storage of fermented products, and conservation conditions of starter cultures, thus enhancing the biotechnological potential of strains for industrial applications. Therefore, the knowledge gained from this work allowed a better understanding of the role of DsrLL in the response of *Lc. lactis* to low temperature and it could contribute to a better future use of strains of the genus *Leuconostoc* as probiotics for the development of new functional foods. Moreover, this work

by the *in vivo* and *in silico* analysis of DsrLL expression should provide a better understanding of the complex regulation of gene expression at low temperatures in *Lc. lactis*.

Data availability statement

The datasets presented in this study are available at the following link: https://www.ebi.ac.uk/pride/archive/projects/PXD037250.

Author contributions

NB-A contributed to all parts of the experimental work and wrote a draft of the manuscript. VL performed the proteomic analysis. MM designed the experiments and interpreted the results. AH-A and AN contributed to the study design. PL participated in the study conception, data interpretation, and generated the final version of the manuscript. H-IO participated in study conception, data interpretation, and manuscript revision. All authors have read and approved the final manuscript.

Funding

This study was supported by the Spanish Ministry of Science, Innovation and Universities (grant no. RTI2018-097114-B-I00) and the Tunisian Ministry of Higher Education and Scientific Research.

Acknowledgments

We thank Guillermo Padilla Alonso for his valuable assistance in the biostatistical analysis and Stephen Elson for the critical reading of the manuscript.

Conflict of interest

The authors declare that the research was conducted in the absence of any commercial or financial relationships that could be construed as a potential conflict of interest.

Publisher's note

Supplementary material

The Supplementary Material for this article can be found online at: https://www.frontiersin.org/articles/10.3389/fmicb.2022.1077375/full#supplementary-material

References

Anastasio, M., Pepe, O., Cirillo, T., Palomba, S., Blaiotta, G., and Villani, F. (2010). Selection and use of phytate-degrading LAB to improve cereal-based products by mineral solubilization during dough fermentation. *J. Food Sci.* 75, 28–35. doi: 10.1111/j.1750-3841.2009.01402.x

Barria, C., Malecki, M., and Arraiano, C. M. (2013). Bacterial adaptation to cold. *Microbiology* 159(Pt 12), 2437–2443. doi: 10.1099/mic.0.052209-0

Beales, N. (2004). Adaptation of microorganisms to cold temperatures, weak acid preservatives, low pH, and osmotic stress: A review. *Compr. Rev. Food Sci. Food Saf.* 3, 1–20. doi: 10.1111/j.1541-4337.2004.tb00057.x

Besrour-Aouam, N., Fhoula, I., Hernández-Alcántara, A. M., Mohedano, M. L., Najjari, A., Prieto, A., et al. (2021). The role of dextran production in the metabolic context of *Leuconostoc* and *Weissella* Tunisian strains. *Carbohydr. Polym.* 253:117254. doi: 10.1016/j.carbpol.2020.117254

Besrour-Aouam, N., Mohedano, M. L., Fhoula, I., Zarour, K., Najjari, A., Aznar, R., et al. (2019). Different modes of regulation of the expression of dextransucrase in *Leuconostoc lactis* AV1n and *Lactobacillus sakei* MN1. *Front. Microbiol.* 10:959. doi: 10.3389/fmicb.2019.00959

Brooijmans, R., Smit, B., Santos, F., van Riel, J., de Vos, W. M., and Hugenholtz, J. (2009). Heme and menaquinone induced electron transport in lactic acid bacteria. *Microb. Cell Factories* 8. doi: 10.1186/1475-2859-8-28

Broglia, L., Lécrivain, A. L., Renault, T. T., Hahnke, K., Ahmed-Begrich, R., Le Rhun, A., et al. (2020). An RNA-seq based comparative approach reveals the transcriptome-wide interplay between 3′-to-5′ exoRNases and RNase Y. *Nat. Commun.* 11:1587. doi: 10.1038/s41467-020-15387-6

Carrión, O., Delgado, L., and Mercade, E. (2015). New emulsifying and cryoprotective exopolysaccharide from Antarctic *Pseudomonas* sp. ID1. *Carbohydr. Polym.* 117, 1028–1034. doi: 10.1016/j.carbpol.2014.08.060

Casillo, A., Parrilli, E., Sannino, F., Mitchell, D. E., Gibson, M. I., Marino, G., et al. (2017). Structure-activity relationship of the exopolysaccharide from a psychrophilic bacterium: A strategy for cryoprotection. *Carbohydr. Polym.* 156, 364–371. doi: 10.1016/j.carbpol.2016.09.037

Champomier-Vergès, M.-C., Zagorec, M., and Fadda, S. (2010). "Proteomics: A tool for understanding lactic acid bacteria adaptation to stressful environments," in *Biotechnology of lactic acid bacteria: Novel applications*, eds F. Mozzi, R. Raya, and G. Vignolo (New York, NY: Wiley-Blackwell), 57–72.

Claverie, M., Cioci, G., Vuillemin, M., Monties, N., Roblin, P., Lippens, G., et al. (2017). Investigations on the determinants responsible for low molar mass dextran formation by DSR-M dextransucrase. *Am. Chem. Soc. Catal.* 7, 7106–7119. doi: 10.1021/acscatal.7b02182

Condon, C. (2010). What is the role of RNase J in mRNA turnover? *RNA Biol.* 7, 316–321. doi: 10.4161/rna.7.3.11913

Cox, J., and Mann, M. (2008). MaxQuant enables high peptide identification rates, individualized p.p.b.-range mass accuracies and proteome-wide protein quantification. *Nat. Biotechnol.* 26, 1367–1372. doi: 10.1038/nbt.1511

Deutsch, E. W., Bandeira, N., Sharma, V., Perez-Riverol, Y., Carver, J. J., Kundu, D. J., et al. (2020). The ProteomeXchange consortium in 2020: Enabling 'big data' approaches in proteomics. *Nucleic Acids Res.* 48, D1145–D1152. doi: 10.1093/nar/gkz984

Dubois, M., Gilles, K. A., Hamilton, J. K., Rebers, P. A., and Smith, F. (1956). Colorimetric method for the determination of sugars and related substances. *Anal. Chem.* 28, 350–356. doi: 10.1021/ac60111a017

Feng, T., and Wang, J. (2020). Oxidative stress tolerance and antioxidant capacity of lactic acid bacteria as probiotic: A systematic review. *Gut Microbes* 12:1801944. doi: 10.1080/19490976.2020.1801944

Galle, S., Schwab, C., Dal Bello, F., Coffey, A., Ganzle, M. G., and Arendt, E. K. (2012). Influence of in-situ synthesized exopolysaccharides on the quality of gluten-free sorghum sourdough bread. *Int. J. Food Microbiol.* 155, 105–112. doi: 10.1016/j.ijfoodmicro.2012.01.009

Germaine, G. R., and Schachtele, C. F. (1976). *Streptococcus mutans* dextransucrase: Mode of interaction with high-molecular-weight dextran and role in cellular aggregation. *Infect. Immun.* 13, 365–372. doi: 10.1128/iai.13.2.365-372.1976

Glow, D., Pianka, D., Sulej, A. A., Kozlowski, L. P., Czarnecka, J., Chojnowski, G., et al. (2015). Sequence-specific cleavage of dsRNA by Mini-III RNase. *Nucleic Acids Res.* 43, 2864–2873. doi: 10.1093/nar/gkv009

Hu, Y., and Ganzle, M. G. (2018). Effect of temperature on production of oligosaccharides and dextran by *Weissella cibaria* 10M. *Int. J. Food Microbiol.* 280, 27–34. doi: 10.1016/j.ijfoodmicro.2018.05.003

Hunger, K., Beckering, C. L., Wiegeshoff, F., Graumann, P. L., and Marahiel, M. A. (2005). Cold-induced putative DEAD box RNA helicases CshA and CshB are essential for cold adaptation and interact with cold shock protein B in *Bacillus subtilis*. *Am. Soc. Microbiol.* 188, 240–248. doi: 10.1128/JB.188.1.240-248.2006

Iost, I., Bizebard, T., and Dreyfus, M. (2013). Functions of DEAD-box proteins in bacteria: Current knowledge and pending questions. *Biochim. Biophys. Acta* 1829, 866–877. doi: 10.1016/j.bbagrm.2013.01.012

Juvonen, R., Honkapaa, K., Maina, N. H., Shi, Q., Viljanen, K., Maaheimo, H., et al. (2015). The impact of fermentation with exopolysaccharide producing lactic acid bacteria on rheological, chemical and sensory properties of pureed carrots (*Daucus carota* L.). *Int. J. Food Microbiol.* 207, 109–118. doi: 10.1016/j.ijfoodmicro.2015.04.031

Katina, K., Maina, N. H., Juvonen, R., Flander, L., Johansson, L., Virkki, L., et al. (2009). *In situ* production and analysis of *Weissella confusa* dextran in wheat sourdough. *Food Microbiol.* 26, 734–743. doi: 10.1016/j.fm.2009.07.008

Kim, W. S., and Dunn, N. W. (1997). Identification of a cold shock gene in lactic acid bacteria and the effect of cold shock on cryotolerance. *Curr. Microbiol.* 35, 59–63. doi: 10.1007/s002849900212

Kim, W. S., Khunajakr, N., Ren, J., and Dunn, N. W. (1998). Conservation of the major cold shock protein in lactic acid bacteria. *Curr. Microbiol.* 37, 333–336.

Klahan, P., Okuyama, M., Jinnai, K., Ma, M., Kikuchi, A., Kumagai, Y., et al. (2018). Engineered dextranase from *Streptococcus mutans* enhances the production of longer isomaltooligosaccharides. *Biosci. Biotechnol. Biochem.* 82, 1480–1487. doi: 10.1080/09168451.2018.1473026

Kothari, D., Das, D., Patel, S., and Goyal, A. (2014). "Dextran and food application," in *Polysaccharides*, eds K. G. Ramawat and J. M. Mérillon (Berlin: Springer), 1–16.

Kullisaar, T., Songisepp, E., Aunapuu, M., Kilk, K., Arend, A., Mikelsaar, M., et al. (2010). Complete glutathione system in probiotic *Lactobacillus fermentum* ME-3. *Prikl. Biokhim. Mikrobiol.* 46, 527–531.

Laalami, S., and Putzer, H. (2011). mRNA degradation and maturation in prokaryotes: The global players. *Biomol. Concepts* 2, 491–506. doi: 10.1515/BMC.2011.042

Liu, S., Ma, Y., Zheng, Y., Zhao, W., Zhao, X., Luo, T., et al. (2020). Cold-stress response of probiotic *Lactobacillus plantarum* K25 by iTRAQ proteomic analysis. *J. Microbiol. Biotechnol.* 30, 187–195. doi: 10.4014/jmb.1909.09021

Liu, Y., Borel, C., Li, L., Muller, T., Williams, E. G., Germain, P. L., et al. (2017). Systematic proteome and proteostasis profiling in human Trisomy 21 fibroblast cells. *Nat. Commun.* 8:1212. doi: 10.1038/s41467-017-01422-6

Llamas-Arriba, M. G., Hernández-Alcántara, A. M., Mohedano, M. L., Chiva, R., Celador-Lera, L., Velázquez, E., et al. (2021). Lactic acid bacteria isolated from fermented doughs in spain produce dextrans and riboflavin. *Foods* 10:2004. doi: 10.3390/FOODS10092004

Lyhs, U., Koort, J. M., Lundstrom, H. S., and Bjorkroth, K. J. (2004). *Leuconostoc gelidum* and *Leuconostoc gasicomitatum* strains dominated the lactic acid bacterium population associated with strong slime formation in an acetic-acid herring preserve. *Int. J. Food Microbiol.* 90, 207–218. doi: 10.1016/s0168-1605(03)00303-9

Makarova, K., Slesarev, A., Wolf, Y., Sorokin, A., Mirkin, B., Koonin, E., et al. (2006). Comparative genomics of the lactic acid bacteria. *Proc. Natl. Acad. Sci.* 103, 15611–15616. doi: 10.1073/pnas.0607117103

Malang, S. K., Maina, N. H., Schwab, C., Tenkanen, M., and Lacroix, C. (2015). Characterization of exopolysaccharide and ropy capsular polysaccharide formation by *Weissella*. *Food Microbiol.* 46, 418–427. doi: 10.1016/j.fm.2014.08.022

Maldonado-Barragan, A., and West, S. A. (2020). The cost and benefit of quorum sensing-controlled bacteriocin production in *Lactobacillus plantarum*. *J. Evol. Biol.* 33, 101–111. doi: 10.1111/jeb.13551

Mohedano, M. L., Hernandez-Recio, S., Yépez, A., Requena, T., Martínez-Cuesta, M. C., Pelaez, C., et al. (2019). Real-time detection of riboflavinproduction by *Lactobacillus plantarum* strains and tracking of their gastrointestinal survival and functionality in vitro and in vivo using mCherry labeling. *Front. Microbiol.* 10:1748. doi: 10.3389/fmicb.2019.01748

Monsan, P., Bozonnet, S., Albenne, C., Joucla, G., Willemot, R. M., and Remaud-Simeon, M. (2001). Homopolysaccharides from lactic acid bacteria. *Int. Dairy J.* 11, 675–685.

Mosso, A. L., Jiménez, M. E., Vignolo, G., LeBlanc, J. G., and Samman, N. C. (2018). Increasing the folate content of tuber based foods using potentially probiotic lactic acid bacteria. *Food Res. Int.* 109, 168–174. doi: 10.1016/j.foodres.2018.03.073

Nácher-Vázquez, M., Ballesteros, N., Canales, A., Rodríguez Saint-Jean, S., Pérez-Prieto, S. I., Prieto, A., et al. (2015). Dextrans produced by lactic acid bacteria exhibit antiviral and immunomodulatory activity against salmonid viruses. *Carbohydr. Polym.* 124, 292–301. doi: 10.1016/j.carbpol.2015.02.020

Nácher-Vázquez, M., Iturria, I., Zarour, K., Mohedano, M. L., Aznar, R., Pardo, M. A., et al. (2017). Dextran production by *Lactobacillus sakei* MN1 coincides with reduced autoagglutination, biofilm formation and epithelial cell adhesion. *Carbohydr. Polym.* 168, 22–31. doi: 10.1016/j.carbpol.2017.03.024

Nielsen, H., Engelbrecht, J., Brunak, S., and von Heijne, G. (1997). Identification of prokaryotic and eukaryotic signal peptides and prediction of their cleavage sites. *Protein Eng.* 10, 1–6.

Oleksy, M., and Klewicka, E. (2016). Exopolysaccharides produced by *Lactobacillus* sp.: Biosynthesis and applications. *Crit. Rev. Food Sci. Nutr.* 58, 450–462. doi: 10.1080/10408398.2016.1187112

Papadimitriou, K., Alegria, A., Bron, P. A., de Angelis, M., Gobbetti, M., Kleerebezem, M., et al. (2016). Stress physiology of lactic acid bacteria. *Microbiol. Mol. Biol. Rev.* 80, 837–890. doi: 10.1128/MMBR.00076-15

Patel, S., and Goyal, A. (2011). Functional oligosaccharides: Production, properties and applications. *World J. Microbiol. Biotechnol.* 27, 1119–1128.

Peláez-García, A., Barderas, R., Batlle, R., Vinas-Castells, R., Bartolome, R. A., Torres, S., et al. (2015). A proteomic analysis reveals that Snail regulates the expression of the nuclear orphan receptor nuclear receptor subfamily 2 group F member 6 (Nr2f6) and interleukin 17 (IL-17) to inhibit adipocyte differentiation. *Mol. Cell. Proteomics* 14, 303–315. doi: 10.1074/mcp.M114.045328

Pérez-Ramos, A., Nácher-Vázquez, M., Notararigo, S., López, P., and Mohedano, M. L. (2015). "Current and future applications of bacterial extracellular polysaccharides," in *Probiotics, prebiotics and symbiotics*, eds V. R. Preedy and R. R. Watson (Oxford: Elsevier), 329–344.

Pérez-Riverol, Y., Bai, J., Bandla, C., Hewapathirana, S., García-Seisdedos, D., Kamatchinathan, S., et al. (2022). The PRIDE database resources in 2022: A Hub for mass spectrometry-based proteomics evidences. *Nucleic Acids Res.* 50, D543–D552. doi: 10.1093/nar/gkab1038

Pérez-Riverol, Y., Csordas, A., Bai, J., Bernal-Llinares, M., Hewapathirana, S., Kundu, D. J., et al. (2019). The pride database and related tools and resources in 2019: Improving support for quantification data. *Nucleic Acids Res.* 47, D442–D450. doi: 10.1093/nar/gky1106

Prosseda, G., Di Martino, M. L., Tielker, D., Micheli, G., and Colonna, B. (2010). A temperature-induced narrow DNA curvature range sustains the maximum activity of a bacterial promoter in vitro. *Biochemistry* 49, 2778–2785. doi: 10.1021/bi902003g

R Core Team (2022). *R: A language and environment for statistical computing*. Vienna: R Foundation for Statistical Computing.

Redko, Y., Bechhofer, D. H., and Condon, C. (2008). Mini-III, an unusual member of the RNase III family of enzymes, catalyses 23 S ribosomal RNA maturation in *B. subtilis*. *Mol. Microbiol.* 68, 1096–1106. doi: 10.1111/j.1365-2958.2008.06207.x

Romero-Gavilán, F., Cerqueira, A., García-Arnáez, I., Azkargorta, M., Elortza, F., Gurruchaga, M., et al. (2022). Proteomic evaluation of human osteoblast responses to titanium implants over time. *J. Biomed. Mater. Res. A* 111, 45–59. doi: 10.1002/jbm.a.37444

Rossi, F., Zotta, T., Iacumin, L., and Reale, A. (2016). Theoretical insight into the heat shock response (HSR) regulation in *Lactobacillus casei* and *L. rhamnosus*. *J. Theor. Biol.* 402, 21–37. doi: 10.1016/j.jtbi.2016.04.029

Rühmkorf, C., Rübsam, H., Becker, T., Bork, C., Voiges, K., and Mischnick, P. (2012). Effect of structurally different microbial homoexopolysaccharides on the quality of gluten-free bread. *Eur. Food Res. Technol.* 235, 139–146. doi: 10.1007/s00217-012-1746-3

Salze, M., Muller, C., Bernay, B., Hartke, A., Clamens, T., Lesouhaitier, O., et al. (2020). Study of key RNA metabolism proteins in *Enterococcus faecalis*. *RNA Biol.* 17, 794–804. doi: 10.1080/15476286.2020.1728103

Singh, A. K., Sad, K., Singh, S. K., and Shivaji, S. (2014). Regulation of gene expression at low temperature: Role of cold-inducible promoters. *Microbiology* 160(Pt 7), 1291–1296. doi: 10.1099/mic.0.077594-0

Solis-Fernández, G., Montero-Calle, A., Martinez-Useros, J., Lopez-Janeiro, A., de Los Rios, V., Sanz, R., et al. (2022). Spatial proteomic analysis of isogenic metastatic colorectal cancer cells reveals key dysregulated proteins associated with lymph node, liver, and lung metastasis. *Cells* 11:447. doi: 10.3390/cells11030447

Ting, L., Williams, T. J., Cowley, M. J., Lauro, F. M., Guilhaus, M., Raftery, M. J., et al. (2010). Cold adaptation in the marine bacterium, *Sphingopyxis alaskensis*, assessed using quantitative proteomics. *Environ. Microbiol.* 12, 2658–2676. doi: 10.1111/j.1462-2920.2010.02235.x

Tribelli, P. M., and Lopez, N. I. (2018). Reporting key features in cold-adapted bacteria. *Life* 8:8. doi: 10.3390/life8010008

Tyanova, S., Temu, T., Sinitcyn, P., Carlson, A., Hein, M. Y., Geiger, T., et al. (2016). The perseus computational platform for comprehensive analysis of (prote)omics data. *Nat. Methods* 13, 731–740. doi: 10.1038/nmeth.3901

van Roosmalen, M. L., Geukens, N., Jongbloed, J. D. H., Tjalsma, H., Dubois, J.-Y. F., Bron, S., et al. (2004). Type I signal peptidases of Gram-positive bacteria. *Biochim. Biophys. Acta* 1694, 279–297. doi: 10.1016/j.bbamcr.2004.05.006

Werning, M. L., Notararigo, S., Nácher, M., Fernández de Palencia, P., Aznar, R., and López, P. (2012). "Biosynthesis, purification and biotechnological use of exopolysaccharides produced by lactic acid bacteria," in *Food additives*, ed. Y. El-Samragy (Rijeka: Intech), 83–114.

Wisselink, H. W., Weusthuis, R., Eggink, G., Hugenholtz, J., and Grobben, G. J. (2002). Mannitol production by lactic acid bacteria: A review. *Int. Dairy J.* 12, 151–161. doi: 10.1016/S0958-6946(01)00153-4

Wouters, J. A., Jeynov, B., Rombouts, F. M., de Vos, W. M., Kuipers, O. P., and Abee, T. (1999). Analysis of the role of 7 kDa cold-shock proteins of *Lactococcus lactis* MG1363 in cryoprotection. *Microbiology* 145(Pt 11), 3185–3194. doi: 10.1099/00221287-145-11-3185

Wouters, J. A., Rombouts, F. M., Kuipers, O. P., de Vos, W. M., and Abee, T. (2000). The role of cold-shock proteins in low-temperature adaptation of food-related bacteria. *Syst. Appl. Microbiol.* 23, 165–173. doi: 10.1016/S0723-2020(00)80001-6

Xiao, Z., and Xu, P. (2007). Acetoin metabolism in bacteria. *Crit. Rev. Microbiol.* 33, 127–140. doi: 10.1080/10408410701364604

Zarour, K., Prieto, A., Pérez-Ramos, A., Kihal, M., and López, P. (2018). Analysis of technological and probiotic properties of Algerian *L. mesenteroides* strains isolated from dairy and non-dairy products. *J. Funct. Foods* 49, 351–361.

Zarour, K., Llamas, M. G., Prieto, A., Ruas-Madiedo, P., Dueñas, M. T., Fernández de Palencia, P. F., et al. (2017a). Rheology and bioactivity of high molecular weight dextrans synthesised by lactic acid bacteria. *Carbohydr. Polym.* 174, 646–657. doi: 10.1016/j.carbpol.2017.06.113

Zarour, K., Vieco, N., Pérez-Ramos, A., Nácher-Vázquez, M., Mohedano, M. L., and López, P. (2017b). "Food ingredients synthesized by lactic acid bacteria," in *Microbial production of ingredients and additives*, eds A. M. Grumezescu and A. M. Holban (Amsterdam: Elsevier), 89–124.

frontiers | Frontiers in Microbiology

TYPE Review
PUBLISHED 02 February 2023
DOI 10.3389/fmicb.2023.1110360

OPEN ACCESS

EDITED BY
Giuseppe Spano,
University of Foggia,
Italy

REVIEWED BY
Beatriz Martínez,
Spanish National Research Council, Spain
Sylvie Françoise Rebuffat,
Muséum National d'Histoire Naturelle,
France

*CORRESPONDENCE
Rubén Cebrián
✉ rcebrian@ibsgranada.es
Manuel Montalbán-López
✉ manuelml@ugr.es

†These authors have contributed equally to this work and share first authorship

SPECIALTY SECTION
This article was submitted to Food Microbiology, a section of the journal Frontiers in Microbiology

RECEIVED 28 November 2022
ACCEPTED 11 January 2023
PUBLISHED 02 February 2023

CITATION
Cebrián R, Martínez-García M, Fernández M, García F, Martínez-Bueno M, Valdivia E, Kuipers OP, Montalbán-López M and Maqueda M (2023) Advances in the preclinical characterization of the antimicrobial peptide AS-48.
Front. Microbiol. 14:1110360.
doi: 10.3389/fmicb.2023.1110360

Advances in the preclinical characterization of the antimicrobial peptide AS-48

Rubén Cebrián[1*†], Marta Martínez-García[2†], Matilde Fernández[3], Federico García[1,4], Manuel Martínez-Bueno[3], Eva Valdivia[3], Oscar P. Kuipers[2], Manuel Montalbán-López[3*] and Mercedes Maqueda[3]

[1]Department of Clinical Microbiology, Instituto de Investigación Biosanitaria Ibs.GRANADA, University Hospital San Cecilio, Granada, Spain, [2]Department of Molecular Genetics, University of Groningen, Groningen, Netherlands, [3]Department of Microbiology, University of Granada, Granada, Spain, [4]Biomedicinal Research Network Center, Infectious Diseases (CIBERINFEC), Madrid, Spain

Antimicrobial resistance is a natural and inevitable phenomenon that constitutes a severe threat to global public health and economy. Innovative products, active against new targets and with no cross- or co-resistance with existing antibiotic classes, novel mechanisms of action, or multiple therapeutic targets are urgently required. For these reasons, antimicrobial peptides such as bacteriocins constitute a promising class of new antimicrobial drugs under investigation for clinical development. Here, we review the potential therapeutic use of AS-48, a head-to-tail cyclized cationic bacteriocin produced by *Enterococcus faecalis*. In the last few years, its potential against a wide range of human pathogens, including relevant bacterial pathogens and trypanosomatids, has been reported using *in vitro* tests and the mechanism of action has been investigated. AS-48 can create pores in the membrane of bacterial cells without the mediation of any specific receptor. However, this mechanism of action is different when susceptible parasites are studied and involves intracellular targets. Due to these novel mechanisms of action, AS-48 remains active against the antibiotic resistant strains tested. Remarkably, the effect of AS-48 against eukaryotic cell lines and in several animal models show little effect at the doses needed to inhibit susceptible species. The characteristics of this molecule such as low toxicity, microbicide activity, blood stability and activity, high stability at a wide range of temperatures or pH, resistance to proteases, and the receptor-independent effect make AS-48 unique to fight a broad range of microbial infections, including bacteria and some important parasites.

KEYWORDS

antimicrobial peptide, bacteriocin, enterocin, AS-48, antimicrobial resistance

Introduction

During the last century, different families of antibiotics and chemotherapeutics have been isolated/synthesized, characterized, and employed in the treatment of human and veterinary infections. Nowadays, antibiotic efficacy is seriously compromised because of several factors including over-prescription, misuse for non-bacterial infections, over-use in livestock and fish farming, poor infection control in hospitals, or poor hygiene and sanitation, among others. This has led to a moment in which the number of multidrug-resistant (MDR) bacteria is alarmingly increasing (Laxminarayan et al., 2013; McCullough et al., 2016). Antibiotic-resistant bacteria constitute one of the main threats to global health since they can affect anyone, of any age, in any

country and lead to longer hospital stays, higher medical costs, and increased mortality (Hofer, 2019; Jit et al., 2020). With this background and according to the WHO, by 2050 MDR bacteria will be the first cause of death in the world, above conditions such as cancer or diabetes (O'Neill, 2014). Additionally, the number of new antibiotics approved for bacterial infection treatment is scarce in comparison with the necessities, and usually, they are chemical modifications of existing compounds, so they represent short-term solutions since the resistance mechanisms are already established in nature (Butler and Paterson, 2020). In the era of antimicrobial resistance development, new leads to fight MDR bacteria are urgently needed (Furuya and Lowy, 2006; Podolsky, 2018). In fact, 32 of the 50 antibiotics in the pipeline target bacteria included in the WHO priority list of pathogens that require urgent development of new treatments (WHO, 2017) but the majority of them have only limited benefits compared to antibiotics in use (WHO, 2022a). Last, investment in new antimicrobial development by the pharmaceutical industry is scarce (less than 5% in R&D) whereas the costs and time necessary for a proper development is extremely expensive and long (May, 2014; O'Neill, 2016).

"Re-discovering" old known molecules with antimicrobial activity to face the antibiotic crisis is an attractive alternative that is gaining the attention of the scientific community. In this sense, antimicrobial peptides (AMPs) are a promising alternative, by themselves or as adjuvants in combined therapy, for the treatment of MDR bacterial infections in both animals and humans (Cruz et al., 2014; Deslouches et al., 2020; Magana et al., 2020; Mookherjee et al., 2020). AMPs are a heterogeneous and ubiquitous group of peptides, posttranslationally modified or not, virtually produced by all the domains of life, that usually act as the first line in the defense against competitors and pathogens (innate immune response). The AMPs produced by bacteria are called bacteriocins. Nowadays, AMPs are pointed as an alternative to antibiotics because of their *in vitro* and *in vivo* potent activity against pathogens, their spectrum of activity (broad or narrow depending on the compound, so they can target specific bacteria reducing the effect over the microbiota), their usually low toxicity, and the ease to engineer them (Cotter et al., 2005, 2013; Montalbán-López et al., 2017, 2020b). In fact, nisin, the first bacteriocin described in 1928, unlike its coetaneous penicillin was relegated to the food industry as a food preservative due mainly to its proteinaceous nature (which raises concerns about the possible administration routes, stability or molecular size). This use has been broadly studied for other bacteriocins, especially those produced by lactic acid bacteria, which are common in the food industry and often present probiotic properties. In the last years, a renewed interest has appeared to study bacteriocins and AMPs to combat clinically relevant species, even though the costs of natural production and purification and/or synthesis, *in vivo* half-life and characterization of their toxicity/immunogenicity, pharmacokinetic-pharmacodynamics, and effect on the host microbiota remain as the main challenges for their development (Cotter et al., 2013; Theuretzbacher et al., 2020; Cesa-Luna et al., 2021).

Several classification schemes have been proposed for bacteriocins from lactic acid bacteria (Alvarez-Sieiro et al., 2016). Among them, lantibiotics and head-to-tail cyclized peptides show high potency against a broad range of microorganisms and have been studied in more detail. Both are ribosomally produced and posttranslationally modified peptides (RiPPs). The group of head-to-tail cyclized peptides (also referred to as circular bacteriocins in literature) is currently integrated by about 20 members (Vezina et al., 2020). They are characterized by the presence of a peptide bond between the N-and C-termini (Montalbán-López et al., 2011; Sánchez-Hidalgo et al., 2011; Dischinger et al., 2014). Head-to-tail cyclization is a rare posttranslational modification occurring in a handful of peptide families that confers them high stability against several physical, chemical, and biological conditions and makes them very interesting as scaffolds for drug design or by re-engineering linear peptides into cyclic ones, thereby increasing their stability and/or activity (Montalbán-López et al., 2012; Strijbis and Ploegh, 2014; Nguyen et al., 2015; Weidmann and Craik, 2016; Stevens et al., 2017).

The first circular bacteriocin (and peptide) discovered and also the best known to date from the genomic point of view to its applicability is the enterocin AS-48 (Gálvez et al., 1986). AS-48 is produced by several *Enterococcus* strains as a 105 amino acids precursor peptide, in which 35 amino acids correspond to the leader peptide that is cleaved before or concomitantly with the head-to-tail cyclization. The mechanisms underneath such a leader peptide cleavage and circularization remain unknown, both for AS-48 and for the rest of the circular bacteriocins described. The diversity in sequences, in leader peptides, or the absence of common motifs among these peptides suggest different ways to obtain the same results, the circular peptide backbone [this is further discussed in Sánchez-Hidalgo et al. (2011) and Gabrielsen et al. (2014)]. This review is focused on the state-of-the-art of clinical development of AS-48, discussing the importance of its mechanism of action reaching new and specific targets in bacteria and/or parasites, the broad spectrum of activity against several intra-and extracellular human pathogens, and its safety as a drug.

AS-48 mechanism of action: Minimizing resistance development

The main target of AS-48 is the cytoplasmic membrane of bacteria. Thus, Gram-positive bacteria are directly exposed to AS-48 whereas its activity is limited in the case of Gram-negative species because of the presence of the outer membrane that acts as a permeability barrier (Maqueda et al., 2004). Structurally, AS-48 is organized in 5 α-helices with a compact globular structure similar to saposin folding (Sánchez-Barrena et al., 2003; Figure 1A). It has a remarkable amphipathic surface where the positively charged residues (helices 4 and 5) are separated from the rest of the hydrophobic or uncharged residues (helices 1, 2, and 3) by a hypothetical plane delimitated by the Cα atoms of 4 glutamic acids (González et al., 2000; Sánchez-Hidalgo et al., 2008, 2011). This asymmetrical charge distribution, the stabilizing interaction of tryptophan residues, and the amphipathicity of the molecule play an essential role in the mechanism of action of the peptide (Cruz et al., 2021).

AS-48 molecules interact with each other in solution. In fact, in water solutions, AS-48 is organized as a dimer called DF-I in which the hydrophobic helices are sandwiched between two layers of cationic polar helices that are exposed to the solvent (Figure 1B; Sánchez-Barrena et al., 2003). In these conditions, the peptide presents a strong dipole moment that drives its approach to the bacterial membranes (Cebrián et al., 2015). At the membrane surface, the acidic pH destabilizes AS-48 DF-I dimer most likely because of the protonation of the glutamic acid side chains, promoting a rearrangement and transition from the water-soluble DF-I to the membrane embedded dimer DF-II (Figure 1B). In the latter, the polar helices are sandwiched in between the hydrophobic ones (exposed to the solvent/membrane). In this model, the protonated glutamic acid could recognize the phosphate group of phospholipids, and the positively charged and hydrophobic residues would interact

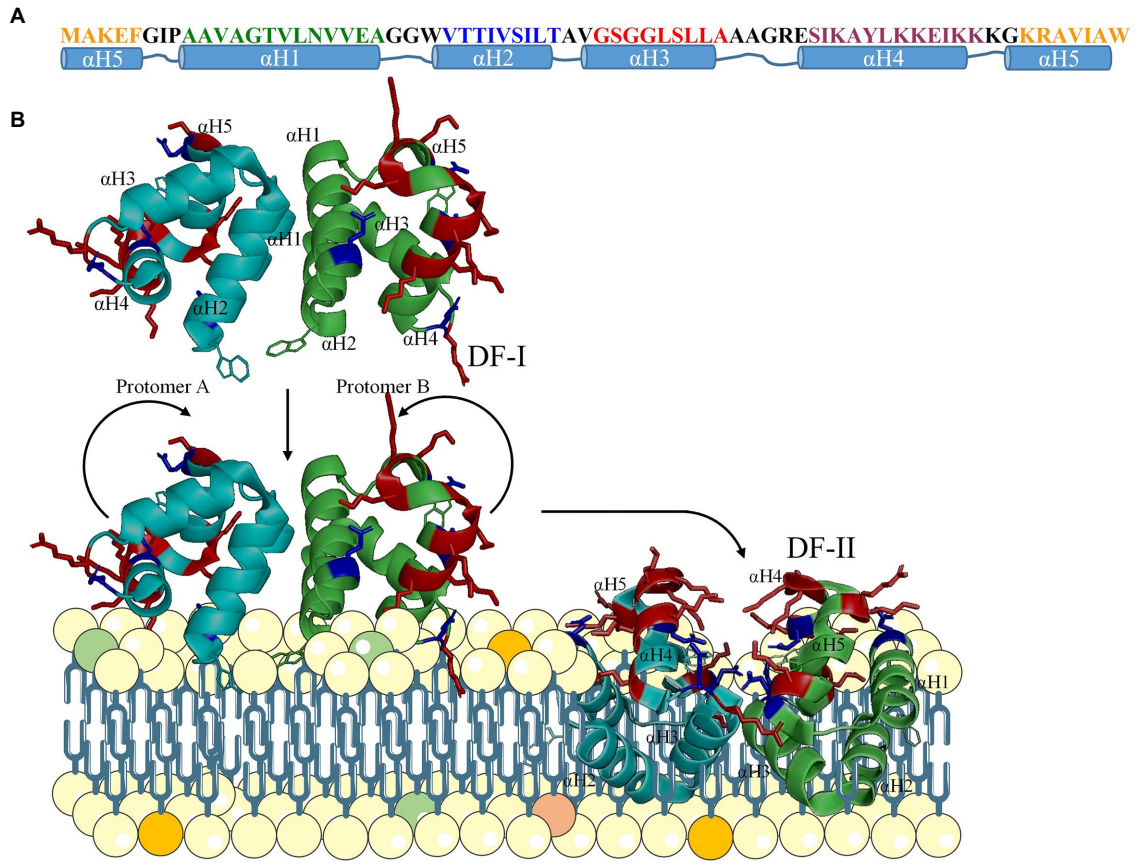

FIGURE 1
Secondary **(A)** and tertiary structure of AS-48 and proposed mode of action **(B)**. The water-soluble DF-I is attracted to the membrane due to electrostatic interactions and flips into the membrane-bound DF-II, that creates pores leading to cell death.

with the polar head groups and the aliphatic chains of phospholipids, respectively (Sánchez-Barrena et al., 2003; Cebrián et al., 2015). The peptide is finally inserted in the membrane where it forms pores, abolishing the membrane potential, and cells lyse (Gálvez et al., 1991; González et al., 2000; Abriouel et al., 2001; Cruz et al., 2013). This mechanism of action is highly specific for bacterial cells due to the abundance of negatively charged phospholipids in their membrane and it is independent of their membrane potential or any receptor, so that even bacterial cells with low or without any metabolic activity may be targeted (Gálvez et al., 1991).

However, the bacterial lysis induced by AS-48 is not the only ultimate cell-death mechanism since in many cases no bacteriolysis has been observed (for instance, members of the Phylum *Actinomycetota* such as *Micrococcus, Mycobacterium*, *Nocardia*, *Cutibacterium, Gardnerella,* or the majority of the susceptible Gram-negative bacteria such as *Agrobacterium tumefaciens*, *Salmonella* spp., or *Escherichia coli*). Recently electronic scanning microscopy images of AS-48-treated *Staphylococcus aureus* showed that the cells remain together after the division septa formation, which suggests alternative unraveled mechanisms of action rather than solely membrane lysis (Velázquez-Suárez et al., 2021).

Most bacteriocins have no effect on eukaryotic cell lines at the concentrations required to inhibit bacteria, which is a positive trait for a clinical application as antibacterial compounds. Surprisingly, and although AS-48 showed no activity against several eukaryotic organisms tested, like the yeast *Saccharomyces* or the amoebas *Naegleria* spp. or *Acanthamoeba* spp. (Gálvez et al., 1989), parasites from the *Trypanosomatidae* family have been reported to be very susceptible (Abengózar et al., 2017; Martínez-García et al., 2018; Martín-Escolano et al., 2019). Interestingly, a deep inspection of the mechanism of action against these cells indicates that the activity involves different targets and mechanisms of action. Thus, two other different mechanisms of action have been proposed to explain the activity of AS-48 against these parasites. As commented before, the specificity of AS-48 to bacterial membranes is determined by the recognition of the negatively charged exposed membrane phospholipids, a feature present also in *Leishmania* (Abengózar et al., 2017; Figure 2A). However, the activity of AS-48 against this parasite cannot be explained just because of pore formation in the cytoplasmic membrane, since the leishmanicidal effect of AS-48 was not completed after 4 h of incubation, while the typical membrane permeation in bacteria is completed in a few minutes (Abengózar et al., 2017). The pores formed by AS-48 in *Leishmania* membrane are used as a gate to access the cytoplasm and, once inside, the peptide reaches the single mitochondrion, binding to the mitochondrial membrane and inducing a fast ATP depletion (Figure 2A). The damage in the functionality of the respiratory chain at the mitochondrion by AS-48 is also supported by the decrease in respiration and a rise in ROS production (Abengózar et al., 2017).

Amazingly, this mechanism is not shared against other trypanosomatids and, unlike *Leishmania*, pore formation in the membrane is not required against *Trypanosoma* spp. *Trypanosoma cruzi* is not permeated by AS-48. However, a similar mitochondrial dysfunction and ROS production were observed, which suggests that AS-48 may

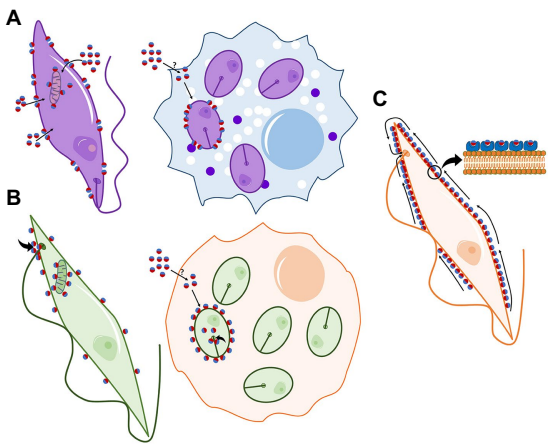

FIGURE 2
Schematic representation of AS-48 mechanisms of action on parasites. **(A)** Activity of AS-48 on *Leishmania* spp. promastigotes (extracellular) and amastigotes (inside macrophages). AS-48 induces pore formation in the cytoplasmic membrane that further grants AS-48 access to the cytoplasm reaching the mitochondria. **(B)** Activity of AS-48 on *T. cruzi* trypomastigotes/epimastigotes (extracelluar) and amastigotes (inside Vero cells). AS-48 is slowly endocytosed by the flagellar pocket and once inside the cells it reaches the mitochondria. **(C)** Activity of AS-48 on *T. brucei*. AS-48 binds VSG proteins on the parasite surface and it is rapidly internalized by the flagellar pocket inducing apoptosis.

be endocytosed by this parasite across the flagellar pocket (Martín-Escolano et al., 2019; Figure 2B). Alterations in the mitochondrial functions were also related to other deleterious effects observed in this parasite such as the blocking of the glycolytic pathway and a decrease in the nucleic acid levels which is related to cell necrosis (Martín-Escolano et al., 2019; Figure 2B). Also, a killing mechanism unrelated to pore formation in the membrane has been described in *Trypanosoma brucei* (Martínez-García et al., 2018). Conversely to *T. cruzi*, in *T. brucei* the endocytic turnover of the surface components across the flagellar pocket is exceptionally high (Porto-Carreiro et al., 2000; Manna et al., 2014). This characteristic is involved in immune system evasion and therefore in the high resistance and survival of the parasite in the host and prevents the development of effective vaccines. However, it is the Achilles' heel against AS-48. In fact, this parasite is the most susceptible pathogen to AS-48 described to date (approx. 1000 times more susceptible than the rest of the susceptible pathogens tested, including bacteria) (Martínez-García et al., 2018). In *T. brucei*, AS-48 enters *via* clathrin-mediated endocytosis after its interaction with the negatively charged variant surface glycoprotein (VSG; Figure 2C). The high number of VSG on the parasite surface (*ca.* 10^7 molecules per cell) and its extremely rapid internalization and recycling by endocytosis (the VSG coat is completely internalized in 12.5 min) allow a fast accumulation of AS-48 inside the parasite. Once there, the bacteriocin can alter the normal structure of the membranous vesicles of the endocytic route inducing death by autophagy (Martínez-García et al., 2018). The parasiticidal activity of AS-48 against *T. brucei* is extremely fast compared to the other trypanosomatids tested, probably because of the prompt entering system (Martínez-García et al., 2018).

Resistance to AS-48

As indicated above, AS-48 interacts with the lipids in the cell membrane and/or eukaryotic membranous organelles without the mediation of a receptor. Therefore, the development of stable resistance against this sort of membrane-active peptides is extremely difficult since it would require extensive modifications on a critical constituent of the cells that may drastically affect the cell physiology and viability. In fact, no resistance against AS-48 has been reported to the best of our knowledge.

Currently, four main mechanisms of adaptive resistance to bacterial AMPs have been described, namely peptide inactivation, surface remodeling, capsule production, or biofilm formation (Band and Weiss, 2015; Magana et al., 2020). So far, the only genetically encoded resistance to AS-48 is provided by the presence of the immunity protein (As-48D1) and the ABC-transporter (As-48EFGH) which are encoded by the *as-48* operon (Martínez-Bueno et al., 1998; Diaz et al., 2003). This transporter is also related to resistance to other similar bacteriocins (Teso-Pérez et al., 2021). Only AS-48 producer strains are fully resistant to the peptide, while the (heterologous) expression of them in other organisms provides partial levels of resistance (Martínez-Bueno et al., 1998; Fernández et al., 2007). Interestingly, cross-resistance to AS-48 was not observed even in the case of *Bacillus pumilus* B4107, which produces pumilarin, a very similar circular peptide that differs only in 10 amino acids compared to AS-48 (van Heel et al., 2017). Furthermore, the compact globular structure and cyclization confer high resistance to diverse proteases, which can provide longer half-life (Montalbán-López et al., 2008; del Castillo-Santaella et al., 2018).

In the case of other bacteriocins, resistance mechanisms are usually related to changes in bacterial outer layers (fluidity, lipid composition, the electrical potential of the membrane; cell wall thickness, and modification extent by, for instance, alanilation of teichoic acids, or a combination of all these factors) but also reducing bacteriocin accessibility to their receptors, downregulating the expression of genes involved in receptors or *via* proteolytic degradation of the bacteriocin (Soltani et al., 2021). Only a transient adaptive response to AS-48 has been detected in the case of *Listeria monocytogenes* at low temperatures and sub-minimum inhibitory concentrations (MIC) of AS-48. Adapted cells show increased resistance to other antimicrobials such as nisin or muramidases. This response is based in part on changes in the cell wall structure but specially on changes in the lipids of the cytoplasmic membrane, in which branched fatty acids and a higher C15:C17 ratio was determined. These adaptations disappear if AS-48 concentration is slightly increased or after repeated subcultivations in absence of the peptide (Mendoza et al., 1999).

Antimicrobial activity of AS-48 against pathogenic bacteria

One of the most promising applications of AS-48 and other bacteriocins is related to their use as a food preservative (Cotter et al., 2005; Silva et al., 2018; O'Connor et al., 2020). In fact, some of them (or their producer strains) have been already approved as food additives by the FDA (Juturu and Wu, 2018). Moreover, enterococcal strains, even AS-48-producing strains, are usually isolated in many fermented products (Cebrián et al., 2012). For this reason, the activity of AS-48 alone or in combination with other antimicrobials as a food preservative against food-spoilage bacteria has been extensively analyzed (Abriouel et al., 2010; Ananou et al., 2014; Grande Burgos et al., 2014; Perales-Adan et al., 2018). Nevertheless, from a clinical point of view, the greatest risks in food safety come from the presence of foodborne pathogens. Bacteria are the most common cause of foodborne diseases.

Foodborne illness occurs in two ways: when the pathogen is ingested with food and establishes itself in the human host, or when the bacteria produce toxins in the food that is ingested (Bintsis, 2017). A broad range of Gram-positive and Gram-negative bacteria such as *Clostridium botulinum, Clostridium perfringens, Clostridioides difficile, Bacillus subtilis, Bacillus cereus, Bacillus anthracis, Staphylococcus aureus*, *Listeria monocytogenes*, *Yersinia enterocolitica*, *Escherichia coli, Campylobacter jejuni, Salmonella* spp., *Shigella* spp., *Vibrio* spp., or *Brucella* spp. are mainly responsible for these diseases, which represent 3.6 million of infections per year just in the United States (Tauxe, 2002; Scallan et al., 2011; Martinović et al., 2016).

On the whole, AS-48 has shown potent activity *in vitro* against most of the Gram-positive bacteria tested including sporulated species as *B. cereus* (MIC 7.5–10 mg/l; Gálvez et al., 1989; Abriouel et al., 2002), although no direct effect on neither the spore viability nor germination initiation has been detected. However, just 10 min after germination, AS-48 was able to effectively kill the growing vegetative cell. Moreover, enterotoxin production by these bacteria was also inhibited by AS-48 (Abriouel et al., 2002; Grande et al., 2006). As an exception, in *Alicyclobacillus acidoterrestris* spore germination was abolished by AS-48 (Grande et al., 2005). Furthermore, a potent activity has been also observed against food-isolated *S. aureus* (MIC 1.14–5.21 mg/l; Caballero Gómez et al., 2013; Perales-Adan et al., 2018) or *L. monocytogenes* (MIC 0.1 mg/l), which is one of the most susceptible species (Mendoza et al., 1999). Because of the importance of *Listeria* as a foodborne pathogen, the effectivity of AS-48 alone or in combination with other antimicrobials or physical treatments against this bacterium (both planktonic or sessile) has been successfully determined in different food models such as ready-to-eat salads, raw fruits, vegetables, sausages or desserts (Gómez et al., 2012; Grande Burgos et al., 2014).

In the case of Gram-negative bacteria, the presence of the outer membrane makes them intrinsically more resistant to AS-48 (Abriouel et al., 1998). However, the combination of this bacteriocin with other treatments (physical or chemical) or with outer membrane disruptive agents has been evaluated in different food models as a good alternative to fight foodborne pathogens such as *Salmonella enterica, E. coli* O157:H7, *Y. enterocolitica*, or *Shigella* spp. (Gálvez et al., 1989; Ananou et al., 2005; Cobo Molinos et al., 2008; Grande Burgos et al., 2014).

In addition to *in vitro* assays and in different foodstuff against food spoilage bacteria and foodborne pathogens, AS-48 has shown potent activity against a wide range of pathogens including both intra- and extracellular bacteria (Table 1). Most of them constitute a main concern in global public health and are discussed below. Remarkably, AS-48 has an intrinsic or potentiated bactericidal action in most of the cases that have been studied.

TABLE 1 Antimicrobial activity of AS-48 against pathogenic bacteria.

	Species/ genus	ARS	Synergy	MIC mg/l	MIC μM
Gram-positive	***Enterococcus***	Yes	Lysozyme antibiotics HT	1.3–7.1	1.81–9.93
	Staphylococcus	Yes	Lysozyme HT	1.17–16.0	1.63–22.38
	Mycobacterium	Yes	Lysozyme antibiotics	2.0–64.0	2.79–89.51
	C. acnes	Yes	Lysozyme	0.62–2.5	0.86–3.49
Gram-negative	***K. pneumoniae***	No	HT[a]	>100	>139.87
	P. aeruginosa	No	HT[a]	>100	>139.87
	E. coli	Yes	HT[a]	>100	>139.87

Genera that are pointed as priority pathogens list for R&D of new antibiotics and specific research programs by the WHO are highlighted. For simplicity, MIC values indicate the concentration of AS-48 before using any synergistic treatment. ARS: antibiotic-resistant strains tested. HT: magnetic-induced hyperthermia. [a]Necessary for sensitization to AS-48.

Activity of AS-48 against the WHO priority list of bacteria

As part of its program in new antimicrobial research and development, the WHO published a list of pathogens for which new antimicrobials are urgently needed (WHO, 2017). Vancomycin-resistant *Enterococcus faecium* or vancomycin and/or methicillin-resistant *S. aureus* are among the bacteria for which new drugs are necessary with a high priority. Both species are intrinsically resistant to several antibiotics and can easily acquire resistance.

In general, enterococci are quite susceptible to AS-48 with MIC values in the low micromolar range. Recently, an enterococcal collection of clinical isolates with a wide range of antibiotics resistance (some of them resistant to 15/20 antibiotics tested) and virulence factors (some of them with 6/7 virulence factor genes) has been tested for its sensitivity to AS-48 (Montalbán-López et al., 2020a). The peptide is active at concentrations ranging between 1.3–7.1 mg/l (3.1 mg/l average) demonstrating an astonishing activity regardless of the virulence factors or antibiotic resistance displayed by the strains tested, including different vancomycin-resistant genotypes (Montalbán-López et al., 2020a). Currently, one of the most promising therapeutical strategies to fight MDR bacteria is based on the combination of two (or more) drugs to obtain a synergistic activity (Tyers and Wright, 2019). Synergism aims at the complete eradication of the infection, reducing the dosage of the drugs (and therefore the side effects) and the treatment timeframe. Also, the boosting effect of the combined treatment reduces the possibility to develop resistance by the bacteria when different mechanisms of action are simultaneously attacking the cell (Xu et al., 2018). For this reason, the combined effect of AS-48 with three well-characterized antibiotics commonly used against enterococci (namely vancomycin, gentamicin, and amoxicillin/clavulanate) has been tested. Interestingly, enterococcal strains that were highly resistant to these antibiotics (MICs >120 mg/l) are generally sensitized to them although not in all the cases, which suggests different resistance mechanisms to the combined treatment (Montalbán-López et al., 2020a).

Similarly, the sensitivity to AS-48 of clinically isolated *S. aureus* ($n = 100$) with a characterized resistance profile to 18 different antibiotics (33 strains were methicillin-resistant, MRSA) has been recently tested. All the strains were susceptible to AS-48 at concentrations ranging from 3 to 16 mg/l with an average resistance of 7.4 ± 0.46 mg/l and, as before, the activity of AS-48 was independent of the antibiotic-resistant profile (Velázquez-Suárez et al., 2021). Differences were neither observed between MRSA and methicillin-susceptible strains (Velázquez-Suárez et al., 2021). Remarkably, although *S. aureus* is intrinsically resistant to lysozyme, the combination of AS-48 with this muramidase significantly reduced the average MIC to 4.23 ± 0.43 mg/l (MIC ranging from 0.5 to 12 mg/l; Velázquez-Suárez et al., 2021). AS-48 was also active in established *S. aureus* biofilms, where important morphological changes were observed during the treatment, on both biofilm matrix structure (almost disappeared) and bacterial morphology (Velázquez-Suárez et al., 2021). Interestingly, clinically isolated *S. aureus* were 4.5 times more resistant to AS-48 than food-isolated *S. aureus*. The MIC of AS-48

against this species was ranging between 1.17 and 3.12 mg/l (average 1.63 mg/l), which suggests that no pathogenic factor could be related to higher AS-48 tolerance (Perales-Adan et al., 2018; Velázquez-Suárez et al., 2021). Besides, in the case of food-isolated *S. aureus*, an additive effect was observed for combinations with other compounds with different mechanisms of action such as the lantibiotic nisin (AS-48 MIC was reduced to 0.36 mg/l in the presence of 0.03 mg/l of nisin) which suggests the absence of cross-resistance for these two bacteriocins (Perales-Adan et al., 2018).

Activity of AS-48 against *Actinomycetota* and *Mycobacterium*

Some species belonging to the phylum *Actinomycetota* (formerly *Actinobacteria*) are pathogens widely distributed worldwide. Acne is a chronic inflammation of the pilosebaceous unit and a recurrent skin condition affecting approximately 10% of the world's population (Hay et al., 2014). The disease has a multifactorial etiology and is triggered initially during adolescence in susceptible individuals, but this condition can continue even in adults (especially in women). Although in general it occurs as a minor infection, in some cases, it can have severe psychological effects (Samuels et al., 2020). The relation of the commensal *Cutibacterium acnes* with the disease is still in question, but available data indicate that the presence of certain genotypes of this bacterium are directly implicated (Dréno et al., 2018). Besides acne, *C. acnes* is also related to other severe medical conditions linked to surgical procedures, foreign bodies, septicemia, and implant-associated infections (Achermann et al., 2014). AS-48 has shown potent activity against 20 clinical isolated *C. acnes* with a MIC between 0.62–2.5 mg/l (average MIC 1.22 mg/l) and this activity has been also achieved inside biofilms of this bacterium (Cebrián et al., 2018). This activity is enhanced by the combination of the peptide with lysozyme (an enzyme present in respiratory tract and ocular secretions as part of the body's defense) commonly used in topical treatments, reducing the MIC of AS-48 to 0.5 mg/l. Remarkably, in this study, eradication of the bacterium was assessed at low concentrations. Unlike other bacteria, the killing kinetics for AS-48 against this species is quite slow (100% of killing effect after 48 h) and no lysis of the cell is observed (Cebrián et al., 2018).

More importantly, AS-48 is effective against mycobacteria, for which an additional specific programme has been developed by the WHO. Around 10 million people fall ill with tuberculosis worldwide each year and 1.5 million die, making tuberculosis one of the top 10 causes of death (WHO, 2022b). About one-quarter of the world's population is estimated to be infected by *M. tuberculosis* but only 5–15% of these people develop the active disease. Tuberculosis infection is curable by a treatment using a combination of antimicrobial drugs for a long time due to the difficulties of the antibiotics to reach the infection sites of this slow-growing intracellular pathogen. Thus, a standard 6-months course of 4 antimicrobial drugs is commonly used. However, most of the people infected with tuberculosis live in low- and middle income countries, which makes access to this treatment difficult. In addition, the number of drug-resistant *M. tuberculosis* is rising and new drugs are urgently needed (WHO|Global Tuberculosis Report, 2019). Interestingly, AS-48 shows bactericidal activity against cultures of *M. tuberculosis* strains at concentrations between 8–64 mg/l without differences between actively replicating cells and the nonreplicative strains (Aguilar-Pérez et al., 2018). Other *Mycobacterium* species such as *M. xenopi* and *M. gordonae* (rarely related to human infections) are quite susceptible to AS-48 (MIC <2 mg/l; Aguilar-Pérez et al., 2018). The combination of AS-48 with lysozyme results in a potent synergistic interaction in all the cases tested. Thus, an astonishing MIC reduction against this bacterium (MIC <0.03 mg/l AS-48 in most cases) was observed (Aguilar-Pérez et al., 2018). Similar to the other actinobacteria tested, i.e., *C. acnes*, the killing kinetics is slower than against other bacterial phyla. Nevertheless, no bacteria are detectable after 6 days of treatment. Besides this, the antimicrobial activity of AS-48 in combination with the first-line antituberculosis drugs (ethambutol, isoniazid, streptomycin, and rifampin) proves an astonishing combined effect with ethambutol which suggests that the arabinogalactans wall may provide resistance against AS-48 in *Mycobacterium* spp. (Aguilar-Pérez et al., 2018). Next to the experiments against *M. tuberculosis* culture activity, the combination of AS-48 and lysozyme or ethambutol has been also tested against *M. tuberculosis*-infected macrophages. In the case of the combination with lysozyme, the synergistic effect is no longer observable but a surprisingly potent synergism was observed for the combination with ethambutol. In this case, a concentration as low as 2 mg/l of AS-48 and ethambutol caused bacterial death, whereas the MIC of each antimicrobial alone against this strain was 32 and 16 mg/l for AS-48 and ethambutol, respectively (Aguilar-Pérez et al., 2018).

Boosting AS-48 activity and antimicrobial spectrum using magnetic nanocarriers

Often, bacterial infections take place in localized foci within the human body. The use of nanocarriers to deliver drugs to these points allows dose reduction and minimizes side effects. Magnetic nanoparticles are superparamagnetic nanocarriers that can be functionalized with diverse compounds depending on their surface characteristics. Those produced *in vitro* mimicking the magnetosome of *Magnetococcus marinus* are enriched in the peptide MamC. This makes the surface negative at physiological pH whereas it is neutral at acidic pH close to 5 (Valverde-Tercedor et al., 2015). Therefore, cationic compounds can be adsorbed at neutral pH and released under mildly acidic conditions such as those around the bacterial surface. Thus, AS-48 has been used to load biomimetic magnetic nanoparticles (BMNPs) and assayed against a broad range of bacteria. As expected AS-48-BMNPs are active against *S. aureus*, *E. faecalis*, and *E. faecium*, but also against the Gram-negative *E. coli*. Such a potent killing effect is not visible with the other Gram-negative species *Pseudomonas aeruginosa* or *Klebsiella pneumoniae* and could be related to the less acidic environment that they cause during growth compared to the former species (Jabalera et al., 2021).

BMNPs can be directed using a magnetic field and, under an alternating magnetic field, they rotate. When the field frequency is high enough, rotation causes a local temperature increase that facilitates drug release and probably a local mechanical damage in the external bacterial structures that potentiates the effect of AS-48 against *E. faecium*, *S. aureus*, *E. coli* but also *P. aeruginosa*, and *K. pneumoniae*. AS-48-BMNPs have been tested under such conditions, therefore, combining the inhibitory effect of AS-48 to that of the higher temperatures (45°C). The reduction in cell viability is already noticeable after just 15 min treatment and can achieve less than 0.5% survivors of *S. aureus* or *E. faecium* and less than 0.15% for the Gram-negative species mentioned above. Remarkably,

avoparcin-resistant *E. faecium* and β–lactam-resistant *E. coli* remain susceptible to this treatment (Jabalera et al., 2021).

Activity of AS-48 against parasites

Although AS-48 is not active against eukaryotic cells some parasites with a negatively charged surface could be susceptible to this bacteriocin. This is the case of *Trypanosomatidae* family, which encompasses several pathogenic species that cause serious diseases in humans and animals (Table 2; Pereira-Chioccola et al., 2000; Souto-Padrón, 2002).

Activity of AS-48 against *Leishmania*

The first member from this family observed to be susceptible to AS-48 was *Leishmania* (Abengózar et al., 2017). Leishmaniases are a group of diseases (cutaneous leishmaniasis, visceral leishmaniasis, also known as kala-azar, and mucocutaneous leishmaniasis) caused by more than 20 *Leishmania* species and is transmitted by the bite of an infected sandfly insect vector. More than 1 billion people live in endemic areas for leishmaniasis (generally low-income countries) and more than 1 million new cases of leishmaniasis (mainly the cutaneous disease) are reported per year. The treatment is complex and should be administered by highly experienced health personnel. Besides, antileishmanial treatments cannot provide a cure, and the parasite remains in the human body causing relapses in case of immunosuppression. Also, some strains are already resistant to antiparasitic drugs (Ponte-Sucre et al., 2017). In their life cycle, the parasites are transmitted by the vector bite to the host as promastigotes that will be endocytosed by macrophages and other types o mononuclear phagocytic cells, and once inside the cell they will be transformed into intracellular amastigotes. In this form, they can multiply and proceed to infect other mononuclear phagocytic cells. When the vector takes the blood meal, the amastigotes change to promastigotes in the gut of the fly. The number is increased by division and then they migrate to the proboscis of the fly to infect a new host in the next blood meal (Bates, 2018). Thus, during its life cycle, both intracellular and extracellular forms are present, so drugs active against both parasite forms are desirable.

TABLE 2 Antimicrobial activity of AS-48 against several members of *Trypanosomatidae* family.

Parasites	Developmental forms	IC_{50} (μM)	Source
Leishmania donovani	Promastigotes	3.9 ± 1.1	Abengózar et al. (2017)
L. pifanoi	Amastigotes	10.2 ± 1.2	
Trypanosoma brucei brucei	Bloodstream	0.0031 ± 0.0002	Martínez-García et al. (2018)
	Procyclic	0.14 ± 0.057	
T. brucei gambiense	Bloodstream	0.0026 ± 0.0001	
T. brucei rhodesiense	Bloodstream	0.0017 ± 0.0002	
Trypanosoma cruzi Arequipa	Epimastigote	0.76 ± 0.11	Martín-Escolano et al. (2019)
	Amastigote	0.99 ± 0.13	
	Trypomastigote	0.17 ± 0.04	
T. cruzi SN3	Epimastigote	1.16 ± 0.18	
	Amastigote	6.81 ± 0.89	
	Trypomastigote	0.11 ± 0.02	
T. cruzi Tulahuen	Epimastigote	0.82 ± 0.11	
	Amastigote	1.98 ± 0.22	
	Trypomastigote	0.19 ± 0.03	

AS-48 can interact with *Leishmania* membranes. In the case of *Leishmania donovani,* the IC_{50} observed for promastigotes is 3.9 μM, while for *Leishmania pifanoi* axenic amastigotes it is 10.2 μM. Nevertheless, AS-48 can avoid the proliferation of the parasite at lower concentrations (1.3 and 7.5 μM, respectively; Abengózar et al., 2017). Remarkably, the leishmanicidal activity of AS-48 is not restricted to extracellular forms and 7 μM AS-48 reduces intracellular amastigotes parasitization index of the macrophage from 3.42 in untreated macrophages to 0.41 in the case of *L. pifanoi* (a reduction close to 90% after 48 h of treatment). Also, the percentage of infected macrophages decreases from 55.3% in untreated to 18.3% in AS-48 treated macrophages (Abengózar et al., 2017). These data suggest an intracellular activity of AS-48 in such phagocytic cells.

Activity of AS-48 against *Trypanosoma cruzi*

Another parasite recently described to be susceptible to AS-48 is *Trypanosoma cruzi*, which causes American trypanosomiasis or Chagas disease. This is a parasitic infection affecting about 7 million people worldwide but mainly in endemic areas of 21 continental Latin American countries, where it is mostly transmitted by contact with feces or urine of infected triatomine bugs (Guhl, 2017). In the cycle of life different parasite forms are found. The infective one is the metacyclic trypomastigotes which are delivered in the feces of the bug and can enter inside the host across the bite of the vector, penetrating the cells of the area where they are transformed into amastigotes. Intracellular amastigotes can multiply and after that, they are delivered and transformed into trypomastigotes which are released into the blood and can infect other cells. When the bug bites, the trypomastigotes change to epimastigotes in the insect gut where they can multiply. Finally, they change to the infective metacyclic trypomastigotes that will be delivered into the feces (Onyekwelu, 2019). Although Chagas disease treatment is 100% effective if it is administered soon after the infection, it usually fails in the chronic phase, and the existence of drug-resistant strains hinders the disease treatment (Campos et al., 2014).

AS-48 has shown to be effective at least against three different strains of this parasite, with IC_{50} ranging between 0.76–1.16 μM for epimastigote forms, 0.11–0.19 μM for trypomastigote forms, and 0.99–6.81 μM for the intracellular amastigote forms (Martín-Escolano et al., 2019). Interestingly, the intracellular test was performed using infected Vero cells instead of phagocytic cells and the results support that AS-48 can enter inside the cells, killing the parasites without affecting the integrity of the Vero cells at the concentrations tested (Martín-Escolano et al., 2019).

Finally, the activity of AS-48 is comparable to marketed drugs such as benznidazole *in vivo* in an experimental mice model of Chagas (Martín-Escolano et al., 2020). In mice infection models, a notable reduction in the parasitemia level was observed when AS-48 was administered at 1 mg/kg while no effect was observed for benznidazole at the same concentrations (although a remarkable activity for this drug was observed when administrated at 100 mg/kg). AS-48 trypanocidal effect is potent from the beginning of the treatment, showing the lowest parasitemia subsequently and being undetectable at 34 days after the infection (Martín-Escolano et al., 2020). The reactivation of the

parasitemia after immunosuppression in the chronic phase has been studied. In this case, a scarce (<10%) reactivation in the infection was noted in immunosuppressed mice treated with AS-48 compared to the benznidazole-treated mice (>50% of reactivation using 100 mg/kg). The presence of parasites was analyzed in 9 different parts of the mice (adipose tissue, bone marrow, brain, esophagus, heart, lung, muscle, spleen, and stomach) after the treatments. AS-48 is able to completely eliminate the parasites from bone marrow, brain, esophagus, lung, and spleen, while benznidazole at 100 mg/kg does the same in adipose tissue, brain, esophagus, spleen, and stomach (Martín-Escolano et al., 2020). These data show the potential of this AMP in the treatment of this infection.

Activity of AS-48 against *Trypanosoma brucei*

The activity of AS-48 has been also tested against *Trypanosoma brucei* which is largely the most susceptible organism to the peptide. It is the etiological agent of African trypanosomiasis also called sleeping sickness which is transmitted by tsetse fly bites. This disease is distributed across 36 countries in sub-Saharan Africa with an estimation of 300.000 cases per year. This parasite causes big economic losses since nagana, the animal trypanosomiasis, is responsible for the inability to establish livestock in the high vector exposed areas (Sutherland and Tediosi, 2019). The treatment is based on old and toxic drugs and is dependent on the state of the disease. The drugs used in the first stage are safer and easier to administer than those required for the second stage when the parasite crosses the hematoencephalic barrier. Three different stages are found in the life cycle of *T. brucei*. Briefly, the infective metacyclic trypomastigotes transferred to the host by the fly bites are transformed into bloodstream trypomastigotes that can multiply in blood escaping from the immune response by the quick switching of the VSG. Unlike *T. cruzi*, *T. brucei* is always in the blood and no intracellular forms exist. When the fly ingests the trypomastigotes from the blood they change to procyclic trypomastigotes in the midgut of the insect and after that, they change to epimastigotes outside of the gut. Finally, they move to the salivary gland of the fly where they are transformed into infective metacyclic trypomastigotes (Matthews, 2005). AS-48 has shown astonishing activity *in vitro* against both, animal and human *Trypanosoma* parasites (*T. brucei brucei*, *T. brucei rhodesiense*, *T. brucei gambiense*), with IC_{50} against bloodstream trypomastigote forms ranging from 1.7 nM for *T. brucei rhodesiense* to 3.12 nM for *T. brucei brucei*, thus more than 1,000-fold reduction compared to other trypanosomatids or even the most susceptible bacteria. In the case of procyclic forms of *T. brucei brucei,* the IC_{50} is 140 nM. This difference could be related to the less endocytic activity of these forms and the importance of this *T. brucei* characteristic in the AS-48 action mechanism.

Toxicity and safety of AS-48

Although bacteriocins are known since 100 years ago, their development and application are largely restricted to the food industry (Cotter et al., 2005). Nevertheless, the current emergency caused by MDR bacteria has given these compounds a renewed interest as new antimicrobial drugs (Cotter et al., 2013). Although their antimicrobial activity *in vitro* is well characterized, no or scarce data about hemolysis, toxicity on eukaryotic cell lines, or toxicity *in vivo* are usually provided, limiting their potential applications in a clinical scenario (Funck et al., 2020).

In the case of AS-48, preclinical characterization of its toxicity has been performed against a broad range of cell lines present in different organs, thus including breast (MCF10A) and colon (CCD18Co) epithelial cells (Cebrián et al., 2019), skin-related cells lines (A2058, CCD25sk; Cebrián et al., 2018), kidney (Vero; Martín-Escolano et al., 2019), immune system cell lines (MHS, J774.2, THP1, Raw264.7; Abengózar et al., 2017; Aguilar-Pérez et al., 2018), lung (MRC-5; Martínez-García et al., 2018) or liver (R1) cell lines (Baños et al., 2019a; Table 3). Similarly to many other cationic AMPs (Oddo and Hansen, 2017), AS-48 displays hemolytic activity against purified red cells. However, this activity disappears in the whole blood, while the antimicrobial activity is retained (Cebrián et al., 2019).

In addition to cells, toxicity has been evaluated in animals. In the case of zebrafish embryos, no visible anomalies were observable at low doses of AS-48 after 48 h, but at concentrations higher than 3 μM several lethal effects were observed. Nevertheless, the absence of data for cationic AMPs toxicity studies in this model suggests that this may not be an appropriate model for these kinds of compounds (Cebrián et al., 2019). In the case of mice, topical and systemic applications of AS-48 have been tested. No adverse reactions have been observed when AS-48 was topically applied and neither any remarkable effect was observed in mice treated intraperitoneally with 5 mg/kg each 8 h during 2 days (Cebrián et al., 2019) or in rainbow trout exposed to 14 μM of AS-48 in baths for 96 h (Baños et al., 2019a). Recently, the subchronic toxicological potential of AS-48 when administrated in the diet has been also evaluated (Baños et al., 2019b). For that purpose, the mice were fed with 200 mg/kg of AS-48 for 90 days and no adverse effects were detected upon food and water intake, body weight, urine, and blood biochemical/hematological parameters. Besides, no alterations in the heart, spleen, thymus, kidneys, and small and large intestines were observed, and only small degenerative changes were observed in the liver. Interestingly, no other abnormal signs were found concerning liver function (including hematological and serum biochemistry tests; Baños et al., 2019b).

AS-48 has been also assayed for mutagenicicity and genotoxicity by means of the bacterial reverse-mutation assay in *Salmonella*

TABLE 3 AS-48 cytotoxicity against several eukaryotic cell lines.

Cell line	Source	IC_{50} (μM)	Source
MRC-5	Human lung fibroblasts	>12.5*	Martínez-García et al. (2018)
Vero	Monkey kidney	93.06 ± 5.67	Martín-Escolano et al. (2019)
CCD18Co	Human colon	>28*	Cebrián et al. (2019)
MCF10A	Human mammary gland	>28*	
A2058	Human skin	>28*	Cebrián et al. (2018)
CCD25sk	Human skin	>28*	
MHS	Murine macrophages	>18*	Aguilar-Pérez et al. (2018)
J774.2	Murine macrophages	>18*	
THP-1	Human monocytes	>18*	
Raw 264.7	Murine macrophages	>50*	Abengózar et al. (2017)
R1	Salmon liver	>14*	Baños et al. (2019a)

*Highest concentration tested.

typhimurium TA97A, TA98, TA100, TA102, TA1535 strains (Ames test) and the micronucleus test, respectively. The results obtained in both tests revealed no mutagenicity or genotoxicity (Cascajosa-Lira et al., 2020).

Conclusion

Thirty-six years have passed since this unique circular bacteriocin was identified for the first time (Gálvez et al., 1986) and during this time it has been fully characterized from the genetical, structural, or biological activity points of view, being the circularization process the main challenge to be resolved yet (Sánchez-Hidalgo et al., 2011; Perez et al., 2018). The applicability of AS-48 has been mainly focused ever since on food preservation because of its potent antimicrobial activity against food spoilage and poisoning bacteria (Grande Burgos et al., 2014). However, the antimicrobial effect on human pathogens has favored numerous studies about toxicity and clinical application of AS-48 during the last few years. AS-48 shows no cross-resistance with other antibiotics and retains the activity against MDR bacteria. Moreover, it can sensitize resistant bacteria to antibiotics in certain synergistic combinations. Thus, the high potential of this peptide, alone or in combination with other drugs, for the treatment of several human (and animal) pathogens extends to multi-drug resistant strains. In fact, even activity against intracellular pathogens (bacteria and parasites) is documented. To the best of our knowledge, this kind of intracellular activity has not been reported for any other bacteriocin to date. An additional feature of AS-48 is its activity against biofilm-embedded bacteria (i.e., *S. aureus* and *C. acnes*) and slow-growing species, which often escape conventional treatments. Remarkably, membrane permeabilization and depolarization can be observed after just 24 h of treatment in the case of *Mycobacterium* spp., which shows the ability of this peptide to kill bacteria with very low metabolic activity. The preliminary studies using nanocarriers loaded with AS-48 open new scenarios to boost the activity against local infections caused by different bacteria, in which the ability to kill cells independently of their metabolic activity and growth rate can constitute a great advance. Preclinical toxicological analyses have shown that AS-48 is a safe molecule with high selectivity for bacteria and low toxicity towards human and animal cell lines at inhibitory concentrations. Its efficacy *in vivo* in mice models encourages us to consider AS-48 as a safe and efficient antimicrobial molecule.

Finally, and despite the effort in the preclinical characterization of AS-48, further analyses are still necessary to understand how AS-48 can enter inside the cell, killing intracellular pathogens, and to fully evaluate the toxicity using different administration routes, to discard an immune response against the peptide. Finally, further establishing the effectivity *in vivo* against additional infection models in both animals and humans is desired.

Author contributions

RC, MM-G, and MM-L wrote the manuscript. RC and MM-G created the figures and tables. MF, FG, MM-B, EV, OK, and MM contributed to reviewing and editing the manuscript. All authors contributed to the article and approved the submitted version.

Funding

MM-L acknowledges funding from FEDER Operational Program B-BIO-268-UGR20 and Proyectos de I+D+I, del Plan Andaluz de Investigación, Desarrollo e Innovación Grant P20_00339. RC acknowledges funding from the Instituto de Salud Carlos III (ISCIII, Miguel Servet program, ref: CP21/00113, Spain).

Acknowledgments

MM-G thanks the Marie Curie program (grant no. 895210).

Conflict of interest

The authors declare that the research was conducted in the absence of any commercial or financial relationships that could be construed as a potential conflict of interest.

Publisher's note

References

Abengózar, M. Á., Cebrián, R., Saugar, J. M., Gárate, T., Valdivia, E., Martínez-Bueno, M., et al. (2017). Enterocin AS-48 AS evidence for the use of bacteriocins as new leishmanicidal agents. *Antimicrob. Agents Chemother.* 61:e02288-16. doi: 10.1128/AAC.02288-16

Abriouel, H., Lucas, R., Omar, N. B., Valdivia, E., and Gálvez, A. (2010). Potential applications of the cyclic peptide enterocin AS-48 in the preservation of vegetable foods and beverages. *Probiotics Antimicrob. Proteins.* 2, 77–89. doi: 10.1007/s12602-009-9030-y

Abriouel, H., Maqueda, M., Gálvez, A., Martínez-Bueno, M., and Valdivia, E. (2002). Inhibition of bacterial growth, enterotoxin production, and spore outgrowth in strains of *Bacillus cereus* by bacteriocin AS-48. *Appl. Environ. Microbiol.* 68, 1473–1477. doi: 10.1128/AEM.68.3.1473-1477.2002

Abriouel, H., Sánchez-González, J., Maqueda, M., Gálvez, A., Valdivia, E., and José Gálvez-Ruiz, M. (2001). Monolayer characteristics of bacteriocin AS-48, pH effect and interactions with dipalmitoyl phosphatidic acid at the air–water interface. *J. Colloid Interface Sci.* 233, 306–312. doi: 10.1006/jcis.2000.7239

Abriouel, H., Valdivia, E., Gálvez, A., and Maqueda, M. (1998). Response of *Salmonella choleraesuis* LT2 spheroplasts and permeabilized cells to the bacteriocin AS-48. *Appl. Environ. Microbiol.* 64, 4623–4626. doi: 10.1128/AEM.64.11.4623-4626.1998

Achermann, Y., Goldstein, E. J. C., Coenye, T., and Shirtliff, M. E. (2014). *Propionibacterium acnes*: from commensal to opportunistic biofilm-associated implant pathogen. *Clin. Microbiol. Rev.* 27, 419–440. doi: 10.1128/CMR.00092-13

Aguilar-Pérez, C., Gracia, B., Rodrigues, L., Vitoria, A., Cebrián, R., Deboosère, N., et al. (2018). Synergy between circular bacteriocin AS-48 and ethambutol against *Mycobacterium tuberculosis*. *Antimicrob. Agents Chemother.* 62, e00359–e00318. doi: 10.1128/AAC.00359-18

Alvarez-Sieiro, P., Montalbán-López, M., Mu, D., and Kuipers, O. P. (2016). Bacteriocins of lactic acid bacteria: extending the family. *Appl. Microbiol. Biotechnol.* 100, 2939–2951. doi: 10.1007/s00253-016-7343-9

Ananou, S., Gálvez, A., Martínez-Bueno, M., Maqueda, M., and Valdivia, E. (2005). Synergistic effect of enterocin AS-48 in combination with outer membrane permeabilizing treatments against *Escherichia coli* O157:H7. *J. Appl. Microbiol.* 99, 1364–1372. doi: 10.1111/j.1365-2672.2005.02733.x

Ananou, S., Zentar, H., Martínez-Bueno, M., Gálvez, A., Maqueda, M., and Valdivia, E. (2014). The impact of enterocin AS-48 on the shelf-life and safety of sardines (*Sardina pilchardus*) under different storage conditions. *Food Microbiol.* 44, 185–195. doi: 10.1016/j.fm.2014.06.008

Band, V. I., and Weiss, D. S. (2015). Mechanisms of antimicrobial peptide resistance in gram-negative bacteria. *Antibiotics (Basel)* 4, 18–41. doi: 10.3390/antibiotics4010018

Baños, A., Ariza, J. J., Nuñez, C., Gil-Martínez, L., García-López, J. D., Martínez-Bueno, M., et al. (2019a). Effects of *Enterococcus faecalis* UGRA10 and the enterocin AS-48 against the fish pathogen *Lactococcus garvieae*. Studies *in vitro* and *in vivo*. *Food Microbiol.* 77, 69–77. doi: 10.1016/j.fm.2018.08.002

Baños, A., García, J. D., Núñez, C., Mut-Salud, N., Ananou, S., Martínez-Bueno, M., et al. (2019b). Subchronic toxicity study in BALBc mice of enterocin AS-48, an anti-microbial peptide produced by *Enterococcus faecalis* UGRA10. *Food Chem. Toxicol.* 132:110667. doi: 10.1016/j.fct.2019.110667

Bates, P. A. (2018). Revising Leishmania's life cycle. *Nat. Microbiol.* 3, 529–530. doi: 10.1038/s41564-018-0154-2

Bintsis, T. (2017). Foodborne pathogens. *AIMS Microbiol* 3, 529–563. doi: 10.3934/microbiol.2017.3.529

Butler, M. S., and Paterson, D. L. (2020). Antibiotics in the clinical pipeline in October 2019. *J. Antibiot.* 73, 329–364. doi: 10.1038/s41429-020-0291-8

Caballero Gómez, N., Abriouel, H., Grande, M. J., Pérez Pulido, R., and Gálvez, A. (2013). Combined treatments of enterocin AS-48 with biocides to improve the inactivation of methicillin-sensitive and methicillin-resistant *Staphylococcus aureus* planktonic and sessile cells. *Int. J. Food Microbiol.* 163, 96–100. doi: 10.1016/j.ijfoodmicro.2013.02.018

Campos, M. C. O., Leon, L. L., Taylor, M. C., and Kelly, J. M. (2014). Benznidazole-resistance in *Trypanosoma cruzi*: evidence that distinct mechanisms can act in concert. *Mol. Biochem. Parasitol.* 193, 17–19. doi: 10.1016/j.molbiopara.2014.01.002

Cascajosa-Lira, A., Prieto, A. I., Puerto, M., Baños, A., Valdivia, E., Jos, A., et al. (2020). Mutagenicity and genotoxicity assessment of a new biopreservative product rich in Enterocin AS-48. *Food Chem. Toxicol.* 146:111846. doi: 10.1016/j.fct.2020.111846

Cebrián, R., Arévalo, S., Rubiño, S., Arias-Santiago, S., Rojo, M. D., Montalbán-López, M., et al. (2018). Control of *Propionibacterium acnes* by natural antimicrobial substances: role of the bacteriocin AS-48 and lysozyme. *Sci. Rep.* 8:11766. doi: 10.1038/s41598-018-29580-7

Cebrián, R., Baños, A., Valdivia, E., Pérez-Pulido, R., Martínez-Bueno, M., and Maqueda, M. (2012). Characterization of functional, safety, and probiotic properties of *Enterococcus faecalis* UGRA10, a new AS-48-producer strain. *Food Microbiol.* 30, 59–67. doi: 10.1016/j.fm.2011.12.002

Cebrián, R., Martínez-Bueno, M., Valdivia, E., Albert, A., Maqueda, M., and Sánchez-Barrena, M. J. (2015). The bacteriocin AS-48 requires dimer dissociation followed by hydrophobic interactions with the membrane for antibacterial activity. *J. Struct. Biol.* 190, 162–172. doi: 10.1016/j.jsb.2015.03.006

Cebrián, R., Rodríguez-Cabezas, M. E., Martín-Escolano, R., Rubiño, S., Garrido-Barros, M., Montalbán-López, M., et al. (2019). Preclinical studies of toxicity and safety of the AS-48 bacteriocin. *J. Adv. Res.* 20, 129–139. doi: 10.1016/j.jare.2019.06.003

Cesa-Luna, C., Alatorre-Cruz, J.-M., Carreño-López, R., Quintero-Hernández, V., and Baez, A. (2021). Emerging applications of bacteriocins as antimicrobials, anticancer drugs, and modulators of the gastrointestinal microbiota. *Pol. J. Microbiol.* 70, 143–159. doi: 10.33073/pjm-2021-020

Cobo Molinos, A., Abriouel, H., López, R. L., Valdivia, E., Omar, N. B., and Gálvez, A. (2008). Combined physico-chemical treatments based on enterocin AS-48 for inactivation of gram-negative bacteria in soybean sprouts. *Food Chem. Toxicol.* 46, 2912–2921. doi: 10.1016/j.fct.2008.05.035

Cotter, P. D., Hill, C., and Ross, R. P. (2005). Bacteriocins: developing innate immunity for food. *Nat. Rev. Microbiol.* 3, 777–788. doi: 10.1038/nrmicro1273

Cotter, P. D., Ross, R. P., and Hill, C. (2013). Bacteriocins — a viable alternative to antibiotics? *Microbiology* 11, 95–105. doi: 10.1038/nrmicro2937

Cruz, J., Ortiz, C., Guzmán, F., Fernández-Lafuente, R., and Torres, R. (2014). Antimicrobial peptides: promising compounds against pathogenic microorganisms. *Curr. Med. Chem.* 21, 2299–2321. doi: 10.2174/0929867321666140217110155

Cruz, V. L., Ramos, J., Martinez-Salazar, J., Montalban-Lopez, M., and Maqueda, M. (2021). The role of key amino acids in the antimicrobial mechanism of a bacteriocin model revealed by molecular simulations. *J. Chem. Inf. Model.* 61, 6066–6078. doi: 10.1021/acs.jcim.1c00838

Cruz, V. L., Ramos, J., Melo, M. N., and Martinez-Salazar, J. (2013). Bacteriocin AS-48 binding to model membranes and pore formation as revealed by coarse-grained simulations. *Biochim. Biophys. Acta Biomembr.* 1828, 2524–2531. doi: 10.1016/j.bbamem.2013.05.036

del Castillo-Santaella, T., Cebrián, R., Maqueda, M., Gálvez-Ruiz, M. J., and Maldonado-Valderrama, J. (2018). Assessing *in vitro* digestibility of food biopreservative AS-48. *Food Chem.* 246, 249–257. doi: 10.1016/j.foodchem.2017.10.149

Deslouches, B., Montelaro, R. C., Urish, K. L., and Di, Y. P. (2020). Engineered cationic antimicrobial peptides (eCAPs) to combat multidrug-resistant bacteria. *Pharmaceutics* 12:501. doi: 10.3390/pharmaceutics12060501

Diaz, M., Valdivia, E., Martínez-Bueno, M., Fernández, M., Soler-González, A. S., Ramírez-Rodrigo, H., et al. (2003). Characterization of a new operon, *as-48EFGH*, from the *as-48* gene cluster involved in immunity to enterocin AS-48. *Appl. Environ. Microbiol.* 69, 1229–1236. doi: 10.1128/AEM.69.2.1229-1236.2003

Dischinger, J., Basi Chipalu, S., and Bierbaum, G. (2014). Lantibiotics: promising candidates for future applications in health care. *Int. J. Med. Microbiol.* 304, 51–62. doi: 10.1016/j.ijmm.2013.09.003

Dréno, B., Pécastaings, S., Corvec, S., Veraldi, S., Khammari, A., and Roques, C. (2018). *Cutibacterium acnes* (*Propionibacterium acnes*) and *Acne vulgaris*: a brief look at the latest updates. *J. Eur. Acad. Dermatol. Venereol.* 32, 5–14. doi: 10.1111/jdv.15043

Fernández, M., Martínez-Bueno, M., Martín, M. C., Valdivia, E., and Maqueda, M. (2007). Heterologous expression of enterocin AS-48 in several strains of lactic acid bacteria. *J. Appl. Microbiol.* 102, 1350–1361. doi: 10.1111/j.1365-2672.2006.03194.x

Funck, G. D., de Lima Marques, J., da Silva Dannenberg, G., dos Santos Cruxen, C. E., Sehn, C. P., Prigol, M., et al. (2020). Characterization, toxicity, and optimization for the growth and production of bacteriocin-like substances by *Lactobacillus curvatus*. *Probiotics Antimicro. Prot.* 12, 91–101. doi: 10.1007/s12602-019-09531-y

Furuya, E. Y., and Lowy, F. D. (2006). Antimicrobial-resistant bacteria in the community setting. *Nat. Rev. Microbiol.* 4, 36–45. doi: 10.1038/nrmicro1325

Gabrielsen, C., Brede, D. A., Nes, I. F., and Diep, D. B. (2014). Circular bacteriocins: biosynthesis and mode of action. *Appl. Environ. Microbiol.* 80, 6854–6862. doi: 10.1128/AEM.02284-14

Gálvez, A., Maqueda, M., Martínez-Bueno, M., and Valdivia, E. (1989). Bactericidal and bacteriolytic action of peptide antibiotic AS-48 against gram-positive and gram-negative bacteria and other organisms. *Res. Microbiol.* 140, 57–68. doi: 10.1016/0923-2508(89)90060-0

Gálvez, A., Maqueda, M., Martínez-Bueno, M., and Valdivia, E. (1991). Permeation of bacterial cells, permeation of cytoplasmic and artificial membrane vesicles, and channel formation on lipid bilayers by peptide antibiotic AS-48. *J. Bacteriol.* 173, 886–892. doi: 10.1128/jb.173.2.886-892.1991

Gálvez, A., Maqueda, M., Valdivia, E., Quesada, A., and Montoya, E. (1986). Characterization and partial purification of a broad spectrum antibiotic AS-48 produced by *Streptococcus faecalis*. *Can. J. Microbiol.* 32, 765–771. doi: 10.1139/m86-141

Gómez, N. C., Abriouel, H., Grande, M. A. J., Pulido, R. P., and Gálvez, A. (2012). Effect of enterocin AS-48 in combination with biocides on planktonic and sessile *Listeria monocytogenes*. *Food Microbiol.* 30, 51–58. doi: 10.1016/j.fm.2011.12.013

González, C., Langdon, G. M., Bruix, M., Gálvez, A., Valdivia, E., Maqueda, M., et al. (2000). Bacteriocin AS-48, a microbial cyclic polypeptide structurally and functionally related to mammalian NK-lysin. *Proc. Natl. Acad. Sci. U. S. A.* 97, 11221–11226. doi: 10.1073/pnas.210301097

Grande Burgos, M. J., Pérez Pulido, R., del López Aguayo, M. C., Gálvez, A., and Lucas, R. (2014). The cyclic antibacterial peptide enterocin AS-48: isolation, mode of action, and possible food applications. *Int. J. Mol. Sci.* 15, 22706–22727. doi: 10.3390/ijms151222706

Grande, M. J., Lucas, R., Abriouel, H., Omar, N. B., Maqueda, M., Martínez-Bueno, M., et al. (2005). Control of *Alicyclobacillus acidoterrestris* in fruit juices by enterocin AS-48. *Int. J. Food Microbiol.* 104, 289–297. doi: 10.1016/j.ijfoodmicro.2005.03.010

Grande, M. J., Lucas, R., Abriouel, H., Valdivia, E., Omar, N. B., Maqueda, M., et al. (2006). Inhibition of toxicogenic *Bacillus cereus* in rice-based foods by enterocin AS-48. *Int. J. Food Microbiol.* 106, 185–194. doi: 10.1016/j.ijfoodmicro.2005.08.003

Guhl, F. (2017). "5- geographical distribution of chagas disease" in *American Trypanosomiasis Chagas Disease*. eds. J. Telleria and M. Tibayrenc. *2nd* ed (London: Elsevier), 89–112.

Hay, R. J., Johns, N. E., Williams, H. C., Bolliger, I. W., Dellavalle, R. P., Margolis, D. J., et al. (2014). The global burden of skin disease in 2010: an analysis of the prevalence and impact of skin conditions. *J. Investig. Dermatol.* 134, 1527–1534. doi: 10.1038/jid.2013.446

Hofer, U. (2019). The cost of antimicrobial resistance. *Nat. Rev. Microbiol.* 17:3. doi: 10.1038/s41579-018-0125-x

Jabalera, Y., Montalban-Lopez, M., Vinuesa-Rodriguez, J. J., Iglesias, G. R., Maqueda, M., and Jimenez-Lopez, C. (2021). Antibacterial directed chemotherapy using AS-48 peptide immobilized on biomimetic magnetic nanoparticles combined with magnetic hyperthermia. *Int. J. Biol. Macromol.* 189, 206–213. doi: 10.1016/j.ijbiomac.2021.08.110

Jit, M., Ng, D. H. L., Luangasanatip, N., Sandmann, F., Atkins, K. E., Robotham, J. V., et al. (2020). Quantifying the economic cost of antibiotic resistance and the impact of related interventions: rapid methodological review, conceptual framework and recommendations for future studies. *BMC Med.* 18:38. doi: 10.1186/s12916-020-1507-2

Juturu, V., and Wu, J. C. (2018). Microbial production of bacteriocins: latest research development and applications. *Biotechnol. Adv.* 36, 2187–2200. doi: 10.1016/j.biotechadv.2018.10.007

Laxminarayan, R., Duse, A., Wattal, C., Zaidi, A. K. M., Wertheim, H. F. L., Sumpradit, N., et al. (2013). Antibiotic resistance—the need for global solutions. *Lancet Infect. Dis.* 13, 1057–1098. doi: 10.1016/S1473-3099(13)70318-9

Magana, M., Pushpanathan, M., Santos, A. L., Leanse, L., Fernandez, M., Ioannidis, A., et al. (2020). The value of antimicrobial peptides in the age of resistance. *Lancet Infect. Dis.* 20, e216–e230. doi: 10.1016/S1473-3099(20)30327-3

Manna, P. T., Boehm, C., Leung, K. F., Natesan, S. K., and Field, M. C. (2014). Life and times: synthesis, trafficking, and evolution of VSG. *Trends Parasitol.* 30, 251–258. doi: 10.1016/j.pt.2014.03.004

Maqueda, M., Gálvez, A., Bueno, M. M., Sanchez-Barrena, M. J., González, C., Albert, A., et al. (2004). Peptide AS-48: prototype of a new class of cyclic bacteriocins. *Curr. Protein Pept. Sci.* 5, 399–416. doi: 10.2174/1389203043379567

Martín-Escolano, R., Cebrián, R., Maqueda, M., Romero, D., Rosales, M. J., Sánchez-Moreno, M., et al. (2020). Assessing the effectiveness of AS-48 in experimental mice models of chagas' disease. *J. Antimicrob. Chemother.* 75, 1537–1545. doi: 10.1093/jac/dkaa030

Martín-Escolano, R., Cebrián, R., Martín-Escolano, J., Rosales, M. J., Maqueda, M., Sánchez-Moreno, M., et al. (2019). Insights into chagas treatment based on the potential of bacteriocin AS-48. *Int. J. Parasitol. Drugs Drug Resist.* 10, 1–8. doi: 10.1016/j.ijpddr.2019.03.003

Martínez-Bueno, M., Valdivia, E., Gálvez, A., Coyette, J., and Maqueda, M. (1998). Analysis of the gene cluster involved in production and immunity of the peptide antibiotic AS-48 in *Enterococcus faecalis*. *Mol. Microbiol.* 27, 347–358. doi: 10.1046/j.1365-2958.1998.00682.x

Martínez-García, M., Bart, J.-M., Campos-Salinas, J., Valdivia, E., Martínez-Bueno, M., González-Rey, E., et al. (2018). Autophagic-related cell death of *Trypanosoma brucei* induced by bacteriocin AS-48. *Int. J. Parasitol. Drugs Drug Resist.* 8, 203–212. doi: 10.1016/j.ijpddr.2018.03.002

Martinović, T., Andjelković, U., Gajdošik, M. Š., Rešetar, D., and Josić, D. (2016). Foodborne pathogens and their toxins. *J. Proteome* 147, 226–235. doi: 10.1016/j.jprot.2016.04.029

Matthews, K. R. (2005). The developmental cell biology of *Trypanosoma brucei*. *J. Cell Sci.* 118, 283–290. doi: 10.1242/jcs.01649

May, M. (2014). Drug development: time for teamwork. *Nature* 509, S4–S5. doi: 10.1038/509S4a

McCullough, A. R., Parekh, S., Rathbone, J., Del Mar, C. B., and Hoffmann, T. C. (2016). A systematic review of the public's knowledge and beliefs about antibiotic resistance. *J. Antimicrob. Chemother.* 71, 27–33. doi: 10.1093/jac/dkv310

Mendoza, F., Maqueda, M., Gálvez, A., Martínez-Bueno, M., and Valdivia, E. (1999). Antilisterial activity of peptide AS-48 and study of changes induced in the cell envelope properties of an AS-48-adapted strain of *Listeria monocytogenes*. *Appl. Environ. Microbiol.* 65, 618–625. doi: 10.1128/AEM.65.2.618-625.1999

Montalbán-López, M., Cebrián, R., Galera, R., Mingorance, L., Martín-Platero, A. M., Valdivia, E., et al. (2020a). Synergy of the bacteriocin AS-48 and antibiotics against uropathogenic enterococci. *Antibiotics* 9:567. doi: 10.3390/antibiotics9090567

Montalbán-López, M., Sánchez-Hidalgo, M., Cebrián, R., and Maqueda, M. (2012). Discovering the bacterial circular proteins: bacteriocins, cyanobactins, and pilins. *J. Biol. Chem.* 287, 27007–27013. doi: 10.1074/jbc.R112.354688

Montalbán-López, M., Sánchez-Hidalgo, M., Valdivia, E., Martínez-Bueno, M., and Maqueda, M. (2011). Are bacteriocins underexploited? Novel applications for old antimicrobials. *Curr. Pharm. Biotechnol.* 12, 1205–1220. doi: 10.2174/138920111796117364

Montalbán-López, M., Scott, T. A., Ramesh, S., Rahman, I. R., Heel, A. J., van Viel, J. H., et al. (2020b). New developments in RiPP discovery, enzymology and engineering. *Nat. Prod. Rep.* 38, 130–239. doi: 10.1039/D0NP00027B

Montalbán-López, M., Spolaore, B., Pinato, O., Martínez-Bueno, M., Valdivia, E., Maqueda, M., et al. (2008). Characterization of linear forms of the circular enterocin AS-48 obtained by limited proteolysis. *FEBS Lett.* 582, 3237–3242. doi: 10.1016/j.febslet.2008.08.018

Montalbán-López, M., van Heel, A. J., and Kuipers, O. P. (2017). Employing the promiscuity of lantibiotic biosynthetic machineries to produce novel antimicrobials. *FEMS Microbiol. Rev.* 41, 5–18. doi: 10.1093/femsre/fuw034

Mookherjee, N., Anderson, M. A., Haagsman, H. P., and Davidson, D. J. (2020). Antimicrobial host defence peptides: functions and clinical potential. *Nat. Rev. Drug Discov.* 19, 311–332. doi: 10.1038/s41573-019-0058-8

Nguyen, G. K. T., Kam, A., Loo, S., Jansson, A. E., Pan, L. X., and Tam, J. P. (2015). Butelase 1: a versatile ligase for peptide and protein macrocyclization. *J. Am. Chem. Soc.* 137, 15398–15401. doi: 10.1021/jacs.5b11014

O'Connor, P. M., Kuniyoshi, T. M., Oliveira, R. P., Hill, C., Ross, R. P., and Cotter, P. D. (2020). Antimicrobials for food and feed; a bacteriocin perspective. *Curr. Opin. Biotechnol.* 61, 160–167. doi: 10.1016/j.copbio.2019.12.023

O'Neill, J. (2014). The Review on Antimicrobial Resistance, Chaired by Jim O'Neill. Antimicrobial Resistance: Tackling a Crisis for the Future Health and Wealth of Nations. Review on Antimicrobial Resistance. Available at: https://amr-review.org/sites/default/files/AMR%20Review%20Paper%20-%20Tackling%20a%20crisis%20for%20the%20health%20and%20wealth%20of%20nations_1.pdf (].

O'Neill, J. (2016). *Tackling Drug-Resistant Infections Globally: Final Report and Recommendations*. The Review on Antimicrobial Resistance. Government of the United Kingdom.

Oddo, A., and Hansen, P. R. (2017). Hemolytic activity of antimicrobial peptides. *Methods Mol. Biol.* 1548, 427–435. doi: 10.1007/978-1-4939-6737-7_31

Onyekwelu, K. C. (2019). Life cycle of *Trypanosoma cruzi* in the invertebrate and the vertebrate hosts. *Biology of Trypanosoma cruzi*. 1–19. doi: 10.5772/intechopen.84639

Perales-Adan, J., Rubiño, S., Martinez-Bueno, M., Valdivia, E., Montalban-Lopez, M., Cebrian, R., et al. (2018). LAB bacteriocins controlling the food isolated (drug-resistant) staphylococci. *Front. Microbiol.* 9:1143. doi: 10.3389/fmicb.2018.01143

Pereira-Chioccola, V. L., Acosta-Serrano, A., Correia de Almeida, I., Ferguson, M. A., Souto-Padron, T., Rodrigues, M. M., et al. (2000). Mucin-like molecules form a negatively charged coat that protects *Trypanosoma cruzi* trypomastigotes from killing by human anti-alpha-galactosyl antibodies. *J. Cell Sci.* 113, 1299–1307. doi: 10.1242/jcs.113.7.1299

Perez, R. H., Zendo, T., and Sonomoto, K. (2018). Circular and leaderless bacteriocins: biosynthesis, mode of action, applications, and prospects. *Front. Microbiol.* 9:2085. doi: 10.3389/fmicb.2018.02085

Podolsky, S. H. (2018). The evolving response to antibiotic resistance (1945–2018). *Palgrave Commun.* 4, 1–8. doi: 10.1057/s41599-018-0181-x

Ponte-Sucre, A., Gamarro, F., Dujardin, J.-C., Barrett, M. P., López-Vélez, R., García-Hernández, R., et al. (2017). Drug resistance and treatment failure in leishmaniasis: a 21st century challenge. *PLoS Negl. Trop. Dis.* 11:e0006052. doi: 10.1371/journal.pntd.0006052

Porto-Carreiro, I., Attias, M., Miranda, K., De Souza, W., and Cunha-e-Silva, N. (2000). *Trypanosoma cruzi* epimastigote endocytic pathway: cargo enters the cytostome and passes through an early endosomal network before storage in reservosomes. *Eur. J. Cell Biol.* 79, 858–869. doi: 10.1078/0171-9335-00112

Samuels, D. V., Rosenthal, R., Lin, R., Chaudhari, S., and Natsuaki, M. N. (2020). *Acne vulgaris* and risk of depression and anxiety: a meta-analytic review. *J. Am. Acad. Dermatol.* 83, 532–541. doi: 10.1016/j.jaad.2020.02.040

Sánchez-Barrena, M. J., Martínez-Ripoll, M., Gálvez, A., Valdivia, E., Maqueda, M., Cruz, V., et al. (2003). Structure of bacteriocin AS-48: from soluble state to membrane bound state. *J. Mol. Biol.* 334, 541–549. doi: 10.1016/j.jmb.2003.09.060

Sánchez-Hidalgo, M., Martínez-Bueno, M., Fernández-Escamilla, A. M., Valdivia, E., Serrano, L., and Maqueda, M. (2008). Effect of replacing glutamic residues upon the biological activity and stability of the circular enterocin AS-48. *J. Antimicrob. Chemother.* 61, 1256–1265. doi: 10.1093/jac/dkn126

Sánchez-Hidalgo, M., Montalbán-López, M., Cebrián, R., Valdivia, E., Martínez-Bueno, M., and Maqueda, M. (2011). AS-48 bacteriocin: close to perfection. *Cell. Mol. Life Sci.* 68, 2845–2857. doi: 10.1007/s00018-011-0724-4

Scallan, E., Hoekstra, R. M., Angulo, F. J., Tauxe, R. V., Widdowson, M.-A., Roy, S. L., et al. (2011). Foodborne illness acquired in the United States—major pathogens. *Emerg. Infect. Dis. J.* 17, 7–15. doi: 10.3201/eid1701.p11101

Silva, C. C. G., Silva, S. P. M., and Ribeiro, S. C. (2018). Application of bacteriocins and protective cultures in dairy food preservation. *Front. Microbiol.* 9:594. doi: 10.3389/fmicb.2018.00594

Soltani, S., Hammami, R., Cotter, P. D., Rebuffat, S., Said, L. B., Gaudreau, H., et al. (2021). Bacteriocins as a new generation of antimicrobials: toxicity aspects and regulations. *FEMS Microbiol. Rev.* 45:fuaa039. doi: 10.1093/femsre/fuaa039

Souto-Padrón, T. (2002). The surface charge of trypanosomatids. *An. Acad. Bras. Cienc.* 74, 649–675. doi: 10.1590/S0001-37652002000400007

Stevens, C. A., Semrau, J., Chiriac, D., Litschko, M., Campbell, R. L., Langelaan, D. N., et al. (2017). Peptide backbone circularization enhances antifreeze protein thermostability. *Protein Sci.* 26, 1932–1941. doi: 10.1002/pro.3228

Strijbis, K., and Ploegh, H. (2014). Secretion of circular proteins using sortase. *Methods Mol. Biol.* 1174, 73–83. doi: 10.1007/978-1-4939-0944-5_5

Sutherland, C. S., and Tediosi, F. (2019). Is the elimination of 'sleeping sickness' affordable? Who will pay the price? Assessing the financial burden for the elimination of human African trypanosomiasis *Trypanosoma brucei gambiense* in sub-Saharan Africa. *BMJ Glob. Health* 4:e001173. doi: 10.1136/bmjgh-2018-001173

Tauxe, R. V. (2002). Emerging foodborne pathogens. *Int. J. Food Microbiol.* 78, 31–41. doi: 10.1016/S0168-1605(02)00232-5

Teso-Pérez, C., Martínez-Bueno, M., Peralta-Sánchez, J. M., Valdivia, E., Maqueda, M., Fárez-Vidal, M. E., et al. (2021). Enterocin cross-resistance mediated by ABC transport systems. *Microorganisms* 9:1411. doi: 10.3390/microorganisms9071411

Theuretzbacher, U., Outterson, K., Engel, A., and Karlén, A. (2020). The global preclinical antibacterial pipeline. *Nat. Rev. Microbiol.* 18, 275–285. doi: 10.1038/s41579-019-0288-0

Tyers, M., and Wright, G. D. (2019). Drug combinations: a strategy to extend the life of antibiotics in the 21st century. *Nat. Rev. Microbiol.* 17, 141–155. doi: 10.1038/s41579-018-0141-x

Valverde-Tercedor, C., Montalbán-López, M., Perez-Gonzalez, T., Sanchez-Quesada, M. S., Prozorov, T., Pineda-Molina, E., et al. (2015). Size control of in vitro synthesized magnetite crystals by the MamC protein of *Magnetococcus marinus* strain MC-1. *Appl. Microbiol. Biotechnol.* 99, 5109–5121. doi: 10.1007/s00253-014-6326-y

van Heel, A. J., Montalban-Lopez, M., Oliveau, Q., and Kuipers, O. P. (2017). Genome-guided identification of novel head-to-tail cyclized antimicrobial peptides, exemplified by the discovery of pumilarin. *Microb Genom* 3:e000134. doi: 10.1099/mgen.0.000134

Velázquez-Suárez, C., Cebrián, R., Gasca-Capote, C., Sorlózano-Puerto, A., Gutiérrez-Fernández, J., Martínez-Bueno, M., et al. (2021). Antimicrobial activity of the circular bacteriocin AS-48 against clinical multidrug-resistant *Staphylococcus aureus*. *Antibiotics* 10:925. doi: 10.3390/antibiotics10080925

Vezina, B., Rehm, B. H. A., and Smith, A. T. (2020). Bioinformatic prospecting and phylogenetic analysis reveals 94 undescribed circular bacteriocins and key motifs. *BMC Microbiol.* 20:77. doi: 10.1186/s12866-020-01772-0

Weidmann, J., and Craik, D. J. (2016). Discovery, structure, function, and applications of cyclotides: circular proteins from plants. *J. Exp. Bot.* 67, 4801–4812. doi: 10.1093/jxb/erw210

WHO (2017). Global Priority List of Antibiotic-Resistant Bacteria to Guide Research, Discovery, and Development of New Antibiotics. WHO. Available at: http://www.who.int/medicines/publications/WHO-PPL-Short_Summary_25Feb-ET_NM_WHO.pdf (Accessed April 30, 2018).

WHO (2022a). 2021 Antibacterial Agents in Clinical and Preclinical Development: An Overview and Analysis. WHO. Available at: http://www.who.int/medicines/areas/rational_use/antibacterial_agents_clinical_development/en/ (Accessed February 27, 2019).

WHO (2022b). Global Tuberculosis Report 2021. Available at: https://www.who.int/publications-detail-redirect/9789240037021 (Accessed January 20, 2022).

WHO|Global Tuberculosis Report (2019). WHO. Available at: http://www.who.int/tb/publications/global_report/en/ (Accessed September 25, 2020).

Xu, X., Xu, L., Yuan, G., Wang, Y., Qu, Y., and Zhou, M. (2018). Synergistic combination of two antimicrobial agents closing each other's mutant selection windows to prevent antimicrobial resistance. *Sci. Rep.* 8:7237. doi: 10.1038/s41598-018-25714-z

frontiers | Frontiers in Microbiology

TYPE Original Research
PUBLISHED 08 February 2023
DOI 10.3389/fmicb.2023.1117684

OPEN ACCESS

EDITED BY
Paloma López,
Spanish National Research Council (CSIC), Spain

REVIEWED BY
Victor Ladero,
Spanish National Research Council (CSIC), Spain
Timothy Meredith,
The Pennsylvania State University, United States

*CORRESPONDENCE
Christian Magni
✉ magni@ibr-conicet.gov.ar

SPECIALTY SECTION
This article was submitted to Food Microbiology, a section of the journal Frontiers in Microbiology

RECEIVED 06 December 2022
ACCEPTED 17 January 2023
PUBLISHED 08 February 2023

CITATION
Acciarri G, Gizzi FO, Torres Manno MA, Stülke J, Espariz M, Blancato VS and Magni C (2023) Redundant potassium transporter systems guarantee the survival of *Enterococcus faecalis* under stress conditions.
Front. Microbiol. 14:1117684.
doi: 10.3389/fmicb.2023.1117684

Redundant potassium transporter systems guarantee the survival of *Enterococcus faecalis* under stress conditions

Giuliana Acciarri[1], Fernán O. Gizzi[1], Mariano A. Torres Manno[1,2], Jörg Stülke[3], Martín Espariz[1,2], Víctor S. Blancato[1,4] and Christian Magni[1,4]*

[1]Laboratorio de Fisiología y Genética de Bacterias Lácticas, Instituto de Biología Molecular y Celular de Rosario (IBR), Sede Facultad de Ciencias Bioquímicas y Farmacéuticas (FBioyF), Universidad Nacional de Rosario (UNR), Consejo Nacional de Ciencia y Tecnología (CONICET), Rosario, Argentina, [2]Área Bioinformática, Departamento de Matemática y Estadística, Facultad de Ciencias Bioquímicas y Farmacéuticas, Universidad Nacional de Rosario, Rosario, Santa Fe, Argentina, [3]Department of General Microbiology, Georg August University, Göttingen, Germany, [4]Laboratorio de Biotecnología e Inocuidad de los Alimentos, Área de Biotecnología de los Alimentos, FBioyF, UNR–Municipalidad de Granadero Baigorria, Rosario, Argentina

Enterococcus is able to grow in media at pH from 5.0 to 9.0 and a high concentration of NaCl (8%). The ability to respond to these extreme conditions requires the rapid movement of three critical ions: proton (H^+), sodium (Na^+), and potassium (K^+). The activity of the proton F_0F_1 ATPase and the sodium Na^+ V_0V_1 type ATPase under acidic or alkaline conditions, respectively, is well established in *these microorganisms*. The potassium uptake transporters KtrI and KtrII were described in *Enterococcus hirae*, which were associated with growth in acidic and alkaline conditions, respectively. In *Enterococcus faecalis*, the presence of the Kdp (potassium ATPase) system was early established. However, the homeostasis of potassium in this microorganism is not completely explored. In this study, we demonstrate that Kup and KimA are high-affinity potassium transporters, and the inactivation of these genes in *E. faecalis* JH2-2 (a Kdp laboratory natural deficient strain) had no effect on the growth parameters. However, in KtrA defective strains (Δ*ktrA*, Δ*kup*Δ*ktrA*) an impaired growth was observed under stress conditions, which was restored to wild type levels by external addition of K^+ ions. Among the multiplicity of potassium transporters identify in the genus *Enterococcus*, Ktr channels (KtrAB and KtrAD), and Kup family symporters (Kup and KimA) are present and may contribute to the particular resistance of these microorganisms to different stress conditions. In addition, we found that the presence of the Kdp system in *E. faecalis* is strain-dependent, and this transporter is enriched in strains of clinical origin as compared to environmental, commensal, or food isolates.

KEYWORDS

***Enterococcus faecalis*, potassium transport, KUP/HAK/KT K+ transporters, Ktr family, Kdp system**

1. Introduction

Enterococcus faecalis is a natural commensal bacterium of the animal gut that can be isolated from diverse niches (water, food, and vegetal; Giraffa, 2002; Byappanahalli et al., 2012). The physiology and genetics of this species are relevant due to its association with infections and diseases, such as bacteremia, endocarditis, urinary tract infections, and dental diseases (Murray, 1990;

García-Solache and Rice, 2019). This group of microorganisms emerges as multi-resistant Gram-positive pathogens and, generally, is not regarded as safe (GRAS; Ogier and Serror, 2008). Despite this categorization, *E. faecalis* is present in fermented food productions, isolated mainly from traditional dairy products around the world where these bacteria contribute to the ripening process in favorable sensorial features (Giraffa, 2002; Franz et al., 2003). Finally, this microorganism is an important fecal contaminant frequently used as biological indicator for assessing recreational water quality (Boehm and Sassoubre, 2014). Like other members of the lactic acid bacteria, *Enterococcus* has the capability to persist, resist, and thrive in harsh conditions that include low and high pH, heat, and hyperosmotic stress. Members of this genus generally grow at temperatures between 10 and 45°C, in NaCl between 0 and 8% and pH values between 4.5 and 9.0 (Giraffa, 2002; Ogier and Serror, 2008; Byappanahalli et al., 2012).

The main biochemistry studies regarding potassium uptake in Enterococci were performed in *Enterococcus hirae* ATCC9790 (Kakinuma, 1998; Krulwich et al., 2011). In this strain, it was well established that the generation of proton-motive force at low pH is generated by proton expulsion *via* the F_0F_1 proton translocating ATPase (*atpIABCDFE* operon), extrusion of Na^+ is catalyzed by NapA antiporter, and the accumulation of cytoplasmic K^+ catalyzed by KtrI system (Kakinuma, 1998; Krulwich et al., 2011; Figure 1). In alkaline conditions, and in the presence of Na^+, *E. hirae* induces the vacuolar V_0V_1 type sodium—ATPase (*ntpFIKECGABDJ* operon) which includes a K^+ transporter KtrII system (last gene of the operon, *ntpJ*). Thus, Na^+ is pumped outside the cells consuming ATP whereas K^+ is accumulated *via* the K^+/Na^+ symporter (Kakinuma, 1998; Krulwich et al., 2011; Figure 1).

In the last decade, different K^+ channels and transporters were characterized in pathogenic and nonpathogenic microorganisms (Stautz et al., 2021). In *Bacillus subtilis*, the KtrAB and KtrCD potassium channels as well as the KimA K+/H+ symporter were characterized (Gundlach et al., 2017). The KtrAB channel and the KimA transporter are high-affinity uptake systems whereas the KtrCD channel has a low affinity unless stimulated by glutamate (Krüger et al., 2020). In *Staphylococcus aureus*, the KdpFABC pump and KtrCB and KtrCD channels are involved in the response to osmotic shock (Gries et al., 2013, 2016; Price-Whelan et al., 2013). In *Streptococcus pneumoniae*, the *trkH cabP* operon encodes a member of the Trk/Ktr/HKT K^+ channel family (Bai et al., 2014), and in *Streptococcus mutans*, coded by the *trkAH* operon (similar to described in *S. pneumoniae*), was defined as the main system involved in the K^+ uptake in the response to acid stress (Binepal et al., 2016). In *Streptococcus agalactiae*, two members of the Trk/Ktr/HKT family are involved in the uptake of K^+ (Devaux et al., 2018). In *Streptococcus pyogenes*, the KtrAB system have a main role in K^+ uptake, while Kup and KimA may have functions under different growth conditions (Faozia et al., 2021). Finally, in *Lactococcus*, two copies of Kup (KupA and KupB) were found in the *Lactococcus lactis* IL1403 strain and only one in the *Lactococcus cremoris* MG1363 (KupB; Pham et al., 2018; Quintana et al., 2019).

The second messenger c-di-AMP was described as involved in the regulation of K^+ homeostasis in Firmicutes (Corrigan and Gründling, 2013; Stülke and Krüger, 2020; Stautz et al., 2021). Specific interactions between potassium transporters and c-di-AMP were found, c-di-AMP binds to the interface of the KtrA dimer, and inactivates the KtrAB channel (Kim et al., 2015; Rocha et al., 2019). Also, direct interaction of c-di-AMP to KimA (Gibhardt et al., 2019; Gundlach et al., 2019), Kup

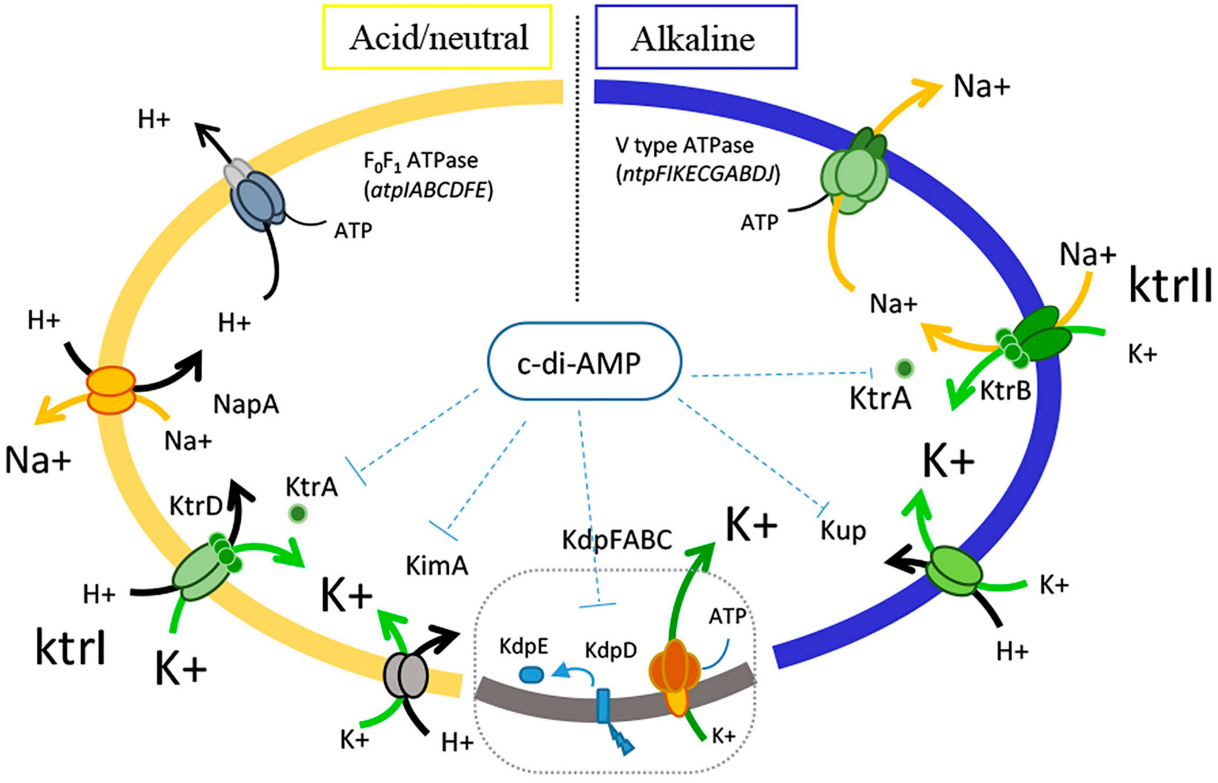

FIGURE 1
Schematic representation of the mechanisms involved ion fluxes in *Enterococcus faecalis*.

(Quintana et al., 2019), and CabP (TrkH; Bai et al., 2014; Devaux et al., 2018) was found (Faozia et al., 2021). Additionally, it has been demonstrated that both c-di-AMP and the K^+ transporters are directly and indirectly involved in the virulence of pathogenic microorganisms (Corrigan and Gründling, 2013; Gries et al., 2013; Stülke and Krüger, 2020; Kundra et al., 2021; Stautz et al., 2021). In *E. faecalis* inactivation of the gene encoding for CdaA (*cdaA*, diadenylate cyclase involved in the synthesis of c-di-AMP) or PDE phosphodiesterases (*gdpP* and *dhh*, encoding the enzymes that degrade c-di-AMP) result in the reduction of virulence and capacity to resist osmotic stress (Kundra et al., 2021).

Initial studies of potassium transport systems in *E. faecalis* V583 identified the *kdpED* operon, which encodes a two-component regulatory system (KdpD sensor kinase and KdpE transcriptional factor) widely distributed in bacteria, responsible for the transcriptional induction of the KdpFABC transporter complex (potassium-transporting ATPase; Hancock and Perego, 2004). It is also known that the transcriptional induction of *kdp* operon is coordinated with the V type *ntp* ATPase operon in response to the increased salt concentration, demonstrating the importance of the K^+ uptake and Na^+ extrusion in the ion homeostasis of the enterococcal cells (Solheim et al., 2014).

The purpose of this study was to study which K^+ transporters are employed in the uptake of this ion in the *kdp*-defective *E. faecalis* JH2-2 strain and analyze the impact of the second messenger c-di-AMP on the activity of these proteins. Bioinformatics analyses were performed to show the distribution of four putative potassium transport systems identified in *E. faecalis* JH2-2: KtrAB, KtrAD, KimA, and Kup. In this study, we show that the *E. faecalis* Kup and KimA proteins are specific high affinity potassium transporters. We also demonstrate that Kup is inhibited by c-di-AMP *in vivo*. Moreover, genetic approaches were performed in the *E. faecalis* JH2-2 strain in order to characterize the multiple physiological roles of each potassium transporter system. We determined that KtrA is required to resist the growth at high pH and concentration of osmolites (NaCl, sorbitol). For the first time, we found evidence that Kup is also required to grow in complex medium at high pH under a limited K^+ concentration and to resist osmotic stress.

2. Materials and methods

2.1. Bacterial strains and cultures

The bacterial strains used in this study are listed in Supplementary Table S1. *Escherichia coli* strain DH5α was used as an intermediate host for cloning, and *E. coli* EC101 was used as host for pBVGh constructs. *Escherichia coli* strains were grown at 37°C under aerobic conditions with vigorous shaking in Lysogeny Broth medium (LB). Potassium transporter deficient *E. coli* LB650 and LB2003 strains were cultivated in LB medium with the addition of 50 mM KCl or in minimal salts M9/M9mod medium supplemented with 50 mM KCl, unless otherwise stated. M9 medium contains 4 mM Na_2HPO_4, 22 mM KH_2PO_4, 18.5 mM NH_4Cl, 1 mM $MgSO_4$, 0.1 mM $CaCl_2$, 0.5 μM $FeCl_3$, 350 μM proline, 3 μM thiamine-di-chloride, 0.66% Casamino Acids, and 0.5% glucose or 0.2% glycerol as sources of carbon. Experiments with defined potassium concentrations were performed in M9mod, in which M9 potassium salts were replaced with equimolar quantities of sodium salts, and KCl was added as indicated. *Enterococcus faecalis* strains were routinely grown at 37°C without shaking in LB medium containing 0.5% w/v glucose (LBG). Alternatively, M17 medium (Oxoid) supplemented with 0.5% w/v glucose (M17G) and M17G supplemented with 0.5 M saccharose (SM17G) were employed when indicated. Experiments requiring low K^+ medium were performed in mLBG, a modified LBG medium in which yeast extract was reduced from 0.5 to 0.025%; the K^+ concentration of mLBG was less than 1 mM (Kawano et al., 2001). KCl, NaCl, and/or sorbitol were added to the growth media at the concentrations indicated in the figure legends. pH adjustments were made with addition of either HCl or NaOH. Suitable antibiotics were added to the media as selective agents when needed. For agar plates, 1.5% agar was added to the medium.

2.2. DNA manipulation

Plasmid DNA from *E. coli* cells was prepared with a Wizard Plus Minipreps DNA purification system (Promega). Chromosomal DNA of *E. faecalis* was extracted using Microbial DNA Kit (Macherey-Nagel). Treatment of DNA with restriction enzymes, T4 DNA ligase, and DNA polymerases was performed as recommended by the suppliers. DNA fragments were purified using the Wizard SV Gel and PCR Clean-Up System (Promega). DNA sequences were checked by sequencing in the World Meridian Venture Center, Macrogen's sequencing service (Seoul, Korea). *Escherichia coli* cells were transformed using standard procedures (Sambrook et al., 1989). *Enterococcus faecalis* transformation was performed by electroporation according to the procedure of Dornan and Collins (1990).

2.3. Plasmid construction

Heterologous expression of the putative potassium transporter proteins in *E. coli* was approached as follows: the *kup* and *kimA* genes from *E. faecalis* JH2-2 were amplified using the oligonucleotide pairs GA1/GA2 and GA3/GA4, respectively. The PCR products were cloned between the BamHI and SalI sites of plasmid pWH844 to allow IPTG-inducible expression. The resulting plasmids were designated as pWH-*kup* and pWH-*kimA*. The pBAD33 and pWH844 expression vectors have compatible selection markers and origin of replications allowing the co-expression of potassium transporter genes (from pWH844) and the *cdaA* variants (from pBAD33; Gibhardt et al., 2019; Quintana et al., 2019).

2.4. Growth of *Escherichia coli* in minimal salt medium

Strains derived from *E. coli* LB650 (Δ*kdpABC5*, Δ*trkD1*, Δ*trkH*,Δ*ktrG*, Km^{50}, and Cm^{30}, see Supplementary Table S1) were propagated twice from −80°C stocks in M9mod medium supplemented with 1% glucose, the corresponding antibiotics, and 50 mM KCl. The overnight culture obtained was used to inoculate fresh M9mod medium supplemented with antibiotics, and 10 mM KCl for strains expressing the Kup and KimA proteins or 100 mM KCl for the strain expressing the empty vector control. At an OD_{600} of 0.5, cells were harvested. The pellet was re-suspended in the initial volume of fresh medium without KCl addition and incubated for 1 h at 37°C. Cultures were harvested again and washed three times with fresh medium. These samples were then used to inoculate fresh M9mod medium in microplates supplemented with 1% glucose, antibiotics, and different KCl concentrations. Microplates were incubated at 37°C with continuous orbital shaking and culture growth was monitored by

measuring OD_{600} in 15-min intervals in a PowerWave™ XS Microplate reader (BioTek, BioTek Instrument Inc., Vermont, United States).

2.5. Co-expression of potassium transporters and diadenylate cyclases

Strain *E. coli* LB2003 (Δ*kdpABC5*, *kupD1*, and Δ*trkA*), a clean deficient in the gene encoding potassium transporter but sensible to antibiotic which allow the introduction of plasmids encoding kanamycin or chloramphenicol resistance determinants was co-transformed with pWH844 or derivatives and the pBAD33 derivatives (see Supplementary Table S1). This strain was inoculated from −80°C stocks in M9mod medium supplemented with 0.2% glycerol as the carbon source, corresponding antibiotics, and 10 mM KCl and propagated twice. At an OD_{600} of 0.5, cultures were harvested and re-suspended in same volume of M9mod medium containing 0.2% glycerol (no KCl added). Samples were incubated at 37°C for 1 h, after which two wash steps were performed. These washed samples were used for microplate inoculation supplemented with 0.075 mM KCl, and 0.05% L-arabinose when indicated. Antibiotics were added as appropriate. Microplates were incubated at 37°C with continuous orbital shaking and culture growth was monitored by measuring OD_{600} in 15-min intervals in a PowerWave™ XS Microplate reader (BioTek Instrument Inc., Vermont, United States).

2.6. Construction of *Enterococcus faecalis* potassium transporter defective strains and complementation of the mutants

Deletion of *kup*, *kimA*, and *ktrA* from *E. faecalis* JH2-2 was carried out using the thermosensitive vector pBVGh (Blancato and Magni, 2010). The oligonucleotides used for the amplification of upstream and downstream fragments of *kup*, *kimA*, and *ktrA* genes are indicated in Supplementary Table S1. Fragments were purified, digested, and ligated into the corresponding sites of the pBVGh vector. Cloned fragments were checked by sequencing. Finally, the protocol to generate the chromosomal deletion in *E. faecalis* was followed as previously described (Blancato and Magni, 2010). The Δ*kup* Δ*kimA*, Δ*kup* Δ*ktrA*, and Δ*kimA* Δ*ktrA* double mutants were obtained by eletroporating the pBVGh-*kimA* plasmid in the Δ*kup* and Δ*ktrA* single mutants, and the pBVGh-*ktrA* plasmid in the Δ*kup* single mutant. All gene deletions were confirmed by PCR sequencing using a pair of primers hybridizing in the adjacent up and downstream genes (Supplementary Table S1). The full-length *ktrA* gene was amplified by PCR using chromosomal DNA extracted from *E. facealis* JH2-2 as template and the pair of primers GA19/GA20 (Supplementary Table S1). The resulting fragment was purified, digested with the appropriate restriction enzymes, and ligated into the pBV153 vector giving rise to plasmid pBV-*ktrA*. The Δ*kup*Δ*ktrA* and Δ*kimA*Δ*ktrA* double mutants were complemented by the plasmid pBV-*ktrA*. Vector pBV153 was also transformed into the wild-type and the mutant strains as a control of any possible effect of plasmid transformation alone.

2.7. Growth of *Enterococcus faecalis* strains under stress conditions

In order to compare the growth curves of wild-type and the different potassium transporter mutant strains, *E. faecalis* was cultivated in microplates at 37°C. For this, overnight cultures grown in LBG medium were used to inoculate fresh LBG medium adjusted to different initial pH values, as indicated. The inoculums were diluted to an initial OD_{600} of 0.1. After the cell culture had reached the exponential growth phase, the cells were harvested and washed twice with fresh medium. These samples were then diluted to an initial OD_{600} of 0.1 in LBG or mLBG medium at different initial pH, and supplemented with 10 mM KCl when indicated. The OD_{600} was registered every 20 min in a PowerWave™ XS Microplate reader.

For osmotolerance assays, cells were cultured as described above except with the addition of either NaCl or sorbitol, and KCl when indicated, at the specified concentrations. The growth rates were calculated and plotted against the NaCl concentrations, which ranged between 0 and 8%.

Growth in urine or blood was analyzed as described previously (Martino et al., 2018). Infection and survival experiments in *Galleria mellonella* were carried out as described (Terán et al., 2022).

2.8. Bioinformatic analysis

Genomic sequence data sets as well as predicted coding sequences of *E. faecalis* strains were retrieved from GenBank[1] using Download Genomes tool.[2] Datasets were composed of sequences submitted until 10 October 2020. Maximum likelihood phylogenetic trees were constructed as reported (Espariz et al., 2016). To counter-select potential paralogues, coverage and identity percentage cut-offs were set at 70% using GeM-Pro tool (Torres Manno et al., 2019). Metadata from NCBI biosample were obtained *via ad hoc* R script.[3] Strains were classified based on these metadata in the categories such as clinical, commensal, environmental, or food sample.

For presence/absence analysis, the sequences of KimA, KupA, KtrA, KtrB, KtrD, KdpFABC, KdpDE, TrkHA, AtpIABCDFE, NtpFIKECGABDJ, and NapA proteins were used as query in TBLASTN (Blast +2.9.0) searches against *E. faecalis* genomes using as thresholds coverages >= 70% and identities >= 50%. In order to determine associations between protein-coding genes and metadata-assigned categories, enrichment statistical analyses were performed with PhyloLM V2.6 (Levy et al., 2018) using "logistic_IG10" method. The multiple comparisons for the statistical tests were corrected with Benjamini–Hochberg approach (Benjamini and Hochberg, 1995).

3. Results

3.1. KimA and Kup of *Enterococcus faecalis* encode high affinity potassium transporters

Potassium transport systems present in *E. faecalis* JH2-2 (a natural deficient in the Kdp system strain) were identified based on homology with the proteins present in strain V583. Strain JH2-2 codes for the KtrAB and KtrAD channels and two members of the Kup family: Kup and KimA (Table 1). To test the functional role of the enterococcal proteins KimA and Kup, the *E. faecalis* JH2-2 *kup* and *kimA* genes were individually cloned in

1 ftp.ncbi.nlm.nih.gov/genomes/
2 https://github.com/torresmanno/Download_Genomes
3 https://github.com/torresmanno/Acciarri_etal_Rscript

the pWH844 vector (Figure 2A). The resulting pWH-*kup* (*kup*) and pWH-*kimA* (*kimA*) plasmids were introduced in the *E. coli* strain LB650 that lacks the main potassium transport systems KdpABC, Kup (formerly TrkD, TrkH, and TrkG and is unable to grow at low K^+ concentrations; Schlosser et al., 1995; Supplementary Table S1). The transformants were used to evaluate whether the expression of these enterococcal proteins could restore growth in minimal salt media when no K^+ salts are added. As shown in Figure 2B, strain LB650 harboring the empty vector pWH844 was unable to grow in M9 minimal salt medium plates (M9mod), in which potassium salts were replaced by equimolar quantities of the respective sodium salts (see the section Materials and methods), without or in the presence of both 1 and 5 mM of KCl. Colonies of the triple mutant LB650 transformed with the vector pWH844 appear on the plates only when the concentration of KCl added reaches 50 mM (Figure 2B, colonies number 1 in each plate). *Escherichia coli* strain LB650/pWH-*kup* grows in M9mod independent of the addition of external K^+ salt (Figure 2B, colonies number 2 in each plate), whereas strain LB650/pWH-*kimA* recovered ability to grow in M9mod in the presence of 1 mM KCl in solid medium (Figure 2B, colonies number 3 in each plate). In all cases, the cells were propagated in M9mod plates without IPTG induction. Thus, the basal expression of each of the enterococcal genes, due to readthrough of the *lac* promoter present in the vector pWH844, is already sufficient to allow potassium uptake and, consequently, growth of the complemented mutant strains.

In addition, growth curves were determined in liquid M9mod medium with external additions of KCl to reach final concentrations between 0.025 and 50 mM. The growth parameters maximum optical density (OD_{max}) and μ_{max} (Supplementary Table S2) were determined for the strains LB650/pWH844, LB650/pWH-*kup*, and LB650/pWH-*kimA*. Then, the μ_{max} were plotted against the potassium concentrations added to the medium (Figure 2C). The strains carrying the full copies of each enterococcal gene, *kup* or *kimA*, showed similar patterns in the variation of the values of μ_{max} vs. the K^+ concentration. Both transporters allowed growth even at very low concentrations of KCl and, furthermore, it can be seen as μ_{max} increases as the concentration of K^+ in the medium increases. However, the latter is not consistent with the OD_{max} values, as this parameter remains constant throughout the curve (Supplementary Table S2). The addition of the inducer IPTG in the medium produces a defect on the growth of the cells containing *kup* or *kimA* genes, that could be because overexpression of membrane proteins is often toxic and interferes with essential functions or because of an accumulation of toxic levels of potassium ions inside the cell (data not shown).

Recent studies have demonstrated that several members of the Kup transporter family (KimA from *B. subtilis* and *Listeria monocytogenes*, KupA and KupB from *L. lactis*) are negatively regulated by direct interaction with the nucleotide second messenger c-di-AMP (Gibhardt et al., 2019; Gundlach et al., 2019; Quintana et al., 2019). To test whether c-di-AMP impacts on the potassium transport activity of Kup and KimA, a co-expression system was established in the defective potassium transporter *E. coli* strain LB2003. Like *E. coli* LB650, this strain is deficient in the Trk, Kup, and Kdp potassium transport systems, hence is unable to grow in low K^+ medium without complementation of a potassium transporter coding gene. A relevant fact is that *E. coli* lacks c-di-AMP synthesizing

TABLE 1 Potassium transport systems present in *Enterococcus faecalis* strains.

	KdpDE	KdpFABC	KtrA	KtrB	KtrD	KimA	Kup
V583	Ef0571-0570	Ef0566-0569	Ef2910	Ef0295	Ef2558	Ef0860	Ef0872
JH2-2	—	—	0994–2329	0994–2501	0994–2056	0994–0592	0994–0603

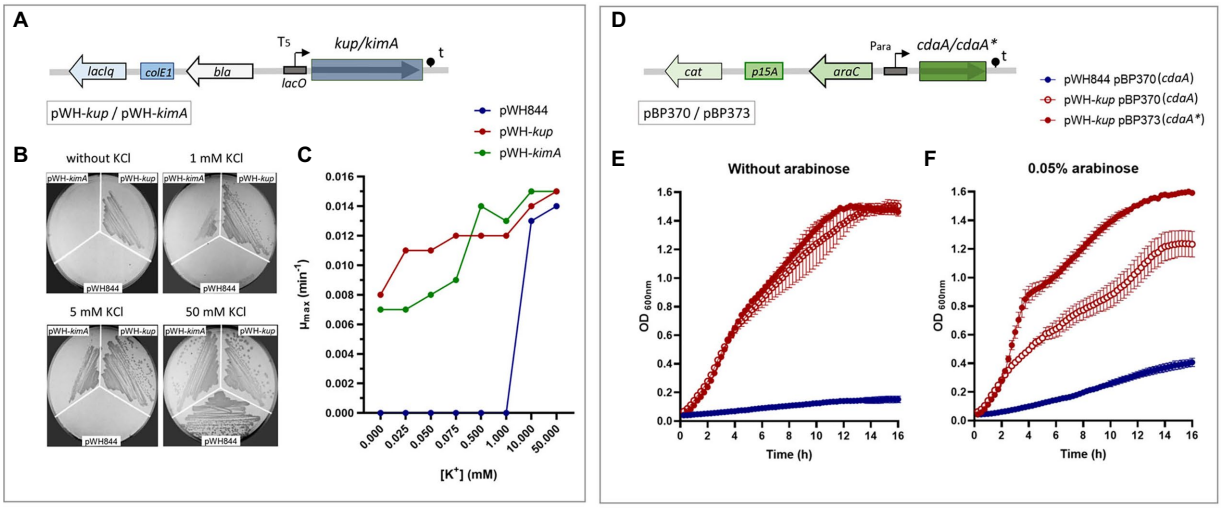

FIGURE 2
KimA and Kup of *Enterococcus faecalis* are potassium transporters. **(A)** pWH844 derived carrying full copy of Kup (pWH-*kup*) or KimA (pWH-*kimA*) used in this study. **(B)** *Escherichia coli* LB650 strains harboring plasmids pWH844, pWH-*kup*, and pWH-*kimA* were grown in M9-mod solid medium with or without supplementation of KCl (1, 5, or 50 mM). **(C)** Growth rate parameters determined at different KCl concentrations of LB650 derived strains, pWH844 (blue dot), pWH-*kup* (red dot), and pWH-*kimA* (green dot). Inhibition of Kup activity by c-di-AMP **(D)** pBAD derived carrying a copy of $cdaA^{lmo}$ (pBP370) or $cdaA^{lmo}$* (pBP373) used in this study. **(E,F)** *Escherichia coli* LB2003 harboring the plasmid combinations pWH844/pBP370 (blue dot), pWH-*kup*/pBP370 (empty red dot), and pWH-*kup*/pBP373 (full red dot), was cultivated in minimal salt M9mod medium, and supplemented without arabinose **(E)** or with arabinose 0.05% **(F)**.

enzymes; therefore, the co-expression system to assess the phenotypic effect of c-di-AMP on the potassium transport systems KimA and Kup, can be carried out without interference of host-synthesized c-di-AMP. To control c-di-AMP recombinant production in *E. coli*, the diadenylate cyclase CdaA from *L. monocytogenes* was used. The $CdaA^{Lmo}$ (carrying the wild type gene of *cdaA*) and the inactive $CdaA^{Lmo*}$variant D171N are encoded by the plasmids pBP370 and pBP373, respectively (Rosenberg et al., 2015). These plasmids are pBAD33 derivatives, allowing expression of genes under control of the arabinose P_{ara} promoter (Figure 2D), and compatible with pWH844 derivatives that were used to express the potassium transporters (Figure 2A). For the co-expression assays, the *E. coli* LB2003 derivative strains carrying pWH844 or derivatives as well as either of the two diadenylate cyclases encoding plasmids were grown in M9mod supplemented with KCl, and L-arabinose when indicated, at the specified concentrations (see the section Materials and methods).

Since in our previous growth experiments performed in *E. coli* LB2003 harboring a copy of *kimA* or *kup*, addition of 0.5 mM KCl to M9mod medium was sufficient for the strains to grow, this concentration was selected for the later co-expression assays. It is important to mention that at this potassium concentration, strain LB2003 harboring empty vector pWH844 was not able to grow (Figure 2E, blue circle). The growth patterns of the strains synthesizing Kup protein, carrying either the plasmid encoding the active $CdaA^{Lmo}$ (Figure 2E, empty red circle) or the inactive $CdaA^{Lmo*}$ (Figure 2E, fill red circle) proteins were similar in the absence of the inducer (arabinose). By contrast, in the presence of 0.05% arabinose the growth of the strain synthesizing Kup was reduced when the functional diadenylate cyclase $CdaA^{Lmo}$ protein was co-produced, and thus in the presence of c-di-AMP (Figure 2F, empty red circle); however, no effect on the growth of the strain was observed when the inactive $CdaA^{Lmo*}$ protein was co-produced, and thus in the absence of c-di-AMP (Figure 2F, fill red circle).

To test the possibility that high intracellular c-di-AMP concentrations or expression of the heterologous diadenylate cyclase affect growth of the strain co-producing Kup and the active $CdaA^{Lmo}$, similar growth curves of *E. coli* LB2003 harboring the empty vector pWH844 and plasmid pBP370 or pBP373 were performed. In this assays, 50 mM KCl was added to the growth media, condition that allows growth of the bacteria. The growth of the strain carrying pWH844 as well as either of the two CdaA encoding plasmids was not reduced both in absence and presence of the inducer arabinose, and both strains exhibited similar growth phenotypes, as observed for the strain carrying the empty vector pWH844.

Similar experiments were performed to assess the effect of c-di-AMP on KimA. Despite different amounts of arabinose were added to de culture medium, the results obtained were unable to show evidence of the specific interaction between the second messenger and the transport system under study (data not shown).

3.2. Inactivation of genes coding for potassium transporter systems belonging to the Kup family in *Enterococcus faecalis* JH2-2

To investigate whether *kup* and *kimA* genes products are involved in K^+ uptake in *E. faecalis*, simple Δ*kup* and Δ*kimA*, and double Δ*kup*Δ*kimA* mutants were generated using the chimeric vector pBVGh (Blancato and Magni, 2010). *Enterococcus faecalis* JH2-2 strain is able to grow in LBG or low K^+ medium mLBG (Kawano et al., 2001) at broad pH values (initial pH 9.0, 7.0, and 5.0 units). In LBG medium, when the initial pH was fixed to 9.0, enterococcal cells reached the maximal OD_{600} and growth rate (1.22 OD and 0.81 h^{-1}, respectively; Supplementary Figure S1). At this pH, in mLBG a decrease of the growth parameters was observed (0.67 OD and 0.46 h^{-1}, respectively; Supplementary Figure S1). At neutral initial pH (7 unit), similar patterns of growth were observed in both media, LB (0.63 OD and 0.88 h^{-1}, respectively) and mLB (0.54 OD and 0.61 h^{-1}, respectively). The reduction of the biomass generation could be due to the rapid acidification of the medium in a batch culture (Supplementary Figure S1). At acidic condition (pH 5.0), a significative reduction in the growth parameters was observed in LB and mLB media (OD = 0.53, growth rate 0.49 h^{-1} and OD = 0.36, growth rate 0.19 h^{-1}, respectively; Supplementary Figure S1). The growth parameters of each enterococcal mutant strain (Δ*kup* and Δ*kimA*, and Δ*kup* Δ*kimA*) were analyzed by testing growth in both LBG or mLBG, and at the same pH values (9.0, 7.0, and 5.0). No differences were observed in the values of biomass and growth rate of the single and double mutants compared to the wild-type strain *E. faecalis* JH2-2 (Supplementary Figure S2).

3.3. Effect of Kup and KimA gene deletion on deficient strain in the Ktr channel systems

Taking into account the results presented above and the pivotal role of the Ktr channel systems in *E. faecalis*, different Ktr deficient strains were generated. Since previous studies in other related microorganisms have demonstrated that one ion-transporting protein (KtrB or KtrD) and the KtrA regulator function together in K^+ uptake (Holtmann et al., 2003; Gries et al., 2013), the suspected major function of Ktr channel was tested by generating a deletion of the *ktrA* gene. A series of different K^+-transporter systems deficient strains was constructed (Δ*ktrA*, Δ*ktrA* Δ*kup*, and Δ*ktrA* Δ*kimA*). The rates of growth of the wild type and the *ktrA*-derived mutants were compared in LB, and mLB at different pH values (Figure 3). In LB medium, only the double mutant Δ*kup* Δ*ktrA* strain shows reduced growth at alkaline pH (Figure 3A, yellow circle), whereas no other mutant showed phenotype at the other pHs in this medium (Figure 3D, pH 7.0 and 2G, pH 5.0). When the concentration of K^+ in the complex medium was reduced (mLB), delayed growth was observed at alkaline conditions (pH 9.0) for all *ktrA* mutants, which was more severe for the double mutant Δ*kup* Δ*ktrA* (Figure 3B, yellow circle). In the same medium at neutral pH, this growth defect was observed only for the Δ*kup* Δ*ktrA* double mutant (Figure 3E, yellow circle). At acidic pH 5.0 in mLB, no growth alterations were observed for the mutant strains as compared to the JH2-2 parent strain (Figure 3H). Growth deficiencies of the KtrA mutants were restored to wild type phenotype by the addition of potassium (10 mM) to the growth medium (Figures 3C,F), strongly suggesting the inability of the mutant strains to concentrate K^+ ions inside the cell.

3.4. Comparison of osmotic response of the *Enterococcus faecalis* potassium transporter deficient strains

As mentioned above, *E. faecalis* is able to resist high concentrations of NaCl. The first response to cope with hyperosmotic stress is K^+ accumulation *via* massive uptake (Stülke and Krüger, 2020). The effect

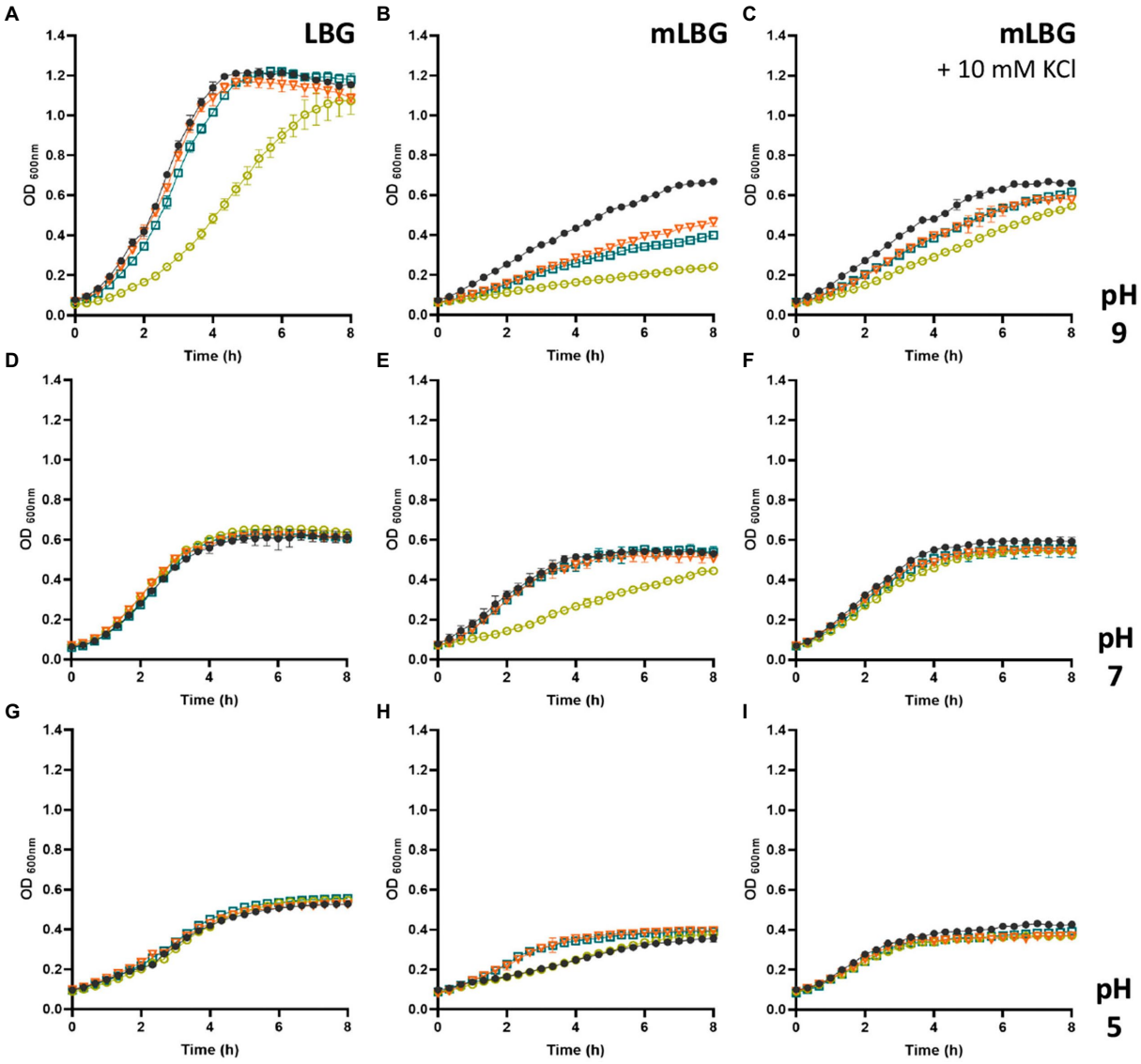

FIGURE 3
Growth curves of *Enterococcus faecalis* JH2-2 mutants under different conditions. Wild type (black dot), Δ*ktrA* (light blue square), Δ*kup*Δ*ktrA* (yellow circle), and Δ*ktimA*Δ*ktrA* (orange triangle) strains were grown in LBG **(A,D,G)**, mLBG **(B,E,H)**, or mLGB medium supplemented with 10 mM KCl **(C,F,I)**. Initial pH was fixed at 9.0 units **(A–C)**, 7.0 **(D–F)**, or 5.0 **(G–I)**.

of salt compound on the growth of the parental and derived potassium transporters deficient strains of *E. faecalis* JH2-2 was analyzed in LBG and mLBG at different starting pH (9.0, 7.0, and 5.0) in the presence of up to 8% NaCl. As shown in Figure 4, during growth under alkaline stress conditions (pH 9.0), the toxic effect of NaCl addition is observed in both media, LB and LBm, for all *ktrA* mutants (Δ*ktrA*, Δ*kup* Δ*ktrA*, and Δ*kimA* Δ*ktrA*). Particularly, in LBG, the double mutant strain Δ*kup* Δ*ktrA* exhibited a more pronounced defect in growth as compared to wild type JH2-2 strain (Figure 4A, yellow circle). When the content of K^+ in the medium is reduced but the pH remained the same, all defective strains were unable to grow at the lowest amount of the salt added (3% NaCl; Figures 4B, 5A), while the JH2-2 strain resisted up to 6% NaCl. As expected, these defects in the growth of all *ktrA* mutant strains were restored by addition of 10 mM KCl (Figure 5B). Growth in LB medium at neutral conditions (pH 7.0) with the addition of increasing concentrations of NaCl (from 0 to 8%), had similar effects for the wild type and the Δ*ktrA* and Δ*kimA* Δ*ktrA* mutant strains, however, a clear inhibition was observed for the double mutant Δ*kup* Δ*ktrA* (Figure 4C). When strains were grown in mLBG and neutral pH, again all *ktrA* mutants exhibited defective growth or sensitivity to the osmotic stressor NaCl, and normal growth was observed with the addition of 10 mM KCl (data not shown). Finally, at low pH condition (5.0), the treatment with NaCl led to drastically reduced growth parameters for all the tested strains; thus, the osmotic effect was not evident (data not shown).

Additionally, the ability of the mutant strains to grow in low K^+ medium mLB supplemented with a low molecular weight osmolyte, different than NaCl, was tested to guarantee that the NaCl-induced effects on growth reported here were due to an osmotic effect and not to an ionic one. Thus, the growth of *ktrA* deficient mutant strains of *E. facecalis* was examined at high concentrations of sorbitol. Both in neutral and alkaline conditions, the addition of 750 mM sorbitol to mLB medium had a severe impact on growth of the Δ*ktrA*, Δ*kimA* Δ*ktrA*, and Δ*kup* Δ*ktrA* strains as compared to the wild type strain (Figure 5C).

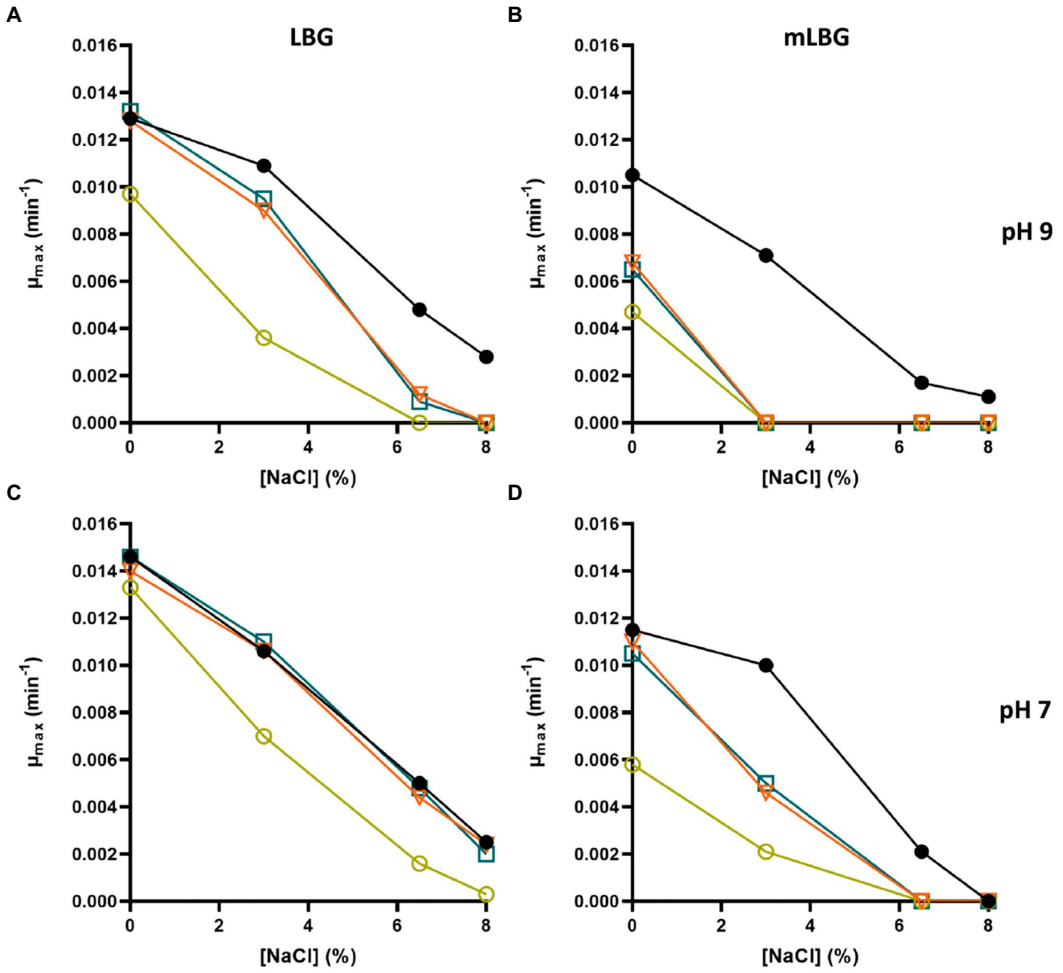

FIGURE 4
Inhibition of growth rate of *Enterococcus faecalis* JH2-2 mutants by NaCl. Wild type (black dot), Δ*ktrA* (light blue square), Δ*kup*Δ*ktrA* (yellow circle), and Δ*ktimA*Δ*ktrA* (orange triangle) strains were grown in LBG **(A,C)** and mLBG medium **(B,D)** at initial pH 9.0 (top) or 7.0 (low) in the presence of increasing concentrations of NaCl.

Similar to the growth in presence of 3% NaCl, addition of 10 mM KCl to the culture medium restored growth of the mutant strains (Figure 5D).

Finally, defective phenotypes found in the Δ*ktrA*-containing mutants were analyzed by complementation with a full copy of the wild type *ktrA* gene, by use of the plasmid vector pBV153 (Figure 5E). Since the phenotype of the single mutant in KtrA and the double mutant in KtrA and KimA was the same in all the conditions examined, the complementation was performed only with the *ktrA* gene on the double mutant strains. Expression of *ktrA* rescued the growth defect of Δ*kimA* Δ*ktrA* and Δ*kup* Δ*ktrA* mutants to wild-type levels in mLBG under alkaline constitions (pH 9.0) and in the presence of 3% NaCl (Figure 5F). This observation demonstrates that the KtrA protein is indeed required to allow growth of *E. faecalis* under alkaline conditions or in the presence of NaCl.

3.5. Diversity of K^+ transporters in *Enterococcus* species

Orthologs of the Kdp pump, Ktr/Trk channels, and Kup symporter family (Stülke and Krüger, 2020; Tascón et al., 2020) were collected from the species with finished whole sequence genomes (NCBI) of the family that include the genus *Enterococcus* (44 species). As shown in the Figure 6A, distribution of the *kdp* operon is limited to 24 of the 44 species of *Enterococcus* analyzed. *kup* was found in 42/44 species studied of *Enterococcus* (mutated in *Enterococcus massiliensis*), whereas *kimA* is present in 38/44 species of *Enterococcus*. In the case of *ktr* genes, both genes encoding for the cytosolic component KtrA and for the membrane component of the system, KtrB, were found encoded in all 44 species analyzed. The *ktrD* gene encoding for the membrane component was found in 41 species. On the other hand, the *trkAH* operon, encoding the cytoplasmatic component TrkA (455 residues) and the membrane component TrkH (479 residues), was found disseminated in only a few species (*Enterococcus asini*, *Enterococcus avium*, *Enterococcus diestrammaneae*, *Enterococcus raffinosus*, *Enterococcus pseudoavium*, and *Enterococcus xiangfangensis*).

In addition to the K^+ transporters, other transporters associated to ion fluxes were sought in *Enterococcus*. Such is the case of the F_0F_1-ATPase complex, a well conserved proton translocator which has an essential function in the establishment of the proton motive force (PFM) and, therefore, it is related to the mechanisms of resistance to low

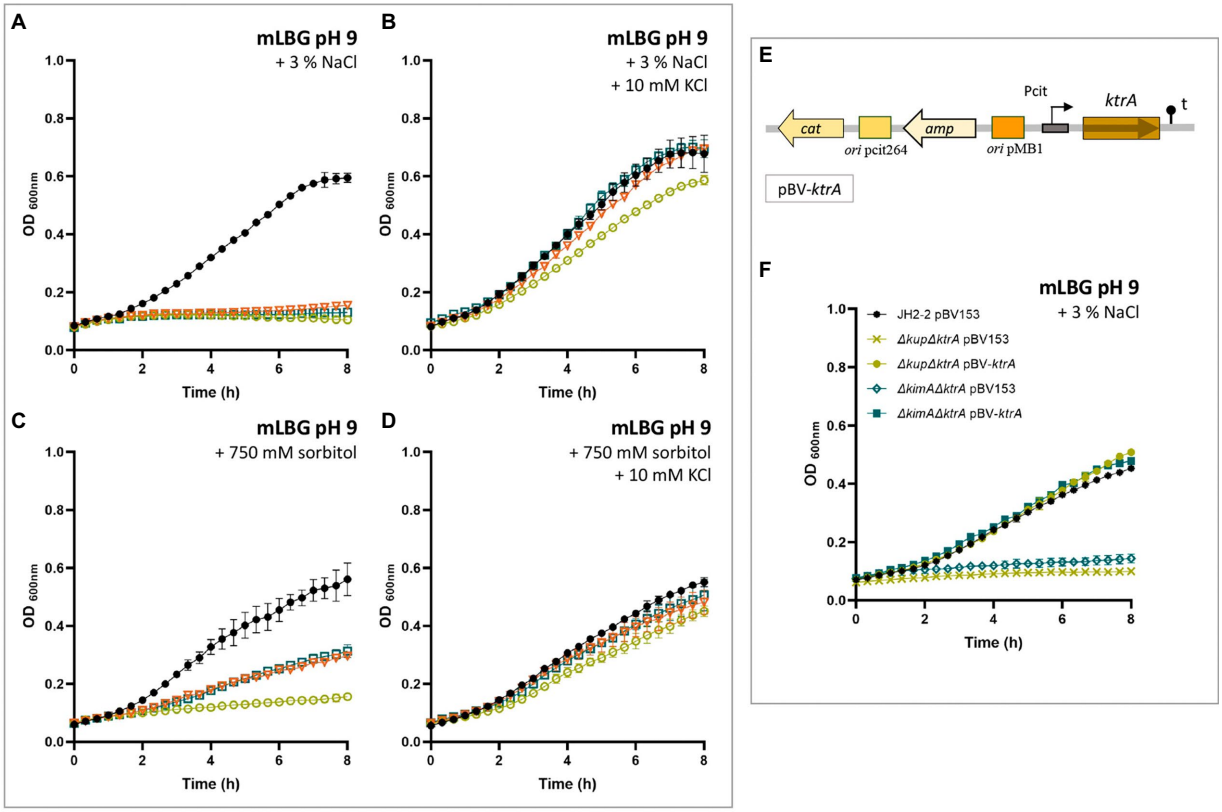

FIGURE 5
KtrA contributes to the osmotic response in *Enterococcus faecalis*. Wild type (black dot), Δ*ktrA* (light blue square), Δ*kup*Δ*ktrA* (yellow circle), and Δ*ktimA*Δ*ktrA* (orange triangle) strains were grown in mLBG at alkaline initial pH and supplemented with 3% NaCl **(A)** or 750 mM sorbitol **(C)**. In both growth conditions, the addition of 10 mM KCl (**B** and **D**, respectively) completely restored defective strains growth to near wild-type levels. **(E)** Schematic representation of the plasmid pBV-*ktrA* used for complementation of a full copy of the wild type *ktrA* gene. **(F)** Expression of *ktrA* from a pBV153 fully complemented the growth defects of the KtrA-mutant strains in mLBG at alkaline initial pH and supplemented with 3% NaCl, and in all conditions tested in this study (data not shown).

pH. Also, the presence of Na^+ transporters, which are involved in the alkaline and osmotic resistance, was identified. The results showed that the *ntp* operon, which encodes for the F_0F_1-ATPase complex, is widespread in *Enterococcus* species (41/44), with few exceptions (*Enterococcus canis*, *E. massilensis*, *and Enterococcus sulfureus*), while *napA*, encoding the Na^+ symporter NapA, is present in 33 species of the 44 analyzed.

Finally, considering that the expression of the Kdp system has been studied in *E. faecalis* V583, and that the induction of this potassium transporter under alkaline and NaCl stress conditions was reported (Solheim et al., 2014), we hypothesized that the requirement of the Kdp system could be involved in the pathogenesis of clinical strain. Though KimA, Kup, and Ktr transporters are homogeneously distributed in nearly all *E. faecalis* strains, the KdpFABC complex and the regulatory KdpDE system were found in only 319 strains out of a total of 1,510 complete genome sequences analyzed (21%) of these species (Figure 6B). The latter indicates that, as in other species, these genes do not belong to the gene core in *E. faecalis*. Then, we classified the strains and tested the hypothesis that the presence of *kdp* genes is correlated with pathogenicity. The phylogenetic tree depicted in Figure 6B showed the existence of clusters of strains with high phylogenetic signal (very related phylogenetically) that have similar *kdp* occurrence. Nevertheless, using phylogeny-aware methods, we observed that the presence of *kdp* genes was significantly positively correlated with *E. faecalis* of clinical origin (*p* value of 2.76 E^{-11}). Taking into account the relevance of the robust physiology of *E. faecalis*, which allows it to persist and thrive in harsh environments that include acid, oxidative and hyperosmotic stress, for its pathogenic potential (Solheim et al., 2014), we investigated whether K^+ transporter systems contribute to the pathogenesis of the natural Kdp defective strain JH2-2. Notably, deletion of the potassium transport systems Kup, KimA, or Ktr in *E. faecalis* JH2-2 did not affect growth and survival in animal fluids associated to common diseases caused by this bacterium (blood and urine) nor the infection and virulence in *Galleria Mellonella* model (Supplementary Figures S3, S4).

4. Discussion

In this study two members of the KUP family, Kup and KimA, present in *E. faecalis* were identified and characterized. Our work demonstrates that both transporters possess a high affinity for the K^+ ion, similar to family members described in *L. lactis* or *B. subtilis* (Gundlach et al., 2019; Quintana et al., 2019). The inhibition of K^+ transport by the second messenger c-di-AMP was demonstrated, by *in vivo* studies in a c-di-AMP producing *E. coli* strain (Figure 2F), for the Kup protein, however, it could not be demonstrated for KimA. In Firmicutes, as mentioned above, regulation of potassium transport by the second messenger c-di-AMP was demonstrated for several members of this phylum; this is the case for the control of the activity of Kup from *L. lactis*, KimA from *B. subtilis* and *L. monocytogenes*, and KtrA/C from *B. subtilis*, *L. monocytogenes*,

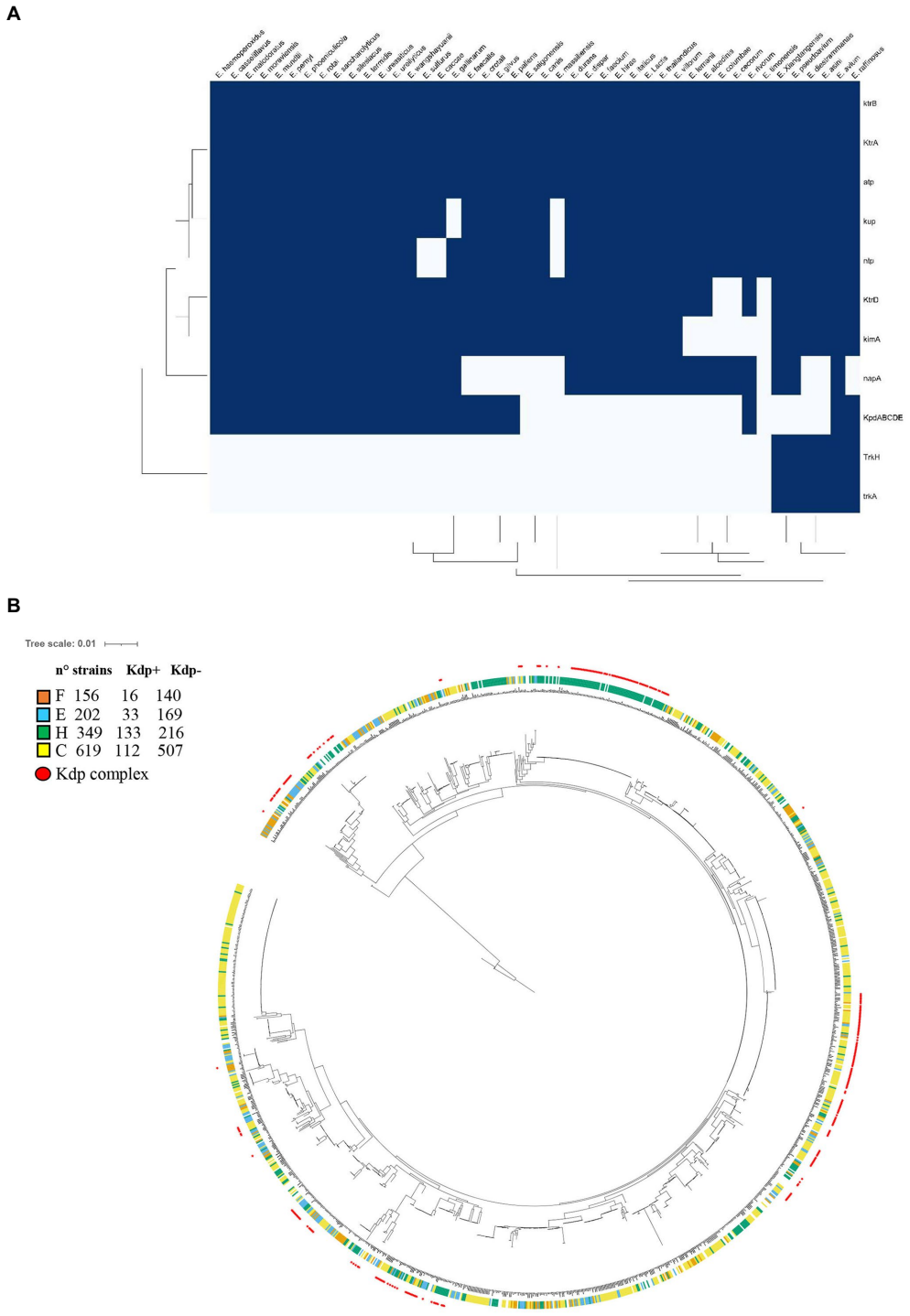

FIGURE 6
(A) Heatmap showing the presence of K^+ transporters and related ATPases in *Enterococcus* species. A presence-absence matrix was constructed and Distance-based clustering was applied. Dark blue indicates presence of the genes analyzed. **(B)** Analysis of the presence of *kdp* genes and the phylogenomic relationships among *E. faecalis* members. 34 common ancestral genes were individually aligned, concatenated, and trimmed resulting in a final alignment containing a total of 4,726 residues. The evolutionary history of the 1,510 *E. faecalis* members was inferred with RAxML algorithm (Stamatakis, 2014) and displayed and annotated using iTOL (Letunic and Bork, 2011). The inner circles colors indicate the source of isolation; F, food (orange); C, commensal (yellow); E, environmental (light blue); and H, clinical (green). The red outside circles indicate the presence of the *kdp* genes within the strains.

S. aureus, *S. pneumoniae*, and *S. mutans*. Considering the high similarity among orthologous transporters in this group of related bacteria, it is strongly suggested that K^+ homeostasis in *E. faecalis* could be controlled by the intracellular c-di-AMP concentration (Figure 1). Also, as stated above, disruptions in both the potassium uptake and the c-di-AMP homeostasis can affect the virulence potential of bacterial pathogens. Recent studies with *E. faecalis* strain OG1RF (Kdp^+ strain) revealed that variations in the intracellular levels of c-di-AMP modify its pathogenic potential (Kundra et al., 2021). In our study, no differences concerning the

growth either in animal fluids or in the *G. mellonella* insect model were detected by using simple and double mutants in the different K^+ transporters (Kup, KimA, and Ktr systems) present in *E. faecalis* JH2-2. This observation differs to findings in other opportunistic pathogen such *S. aureus*, where a KtrA deficient strain showed a deficiency in the capacity to infect mice (Gries et al., 2013). Here, it is important to mention that, in this study we were unable to obtain a K^+ transporter-free triple mutant (Δ*kup* Δ*kimA* Δ*ktrA*) using our gene deletion methodology. Therefore, although further studies will be required, this impossibility suggests that at least one potassium transport system is necessary and sufficient to satisfy the demand for this ion in the cellular interior, in the media and conditions studied. On the other hand, a detailed analysis of the distribution of transport systems in clinical and non-clinical isolates of *E. faecalis* showed that the *kdp* genes were enriched significantly in clinical isolate samples.

Given that the robust nature of *E. faecalis* facilitates its tolerance to hostile environments, and the fact that bacterial cells are known to import K^+ to help resist and survive under various stressful conditions, growth of simple and double potassium transport mutants derived from *E. faecalis* JH2-2 parental strain was assayed under different conditions. Interestingly, the inactivation of KtrA - dependent K^+ channels contribute to the sensitivity to both alkaline growth condition and osmotic stress. These phenotypes were increased in a low K^+ medium, and recovered by the external addition of potassium salt or by the introduction of a plasmid carrying a full copy of the wild type *ktrA* gene. We also found that inactivation of the K^+ transporter Kup, but not KimA, in the KtrA—deficient mutant strain increases both the sensitivity to alkaline stress and the toxicity by NaCl. From the latter data, we propose that the Ktr system plays an important role in the ability of *E. faecalis* to adapt to hyperosmotic stress, and that Kup functions secondarily to Ktr. However, altogether the growth assays of the potassium transporter defective strains indicate that *E. faecalis* uses different transporters systems with capacity to replace one to the others in different stress conditions, such as low K^+, extreme pH, and salt concentrations.

Based on the results of this study, we propose a general mechanism of *Enterococcus* resistance, which as shown in Figure 1 involves the expression of different ATPases for the movement of the essential ions. Proton extrusion is carried out by the F_0F_1 ATPase complex, which is functional at neutral and acidic pH. Sodium ions are pumped outside cells by the V_0V_1 ATPase complex, which is active at low H^+ concentrations. Concerning to the homeostasis of K^+, multiple channels and transporters are present in *E. faecalis*, but the specific physiological roles of each transporter are poorly studied. Diversity analysis of the potassium transporters performed in the *Enterococcus* species revealed that the channels KtrA/B is the most widely disseminated of the K^+ transporters. The two members of the H^+/K^+ symporter KUP family, Kup and KimA, described here, are widely disseminated in the *Enterococcus* genera. Taking into account how the ion flux of H^+, Na^+, and K^+ involved in alkaline stress occurs in this microorganism (Figure 1), and the results obtained in this work with respect to the mutant strains in potassium transport, we hypothesize that the KtrAB system is involved in the symport of K^+ and Na^+, and function together, under alkaline pH growth, with the Na^+ ATPase, responsible to expel out the Na^+. In addition, we found that Kup could mediate the intracellular import of K^+ and H^+, which could contribute to not only the homeostasis of potassium, but also to hold protons inside the cells. This participation of the Kup transporter in alkaline conditions is highly relevant, and its contribution could be that this protein can transport K^+ ions with H^+, thus contributing not only to K^+ uptake but also to the acidification of the cytoplasm in extreme alkaline conditions.

5. Conclusion

Enterococcus faecalis is able to resist and grow in different conditions. By using genetic techniques, we conclude that KtrA is required for the functionality of the uptake system in alkaline and high osmolarity, in this condition also Kup increase the resistance to this stress conditions to the concentration of K^+. Finally, simple or double mutans in the K^+ transporter did not produce significative modification in the virulence of the strains.

Data availability statement

The original contributions presented in the study are included in the article/Supplementary material, further inquiries can be directed to the corresponding author.

Author contributions

GA done experimental design and performed experiments. FG performed experiments. MT contributed to bioinformatic analysis. ME contributed to experimental design and bioinformatic analysis. VB designed and performed experiments and bioinformatic analysis. JS designed experiments. CM designed experiments and performed bioinformatic analysis. All authors contributed to the article and approved the submitted version.

Funding

This work was supported by Ministerio de Ciencia y Tecnologia PICT 2020–3227 (Prest BID) and PIP 11220200101356CO, CONICET.

Conflict of interest

The authors declare that the research was conducted in the absence of any commercial or financial relationships that could be construed as a potential conflict of interest.

Publisher's note

Supplementary material

The Supplementary material for this article can be found online at: https://www.frontiersin.org/articles/10.3389/fmicb.2023.1117684/full#supplementary-material

References

Bai, Y., Yang, J., Zarrella, T. M., Zhang, Y., Metzger, D. W., and Bai, G. (2014). Cyclic Di-AMP impairs potassium uptake mediated by a cyclic Di-AMP binding protein in streptococcus pneumoniae. *J. Bacteriol.* 196, 614–623. doi: 10.1128/JB.01041-13

Benjamini, Y., and Hochberg, Y. (1995). Controlling the false discovery rate: a practical and powerful approach to multiple testing. *J. R. Stat. Soc. Ser. B* 57, 289–300.

Binepal, G., Gill, K., Crowley, P., Cordova, M., Brady, J. L., Senadheera, D. B., et al. (2016). Trk2 potassium transport system in Streptococcus mutans and its role in potassium homeostasis, biofilm formation, and stress tolerance. *J. Bacteriol.* 198, 1087–1100. doi: 10.1128/JB.00813-15

Blancato, V. S., and Magni, C. (2010). A chimeric vector for efficient chromosomal modification in enterococcus faecalis and other lactic acid bacteria. *Lett. Appl. Microbiol.* 50, 542–546. doi: 10.1111/j.1472-765X.2010.02815.x

Boehm, A. B., and Sassoubre, L. M. (2014). "Enterococci as indicators of environmental fecal contamination," in *Enterococci: From Commensals to Leading Causes of Drug Resistant Infection [Internet]*. eds. M. S. Gilmore, D. B. Clewell, Y. Ike and N. Shankar (Boston: Massachusetts Eye and Ear Infirmary).

Byappanahalli, M. N., Nevers, M. B., Korajkic, A., Staley, Z. R., and Harwood, V. J. (2012). Enterococci in the environment. *Microbiol. Mol. Biol. Rev.* 76, 685–706. doi: 10.1128/MMBR.00023-12

Corrigan, R. M., and Gründling, A. (2013). Cyclic di-AMP: another second messenger enters the fray. *Nat. Rev. Microbiol.* 11, 513–524. doi: 10.1038/nrmicro3069

Devaux, L., Sleiman, D., Mazzuoli, M. V., Gominet, M., Lanotte, P., Trieu-Cuot, P., et al. (2018). Cyclic di-AMP regulation of osmotic homeostasis is essential in group B streptococcus. *PLoS Genet.* 14, e1007342–e1007353. doi: 10.1371/journal.pgen.1007342

Dornan, S., and Collins, M. A. (1990). High efficiency electroporation of Lactococcus lactis subsp. lactis LM0230 with plasmid pGB301. *Lett. Appl. Microbiol.* 11, 62–64. doi: 10.1111/j.1472-765X.1990.tb01275.x

Espariz, M., Zuljan, F. A., Esteban, L., and Magni, C. (2016). Taxonomic identity resolution of highly phylogenetically related strains and selection of phylogenetic markers by using genome-scale methods: the bacillus pumilus group case. *PLoS One* 11:e0163098. doi: 10.1371/journal.pone.0163098

Faozia, S., Fahmi, T., Port, G. C., and Cho, K. H. (2021). C-di-AMP-regulated K+ importer KtrAB affects biofilm formation, stress response, and SpeB expression in *Streptococcus* pyogenes. *Infect. Immun.* 89, e00317–e00320. doi: 10.1128/IAI.00317-20

Franz, C. M. A. P., Stiles, M. E., Schleifer, K. H., and Holzapfel, W. H. (2003). Enterococci in foods—a conundrum for food safety. *Int. J. Food Microbiol.* 88, 105–122. doi: 10.1016/S0168-1605(03)00174-0

García-Solache, M., and Rice, L. B. (2019). The enterococcus: a model of adaptability to its environment. *Clin. Microbiol. Rev.* 32, 1–28. doi: 10.1128/CMR.00058-18

Gibhardt, J., Hoffmann, G., Turdiev, A., Wang, M., Lee, V. T., and Commichau, F. M. (2019). C-di-AMP assists osmoadaptation by regulating the listeria monocytogenes potassium transporters KimA and KtrCD. *J. Biol. Chem.* 294, 16020–16033. doi: 10.1074/jbc.RA119.010046

Giraffa, G. (2002). Enterococci from foods. *FEMS Microbiol. Rev.* 26, 163–171. doi: 10.1111/j.1574-6976.2002.tb00608.x

Gries, C. M., Bose, J. L., Nuxoll, A. S., Fey, P. D., and Bayles, K. W. (2013). The Ktr potassium transport system in Staphylococcus aureus and its role in cell physiology, antimicrobial resistance and pathogenesis. *Mol. Microbiol.* 89, 760–773. doi: 10.1111/mmi.12312

Gries, C. M., Sadykov, M. R., Bulock, L. L., Chaudhari, S. S., Thomas, V. C., Bose, J. L., et al. (2016). Potassium uptake modulates Staphylococcus aureus metabolism. *mSphere*:1. doi: 10.1128/msphere.00125-16

Gundlach, J., Herzberg, C., Kaever, V., Gunka, K., Hoffmann, T., Weiß, M., et al. (2017). Control of potassium homeostasis is an essential function of the second messenger cyclic di-AMP in Bacillus subtilis. *Sci. Signal.* 10, 1–10. doi: 10.1126/scisignal.aal3011

Gundlach, J., Krüger, L., Herzberg, C., Turdiev, A., Poehlein, A., Tascón, I., et al. (2019). Sustained sensing in potassium homeostasis: cyclic di-AMP controls potassium uptake by KimA at the levels of expression and activity. *J. Biol. Chem.* 294, 9605–9614. doi: 10.1074/jbc.RA119.008774

Hancock, L. E., and Perego, M. (2004). Systematic inactivation and phenotypic characterization of two-component signal transduction systems of enterococcus faecalis V583. *J. Bacteriol.* 186, 7951–7958. doi: 10.1128/JB.186.23.7951-7958.2004

Holtmann, G., Bakker, E. P., Uozumi, N., and Bremer, E. (2003). KtrAB and KtrCD: two K. *Society* 185, 1289–1298. doi: 10.1128/JB.185.4.1289

Kakinuma, Y. (1998). Inorganic cation transport and energy transduction in enterococcus hirae and other streptococci. *Microbiol. Mol. Biol. Rev.* 62, 1021–1045. doi: 10.1128/MMBR.62.4.1021-1045.1998

Kawano, M., Abuki, R., Igarashi, K., and Kakinuma, Y. (2001). Potassium uptake with low affinity and high rate in enterococcus hirae at alkaline pH. *Arch. Microbiol.* 175, 41–45. doi: 10.1007/s002030000234

Kim, H., Youn, S. J., Kim, S. O., Ko, J., Lee, J. O., and Choi, B. S. (2015). Structural studies of potassium transport protein KtrA regulator of conductance of K^+ (RCK) C domain in complex with cyclic diadenosine monophosphate (c-di-AMP). *J. Biol. Chem.* 290, 16393–16402. doi: 10.1074/jbc.M115.641340

Krüger, L., Herzberg, C., Warneke, R., Poehlein, A., Stautz, J., Weiß, M., et al. (2020). Two ways to convert a low-affinity potassium channel to high affinity: control of Bacillus subtilis KtrCD by glutamate. *J. Bacteriol.* 202, e00138–e00158. doi: 10.1128/JB.00138-20

Krulwich, T. A., Sachs, G., and Padan, E. (2011). Molecular aspects of bacterial pH sensing and homeostasis. *Nat. Rev. Microbiol.* 9, 330–343. doi: 10.1038/nrmicro2549

Kundra, S., Lam, L. N., Kajfasz, J. K., Casella, L. G., Andersen, M. J., Abranches, J., et al. (2021). C-di-AMP is essential for the virulence of *Enterococcus faecalis*. *Infect. Immun.* 89:e0036521. doi: 10.1128/IAI.00365-21

Letunic, I., and Bork, P. (2011). Interactive tree of life v2: online annotation and display of phylogenetic trees made easy. *Nucleic Acids Res.* 39, W475–W478. doi: 10.1093/nar/gkr201

Levy, A., Salas Gonzalez, I., Mittelviefhaus, M., Clingenpeel, S., Herrera Paredes, S., Miao, J., et al. (2018). Genomic features of bacterial adaptation to plants. *Nat. Genet.* 50, 138–150. doi: 10.1038/s41588-017-0012-9

Martino, G. P., Perez, C. E., Magni, C., and Blancato, V. S. (2018). Implications of the expression of enterococcus faecalis citrate fermentation genes during infection. *PLoS One* 13:e0205787. doi: 10.1371/journal.pone.0205787

Murray, B. E. (1990). The life and times of the enterococcus. *Clin. Microbiol. Rev.* 3, 46–65. doi: 10.1128/CMR.3.1.46

Ogier, J. C., and Serror, P. (2008). Safety assessment of dairy microorganisms: the enterococcus genus. *Int. J. Food Microbiol.* 126, 291–301. doi: 10.1016/j.ijfoodmicro.2007.08.017

Pham, H. T., Nhiep, N. T. H., Vu, T. N. M., Huynh, T. A. N., Zhu, Y., Huynh, A. L. D., et al. (2018). Enhanced uptake of potassium or glycine betaine or export of cyclic-di-AMP restores osmoresistance in a high cyclic-di-AMP Lactococcus lactis mutant. *PLoS Genet.* 14:e1007574. doi: 10.1371/journal.pgen.1007574

Price-Whelan, A., Poon, C. K., Benson, M. A., Eidem, T. T., Roux, C. M., Boyd, J. M., et al. (2013). Tanscriptional profiling of staphylococcus aureus during growth in 2 M NaCl leads to clarification of physiological roles for Kdp and Ktr K+ uptake systems. *MBio* 4, e00407–e00413. doi: 10.1128/mBio.00407-13

Quintana, I. M., Gibhardt, J., Turdiev, A., Hammer, E., Commichau, F. M., Lee, V. T., et al. (2019). The KupA and KupB proteins of *Lactococcus lactis* IL1403 are novel c-di-AMP receptor proteins responsible for potassium uptake. *J. Bacteriol.* 201, 1–13. doi: 10.1128/JB.00028-19

Rocha, R., Teixeira-Duarte, C. M., Jorge, J. M. P., and Morais-Cabral, J. H. (2019). Characterization of the molecular properties of KtrC, a second RCK domain that regulates a Ktr channel in Bacillus subtilis. *J. Struct. Biol.* 205, 34–43. doi: 10.1016/j.jsb.2019.02.002

Rosenberg, J., Dickmanns, A., Neumann, P., Gunka, K., Arens, J., Kaever, V., et al. (2015). Structural and biochemical analysis of the essential diadenylate cyclase CdaA from listeria monocytogenes. *J. Biol. Chem.* 290, 6596–6606. doi: 10.1074/jbc.M114.630418

Sambrook, J., Fritsch, E. F., and Maniatis, T. (1989). *Molecular Cloning: A Laboratory Manual. 2nd Edn.* Cold Spring Harbor, NY: Cold Spring Harbor Laboratory Press.

Schlosser, A., Meldorf, M., Stumpe, S., Bakker, E. P., and Epstein, W. (1995). TrkH and its homolog, TrkG, determine the specificity and kinetics of cation transport by the Trk system of Escherichia coli. *J. Bacteriol.* 177, 1908–1910. doi: 10.1128/jb.177.7.1908-1910.1995

Solheim, M., La Rosa, S. L., Mathisen, T., Snipen, L. G., Nes, I. F., and Brede, D. A. (2014). Transcriptomic and functional analysis of NaCl-induced stress in enterococcus faecalis. *PLoS One* 9, 1–13. doi: 10.1371/journal.pone.0094571

Stamatakis, A. (2014). RAxML version 8: a tool for phylogenetic analysis and post-analysis of large phylogenies. *Bioinformatics* 30, 1312–1313. doi: 10.1093/bioinformatics/btu033

Stautz, J., Hellmich, Y., Fuss, M. F., Silberberg, J. M., Devlin, J. R., Stockbridge, R. B., et al. (2021). Molecular mechanisms for bacterial potassium homeostasis. *J. Mol. Biol.* 433:166968. doi: 10.1016/j.jmb.2021.166968

Stülke, J., and Krüger, L. (2020). Cyclic di-AMP signaling in bacteria. *Annu. Rev. Microbiol.* 74, 159–179. doi: 10.1146/annurev-micro-020518-115943

Tascón, I., Sousa, J. S., Corey, R. A., Mills, D. J., Griwatz, D., Aumüller, N., et al. (2020). Structural basis of proton-coupled potassium transport in the KUP family. *Nat. Commun.* 11:626. doi: 10.1038/s41467-020-14441-7

Terán, L. C., Mortera, P., Tubio, G., Alarcón, S. H., Blancato, V. S., Espariz, M., et al. (2022). Genomic analysis revealed conserved acid tolerance mechanisms from native micro-organisms in fermented feed. *J. Appl. Microbiol.* 132, 1152–1165. doi: 10.1111/jam.15292

Torres Manno, M. A., Pizarro, M. D., Prunello, M., Magni, C., Daurelio, L. D., and Espariz, M. (2019). GeM-pro: a tool for genome functional mining and microbial profiling. *Appl. Microbiol. Biotechnol.* 103, 3123–3134. doi: 10.1007/s00253-019-09648-8

frontiers | Frontiers in Microbiology

TYPE Original Research
PUBLISHED 14 February 2023
DOI 10.3389/fmicb.2023.1111652

OPEN ACCESS

EDITED BY
Paloma López,
Spanish National Research Council (CSIC),
Spain

REVIEWED BY
Mangesh Vasant Suryavanshi,
Cleveland Clinic,
United States
Xin Tang,
Jiangnan University,
China

*CORRESPONDENCE
Leónides Fernández
✉ leonides@ucm.es
Juan M. Rodríguez
✉ jmrodrig@ucm.es

SPECIALTY SECTION
This article was submitted to Food Microbiology, a section of the journal Frontiers in Microbiology

RECEIVED 29 November 2022
ACCEPTED 17 January 2023
PUBLISHED 14 February 2023

CITATION
Rodríguez JM, Garranzo M, Segura J, Orgaz B, Arroyo R, Alba C, Beltrán D and Fernández L (2023) A randomized pilot trial assessing the reduction of gout episodes in hyperuricemic patients by oral administration of *Ligilactobacillus salivarius* CECT 30632, a strain with the ability to degrade purines. *Front. Microbiol.* 14:1111652. doi: 10.3389/fmicb.2023.1111652

A randomized pilot trial assessing the reduction of gout episodes in hyperuricemic patients by oral administration of *Ligilactobacillus salivarius* CECT 30632, a strain with the ability to degrade purines

Juan M. Rodríguez[1]*, Marco Garranzo[2], José Segura[2], Belén Orgaz[2], Rebeca Arroyo[1], Claudio Alba[1], David Beltrán[3] and Leónides Fernández[2]*

[1]Department of Nutrition and Food Science, Complutense University of Madrid, Madrid, Spain, [2]Department of Galenic Pharmacy and Food Technology, Complutense University of Madrid, Madrid, Spain, [3]Centro de Diagnóstico Médico, Ayuntamiento de Madrid, Madrid, Spain

Introduction: Hyperuricemia and gout are receiving an increasing scientific and medical attention because of their relatively high prevalence and their association with relevant co-morbidities. Recently, it has been suggested that gout patients have an altered gut microbiota. The first objective of this study was to investigate the potential of some *Ligilactobacillus salivarius* strains to metabolize purine-related metabolites. The second objective was to evaluate the effect of administering a selected potential probiotic strain in individuals with a history of hyperuricemia.

Methods: Inosine, guanosine, hypoxanthine, guanine, xanthine, and uric acid were identified and quantified by high-performance liquid chromatography analysis. The uptake and biotransformation of these compounds by a selection of *L. salivarius* strains were assessed using bacterial whole cells and cell-free extracts, respectively. The efficacy of *L. salivarius* CECT 30632 to prevent gout was assessed in a pilot randomized controlled clinical trial involving 30 patients with hyperuricemia and a history of recurrent gout episodes. Half of the patients consumed *L. salivarius* CECT 30632 (9 $\log_{10}$ CFU/day; probiotic group; n = 15) for 6 months while the remaining patients consumed allopurinol (100–300 mg/daily; control group; n = 15) for the same period. The clinical evolution and medical treatment received by the participants were followed, as well as the changes in several blood biochemical parameters.

Results: L. salivarius CECT 30632 was the most efficient strain for inosine (100%), guanosine (100%) and uric acid (50%) conversion and, therefore, it was selected for the pilot clinical trial. In comparison with the control group, administration of *L. salivarius* CECT 30632 resulted in a significant reduction in the number of gout episodes and in the use of gout-related drugs as well as an improvement in some blood parameters related to oxidative stress, liver damage or metabolic syndrome.

Conclusion: Regular administration of *L. salivarius* CECT 30632 reduced serum urate levels, the number of gout episodes and the pharmacological therapy required to control both hyperuricemia and gout episodes in individuals with a history of hyperuricemia and suffering from repeated episodes of gout.

KEYWORDS

probiotics, *Ligilactobacillus salivarius*, gout, hyperuricemia, uric acid, inosine, guanosine

Introduction

Purines are part of nucleosides (adenosine and guanosine) from which adenosine monophosphate (AMP) and guanosine monophosphate (GMP) are synthesized and, in turn, used for nucleic acids (DNA/RNA) synthesis. Also, purine derivatives are metabolically relevant molecules involved in cell survival and proliferation, as they act as energy cofactors (ATP, GTP), intracellular signal transduction molecules (cyclic AMP, cyclic GMP), part of coenzymes [nicotinamide adenine dinucleotide (NAD^+), nicotinamide adenine dinucleotide phosphate ($NADP^+$), and coenzyme A] and universal methyl donors (S-adenosylmethionine; Rosemeyer, 2004). Most of the purines present in cells come from the recycling of derivatives of cellular metabolism (the savage pathway), but they can also arise from *de novo* biosynthesis (a process that happens mainly in the liver although small amounts are also produced in the intestine and the vascular endothelium, among other tissues) or from the diet (Pareek et al., 2021). Excess purine nucleosides are removed by breakdown to uric acid involving the sequential action of several enzymes. Adenosine deaminase transforms adenosine into inosine, and the enzyme purine nucleoside phosphorylase converts inosine and guanosine into hypoxanthine and guanine, respectively, which are further transformed to xanthine by xanthine oxidase (acting on hypoxanthine) and guanine deaminase (acting on guanine). In addition, xanthine oxidase, also known as xanthine oxidoreductase, also converts xanthine into uric acid.

Uric acid exists as urate (deprotonated form; pKa = 5.8) at physiological pH (Mandal and Mount, 2015). The normal concentration ranges for urate in human blood are 1.5–6.0 mg/dL in women and 2.5–7.0 mg/dL in men, which are close to saturation levels and are unusually high concentrations compared to other mammalian species due to the lack of uricase, the enzyme responsible of urate degradation (Álvarez-Lario and Macarrón-Vicente, 2010). Urate concentration in the blood depends on the balance between its rate of synthesis in the body, the amount of xanthine of purines from the diet, and on the rate of urate excretion (Lane and Fan, 2015). Approximately, two-thirds of urate elimination takes place in the kidneys, being excreted in the urine, while the remaining one-third occurs in the gastrointestinal tract (Sorensen, 1965; Maesaka and Fishbane, 1998). When there is an imbalance between urate production and excretion, hyperuricemia, defined as an elevated serum urate concentration (>6.0 mg/dL in women and >7.0 mg/dL in men), occurs (Li et al., 2019; George and Minter, 2022). Hyperuricemia increases the risk of precipitation of monosodium urate crystals (solubility limit at 6.8 mg/dL), which can cause gout and urate kidney stones, and also has been associated with the development and severity of many other conditions including chronic renal disease, cardiovascular diseases and metabolic syndrome due to its role in inducing inflammation, endothelial dysfunction, the proliferation of vascular smooth muscle cells and the activation of the renin-angiotensin system (Yanai et al., 2021).

Some risk factors for hyperuricemia and gout development are non-modifiable factors, such as sex (men are at a higher risk than women), age (risk increases with age), race and/or ethnicity, and genetics (due to genetic variants of renal urate transporters), but others are modifiable factors including diet (alcohol consumption, purine-rich foods, fructose-sweetened beverages), medication, and lifestyle (physical activity, body mass index [BMI]) (MacFarlane and Kim, 2014). However, the two main causes for hyperuricemia and gout are, first, a purine-rich diet (seafood, meat, animal offal, alcoholic beverages, and fructose-containing drinks) which induces urate overproduction and, second, a deficient excretion by kidneys and gut.

In the United States, the prevalence rates of hyperuricemia (defined as a serum urate level of >7.0 mg/dL regardless of sex) and gout were 11.9 and 3.9%, respectively, and about one-third of gout patients reported the use of urate-lowering therapy (Chen-Xu et al., 2019). Among non-United States populations, the prevalence of hyperuricemia and gout is higher in Asian than in European populations, although wide variability has been reported due to differences in genetic background and non-genetic factors (Butler et al., 2021).

Most treatments for patients affected by hyperuricemia are based on three strategies: (a) uricostatic drugs inhibiting the production of urate (e.g., allopurinol, febuxostat, and topiroxostat) by modulating the activity of a key enzyme (xanthine oxidase) involved in the production of uric acid; (b) uricosuric drugs that promote the excretion of urate in the kidneys by reducing its reabsorption in the renal tubules (e.g., benzbromarone, probenecid, sulfinpyrazone, and lesinurad); or (c) promoting the transformation of urate to more soluble allantoin and hydrogen peroxide (injectable recombinant uricases, such as pegloticase) but, while showing different effectiveness in reducing serum urate levels, most of them are known to have a myriad of side effects (Strilchuk et al., 2019). Unlike other conditions, dietary restriction alone does not always lead to resolution or improvement of hyperuricemia symptoms. Only a few dietary interventions have been described in the literature that resulted in a small decrease in serum urate levels (Vedder et al., 2019).

In the last decade, a wealth of information has arisen on the important role that the human microbiota plays in health and disease (reviewed in Requena and Velasco, 2021; Afzaal et al., 2022). Because alterations in the human microbiota could play a role in the development of various diseases, modifications of the microbiota (probiotics, prebiotics, antibiotics, and fecal microbiota transference) have been proposed as strategies to prevent and treat some illnesses, including hyperuricemia (Rizzatti et al., 2018; Martín and Langella, 2019; Antushevich, 2020; Fan and Pedersen, 2021; Wang et al., 2022). In fact, gout has been linked to gut bacterial dysbiosis: *Bacteroides caccae* and *Bacteroides xylanisolvens* were enriched in the gut microbiota of patients with clinically diagnosed gout while, simultaneously, *Faecalibacterium prausnitzii* was depleted resulting in reduced butyrate biosynthesis and altered purine degradation in the gut (Guo et al., 2016). More recent studies have confirmed that the profiles of gut microbiota and bacterial metabolites were altered in gout patients, and that they may be partly reversed after urate-lowering treatment with febuxostat (Shao et al., 2017; Chu et al., 2021; Lin et al., 2021). At present, the exact mechanisms relating gut microbiota and purine metabolism are unknown. Modulation of gut microbiota composition using probiotics may be a promising intervention to regulate serum urate levels as it has been shown in animal studies with bacterial strains isolated from fermented foods (Li et al., 2014; Cao et al., 2017; Yamada et al., 2017; Wu et al., 2021). Human vagina and milk have been shown to contain unique microbiotas playing key roles in the initial colonization of the infant gut and, most probably, in the short- and long-term health of the human host (Fernández et al., 2020; France et al., 2022). In the past years, our group has characterized bacterial isolates from both milk and vaginal samples from healthy individuals and some of them were revealed to be good probiotic candidates in clinical trials (Arroyo et al., 2010; Fernández et al., 2016; Cárdenas et al., 2019; Martín et al., 2019; Fernández et al., 2021; Jiménez et al., 2021). Therefore, the objective of this study was, first, to select a potential probiotic strain with the ability to metabolize purine-related metabolites and, second, to evaluate the effect of the administration of this potential probiotic strain on individuals with a history of hyperuricemia in order to evaluate the feasibility of a future multicenter randomized controlled trial.

Materials and methods

Bacterial strains and culture conditions

A collection of 13 *Ligilactobacillus salivarius* strains were initially included in this study. Such strains had been previously isolated from human milk or vaginal exudate samples obtained from healthy individuals. Routinely, bacterial cultures were transferred (1.5%, v/v) from frozen stock cultures to de Man, Rogosa and Sharpe (MRS, Oxoid, Basingstoke, United Kingdom) broth and incubated aerobically at 37°C for 24 h. Viable bacteria were quantified by spreading decimal dilutions onto MRS agar (1.5%, w/v) plates incubated aerobically at 37°C for 24 h. The results were expressed as the number of colony-forming units (CFU).

Evaluation of the uptake of guanosine, inosine, and uric acid by whole bacterial cells

The initial screening of the bacterial collection was carried out by using the method described by Li et al. (2014) with some modifications. In brief, bacterial cells were collected from overnight broth cultures (stationary phase) by centrifugation at 4°C and 19,000 ×*g* for 10 min and washed once with the same volume of cold saline (0.85% NaCl, w/v) solution. Then, the cell pellet was suspended in 0.2 mL of phosphate buffer (100 mM K_3PO_4, pH 7) and an aliquot was taken to determine the number of viable cells. 0.8 mL of 1.3 mM solution of either guanosine, inosine, and/or uric acid, sterilized by filtration (0.22 µm pore size; Nalgene 176–0020 nylon), were mixed with 100 or 25 µL of the suspension of washed cells (about 10^{10} CFU of viable cells) and the required volume of the phosphate buffer to reach a final volume of 1.4 mL. When indicated, 0.1 mL of either sterile 4 mM glucose or distilled water were added to the mixture to evaluate the uptake of inosine, guanosine, and uric acid in the presence of glucose. The mixtures were incubated in a water bath at 37°C for 60 min. Afterwards, the mixture was centrifuged as above and 540 µL of the cell-free supernatant were mixed with 60 µL of 0.1 M $HClO_4$. Following filtration (0.22 µm pore size; Nalgene 176–0020 nylon) to remove particulate material, the filtrate was kept frozen at −20°C until the determination of the concentration of guanosine, inosine, and uric acid by high-performance liquid chromatography (HPLC) analysis.

Evaluation of the biotransformation of guanosine, inosine, and uric acid

For this purpose, the same procedure described in the previous section was used but, in this case, cells were substituted by cell-free extracts (CFE). To prepare the CFE, concentrated washed cells suspended in 0.2 mL of cold 0.1 M phosphate buffer (pH 7) were mixed with the same volume of glass beads (0.1 mM bead size; Sigma-Aldrich) and lysed by mechanical disruption in an FP120 FastPrep® Instrument (QbioGene, Irvine, California, United Sates). The mixture was subjected to three processing cycles of 20 s of bead-beating at 5 m s^{-1} followed by 2 min incubation in an ice bath to avoid protein denaturalization. After bead-beating, the tubes were centrifuged at 4°C and 19,000 ×*g* for 10 min to sediment cell debris and glass beads. The supernatant (CFE) was transferred to clean tubes and 25 µL were used instead of whole cell suspensions as described above to determine the transformation of guanosine, inosine, and uric acid.

The protein content in the CFE was determined by the Bradford method using a Coomassie Plus (Bradford) Assay Reagent (Thermo Scientific™) and bovine serum albumin (Sigma-Aldrich) as the standard and the microplate procedure in 96-well plates.

Identification and quantification of inosine, guanosine, hypoxanthine, guanine, xanthine, and uric acid

Inosine, guanosine, hypoxanthine, guanine, xanthine, and uric acid were quantified by HPLC using the method described by Li et al. (2014), with slight modifications. Analyses were carried out using a Zorbax SB-C18 (5 µm, 4.6 × 250 mM) column connected to an HPLC device (Agilent 1,260 Infinity Quaternary LC) with a diode array detector (Agilent Technologies, Waldbronn, Germany). Working solutions (1.3 mM) of all compounds were prepared in phosphate buffer (K_3PO_4, 100 mM, pH 7), cleaned and sterilized by passing the solution through a filter (0.22 µm pore size; Nalgene 176–0020 nylon), and degassed by sonication. The separation of the compounds was achieved by using an isocratic flow (0.5 mL/min) of methanol and 0.1% of acetic acid in Milli-Q water (3:97, v/v). The retention times at 245 nm were 5.00, 4.75, 2.46, 2.36, 2.24, and 2.09 min for guanosine, inosine, xanthine, hypoxanthine, guanine, and uric acid, respectively.

Compound quantification was carried out by developing standard curves built using the corresponding pure compounds (Sigma, Alcobendas, Madrid). The analyses were carried out in triplicate.

Efficacy of *Ligilactobacillus salivarius* CECT 30632 to prevent gout: A pilot randomized controlled clinical trial

A total of 30 patients participated in the study and were recruited at Centro de Diagnóstico Médico (Madrid, Spain). All of them shared hyperuricemia (>7 mg/dL), a history of recurrent gout episodes (≥3 episodes/year), characterized by acute arthritis and requiring treatment with colchicine despite taking allopurinol (100–300 mg/day) as a preventive measure. The definition of case (gout) was performed following the criteria of the Spanish Society for Rheumatology. Exclusion criteria included antibiotic or probiotic treatment within the previous 2 months or suffering a gout episode at recruitment. Sample size for this trial was calculated accepting an alpha risk of 0.05 and a beta risk of 0.2 in a one-side test to find a 400% increase in the number of individuals without gout episodes during the 6-month period of the trial and anticipating a drop-out rate of 4%. Participants were allocated by simple randomization using a computer-generated list of random numbers prepared by an independent researcher who also prepared the envelopes containing the treatment but with no clinical involvement in the trial. Then, half of the patients ($n = 15$; probiotic group) consumed daily, for 6 months, a sachet containing ~9 $\log_{10}$ CFU of *L. salivarius* CECT 30632 while the other half of the patients ($n = 15$; control group) consumed allopurinol (100–300 mg/day) for the same period. Physicians and data analysts were kept blinded to the allocation.

Consumption of drugs used for prevention (allopurinol) or treatment (colchicine, non-steroidal inflammatory drugs [NSAIDs]) of gout was recorded throughout the study. BMI was calculated as weight divided by the square of the height (kg/m^2). Blood samples were obtained at the beginning (T1) and at the end (T2; 6 months) of the study. Blood samples

were extracted at Unilabs (Madrid, Spain). The first 8 mL-fraction was collected into a Na-heparin tube to analyze oxidative stress (OS)-related parameters in plasma, including markers of oxidative stress (advanced oxidation protein products [AOPPs], sulfhydryl [SH] groups, thiobarbituric acid reactive substances [TBARS], malondialdehyde [MDA], 8-isoprostaglandin F2α) and indicators of vascular function and blood pressure modulation (nitric oxide, nitrite, nitrate); a second 4 mL-fraction was used to obtain serum for standard biochemistry (serum urate, triglycerides, total cholesterol, aspartate transaminase [AST or GOT], alanine transaminase [ALT or GPT]). Hematology and biochemical analyses of blood samples were performed by Unilabs. Metabolites related to OS and nitric oxide metabolism end products (NOx) were measured in duplicate as described previously (Codoñer-Franch et al., 2011, 2012).

This study was conducted according to the guidelines laid down in the Declaration of Helsinki and was approved by the Ethics Committee of the Hospital Clínico San Carlos (Madrid, Spain) (protocol: CEIC 20/263-E; date of approval: 01/04/2020, act 4.1/20).

Statistical analysis

The normality of data distribution was analyzed using the Shapiro–Wilks test. Quantitative variables are presented as mean and 95% confidence interval (CI) or standard deviation (SD). The Student's t-test was used to compare the means of continuous variables having a normal distribution. The χ^2 test, the Fisher exact test or the Freeman–Halton extension of the Fisher exact probability test for a 2×4 contingency table were used to compare percentages. One-way repeated measures ANOVA was used to compare the changes in the mean values of blood parameters during the study. Differences were considered significant when the value of $p < 0.05$. Statistical calculations were performed using Statgraphics Centurion 19 version 19.2.01 (Statgraphics Technologies, Inc., The Plains, VA, United States).

Results

Initial screening of *Ligilactobacillus salivarius* strains for nucleoside and uric acid uptake

Most of 13 *L. salivarius* strains included in this study showed a high ability for guanosine and inosine uptake (Supplementary Table S1). The results of uptake capacity of inosine, guanosine, and uric acid in the presence or not of 4 mM glucose of the most active purine-uptaking strains (5 strains) is shown in Figure 1. The five strains transported inosine, guanosine and uric acid into the cytoplasm, although some variability was observed among them. Most of the strains transported lower amounts of uric acid compared to inosine and guanosine, except MPac90 which showed no preference for any of the three compounds. In the presence of glucose, the transport of the three compounds into the cells increased, being *L. salivarius* CECT 30632 the only strain that depleted all the inosine, guanosine, and uric acid (Figure 1).

Biotransformation of inosine and guanosine by whole cells of *Ligilactobacillus salivarius*

Subsequently, both the transformation of inosine and guanosine inside the cells and the release into the extracellular medium of related metabolites were investigated. The concentrations (as % of transformation) of hypoxanthine, xanthine, and uric acid in the extracellular media when the cells had been incubated in the presence of either inosine or guanosine are shown in Table 1. Guanine was not detected in any sample under these assay conditions.

Except for the strain MPac32, inosine was efficiently transformed into hypoxanthine (>89%) and released into the extracellular media by the rest of selected strains (Table 1). When glucose was present in the reaction mixture, the release of hypoxanthine decreased in all the strains, although to a different extent; hypoxanthine was not even detected in the extracellular media of *L. salivarius* CECT 30632 and MPac90. Xanthine was found only in some samples and at a very low concentration (≤ 2% transformation), regardless of the presence of glucose. On the other hand, *L. salivarius* MPac40 and MPac91 secreted also uric acid in addition to hypoxanthine when inosine was supplied in the reaction mixture. *L. salivarius* MPac91 was the most efficient at metabolizing guanosine to uric acid and releasing it from cells (Table 1).

Biotransformation of inosine and guanosine by cell extracts of *Ligilactobacillus salivarius*

The products obtained after incubation of cell-free intracellular extracts of selected *L. salivarius* strains with inosine and guanosine are shown in Table 2. *L. salivarius* CECT 30632 and MPac32 extracts efficiently transformed inosine and guanosine to hypoxanthine and xanthine (>90%), respectively, which were no further converted to uric acid in a large proportion (<10%). The yield of xanthine from guanosine was lower (<35%) and that of uric acid was higher (>20%) in *L. salivarius* MPac40, MPac90, and MPac91 than in CECT 30632 and MPac32. Most of the inosine present in the reaction mixture containing *L. salivarius* MPac90 extracts was converted to uric acid (>90%) without accumulation of the intermediates hypoxanthine and xanthine, but a lower efficiency of the guanosine transformation was found, yielding 30–45% of xanthine and 8–26% of uric acid. Remarkably, the inclusion of glucose in the reaction mixture did not modify the type and yield of the obtained compounds (Table 2).

When considering the protein concentration in the reaction mixtures, to somehow relate the extent of transformation to the bacterial enzyme amount, *L. salivarius* CECT 30632 was the most efficient for inosine (100%), guanosine (100%) and uric acid (50%) conversion (Table 3). For this reason, this strain was selected for a pilot clinical trial.

Clinical outcomes of the study

This study was conducted between July 2020 and December 2021. A total of 30 volunteers were enrolled and assigned to the probiotic ($n = 15$) or the control (allopurinol) ($n = 15$) groups. There were no withdrawals during the assay and the compliance rate was high (>93%). Baseline characteristics of the participants were comparable, and no significant differences were identified in terms of age, BMI, and the number of gout episodes in the 9 previous months (Table 4).

The main outcomes of this pilot study are shown in Tables 5, 6 and Figure 2. Daily administration of the probiotic *L. salivarius* CECT 30632 to hyperuricemic individuals was well tolerated and resulted in a significant reduction of the number of gout episodes reported during the period that lasted the study in comparison to the participants that received allopurinol in the control group (the Freeman–Halton

10.3389/fmicb.2023.1111652

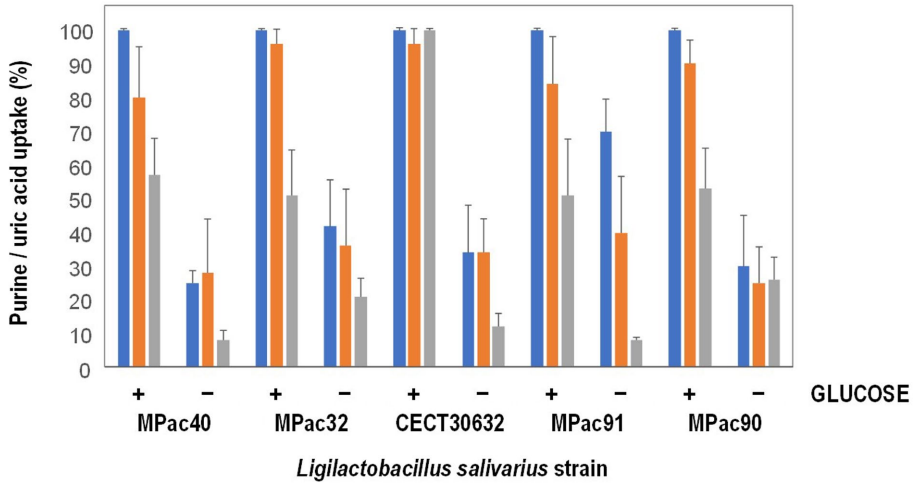

FIGURE 1
Inosine (blue), guanosine (orange), and uric acid (grey) uptake by whole cells of selected *Ligilactobacillus salivarius* strains in the presence (+) or not (–) of 4 mM glucose.

TABLE 1 Biotransformation of inosine and guanosine by whole cells of selected *Ligilactobacillus salivarius* strains in the presence (+) or not (–) of 4 mM glucose.

			Transformation (%)		
			Product in the extracellular medium		
Strain	Substrate	Glucose (4 mM)	Hypoxanthine	Xanthine	Uric acid
CECT 30632	Inosine	–	97 ± 10	<1	8 ± 3
		+	ND	ND	ND
	Guanosine	–	ND	<1	<1
		+	ND	ND	ND
MPac32	Inosine	–	58 ± 1	<1	19 ± 9
		+	33 ± 11	<1	<1
	Guanosine	–	<1	<1	22 ± 6
		+	<1	<1	<1
MPac40	Inosine	–	89 ± 2	ND	89 ± 1
		+	6 ± 1	ND	<1
	Guanosine	–	ND	ND	2 ± 1
		+	<1	1	1
MPac90	Inosine	–	90 ± 9	2	<1
		+	ND	ND	<1
	Guanosine	–	ND	1	<1
		+	ND	ND	ND
MPac91	Inosine	–	99 ± 9	<1	60 ± 12
		+	83 ± 9	ND	3 ± 2
	Guanosine	–	<1	5 ± 3	99 ± 5
		+	<1	ND	13 ± 4

ND, not detected.

extension of the Fisher Exact Probability Test for a 2 × 4 contingency table; $p = 0.006$). In the probiotic group, only 5 out of the 15 volunteers reported a gout episode (only one episode for each of these 5 participants during the trial). In the control group, 13 out of 15 individuals reported gout episodes, and one third of them suffered at least two episodes during the study; the frequency rates reported in the control group during the study were similar to those registered during the 9 months previous to the study (Tables 4, 5).

10.3389/fmicb.2023.1111652

TABLE 2 Biotransformation of inosine and guanosine by cell-free extracts of selected *Ligilactobacillus salivarius* strains.

			Transformation (%)		
Strain	Substrate	Glucose (4 mM)	Hypoxanthine	Xanthine	Uric acid
CECT 30632	Inosine	–	92 ± 11	ND	8 ± 6
		+	89 ± 9	ND	8 ± 2
	Guanosine	–	ND	97 ± 7	9
		+	ND	94 ± 8	7 ± 5
MPac32	Inosine	–	92 ± 9	9 ± 7	1
		+	98 ± 8	ND	13 ± 9
	Guanosine	–	ND	89 ± 10	9 ± 5
		+	ND	75 ± 13	7 ± 5
MPac40	Inosine	–	89 ± 24	12 ± 9	30 ± 13
		+	81 ± 1	5 ± 2	18 ± 5
	Guanosine	–	3	33 ± 18	19 ± 9
		+	ND	32 ± 23	ND
MPac90	Inosine	–	10 ± 5	ND	95 ± 11
		+	9 ± 4	ND	93 ± 11
	Guanosine	–	3 ± 1	30 ± 6	8 ± 5
		+	3 ± 1	45 ± 12	26 ± 5
MPac91	Inosine	–	85 ± 18	ND	21 ± 9
		+	100 ± 20	14 ± 9	9
	Guanosine	–	1	25 ± 8	5 ± 3
		+	4 ± 1	35 ± 18	6 ± 3

ND, not detected.

TABLE 3 Extent of inosine, guanosine, and uric acid transformation by cell-free extracts of selected *Ligilactobacillus salivarius* strains.

			Transformation of		
Strain	Protein in CFE* (μg/mL)	Glucose (mM)	Inosine (%)	Guanosine (%)	Uric acid (%)
CECT 30632	11.1 ± 1.20	-	100 ± 12	100 ± 8	51 ± 8
		4	100 ± 12	100 ± 8	51 ± 14
MPac32	16.3 ± 0.48	-	36 ± 26	24 ± 23	51 ± 14
		4	43 ± 25	37 ± 19	51 ± 12
MPac40	8.1 ± 1.57	-	100 ± 12	100 ± 8	14 ± 3
		4	100 ± 12	100 ± 8	13 ± 6
MPac90	26.4 ± 7.32	-	100 ± 12	100 ± 8	4 ± 2
		4	100 ± 12	100 ± 8	6 ± 4
MPac91	14.2 ± 0.44	-	24 ± 18	30 ± 21	51 ± 15
		4	24 ± 22	37 ± 4	53 ± 12

*CFE, cell-free extract.

Colchicine and ibuprofen (or related NSAIDs) doses used during the study by the participants of the control (allopurinol) group (70 and 87 total doses, respectively) were much higher than those required by the volunteers of the probiotic group (30 and 33, respectively) (one-way ANOVA; $p = 0.023$ for colchicine and $p = 0.022$ for ibuprofen or related NSAIDs; Figure 2).

There were no differences in the number of doses of either colchicine (*t*-test: $p = 0.669$) or NSAIDs (*t*-test: $p = 0.964$) taken per individual between the individuals in the control group ($n = 13$) or those in the probiotic group ($n = 5$) who suffered gout episodes. Among such participants, the mean (95% CI) of the number of doses per participant was 5.4 (3.6–7.1) doses and 6.7 (4.1–9.3) doses for colchicine or ibuprofen (and related NSAIDs), respectively, in the control group, and 6.0 (3.5–8.5) doses and 6.6 (4.0–9.2) doses for colchicine or ibuprofen (and related NSAIDs), respectively, in the probiotic group. While all the individuals in the control group daily received allopurinol throughout

TABLE 4 Baseline characteristics of the hyperuricemic volunteers (n=30) that participated in this study.

	Control group (n=15)	Probiotic group (n=15)	p-value*
	Mean [95% CI] or n (%)	Mean [95% CI] or n (%)	
Age (years)	54.2 [52.2–56.2]	53.9 [51.9–55.9]	0.802
BMI (kg/m^2)	32.0 [30.5–33.5]	31.7 [30.2–33.3]	0.784
Gout episodes in the previous 9 months			
0	1 (7)	1 (7)	0.772
1	5 (33)	7 (47)	
2	8 (53)	5 (33)	
3	1 (7)	2 (13)	

*Student's t-tests for age and BMI variables; the Freeman–Halton extension of the Fisher exact probability test for a 2 × 4 contingency table was used to compare the number of gout episodes in the 9 months previous to the study. BMI, body mass index.

TABLE 5 Effect of the probiotic treatment with *Ligilactobacillus salivarius* CECT 30632 on the number of gout episodes and the use of hyperuricemic- or gout-related medication during the study.

	Control group (n=15)	Probiotic group (n=15)	p-value
	n (%)	n (%)	
Number of gout episodes during the study			
0	2 (13)	10 (67)	0.006[a]
1	8 (53)	5 (33)	
2	4 (27)	-	
3	1 (7)	-	
Use of allopurinol			
No	0	12 (80)	<0.001[b]
Yes	15 (100)	3 (20)	
Use of colchicine			
No	1 (7)	10 (67)	<0.001[b]
Yes	14 (93)	5 (33)	
Use of ibuprofen and similar NSAIDs			
No	2 (13)	10 (67)	0.004[b]
Yes	13 (93)	5 (33)	

[a]The Freeman–Halton extension of the fisher exact probability test for a 2 × 4 contingency table. [b]Fisher exact probability test (one-tailed). NSAIDs, non-steroidal anti-inflammatory drugs.

the study, the use of this drug was prescribed for only 5 participants of the probiotic group (Figure 2).

Results of blood analyses performed before the start and at the end of the study to determine the effect of the probiotic intervention in serum urate, markers of oxidative stress (AOPPs, SH groups, TBARS, MDA, 8-isoprostaglandin F2α), indicators of vascular function and blood pressure modulation (NOx, nitrite, nitrate), lipid profile (triglycerides, total cholesterol) and indicators of damage of liver and/or other tissues (AST, ALT) are shown in Table 6. There were no significant changes in the levels of any of the blood parameters tested in the control group individuals. However, relevant changes were observed in the probiotic group in most of the parameters analyzed after the probiotic intervention. Serum urate level was reduced from a mean (95% CI) value of 9.04 (8.72–9.36) mg/dL to 7.90 (7.58–8.22) mg/dL (one-way repeated measures ANOVA; p < 0.001). The levels of AOPPs, MDA, and 8-isoprostaglandin F2α were reduced by 16, 6, and 12% (one-way repeated measures ANOVA; p < 0.001) in the participants of the probiotic group at the end of the study. In contrast, the levels of SH groups and TBARS did not changed. Serum nitrite and nitrate concentrations did not experience variation but that of NOx decreased by a mean value of 0.83 μmol/L (one-way repeated measures ANOVA; p = 0.027). Differences were also found in the mean value of serum triglycerides and total cholesterol that were reduced by 29.52 and 27.88 mg/dL, respectively (one-way repeated measures ANOVA; p = 0.000). Individuals in the probiotic group also experienced an improvement in their serum AST and ALT levels since they were significantly reduced by 1.92 and 2.13 IU/L, respectively (one-way repeated measures ANOVA; p = 0.037 and p = 0.028).

The CONSORT 2010 checklist of information to include when reporting a pilot or feasibility trial[1] can be found as Supplementary material (Supplementary Table S2; Eldridge et al., 2016).

1 www.consort-statement.org

10.3389/fmicb.2023.1111652

TABLE 6 Effect of the probiotic intervention with *Ligilactobacillus salivarius* CECT 30632 on the blood parameters of hyperuricemic participants in the control (*n*=15) and the probiotic (*n*=15) groups.

Blood parameter	Control group (*n*=15)			Probiotic group (*n*=15)		
	Initial	Final	*p*-value*	Initial	Final	*p*-value*
	Mean (95% CI)	Mean (95% CI)		Mean (95% CI)	Mean (95% CI)	
Uric acid (mg/dL)	9.04 (8.90–9.18)	9.03 (8.89–9.17)	0.922	9.04 (8.72–9.36)	7.90 (7.58–8.22)	<0.001
AOPPs (μmol/L)	61.39 (61.21–61.57)	61.21 (61.03–61.40)	0.163	60.35 (59.41–61.29)	50.84 (49.90–51.78)	<0.001
SH groups (μmol/L)	434.18 (432.96–435.40)	434.17 (432.95–435.40)	0.994	434.28 (432.22–436.34)	432.87 (430.81–434.92)	0.315
TBARS (μmol/L)	26.46 (26.00–26.93)	26.63 (26.17–27.09)	0.583	26.42 (26.11–26.73)	26.06 (25.75–26.37)	0.106
MDA (μmol/L)	2.01 (1.97–2.04)	2.01 (1.98–2.04)	0.872	2.00 (1.97–2.04)	1.89 (1.92–1.97)	<0.001
8–Isoprostaglandin F2α (pg/mL)	184.12 (183.08–185.16)	184.24 (183.02–185.28)	0.863	183.85 (181.74–185.97)	161.03 (158.91–163.14)	<0.001
NOx (μmol/L)	23.58 (23.00–24.17)	23.87 (23.28–24.45)	0.471	23.66 (23.15–24.17)	22.83 (22.31–23.34)	0.027
Nitrite (μmol/L)	2.02 (1.98–2.01)	2.04 (2.00–2.08)	0.637	2.01 (1.98–2.05)	2.01 (1.98–2.04)	0.833
Nitrate (μmol/L)	21.97 (21.51–22.42)	21.88 (21.43–22.34)	0.794	22.11 (21.70–22.53)	21.89 (21.47–22.30)	0.425
Triglycerides (mg/dL)	164.85 (163.52–166.19)	164.75 (163.42–166.09)	0.911	164.47 (161.03–167.92)	134.95 (131.50–138.40)	<0.001
Total cholesterol (mg/dL)	188.86 (187.82–189.91)	188.36 (187.31–189.40)	0.475	189.00 (185.84–193.27)	161.67 (157.95–165.39)	<0.001
GOT (IU/L)	32.93 (32.26–33.60)	33.00 (32.26–33.66)	0.884	32.19 (30.93–33.45)	30.27 (29.01–31.53)	0.037
GPT (IU/L)	37.65 (36.62–38.67)	38.21 (37.19–39.24)	0.413	38.79 (37.47–40.10)	36.66 (35.35–37.98)	0.028

*One-way repeated measures ANOVA. AOPPs, advanced oxidation protein products; SH groups, sulfhydryl groups; TBARS, thiobarbituric acid-reactive substances; MDA, malondialdehyde; GOT, glutamic oxoloacetic transaminase; GPT, glutamic pyruvic transaminase; NOx, nitric oxides; IU, international units.

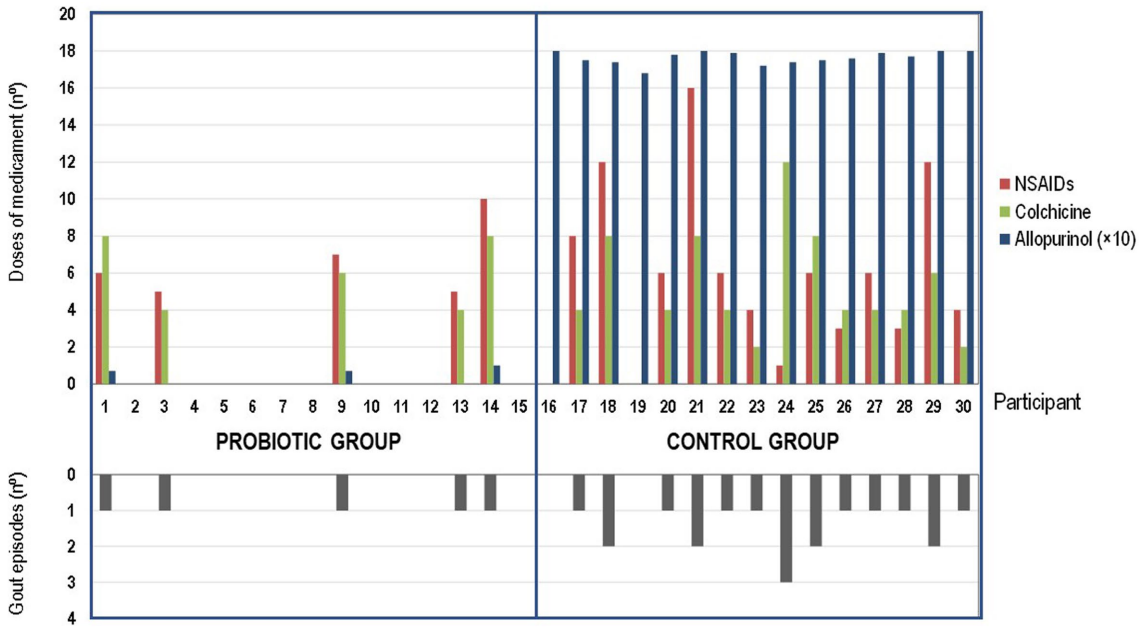

FIGURE 2
Effect of the probiotic treatment with *Ligilactobacillus salivarius* CECT 30632 on gout-associated symptomatology and use of hyperuricemic-related drugs during the study in the probiotic group (participants 1 to 15) and in the control group (participants 16–30).

Discussion

Gout is a painful arthritis that may occur in hyperuricemic patients and is caused by the precipitation of monosodium urate crystals in joints and soft tissues, which activates the inflammasome with the concomitant release of IL-1βb (Dalbeth et al., 2021). The intestinal tract is the second organ responsible for the excretion of urate (20–30%) and this process is driven by efflux transporters such as BCRP/ABCG2, which in addition to being present in the kidney is also highly expressed at the apical membrane of the small intestine (Hosomi et al., 2012). It has been hypothesized that the intestinal microbiota might contribute to the reduction of the serum urate levels by different mechanisms: promoting catabolism of purines and

urate, secreting microbial metabolites that facilitate urate excretion, and alleviating the intestinal inflammation that is associated with hyperuricemia (Wang et al., 2022). Considering that the gut microbiota profile of gout patients is usually altered, probiotics have been proposed as an interesting alternative to treat hyperuricemia and deposition of urate crystals, without the adverse effects of classical pharmacological therapies (Guo et al., 2016). Different lactobacilli strains have been proven to effectively prevent hyperuricemia and/or reduce serum urate levels in human trials (Li et al., 2014; Yamada et al., 2017; Wang et al., 2019). The results of our pilot study show that serum urate levels and, of utmost relevance, the number of gout episodes and the amount of medication used to prevent or treat acute gout episodes were significantly reduced in individuals with hyperuricemia after the consumption of the probiotic strain *L. salivarius* CECT 30632, at a daily dose of 10^9 UFC for 6 months.

Similarly to Li et al. (2014), in this study, uric acid and two precursors for uric acid generation (guanosine and inosine) were used as substrates to select potential gout-preventing strains. Our working hypothesis was that increased intestinal clearance of uric acid and/or its precursors by potential probiotic bacteria would eventually lead to lower serum urate levels. Our results showed that almost all of the 13 *L. salivarius* strains included in the first screening had high inosine and guanosine uptake capacity. Lactic acid bacteria are ubiquitous in rich ecological niches, such as plants, raw and processed foods, wastewater sludge, and the gastrointestinal tract and other mucosal surfaces of a wide variety of host species (George et al., 2018). The adaptation of many lactic acid bacteria to nutrient-rich environments has resulted in an auxotrophy for purines and pyrimidines (Kilstrup et al., 2005). Dedicated transporters have been described for both nucleosides and purine bases, whereas nucleotides (the first degradation product of nucleic acids) must be dephosphorylated by phosphatases before being transported into the bacterial cell. The nucleoside and/or the purine base, once inside the bacterial cell, enter the salvage pathway for nucleotide synthesis or are degraded to purine metabolites (Kilstrup et al., 2005). Nucleoside transport has been proven in many different species of lactic acid bacteria (Li et al., 2014; Hsieh et al., 2021; Lee et al., 2022), but the incorporation of inosine and guanosine by *L. salivarius* strains of human origin is described for the first time in this study. Additionally, it shows that whole cells of 5 selected *L. salivarius* strains also uptake uric acid, although to a lesser extent than nucleosides. Under the assay conditions, only one strain, *L. salivarius* CECT 30632, incorporated all the inosine, guanosine and uric acid present in the extracellular media when abundant glucose was provided. The availability of an easily metabolizable carbon source (glucose) may increase the transport of adenosine, guanosine and uric acid, which will be subsequently used as a nitrogen source for the bacterial cells.

A more detailed characterization of the fate of the nucleosides inosine and guanosine revealed that inosine was metabolized to hypoxanthine which was, then, excreted outside the cell under glucose restriction conditions but not in a glucose-rich medium. Therefore, the absence of glucose will favor the use of the pentose sugar of the nucleosides as a carbon source for *L. salivarius* CECT 30632, MPac32, and MPac90, as it has been reported in *Lactilactobacillus sakei* CTC 494 (Rimaux et al., 2011). These strains also transported efficiently guanosine, but xanthine was not detected in the extracellular medium, and glucose availability did not modify this result. Uric acid was not detected in the extracellular media following the uptake of inosine and guanosine by *L. salivarius* CECT 30632 and MPac90, but different amounts of this metabolite were detected in the case of *L. salivarius* MPac32, MPac40 and MPac91.

This study also explored the enzymatic potential of the strains to transform inosine, guanosine and uric acid. All the strains, except MPac90, transformed efficiently inosine into hypoxantine. In an animal model, it has been shown that hypoxanthine in the colon modulates energy metabolism (promoting the purine savage pathway) and improves the barrier function in intestinal epithelial cells (Lee et al., 2018). In addition, *L. salivarius* CECT 30632 and MPac32 also metabolized guanosine to xanthine. This transformation in the gut lumen could be advantageous if purine bases are less efficiently transported across the apical membrane of human intestinal epithelial as it has been reported in animal models (Stow and Bronk, 1993). The transformation of inosine and guanosine into hypoxanthine and xanthine suggests that these strains possess purine nucleosidases (Kilstrup et al., 2005). This transformation would be advantageous because some bacteria favor the uptake of purine bases over purine nucleosides to be incorporated into the savage pathway for the synthesis of nucleotides (Yamada et al., 2017).

The administration of *L. salivarius* CECT 30632 for 6 months to individuals with hyperuricemia and a history of acute gout episodes included in this study resulted in a significant reduction (~1 mg/dL) of serum uric acid. This reduction was not enough to reset uric acid concentration to normal reference range values, but it was highly effective in terms of reducing the number of gout attacks. This indicates that the mechanism involved in the reduction of gout episodes by *L. salivarius* CECT 30632 may be related, at least partly, to effects other than the metabolism of nucleosides, purine bases and uric acid. Provision of nutrients to intestinal epithelial cells for energy that promote intestinal uric acid excretion, alleviating inflammation associated with gout and regulation of the expression of uric acid transporters are alternative mechanisms by which intestinal microbiota could reduce hyperuricemia and gout (Yin et al., 2022). Very recently, a study has also described the potential of *Limosilactobacillus fermentum* GR-3 as a therapeutic adjuvant in humans for probiotic treatment of hyperuricemia (Zhao et al., 2022).

The lower requirement of pharmacotherapy is another benefit derived from the administration of the probiotic since adverse events have been linked to most of the current long-term pharmacological strategies to lower serum urate levels, including allopurinol and colchicine (Benn et al., 2018). High doses of allopurinol, a competitive xanthine oxidase inhibitor, can result in severe cutaneous adverse reactions that are associated in some patients with drug-induced liver injury leading to high mortality rates as demonstrated in a 10-year multi-center prospective study (Huang et al., 2021). In patients who experience adverse events related to allopurinol treatment, the alternative is febuxostat (a noncompetitive xanthine oxidase inhibitor), but it has been associated with an increased cardiac risk (White et al., 2018). Colchicine is the most widely used anti-inflammatory drug as a pharmacologic approach to acute gout and is associated with gastrointestinal adverse effects (diarrhea, nausea, vomiting, cramps, and pain) (Qaseem et al., 2017).

In addition, the intake of *L. salivarius* CECT 30632 resulted in a significant decrease in the blood levels of some markers of oxidative stress (AOPPs, MDA and 8-isoprostaglandin F2α), nitric oxide, triglycerides, total cholesterol, GOT and GPT. Decreases in such parameters are relevant because of the close association between gout and metabolic syndrome (Raya-Cano et al., 2022). Gout is an increasingly relevant condition because of its relatively high prevalence, its impact on well-being and healthcare costs and, most importantly, its association with important co-morbidities that are usually considered as manifestations of the metabolic syndrome including hypertension, hyperlipidemia, cardiovascular disease, liver disease, renal disease, type

2 diabetes, and obesity (Thottam et al., 2017; Kimura et al., 2021). Interestingly, the administration of another *L. salivarius* strain for lactational mastitis (another inflammatory condition) also led to a significant reduction in the same blood parameters (Espinosa-Martos et al., 2016). Other studies have shown that different *L. salivarius* strains are able to reduce the blood levels of total cholesterol, low-density lipoprotein (LDL) cholesterol, and triglycerides in broiler chicken (Shokryazdan et al., 2017) or healthy young humans (Rajkumar et al., 2015), or to attenuate their normal pregnancy-induced rise in women with gestational diabetes, who are at risk of future metabolic syndrome (Lindsay et al., 2015). Chuang et al. (2016) evaluated whether heat-killed cells obtained from either a *L. salivarius* or a *Lactobacillus johnsonii* strain were able to prevent alcoholic liver damage in rats after acute alcohol exposure and found that only those obtained from the *L. salivarius* strain reduced serum AST and triglyceride levels.

The clinical study presented in this work was an initial pilot trial and, therefore, it has the inherent limitation of the relatively low number of individuals included and, as consequence, the results must be confirmed in future multicenter randomized placebo-controlled trials. Moreover, the treatment was limited to 6 months and the analyses were performed immediately at its end, with no follow-up of participants to check the endurance of the observed positive effects. However, this pilot trial has revealed the high potential of *L. salivarius* CECT 30632 to reduce the burden associated with hyperuricemia and gout. Measured parameters in this study to assess the potential benefits of the strain for gout prevention were related to clinical or metabolic outcomes (gout episodes, gout-related medication, and standard blood analyses). Such parameters are more appealing or understandable for medical purposes that changes in the fecal microbiome, whose interpretation is frequently very difficult or even impossible for medical practitioners. In future trials, however, it should be evaluated whether changes in the fecal microbiome occur, since the alteration of the intestinal microbiome balance may favor multiple changes in gastrointestinal physiology and inflammatory status. This knowledge may reveal the involvement of specific microorganisms or consortia in the onset and/or progression of hyperuricemia, improve the diagnosis and treatment of this pathology, and help to develop more effective therapeutic strategies by manipulating the gut microbiota, including the selection of probiotics than are even more effective.

In conclusion, in this study, it was shown that the regular administration of *L. salivarius* CECT 30632 did reduce serum urate levels, the number of gout episodes and, the pharmacological therapy required to control both the hyperuricemia and the gout episodes involving individuals with a history of hyperuricemia and suffering repeated gout episodes.

Data availability statement

The raw data supporting the conclusions of this article will be made available by the authors, without undue reservation.

Ethics statement

The studies involving human participants were reviewed and approved by The Ethics Committee of the Hospital Clínico San Carlos (Madrid, Spain). The patients/participants provided their written informed consent to participate in this study.

Author contributions

LF and JR designed and coordinated the study. DB directed the recruitment of participants and the diagnosis of gout episodes. MG, JS, and BO processed the samples and performed the *in vitro* assays. CA and LF performed the statistical analysis. LF, BO, and JR drafted the manuscript. All authors contributed to the article and approved the submitted version.

Funding

This work was funded by a grant conceded by the Complutense University of Madrid (Spain) to the research group.

Acknowledgments

We sincerely thank all the patients that participated in the assay.

Conflict of interest

The authors declare that the research was conducted in the absence of any commercial or financial relationships that could be construed as a potential conflict of interest.

Publisher's note

Supplementary material

The Supplementary material for this article can be found online at: https://www.frontiersin.org/articles/10.3389/fmicb.2023.1111652/full#supplementary-material

References

Afzaal, M., Saeed, F., Shah, Y. A., Hussain, M., Rabail, R., Socol, C. T., et al. (2022). Human gut microbiota in health and disease: unveiling the relationship. *Front. Microbiol.* 13:999001. doi: 10.3389/fmicb.2022.999001

Álvarez-Lario, B., and Macarrón-Vicente, J. (2010). Uric acid and evolution. *Rheumatology (Oxford)*. 49, 2010–2015. doi: 10.1093/rheumatology/keq204

Antushevich, H. (2020). Fecal microbiota transplantation in disease therapy. *Clin. Chim. Acta* 503, 90–98. doi: 10.1016/j.cca.2019.12.010

Arroyo, R., Martín, V., Maldonado, A., Jiménez, E., Fernández, L., and Rodríguez, J. M. (2010). Treatment of infectious mastitis during lactation: antibiotics versus oral administration of lactobacilli isolated from breast milk. *Clin. Infect. Dis.* 50, 1551–1558. doi: 10.1086/652763

Benn, C. L., Dua, P., Gurrell, R., Loudon, P., Pike, A., Storer, R. I., et al. (2018). Physiology of hyperuricemia and urate-lowering treatments. *Front. Med (Lausanne).* 5:160. doi: 10.3389/fmed.2018.00160

Butler, F., Alghubayshi, A., and Roman, Y. (2021). The epidemiology and genetics of hyperuricemia and gout across major racial groups: a literature review and population genetics secondary database analysis. *J. Pers. Med.* 11:231. doi: 10.3390/jpm11030231

Cao, T., Li, X., Mao, T., Liu, H., Zhao, Q., Ding, X., et al. (2017). Probiotic therapy alleviates hyperuricemia in C57BL/6 mouse model. *Biomed. Res.* 28, 2244–2249.

Cárdenas, N., Martín, V., Arroyo, R., López, M., Carrera, M., Badiola, C., et al. (2019). Prevention of recurrent acute otitis media in children through the use of *Lactobacillus salivarius* PS7, a target-specific probiotic strain. *Nutrients* 11:376. doi: 10.3390/nu11020376

Chen-Xu, M., Yokose, C., Rai, S. K., Pillinger, M. H., and Choi, H. K. (2019). Contemporary prevalence of gout and hyperuricemia in the United States and decadal trends: the National Health and nutrition examination survey, 2007-2016. *Arthritis Rheumatol.* 71, 991–999. doi: 10.1002/art.40807

Chu, Y., Sun, S., Huang, Y., Gao, Q., Xie, X., Wang, P., et al. (2021). Metagenomic analysis revealed the potential role of gut microbiome in gout. *NPJ Biofilms Microbiomes.* 7:66. doi: 10.1038/s41522-021-00235-2

Chuang, C. H., Tsai, C. C., Lin, E. S., Huang, C. S., Lin, Y. Y., Lan, C. C., et al. (2016). Heat-killed *Lactobacillus salivarius* and *Lactobacillus johnsonii* reduce liver injury induced by alcohol in vitro and in vivo. *Molecules* 21:1456. doi: 10.3390/molecules21111456

Codoñer-Franch, P., Tavárez-Alonso, S., Murria-Estal, R., Megías-Vericat, J., Tortajada-Girbés, M., and Alonso-Iglesias, E. (2011). Nitric oxide production is increased in severely obese children and related to markers of oxidative stress and inflammation. *Atherosclerosis* 215, 475–480. doi: 10.1016/j.atherosclerosis.2010.12.035

Codoñer-Franch, P., Tavárez-Alonso, S., Murria-Estal, R., Tortajada-Girbés, M., Simó-Jordá, R., and Alonso-Iglesias, E. (2012). Elevated advanced oxidation protein products (AOPPs) indicate metabolic risk in severely obese children. *Nutr. Metab. Cardiovasc. Dis.* 22, 237–243. doi: 10.1016/j.numecd.2010.06.002

Dalbeth, N., Gosling, A. L., Gaffo, A., and Abhishek, A. (2021). Gout. *Lancet* 397, 1843–1855. doi: 10.1016/S0140-6736(21)00569-9

Eldridge, S. M., Chan, C. L., Campbell, M. J., Bond, C. M., Hopewell, S., Thabane, L., et al. (2016). CONSORT 2010 statement: extension to randomised pilot and feasibility trials. *BMJ* 355:i5239. doi: 10.1136/bmj.i5239

Espinosa-Martos, I., Jiménez, E., de Andrés, J., Rodríguez-Alcalá, L. M., Tavárez, S., Manzano, S., et al. (2016). Milk and blood biomarkers associated to the clinical efficacy of a probiotic for the treatment of infectious mastitis. *Benef. Microbes.* 7, 305–318. doi: 10.3920/BM2015.0134

Fan, Y., and Pedersen, O. (2021). Gut microbiota in human metabolic health and disease. *Nat. Rev. Microbiol.* 19, 55–71. doi: 10.1038/s41579-020-0433-9

Fernández, L., Cárdenas, N., Arroyo, R., Manzano, S., Jiménez, E., Martín, V., et al. (2016). Prevention of infectious mastitis by oral administration of *Lactobacillus salivarius* PS2 during late pregnancy. *Clin. Infect. Dis.* 62, 568–573. doi: 10.1093/cid/civ974

Fernández, L., Castro, I., Arroyo, R., Alba, C., Beltrán, D., and Rodríguez, J. M. (2021). Application of *Ligilactobacillus salivarius* CECT5713 to achieve term pregnancies in women with repetitive abortion or infertility of unknown origin by microbiological and immunological modulation of the vaginal ecosystem. *Nutrients* 13:162. doi: 10.3390/nu13010162

Fernández, L., Pannaraj, P. S., Rautava, S., and Rodríguez, J. M. (2020). The microbiota of the human mammary ecosystem. *Front. Cell. Infect. Microbiol.* 10:586667. doi: 10.3389/fcimb.2020.586667

France, M., Alizadeh, M., Brown, S., Ma, B., and Ravel, J. (2022). Towards a deeper understanding of the vaginal microbiota. *Nat. Microbiol.* 7, 367–378. doi: 10.1038/s41564-022-01083-2

George, F., Daniel, C., Thomas, M., Singer, E., Guilbaud, A., Tessier, F. J., et al. (2018). Occurrence and dynamism of lactic acid bacteria in distinct ecological niches: a multifaceted functional health perspective. *Front. Microbiol.* 9:2899. doi: 10.3389/fmicb.2018.02899

George, C., and Minter, D. A. (2022). "Hyperuricemia" in *StatPearls* (Treasure Island, (FL): StatPearls Publishing)

Guo, Z., Zhang, J., Wang, Z., Ang, K. Y., Huang, S., Hou, Q., et al. (2016). Intestinal microbiota distinguish gout patients from healthy humans. *Sci. Rep.* 6:20602. doi: 10.1038/srep20602

Hosomi, A., Nakanishi, T., Fujita, T., and Tamai, I. (2012). Extra-renal elimination of uric acid via intestinal efflux transporter BCRP/ABCG2. *PLoS One* 7:e30456. doi: 10.1371/journal.pone.0030456

Hsieh, M.-W., Chen, H.-Y., and Tsai, C. -C. (2021). Screening and evaluation of purine-nucleoside-degrading lactic acid bacteria isolated from winemaking byproducts in vitro and their uric acid-lowering effects in vivo. *Fermentation* 7:74. doi: 10.3390/fermentation7020074

Huang, Y. S., Wu, C. Y., Chang, T. T., Peng, C. Y., Lo, G. H., Hsu, C. W., et al. (2021). Drug-induced liver injury associated with severe cutaneous adverse drug reactions: a nationwide study in Taiwan. *Liver Int.* 41, 2671–2680. doi: 10.1111/liv.14990

Jiménez, E., Manzano, S., Schlembach, D., Arciszewski, K., Martin, R., Ben Amor, K., et al. (2021). *Ligilactobacillus salivarius* PS2 supplementation during pregnancy and lactation prevents mastitis: a randomised controlled trial. *Microorganisms* 9:1933. doi: 10.3390/microorganisms9091933

Kilstrup, M., Hammer, K., Ruhdal Jensen, P., and Martinussen, J. (2005). Nucleotide metabolism and its control in lactic acid bacteria. *FEMS Microbiol. Rev.* 29, 555–590. doi: 10.1016/j.femsre.2005.04.006

Kimura, Y., Tsukui, D., and Kono, H. (2021). Uric acid in inflammation and the pathogenesis of atherosclerosis. *Int. J. Mol. Sci.* 22:12394. doi: 10.3390/ijms222212394

Lane, A. N., and Fan, T. W. (2015). Regulation of mammalian nucleotide metabolism and biosynthesis. *Nucleic Acids Res.* 43, 2466–2485. doi: 10.1093/nar/gkv047

Lee, J. S., Wang, R. X., Alexeev, E. E., Lanis, J. M., Battista, K. D., Glover, L. E., et al. (2018). Hypoxanthine is a checkpoint stress metabolite in colonic epithelial energy modulation and barrier function. *J. Biol. Chem.* 293, 6039–6051. doi: 10.1074/jbc.RA117.000269

Lee, Y., Werlinger, P., Suh, J.-W., and Cheng, J. (2022). Potential probiotic *Lacticaseibacillus paracasei* MJM60396 prevents hyperuricemia in a multiple way by absorbing purine, suppressing xanthine oxidase and regulating urate excretion in mice. *Microorganisms* 10:851. doi: 10.3390/microorganisms10050851

Li, Q., Li, X., Wang, J., Liu, H., Kwong, J. S., Chen, H., et al. (2019). Diagnosis and treatment for hyperuricemia and gout: a systematic review of clinical practice guidelines and consensus statements. *BMJ Open* 9:e026677. doi: 10.1136/bmjopen-2018-026677

Li, M., Yang, D., Mei, L., Yuan, L., Xie, A., and Yuan, J. (2014). Screening and characterization of purine nucleoside degrading lactic acid bacteria isolated from Chinese sauerkraut and evaluation of the serum uric acid lowering effect in hyperuricemic rats. *PLoS One* 9:e105577. doi: 10.1371/journal.pone.0105577

Lin, S., Zhang, T., Zhu, L., Pang, K., Lu, S., Liao, X., et al. (2021). Characteristic dysbiosis in gout and the impact of a uric acid-lowering treatment, febuxostat on the gut microbiota. *J. Genet. Genomics* 48, 781–791. doi: 10.1016/j.jgg.2021.06.009

Lindsay, K. L., Brennan, L., Kennelly, M. A., Maguire, O. C., Smith, T., Curran, S., et al. (2015). Impact of probiotics in women with gestational diabetes mellitus on metabolic health: a randomized controlled trial. *Am. J. Obstet. Gynecol.* 212, 496.e1–496.e11. doi: 10.1016/j.ajog.2015.02.008

MacFarlane, L. A., and Kim, S. C. (2014). Gout: a review of nonmodifiable and modifiable risk factors. *Rheum. Dis. Clin. N. Am.* 40, 581–604. doi: 10.1016/j.rdc.2014.07.002

Maesaka, J. K., and Fishbane, S. (1998). Regulation of renal urate excretion: a critical review. *Am. J. Kidney Dis.* 32, 917–933. doi: 10.1016/s0272-6386(98)70067-8

Mandal, A. K., and Mount, D. B. (2015). The molecular physiology of uric acid homeostasis. *Annu. Rev. Physiol.* 77, 323–345. doi: 10.1146/annurev-physiol-021113-170343

Martín, V., Cárdenas, N., Ocaña, S., Marín, M., Arroyo, R., Beltrán, D., et al. (2019). Rectal and vaginal eradication of *Streptococcus agalactiae* (GBS) in pregnant women by using *Lactobacillus salivarius* CECT 9145, a target-specific probiotic strain. *Nutrients* 11:810. doi: 10.3390/nu11040810

Martín, R., and Langella, P. (2019). Emerging health concepts in the probiotics field: streamlining the definitions. *Front. Microbiol.* 10:1047. doi: 10.3389/fmicb.2019.01047

Pareek, V., Pedley, A. M., and Benkovic, S. J. (2021). Human de novo purine biosynthesis. *Crit. Rev. Biochem. Mol. Biol.* 56, 1–16. doi: 10.1080/10409238.2020.1832438

Qaseem, A., Harris, R. P., Forciea, M. A., Clinical Guidelines Committee of the American College of PhysiciansDenberg, T. D., Barry, M. J., et al. (2017). Management of acute and recurrent gout: a clinical practice guideline from the American College of Physicians. *Ann. Intern. Med.* 166, 58–68. doi: 10.7326/M16-0570

Rajkumar, H., Kumar, M., Das, N., Kumar, S. N., Challa, H. R., and Nagpal, R. (2015). Effect of probiotic *Lactobacillus salivarius* UBL S22 and prebiotic fructo-oligosaccharide on serum lipids, inflammatory markers, insulin sensitivity, and gut bacteria in healthy young volunteers: a randomized controlled single-blind pilot study. *J. Cardiovasc. Pharmacol. Ther.* 20, 289–298. doi: 10.1177/1074248414555004

Raya-Cano, E., Vaquero-Abellán, M., Molina-Luque, R., De Pedro-Jiménez, D., Molina-Recio, G., and Romero-Saldaña, M. (2022). Association between metabolic syndrome and uric acid: a systematic review and meta-analysis. *Sci. Rep.* 12:18412. doi: 10.1038/s41598-022-22025-2

Requena, T., and Velasco, M. (2021). The human microbiome in sickness and in health. *Rev. Clin. Esp. (Barc).* 221, 233–240. doi: 10.1016/j.rceng.2019.07.018

Rimaux, T., Vrancken, G., Vuylsteke, B., De Vuyst, L., and Leroy, F. (2011). The pentose moiety of adenosine and inosine is an important energy source for the fermented-meat starter culture *Lactobacillus sakei* CTC 494. *Appl. Environ. Microbiol.* 77, 6539–6550. doi: 10.1128/AEM.00498-11

Rizzatti, G., Ianiro, G., and Gasbarrini, A. (2018). Antibiotic and modulation of microbiota: a new paradigm? *J. Clin. Gastroenterol.* 52, S74–S77. doi: 10.1097/MCG.0000000000001069

Rosemeyer, H. (2004). The chemodiversity of purine as a constituent of natural products. *Chem. Biodivers.* 1, 361–401. doi: 10.1002/cbdv.200490033

Shao, T., Shao, L., Li, H., Xie, Z., He, Z., and Wen, C. (2017). Combined signature of the fecal microbiome and metabolome in patients with gout. *Front. Microbiol.* 8:268. doi: 10.3389/fmicb.2017.00268

Shokryazdan, P., Faseleh Jahromi, M., Liang, J. B., Ramasamy, K., Sieo, C. C., and Ho, Y. W. (2017). Effects of a *Lactobacillus salivarius* mixture on performance, intestinal health and serum lipids of broiler chickens. *PLoS One* 12:e0175959. doi: 10.1371/journal.pone.0175959

Sorensen, L. B. (1965). Role of the intestinal tract in the elimination of uric acid. *Arthritis Rheum.* 8, 694–706. doi: 10.1002/art.1780080429

Stow, R. A., and Bronk, J. R. (1993). Purine nucleoside transport and metabolism in isolated rat jejunum. *J. Physiol.* 468, 311–324. doi: 10.1113/jphysiol.1993.sp019773

Strilchuk, L., Fogacci, F., and Cicero, A. F. (2019). Safety and tolerability of available urate-lowering drugs: a critical review. *Expert Opin. Drug Saf.* 18, 261–271. doi: 10.1080/14740338.2019.1594771

Thottam, G. E., Krasnokutsky, S., and Pillinger, M. H. (2017). Gout and metabolic syndrome: a tangled web. *Curr. Rheumatol. Rep.* 19:60. doi: 10.1007/s11926-017-0688-y

Vedder, D., Walrabenstein, W., Heslinga, M., de Vries, R., Nurmohamed, M., van Schaardenburg, D., et al. (2019). Dietary interventions for gout and effect on cardiovascular risk factors: a systematic review. *Nutrients* 11:2955. doi: 10.3390/nu11122955

Wang, J., Chen, Y., Zhong, H., Chen, F., Regenstein, J., Hu, X., et al. (2022). The gut microbiota as a target to control hyperuricemia pathogenesis: potential mechanisms and therapeutic strategies. *Crit. Rev. Food Sci. Nutr.* 62, 3979–3989. doi: 10.1080/10408398.2021.1874287

Wang, H., Mei, L., Deng, Y., Liu, Y., Wei, X., Liu, M., et al. (2019). *Lactobacillus brevis* DM9218 ameliorates fructose-induced hyperuricemia through inosine degradation and manipulation of intestinal dysbiosis. *Nutrition* 62, 63–73. doi: 10.1016/j.nut.2018.11.018

White, W. B., Saag, K. G., Becker, M. A., Borer, J. S., Gorelick, P. B., Whelton, A., et al. (2018). Cardiovascular safety of febuxostat or allopurinol in patients with gout. *N. Engl. J. Med.* 378, 1200–1210. doi: 10.1056/NEJMoa1710895

Wu, Y., Ye, Z., Feng, P., Li, R., Chen, X., Tian, X., et al. (2021). *Limosilactobacillus fermentum* JL-3 isolated from "Jiangshui" ameliorates hyperuricemia by degrading uric acid. *Gut Microbes* 13, 1–18. doi: 10.1080/19490976.2021.1897211

Yamada, N., Saito-Iwamoto, C., Nakamura, M., Soeda, M., Chiba, Y., Kano, H., et al. (2017). *Lactobacillus gasseri* PA-3 uses the purines IMP, inosine and hypoxanthine and reduces their absorption in rats. *Microorganisms* 5:10. doi: 10.3390/microorganisms5010010

Yanai, H., Adachi, H., Hakoshima, M., and Katsuyama, H. (2021). Molecular biological and clinical understanding of the pathophysiology and treatments of hyperuricemia and its association with metabolic syndrome, cardiovascular diseases and chronic kidney disease. *Int. J. Mol. Sci.* 22,:9221. doi: 10.3390/ ijms22179221, doi: 10.3390/ijms22179221

Yin, H., Liu, N., and Chen, J. (2022). The role of the intestine in the development of hyperuricemia. *Front. Immunol.* 13:845684. doi: 10.3389/fimmu.2022.845684

Zhao, S., Feng, P., Hu, X., Cao, W., Liu, P., Han, H., et al. (2022). Probiotic *Limosilactobacillus fermentum* GR-3 ameliorates human hyperuricemia via degrading and promoting excretion of uric acid. *iScience* 25:105198. doi: 10.1016/j.isci.2022.105198

frontiers | Frontiers in Microbiology

TYPE Original Research
PUBLISHED 20 February 2023
DOI 10.3389/fmicb.2023.1128275

OPEN ACCESS

EDITED BY
Giuseppe Spano,
University of Foggia,
Italy

REVIEWED BY
Samuele Maramai,
University of Siena,
Italy
Angela Casillo,
University of Naples Federico II, Italy

*CORRESPONDENCE
Rossella Grande
✉ rossella.grande@unich.it

†These authors have contributed equally to this work

SPECIALTY SECTION
This article was submitted to Food Microbiology, a section of the journal Frontiers in Microbiology

RECEIVED 20 December 2022
ACCEPTED 20 January 2023
PUBLISHED 20 February 2023

CITATION
Vitale I, Spano M, Puca V, Carradori S, Cesa S, Marinacci B, Sisto F, Roos S, Grompone G and Grande R (2023) Antibiofilm activity and NMR-based metabolomic characterization of cell-free supernatant of *Limosilactobacillus reuteri* DSM 17938.
Front. Microbiol. 14:1128275.
doi: 10.3389/fmicb.2023.1128275

Antibiofilm activity and NMR-based metabolomic characterization of cell-free supernatant of *Limosilactobacillus reuteri* DSM 17938

Irene Vitale[1†], Mattia Spano[2†], Valentina Puca[1], Simone Carradori[1], Stefania Cesa[2], Beatrice Marinacci[1,3], Francesca Sisto[4], Stefan Roos[5,6], Gianfranco Grompone[6] and Rossella Grande[1,7*]

[1]Department of Pharmacy, "G. d'Annunzio" University of Chieti-Pescara, Chieti, Italy, [2]Department of Drug Chemistry and Technology, Sapienza University of Rome, Rome, Italy, [3]Department of Innovative Technologies in Medicine & Dentistry, "G. d'Annunzio" University of Chieti-Pescara, Chieti, Italy, [4]Department of Biomedical, Surgical and Dental Sciences, University of Milan, Milan, Italy, [5]Department of Molecular Sciences, Swedish University of Agricultural Sciences, Uppsala, Sweden, [6]BioGaia AB, Stockholm, Sweden, [7]Center for Advanced Studies and Technology (CAST), G. d'Annunzio University of Chieti-Pescara, Chieti, Italy

The microbial biofilm has been defined as a "key virulence factor" for a multitude of microorganisms associated with chronic infections. Its multifactorial nature and variability, as well as an increase in antimicrobial resistance, suggest the need to identify new compounds as alternatives to the commonly used antimicrobials. The aim of this study was to assess the antibiofilm activity of cell-free supernatant (CFS) and its sub-fractions (SurE 10K with a molecular weight <10kDa and SurE with a molecular weight <30kDa), produced by *Limosilactobacillus reuteri* DSM 17938, vs. biofilm-producing bacterial species. The minimum inhibitory biofilm concentration (MBIC) and the minimum biofilm eradication concentration (MBEC) were determined *via* three different methods and an NMR metabolomic analysis of CFS and SurE 10K was performed to identify and quantify several compounds. Finally, the storage stability of these postbiotics was evaluated by a colorimetric assay by analyzing changes in the CIEL*a*b parameters. The CFS showed a promising antibiofilm activity against the biofilm developed by clinically relevant microorganisms. The NMR of CFS and SurE 10K identifies and quantifies several compounds, mainly organic acids and amino acids, with lactate being the most abundant metabolite in all the analyzed samples. The CFS and SurE 10K were characterized by a similar qualitative profile, with the exception of formate and glycine detected only in the CFS. Finally, the CIEL*a*b parameters assess the better conditions to analyze and use these matrices for the correct preservation of bioactive compounds.

KEYWORDS

***Lactobacillus reuteri*, *Limosilactobacillus reuteri*, cell-free supernatant, NMR, color analysis, antibiofilm activity, probiotics, postbiotics**

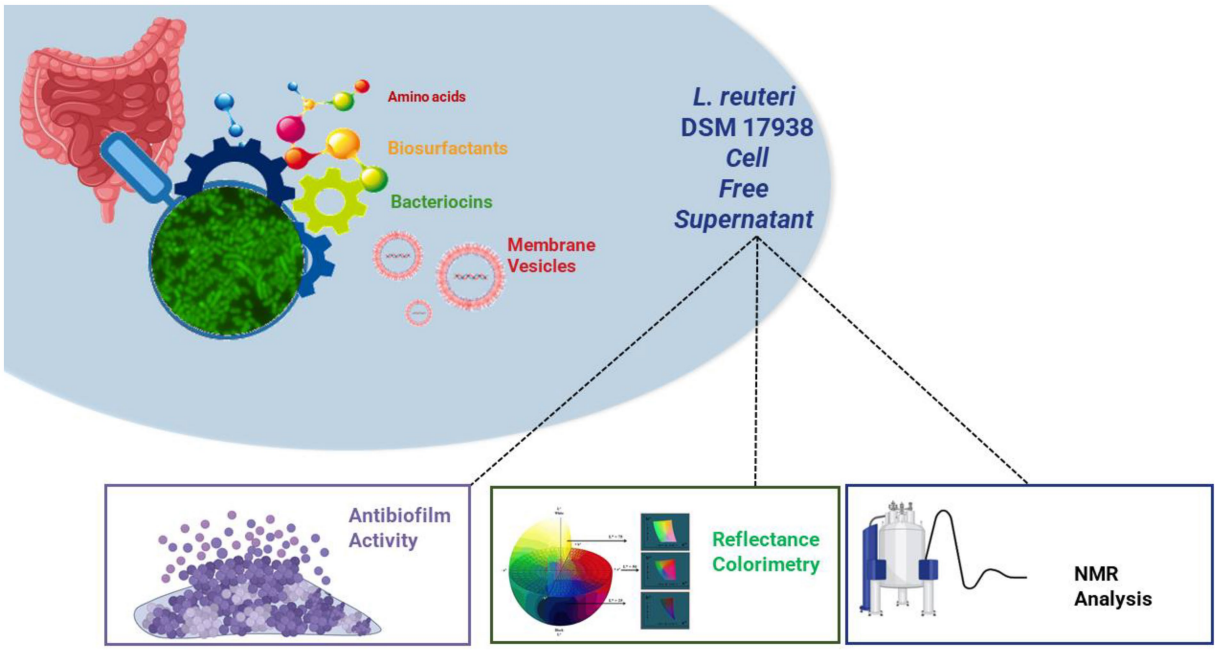

GRAPHICAL ABSTRACT

Introduction

The microbial biofilm represents a microbial strategy of cooperation in which the microorganisms aggregate, communicate, and defend themselves thanks to the extracellular polymeric substances (EPS) that constitute a protective barrier (Hall-Stoodley et al., 2004; Flemming et al., 2016). It has always been believed that the formation of biofilm began following the adhesion of "pioneer microorganisms" on a biotic or abiotic surface; therefore, biofilms are defined as "manifestations of microbial life, not only growing on surfaces, but developing at any solid–liquid, liquid–liquid, liquid–gas, and solid–gas interfaces" (Flemming et al., 2021). The EPS matrix is very heterogeneous and complex and depends on many environmental factors as well as on bacterial strains, culture conditions, and biofilm age (Allesen-Holm et al., 2006; Grande et al., 2014). It can be constituted from polysaccharides, proteins, lipids, insoluble components such as amyloids, fimbriae, pili, flagella, and nucleic acids, in particular extracellular DNA (eDNA), released as free components or associated with extracellular vesicles (Hall-Stoodley et al., 2004; Grande et al., 2015). Regarding the eDNA, we showed in our previous work that it can play a different role in membrane vesicles, depending on the bacterial phenotype (Grande et al., 2015, 2017).

Koo et al. (2017) recognized microbial biofilm formation as a "key virulence factor" for numerous microorganisms responsible for chronic infections. The tolerance expressed by biofilms against traditional antimicrobial drugs as well as the host immune defenses makes them difficult to eradicate, contributing to the spread of the antibiotic resistance phenomenon (Grande et al., 2021). A wide range of microorganisms that possess different characteristics (Gram-positive and Gram-negative, motile and non-motile, aerobic, anerobic, and microaerophilic) are biofilm producers, and many of them are opportunistic pathogens associated with hospital-acquired infections. Based on the consideration that biofilm infections can be derived from dysbiosis, the characterization of natural compounds produced by probiotic strains could represent a new goal to achieve (Grande et al., 2020). The cell-free supernatant (CFS) produced by many probiotic strains (e.g., *Limosilactobacillus reuteri*) contains many bioactive compounds such as biosurfactants, bacteriocins, and antimicrobial peptides, free or delivered by extracellular vesicles, with inhibitory effects on the growth of the pathogen (Alakomi et al., 2000; Aminnezhad et al., 2015; Grande et al., 2017; Maccelli et al., 2020). However, each probiotic strain produces its own compounds. In a previous report, we demonstrated that *Limosilactobacillus reuteri* DSM 17938 CFS has antimicrobial activity vs. both Gram-negative and Gram-positive bacteria, while membrane vesicles of planktonic phenotype (pMVs) and biofilm phenotype (bMVs) were not active (Maccelli et al., 2020). The CFS and its subfraction SurE 10 K, which contains molecules or compounds with a molecular size lower than 10 kDa, were tested at different concentrations against reference and clinical strains of *Escherichia coli*, *Pseudomonas aeruginosa*, *Fusobacterium nucleatum*, *Staphylococcus aureus*, and *Streptococcus mutans* characterized by different antimicrobial susceptibility patterns. The results demonstrated that the CFS contained antimicrobial compounds, in addition to the well-known reuterin, showing greater activity against Gram-negative bacteria than Gram-positive bacteria, and the efficacy was related to the species rather than to the individual strains (Maccelli et al., 2020). Moreover, the data obtained supported the hypothesis that the antimicrobial effect could be associated with synergistic activity between several compounds contained in the CFS, as previously demonstrated by other authors (Poppi et al., 2015).

On the basis of the results previously obtained and considering the clinical relevance of microbial biofilms, the first aim of this study was to evaluate the antibiofilm activity of the CFS and some of its fractions (SurE 10 K and 30 K). We chose clinically relevant species that form biofilms to test the capability of the CFS to both inhibit biofilm formation and eradicate mature biofilms. Successively, to better comprehend the potential of this probiotic, we aimed at improving our previous mass spectrometry-based knowledge of the metabolic content by means of qualitative and quantitative NMR analyses. Given that the chemical composition of the entire set of metabolites of a probiotic is very complex, an untargeted metabolite profile characterization of this matrix can be useful to identify

the main metabolites of the considered system and potentially correlate them with the biological activity. In this context, NMR spectroscopy represents a very powerful tool for this kind of analysis since this methodology can be used to obtain a chemical profile of a biological system (Bianchi et al., 2020). Finally, we monitored the stability of microbial products with an affordable and fast color analysis assay. Previous studies on cyanobacteria monitored biofilm formation and how pigment production was affected by the environment (Sanmartín et al., 2010, 2012). Our previous studies demonstrated how color could be useful to monitor the shelf-life of different systems, providing useful information about oxidative stability and, more generally, about browning, which represents the main modification induced by aging on the biological matrices (Cesa et al., 2015; Menghini et al., 2021). In this view, a preliminary shelf-life stability study to monitor the chemical composition of CFS was performed by CIEL*a*b colorimetric analysis for a period of 4 weeks. The workflow described earlier is shown in Figure 1.

Materials and methods

Bacterial strains and culture conditions

Limosilactobacillus reuteri DSM 17938 (Rosander et al., 2008), provided by BioGaia AB (Stockholm, Sweden), was used in the study. The bacteria were plated on DeMan, Rogosa, and Sharpe agar (MRSA; Oxoid Limited, Hampshire, United Kingdom), and incubated at 37°C for 24 h in an anaerobic atmosphere (Anaerogen Pak Jar, Oxoid Ltd.). The CFS and its fractions, SurE 10 K and 30 K, were obtained following the procedure described by Maccelli et al. (2020). Regarding the other bacterial strains used, different media and growth conditions were used on the basis of the species.

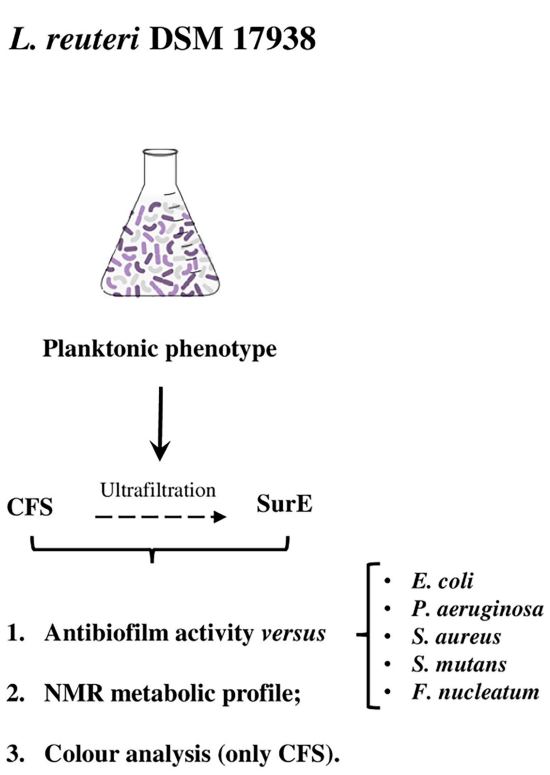

FIGURE 1
Flowchart of this study. CFS, cell-free supernatant; SurE, eluted supernatant <10kDa.

Biofilm formation assay

The biofilms were developed on 96-well flat-bottomed polystyrene microtitre plates (Eppendorf, Hamburg, Germany) by using different media and growth conditions depending on the species. The OD_{600} of each inoculum was read and adjusted to reach a final concentration in each well of 1.0×10^5 CFU/mL. More details are given as follows:

- *Escherichia coli* ATCC 25922 was grown in Mueller Hinton Broth (MHB; Oxoid Limited, Hampshire, United Kingdom), and the biofilm was developed in MHB for 24 h of incubation at 37°C in static and aerobic conditions;
- *Pseudomonas aeruginosa* ATCC 27853 growth and biofilm formation were conducted in Luria Bertani Broth (LB; Oxoid Limited, Hampshire, United Kingdom) for 24 h of incubation at 37°C in static and aerobic conditions;
- *Streptococcus mutans* UA 159 was grown in Brain Heart Infusion (BHI; Oxoid Limited, Hampshire, United Kingdom), and the biofilm was developed in BHI + 1% of sucrose (BHIS) for 24 h of incubation at 37°C in static and anaerobic conditions;
- *Staphylococcus aureus* ATCC 29213 was grown in Tryptic Soy Broth (TSB; Oxoid Limited, Hampshire, United Kingdom), and the biofilm was developed in TSB + 1% of glucose (TSBG) for 24 h of incubation at 37°C in static and aerobic conditions;
- *Fusobacterium nucleatum* ATCC 25586 growth and biofilm formation were conducted in BHI for 48 h of incubation at 37°C in static and anaerobic conditions.

Determination of CFS and SurE 10K minimum biofilm eradication concentration

The MIC and MBC of the CFS and SurE 10 K vs. *P. aeruginosa* ATCC 27853, *F. nucleatum* ATCC 25586, *E. coli* ATCC 25922, *S. aureus* ATCC 29213, and *S. mutans* UA159 were previously determined (Maccelli et al., 2020).

Regarding the determination of the Minimum Biofilm Eradication Concentration (MBEC), the biofilms were developed depending on the bacterial species. The MBEC was defined as the lowest concentration, which completely eradicated bacterial biofilms developed in 96-well flat-bottomed polystyrene microtiter plates. At the end of incubation, the biofilms were washed with phosphate-buffered saline (PBS), and the CFS and SurE 10 K were added to the pre-formed biofilms at concentrations corresponding to 1×MIC, 2×MIC, 3×MIC, and 4×MIC of each test sample, except for the *F. nucleatum* biofilm that was treated with 2×MIC, 3×MIC, 4×MIC, and 5×MIC. Controls consist of (i) non-treated biofilms and (ii) biofilms with the addition of MRS broth (the medium in which CFS and SurE are resuspended). The microtiter plates were then incubated at 37°C for the time of incubation chosen on the basis of bacterial species under static conditions. The eradication effects of CFS and SurE 10 K were measured using three different methods, namely Colony Forming Units (CFU) counting; metabolic assays such as alamarBlue® (AB) (Thermo Fisher Scientific, Waltham, MA, United States) or XTT (sodium 3'-[1-(phenylaminocarbonyl)-3,4-tetrazolium]-bis-(4-methoxy-6-nitro) benzene sulfonic acid hydrate; Cell Proliferation Kit II XTT, Roche Diagnostic, Mannheim, Germany); and Crystal Violet (CV) assay.

Cell viability evaluation through colony-forming unit count

The CFU enumeration was performed to evaluate the bacterial cell viability in the treated and non-treated biofilms with different concentrations of CFS and SurE 10 K. A volume of 100 µL of the sample was taken from each well and used for CFU counts. Serial dilutions of the stock were performed in PBS (pH 7.2) and plated on the suitable agar media at 37°C for 18–24 h. The same evaluation was performed in the case of the AB assay due to its non-toxic nature.

Cell viability assays

The MBEC was confirmed using the XTT metabolic assay and/or AB assay according to the manufacturer's recommendations (Zengin et al., 2018; Maccelli et al., 2020). Given that we noticed that some components or supplements present in the media that were used interfered with the dyes present in the kits, it was decided to use both kits and compare the data obtained.

The absorbances corresponding to 490 nm for XTT and 570 and 600 nm for AB were then read with a microplate reader (Synergy H1 Multi-Mode Reader, BioTek, Winooski, VT, United States). The XTT and Alamar Blue MBEC were defined as the lowest concentrations of the sample, resulting in a detectable colorimetric change in the assays. The colorimetric change is a direct correlation with the metabolic activity of the biofilm. Two independent experiments were performed in triplicate.

Crystal violet assay

The Crystal Violet assay was used to stain the biofilm biomass. The treated and non-treated biofilms were rinsed with 100 µL of PBS and fixed for 1 h at 60°C. Then, 100 µL of crystal violet at 0.1% diluted in MilliQ water was added for 5 min to *P. aeruginosa*, *S. mutans*, *E. coli*, and *S. aureus* pre-formed biofilms. Crystal violet at 0.5% diluted in MilliQ water was added for 2 min to pre-formed biofilm of *F. nucleatum*. The biofilms were washed with 200 µL of MilliQ water and dried at room temperature (RT) for 30 min. In the end, 100 µL of 33% acid acetic was added to each well for 10 min and absorbance was read at 590 nm.

Live/dead assay

The qualitative analysis of the CFS-treated and untreated biofilms developed by the different bacterial species was performed using live/dead staining (BacLight kit; Thermo Fisher Scientific, Waltham, MA, United States) as indicated by the manufacturers and fluorescent microscopy evaluation with a Leica DMR Fluorescent Microscope (Leica Microsystem, Wetzlar, Germany). Two experiments were performed in triplicate.

Determination of SurE 30K minimum biofilm eradication concentration vs. *Pseudomonas aeruginosa* ATCC 27853

SurE 30 K was obtained *via* ultrafiltration of CFS with Amicon Ultra-15 30 K (30000 MWCO) Centrifugal Filter Devices (Merck KGaA, Darmstadt, Germany). The MIC of SurE 30 K was determined as for SurE 10 K (data not shown; Maccelli et al., 2020). After determining the MIC, a *P. aeruginosa* biofilm was developed in LB, and after 24 h, the mature biofilm was treated with SurE 30 K at 1 × MIC, 2 × MIC, 3 × MIC, and 4 × MIC. The MBEC was evaluated with an AB assay, CFU counting, and CV assay.

Minimum biofilm inhibitory concentration of CFS and SurE 10K

To determine the MBIC, the CFS and SurE 10 K were diluted into each well until reaching a concentration of half of the Minimum Inhibitory Concentration (MIC). The MIC values of *L. reuteri* CFS and SurE 10 K vs. the bacterial species used were previously described (Maccelli et al., 2020). Then, the OD_{600} of each inoculum was read and adjusted to reach a final concentration in each well of 1.0×10^5 CFU/mL. The plates were incubated at 37°C for 24 h for *P. aeruginosa*, *S. mutans*, *S. aureus*, and *E. coli* and for 48 h for *F. nucleatum*. The valuation of the MBIC was determined by both CFU counts and metabolic assays previously described.

Determination of minimum inhibitory concentration of CFS and SurE 10K vs. *Lactobacillus rhamnosus* ATCC 53103, *Lactobacillus paracasei* CNCM I-1572, and *Lactobacillus acidophilus* LA14 ATCC SD 5212

The minimum inhibitory concentration was determined using the broth microdilution assay in 96-well polystyrene microtiter plates and CFU counting. Briefly, *Lactobacillus rhamnosus*, *Lactobacillus paracasei*, and *Lactobacillus acidophilus* were grown in MRSB for 17 h at 37°C under shaking conditions at 125 rpm. The overnight cultures were resuspended until reaching an optical density of 0.1 nm (OD_{600}) that corresponds to 10^7 CFU/mL and then diluted to 10^5 CFU/mL in the 96-well plate. CFS and SurE 10 K were tested from a maximum concentration of 88 µL/100 µL to a minimum concentration of 5.5 µL/100 µL. The plates were incubated in static and anaerobic conditions for 24 h at 37°C. The MIC was defined as the lowest concentration without visible growth, and it was determined both visually and *via* CFU counting. Controls consisted of MRSB media without the addition of CFS. Two independent experiments were performed in triplicate.

Determination of MIC and MBC values of lactic acid vs. *Staphylococcus aureus*

The antimicrobial activity of lactic acid (Puraq Bioquimica SRL, Spain) was tested vs. *Staphylococcus aureus* ATCC 29213 *via* the broth microdilution method in 96-well plates according to the CLSI guidelines and confirmed by XTT assay, following the methods previously described (Maccelli et al., 2020). Lactic acid was diluted in MHB and tested in the range of 0.05–6.4 µL/100 µL.

Statistical analysis

The differences in the means of the results between untreated and treated bacterial strains were evaluated by one-way ANOVA (GraphPad Software, San Diego, CA, United States) and Dunnet's multiple

comparison test. Media supplemented with MRS broth at the maximum concentration of CFS tested was used as the control. The probability value of $p \leq 0.05$ was considered significantly different. Analysis of cytotoxicity data (expressed as mean ± standard error) was performed by the GraphPad Prism TM 6.00 software (GraphPad Software, San Diego, CA, United States).

NMR-based qualitative and quantitative analyses

A volume of 1 mL of each sample was lyophilized and then dissolved in 750 µL of 200 mM phosphate buffer/D_2O, containing 1.4 mM TSP (3-(trimethylsilyl)propionic acid sodium salt) as internal standard. Finally, 700 µL of the solution was transferred into a 5 mm NMR tube. NMR analyses were carried out on a Jeol JNM-ECZ 600R operating at the proton frequency of 600.17 MHz and equipped with a Jeol 5 mm FG/RO DIGITAL AUTOTUNE probe. ^{1}H NMR experiments were carried out by using the following parameters: 298 K, 256 scans, residual water signal suppression with a presaturation pulse, 7.7 s relaxation delay, 90° pulse of 8.3 µs, 64 k data points, and 9,000 Hz spectral width. ^{1}H spectra were referenced to methyl group signals of TSP ($\delta_H = 0.00$ ppm) in D_2O. Homonuclear ^{1}H-^{1}H TOCSY experiment was acquired with 96 scans, 8 k data points in *f*2 and 128 in *f*1, 50 ms mixing time, 2 s relaxation delay, and 9,000 Hz spectral width in both dimensions. Heteronuclear ^{1}H-^{13}C HSQC experiment was acquired with 88 scans, 8 k data points in *f*2 and 256 in *f*1, 3 s relaxation delay, and a spectral width of 9,000 Hz and 33,000 Hz for *f*2 and *f*1, respectively. ^{1}H-^{13}C HMBC experiment was acquired with 64 scans, 8 k data points in *f*2 and 256 in *f*1, 2.8 s relaxation delay, and a spectral width of 9,000 Hz and 39,000 Hz for *f*2 and *f*1, respectively. Spectra processing and signal integration were carried out with the JEOL Delta software (v5.3.1). For each metabolite, a characteristic signal was considered and integrated, normalizing the area to those of the methyl group signals of TSP, set to 100. Results were expressed as µg/mL of sample.

Colorimetric analysis

The samples were analyzed at the initial time (t^0) for their color character, with a colorimeter X-Rite MetaVue™ (X-Rite, Prato, Italy), equipped with full spectrum LED illuminant and an observer angle of 45°/0° imaging spectrophotometer. Samples that were stored in a refrigerator (4°C) were analyzed again in the same conditions after 2 (t^{2w}) and 4 weeks (t^{4w}). Cylindrical coordinates C^*_{ab} and h_{ab} and the color distances (ΔE) were calculated according to the reference samples at t° sample, as known by the literature (Cairone et al., 2020).

Results

Determination of the minimum biofilm eradication concentration

The ability of factors secreted by *L. reuteri* DSM 17938 to eradicate biofilms produced by different pathogenic bacteria was evaluated by using three different methods to obtain more reliable results. Two independent experiments, performed in triplicate, have been carried out for each method. The methods used were: CFU counting, biofilm metabolic activity, and crystal violet (CV) assay, followed by fluorescent microscopy qualitative analysis (data not shown), which represented an additional confirmation. The exact correspondence of the results obtained guarantees us the accuracy and reproducibility of the data. The CFS showed the capability to eradicate pre-formed biofilms developed by *E. coli* ATCC 25922, *P. aeruginosa* ATCC 27853, *S. aureus* ATCC 29213, and *F. nucleatum* ATCC 25585 (Figure 2). In particular, the effect of the CFS at 2 × MIC (corresponding to 20 µL/100 µL) on the eradication of *E. coli* pre-formed biofilm was confirmed by the significant reduction in CFU counts and metabolic activity, as well as a statistically significant reduction in the biofilm biomass, as shown in Figure 2A. While the effect of CFS on the eradication of *P. aeruginosa* and *S. aureus* mature biofilms was detected at 2 × MIC or at MIC (corresponding to 11 µL/100 µL and 25 µL/100 µL, respectively; Figures 2B,C). On the contrary, CFS was not capable of eradicating the biofilm developed by *S. mutans* UA 159 (Figure 2C). Regarding the SurE 10 K, it showed a value of MBEC comparable to those of CFS vs. *E. coli* and *S. aureus* (see Figures 2A,C). On the contrary, it did not work against *P. aeruginosa*, suggesting that the molecules responsible for the inhibitory activity are contained in the CFS fraction (Figure 2B). To demonstrate this, we performed an intermediate fractionation by using 30 K columns. The results obtained demonstrated that SurE 30 K is capable of eradicating *P. aeruginosa* mature biofilm at 3 × MIC (corresponding to 33 µL/100 µL; Figure 3). Finally, SurE 10 K, as previously demonstrated for CFS, did not eradicate *S. mutans* biofilm (Figure 2D). Regarding the antibiofilm activity of the CFS against the *F. nucleatum* ATCC 27853 biofilm, the results showed a statistical reduction at 4 × MIC for CFS and 5 × MIC for SurE 10 K, demonstrating a more powerful eradication ability of the CFS.

SurE 30K MIC and MBEC vs. *Pseudomonas aeruginosa* ATCC 27853

Since SurE 10 K did not show any antibiofilm effect toward *P. aeruginosa*, it was decided to test SurE ultrafiltrated through a 30 kDa (SurE 30 K) filter to check if the 10 kDa filtration did not allow the passage into the eluted sample of the compound(s) responsible for the antibiofilm activity. SurE 30 K showed a MIC of 11 µL/100 µL toward *P. aeruginosa*, the same as in CFS. The MBEC value corresponded to 33 µL/100 µL (3 × MIC; Figure 3).

Determination of the minimum biofilm inhibitory concentration

We next evaluated the ability of the secreted factors to inhibit biofilm formation. In particular, the capability of the CFS and SurE 10 K to inhibit the biofilm formation of the species previously mentioned was determined by the evaluation of the Minimum Biofilm Inhibitory Concentration (MBIC) by using, as previously mentioned, the CFU counting, biofilm metabolic activity, and CV assay. Both the CFS and SurE 10 K were not capable of inhibiting biofilm formation in any of the microorganisms tested. No significant reduction in the number of CFUs, biofilm metabolic activity, or biomass of the biofilm was detected (Supplementary Figure S1).

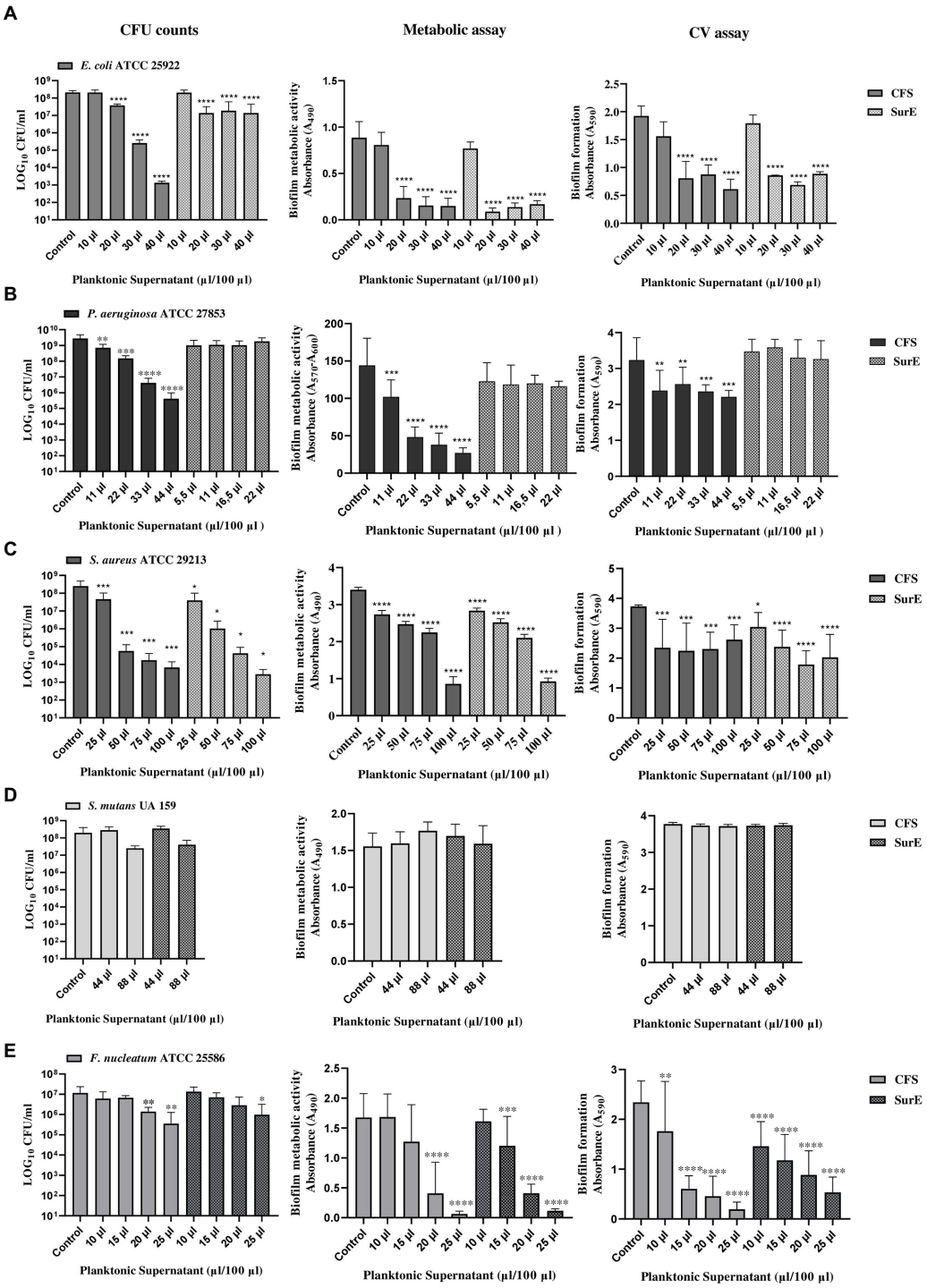

FIGURE 2
Determination of MBEC of CFS and SurE 10K through CFU counts, metabolic assay, and CV assay vs. *Escherichia coli* ATCC 25922 **(A)**, *Pseudomonas aeruginosa* ATCC 27853 (metabolic assay) **(B)**, *Staphylococcus aureus* ATCC 29213 **(C)**, *Streptococcus mutans* UA 159 **(D)**, and *Fusobacterium nucleatum* ATCC25586 **(E)**. Data are presented as the mean of three replicates from two independent experiments. The statistical comparison between the control and treated samples was determined with a one-way ANOVA. The control was composed of media with the supplement of MRS broth. The error bars represent the standard deviation. The asterisks stand for *p*-value: *$p<0.05$, **$p<0.01$, ***$p<0.001$, and ****$p<0.0001$.

Minimum inhibitory concentration of CFS and SurE 10K vs. *Lacticaseibacillus rhamnosus* ATCC 53103, *Lacticaseibacillus paracasei* CNCM I-1572, and *Lactobacillus acidophilus* LA14 ATCC SD 5212

We also tested the potential antimicrobial activity of CFS and SurE 10 K vs. other probiotic strains such as *L. rhamnosus* ATCC 53103, *L. paracasei* CNCM I-1572, and *L. acidophilus* LA14ATCC SD 5212 to evaluate the selective toxicity of these postbiotics against pathogenic bacteria with respect to probiotic strains. CFS and SurE 10 K did not show any inhibitory effect toward *L. rhamnosus* and *L. paracasei*. Regarding *L. acidophilus*, the MIC was 88 µL/100 µL for both CFS and SurE 10 K (Table 1).

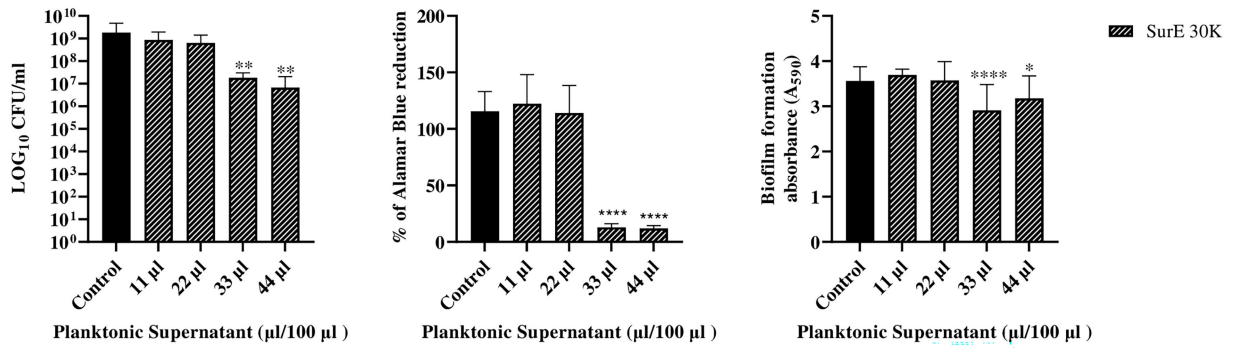

FIGURE 3
Determination of MBEC of SurE 30K through CFU counts, metabolic assay, and CV assay vs. *P. aeruginosa* ATCC 27853. Data are presented as the mean of three replicates from two independent experiments. The statistical comparison between the control and treated samples was determined with a one-way ANOVA. The control was made up of media with the supplement of MRS broth. The error bars represent the standard deviation. The asterisks stand for *p*-value: **p*<0.05, ***p*<0.01, and *****p*<0.0001.

TABLE 1 Evaluation of the MIC of CFS and SurE 10K, obtained by *L. reuteri* DSM 17938, toward three probiotic strains.

Bacterial strains	CFS MIC (µL/100µL)	SurE 10K MIC (µL/100µL)
L. rhamnosus ATCC 53103	>88	>88
L. paracasei CNCM I-1572	>88	>88
L. acidophilus LA14 ATCC SD 5212	88	88

NMR-based metabolomic profile

The NMR analysis of the considered samples (including MRS broth as the blank) allows identifying two organic acids (lactate and formate), nine amino acids (alanine, valine, glycinebetaine, isoleucine, leucine, glycine, phenylalanine, tyrosine, and tryptophan), and choline by means of 2D experiments and literature data (Di Matteo et al., 2021; Spano et al., 2021) as reported in Supplementary Table S1 and Supplementary Figures S2–S6. Comparing the NMR results obtained in Table 2, lactate and formate were identified among organic acids, whereas leucine, isoleucine, valine, alanine, glycine, tyrosine, phenylalanine, tyrosine, and tryptophan were revealed among amino acids. Choline and glycinebetaine were also present. Formate and glycine were detected in CFS samples only.

Determination of the MIC of lactic acid vs. *Staphylococcus aureus*

Due to the well-known antimicrobial activity of lactic acid-producing bacteria and the high content of this organic acid detected by quantitative NMR analyses (Table 2), lactic acid MIC was detected by unaided eye at 0.2 µL/100 µL and was also confirmed by XTT assay (Figure 4A). The minimum bactericidal concentration of lactic acid was determined at 0.4 µL/100 µL through the CFU count (Figure 4B).

Stability studies using reflectance colorimetry

The shelf-life of the samples was monitored after 2 and 4 weeks of storage at 4°C. All the detected color parameters are reported in Supplementary Table S2. Data showed the color differences existing among samples, both in terms of elapsed time and different analyzed samples. This is also shown by the sample reflectance curves reported in Figure 5. In the CFS (A), the variation with respect to t° is particularly marked at t^{2w} and assumes the mean of a powerful whitening. This trend, however, is well delineated also in the medium used as reference (MRSB, B) at t^{2w}, so that the difference between the two systems remains low ($\Delta E = 4.87$, CFS t^{2w} vs. MRSB t^{2w}). On the contrary, an evident change is denoted after 4 weeks because the color of the supernatant is turning toward blue and green rather than increasing in red and yellow as in the medium ($\Delta E = 18.56$ CFS t^{4w} vs. MRSB t^{4w}).

TABLE 2 Quantitative results obtained from the NMR analysis of samples subtracted from their blank (MRSB).

Metabolite	CFS	SurE 10K
Lactate	6746.00	8427.49
Formate	28.49	–
Leucine	236.04	308.93
Isoleucine	92.08	114.03
Valine	158.56	213.97
Alanine	380.62	523.70
Glycinebetaine	63.33	75.71
Glycine	550.09	–
Tyrosine	29.19	38.09
Phenylalanine	113.28	151.04
Tryptophan	3.20	8.38
Choline	10.72	15.55

Results are expressed as µg/ml of sample. "–" means "not detected."

Discussion

Probiotics are considered an effective approach for treating infections and inhibiting the spread of antibiotic resistance. In particular, lactobacilli are involved in the process of biofilm formation on oral surfaces, exerting anti-adhesive activity against different pathogens given that they interfere with adhesion and microbial cells'

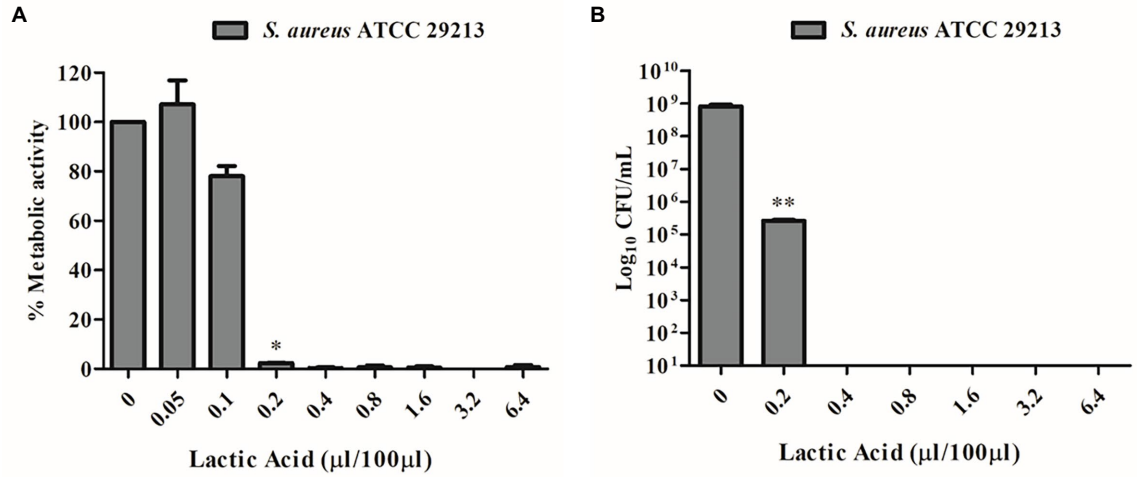

FIGURE 4
(A) MIC determination of lactic acid vs. *S. aureus* ATCC 29213 using the XTT assay. **(B)** MBC determination of lactic acid vs. *S. aureus* ATCC 29213 using the CFU count.

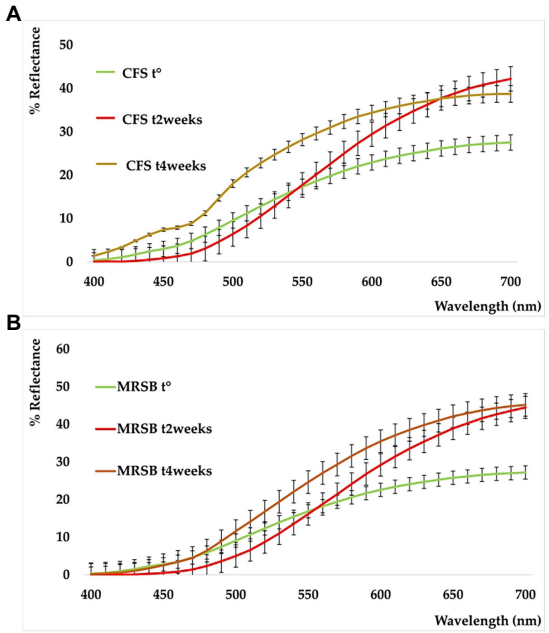

FIGURE 5
Reflectance curves of CFS **(A)** and planktonic supernatant blank (MRSB) **(B)**, at t^0 (green), t^{2weeks} (red), and t^{4weeks} (ocher).

co-aggregation *via* the secretion of antagonistic substances such as bacteriocins, organic acids, enzymes, and biosurfactants (Söderling et al., 2011; Barzegari et al., 2020).

Different articles have shown that probiotics like *Limosilactobacillus fermentum* and *Lactiplantibacillus plantarum* and some of their derivatives possess an antibiofilm effect on *P. aeruginosa* (Sharma et al., 2018; Shokri et al., 2018). In particular, Sharma et al. demonstrated that postbiotics, produced by *L. fermentum*, can reduce quorum sensing signals needed for biofilm formation, confirming results from previous studies (Kanmani et al., 2011; Bulgasem et al., 2015; Sharma et al., 2018). Here, we demonstrated that CFS from *L. reuteri* can eradicate *P. aeruginosa* biofilm at 1 × MIC, even if its 10 kDa filtered fraction is not able to exert any eradication activity, suggesting that the molecules/compounds responsible for its action, have a molecular weight higher than 10 kDa. As previously mentioned, the antimicrobial activity of CFS is probably due to the synergistic effect of different molecules/compounds (Maccelli et al., 2020). These data confirm our hypothesis, according to which, in this case, the antibiofilm activity is associated with several compounds, some of them with a size higher than 30 kDa, potentially involved either in the disintegration or in the permeabilization of the biofilm EPS matrix, facilitating the penetration of other components with antimicrobial activity. Regarding this hypothesis, Sharma et al. proposed that some bacteriocins from different probiotics are able to create pores through the *P. aeruginosa* cell membrane, leading to a change in cell membrane integrity and inducing cell death; similarly, some bacteriocins produced by *Streptococcus pyogenes* FF22 are able to disrupt the membrane potential of a *S. aureus* biofilm by forming short-lived pores that allow the passage of ions, leading to a major ATP efflux from biofilms which is correlated with the antimicrobial activity of bacteriocins (Okuda et al., 2013; Sharma et al., 2018). Tunçer et al. also showed very interesting results related to the action of CFS from *S. salivarius* M18. The authors demonstrated that CFS increases the lipid unsaturation index of *P. aeruginosa* and decreases the content of cellular polysaccharides, factors that have a crucial role in the formation of *P. aeruginosa* biofilm (Tunçer and Karaçam, 2020).

Ghane et al. showed that CFS produced from different probiotics, in particular, *Lactobacillus rhamnosus* and *Lactobacillus paracasei*, had a strong uropathogenic *E. coli* (UPEC) biofilm inhibitory effect (Ghane et al., 2020). On the contrary, Al-Dhabi et al. showed that *L. reuteri* LR12 has an inhibition rate of 53% on *E. coli* biofilm, a 68% inhibition rate against *P. aeruginosa* biofilm, and a 100% inhibition rate vs. *S. aureus* biofilm (Al-Dhabi et al., 2020). These data support our results, although the efficacy is known to be strain-specific. In fact, we demonstrated a more powerful eradication by *L. reuteri* DSM 17938 CFS against *S. aureus* and *P. aeruginosa* biofilms (1 × MIC), with respect to *E. coli*, where the MBEC value was higher (2× MIC). In contrast to our findings, Melo et al. showed that *L. fermentum* TCUESC01 can reduce the formation of *S. aureus* biofilm under sub-inhibitory concentrations, at 50% of the MIC, confirming that the

inhibition growth ability of probiotics differs among strains (Keller et al., 2011; Melo et al., 2016).

Concerning *S. mutans*, our findings showed both that the MIC value is higher (44 μL/100 μL) when compared to other bacterial strains, including *F. nucleatum* (5 μL/100 μL), and that CFS does not have any biofilm eradication action until 2 × MIC concentration. It is important to take into consideration that the biofilm was developed in BHI supplemented with 1% of sucrose and that *S. mutans* uses sucrose from dietary sources for the synthesis of EPS, which act as a scaffold and contribute to its pathogenicity and antimicrobial resistance (Yang et al., 2019). We never supplemented MRSB media with glycerol, which is required by *L. reuteri* to produce reuterin (Maccelli et al., 2020). When considering the action of reuterin, it is important to consider that the amount of glycerol in the plaque is very low, therefore it may not be so important for oral health (Söderling et al., 2011). Yang et al. demonstrated that *L. reuteri* AN417 CFS is able to reduce *S. mutans* biofilm formation in the absence of reuterin. The authors developed *S. mutans* biofilm in the absence of sucrose, which was capable of increasing its pathogenicity, and water-insoluble glucan, derived from sucrose metabolism, and involved in *S. mutans* biofilm formation (Hasibul et al., 2018; Yang et al., 2021). The results in the literature are controversial, but it is known that considerable genotypic and phenotypic differences exist between *S. mutans* strains (Senpuku et al., 2018).

Besides reuterin, *L. reuteri* strains can produce different antimicrobial substances, including lactic acid, acetic acid, and ethanol. Data have evidenced the importance of the acidic environment in the interactions between *L. reuteri* and other microorganisms, in particular with the effect of lactic acid (Geraldo et al., 2020). To ensure that lactic acid was not the only player responsible for the antimicrobial activity despite its high content in both *L. reuteri* CFS and SurE 10 K, we evaluated the MIC of lactic acid against *S. aureus*. The results showed a MIC value of 0.2 μL/100 μL. Conversely, the MIC of *L. reuteri* CFS was 25 μL/100 μL, demonstrating that the inhibitory activity was not associated with the action of lactic acid alone but was derived from a synergistic effect among different molecules or compounds present in the supernatant and characterized by a molecular size lower than 10 kDa. In fact, 0.025 mL of CFS or SurE 10 K should contain 0.16 mg and 0.21 mg of lactic acid, respectively, based on the amounts reported in Table 2, whereas 0.2 μL of lactic acid corresponds to 0.24 mg (lactic acid density = 1,209 mg/mL). It is well-known that probiotics can produce some bacteriocin-like compounds that have been claimed to be more active at acid pH than at neutral or alkaline pH (Li et al., 2015); therefore, we could also hypothesize the presence of such compounds in CFS. Further studies are needed to better understand which molecules could contribute to the efficacy of CFS.

With regards to *F. nucleatum*, some articles in the literature have shown that some probiotics like *Bifidobacterium lactis* and *Bifidobacterium infantis* are able to cause an antagonistic effect toward periodontopathogens like *F. nucleatum* (Valdez et al., 2021). *Fusobacterium nucleatum* has the ability to co-aggregate with other bacteria, and this may be due to its long rod morphology that acts as a bridge in dental plaque (Kolenbrander and London, 1993). Moreover, *F. nucleatum* is able to reduce oxygen levels, contributing to the growth of less aerotolerant and more pathogenic bacterial species like *Porphyromonas gingivalis* (Bradshaw and Marsh, 1998; Llama-Palacios et al., 2020).

Many studies have demonstrated the efficacy of CFS and probiotic cells on *F. nucleatum* growth. Yang et al., for example, showed that the CFS produced by *L. reuteri* AN 417 was very effective against *P. gingivalis* growth but less effective on *F. nucleatum* and *S. mutans* (Yang et al., 2021). With regards to the antibiofilm activity toward *F. nucleatum*, a limited number of details are reported. Jiang et al. proved that *S. mutans* and *F. nucleatum* have a poorer ability to grow in mono-species biofilms and they demonstrated better abilities of adhesion and reproduction in dual-and/or multispecies biofilms (Jiang et al., 2016). In multi-species biofilms, neighbors can take advantage of the productivity of the community, in particular in the oral cavity, in which they develop dental plaque (Elias and Banin, 2012). In the end, the evaluation of the effect of *L. reuteri* DSM 17938 vs. other probiotic strains showed promising results given that the CFS did not demonstrate any inhibitory activity toward the probiotic strains tested but only toward pathogens. The results reported represent the first contribution to the evaluation of the antibiofilm activity of CFS produced by *L. reuteri* DMS 17938 vs. *F. nucleatum* mono-species biofilm. The capability of *L. reuteri* DSM 17938 CFS to inhibit *F. nucleatum* growth and eradicate its biofilm could represent a strategy to prevent the formation of polymicrobial dental plaque, avoiding the development of biofilm-related pathologies in the oral cavity. Further studies should be performed in order to determine the activity of CFS in multi-species biofilms, especially from species of clinical relevance that colonize the oral cavity, such as *S. mutans* and *P. gingivalis*.

The application of NMR spectroscopy for the metabolomic analysis of these matrices was effective for the identification and quantification of primary and secondary metabolites, giving important information with regards to the potential role of some of them in the observed anti-biofilm activity. Only one article regarding the NMR analysis of *Lactobacillus* vesicles has been found (Ñahui Palomino et al., 2019). In respect to the assignments present, a further identification was observed in this work by detecting citrate, malate, and glycinebetaine. The latter is an osmoprotectant metabolite that usually improves adaptation to environmental salt stresses, especially for those bacteria living in the mammalian gut (e.g., *C. difficile*), where salinity could hamper bacterial growth (Michel et al., 2022). This is the first report revealing the presence of this compound in probiotic species as well. Generally, Sur E 10 K was richer in terms of all detected metabolites, despite the fact that formate and glycine were present only in the CFS. Lactic acid was the most abundant metabolite. Among amino acids, we found the following substances in the order of decreasing amounts: glycine > alanine > leucine > valine > phenylalanine. All these compounds were also detected *via* untargeted metabolomic profiling by means of high-resolution fourier transform ion cyclotron resonance mass spectrometry (FT-ICR MS) coupled with electrospray ionization source (ESI; Maccelli et al., 2020), but without any knowledge of the content.

To assess the stability of CFS and Sur E 10 K, we performed a fast, affordable, and non-destructive analysis based on reflectance colorimetry. Besides a well-known role in the consumer's compliance toward a product, color could play a main role in assessing differences and peculiarities among the commodity class, as well as give information related to stability and allow the evaluation of their shelf-life. As previously explained, this is of particular significance in the case of rapidly evolving biological systems. In fact, color is influenced and quickly modified by humidity, temperature, oxygen content, and metal presence, apart from many other factors correlated to the nature of the analyzed matrix, its solid or liquid state, the presence of

enzymes, the molecular composition, and light exposure (Cesa et al., 2017).

To the best of our knowledge, the tristimulus colorimetric analysis was applied for the first time to evaluate the color characters, the differences, and the stability of CFS derived from *L. reuteri*. Only some articles are available in the literature which deal with the color onset in cyanobacteria forming biofilm (Sanmartín et al., 2010, 2012), while some other articles deal with the color evaluation of fermented foods in which lactobacilli were grown (Pelicano et al., 2003; Antunes et al., 2013; Zhu et al., 2020; Wang et al., 2021). In previous studies, the change of color in milk was evaluated in relation to the microorganism growth based on time and temperature (Ziyaina et al., 2019), and the ΔE scale, as proposed by Limbo and Piergiovanni (2006), was used to discriminate colors. The results confirmed that these natural matrices can be subjected to degradation phenomena after 2 and 4 weeks of storage and that they must be conserved at temperatures below 4°C to preserve the bioactive components.

The results indicated that CFS and its sub-fractions from *L. reuteri* DSM 17938 have a promising potential for the eradication of biofilms produced by clinically relevant species that are biofilm producers and responsible for nosocomial and oral infections. The potential of CFS should be thoroughly investigated in order to understand novel inhibitory compounds as new antibiofilm agents. The NMR metabolomic profile discriminated specific metabolites, which, along with MS data, can be considered the fingerprint of these natural matrices. Their stability tested spectrophotometrically for up to 4 weeks also gave new insights concerning storage time within the performance of biological experiments.

Data availability statement

The original contributions presented in the study are included in the article/Supplementary material, further inquiries can be directed to the corresponding author.

Author contributions

RG and SCa designed the project. RG and SCa designed the experiments, discussed the results, and drafted the manuscript. IV, VP, BM, MS, SCe, and FS performed the experiment consisting of the isolation of CFS, evaluation of the antibiofilm activity, and analysis of metabolomic/color profiles. RG, SCa, GG, and SR drafted the final editing of the manuscript and critically revised it. All authors contributed to the article and approved the submitted version.

Funding

This study was supported by the company BioGaia AB, Stockholm Sweden, and the Ministero Italiano dell'Università e della Ricerca (MIUR) FAR2020 Grant, held by RG.

Acknowledgments

The authors gratefully acknowledge BioGaia AB (Stockholm, Sweden) for the donation of the strain used in the present study as well as for supporting the research project. We thank Paul Stoodley for providing *S. mutans* UA159.

Conflict of interest

SR and GG are currently employed by the company BioGaia AB. RG and SCa have received a research grant from Company BioGaia which partially supported the project.

The remaining authors declare that the research was conducted in the absence of any commercial or financial relationships that could be construed as a potential conflict of interest.

Publisher's note

Supplementary material

The Supplementary material for this article can be found online at: https://www.frontiersin.org/articles/10.3389/fmicb.2023.1128275/full#supplementary-material

References

Alakomi, H. L., Skyttä, E., Saarela, M., Mattila-Sandholm, T., Latva-Kala, K., and Helander, I. M. (2000). Lactic acid permeabilizes gram-negative bacteria by disrupting the outer membrane. *Appl. Environ. Microbiol.* 66, 2001–2005. doi: 10.1128/AEM.66.5.2001-2005.2000

Al-Dhabi, N. A., Valan Arasu, M., Vijayaraghavan, P., Esmail, G. A., Duraipandiyan, V., Kim, Y. O., et al. (2020). Probiotic and antioxidant potential of *Lactobacillus reuteri* LR12 and lactobacillus lactis LL10 isolated from pineapple puree and quality analysis of pineapple-flavored goat milk yoghurt during storage. *Microorganisms* 8:1461. doi: 10.3390/microorganisms8101461

Allesen-Holm, M., Barken, K. B., Yang, L., Klausen, M., Webb, J. S., Kjelleberg, S., et al. (2006). A characterization of DNA release in *Pseudomonas aeruginosa* cultures and biofilms. *Mol. Microbiol.* 59, 1114–1128. doi: 10.1111/j.1365-2958.2005.05008.x

Aminnezhad, S., Kermanshahi, R. K., and Ranjbar, R. (2015). Evaluation of synergistic interactions between cell-free supernatant of lactobacillus strains and amikacin and gentamicin against *Pseudomonas aeruginosa*. *Jundishapur J. Microbiol.* 8:e16592. doi: 10.5812/jjm.8(4)2015.16592

Antunes, A. E. C., Liserre, A. M., Coelho, A. L. A., Menezes, C. R., Moreno, I., Yotsuyanagi, K., et al. (2013). Acerola nectar with added microencapsulated probiotic. *LWT-Food Sci. Technol.* 54, 125–131. doi: 10.1016/J.LWT.2013.04.018

Barzegari, A., Kheyrolahzadeh, K., Hosseiniyan Khatibi, S. M., Sharifi, S., Memar, M. Y., and Zununi Vahed, S. (2020). The battle of probiotics and their derivatives against biofilms. *Infect. Drug Resist.* 13, 659–672. doi: 10.2147/IDR.S232982

Bianchi, L., Laghi, L., Correani, V., Schifano, E., Landi, C., Uccelletti, D., et al. (2020). A combined proteomics, metabolomics and in vivo analysis approach for the characterization of probiotics in large-scale production. *Biomol. Ther.* 10:157. doi: 10.3390/biom10010157

Bradshaw, D. J., and Marsh, P. D. (1998). Analysis of pH-driven disruption of oral microbial communities in vitro. *Caries Res.* 32, 456–462. doi: 10.1159/000016487

Bulgasem, B. Y., Hassan, Z., Abdalsadiq, N. K., Yusoff, W. M., and Lani, M. N. (2015). Anti-adhesion activity of lactic acid bacteria supernatant against human pathogenic Candida species biofilm. *Health Sci. J.* 9, 1–9.

Cairone, F., Carradori, S., Locatelli, M., Casadei, M. A., and Cesa, S. (2020). Reflectance colorimetry: a mirror for food quality—a mini review. *Eur. Food Res. Technol.* 246, 259–272. doi: 10.1007/s00217-019-03345-6

Cesa, S., Carradori, S., Bellagamba, G., Locatelli, M., Casadei, M. A., Masci, A., et al. (2017). Evaluation of processing effects on anthocyanin content and colour modifications of blueberry (*Vaccinium* spp.) extracts: comparison between HPLC-DAD and CIELAB analyses. *Food Chem.* 232, 114–123. doi: 10.1016/j.foodchem.2017.03.153

Cesa, S., Casadei, M. A., Cerreto, F., and Paolicelli, P. (2015). Infant milk formulas: effect of storage conditions on the stability of powdered products towards autoxidation. *Foods* 4, 487–500. doi: 10.3390/foods4030487

Di Matteo, G., Spano, M., Esposito, C., Santarcangelo, C., Baldi, A., Daglia, M., et al. (2021). NMR characterization of ten apple cultivars from the Piedmont region. *Foods* 10:289. doi: 10.3390/foods10020289

Elias, S., and Banin, E. (2012). Multi-species biofilms: living with friendly neighbors. *FEMS Microbiol. Rev.* 36, 990–1004. doi: 10.1111/j.1574-6976.2012.00325.x

Flemming, H. C., Baveye, P., Neu, T. R., Stoodley, P., Szewzyk, U., Wingender, J., et al. (2021). Who put the film in biofilm? The migration of a term from wastewater engineering to medicine and beyond. *NPJ Biofilms Microbiomes.* 7:10. doi: 10.1038/s41522-020-00183-3

Flemming, H. C., Wingender, J., Szewzyk, U., Steinberg, P., Rice, S. A., and Kjelleberg, S. (2016). Biofilms: an emergent form of bacterial life. *Nat. Rev. Microbiol.* 14, 563–575. doi: 10.1038/nrmicro.2016.94

Geraldo, B. M. C., Batalha, M. N., Milhan, N. V. M., Rossoni, R. D., Scorzoni, L., and Anbinder, A. L. (2020). Heat-killed *Lactobacillus reuteri* and cell-free culture supernatant have similar effects to viable probiotics during interaction with Porphyromonas gingivalis. *J. Periodiodontal. Res.* 55, 215–220. doi: 10.1111/jre.12704

Ghane, M., Babaeekhou, L., and Ketabi, S. S. (2020). Antibiofilm activity of kefir probiotic lactobacilli against uropathogenic Escherichia coli (UPEC). *Avicenna J. Med. Biotechnol.* 12, 221–229.

Grande, R., Carradori, S., Puca, V., Vitale, I., Angeli, A., Nocentini, A., et al. (2021). Selective inhibition of helicobacter pylori carbonic anhydrases by carvacrol and thymol could impair biofilm production and the release of outer membrane vesicles. *Int. J. Mol. Sci.* 22:11583. doi: 10.3390/ijms222111583

Grande, R., Celia, C., Mincione, G., Stringaro, A., Di Marzio, L., Colone, M., et al. (2017). Detection and physicochemical characterization of membrane vesicles (MVs) of *Lactobacillus reuteri* DSM 17938. *Front. Microbiol.* 8:1040. doi: 10.3389/fmicb.2017.01040

Grande, R., Di Marcantonio, M. C., Robuffo, I., Pompilio, A., Celia, C., Di Marzio, L., et al. (2015). Helicobacter pylori ATCC 43629/NCTC 11639 outer membrane vesicles (OMVs) from biofilm and planktonic phase associated with extracellular DNA (eDNA). *Front. Microbiol.* 6:1369. doi: 10.3389/fmicb.2015.01369

Grande, R., Nistico, L., Sambanthamoorthy, K., Longwell, M., Iannitelli, A., Cellini, L., et al. (2014). Temporal expression of agrB, cidA, and alsS in the early development of Staphylococcus aureus UAMS-1 biofilm formation and the structural role of extracellular DNA and carbohydrates. *Pathog. Dis.* 70, 414–422. doi: 10.1111/2049-632X.12158

Grande, R., Puca, V., and Muraro, R. (2020). Antibiotic resistance and bacterial biofilm. *Expert Opin. Ther. Pat.* 30, 897–900. doi: 10.1080/13543776.2020.1830060

Hall-Stoodley, L., Costerton, J. W., and Stoodley, P. (2004). Bacterial biofilms: from the natural environment to infectious diseases. *Nat. Rev. Microbiol.* 2, 95–108. doi: 10.1038/nrmicro821

Hasibul, K., Nakayama-Imaohji, H., Hashimoto, M., Yamasaki, H., Ogawa, T., Waki, J., et al. (2018). D-Tagatose inhibits the growth and biofilm formation of Streptococcus mutans. *Mol. Med. Rep.* 17, 843–851. doi: 10.3892/mmr.2017.8017

Jiang, Q., Stamatova, I., Kainulainen, V., Korpela, R., and Meurman, J. H. (2016). Interactions between lactobacillus rhamnosus GG and oral micro-organisms in an in vitro biofilm model. *BMC Microbiol.* 16:149. doi: 10.1186/s12866-016-0759-7

Kanmani, P., Satish Kumar, R., Yuvaraj, N., Paari, K. A., Pattukumar, V., and Arul, V. (2011). Production and purification of a novel exopolysaccharide from lactic acid bacterium Streptococcus phocae PI80 and its functional characteristics activity in vitro. *Bioresour. Technol.* 102, 4827–4833. doi: 10.1016/j.biortech.2010.12.118

Keller, M. K., Hasslöf, P., Stecksén-Blicks, C., and Twetman, S. (2011). Co-aggregation and growth inhibition of probiotic lactobacilli and clinical isolates of mutans streptococci: an in vitro study. *Acta Odontolol. Scand.* 69, 263–268. doi: 10.3109/00016357.2011.554863

Kolenbrander, P. E., and London, J. (1993). Adhere today, here tomorrow: oral bacterial adherence. *J. Bacteriol.* 175, 3247–3252. doi: 10.1128/jb.175.11.3247-3252.1993

Koo, H., Allan, R. N., Howlin, R. P., Stoodley, P., and Hall-Stoodley, L. (2017). Targeting microbial biofilms: current and prospective therapeutic strategies. *Nat. Rev. Microbiol.* 15, 740–755. doi: 10.1038/nrmicro.2017.99

Li, B., Liu, F., Tang, Y., Luo, G., Evivie, S., Zhang, D., et al. (2015). Complete genome sequence of lactobacillus helveticus KLDS1.8701, a probiotic strain producing bacteriocin. *J. Biotechnol.* 212, 90–91. doi: 10.1016/j.jbiotec.2015.08.014

Limbo, S., and Piergiovanni, L. (2006). Shelf life of minimally processed potatoes part 1. Effects of high oxygen partial pressures in combination with ascorbic and citric acids on enzymatic browning. *Postharvest Biol. Technol.* 39, 254–264. doi: 10.1016/j.postharvbio.2005.10.016

Llama-Palacios, A., Potupa, O., Sánchez, M. C., Figuero, E., Herrera, D., and Sanz, M. (2020). Proteomic analysis of Fusobacterium nucleatum growth in biofilm versus planktonic state. *Mol Oral Microbiol* 35, 168–180. doi: 10.1111/omi.12303

Maccelli, A., Carradori, S., Puca, V., Sisto, F., Lanuti, P., Crestoni, M. E., et al. (2020). Correlation between the antimicrobial activity and metabolic profiles of cell free supernatants and membrane vesicles produced by *Lactobacillus reuteri* DSM 17938. *Microorganisms* 8:1653. doi: 10.3390/microorganisms8111653

Melo, T. A., Dos Santos, T. F., de Almeida, M. E., Junior, L. A., Andrade, E. F., Rezende, R. P., et al. (2016). Inhibition of Staphylococcus aureus biofilm by lactobacillus isolated from fine cocoa. *BMC Microbiol.* 16:250. doi: 10.1186/s12866-016-0871-8

Menghini, L., Ferrante, C., Carradori, S., D'Antonio, M., Orlando, G., Cairone, F., et al. (2021). Chemical and bioinformatics analyses of the anti-Leishmanial and anti-oxidant activities of hemp essential oil. *Biomol. Ther.* 11:272. doi: 10.3390/biom11020272

Michel, A. M., Borrero-de Acuña, J. M., Molinari, G., Ünal, C. M., Will, S., Derksen, E., et al. (2022). Cellular adaptation of Clostridioides difficile to high salinity encompasses a compatible solute-responsive change in cell morphology. *Environ. Microbiol.* 24, 1499–1517. doi: 10.1111/1462-2920.15925

Ñahui Palomino, R. A., Vanpouille, C., Laghi, L., Parolin, C., Melikov, K., Backlund, P., et al. (2019). Extracellular vesicles from symbiotic vaginal lactobacilli inhibit HIV-1 infection of human tissues. *Nat. Commun.* 10:5656. doi: 10.1038/s41467-019-13468-9

Okuda, K., Zendo, T., Sugimoto, S., Iwase, T., Tajima, A., Yamada, S., et al. (2013). Effects of bacteriocins on methicillin-resistant Staphylococcus aureus biofilm. *Antimicrob. Agents Chemother.* 57, 5572–5579. doi: 10.1128/AAC.00888-13

Pelicano, E., Souza, P. T., Souza, H., Oba, A., Norkus, E., Kodawara, L., et al. (2003). Effect of different probiotics on broiler carcass and meat quality. *Braz. J. Poult. Sci.* 5, 207–214. doi: 10.1590/S1516-635X2003000300009

Poppi, L. B., Rivaldi, J. D., Coutinho, T. S., Astolfi-Ferreira, C. S., Ferreira, A. J. P., and Mancilha, I. M. (2015). Effect of lactobacillus sp. isolates supernatant on Escherichia coli O157:H7 enhances the role of organic acids production as a factor for pathogen control. *Pesqui. Vet. Bras.* 35, 353–359. doi: 10.1590/S0100-736X2015000400007

Rosander, A., Connolly, E., and Roos, S. (2008). Removal of antibiotic resistance gene-carrying plasmids from *Lactobacillus reuteri* ATCC 55730 and characterization of the resulting daughter strain, *L. reuteri* DSM 17938. *Appl. Environ. Microbiol.* 74, 6032–6040. doi: 10.1128/AEM.00991-08

Sanmartín, P., Aira, N., Devesa-Rey, R., Silva, B., and Prieto, B. (2010). Relationship between color and pigment production in two stone biofilm-forming cyanobacteria (Nostoc sp. PCC 9104 and Nostoc sp. PCC 9025). *Biofouling* 26, 499–509. doi: 10.1080/08927011003774221

Sanmartín, P., Vázquez-Nion, D., Silva, B., and Prieto, B. (2012). Spectrophotometric color measurement for early detection and monitoring of greening on granite buildings. *Biofouling* 28, 329–338. doi: 10.1080/08927014.2012.673220

Senpuku, H., Yonezawa, H., Yoneda, S., Suzuki, I., Nagasawa, R., and Narisawa, N. (2018). SMU.940 regulates dextran-dependent aggregation and biofilm formation in Streptococcus mutans. *Mol Oral Microbiol* 33, 47–58. doi: 10.1111/omi.12196

Sharma, V., Harjai, K., and Shukla, G. (2018). Effect of bacteriocin and exopolysaccharides isolated from probiotic on *P. aeruginosa* PAO1 biofilm. *Folia Microbiol.* 63, 181–190. doi: 10.1007/s12223-017-0545-4

Shokri, D., Khorasgani, M. R., Mohkam, M., Fatemi, S. M., Ghasemi, Y., and Taheri-Kafrani, A. (2018). The inhibition effect of lactobacilli against growth and biofilm formation of *Pseudomonas aeruginosa*. *Probiotics Antimicrob. Proteins* 10, 34–42. doi: 10.1007/s12602-017-9267-9

Söderling, E. M., Marttinen, A. M., and Haukioja, A. L. (2011). Probiotic lactobacilli interfere with Streptococcus mutans biofilm formation in vitro. *Curr. Microbiol.* 62, 618–622. doi: 10.1007/s00284-010-9752-9

Spano, M., Maccelli, A., Di Matteo, G., Ingallina, C., Biava, M., Crestoni, M. E., et al. (2021). Metabolomic profiling of fresh goji (Lycium barbarum L.) berries from two cultivars grown in Central Italy: a multi-methodological approach. *Molecules* 26:5412. doi: 10.3390/molecules26175412

Tunçer, S., and Karaçam, S. (2020). Cell-free supernatant of streptococcus salivarius M18 impairs the pathogenic properties of *Pseudomonas aeruginosa* and *Klebsiella pneumoniae*. *Arch. Microbiol.* 202, 2825–2840. doi: 10.1007/s00203-020-02005-8

Valdez, R. M. A., Ann Ximenez-Fyvie, L., Caiaffa, K. S., Dos Santos, V. R., Cervantes, R. M. G., Almaguer-Flores, A., et al. (2021). Antagonist effect of probiotic bifidobacteria on biofilms of pathogens associated with periodontal disease. *Microb. Pathog.* 150:104657. doi: 10.1016/j.micpath.2020.104657

Wang, J., Xie, B., and Sun, Z. (2021). Quality parameters and bioactive compound bioaccessibility changes in probiotics fermented mango juice using ultraviolet-assisted ultrasonic pre-treatment during cold storage. *LWT-Food Sci. Technol.* 137:110438. doi: 10.1016/J.LWT.2020.110438

Yang, K. M., Kim, J. S., Kim, H. S., Kim, Y. Y., Oh, J. K., Jung, H. W., et al. (2021). *Lactobacillus reuteri* AN417 cell-free culture supernatant as a novel antibacterial agent targeting oral pathogenic bacteria. *Sci. Reports* 11:1631. doi: 10.1038/s41598-020-80921-x

Yang, Y., Mao, M., Lei, L., Li, M., Yin, J., Ma, X., et al. (2019). Regulation of water-soluble glucan synthesis by the Streptococcus mutans dexA gene effects biofilm aggregation and cariogenic pathogenicity. *Mol Oral Microbiol* 34, 51–63. doi: 10.1111/omi.12253

Zengin, G., Menghini, L., Di Sotto, A., Mancinelli, R., Sisto, F., Carradori, S., et al. (2018). Chromatographic analyses, in vitro biological activities and cytotoxicity of Cannabis sativa L. essential oil: a multidisciplinary study. *Molecules* 23:3266. doi: 10.3390/molecules23123266

Zhu, Y., Guo, L., and Yang, Q. (2020). Partial replacement of nitrite with a novel probiotic lactobacillus plantarum on nitrate, color, biogenic amines and gel properties of Chinese fermented sausages. *Food Res. Int.* 137:109351. doi: 10.1016/j.foodres.2020.109351

Ziyaina, M., Rasco, B., Coffey, T., Mattinson, D. S., and Sablani, S. (2019). Correlation of volatile compound concentrations with bacterial counts in whole pasteurised milk under various storage conditions. *Int. J. Dairy Technol.* 72, 36–46. doi: 10.1111/1471-0307.12557

frontiers | Frontiers in Microbiology

TYPE Original Research
PUBLISHED 24 February 2023
DOI 10.3389/fmicb.2023.1110177

OPEN ACCESS

EDITED BY
Giuseppe Spano,
University of Foggia,
Italy

REVIEWED BY
Zhenshang Xu,
Qilu University of Technology, China
Maria Aponte,
University of Naples Federico II, Italy

*CORRESPONDENCE
Analía G. Abraham
✉ aga@biol.unlp.edu.ar;
✉ analiaabraham@gmail.com

SPECIALTY SECTION
This article was submitted to Microbial Symbioses, a section of the journal Frontiers in Microbiology

Received 28 November 2022
ACCEPTED 31 January 2023
PUBLISHED 24 February 2023

CITATION
Bengoa AA, Dueñas MT, Prieto A, Garrote GL and Abraham AG (2023) Exopolysaccharide-producing *Lacticaseibacillus paracasei* strains isolated from kefir as starter for functional dairy products.
Front. Microbiol. 14:1110177.
10.3389/fmicb.2023.1110177

Exopolysaccharide-producing *Lacticaseibacillus paracasei* strains isolated from kefir as starter for functional dairy products

Ana Agustina Bengoa[1], María Teresa Dueñas[2], Alicia Prieto[3], Graciela L. Garrote[1] and Analía G. Abraham[1,4]*

[1]Centro de Investigación y Desarrollo en Criotecnología de Alimentos (CIDCA) (CONICET-UNLP-CIC), Buenos Aires, Argentina, [2]Dpto. de Química Aplicada, Facultad de Química, Universidad del País Vasco (UPV/EHU), San Sebastián, Spain, [3]Grupo de Sistemas Microbianos e Ingeniería de Proteínas, Dpto. de Biotecnología Microbiana y de Plantas, Centro de Investigaciones Biológicas Margarita Salas, Consejo Superior de Investigaciones Científicas, Madrid, Spain, [4]Area Bioquímica y Control de Alimentos (Dto de Ciencias Biológicas - Facultad de Ciencias Exactas, UNLP), Buenos Aires, Argentina

Exopolysaccharides (EPS) produced by lactic acid bacteria are molecules of great interest for the dairy food industry. *Lacticaseibacillus paracasei* CIDCA 8339, CIDCA 83123, and CIDCA 83124 are potentially probiotic strains isolated from kefir grains whose EPS-production on MRS broth is dependent on incubation temperature. The aim of the present work is to evaluate the effect of fermentation temperature on the characteristics of EPS produced in milk by *L. paracasei* strains and the consequent impact on the rheological properties of the fermented products. Additionally, the protective effect of these EPS against *Salmonella* infection was evaluated *in vitro*. Acid gels with each strain were obtained by milk fermentation at 20°C, 30°C, and 37°C evidencing for all the strains a reduction in growth and acidification rate at lower temperature. *Lacticaseibacillus paracasei* CIDCA 83123 showed low fermentation rate at all temperatures requiring between 3 and 8 days to obtain acids gels, whereas CIDCA 8339 and 83124 needed between 24 and 48 h even when the temperature was 20°C. Fermentation temperature led to changes in crude EPS characteristics of the three strains, observing an increase in the relative amount of the high molecular weight fraction when the fermentation temperature diminished. Additionally, EPS_{83124} and EPS_{83123} presented modifications in monosaccharide composition, with a reduction of rhamnose and an increase of amino-sugars as temperature rise. These changes in the structure of EPS_{83124} resulted in an increase of the apparent viscosity of milks fermented at 20°C (223mPa.s) and 30°C (217mPa.s) with respect to acid gels obtained at 37°C (167mPa.s). In order to deepen the knowledge on EPS characteristics, monosaccharide composition of low and high molecular weight EPS fractions were evaluated. Finally, it was evidenced that the preincubation of intestinal epithelial cells Caco-2/TC-7 with EPS_{8339} and EPS_{83124} partially inhibit the association and invasion of *Salmonella*. In light of these results, it can be concluded that the selection of the EPS-producing strain along with the appropriate fermentation conditions could be an interesting strategy to improve the technological properties of these *L. paracasei* fermented milks with potential protective effects against intestinal pathogens.

KEYWORDS

exopolysaccharides, *Lacticaseibacillus paracasei*, kefir, fermented milks, functionality

1. Introduction

The selection of lactic acid bacteria (LAB) for dairy manufacturing includes the search for exopolysaccharides-producing strains to fulfill consumer demand of pleasant and healthy products without additives. Exopolysaccharides are produced *in situ* during fermentation, having a great impact on the physico-chemical characteristics of the final product and contributing to enhance sensorial attributes on account of their techno-functional properties (Lynch et al., 2018; Dedhia et al., 2022). These biopolymers can act as bio-thickeners improving rheological properties such as viscosity of fermented beverages or viscoelastic properties of acid milk gels (Rimada and Abraham, 2006; Xu et al., 2019). Additionally, they can prevent syneresis due to their water holding capacity and may act as emulsion stabilizing agents (Torino et al., 2015; Piermaria et al., 2021). Exopolysaccharides produced by LAB can be secreted into the growth media and/or form a slime layer loosely bound to the bacterial surface (EPS) or remain tightly linked to the cell surface forming a capsular polysaccharide (CPS) (Ruas-Madiedo et al., 2009; Oleksy and Klewicka, 2018; Bachtarzi et al., 2020). This extracellular location of EPS allows the interaction of these polymers with the matrix improving the physico-chemical properties of products obtained by fermentation with EPS-producing strains.

Some LAB strains with demonstrated probiotic properties are able to produce EPS. In fact, surface EPS plays a key role in the interaction of the probiotic bacteria with epithelial cells, triggering the biological effect (Bengoa et al., 2018a; Sabater et al., 2020). In fact, the health-promoting effect attributed to the probiotic bacteria has been ascribed to the presence of these biopolymers in many cases (Ale et al., 2020; Bengoa et al., 2021; Werning et al., 2022). Among the diverse health promoting properties ascribed to EPS produced by LAB it can be mentioned their ability to modulate intestinal microbiota, exert immunomodulatory and/or antitumor effect, or reduce cholesterol level (Laiño et al., 2016; Ale et al., 2020; Medrano et al., 2020; Bengoa et al., 2020a; Oerlemans et al., 2021; Simonelli et al., 2022).

It has been previously demonstrated that there is a direct relationship between EPS structure and its functionality, both technological and biological (Welman and Maddox, 2003; Chen et al., 2019; Bengoa et al., 2020a). In this direction, EPS-producing LAB are consider special suppliers of a variety of novel polysaccharides whose monomer composition, anomeric configuration, glycosidic linkage and structure is defined by specific biosynthesis enzymes present in each microorganism, resulting in an enormous EPS diversity with potentially different applications (Zeidan et al., 2017).

Since remotes times, fermented foods have been widely produced and consumed as part of a healthy diet, not only because of their enhanced food safety and extended shelf-life but also due to their human health benefits associated (Leeuwendaal et al., 2022). Recently, scientific attention was focused on artisanal fermented foods such as kefir, sugary kefir, kimchi, among others as sources of novel LAB strains with promising technological properties and probiotic potential (Tamang et al., 2016; Bengoa et al., 2019b; Pendón et al., 2021). Isolation of novel strains from these fermented foods would increase microbial biodiversity in the development of selected starter cultures with defined properties (Bachtarzi et al., 2020; Galli et al., 2022). Moreover, they can be the source of novel EPS to fulfill expectation of technological progress for their application in dairy foods (Bachtarzi et al., 2019), non-dairy food (Llamas-Arriba et al., 2019), or biotherapeutic products (de Carvalho and Conte-Junior, 2021; Nadzir et al., 2021).

In previous reports, the isolation of several EPS-producing strains from kefir grains was described by our group (Hamet et al., 2013, 2015; Gangoiti et al., 2017). Among them, *Lacticaseibacillus paracasei* CIDCA 8339, CIDCA 83123 and CIDCA 83124 have proven to be promising probiotic strains that have the ability to adhere to gastric and intestinal epithelial cells even after the passage through the gastrointestinal tract (Zavala et al., 2016; Bengoa et al., 2018b, 2020b) and also meet the requirements established by the regulations about safety for food application (Bengoa et al., 2019a).

One of the effectors ascribed to health-promoting properties of *L. paracasei* strains are exopolysaccharides (Bengoa et al., 2021). In particular, exopolysaccharide produced in milk by *L. paracasei* CIDCA 8339 and CIDCA 83124 strains have demonstrated their potential to modulate the fecal microbiota of children *in vitro* inducing changes in microbial populations and increasing the production of propionic and/or butyric acid depending on the EPS used (Bengoa et al., 2020a). Additionally, it was evidenced that EPS-production by these strains on MRS broth is dependent on incubation temperature with an increment of high molecular weight fractions at low temperature, along with an increase in the total amount of EPS produced (Bengoa et al., 2018a).

Taking in consideration the previous results in MRS medium and the biological effect of EPS produced in milk by these strains, the aim of the present work is to evaluate the effect of fermentation temperature on the characteristics of EPS produced by *L. paracasei* strains in milk and the consequent impact on the rheological and functional properties of the fermented products.

2. Materials and methods

2.1. Bacterial strains and culture conditions

Stock cultures of EPS-producing *Lacticaseibacillus paracasei* CIDCA 8339, CIDCA 83123 and CIDCA 83124 isolated from kefir grains were stored in 12% w/v non-fat milk solids at −80°C. Strains were grown in MRS broth (Difco Laboratories, Detroit, MI, USA) at 20°C (48 h), 30°C (24 h) and 37°C (24 h) under aerobic conditions previous to each experiments (Bengoa et al., 2018a). *Salmonella enterica* serovar Enteritidis CIDCA 101 (Zavala et al., 2016) used for association/invasion experiments was grown in nutrient broth (Biokar Diagnostics, Beauvais, France) for 18 h at 37°C.

2.2. Fermented milks preparation and characterization

Fresh pure cultures of each strain were inoculated in 10 mL of ultra-high temperature low fat milk (La Serenisima, Mastellone Hnos S.A, Argentina) at 5% v/v and incubated at 20°C, 30°C or 37°C. pH and viable bacteria were evaluated at different fermentation times until pH was lower than 4.0. The number of viable bacteria in the fermented milks (CFU/mL) was determined in MRS agar plates. Temperatures selected were between the range of temperature previously described for this species (Zheng et al., 2020).

Organic acids levels in the fermented milks were determined qualitatively and quantitatively by high pressure liquid chromatography (HPLC) when the culture reached pH ≤ 4.0 according to Bengoa et al. (2019a). Briefly, 1 mL of the fermented product was centrifuged for 10 min at 10,000 × *g*. The supernatant obtained was filtered through a 0.45 μm membrane (Millipore Corporation, USA) and 20 μL of the filtrate were injected into the chromatograph. Organic acids were separated on an AMINEX HPX-87H ion exchange column (BioRad Labs, USA) and detected at 214 nm (Waters ™ 996, Millipore Corporation, Milford, MA 01757, USA). The determination was carried out at a flow rate of 0.7 mL/min at 60°C using 0.009 N H_2SO_4 as mobile phase for 30 min. Acids were identified by comparison of the retention times with HPLC-grade standard solutions (Sigma Chemical Co, USA). Additionally, calibration curves of lactic and acetic acid standards were used to determine the concentration of these acids in the samples.

Flow behavior at 25°C of fermented milks was determined in a Haake ReoStress 600 rheometer (Haake, Karlsruhe, Germany) in its rotational mode using a 1 mm gap plate-rough plate sensor system PP35 (Thermo Haake, Karlsruhe, Germany) according to Hamet et al. (2015). The samples were subjected to a cycle that consisted of an increase of shear rate up to 500 s^{-1} using an acceleration of 4,167 s^{-2}. Then, the same but negative acceleration value was used to return the shear rate to 0 s^{-1}. Flow curves were obtained and the apparent viscosity at 300 s^{-1} (mPa.s) was determined for each sample. The flow behavior of fermented milks adjusted with Ostwald de Waele model: $\tau = k.\dot{\gamma}^{n}$, where τ is the shear stress (Pa), k is the consistency index (Pa s^n), $\dot{\gamma}$ is the shear rate (s^{-1}) and n is the flow index (non-dimensional); or Carreau-Yasuda model: $\tau = \dot{\gamma}\ [\eta_\infty + (\eta_0 - \eta_\infty) / (1 + (\lambda\ \dot{\gamma})^{a})^{(1-n)/a}]$, where τ is the shear stress (Pa), $\dot{\gamma}$ is the shear rate (s^{-1}), η_0 is the initial viscosity expressed in Pa·s, η_∞ is the viscosity to infinite time expressed in Pa·s and its constant value is 0, n is the flow behavior index, λ is time parameters in s^{-1} and a is a constant (non-dimensional). Glucono δ lactone (GDL) acid milk gels were obtained according to Rimada and Abraham (2006) and used as controls.

2.3. EPS extraction

For EPS extraction, 500 mL of commercial UHT low fat milk (La Serenisima, Mastellone Hnos S.A, Argentina) were individually inoculated with fresh pure cultures (1% v/v) and incubated at 20°C, 30°C or 37°C until the acid gels were formed. The fermented milks obtained were heated for 30 min at 100°C in order to favor the detachment and dissolution of the polysaccharide bound to the cells and allow enzymes denaturalization. Trichloroacetic acid 8% w/v (Ciccarelli, Argentina) was added to precipitate the proteins. Then, the samples were centrifuged at 10,000 *g* for 20 min at 20°C in an Avanti J25 centrifuge (Beckman Coulter Inc., USA) and two volumes of cold ethanol were added to the supernatant obtained. The samples were placed at-20°C overnight and centrifuged at 10,000 *g* for 20 min at 4°C. EPS pellets were dissolved in hot distilled water and dialyzed against bi-distilled water through a 1 kDa cut-off dialysis membrane (Spectra/Por, The Spectrum Companies, Gardena, CA) for 48 h at 4°C. Finally, the samples were lyophilized. EPS extraction was performed from two independent cultures. The absence of other sugars was determined by thin-layer chromatography and the absence of proteins was evaluated by the Bradford method (Rimada and Abraham, 2003). EPS amount was estimated by weight of crude EPS lyophilized and expressed as mg/L.

2.4. Evaluation of molecular weight distribution and monosaccharide composition of EPS

Molecular weight distributions of lyophilized crude EPS were determined by size exclusion chromatography. In brief, crude EPS powder was suspended in 0.1 M $NaNO_3$ (0.5 mg/mL) and then filtered through a 0.45 μm pore diameter polyvinylidene fluoride membrane (Millipore Corporation, USA). The average molecular weight (MW) was determined by high-performance molecular exclusion chromatography (HPLC-SEC, Agilent 1,100 Series System, Hewlett-Packard, Germany) associated with a refractive index (IR) detector (Ibarburu et al., 2015). 50 μL of the samples were injected and eluted at a flow rate of 0.95 mL/min (pressure: 120:130 psi) at room temperature using 0.1 M $NaNO_3$ as mobile phase. Dextrans (0.5 mg/mL) with a molecular weight between 10^3 and 2.10^6 Da (Sigma-Aldrich, USA) were used as standards.

Once the molecular weight distributions were determined, low and high molecular weight fractions that composed the crude EPS obtained at 20°C were separated. For this purpose, EPS solutions (0.2% w/v) were centrifuged through a Vivaspin™ ultrafiltration spin column 100 KDa MWCO, (Sartorious, Goettingen, Germany) for 20 min at 6000 *g*, eluting only the low MW fraction. Subsequently, high MW fraction retained in the column was eluted using hot distilled water. The eluted fractions were passed through a Vivaspin column (cut-off 30KDa) in order to separate the middle and low MW fraction of EPS.

Monosaccharide composition of crude EPS and their fractions were determined by gas chromatography as previously described (Notararigo et al., 2013). Briefly, 1–2 mg of EPS were hydrolyzed in 1 mL of 3 M trifluoroacetic acid (1 h at 120°C). The monosaccharides obtained were converted into alditol acetates by reduction with $NaBH_4$ and subsequent acetylation. The samples were analyzed by gas chromatography in an Agilent 7890A coupled to a 5975C mass detector, using an HP5-MS column with helium as carrier gas at a flow rate of 1 mL/min. For each run, 1 μL of sample was injected (with a Split 1:50) and the following temperature program was performed: the oven was heat to 175°C for 1 min; the temperature was increased to 215°C at a rate of 2.5°C/min and then increased to 225°C at 10°C/min, keeping it constant at this temperature for 1.5 min. Monosaccharides were identified by comparison of retention times with standards (arabinose, xylose, rhamnose, galactose, glucose, mannose, glucosamine and galactosamine) analyzed under the same conditions. Calibration curves were also processed for monosaccharide quantification. Myo-inositol was added to each sample as internal standard.

2.5. *Salmonella* association and invasion assays

Salmonella association and invasion assays were performed according to Zavala et al. (2016). Caco-2/TC-7 cells that were routinely

grown in Dulbecco's modified Eagle's minimal essential medium (DMEM) (GIBCO BRL Life Technologies Rockville, MD. USA), supplemented with 15% heat-inactivated (30 min at 60°C) fetal bovine serum (FBS, PAA, GE Healthcare Bio-Sciences Corp., USA), 1% non-essential amino acids (GIBCO BRL Life Technologies Rockville, MD. USA), and the following antibiotics (Parafarm, Saporiti SACIFIA, Buenos Aires, Argentina): penicillin (12 UI/mL), streptomycin (12 µg/mL), gentamicin (50 µg/mL). Cells were seeded in 24-well culture plates (Corning, NY, USA) at 2.5×10^5cells per well and incubated at 37°C in a 5% CO_2 — 95% air atmosphere. Caco-2/TC-7 cells were used at post-confluence after 7 days of culture.

Salmonella enteritidis serovar enteritidis CIDCA 101, provided by Dr. H. Lopardo, was grown in nutritive broth (Biokar Diagnostics, Beauvais, France) for 18 h at 37°C (Golowczyc et al., 2007). Confluent Caco-2/TC-7 monolayers were washed twice with sterile PBS (pH 7.2). Cells were pre incubated for 1 h at 37°C in a 5% CO_2—95% air atmosphere with 250 µL EPS solutions (300, 500 and 800 mg/L in DMEM) or 250 µL DMEM in the case of *Salmonella* association and invasion controls. Afterwards, 250 µL of *Salmonella* suspension (1×10^7 CFU/mL) were added to each well and incubated 1 h at 37°C in a 5% CO_2—95% air atmosphere. For association assays, cells were washed three times with PBS and lysed with 500 µL/well of bi-destilled water. The number of associated *Salmonella* (adhering and invading) was determined by serial dilutions on 0.1% w/v tryptone followed by colony counts on nutrient agar. *Salmonella* invasion was determined by counting only bacteria located in the Caco-2/TC-7 cells. For this purpose, the monolayer incubated with *Salmonella* as previously described, were treated with 0.5 mL/well of gentamicin (100 µg/mL PBS) for 1 h at 37°C. Subsequently, cells were lysed and colony counts performed as described above.

2.6. Statistical analysis

All experiments were performed at least in triplicate. Quantitative data were analyzed by using one-way analysis of variance (ANOVA) followed by Tukey's Tests for multiple mean comparisons. A value of $p < 0.05$ indicates significant differences. GraphPad Prism version 5.01 software for Windows (GraphPad®, California, USA) was used for data analysis. The results are expressed as mean ± standard deviation (SD).

3. Results

3.1. Milk fermentation with *Lacticaseibacillus paracasei* strains at different temperatures

As a first characterization, the growth and acidification kinetics of *L. paracasei* strains in milk at 20, 30 and 37°C were evaluated (Table 1; Figure 1) and the fermented milks obtained were characterized. Table 1 shows the growth rate and yield of the strains, and organic acids concentration in all cases. It was clearly evidenced that growth and acidification rate were influenced by incubation temperature, observing an increase with temperature for the three strains without showing significant differences in the growth yield. *L. paracasei* CIDCA 8339 and CIDCA 83124 showed an acceptable growth and acidification rate even at 20°C, requiring between 24 h at 30 and 37°C, and 48 h at 20°C to reach the maximum growth and a pH ≤ 4.0. On the other hand, *L. paracasei* CIDCA 83123 showed low growth and acidification rates at all temperatures assayed, demanding a longer fermentation period to form the acid gels and reach the maximum growth. In fact, the pH of the milk fermented with *L. paracasei* CIDCA 83123 at 20°C began to decrease only after 125 h of fermentation, requiring 192 h (8 days) to obtain the acid gel at this temperature. These differences in growth and acidification kinetics between *L. paracasei* strains at 20°C can be clearly evidenced in Supplementary Figure S1. The slow growth of CIDCA 83123 in milk constitutes a technological disadvantage for this strain since the food industry usually prefers the application of fast-growing acidifying microorganisms for the development of fermented dairy products.

Subsequently, the fermented products obtained at different temperatures were characterized with regard to macroscopic aspect, pH and organic acids levels. The fermented products obtained with the strains at all three temperatures were firm acid gels with pleasant appearance that did not presented syneresis. Those obtained with CIDCA 8339 and CIDCA 83123 strains did not show a ropy character. However, milks fermented with CIDCA 83124, at 20°C and 30°C showed a marked ropy character (Supplementary Figure S2) that was not evidenced when milk was fermented at 37°C.

Moreover, it could be evidenced that lactic acid levels (120–150 mM) in the milks fermented with different *L. paracasei* strain did not present significant differences (Table 1). On the other hand, *L. paracasei* CIDCA 83123 produced higher levels of acetic acid than CIDCA 8339 and CIDCA 83124 strains. However, for a specific strain, no significant differences were observed in lactic or acetic acid levels with fermentation temperature.

The results obtained indicate that although temperature incubation has a significant impact on the growth and acidification kinetics of *L. paracasei* strains, at the end of fermentation organic acid levels, pH and probiotic concentration result equivalent. At this point, *L. paracasei* CIDCA 8339 produces 130–145 mg of EPS per liter of fermented milk obtained at 30°C, CIDCA 83123 produces 155–160 mg/L and CIDCA 83124 about 140–160 mg/L, being these values not significantly different.

Flow behavior and apparent viscosity of the fermented products were analyzed (Figure 2). All acid gels obtained presented a non-Newtonian pseudoplastic behavior with a hysteresis loop that was higher in the milks fermented with CIDCA 83124 at all temperatures (Figure 2A). The hysteresis is a measure of the extent of structural breakdown during the shearing cycle. The evidence of this structural breakdown was demonstrated by analyzing the flow behavior in the up and down curve. Fermented milk with *L. paracasei* CIDCA 8339 at 20°C and CIDCA 83123 at 20°C or 30°C presented a flow behavior that fitted the Ostwald de Waele model with n values ranging from 0.08 to 0.2 in the up curve while fermented milks with *L. paracasei* CIDCA 8339 at 30°C and 37°C or *L. paracasei* CIDCA 83123 at 37°C did not fit this model (Supplementary Table S1). However, after the first structural breakdown (flow behavior of the down curve) all the acid gels obtained with these strains fitted Ostwald de Waele model with n values between 0.41 and 0.47. On the other hand, all the acid gels obtained by fermentation with CIDCA 83124 did not fit Otswald de Waele model indicating that

TABLE 1 Bacteria growth rate and yield, lactic and acetic acid concentration of milk fermented with *Lacticaseibacillus paracasei* CIDCA 8339, CIDCA 83123, and CIDCA 83124 at 20°C, 30°C, and 37°C.

L. paracasei strain	Temperature	Growth rate (h^{-1})	Growth yield (log CFU/mL)	Lactic acid (mM)	Acetic acid (mM)
CIDCA 8339	20°C	0.0718	9.45 ± 0.08	142.54 ± 15.02 [a]	9.05 ± 1.85 [a]
	30°C	0.1088	9.38 ± 0.05	150.15 ± 11.07 [a]	12.38 ± 4.94 [ac]
	37°C	0.1645	9.28 ± 0.11	143.57 ± 11.77 [a]	7.85 ± 1.12 [a]
CIDCA 83123	20°C	0.0055	9.68 ± 0.08	126.58 ± 7.77 [a]	20.66 ± 1.29 [b]
	30°C	0.0138	9.63 ± 0.02	124.72 ± 26.08 [a]	21.43 ± 0.53 [b]
	37°C	0.0178	9.79 ± 0.09	122.78 ± 4.61 [a]	19.46 ± 3.59 [bc]
CIDCA 83124	20°C	0.0556	9.75 ± 0.11	119.55 ± 9.61 [a]	8.62 ± 2.11 [a]
	30°C	0.1703	9.80 ± 0.08	132.76 ± 24.39 [a]	10.23 ± 1.56 [a]
	37°C	0.2387	9.79 ± 0.04	154.64 ± 28.64 [a]	11.52 ± 1.27 [a]

Different letters indicate significant differences ($p < 0.05$).

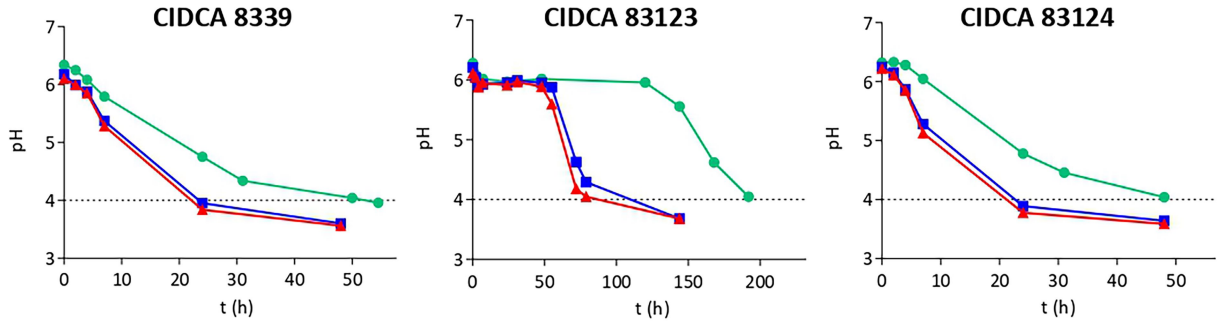

FIGURE 1
Acidification kinetics of *Lacticaseibacillus paracasei* CIDCA 8339, CIDCA 83123 and CIDCA 83124 in milk at 20°C (●), 30°C (●), and 37°C (●). Dotted line indicates the pH selected for characterization of fermented milks.

these acid gels have a different texture, may be due to differences in the characteristic of EPS produced by this strain. These acid gels fitted to Carreau-Yasuda model (Supplementary Table S2) which describes a pseudoplastic fluid with asymptotic viscosities at zero (η_0) and infinite (η_∞) shear rates with no yield stress (Hackley and Ferraris, 2001).

Moreover, the acid gels obtained by fermentation with CIDCA 83124 were significantly more viscous, compared to those fermented by *L. paracasei* CIDCA 8339 and CIDCA 83123 (Figure 2B; Supplementary Table S3). Regarding the effect of fermentation temperature, significant changes in the apparent viscosity of the fermented milk were only observed with *L. paracasei* CIDCA 83124, obtaining values significantly higher at 20°C and 30°C. These results indicate that the fermentation temperature could be modifying the physico-chemical characteristics of the EPS synthesized by this strain.

Flow curve of milk gel acidified with GDL used as control fitted Otswald de Waele model having a lower consistence index and a flow index (n) of 0.8 (Supplementary Table S2). The smaller value of n of acid gels obtained by milk fermentation with *L paracasei*, may indicate that EPS affects structure of the acid gels and consequently modify their flow behavior.

3.2. Temperature fermentation modified the molecular weight of exopolysaccharides produced by *Lacticaseibacillus paracasei* strains

Crude EPS synthesized by the strains at 20, 30 and 37°C in milk were extracted and subsequently characterized in terms of molecular weight distribution (MW). Table 2 shows the molecular weight fractions evidenced for the EPS produced at different temperatures and the percentage relative area of the MW fractions in each condition. *Lacticaseibacillus paracasei* CIDCA 8339 synthesizes an EPS that is made up of two fractions, a high MW fraction in the order of 10^5 Da and a low MW fraction of about 10^4 Da. These two fractions are present at the three temperatures studied, observing a change in the relative abundance of each fraction depending on the temperature. The low MW fraction is the most abundant when fermentation temperature is 37°C. At 30°C, the proportion of both fractions is equivalent; meanwhile the high MW fraction becomes predominant at 20°C. The polysaccharide produced by CIDCA 83124 at 20 and 37°C is composed by two fractions, a low MW fraction of 10^4 Da and a high MW of $1–4 \times 10^6$ Da. This last fraction has a higher MW than the

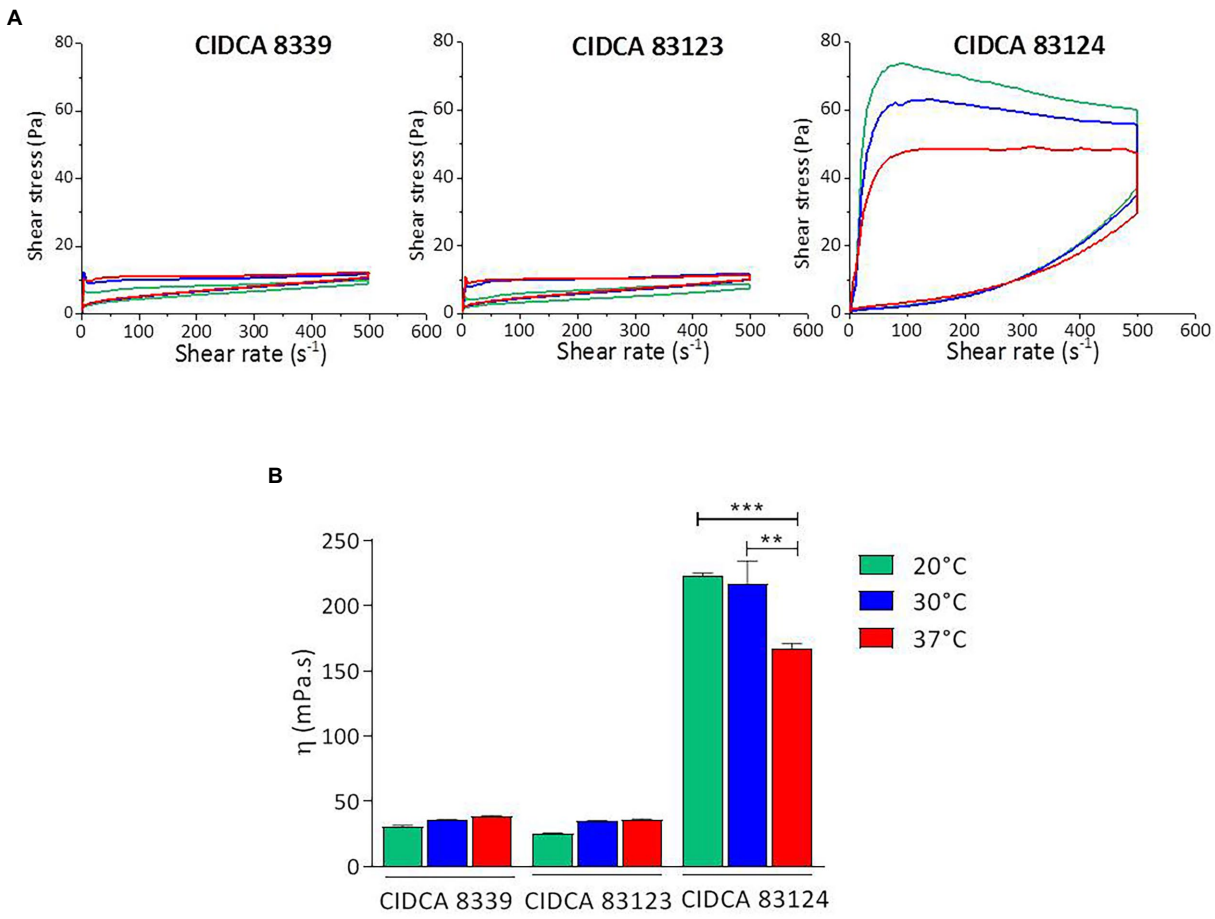

FIGURE 2
Flow curves **(A)** and apparent viscosity at 300s^{-1} **(B)** of milks fermented with *L. paracasei* CIDCA 8339, CIDCA 83123, and CIDCA 83124 at 20°C (●), 30°C (●), and 37°C (●). Significant differences ** p<0.01, *** p<0.001.

TABLE 2 Molecular weight and relative abundance (percentual expression) of EPS fractions produced by *L paracasei* strains in milk at different temperatures.

L. paracasei strain	Temperature	EPS molecular weight (Da)							
		High MW fraction (>1×10^5)				Middle MW fraction (3×10^4 <PM>1×10^5)		Low MW fraction (<3×10^4)	
		Mw	Relative abundance %	Mw	Relative abundance %	Mw	Relative abundance %	Mw	Relative abundance %
CIDCA 8339	20°C	-	-	1.4×10^5	57.1	-	-	9.0×10^3	42.9
	30°C	-	-	3.9×10^5	50.0	-	-	1.0×10^4	50.0
	37°C	-	-	5.4×10^5	33.3	-	-	1.2×10^4	66.7
CIDCA 83123	20°C	3.4×10^6	85.1	6.0×10^5	6.4	7.4×10^4	2,1	1.0×10^4	6.8
	30°C	3.3×10^6	17.6	6.8×10^5	17.6	7.1×10^4	5.9	1.1×10^4	58.9
	37°C	3.5×10^6	9.5	4.5×10^5	14.3	7.8×10^4	9.5	1.2×10^4	66.7
CIDCA 83124	20°C	3.7×10^6	80.0	-	-	-	-	1.1×10^4	20.0
	30°C	5.7×10^6	21.0	6.9×10^5	10.5	7.0×10^4	5.3	1.1×10^4	63.1
	37°C	1.1×10^6	14.3	-	-	-	-	1.5×10^4	85.7

Relative abundance is calculated considering the percentage of the area of each peak referred to the total area of the chromatogram. Standard deviation ranged between 0.05 and 0.2. Standard deviation in retention time of peak ranged from 0.04 to 0.06.

corresponding produced by CIDCA 8339. The EPS produced by *L. paracasei* CIDCA 83124 at 30°C presents two additional fractions that include an intermediate MW fraction of 7×10^4 Da and another high MW fraction of 7×10^5, being composed by a total of four fractions. When analyzing the EPS produced by *L. paracasei* CIDCA 83123, it can be evidenced that there are four distributions of different MW at all three temperatures. As evidenced with CIDCA 8339, a clear increase in the proportion of the high MW fractions at lower fermentation temperatures was also observed for CIDCA 83123 and CIDCA 83124 when grown in milk.

3.3. Monosaccharide composition of exopolysaccharide produced by *Lacticaseibacillus paracasei* was affected by temperature fermentation depending on the strain

Monosaccharide composition of the crude EPS produced in milk by the three *L. paracasei* strains was evaluated, evidencing that all of them contain glucose, galactose and rhamnose as major sugars, and to a lesser extent amino sugars such as glucosamine and galactosamine. However, the relative amount of each monosaccharide depended on the strain and growth temperature (Figure 3).

EPS from *L. paracasei* CIDCA 8339 is mainly composed of galactose and rhamnose and to a lesser extent glucose, keeping the proportion of sugars constant at the three temperatures studied. On the contrary, EPS from CIDCA 83123 and CIDCA 83124 strains are mainly composed by glucose. Moreover, changes in the proportion of sugar composition with temperature were evidenced for these two stains. EPS produced by CIDCA 83123 at 20°C has glucose as the most abundant sugar, followed by galactose and rhamnose. However, the proportion of glucose and rhamnose decreases when temperature fermentation increases, accompanied by a rise in glucosamine and galactosamine proportion. Similarly, EPS of *L. paracasei* CIDCA 83124 also showed a reduction in rhamnose at higher temperatures, along with an increase in galactose and amino sugars. In summary, it can be state that in the case of EPS produced by CIDCA 83123 and CIDCA 83124 the incorporation of rhamnose is favored at 20°C, while the proportion of amino sugars increases at higher temperatures.

Then, monosaccharide compositions of high and low molecular weight fractions of EPS were studied (Figure 4). For this purpose, EPS produced at 20°C were selected since high and low molecular weight fractions were clearly defined in the chromatograms, facilitating their separation and purification. At 20°C the two fractions of EPS produced by *L. paracasei* CIDCA 8339 (EPS_{8339}) presented similar monosaccharide composition showing only small differences in the proportion of galactose and rhamnose. Similar results were observed in the case of EPS_{83124}. The similarity in monosaccharide composition of low and high molecular weight fraction of these EPS could be indicating that both fractions correspond to the same polymer but with different polymerization grade.

3.4. EPS from *Lacticaseibacillus paracasei* CIDCA 8339 and CIDCA 83124 protected against *Salmonella* invasion *in vitro*

The protective effect of EPS against *Salmonella enteritidis* infection to Caco-2/TC-7 cells was evaluated. Considering all previous results and in sight of applying these strains for the development of a fermented product, EPS produced by CIDCA 8339 and CIDCA 83124 at 30°C were selected since these strains presented an adequate fermentation time to reach pH <4.0 at this temperature. Moreover, the comparison of these two EPS results particularly interesting due to the differences evidenced in crude EPS molecular weight distribution and monosaccharide composition which could imply differences in the biological activity.

To evaluate the protective effect of EPS_{8339} and EPS_{83124}, cells were pre-incubated with EPS solutions before *Salmonella* infection. As shown in Table 3, when the concentration was 800 mg/L, the presence of EPS_{8339} and EPS_{83124} led to a reduction of 0.5 log of the pathogenic bacteria associated to Caco-2/TC-7 cells when compared to the control. Moreover, the internalization of *Salmonella* strain to these intestinal epithelial cells was affected by EPS observing a significant decrease of 1.5 log in the number of *Salmonella* internalized to the cells. Nevertheless, lower concentrations of EPS (300 or 500 mg/L) did not exert a protective effect. These results could be explained by a barrier effect ejected by EPS that prevents the interaction of the bacteria with specific cell receptors hindering the adhesion and invasion of *Salmonella* and avoiding the setting up of the infection.

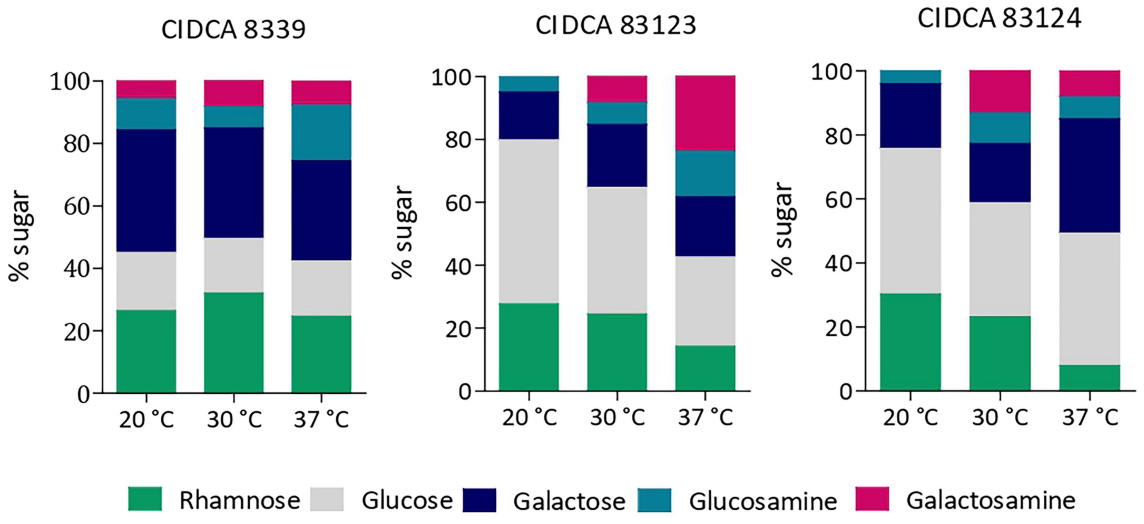

FIGURE 3
Monosaccharide composition of EPS produced by *L. paracasei* CIDCA 8339, CIDCA 83123 and CIDCA 83124 in milk at 20°C, 30°C, and 37°C. Standard deviation in monosaccharide composition was between 0.2 and 4 depending on the percentage of each monosaccharide.

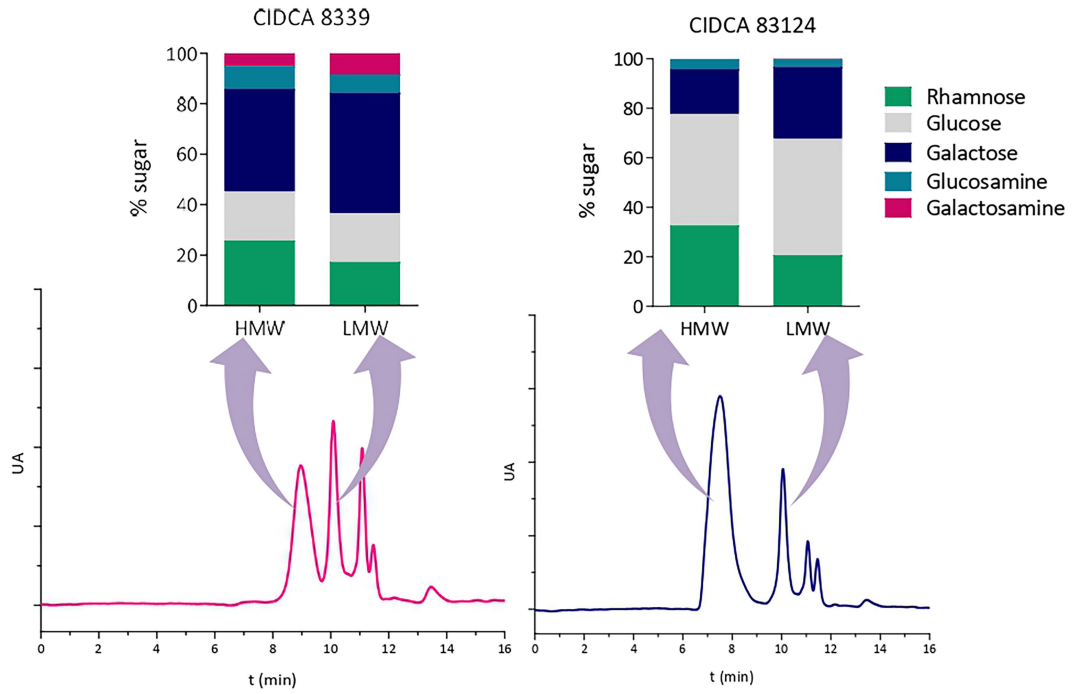

FIGURE 4
High-performance size exclusion chromatograms of EPS isolated from milk produced by *L. paracasei* CIDCA 8339 and CIDCA 83124 at 20°C, and monosaccharide composition of the corresponding high and low molecular weight fractions. AU: arbitrary units. Standard deviation in monosaccharide composition was between 0.4 and 4 depending on the percentage of each monosaccharide.

TABLE 3 Association and invasion of *Salmonella enteritidis* to Caco-2/TC-7 cells preincubated (1h, 37°C) with EPS produced by *L. paracasei* CIDCA 8339 and CIDCA 83124 at 30°C in milk.

	Concentration (mg/L)	Association (log CFU/mL)	Invasion (log CFU/mL)
Control	-	6.07 ± 0.06^{a}	4.60 ± 0.05^{a}
EPS 8339	300	6.07 ± 0.01^{a}	4.69 ± 0.09^{a}
	500	6.14 ± 0.03^{a}	4.57 ± 0.08^{a}
	800	5.49 ± 0.04^{b}	3.50 ± 0.04^{b}
EPS 83124	300	6.03 ± 0.12^{a}	4.63 ± 0.04^{a}
	500	6.08 ± 0.02^{a}	4.55 ± 0.11^{a}
	800	5.54 ± 0.03^{b}	3.43 ± 0.08^{b}

Control corresponds to cells preincubated with DMEM. Different letters within columns indicate significant differences ($p < 0.05$, Tukey's multiple comparison test).

4. Discussion

In the present research the growth in milk at different temperatures of three EPS-producing *L. paracasei* strains isolated from kefir was evaluated focusing the study on the characterization of EPS. The response of microorganisms to environmental conditions has been extensively investigated. Particularly for LAB, the physiological and molecular mechanisms in response to growth temperature have been studied due to the impacts on food processing (De Angelis and Gobbetti, 2004). According to König and Berkelmann-Löhnertz (2017) and Sánchez et al. (2019), in general the optimal growth temperature of lactobacilli is between 30 to 40°C; however, there are strains that can grow at temperatures ranging from 2 at 53°C as was observed for *L. plantarum* strains that were able to grow at low temperatures (4°C to 16°C) (Dalcanton et al., 2018). Likewise, other authors have found that some *Lactobacillus* spp. can grow at high temperatures (Yang et al., 2018; Śliżewska and Chlebicz-Wójcik, 2020). The effect of temperature on LAB growth has also been studied in different food matrices such as fruit juice (Mustafa et al., 2019) or coconut milk (Saori Ishii Mauro and Garcia, 2019). When evaluating the growth of different strains of LAB in fruit juice at 30, 35 and 37°C, a strain-dependent effect was observed since some strains had an equivalent growth at different temperatures while others showed better development at 30°C. However, none of the strains presented marked changes in lactic acid production with temperature (Mustafa et al., 2019). This is in concordance with our results where temperature affected growth rate in a strain specific manner. When studying the effect of temperature on milk fermentation, it has been evidenced that the production of metabolites by probiotic strains occurs in different amounts depending on the temperature and time of fermentation, which illustrates the relevance of controlling these parameters (Østlie et al., 2005). Organic acids constitute one of the main metabolites produced by LAB during milk fermentation. In the present work, it was evidenced an influence of temperature in acidification kinetics. However, as organic acids were determined at the end of the fermentation process which was defined by a pH ≤ 4.0, the concentration of viable microorganisms as well as organic acids concentrations showed no significant differences with temperature fermentation.

As previously mentioned, some LAB are able to produce exopolysaccharides, which are relevant metabolites in food due to

their potential biological and techno-functional properties. To deepen the knowledge about the characteristics of EPS produced by *L. paracasei* CIDCA strains and understand the relationship between EPS features and their functional properties, the degree of polymerization and the monomer composition of each EPS were studied.

EPS produced by LAB present a wide range of molecular weight that varies between 10^4 and 10^6 Da for heteropolysaccharides (HePS) and up to 10^8 for homopolysaccharides (HoPS) (Ryan et al., 2015; Daba et al., 2021; Werning et al., 2022), as it was evidenced for *L. paracasei* strains reported in the literature (Liu et al., 2013; Wang et al., 2022). When studying the molecular weight of EPS from *L. paracasei* CIDCA strains, it was observed that these EPS have fractions with different molecular weight that goes from low MW fractions of 1×10^4 Da to high MW fractions of 5.10^6 Da. It has been described that some LAB produce EPS fractions that could be ascribed to different EPS (Ibarburu et al., 2015; Llamas-Arriba et al., 2019) while others usually produce fractions that only differ in the degree of polymerization, in agreement with our results (Zeidan et al., 2017).

With regard to EPS-producing *L. paracasei* strains, most of the studies report the monosaccharide composition of EPS synthetized in MRS or chemically defined medium added with different sugars. In general, EPS from *L. paracasei* strains are heteropolysaccharides mainly composed by glucose, mannose and galactose, along with some minor sugars such as fucose, xylose, rhamnose, arabinose, N-acetylgalactosamine, galacturonic and glucuronic acid, depending on the strain (Hee et al., 2011; Liu et al., 2013; Balzaretti et al., 2017; Bhat and Bajaj, 2019; Xiao et al., 2021; Zhang et al., 2021; Amini et al., 2022; Wang et al., 2022). In agreement with our results, EPS produced by *L. paracasei* DG (Balzaretti et al., 2017), *L. paracasei* KB28 (Hee et al., 2011) and *L. paracasei* KL1 (Liu et al., 2013) have also shown the presence of rhamnose in their composition. The presence of this monosaccharide as a constituent of EPS from *L. paracasei* strains seems to be a common feature. Smokvina et al. (2013) analyzed the genome of *L. paracasei* strains from different niches, evidencing that most of the studied strains presented two cluster that contain genes that encode rhamnosyltransferases and enzymes involved in the conversion of D-glucose-1-phosphate into dTDP-L-rhamnose. In fact, it has been proposed that the presence of rhamnose in EPS is relevant with regard to their biological effect since several rhamnose-rich EPS produced by species of *Lacticaseibacillus* have the ability to stimulate the production of proinflammatory cytokines by antigen-presenting cells (Balzaretti et al., 2017).

On the other hand, little is known about monosaccharide composition of EPS produced by *L. paracasei* strains in milk. Recently, Li et al. (2020) reported an HePS from *L. paracasei* H9 produced in milk that was composed by mannose, glucose, galactose and glucuronic acid. When analyzing the monomer composition of EPS produced by LAB in milk, the presence of glucose and galactose and their amino derivatives can be evidenced in most biopolymers, which is expected considering that lactose constitutes the main sugar present in milk (Zhu et al., 2019; Bachtarzi et al., 2020; You et al., 2020a, 2020b). These results are in line with HePS of *L. paracasei* CIDCA strains studied in the present work.

The characteristics of EPS produced by LAB are highly dependent on culture conditions, including temperature, medium composition and incubation time (Ibarburu et al., 2015). In a previous work, the EPS produced by these *L. paracasei* CIDCA strains in MRS agar was evaluated (Bengoa et al., 2018a). When comparing the molecular weight distribution of EPS produced in milk with those obtained in MRS, it can be clearly evidenced that they are composed by different fractions, showing the influence of the culture medium on the polymer characteristics. Interestingly, the temperature influence on the molecular weight distribution of EPS was equivalent both in MRS (Bengoa et al., 2018a) and milk, showing that low temperatures increase the proportion of high molecular weight fractions, favoring EPS polymerization. Furthermore, in the case of HePS produced by *L. paracasei* CIDCA 83123 and CIDCA 83124 in milk, it was evidenced that temperature also induced changes in the monosaccharide composition. In contrast to our results, Khanal and Lucey (2018) studied the effect of temperature fermentation in the molecular weight of EPS synthetized by two *Streptococcus thermophilus* strains and no significant changes in molecular weight were observed. Many studies have evaluated the effect of different culture conditions (incubation time and temperature, carbon, nitrogen, and mineral sources) on EPS yield (Amiri et al., 2019; Zhang et al., 2020; Chen et al., 2022). However, the influence of these factors on EPS characteristics, including molecular weight distribution and monosaccharide composition, has not been extensively studied. In fact, to our knowledge, the present work constitutes the first report of the effect of temperature fermentation on monosaccharide composition of EPS produced by LAB.

The structural diversity of EPS produced by *L. paracasei* provides a variety of rheological properties that can be exploited for diverse commercial applications in the food or medical industry. Moreover, the impact of culture conditions on EPS characteristics allows obtaining products with different technological properties simply by modifying the fermentation temperature. Acid milk gels obtained with *L. paracasei* strains at three fermentation temperatures presented a non-Newtonian flow behavior. Growth temperature did not significantly affect the apparent viscosity or the shear-thinning flow behavior of acids gels obtained with *L. paracasei* CIDCA 8339 and CIDCA 83123. This indicates that the changes on molecular weight distribution induced with temperature in the EPS synthesized by these strains did not generate a significant impact on the viscosity of the fermented product. On the other hand, acid gels obtained with *L. paracasei* CIDCA 83124 presented a significant increase in viscosity when temperature decreased, which is in line with the increment in the proportion of the high MW fraction. Moreover, differences in hysteresis area of the flow curves were also observed. These results are in agreement with those previously reported that indicated the relationship between EPS structure and its techno-functional properties. Bachtarzi et al. (2020) compared EPS produced by *L. plantarum* strains and demonstrated a correlation between a ropy phenotype and the presence of a high MW fraction, which also contributed to the viscosity of the fermented product.

Comparing flow curves and viscosity of the acid gels obtained with *L. paracasei* CIDCA strains at a given temperature, differences were observed. When grown at 30°C, the three strains produced the same amount of EPS indicating that, although the amount of EPS produced *in situ* is one of the factor affecting rheological properties, the physicochemical properties of the biopolymer are also of great relevance since the structure of EPS may significantly affect its interaction with milk proteins (Ruas-Madiedo et al., 2009). Considering the molecular weight distribution of the EPS produced by the three *L. paracasei* strains, the lower viscosity values of acid gels

obtained with CIDCA 8339 correlated with the structural characteristic of the EPS as the high MW fraction produced by this strain is smaller than the corresponding high MW fraction produced by CIDCA 83123 and CIDCA 83124. On the other hand, *L. paracasei* CIDCA 83123 and CIDCA 83124 produce EPS that have similar molecular weight distribution, but their acid gels present different viscosity and flow behavior. While acid gels obtained with *L. paracasei* CIDCA 83123 have low apparent viscosity with flow curves that fit the Oswald de Waele model, acid gels obtained with CIDCA 83124 strain fit the Carreau-Yasuda model. Acidification rate along with fermentation temperature are factors that affect the texture of acid gels (Cobos et al., 1995; Lucey and Singh, 1997; Ruas-Madiedo and Zoon, 2003). Acidification rate determines the aggregation of casein micelles to form acid gels, together with the *in situ* production of EPS that may differentially affect protein network depending on the polymer physicochemical properties (Mende et al., 2016). Observing acidification curves for both strains at a specific temperature, it can be clearly evidenced that CIDCA 83124 strain has higher growth and acidification rates, which could be one of the factors that explain the differences evidenced in acid gels obtained with these two strains. Furthermore, these HePS could have different ramification degree that determines flow properties and macromolecules interaction.

Another important feature ascribed to bacterial EPS are their health-promoting properties since they are one of the molecules that may act as effectors of the biological role of probiotic microorganisms (Caggianiello et al., 2016; Laiño et al., 2016). One of the health effects attributed to EPS produced by probiotics is their prebiotic potential acting as compounds that can be selectively fermented by gut microbiota leading to the production of bioactive metabolites such as short chain fatty acids (acetate, propionate, and butyrate) (Ale et al., 2020; Sabater et al., 2020). This was the case of EPS produced by *L. paracasei* CIDCA 8339 and CIDCA 83124 in milk at 30°C, which have the ability to be metabolized by infant fecal microbiota differentially modifying the microbial populations as well as their metabolic activity (Bengoa et al., 2020a). While fermentation of EPS_{8339} increased propionate and butyrate levels, fermentation of EPS_{83124} only raised butyrate levels indicating that EPS molecular weight or monomer composition have a crucial role in the stimulation of gut bacteria growth and activity.

On the contrary, the results obtained in the present work with regard of *Salmonella enteritidis* invasion to intestinal epithelial cells in the presence of crude EPS, demonstrated that this effect was not dependent on the biopolymer structure since both EPS tested performed a similar barrier effect at the highest concentration. It has been previously evidenced that *L. paracasei* CIDCA 8339 and CIDCA 83124 grown in MRS medium can decrease *Salmonella* invasion. With regard to the mechanism involved, both strains inhibited *Salmonella* invasion by interaction with the pathogen meanwhile, only CIDCA 8339 protects through a barrier effect (Zavala et al., 2016). Therefore, it can be consider that EPS is not the only factor involved in epithelium protection from pathogen damage.

5. Conclusion

The present results demonstrate that temperature affects the growth and acidification rate of *L. paracasei* CIDCA strains affecting the time require to form the acid gel. At this point, an equivalent concentration of the three lactobacilli is obtained in the product without changes in organic acids levels. Given that *L. paracasei* CIDCA 83123 has low growth rates at all temperatures assayed, it could be considered the least attractive strain for its application at an industrial level. On the other hand, the ability of CIDCA 8339 and CIDCA 83124 strains to grow well in a wide range of temperatures could be relevant for the industry, since it enables their application in the development of a wide variety of foods without limitations in the product manufacturing conditions. Furthermore, milk fermentation with *L. paracasei* CIDCA 83124 at 20 or 30°C would constitute an alternative to improve the rheological properties of the product. The production *in situ* of EPS will also contribute to the healthy properties attributed to the fermented milk obtained with these strains by promoting the protection against *Salmonella* infection.

In light of these results, it can be concluded that the selection of the EPS-producing strain along with the appropriate fermentation conditions could be an interesting strategy to improve the technological properties of these *L. paracasei* fermented milks with potential health benefits. Deepening the knowledge of EPS structure of these strains would contribute to maximally exploit them for food application.

Data availability statement

The original contributions presented in the study are included in the article/Supplementary material, further inquiries can be directed to the corresponding author.

Author contributions

AB contributed in study design and conception, and performed experimental work, data interpretation, and manuscript writing. AP and MD participated in data discussion and manuscript revising. GG and AA participated in study design and conception, funding, and manuscript revising. All authors contributed to the article and approved the submitted version.

Funding

The present work was supported by CONICET (PIP 2786), Universidad Nacional de La Plata (UNLP 18/X813), ANPCyT (PICT 2020–03973 and PICT 2020–3239), and the Basque Government (IT1662-22 and PIBA 2020_1_0032).

Acknowledgments

AB is fellow of Consejo Nacional de Ciencia y Tecnología (CONICET). MD is member of University of the Basque Country (UPV/EHU), AP is a member of SCIC; GG and AA are members of Scientific Career of CONICET. We thanks C. Reyes Cantera for chromatographic technical assistance and H. Lopardo for providing *Salmonella enteritidis* strain used in the present work.

Conflict of interest

The authors declare that the research was conducted in the absence of any commercial or financial relationships that could be construed as a potential conflict of interest.

Publisher's note

All claims expressed in this article are solely those of the authors and do not necessarily represent those of their affiliated organizations, or those of the publisher, the editors and the reviewers. Any product that may be evaluated in this article, or claim that may be made by its manufacturer, is not guaranteed or endorsed by the publisher.

Supplementary material

The Supplementary material for this article can be found online at: https://www.frontiersin.org/articles/10.3389/fmicb.2023.1110177/full#supplementary-material

References

Ale, E. C., Rojas, M. F., Reinheimer, J. A., and Binetti, A. G. (2020). *Lactobacillus fermentum*: could EPS production ability be responsible for functional properties? *Food Microbiol.* 90:103465. doi: 10.1016/J.FM.2020.103465

Amini, E., Salimi, F., Imanparast, S., and Mansour, F. N. (2022). Isolation and characterization of exopolysaccharide derived from *Lacticaseibacillus paracasei* AS20(1) with probiotic potential and evaluation of its antibacterial activity. *Lett. Appl. Microbiol.* 75, 967–981. doi: 10.1111/LAM.13771

Amiri, S., Rezaei Mokarram, R., Sowti Khiabani, M., Rezazadeh Bari, M., and Alizadeh Khaledabad, M. (2019). Exopolysaccharides production by *lactobacillus acidophilus* LA5 and *Bifidobacterium animalis* subsp. *lactis* BB12: optimization of fermentation variables and characterization of structure and bioactivities. *Int. J. Biol. Macromol.* 123, 752–765. doi: 10.1016/J.IJBIOMAC.2018.11.084

Bachtarzi, N., Kharroub, K., and Ruas-Madiedo, P. (2019). Exopolysaccharide-producing lactic acid bacteria isolated from traditional Algerian dairy products and their application for skim-milk fermentations. *LWT* 107, 117–124. doi: 10.1016/J.LWT.2019.03.005

Bachtarzi, N., Speciale, I., Kharroub, K., De Castro, C., Ruiz, L., and Ruas-Madiedo, P. (2020). Selection of exopolysaccharide-producing *lactobacillus plantarum* (*Lactiplantibacillus plantarum*) isolated from algerian fermented foods for the manufacture of skim-milk fermented products. *Microorganisms* 8:1101. doi: 10.3390/MICROORGANISMS8081101

Balzaretti, S., Taverniti, V., Guglielmetti, S., Fiore, W., Minuzzo, M., Ngo, H. N., et al. (2017). A novel rhamnose-rich hetero-exopolysaccharide isolated from *lactobacillus paracasei* DG activates THP-1 human monocytic cells. *Appl. Environ. Microbiol.* 83, e02702–e02716. doi: 10.1128/aem.02702-16

Bengoa, A. A., Dardis, C., Gagliarini, N., Garrote, G. L., and Abraham, A. G. (2020a). Exopolysaccharides from *lactobacillus paracasei* isolated from kefir as potential bioactive compounds for microbiota modulation. *Front. Microbiol.* 11:583254. doi: 10.3389/FMICB.2020.583254/BIBTEX

Bengoa, A. A., Dardis, C., Garrote, G. L., and Abraham, A. G. (2021). Health-promoting properties of *Lacticaseibacillus paracasei*: a focus on kefir isolates and exopolysaccharide-producing strains. *Foods* 10:2239. doi: 10.3390/FOODS10102239

Bengoa, A. A., Errea, A. J., Rumbo, M., Abraham, A. G., and Garrote, G. L. (2020b). Modulatory properties of *lactobacillus paracasei* fermented milks on gastric inflammatory conditions. *Int. Dairy J.* 111:104839. doi: 10.1016/j.idairyj.2020.104839

Bengoa, A. A., Iraporda, C., Acurcio, L. B., de Cicco Sandes, S. H., Costa, K., Moreira Guimarães, G., et al. (2019a). Physicochemical, immunomodulatory and safety aspects of milks fermented with *lactobacillus paracasei* isolated from kefir. *Food Res. Int.* 123, 48–55. doi: 10.1016/j.foodres.2019.04.041

Bengoa, A. A., Iraporda, C., Garrote, G. L., and Abraham, A. G. (2019b). Kefir micro-organisms: their role in grain assembly and health properties of fermented milk. *J. Appl. Microbiol.* 126, 686–700. doi: 10.1111/jam.14107

Bengoa, A. A., Llamas, M. G., Iraporda, C., Dueñas, M. T., Abraham, A. G., and Garrote, G. L. (2018a). Impact of growth temperature on exopolysaccharide production and probiotic properties of *lactobacillus paracasei* strains isolated from kefir grains. *Food Microbiol.* 69, 212–218. doi: 10.1016/J.FM.2017.08.012

Bengoa, A. A., Zavala, L., Carasi, P., Trejo, S. A., Bronsoms, S., de los Serradell, M. Á., et al. (2018b). Simulated gastrointestinal conditions increase adhesion ability of *lactobacillus paracasei* strains isolated from kefir to Caco-2 cells and mucin. *Food Res. Int.* 103, 462–467. doi: 10.1016/j.foodres.2017.09.093

Bhat, B., and Bajaj, B. K. (2019). Hypocholesterolemic potential and bioactivity spectrum of an exopolysaccharide from a probiotic isolate *lactobacillus paracasei* M7. *Bioact. Carbohydr. Diet. Fibre* 19:100191. doi: 10.1016/j.bcdf.2019.100191

Caggianiello, G., Kleerebezem, M., and Spano, G. (2016). Exopolysaccharides produced by lactic acid bacteria: from health-promoting benefits to stress tolerance mechanisms. *Appl. Microbiol. Biotechnol.* 100, 3877–3886. doi: 10.1007/S00253-016-7471-2/FIGURES/2

Chen, L., Gu, Q., and Zhou, T. (2022). Statistical optimization of novel medium to maximize the yield of exopolysaccharide from *Lacticaseibacillus rhamnosus* ZFM216 and its immunomodulatory activity. *Front. Nutr.* 9:1124. doi: 10.3389/FNUT.2022.924495/BIBTEX

Chen, Y. C., Wu, Y. J., and Hu, C. Y. (2019). Monosaccharide composition influence and immunomodulatory effects of probiotic exopolysaccharides. *Int. J. Biol. Macromol.* 133, 575–582. doi: 10.1016/J.IJBIOMAC.2019.04.109

Cobos, A., Horne, D. S., and Muir, D. D. (1995). Rheological properties of acid milk gels. I. Effect of composition, process and acidification conditions on products from recombined milks. *Milchwissenschaft* 50, 444–448.

Daba, G. M., Elnahas, M. O., and Elkhateeb, W. A. (2021). Contributions of exopolysaccharides from lactic acid bacteria as biotechnological tools in food, pharmaceutical, and medical applications. *Int. J. Biol. Macromol.* 173, 79–89. doi: 10.1016/j.ijbiomac.2021.01.110

Dalcanton, F., Carrasco, E., Pérez-Rodríguez, F., Posada-Izquierdo, G. D., Falcão De Aragão, G. M., and García-Gimeno, R. M. (2018). Modeling the combined effects of temperature, pH, and sodium chloride and sodium lactate concentrations on the growth rate of *lactobacillus plantarum* ATCC 8014. *J. Food Qual.* 2018, 1–10. doi: 10.1155/2018/1726761

De Angelis, M., and Gobbetti, M. (2004). Environmental stress responses in *lactobacillus*: a review. *Proteomics* 4, 106–122. doi: 10.1002/PMIC.200300497

de Carvalho, A. P. A., and Conte-Junior, C. A. (2021). Food-derived biopolymer kefiran composites, nanocomposites and nanofibers: emerging alternatives to food packaging and potentials in nanomedicine. *Trends Food Sci. Technol.* 116, 370–386. doi: 10.1016/J.TIFS.2021.07.038

Dedhia, N., Marathe, S. J., and Singhal, R. S. (2022). Food polysaccharides: a review on emerging microbial sources, bioactivities, nanoformulations and safety considerations. *Carbohydr. Polym.* 287:119355. doi: 10.1016/J.CARBPOL.2022.119355

Galli, V., Venturi, M., Mari, E., Guerrini, S., and Granchi, L. (2022). Selection of yeast and lactic acid bacteria strains, isolated from spontaneous raw milk fermentation, for the production of a potential probiotic fermented milk. *Fermentation* 8:407. doi: 10.3390/FERMENTATION8080407

Gangoiti, M. V., Puertas, A. I., Hamet, M. F., Peruzzo, P. J., Llamas, M. G., Medrano, M., et al. (2017). *Lactobacillus plantarum* CIDCA 8327: an α-glucan producing-strain isolated from kefir grains. *Carbohydr. Polym.* 170, 52–59. doi: 10.1016/J.CARBPOL.2017.04.053

Golowczyc, M. A., Mobili, P., Garrote, G. L., Abraham, A. G., and De Antoni, G. L. (2007). Protective action of *lactobacillus kefir* carrying S-layer protein against *salmonella enterica* serovar Enteritidis. *Int. J. Food Microbiol.* 118, 264–273. doi: 10.1016/J.IJFOODMICRO.2007.07.042

Hackley, V. A., and Ferraris, C. F. (2001). *Guide to Rheological Nomenclature: Measurement in Ceramic Particulate Systems*. Gaithersburg, MD: Special Publication (NIST SP), National Institute of Standards and Technology.

Hamet, M. F., Londero, A., Medrano, M., Vercammen, E., Van Hoorde, K., Garrote, G. L., et al. (2013). Application of culture-dependent and culture-independent methods for the identification of *lactobacillus kefiranofaciens* in microbial consortia present in kefir grains. *Food Microbiol.* 36, 327–334. doi: 10.1016/j.fm.2013.06.022

Hamet, M. F., Piermaria, J. A., and Abraham, A. G. (2015). Selection of EPS-producing *lactobacillus* strains isolated from kefir grains and rheological characterization of the fermented milks. *LWT-Food Sci. Technol.* 63, 129–135. doi: 10.1016/j.lwt.2015.03.097

Hee, K., Choi, H. S., Kim, J. E., and Han, N. S. (2011). Exopolysaccharide-overproducing *lactobacillus paracasei* KB28 induces cytokines in mouse peritoneal macrophages via modulation of NF-kB and MAPKs. *J. Microbiol. Biotechnol.* 21, 1174–1178. doi: 10.4014/JMB.1105.05026

Ibarburu, I., Puertas, A. I., Berregi, I., Rodríguez-Carvajal, M. A., Prieto, A., and Dueñas, M. T. (2015). Production and partial characterization of exopolysaccharides produced by two *lactobacillus suebicus* strains isolated from cider. *Int. J. Food Microbiol.* 214, 54–62. doi: 10.1016/j.ijfoodmicro.2015.07.012

Khanal, S. N., and Lucey, J. A. (2018). Effect of fermentation temperatur re on the properties of exopolysaccharides and the acid gelation behavior for milk fermented by *Streptococcus thermophilus* strains DGCC7785 and St-143. *J. Dairy Sci.* 101, 3799–3811. doi: 10.3168/JDS.2017-13203

König, H., and Berkelmann-Löhnertz, B. (2017). "Maintenance of Wine-Associated Microorganisms," in *Biology of Microorganisms on Grapes, in Must and in Wine*. eds. H. König, G. Unden and J. Fröhlich (Cham: Springer).

Laiño, J., Villena, J., Kanmani, P., and Kitazawa, H. (2016). Immunoregulatory effects triggered by lactic acid bacteria exopolysaccharides: new insights into molecular interactions with host cells. *Microorganisms* 4:27. doi: 10.3390/MICROORGANISMS4030027

Leeuwendaal, N. K., Stanton, C., O'Toole, P. W., and Beresford, T. P. (2022). Fermented foods, health and the gut microbiome. *Nutrients* 14:1527. doi: 10.3390/NU14071527

Li, X. W., Lv, S., Shi, T. T., Liu, K., Li, Q. M., Pan, L. H., et al. (2020). Exopolysaccharides from yoghurt fermented by *lactobacillus paracasei*: production, purification and its binding to sodium caseinate. *Food Hydrocoll.* 102:105635. doi: 10.1016/J.FOODHYD.2019.105635

Liu, H., Xie, Y. H., Han, T., and Zhang, H. X. (2013). Purification and structure study on exopolysaccharides produced by *Lactobacillus paracasei* KL1-Liu from Tibetan kefir. *Adv. Mater. Res.* 781–784, 1513–1518. doi: 10.4028/WWW.SCIENTIFIC.NET/AMR.781-784.1513

Llamas-Arriba, M. G., Puertas, A. I., Prieto, A., López, P., Cobos, M., Miranda, J. I., et al. (2019). Characterization of dextrans produced by *lactobacillus Mali* CUPV271 and *Leuconostoc carnosum* CUPV411. *Food Hydrocoll.* 89, 613–622. doi: 10.1016/J.FOODHYD.2018.10.053

Lucey, J. A., and Singh, H. (1997). Formation and physical properties of acid milk gels: a review. *Food Res. Int.* 30, 529–542. doi: 10.1016/S0963-9969(98)00015-5

Lynch, K. M., Zannini, E., Coffey, A., and Arendt, E. K. (2018). Lactic acid bacteria exopolysaccharides in foods and beverages: Isolation, properties, characterization, and health benefits. *Annu. Rev. Food Sci. Technol.* 9, 155–176.

Medrano, M., Gangoiti, M. V., Simonelli, N., and Abraham, A. G. (2020). Kefiran fermentation by human faecal microbiota: organic acids production and in vitro biological activity. *Bioact. Carbohydr. Diet. Fibre* 24:100229. doi: 10.1016/J.BCDF.2020.100229

Mende, S., Rohm, H., and Jaros, D. (2016). Influence of exopolysaccharides on the structure, texture, stability and sensory properties of yoghurt and related products. *Int. Dairy J.* 52, 57–71. doi: 10.1016/J.IDAIRYJ.2015.08.002

Mustafa, S. M., Chua, L. S., El-Enshasy, H. A., Abd Majid, F. A., Hanapi, S. Z., and Abdul Malik, R. (2019). Effect of temperature and pH on the probiotication of Punica granatum juice using *lactobacillus* species. *J. Food Biochem.* 43:e12805. doi: 10.1111/JFBC.12805

Nadzir, M. M., Nurhayati, R. W., Idris, F. N., and Nguyen, M. H. (2021). Biomedical applications of bacterial exopolysaccharides: a review. *Polymers* 13:530. doi: 10.3390/POLYM13040530

Notararigo, S., Nácher-Vázquez, M., Ibarburu, I., Werning, M., De Palencia, P. F., Dueñas, M. T., et al. (2013). Comparative analysis of production and purification of homo-and hetero-polysaccharides produced by lactic acid bacteria. *Carbohydr. Polym.* 93, 57–64. doi: 10.1016/J.CARBPOL.2012.05.016

Oerlemans, M. M. P., Akkerman, R., Ferrari, M., Walvoort, M. T. C., and de Vos, P. (2021). Benefits of bacteria-derived exopolysaccharides on gastrointestinal microbiota, immunity and health. *J. Funct. Foods* 76:104289. doi: 10.1016/J.JFF.2020.104289

Oleksy, M., and Klewicka, E. (2018). Exopolysaccharides produced by *lactobacillus* sp.: biosynthesis and applications. *Crit. Rev. Food Sci. Nutr.* 58, 450–462. doi: 10.1080/10408398.2016.1187112

Østlie, H. M., Treimo, J., and Narvhus, J. A. (2005). Effect of temperature on growth and metabolism of probiotic bacteria in milk. *Int. Dairy J.* 15, 989–997. doi: 10.1016/J.IDAIRYJ.2004.08.015

Pendón, M. D., Bengoa, A. A., Iraporda, C., Medrano, M., Garrote, G. L., and Abraham, A. G. (2021). Water kefir: factors affecting grain growth and health-promoting properties of the fermented beverage|enhanced reader. *J. Appl. Microbiol.* 133, 162–180. doi: 10.1111/jam.15385

Piermaria, J., López-Castejón, M. L., Bengoechea, C., Guerrero, A., and Abraham, A. G. (2021). Prebiotic emulsions stabilised by whey protein and kefiran. *Int. J. Food Sci. Technol.* 56, 76–85. doi: 10.1111/ijfs.14601

Rimada, P. S., and Abraham, A. G. (2003). Comparative study of different methodologies to determine the exopolysaccharide produced by kefir grains in milk and whey. *Lait* 83, 79–87. doi: 10.1051/LAIT:2002051

Rimada, P. S., and Abraham, A. G. (2006). Kefiran improves rheological properties of glucono-δ-lactone induced skim milk gels. *Int. Dairy J.* 16, 33–39. doi: 10.1016/J.IDAIRYJ.2005.02.002

Ruas-Madiedo, P., Abraham, A. G., Mozzi, F., and de los Reyes-Gavilán, C. G. (2009). Functionality of exopolysaccharides produced by lactic acid bacteria in an in vitro gastric system. *J. Appl. Microbiol.* 107, 56–64. doi: 10.1111/j.1365-2672.2009.04182.x

Ruas-Madiedo, P., and Zoon, P. (2003). Effect of exopolysaccharide-producing *Lactococcus lactis* strains and temperature on the permeability of skim milk gels. *Colloids Surf. A Physicochem. Eng. Asp.* 213, 245–253. doi: 10.1016/S0927-7757(02)00517-4

Ryan, P. M., Ross, R. P., Fitzgerald, G. F., Caplice, N. M., and Stanton, C. (2015). Sugar-coated: exopolysaccharide producing lactic acid bacteria for food and human health applications. *Food Funct.* 6, 679–693. doi: 10.1039/c4fo00529e

Sabater, C., Molinero-García, N., Castro-Bravo, N., Diez-Echave, P., Hidalgo-García, L., Delgado, S., et al. (2020). Exopolysaccharide producing Bifidobacterium animalis subsp. lactis strains modify the intestinal microbiota and the plasmatic cytokine levels of BALB/c mice according to the type of polymer synthesized. *Front. Microbiol.* 11:601233. doi: 10.3389/FMICB.2020.601233/BIBTEX

Sánchez, Ó. J., Barragán, P. J., and Serna, L. (2019). Review of *lactobacillus* in the food industry and their culture media. *Rev. Colomb. Biotecnol.* 21, 63–76. doi: 10.15446/REV.COLOMB.BIOTE.V21N2.81576

Saori Ishii Mauro, C., and Garcia, S. (2019). Coconut milk beverage fermented by *lactobacillus reuteri*: optimization process and stability during refrigerated storage. *J. Food Sci. Technol.* 56, 854–864. doi: 10.1007/S13197-018-3545-8

Simonelli, N., Gagliarini, N., Medrano, M., Piermaria, J. A., and Abraham, A. G. (2022). "Kefiran" in *Polysaccharides of Microbial Origin*. eds. J. M. Oliveira, H. Radhouani and R. L. Reis (Cham, 116: Springer).

Śliżewska, K., and Chlebicz-Wójcik, A. (2020). Growth kinetics of probiotic *lactobacillus* strains in the alternative, cost-efficient semi-solid fermentation medium. *Biol.* 9:423. doi: 10.3390/BIOLOGY9120423

Smokvina, T., Wels, M., Polka, J., Chervaux, C., Brisse, S., Boekhorst, J., et al. (2013). *Lactobacillus paracasei* comparative genomics: towards species pan-genome definition and exploitation of diversity. *PLoS One* 8:e68731. doi: 10.1371/JOURNAL.PONE.0068731

Tamang, J. P., Watanabe, K., and Holzapfel, W. H. (2016). Review: diversity of microorganisms in global fermented foods and beverages. *Front. Microbiol.* 7:337. doi: 10.3389/fmicb.2016.00377

Torino, M. I., de Valdez, G. F., and Mozzi, F. (2015). Biopolymers from lactic acid bacteria. Novel applications in foods and beverages. *Front. Microbiol.* 6:834. doi: 10.3389/FMICB.2015.00834/BIBTEX

Wang, X., Tian, J., Zhang, X., Tang, N., Rui, X., Zhang, Q., et al. (2022). Characterization and immunological activity of exopolysaccharide from *Lacticaseibacillus paracasei* GL1 isolated from Tibetan kefir grains. *Foods* 11:3330. doi: 10.3390/FOODS11213330

Welman, A. D., and Maddox, I. S. (2003). Exopolysaccharides from lactic acid bacteria: perspectives and challenges. *Trends Biotechnol.* 21, 269–274. doi: 10.1016/S0167-7799(03)00107-0

Werning, M. L., Hernández-Alcántara, A. M., Ruiz, M. J., Soto, L. P., Dueñas, M. T., López, P., et al. (2022). Biological functions of exopolysaccharides from lactic acid bacteria and their potential benefits for humans and farmed animals. *Foods* 11:1284. doi: 10.3390/FOODS11091284

Xiao, L., Xu, D., Tang, N., Rui, X., Zhang, Q., Chen, X., et al. (2021). Biosynthesis of exopolysaccharide and structural characterization by *Lacticaseibacillus paracasei* ZY-1 isolated from Tibetan kefir. *Food Chem. Mol. Sci.* 3:100054. doi: 10.1016/J.FOCHMS.2021.100054

Xu, Y., Cui, Y., Yue, F., Liu, L., Shan, Y., Liu, B., et al. (2019). Exopolysaccharides produced by lactic acid bacteria and Bifidobacteria: structures, physiochemical functions and applications in the food industry. *Food Hydrocoll.* 94, 475–499. doi: 10.1016/j.foodhyd.2019.03.032

Yang, E., Fan, L., Yan, J., Jiang, Y., Doucette, C., Fillmore, S., et al. (2018). Influence of culture media, pH and temperature on growth and bacteriocin production of bacteriocinogenic lactic acid bacteria. *AMB Express* 8, 1–14. doi: 10.1186/S13568-018-0536-0/FIGURES/6

You, X., Li, Z., Ma, K., Zhang, C., Chen, X., Wang, G., et al. (2020a). Structural characterization and immunomodulatory activity of an exopolysaccharide produced by *lactobacillus helveticus* LZ-R-5. *Carbohydr. Polym.* 235:115977. doi: 10.1016/J.CARBPOL.2020.115977

You, X., Yang, L., Zhao, X., Ma, K., Chen, X., Zhang, C., et al. (2020b). Isolation, purification, characterization and immunostimulatory activity of an exopolysaccharide produced by *lactobacillus pentosus* LZ-R-17 isolated from Tibetan kefir. *Int. J. Biol. Macromol.* 158, 408–419. doi: 10.1016/J.IJBIOMAC.2020.05.027

Zavala, L., Golowczyc, M. A., Van Hoorde, K., Medrano, M., Huys, G., Vandamme, P., et al. (2016). Selected *lactobacillus* strains isolated from sugary and milk kefir reduce *salmonella* infection of epithelial cells *in vitro*. *Benef. Microbes* 7, 585–595. doi: 10.3920/BM2015.0196

Zeidan, A. A., Poulsen, V. K., Janzen, T., Buldo, P., Derkx, P. M. F., Øregaard, G., et al. (2017). Polysaccharide production by lactic acid bacteria: from genes to industrial applications. *FEMS Microbiol. Rev.* 41, S168–S200. doi: 10.1093/FEMSRE/FUX017

Zhang, Y., Dai, X., Jin, H., Man, C., and Jiang, Y. (2021). The effect of optimized carbon source on the synthesis and composition of exopolysaccharides produced by *lactobacillus paracasei*. *J. Dairy Sci.* 104, 4023–4032. doi: 10.3168/JDS.2020-19448

Zhang, L., Zhao, B., Liu, C. J., and Yang, E. (2020). Optimization of biosynthesis conditions for the production of exopolysaccharides by *lactobacillus plantarum* SP8 and the exopolysaccharides antioxidant activity test. *Indian J. Microbiol.* 60, 334–345. doi: 10.1007/S12088-020-00865-8/FIGURES/5

Zheng, J., Wittouck, S., Salvetti, E., Franz, C. M. A. P., Harris, H. M. B., Mattarelli, P., et al. (2020). A taxonomic note on the genus *lactobacillus*: description of 23 novel genera, emended description of the genus *lactobacillus* Beijerinck 1901, and union of *Lactobacillaceae* and *Leuconostocaceae*. *Int. J. Syst. Evol. Microbiol.* 70, 2782–2858. doi: 10.1099/ijsem.0.004107

Zhu, Y., Wang, X., Pan, W., Shen, X., He, Y., Yin, H., et al. (2019). Exopolysaccharides produced by yogurt-texture improving *lactobacillus plantarum* RS20D and the immunoregulatory activity. *Int. J. Biol. Macromol.* 121, 342–349. doi: 10.1016/J.IJBIOMAC.2018.09.201

frontiers | Frontiers in Microbiology

TYPE Original Research
PUBLISHED 24 February 2023
DOI 10.3389/fmicb.2023.1111516

OPEN ACCESS

EDITED BY
Paloma López,
Margarita Salas Center for Biological Research (CSIC), Spain

REVIEWED BY
John Renye,
Agricultural Research Service (USDA), United States
Rodney Honrada Perez,
University of the Philippines Los Baños, Philippines

*CORRESPONDENCE
Guorong Liu
✉ liuguorong1983@126.com

†These authors have contributed equally to this work and share first authorship

SPECIALTY SECTION
This article was submitted to Food Microbiology, a section of the journal Frontiers in Microbiology

RECEIVED 29 November 2022
ACCEPTED 30 January 2023
PUBLISHED 24 February 2023

CITATION
Nie R, Zhu Z, Qi Y, Wang Z, Sun H and Liu G (2023) Bacteriocin production enhancing mechanism of *Lactiplantibacillus paraplantarum* RX-8 response to *Wickerhamomyces anomalus* Y-5 by transcriptomic and proteomic analyses. *Front. Microbiol.* 14:1111516. doi: 10.3389/fmicb.2023.1111516

Bacteriocin production enhancing mechanism of *Lactiplantibacillus paraplantarum* RX-8 response to *Wickerhamomyces anomalus* Y-5 by transcriptomic and proteomic analyses

Rong Nie[1†], Zekang Zhu[1†], Yanwei Qi[2], Zhao Wang[1], Haoxuan Sun[1] and Guorong Liu[1*]

[1]Beijing Advance Innovation Center for Food Nutrition and Human Health, Beijing Laboratory of Food Quality and Safety, Beijing Engineering and Technology Research Center of Food Additives, Beijing Technology and Business University, Beijing, China, [2]School of Control and Computer Engineering, North China Electric Power University, Beijing, China

Plantaricin is a kind of bacteriocin with broad-spectrum antibacterial activity on several food pathogens and spoilage microorganisms, showing potential in biopreservation applications. However, the low yield of plantaricin limits its industrialization. In this study, it was found that the co-culture of *Wickerhamomyces anomalus* Y-5 and *Lactiplantibacillus paraplantarum* RX-8 could enhance plantaricin production. To investigate the response of *L. paraplantarum* RX-8 facing *W. anomalus* Y-5 and understand the mechanisms activated when increasing plantaricin yield, comparative transcriptomic and proteomic analyses of *L. paraplantarum* RX-8 were performed in mono-culture and co-culture. The results showed that different genes and proteins in the phosphotransferase system (PTS) were improved and enhanced the uptake of certain sugars; the key enzyme activity in glycolysis was increased with the promotion of energy production; arginine biosynthesis was downregulated to increase glutamate mechanism and then promoted plantaricin yield; and the expression of several genes/proteins related to purine metabolism was downregulated and those related to pyrimidine metabolism was upregulated. Meanwhile, the increase of plantaricin synthesis by upregulation of *plnABCDEF* cluster expression under co-culture indicated that the PlnA-mediated quorum sensing (QS) system took part in the response mechanism of *L. paraplantarum* RX-8. However, the absence of AI-2 did not influence the inducing effect on plantaricin production. Mannose, galactose, and glutamate were critical metabolites and significantly simulate plantaricin production ($p < 0.05$). In summary, the findings provided new insights into the interaction between bacteriocin-inducing and bacteriocin-producing microorganisms, which may serve as a basis for further research into the detailed mechanism.

KEYWORDS

bacteriocin, co-culture, microorganism interaction, quorum sensing, response mechanism

Introduction

Bacteriocins are proteins or peptides that display antibacterial activity against various spoilage and pathogenic bacteria (Bu et al., 2021b). Bacteriocins from lactic acid bacteria (LAB) are regarded as safe, natural antimicrobials for food biological preservatives (Bu et al., 2021a). However, the manufacturing and secretion of bacteriocin have high metabolic costs; therefore, bacteria have developed regulatory mechanisms that relay quorum sensing (QS) signals to generate bacteriocins only upon necessity (Kern et al., 2021). As they lack competitors, bacteriocin production is low and may be gradually lost in ideal laboratory conditions. To increase bacteriocin production, it is useful to add certain microorganisms to induce bacteriocin-producing bacteria to produce more bacteriocins. This approach uses the interaction between different strains in mixed culture and was widespread in the area of natural bacteriocin production (Chanos and Mygind, 2016).

Plantaricin, a class IIb bacteriocin produced by *Lactiplantibacillus plantarum*, is often induced by the bacteria–bacteria interactions. The mechanism of induction regulation behind plantaricin production under co-culturing with other bacteria is associated with QS, the regulation of specific genes in a bacterial population. Specifically, it was reported that the plantaricin production of *L. plantarum* NC8 by co-culture is mediated by the three-component regulatory system, compounded by an autoinduction factor (PlNC8IF), the histidine kinase (PlNC8HK), and the response regulator (RR; PlnD) (Maldonado-Barragán et al., 2013). Furthermore, the interspecies QS molecule AI-2 and its related gene *LuxS* both increased in *L. plantarum* DC400 under co-culture (Calasso et al., 2013). Meanwhile, the two QS signals (PlnA and AI-2) independently participate in the plantaricin induction mechanism of the co-culture system (*L. paraplantarum* RX-8 and *Bacillus subtilis* BS-15) (Liu et al., 2022).

However, the inducing mechanism of bacteriocin production when bacteriocin-producing strains co-culture with fungi remains unknown, especially for plantaricin. It has been reported that undissociated lactate and a low pH strongly inhibit the growth of *Lactococcus lactis* and lead to a low yield of nisin, while *Kluyveromyces marxianus* MS1 (Wardani et al., 2006), *Yarrowia lipolytica* ATCC 18942 (Ariana and Hamedi, 2017), and *Saccharomyces cerevisiae* W303-1A (Liu et al., 2021) could increase nisin production by consuming lactate. However, research involving a detailed mechanism at the gene level is still inadequate. Unlike that in bacteria, the QS system in fungi has different models and the bacteria–fungi interaction has yet to be studied in detail. A deeper understanding of interaction networks between microbes, including bacteria–bacteria, bacteria–fungi, and fungi–fungi, will help in the exploration of the induction mechanism of yeast, which has an inducing effect on bacteriocin production, and provide a new method for control.

Plantaricin RX-8 produced by *L. paraplantarum* RX-8 was proven to exhibit broad-spectrum antibacterial activity, and the yield of plantaricin RX-8 was improved by *Wickerhamomyces anomalus* Y-5. In this study, interactions between *L. paraplantarum* RX-8 and *W. anomalus* Y-5, the pH, the plantaricin production, and the transcription levels of related bacteriocin biosynthesis genes from 4 to 32 h in co-culture/mono-culture were investigated. Furthermore, transcriptomic and proteomic technologies were used to compare the difference in gene and protein expression between the *L. paraplantarum* RX-8 cells under a co-culture and mono-culture.

Methods and materials

2.1. Co-culture experiment

L. paraplantarum RX-8 (CGMCC 20852) was isolated from the traditional pickle in Chengdu, Sichuan Province, China. *W. anomalus* Y-5 was isolated from fermented grains of Chinese liquor and stored in the food quality and safety laboratory at Beijing Technology and Business University (Beijing, China). In brief, *L. paraplantarum* RX-8 and *W. anomalus* Y-5 were cultured overnight in De Man–Rogosa–Sharp (MRS) medium at 37°C and Yeast Peptone Dextrose (YPD) medium at 30°C under aerobic conditions, respectively. Then, 1 ml of *L. paraplantarum* RX-8 and *W. anomalus* Y-5 were singly inoculated into 100 ml of MRS liquid media for 24 h at 37°C as mono-cultured samples. Then, 1 ml of *L. paraplantarum* RX-8 and *W. anomalus* Y-5 were simultaneously inoculated into 100 ml of MRS liquid media for 24 h at 37°C as co-cultured samples.

2.2. Determination of viable cells and pH

The viable cells were counted every 4 h from 0 to 32 h, and the assay of viable cell counts was carried out according to the method of Zhang et al. (2021). At the same fermentation time points, the cell-free supernatants (CFSs) were obtained by removing cells through centrifugation (10,000 rpm, 10 min, 4°C). Then, the pH value of the CFSs was measured with a pH meter (PH400, Alalis, USA).

2.3. Plantaricin production assay

The yield of plantaricin in mono-culture/co-culture was assayed through agar well diffusion. After every 4 h (4–32 h) fermentation, the CFSs were obtained by centrifugation at 10,000 rpm for 10 min at 4°C; then, the pH of CFSs was adjusted to 6.0 with 1 mol/L NaOH, and these CFS samples were concentrated by vacuum centrifugal concentration (1,500 rpm, 45°C, 5 h). Wells of 6 mm were loaded with 100 μl of 5-fold concentrated plantaricin in the agar, which was inoculated at about 10^7 CFU *Listeria monocytogenes* 35152. The plates were stored at 4°C overnight to allow for the plantaricin to completely diffuse; then, these plates were cultured for 8 h at 37°C. The bacteriocin activity was expressed in arbitrary units (AU/ml), which are represented as the reciprocal of the highest dilution, showing distinct zones of inhibition, and calculated according to the equation:

$$\text{Bacteriocin activity}\left(\frac{\text{AU}}{\text{mL}}\right) = \frac{a^n}{b \times c}$$

where a is 2 (dilution factor), n is the reciprocal of the highest dilution that resulted in inhibition of the indicator strain, b is 100 μl (sample volume in each well), and c is 5 (sample concentration fold). Furthermore, the relative bacteriocin activity was defined as the ratio of bacteriocin activity in co-culture to that in mono-culture. This was used to evaluate the influence of *W. anomalus* Y-5 on plantaricin production in co-culture.

To verify the role of bacteriocin in the competition of bacteria and yeast, the inhibiting effect of plantaricin on *W. anomalus* Y-5 was determined according to Section 2.3.

2.4. RT-qPCR analysis of plantaricin locus and AI-2 synthesis-related gene

To determine the expression level of plantaricin biosynthesis gene clusters (*plnABCDEF*) and AI-2 synthesis-related genes (*pfs* and *luxS*), cells of *L. paraplantarum* RX-8 were harvested through centrifugation (10,000 rpm, 2 min, 4°C) at every 4 h in mono-culture/co-culture (4–32 h). RNA was extracted from cells using the RNAprep Pure Cell/Bacteria Kit according to the manufacturer's instructions (DP430, Tiangen Biotech, China). The extracted RNA was reverse-transcribed into cDNA using the FastQuant RT Kit (with gDNase) (KR116, Tiangen Biotech, China). The transcriptional levels of *plnABCDEF*, *pfs*, and *luxS* were realized by CFX96 Real-Time PCR Detection System (Bio-Rad, Hercules, CA, USA) using SYBR Green PCR master mix (FP205, Tiangen Biotech, China). The reaction mixture consists of 10 μl 2×SuperReal PreMix Plus, 0.6 μl each of the forward and reverse primer, 1.0 μl cDNA (100 ng), and 7.8 μl nuclease-free H_2O. The amplification program was performed at 95°C for 15 min, followed by 39 cycles of 95°C for 10 s, 55°C for 20 s, and 72°C for 30 s. Primers were designed based on the genome sequence of *L. paraplantarum* RX-8 and synthesized by Beijing Genomics Institute (Table 1). 16S rRNA genes were used as the reference gene. The relative expression levels of target genes at each sampling point for *L. paraplantarum* RX-8 in mono-culture/co-culture were calculated by the ΔΔCt method.

TABLE 1 Primer sequences used for RT-qPCR.

Primer	Sequence (5′-3′)
16S rRNA-F	GCATTAAGCATTCCGCCTGG
16S rRNA-R	ACCTGTATCCATGTCCCCGA
RT-*plnA*-F	CGCTGCGCTTAAGTTAATGT
RT-*plnA*-R	TTTTGAGGTACGCTGGGATT
RT-*plnB*-F	CGATACACAGGCTCGTTTGA
RT-*plnB*-R	GCCCAAGCATCAAAACAAAT
RT-*plnC*-F	GGATTGCACCGTTGGATTAT
RT-*plnC*-R	AGAAACGCGTTCCGATTTTA
RT-*plnD*-F	GTTGCAACGGATGATCAAAA
RT-*plnD*-R	ATAATCCAACGGTGCAATCC
RT-*plnE*-F	TTGAGAAGTTACAATATTCCAGGTTG
RT-*plnE*-R	CCCCTAATATTCAAAATACCACGA
RT-*plnF*-F	TGCTATTTCAGGTGGCGTTT
RT-*plnF*-R	GACAGCGCTAATGACCCAAT
RT-*luxS*-F	CGGATGGATGGCGTGATTGACTG
RT-*luxS*-R	CTTAGCAACTTCAACGGTGTCATGTTC
RT-*pfs*-F	GAATTATTTGTGCGATGGAAGAAGA
RT-*pfs*-R	CGCAAATAATGCAAGTAACATCGCT

2.5. Transcriptomic analysis

2.5.1. RNA extraction, library construction, and transcriptome sequencing

Cell samples of *L. paraplantarum* RX-8 were obtained in co-culture and mono-culture at 24 h by centrifugation (10,000 rpm, 10 min, 4°C). After removing the supernatant, cells were immediately cleaned by phosphate buffered saline (PBS) two times, frozen in liquid nitrogen for 15 min, and then stored at −80°C.

Total RNA extractions were performed using Magen HiPure Universal RNA Kit (Magen, China). RNA concentration and purity were measured using Qubit 3.0 (Thermo Fisher Scientific, MA, USA) and Nanodrop One (Thermo Fisher Scientific, MA, USA), and integrity was confirmed using the Agilent 4200 system (Agilent Technologies, Waldbron, Germany). The RNA samples with an RNA integrity number (RIN) >6.5, and 280/260 ratios >1.5 were further used for RNA-sequencing purposes. Libraries were generated from three replicates using NEB Next® Ultra™ Directional RNA Library Prep Kit for Illumina® (New England Biolabs, MA, USA). From these libraries, the PE150 reads were produced with the Illumina Novaseq6000 platform by Guangdong Magigene Biotechnology Co., Ltd. (Guangzhou, China). All raw RNA-Seq data were submitted to NCBI under BioProject PRJNA901346.

2.5.2. Sequencing data processing

The raw reads were trimmed using Trimmomatic (version 0.36) to obtain the qualified reads (Bolger et al., 2014). Then, the rRNA sequences were removed in the qualified reads mapping with NCBI Rfam datasets using Bowtie2 (version 2.33) (Langdon, 2015). Initially, we mapped the mRNA reads of these samples to the reference genome *L. plantarum* WCFS1 downloaded from NCBI, which was the strain that was most closely related to *L. paraplantarum* RX-8, but the acquired alignment rate was mostly low at around 50% and limited to transcriptomic analysis. Therefore, to obtain a higher mapping rate, we assembled the draft genome of *L. paraplantarum* RX-8 using Unicycler (version 0.4.7) to assemble the combined Illumina NovaSeq PE150 data and Nanopore PromethION data (Wick et al., 2017). The new reference genome was uploaded to the NCBI shared database for research retrieval in NCBI GenBank CP111117-CP111119. Eventually, the transcriptomic data were mapped to the new reference genome using Hisat2 (version 2.1.0) (Kim et al., 2019), and the mapping rate was improved to above 90%. Read counts per genome assembly annotated transcript were calculated using HTseq (version 0.9.1) (Anders et al., 2015).

2.5.3. Differential expression genes detection

The differentially expressed genes (DEGs) between groups (RY and R, three biological replicates) were identified from all genes according to the expression levels of the transcripts, based on the statistics of the fragments per kilobase of each reading, per million mapped reads (FPKM). The DEGs were detected using edgeR (version 3.16.5) with default parameters (Robinson et al., 2010). We then used Benjamini and Hochberg's correction approach to adjust the *p*-values to control the false discovery rate (FDR). The genes were regarded as DEGs if they satisfied the threshold with $FDR \leq 0.05$ and $\left|Log_2FC\right| \geq 1$. These genes were used for further enrichment analysis.

2.5.4. Enrichment analysis

The enrichment analyses of DEGs with Gene Ontology (GO) and Kyoto Encyclopedia of Genes and Genomes (KEGG) databases were implemented using clusterProfiler (version 3.4.4), in which gene length bias was corrected. The GO terms and KEGG pathways with FDR $\leq$ 0.05 were regarded as candidates for enrichment functional annotation *via* the DEGs.

2.6. Proteomic analysis

2.6.1. Cytosolic protein extraction and in-solution protein digestion

Cell samples of *L. paraplantarum* RX-8 in co-culture and mono-culture were collected at 24 h according to Section 2.5.1. The protein was extracted by using a lysis buffer (8 M urea, 50 mM Tris8.0, 1% NP40, 1% sodium deoxycholate, 5 mM dithiothreitol (DTT), 2 mM EDTA, 30 mM nicotinamide, and 3 μm trichostatin A), and, after sonication on ice, the total protein concentration of the supernatant, which was obtained by centrifugation (20,000 rpm, 10 min, 4°C), was determined by using a BCA Protein Assay kit. The protein sample was reduced by DTT (5 mM, 45 min, 30°C), later alkylated with 30 mM iodoacetamide (30 mM, 1 h, RT) in darkness, and then precipitated with ice-cold acetone. After being washed thrice with acetone, the precipitate was suspended in 0.1 M triethylammonium bicarbonate (TEAB) and digested with trypsin (1/25 protein mass, Promega) for 12 h at 37°C. Finally, the reaction was ended with 1% trifluoroacetic acid (TFA), and the resulting peptide was desalted with Strata X C18 SPE column (Phenomenex, Torrance, CA, USA) and vacuum-dried in Scanvac maxi-beta (Labogene, Alleroed, Denmark).

2.6.2. TMT labeling and HPLC fractionation

After reduction and alkylation, six digested peptide samples (RY and R, three biological replicates, 100 μg/sample) were transferred to the TMT Reagent vial (Thermo Fisher Scientific, 90066) and incubated for 2 h at room temperature. Then, 8 μl of 5% hydroxylamine was added to the mixture and incubated for 15 min to quench the reaction. Finally, the labeled samples were fractionated into 15 fractions by XBridge Shield C18 RP column (Waters, Milford, MA, USA) in an LC20AD HPLC system (Shimadzu, Kyoto, Japan) for proteomic analysis.

2.6.3. LC-MS analysis

The sample was loaded to the column equilibrated with buffers A (0.1% formic acid in water) and B (0.1% formic acid in acetonitrile). The Acclaim PepMap 100 C18 trap column (75 μm × 2 cm, Dionex) was equilibrated with liquid A by Ultimate 3000 nanoUPLC (Dionex), and the sample was eluted onto an Acclaim PepMap RSLC C18 analytical column (75 μm × 25 cm, Dionex) at a flow rate of 300 nl/min. The liquid-phase gradient was given as follows: 0–6 min, where the linear gradient of buffer B was from 2 to 10%; 7–51 min, where the linear gradient of buffer B was from 10 to 20%; 51–53 min, where the linear gradient of buffer B was from 20 to 80%; 53–57 min, where the linear gradient of buffer B solution was held at 80%.

Mass analysis was performed by nano-spray ionization-mass spectrometry (NSI-MS) and Q-Exactive HF mass spectrometry (Thermo Scientific). The intact peptide was detected by the Orbitrap, the scanning range was set to 250–1,500 m/z, the automatic gain control (AGC) target was 3E6, the resolution was 70,000, the max injection time (IT) was 250 ms, and the dynamic exclusion time was 15 s. The peptide was selected and fragmented for MS/MS using 28% NCE; ion fragments were detected in the Orbitrap, the resolution was 17,500, AGC was 1E5 or 5E4, and the maximum IT was 100 or 200 ms. LC-MS was performed by Micrometer Biotech (Hangzhou, China).

2.6.4. Protein database search and protein quantification

To improve the accuracy of protein identification, RNA-Seq data as mentioned earlier were used to construct specific reference protein databases using DIAMOND (version 2.0.15) (Buchfink et al., 2015). The MS files were searched against the sample-specific *L. paraplantarum* RX-8 database using MaxQuant (version 1.5.2.8) (Tyanova et al., 2016). The mass error of precursor and fragment ions was set as 10 ppm and 0.02 Da, respectively. Trypsin was selected for enzyme specificity and two missed cleavages were allowed. Carbamidomethylation on Cys, TMT 6-plex tag of Lys, and peptide N-terminal was specified as a fixed modification. The variable modifications were oxidation on Met and TMT 6-plex tag on Tyr. FDR was estimated by reverse-decoy strategy, percolator algorithm, and peptide–spectrum match (PSM). $P < 0.05$ and $e < 0.05$ were used to calculate the results. For quantitation, a protein must have at least two unique peptides with the above identity. The protein ratio type was median, and the normalization method was median. All the raw files were uploaded to PRIDE with the accession number PXD038315.

2.6.5. Bioinformatics analysis

The proteins identified as differentially expressed proteins (DEPs) should satisfy the threshold of $p \leq 0.05$ and $\left|Fold\ Change\right| \geq 1.3$. The enrichment analysis of DEPs used the clusterProfiler (version 3.4.4) for GO function annotation and KEGG pathways (Yu et al., 2012). The GO terms and KEGG pathways were regarded as significant protein enrichment annotations using the DEPs.

TABLE 2 Primers used for key differential genes verification.

Primer	Sequence (5′-3′)
16S rRNA-F	GCATTAAGCATTCCGCCTGG
16S rRNA-R	ACCTGTATCCATGTCCCCGA
RT-*oppA*-F	ATACGACGATGCTGTGAAGAAG
RT-*oppA*-R	GTTGCTGAGGCTTGTTGATAGA
RT-*agrA*-F	GCCATTGTCAATCGCCGTAA
RT-*agrA*-R	TTAGATGATGGTGAACTGGAGTAC
RT-*pstS*-F	GGCACAAGGCTCTGGAACT
RT-*pstS*-R	TTAACGGTCTGTACGGACTGAT
RT-*glnA*-F	GGTATCGCTGACTTGCCATC
RT-*glnA*-R	GCTAACTTGCTGACGGTATGAT
RT-*agrH*-F	TGTCAGTTGGAGTAGTTATGAGTTC
RT-*agrH*-R	CCTTCATCACGGTCAATAGCC
RT-*purD*-F	CGGTCACATAATCTTCAATCAACAC
RT-*purD*-R	AGGCGGCAACGGCAATT

2.7. Key differential genes verification

To validate the transcriptomic and proteomic data, RT-qPCR was employed to measure the expression of selected genes in mRNA, according to Section 2.4. The primers for selected genes were synthesized by the Beijing Genomics Institute, and the sequences are listed in Table 2.

2.8. Key inducing metabolite verification

According to the results of transcriptomic and proteomic analyses, the carbohydrate substance (mannose, galactose, cellobiose, and D-ribose) was added to the mono-culture of *L. paraplantarum* RX-8 at the concentrations of 2, 20, and 200 mM. Meanwhile, the amino acid substance (arginine, cysteine, glutamate, and glutamine) was added to the mono-culture of *L. paraplantarum* RX-8 at the concentrations of 0.5, 1.25, and 2.5 g/L. After being cultured for 24 h at 37°C, the supernatants of each sample were collected for the plantaricin production assay. The mono-culture of *L. paraplantarum* RX-8 was used as a control.

2.9. Determination of AI-2 activity on inducing effect

To determine AI-2's role in inducing effect, AI-2 inhibitor D-ribose (0, 200, 300, and 400 mM) was added to the co-culture system; then, the plantaricin production of these samples at 24 h was detected according to Section 2.2, as described earlier. The plantaricin production in co-culture was used as the positive control, and that in mono-culture was used as the negative control.

The AI-2 activity was detected by the bioluminescence of *Vibrio harveyi* BB170. After overnight culture at 30°C, *V. harveyi* BB170 was diluted in a ratio of 1:5,000 with fresh AB medium. The CFSs of the above samples were adjusted to pH 7.0, then filtrated with a 0.22-μm sterile filter, and added to the diluted BB170 culture at the percentage of 10%. The mixture was incubated at 30°C for 4 h under aerobic conditions (180 rpm), and 200 μl of aliquots were added to white 96-well plates (Thermo, USA) to measure relative luminescence units (RLUs) using the Multi-Detection Plate Reader (SpectraMax i3, Molecular Devices, USA). The suspension of strain BB170 in AB medium (1:5,000) was used as a blank control.

Results and discussion

3.1. Growth dynamics and bacteriocin production of *L. paraplantarum* RX-8 and *W. anomalus* Y-5 under co-culture

The growths of *L. paraplantarum* RX-8/*W. anomalus* Y-5, the pH, and bacteriocin production in co-culture and every mono-culture from 4 to 32 h are shown in Figure 1. The viable cell numbers for the bacteria and yeast in co-culture were tested using different antibiotic susceptibilities of *L. paraplantarum* RX-8/*W. anomalus* Y-5. Up to 16 h, the growth rate of *L. paraplantarum* RX-8 was very consistent between the mono-culture and co-culture. However, a decline in *L. paraplantarum* RX-8 cell number was evident during 20–32 h. *W. anomalus* Y-5 grew poorly in liquid MRS media, as it lacked adequate oxygen and an appropriate temperature. The growth of *W. anomalus* Y-5 was also significantly reduced when *L. paraplantarum* RX-8 was present for 4–20 h, while *W. anomalus* Y-5 began to regrow over 24–32 h. The results of the antimicrobial assay show that plantaricin from *L. paraplantarum* RX-8 could not inhibit the growth of *W. anomalus* Y-5 (Supplementary Figure 1). A suitable pH for *W. anomalus* Y-5 growth was about 5.5. It was also reported that *W. anomalus* could not grow well under low pH conditions (Tian et al., 2020). The competitive effect of the two strains may be caused by nutrient competition and acid stress.

In the fermentation, *L. paraplantarum* RX-8 produced lactic acid and other organic acids, which rapidly decreased the pH value. The pH value of *L. paraplantarum* RX-8 under co-culture and mono-culture was similar from 4 to 12 h and rapidly declined from pH 5.7 to pH 3.8. The pH value in co-culture (pH 3.79–3.99) was slightly higher than that in mono-culture (pH 3.57–3.70) of *L. paraplantarum* RX-8 from 16 to 32 h. The pH value of *W. anomalus* Y-5 under mono-culture was maintained at 5.5–6.0. A reason for the increased pH in co-culture from 16 to 32 h may be that less organic acid is produced by *L. paraplantarum* RX-8, or it may be due to ammonia and proton production *via W. anomalus* Y-5.

Similarly, the bacteriocin production in co-culture did not increase until 16 h compared with that in mono-culture, then reached the highest point at 20 h, and stabilized in the 20–24 h period before declining at 28 h. Compared with the decrease in the population of *L. paraplantarum* RX-8, the bacteriocin activity of *L. paraplantarum* RX-8 in co-culture was promoted effectively. This suggests that the inducing effect of bacteriocin production is not due to an increase in cell number. Specifically, bacteriocin production at 24 h in co-culture finally reached 512 AU/ml and showed the most significant

10.3389/fmicb.2023.1111516

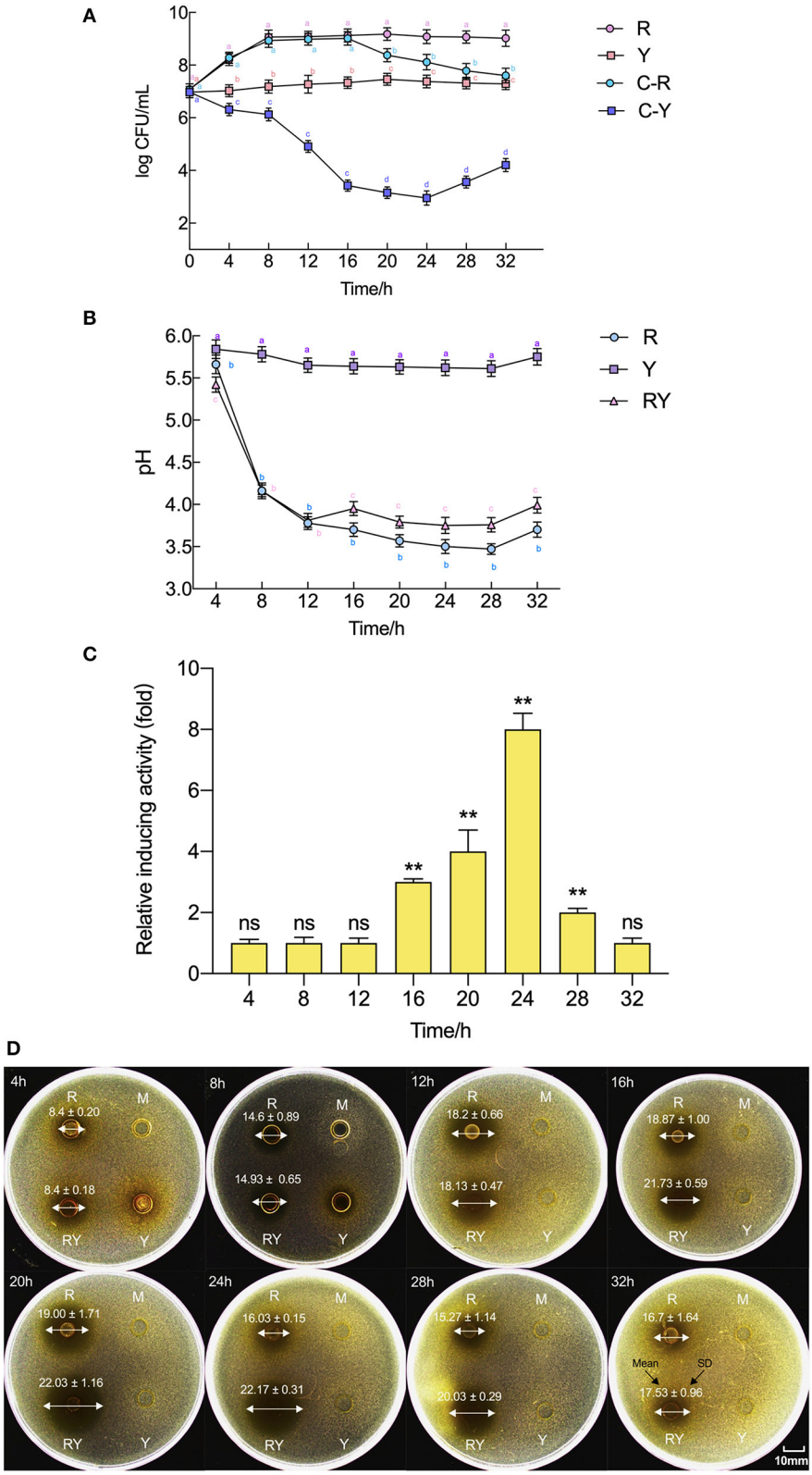

FIGURE 1
Evolution of pH, plantaricin production, and viable cell counts of *L. paraplantarum* RX-8/*W. anomalus* Y-5 in co-culture. **(A)** Indicates viable counts of *L. paraplantarum* RX-8/*W. anomalus* Y-5 at every 4 h from 4 to 32 h in mono-culture and co-culture, **(B)** indicates the pH value of CFS from mono-culture and co-culture at every 4 h from 4 to 32 h, **(C)** indicates the relative inducing activity in co-culture at every 4 h from 4 to 32 h compared with the mono-culture, **(D)** were images of inhibition zone of CFSs from mono-culture and co-culture against *L. monocytogenes* 35152. Mean diameter of inhibition zone (mm) ± standard deviation. R means mono-culture of *L. paraplantarum* RX-8 at 37°C in 4–32 h, Y means mono-culture of *W. anomalus* Y-5 at 37°C in 4–32 h, RY means bacteriocin-inducing co-culture of *L. paraplantarum* RX-8 and *W. anomalus* Y-5 at 37°C in 4–32 h, and M means blank control (MRS, pH 6.0). C-R means the viable cell count of *L. paraplantarum* RX-8 in co-culture, and C-Y means the viable cell count of *W. anomalus* Y-5 in co-culture. ns, not significant, $*p < 0.05$, $**p < 0.01$. Bars with no letter in common for each treatment are significantly different ($p < 0.01$).

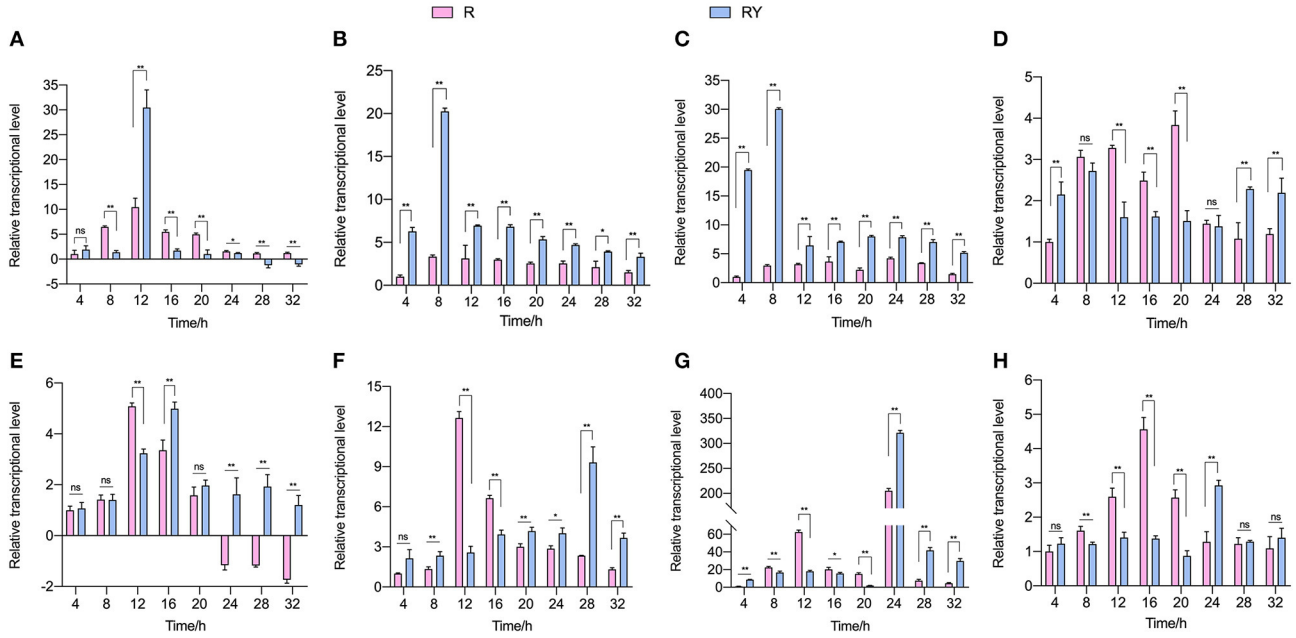

FIGURE 2
Transcriptional level of plantaricin biosynthesis (*plnABCDEF*; **A–F**) and AI-2 synthesis-related gene (*pfs* and *luxS*; **G, H**). R means mono-culture of *L. paraplantarum* RX-8 at 37°C in 4–32 h, and RY means bacteriocin-inducing co-culture of *L. paraplantarum* RX-8 and *W. anomalus* Y-5 at 37°C in 4–32 h. ns, not significant, $*p < 0.05$, $**p < 0.01$.

increase (8-fold) compared to that in mono-culture. Therefore, the sampling point (24 h) was selected for transcriptomic and proteomic analyses to determine the interaction between the two strains.

3.2. Effects of *W. anomalus* Y-5 on the transcription of plantaricin biosynthesis and AI-2 synthesis-related gene

To explore *L. paraplantarum* RX-8's response to the inducing effect from *W. anomalus* Y-5, the plantaricin gene cluster *plnABCDEF* and AI-2 biosynthesis genes *pfs* and *luxS* in *L. paraplantarum* RX-8 were detected by RT-qPCR from 4 to 32 h. As shown in Figure 2, the transcriptional levels of the *L. paraplantarum* RX-8 genes in mono-culture (R) and co-culture (RY) increased over time and then decreased toward the end of their growth. The QS signal PlnA was encoded by *plnA*, which markedly increased in RY compared to that in sample R at 12 h, while the expression of *plnA* showed a decrease at 28 and 32 h in RY (Figure 2A). The reason for these phenomena is that the autoinducing peptide PlnA was secreted at an early stage before the production of bacteriocin. When the concentration of PlnA reached a critical threshold, it would activate the histidine protein kinase (HPK, encoded by *plnB*) on the cell membrane (Liu et al., 2022). However, the *plnB* trend was not consistent with the change of *plnA* in RY (Figure 2B). This indicates that some factors may induce an increase in *plnA*, and signal-transduction proteins may work with *plnB* on plantaricin production under co-culture. For instance, the overexpression of gene *Lp_2642*, belonging to the TetR family, and its regulatory factors could enhance plantaricin EF synthesis in *L. plantarum* 163, and the Lp_2642 protein can bind to the promoter sequence of the *plnA* gene *in vitro* experiments (Zhao et al., 2022). It was predicted that gene *lamK* (HPK) and *lamR* (RRs) would enhance the transcription of genes *plnB* and *plnD*, resulting in an increase in plantaricin EF production (Zhao et al., 2021). Then, the two RRs PlnC and PlnD were phosphorylated by HPK and bound to the promoters of *plnEF* to activate (by *plnC*) or repress (by *plnD*) the production of plantaricin EF (Straume et al., 2009). The transcriptional level of *plnC* in RY was higher than that in R over 4–32 h, and the transcriptional level of *plnD* in RY was lower than that in R over 12–20 h (Figures 2C, D). As for *plnEF*, the transcription expressions of *plnE* and *plnF* in RY were both obviously higher than those in R over 20–32 h, which was consistent with the changes in the plantaricin production (Figures 2E, F). The maximum transcriptional level of *plnE* in R was reached at 12 h; then, it was downregulated from 24 to 32 h. However, the expression of *plnE* in RY was the highest at 16 h, and it remained upregulated at 24–32 h. The maximum transcriptional level of *plnF* in R was reached at 12 h, while it reached the maximum point at 28 h in RY. For the gene of AI-2 biosynthesis' key enzymes, the transcriptional level of *pfs* and *luxS* decreased more in RY compared to R from 8 to 20 h, while they increased in RY at 24 and 28 h (Figures 2G, H). The AI-2 activity at 4–32 h showed the same trend in R and RY (Supplementary Figure 2). However, the effect of AI-2 on the induction process under co-culture is still unclear.

3.3. Transcriptomic and proteomic analyses of *L. paraplantarum* RX-8 in co-culture

To identify the DEGs and DEPs of *L. paraplantarum* RX-8 in response to *W. anomalus* Y-5 under co-culture, the cells of *L. paraplantarum* RX-8 in co-culture and mono-culture were harvested at 24 h for transcriptomic and proteomic analyses. Due to a large amount of transcriptomic data and to reduce the false-positive rate, candidate genes of *L. paraplantarum* RX-8 involved in co-culture were chosen according to the following criteria: (1) more than 2-fold change after normalization; (2) Benjamini and Hochberg's correction approach was used to adjust the *p*-values; and (3) statistically significant level of $p < 0.05$. Finally, the transcription of 580 genes was detected, including 199 upregulated genes and 381 downregulated genes (Figure 3). In addition, iTRAQ was further performed to identify the DEPs of *L. paraplantarum* RX-8 in co-culture and mono-culture. Compared with the transcriptomic data, the amount of proteomic data was relatively small; therefore, FDR verification of the *p*-value was not needed. Compared to the mono-culture group, 339 DEPs (fold change ≥ 1.3, $p < 0.05$) were identified, including 244 upregulated proteins and 95 downregulated proteins (Figure 3). In the Venn diagrams, consistency between the significantly expressed genes and proteins was low. The correlation coefficient between mRNAs and proteins was 0.44 (Figure 3). This can be explained by some biological reasons, including weak ribosome-binding sites, regulatory proteins, codon usage bias, and the half-life difference between protein and mRNA, resulting in gene and protein expression levels that are not always perfectly correlated (Kumar et al., 2016). The 580 DEGs and 339 DEPs were subsequently applied to functional analysis in the functional enrichment of the KEGG pathway. After KEGG analysis, these pathways were remarkably upregulated under co-culture, which included the phosphotransferase system (PTS), glycolysis, galactose metabolism, and pyruvate metabolism (Figure 4). Other pathways were significantly downregulated under co-culture, which included purine metabolism and arginine biosynthesis (Figure 4).

3.3.1 Carbohydrate transport and metabolism of *L. paraplantarum* RX-8 in co-culture

Compared with *L. paraplantarum* RX-8 in mono-culture, *L. paraplantarum* RX-8 in co-culture presented a much stronger carbohydrate utilization ability, which contributes to its great adaptability in competition with *W. anomalus* Y-5. In the process of carbohydrate transport and metabolism, the following metabolic pathways are involved in *L. paraplantarum* RX-8, with or without co-culture: PTS, fructose and mannose metabolism, galactose metabolism, glycolysis, TCA cycle, and amino sugar and nucleotide sugar metabolism.

The phosphotransferase system is responsible for the absorption of sugars, which depends on ATP and the 50 DEGs and 13 DEPs enriched in the PTS. In the PTS, the genes and proteins of mannose transport (*manXaYZ*) and galactitol transport (*gatABC*) are upregulated, while genes and proteins of fructose transport (*FruA/B*) are downregulated. In *Lactobacillus pentosus*, the mannose PTS EIIB participates in the inhibition of the fructose PTS (Chaillou et al., 2001). The mannose PTS in *L. paraplantarum* RX-8 may have a similar effect on inhibiting fructose transport (*FruA/B*). Aside from mannose, other carbohydrates, such as glucose, cellobiose, and maltose, could be transported by the mannose PTS. The sensing of exogenous AI-2 in *Streptococcus pneumoniae* is dependent on FruA; then, AI-2 promotes the transition of the pneumococcus from colonization to invasion by facilitating the utilization of galactose (Trappetti et al., 2017). In *Escherichia coli*, the internalization of AI-2 also depends on the PTS (Ha et al., 2018). AI-2 plays an important role in the inducing effect under a bacteria–bacteria co-culture (Chanos and Mygind, 2016; Liu et al., 2022), while AI-2's role in inducing this effect under fungi–bacteria co-culture needs further investigation. The proteins celA, celB, and celC, comprising the cellobiose transport system permease, take charge of the cellobiose utilization in *L. paraplantarum* RX-8, and are significantly upregulated, by 2.639-, 1.375-, and 2.71-fold, compared to that in mono-culture. However, the gene *celA* showed the opposite expression trend and the gene *celC* did not change. This indicates that post-transcriptional regulation may occur in *L. paraplantarum* RX-8. The gene *crr* encodes the sugar PTS EIIA component; when it is non-phosphorylated, Crr can inhibit the uptake of certain sugars, such as maltose, melibiose, lactose, and glycerol. However, when Crr is phosphorylated, it may activate adenylate cyclase (Saier and Roseman, 1976). The downregulation of the gene *crr* suggests that sugar uptake restrictions are lifted. Moreover, the mannose PTS EIIC acts as a target protein to confer class II bacteriocin sensitivity in *L. monocytogenes*, *Enterococcus faecalis*, and *Latilactobacillus sakei* (Kjos et al., 2009; Jeckelmann and Erni, 2020). The class IIa bacteriocin, immunity protein, and receptor proteins (mannose PTS EIIC and EIID) build up a tight complex to prevent pore formation and block cell death (Diep et al., 2007). However, the relationship between the mannose PTS and the immunity of class IIb bacteriocin produced by *L. plantarum* has not been reported to date (Kjos et al., 2010). Apart from its dual role in carbohydrate transport, the PTS is involved in the coupling of the sensory and regulatory mechanisms (Lengeler and Jahreis, 2009). The PTS transporter subunit IIB may be related to the effect of β-glucooligosaccharides on enhancing nisin production in *L. lactis* I2 (Lee et al., 2020). According to the results of transcriptomic and proteomic analyses, the PTS seems to be involved in the regulation of the response of *L. paraplantarum* to *W. anomalus* Y-5, leading to an increase in bacteriocin production.

Under co-culture conditions, the genes and proteins responsible for the utilization of cellobiose, lactose, galactose, fructose, sorbitol, galactitol, and ribose were also upregulated in *L. paraplantarum* RX-8. These sugars undergo glycolysis to pyruvate and ATP. Glucose-6-phosphate isomerase (GPI) was upregulated by 2.63-fold, which catalyzed the mutual conversion of glucose-6-phosphate and fructose-6-phosphate and helped sugars to enter the glycolysis pathway. The upregulated phosphoglycerate kinase (PGK), which directly generates ATP by phosphorylating the ADP, suggested that *L. paraplantarum* RX-8 produced more energy under co-culture. The pyruvate produced by glycolysis is a major metabolic intersection connecting the utilization and biosynthetic pathways of carbohydrates or amino acids; it linked the L-cysteine

10.3389/fmicb.2023.1111516

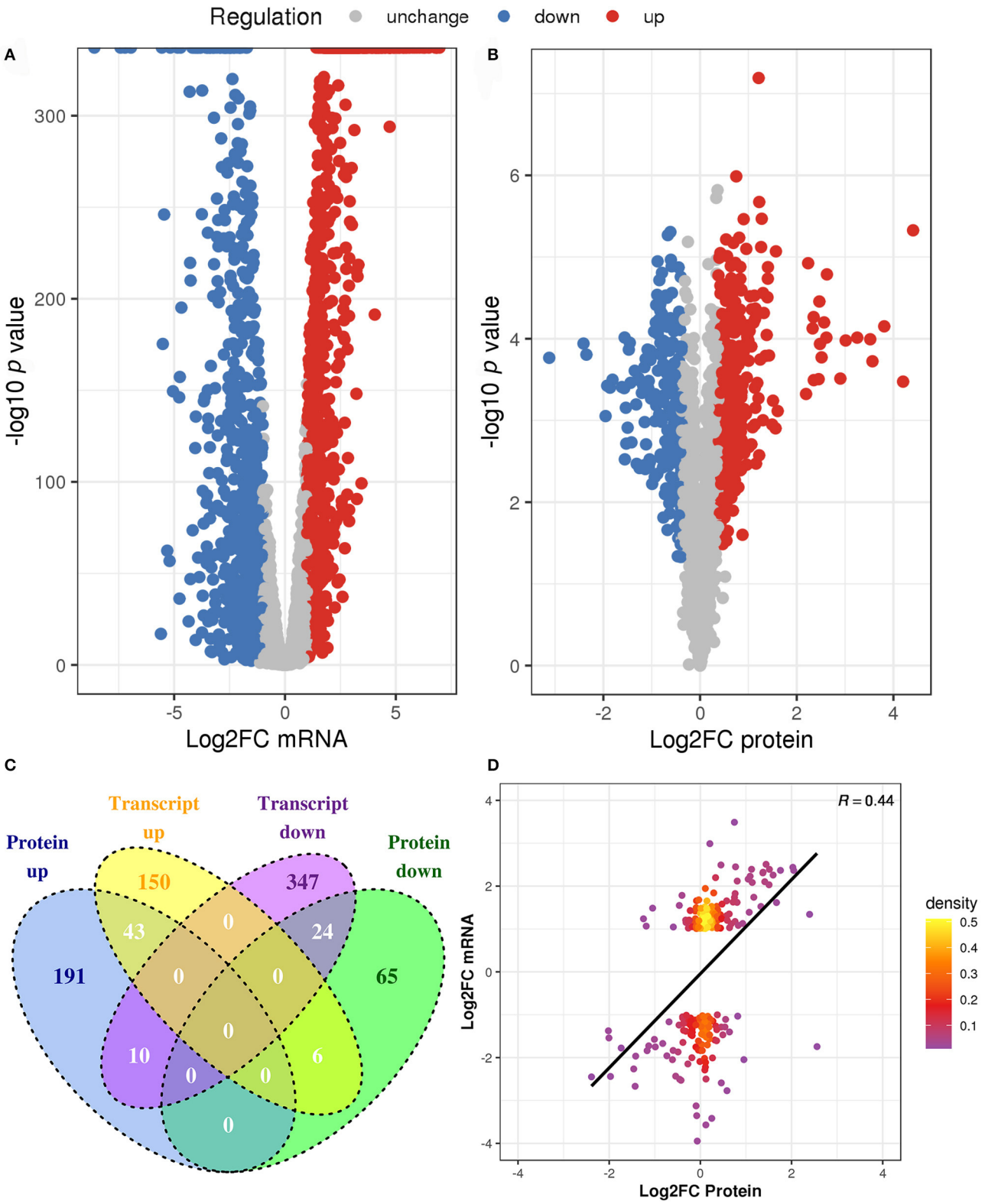

FIGURE 3
The changes of *L. paraplantarum* RX-8 under co-culture in transcriptional and protein levels. **(A)** Indicates volcano plots in the DEGs of *L. paraplantarum* RX-8 under co-culture. **(B)** Indicates volcano plots in the DEPs of *L. paraplantarum* RX-8 under co-culture. **(C)** Venn diagram illustrates the count of DEGs and DEPs coherence regulation, when comparing *L. paraplantarum* RX-8 in co-culture and mono-culture. **(D)** Correlation between DEGs and DEPs *L. paraplantarum* RX-8 under co-culture.

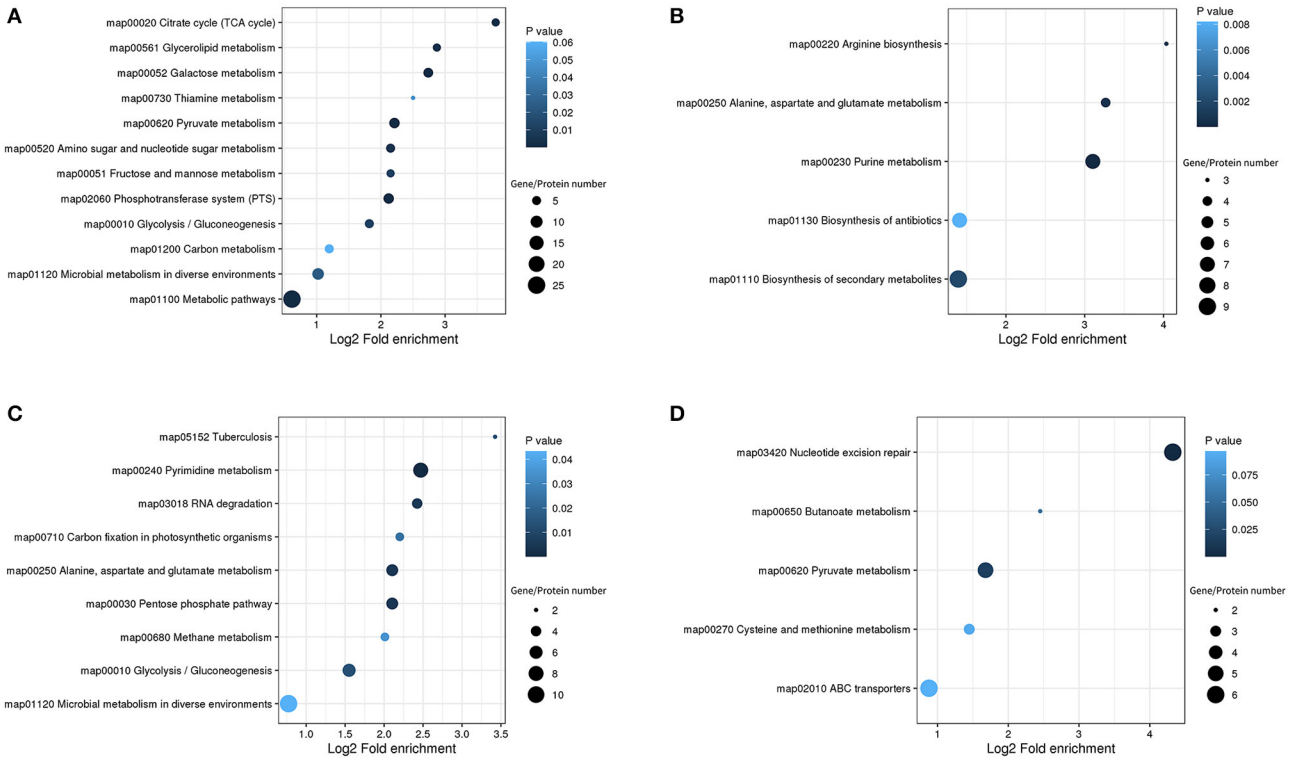

FIGURE 4
KEGG pathway enrichment bubble diagrams in the DEGs/DEPs of *L. paraplantarum* RX-8 under co-culture. **(A)** Indicates KEGG pathway enrichment of upregulated genes and upregulated proteins, **(B)** indicates KEGG pathway enrichment of downregulated genes and downregulated proteins, **(C)** indicates KEGG pathway enrichment of upregulated genes and unchanged proteins, and **(D)** indicates KEGG pathway enrichment of downregulated genes and unchanged proteins.

and carbon metabolism (Figure 5). After pyruvate dehydrogenase complex catalysis, pyruvate is oxidatively decarboxylated with the loss of one carbon and converted into acetyl-CoA, before entering the TCA cycle (Tian et al., 2022). The upregulation of DEPs in the TCA cycle enhances glucose oxidation and energy production. However, the increase in TCA decreased the transformation from phosphoenolpyruvate to aspartate, thereby weakening the serine synthesis. This leads to the downregulation of aspartate, serine, and L-cysteine metabolism.

3.3.2. Amino acid metabolism of *L. paraplantarum* RX-8 in co-culture

Amino acids could serve as the materials in plantaricin synthesis. Aminoacyl-tRNA was responsible for the transportation of amino acids to ribosomes for incorporation into polypeptide chains of plantaricin. Under co-culture, the aspartate–ammonia ligase (*asnA*) and asparagine–tRNA ligase (*asnS*) increased by 2.02- and 2.35-fold, respectively. The aspartate–ammonia ligase catalyzed the production of L-asparagine; then, it was converted by asparaginyl–tRNA synthetase into L-asparaginyl–tRNA, which played a vital role in the translation of RNA into protein (Yeom et al., 2020). In addition, the enzymes that catalyzed the conversion of L-aspartate into fumarate were downregulated. The L-aspartate concentration in *Lactobacillus casei* increased when it faced acid resistance, and the transcriptional levels of *argG* and *argH* in *L. casei* increased with the decrease in pH (Wu et al., 2013). In our study, the pH of *L. paraplantarum* RX-8 in mono-culture was lower than that in co-culture, and a higher expression of *argG* and *argH* was detected in mono-culture.

At the same time, glutamate decarboxylase (*gad*), which was responsible for the mutual conversion of L-glutamate and γ-aminobutyrate (GABA), increased by 2.02-fold. The *gad* process converted L-glutamate into GABA, accompanied by the consumption of H^+. This may explain why the pH of the co-culture was higher than that of the mono-culture of *L. paraplantarum* RX-8. Considering the upregulation of glutamate decarboxylase (*gdhA*), it is possible that *L. paraplantarum* RX-8 under co-culture produces more ammonia or proton consumption *via* glutamate decarboxylase (Teixeira et al., 2014). Moreover, the repression of GlnR could increase the expression of glutamine- and glutamate-metabolism-related genes (*glnP*, *glnQ*, *amtB*, *glnK*, *gltB*, and *gad*), promoting cell growth, acid resistance, and nisin yield (Miao et al., 2018). However, direct interactions between the anti41, an sRNA with a strong inhibitory effect on *glnR*, and the nisin gene cluster were not found (Miao et al., 2018). In addition, purine metabolism was weakened when the gene *purF* was downregulated, while pyrimidine metabolism was enhanced when the gene *CAD* was upregulated (Figure 5). The expression of carbamoyl–phosphate synthase (CAD) converted L-glutamine into carbamoyl phosphate,

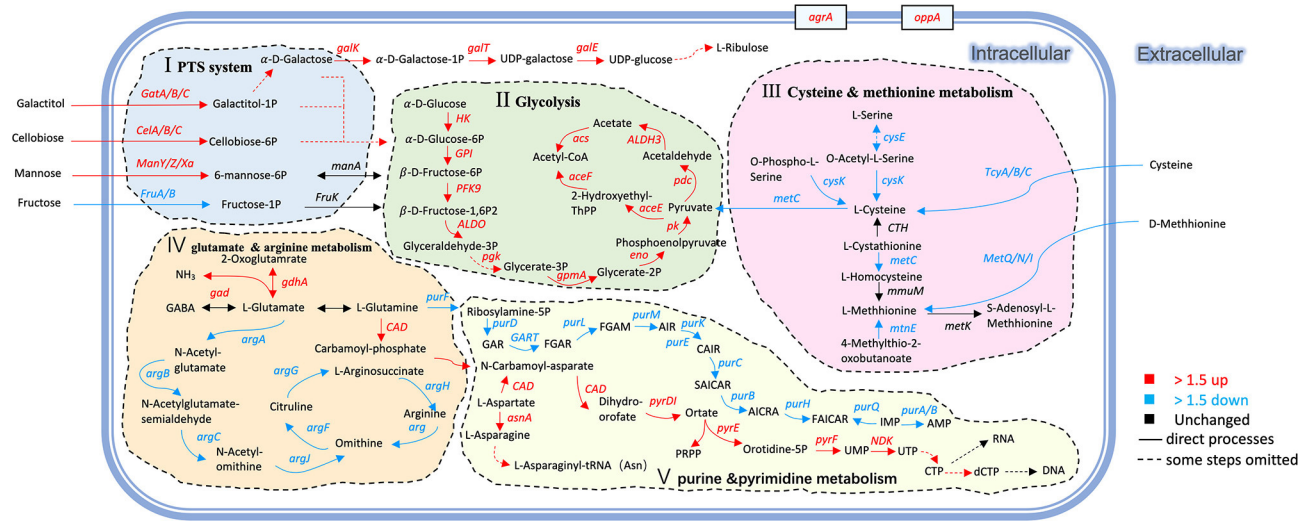

FIGURE 5
Changes of genes and proteins in *L. paraplantarum* RX-8 response to inducing effect from *W. anomalus* Y-5. The serial number (I, II, III, IV, V) indicates the response pathways of *L. paraplantarum* RX-8 under co-culture. (I) improving PTS and enhancing the uptake of certain sugars; (II) increasing the key enzyme activity in glycolysis, then promoting the energy production; (III) repressing the precursor of QS signal AI-2; (IV) decreasing arginine biosynthesis to increase glutamate mechanism, then promote plantaricin yield; (V) changing the expression of several genes/proteins related to purine metabolism (downregulation) and pyrimidine metabolism (upregulation). Pathways were constructed based on information provided in the KEGG database and previous studies.

which is an intermediate in the biosynthesis of nucleotides through the orotate pathway (Namrak et al., 2022).

Meanwhile, the related arginine biosynthesis (*argACDJGH*) genes were downregulated, especially the genes controlling the transportation from glutamate to arginine (Figure 5). It was indicated that *L. paraplantarum* RX-8, under co-culture, led to the accumulation of glutamate by reducing arginine biosynthesis. The gene *metC*, which converted L-cysteine into L-methionine and was a precursor of S-ribosomal homocysteine (SRH), was downregulated. The gene *luxS*, a key enzyme, converted SRH into 4,5-dihydroxy-2,3-pentanedione (DPD). Then, DPD underwent spontaneous rearrangements to form AI-2. The downregulation of *luxS* influences the biosynthesis of AI-2, and a similar tendency was observed in co-culture AI-2 activity (Supplementary Figure 2). It was reported that the decrease in the L-methionine and L-cysteine cycling pathways was caused by the knockout of the *luxS* gene (Qian et al., 2022b). Similar results of changes in L-methionine- and L-cysteine-related genes were found in co-culture.

3.3.3. Quorum sensing system of *L. paraplantarum* RX-8 in co-culture

Some genes related to the quorum-sensing system and ABC-transport system were upregulated in *L. paraplantarum* RX-8 under co-culture. OppA is an oligopeptide-binding protein that is responsible for peptides' capture (Kieliszek et al., 2021). Therefore, the strong upregulation of *oppA* suggested an increase in the transportation of oligopeptides. OppA could increase Ox-bile resistance in *L. salivarius* Ren and salt resistance in *Lactobacillus paracasei* ATCC 334 (Ma et al., 2018). It is possible that OppA helps *L. paraplantarum* RX-8 to survive in the presence of yeast. When PlnA or *Lactobacillus sanfranciscensis* DPPMA174 is co-cultured with *L. plantarum* DC400, OppA is upregulated compared with *L. plantarum* DC400 mono-culture (Calasso et al., 2013). Although *oppA* did not show a difference in the plantaricin Q7 biosynthesis of *L. plantarum* Q7, *oppD*-, and *oppF*-encoding intracellular ATPases were upregulated when plantaricin Q7 production increased and downregulated when plantaricin Q7 was hydrolyzed to support the nutrients needed to promote the growth of *L. plantarum* Q7 (Bu et al., 2021a). Moreover, the Opp system in *E. faecalis* and *Streptococcus mutans* has specific pheromone binding activity (Leonard et al., 1996; Li and Tian, 2012). It can be hypothesized that *L. plantarum* DC400 transports PlnA *via* the Opp system (Calasso et al., 2013). The upregulation of phosphate-inducible transport system (*pstSCAB*) suggested that the phosphate uptake was increased to meet the increase in the phosphorylated nucleotides and proteins, which control the biosynthesis of many secondary metabolites. In addition, fructose, galactose, or mannose in media could promote the expression of the *pstSCAB* operon and significantly increase the formation of PstS (Martín and Liras, 2021). In this result, the mannose transport system and galactose metabolism were also upregulated.

The production of plantaricin was regulated by the quorum-sensing system (encoded by *plnABCDEF* gene clusters) (Zhao et al., 2021; Liu et al., 2022). Although *plnABCDEF* gene clusters synthesizing bacteriocin did not show significant differences ($|Log_2FC| \geq 1$, $p < 0.05$) in transcriptomic analysis, the *plnABCDEF* gene clusters were found to show 2.51-, 1.61-, 1.45-, 1.27-, 1.03-, and 1.41-fold changes at 24 h in transcriptomic analysis, and the results of RT-qPCR indicated that *W. anomalus* Y-5 stimulated plantaricin production *via* *plnABCDEF*. In the QS system, the gene *agrA*, an RR, was upregulated under co-culture. The Agr-mediated QS system (*agrBDCA*) might participate

in commensal host–microbe interactions, especially *agrA*-encoded RR, which performs important functions in cell adhesion and biofilm formation in *L. plantarum* WCFS1 (Sturme et al., 2005). In addition, the expression of *agrA* was related to a global cellular response, such as the upregulated pyrimidine biosynthesis genes (*pyrB*, *pyrD*, *pyrF*, and *pyrR*) in *L. plantarum* WCFS1 (Sturme et al., 2005). Interestingly, similar results were also found for *L. paraplantarum* RX-8 in co-culture, suggesting that *agrA* controls pyrimidine biosynthesis under the interactions of *L. paraplantarum* RX-8 and *W. anomalus* Y-5. *agrBDCA* may influence plantaricin Q7 biosynthesis; specifically, *agrC* and *agrA* were upregulated in the synthesis of plantaricin Q7 (Bu et al., 2021a). The gene *agrB* of *L. paraplantarum* RX-8 was upregulated by 1.5-fold under co-culture. Protein AgrB also increased when *L. plantarum* DC400 was co-cultured with *L. plantarum* DPPMA20 or *L. sanfranciscensis* DPPMA174 (Calasso et al., 2013). This indicates that the *agrBCDA* quorum-sensing system might enhance plantaricin production when *L. paraplantarum* RX-8 is induced by *W. anomalus* Y-5.

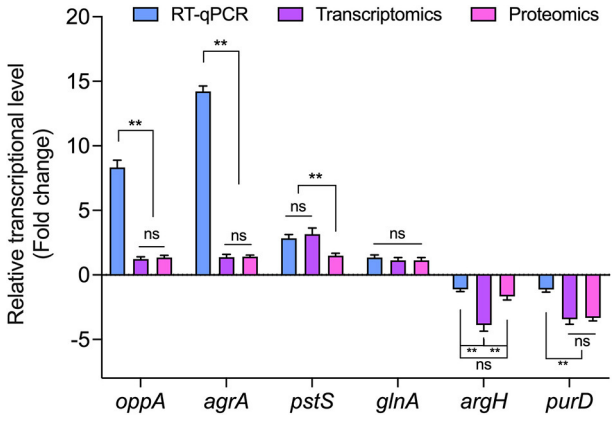

FIGURE 6
The relative expression of genes encoding DEPs in *L. paraplantarum* RX-8 under co-culture. ns, not significant, $^{**}p < 0.01$.

3.3.4. RNA degradation and nucleotide repair of *L. paraplantarum* RX-8 in co-culture

To repair DNA damage, there are different classes of DNA repair systems. The nucleotide excision repair (*uvrABCD*) system recognizes the damaged strand, removes it, and then fills the gap (Goosen and Moolenaar, 2001). The gene *uvrABCD* was downregulated, which indicates that there is less DNA synthesis or less DNA damage when *L. paraplantarum* RX-8 is under co-culture. It is important for a tightly regulated RNA metabolism to adapt to environmental change and utilize nutrients. RNA helicases could locally unwind double-stranded RNA, or they can clamp protein complexes to a substrate RNA in an ATP-dependent manner. Gene *cshA*-encoded RNA helicase was downregulated in *L. paraplantarum* RX-8 under co-culture. It was reported that the *cshA* mutant of *Staphylococcus aureus* SA564 led to increased stability in *agr* mRNA, and it was hypothesized that the *agrBDCA* mRNAs were unable to correctly degrade in the absence of *cshA* (Oun et al., 2013). This would account for the lower *cshA* and higher *agrA* expression in *L. paraplantarum* RX-8 under co-culture. GroEL could partially unfold the misfolded RNA or proteins in an ATP-dependent manner. DnaK is a major chaperone, and the binding and release of protein clients by DnaK are regulated by ATP's hydrolytic activity. The downregulation of *groEL* and *dnaK* may indicate that there is less RNA degradation and a more stable RNA in co-culture.

3.4. Transcription- and protein-level validation

Based on the results of transcriptomic and proteomic analyses, *oppA*, *agrA*, *pstS*, *glnA*, *argH*, and *purD* (four upregulated and two downregulated) were selected for validation by RT-qPCR. Although the value of the obtained fold-change was different between RT-qPCR and transcriptomic and proteomic data, the expressions of the tested genes were entirely consistent in the direction of regulation (Figure 6). The concordance between RT-qPCR and transcriptomic and proteomic data suggests high reliability in transcriptomic and proteomic data.

3.5. Inducing effects of key metabolites on plantaricin production

The effects of key-inducing metabolites on the plantaricin production of *L. paraplantarum* RX-8 were studied. It was found that the addition of galactose, mannose, arginine, cysteine, glutamate, and glutamine could induce plantaricin production, while cellobiose and D-ribose had little less effect on plantaricin production (Figure 7). It was indicated that galactose, mannose, arginine, cysteine, glutamate, and glutamine could be essential to the plantaricin production of *L. paraplantarum* RX-8. The production of plantaricin was significantly enhanced in mono-culture with the addition of 200 mM, but lower concentrations of galactose (2 and 20 mM) did not induce any effects on plantaricin yield (Figure 7A). The exogenous addition of mannose could increase the plantaricin synthesis at concentrations of 2, 20, and 200 mM (Figure 7B). The yield of plantaricin was strengthened at 24 h by adding arginine to mono-culture (Figure 7E). The addition of arginine, 2.5 g/L of cysteine, 0.5 g/L of glutamate, and 0.5 g/L of glutamine had significant effects on plantaricin production (Figures 7E, F, H), while cysteine, glutamate, and glutamine at other concentrations did not show a significant impact on plantaricin production.

Interestingly, the stimulus effects of glutamate and glutamine were not exhibited at higher concentrations. Considering the upregulation of related genes and proteins in galactose metabolism, this could because the significant induction that occurs at low concentrations of glutamate and glutamine makes them the most economic strategy for enhancing plantaricin production in *L. paraplantarum* RX-8. Bu et al. (2021b) reported that the plantaricin synthesis of *L. plantarum* Q7 was promoted by the exogenous addition of glutamate at 16 h, but plantaricin Q7 production

10.3389/fmicb.2023.1111516

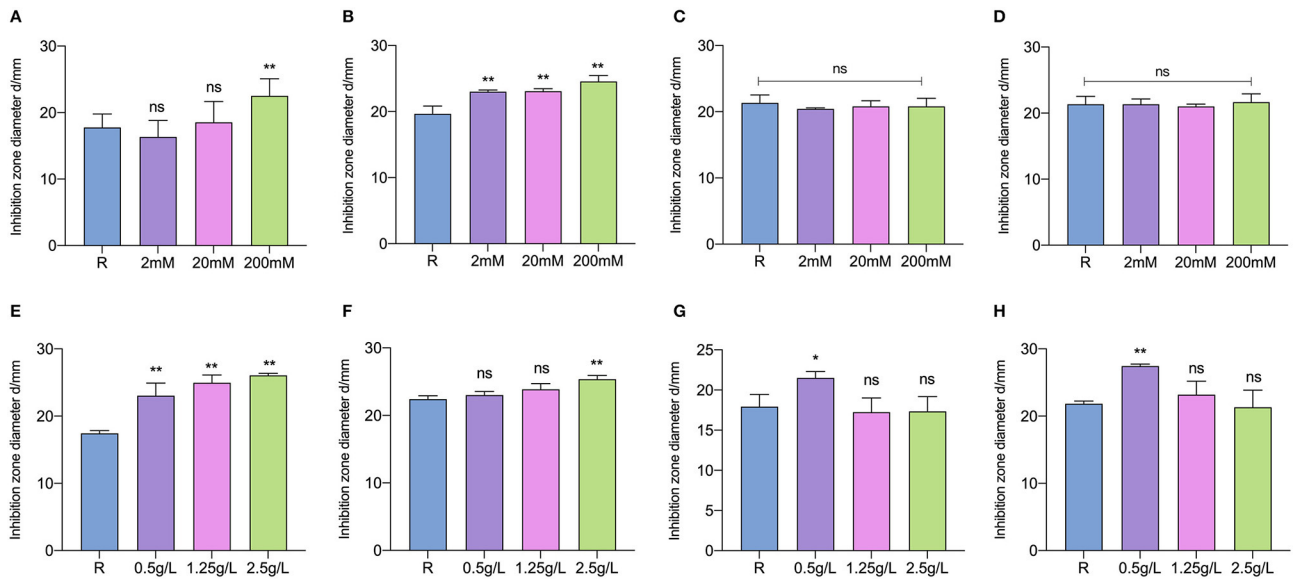

FIGURE 7
Inducing effects of different concentrations of galactose **(A)**, mannose **(B)**, cellobiose **(C)**, D-ribose **(D)**, arginine **(E)**, cysteine **(F)**, glutamate **(G)**, and glutamine **(H)** on plantaricin production. ns: not significant, $*p < 0.05$, $**p < 0.01$.

was not stimulated by glutamate at 2, 6, and 12 h. Although *S. cerevisiae* could secrete different kinds of amino acids that are crucial to the survival of *L. plantarum*, the supplementing CDM35 medium with glutamine, threonine, phenylalanine, tryptophan, and serine, which were under the observed concentrations, had only a minimal impact on *L. plantarum* growth (Ponomarova et al., 2017). This is because the synergistic nature of multi-component cross-feeding was challenging to characterize. In addition, the nutritional competition was one of the reasons that *L. plantarum* SS-128 inhibits the growth of *Shewanella baltica* (Qian et al., 2022a). To further demonstrate the advantage of using *W. anomalus* Y-5 to induce bacteriocin production, metabolomics would be performed on quantified amino acids, sugar, and other metabolites secreted by *L. paraplantarum* RX-8 and *W. anomalus* Y-5. Then, the induction effect of the target metabolite at the observed concentrations in mono-culture would be analyzed.

3.6. The role of AI-2 activity in inducing effect

D-ribose, as a competitive inhibitor of AI-2, could cut the intracellular communication mediated by AI-2 among bacteria. AI-2 activity in co-culture was inhibited by D-ribose at all selected concentrations (Figure 8A). All samples whose AI-2 activity was cut still showed antibacterial activity and did not show a significant difference compared with co-culture samples without D-ribose (Figure 8B). It was suggested that AI-2 does not play an important role in inducing bacteriocin production when the bacteriocin-producing strain is co-cultured with *W. anomalus* Y-5.

Conclusion

In this study, the plantaricin production and response mechanisms that occur when *L. paraplantarum* RX-8 is co-cultured with *W. anomalus* Y-5 were investigated. The results indicated that *W. anomalus* Y-5 could enhance plantaricin production by activating the expression of *plnABCDEF* cluster in *L. paraplantarum* RX-8. Then, the differences between *L. paraplantarum* RX-8 at transcriptomic and protein levels were analyzed under co-culture and mono-culture. The data showed that multiple metabolic pathways of *L. paraplantarum* RX-8 were significantly affected in the co-culture including (i) upregulation of the PTS in mannose, galactitol, and cellobiose transport, and downregulation of the PTS in fructose transport; (ii) modulation of the expression of several enzymes involved in glycolysis and other carbohydrate pathways; (iii) upregulation of key enzymes involved in glutamate metabolism and downregulation of multiple enzymes involved in aspartate, arginine, and cysteine metabolisms; (iv) modulation of the expression of several enzymes involved in the quorum-sensing system and ABC-transport system; and (v) upregulation of several enzymes involved in pyrimidine metabolism and downregulation of several enzymes involved in purine metabolism. In combination with the induction of metabolites' validation during plantaricin production and previous studies, we predicted that *L. paraplantarum* RX-8 mechanisms would occur in response to *W. anomalus* Y-5; that the changes in the PTS led to an increase in mannose and galactose uptake; that the glycolysis and fermentative pathways would be promoted and generated energy to support plantaricin production. The increase in glutamate metabolism and decrease in arginine biosynthesis may replenish the glutamate and then enhance the plantaricin yield, and the upregulation of the *agrA* and *oppA* genes may help

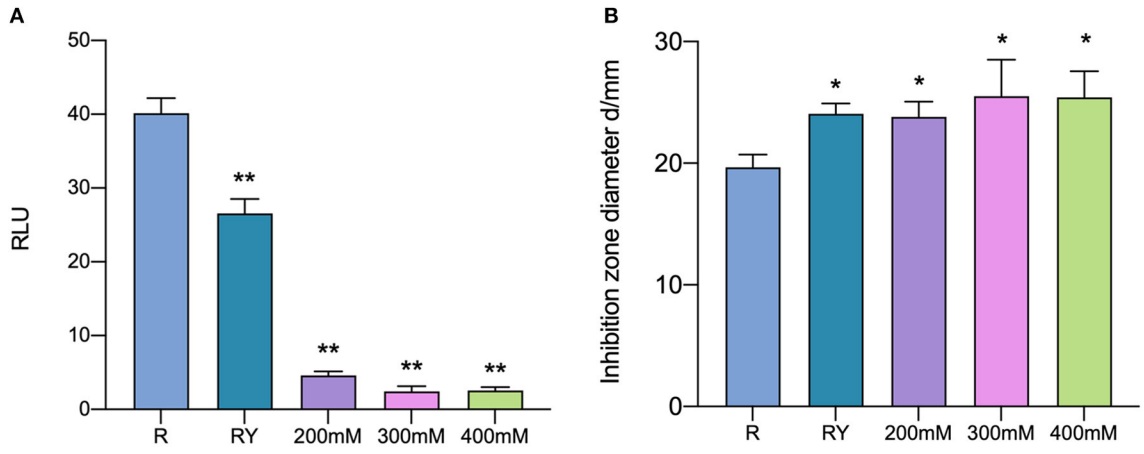

FIGURE 8
AI-2 activity **(A)** and the antibacterial activity **(B)** in co-culture with the addition of D-ribose. R means mono-culture of *L. paraplantarum* RX-8 at 37°C; RY means bacteriocin-inducing co-culture of *L. paraplantarum* RX-8 and *W. anomalus* Y-5 at 37°C as a positive control; 200/300/400 mM means co-culture of *L. paraplantarum* RX-8 and *W. anomalus* Y-5 at 37°C with 200, 300, and 400 mM D-ribose. *$p < 0.05$, **$p < 0.01$.

transport PlnA and regulate plantaricin production. Our study provides a novel insight into the mechanisms of bacteriocin-producing bacteria's response to bacteriocin-inducing yeast and offers a reference for the interaction between *L. paraplantarum* and *W. anomalus*. In the future, a detailed study of the bacteriocin-inducing regulatory mechanism in co-culture could be undertaken using metabolomics methods.

Data availability statement

The datasets presented in this study can be found in online repositories. The names of the repository/repositories and accession number(s) can be found in the article/Supplementary material.

Author contributions

RN and GL conceptualized the idea and designed the experiments. RN wrote the manuscript. GL, RN, and YQ revised, make corrections, and approved the research article for publication. RN, ZZ, ZW, and HS performed the experiments. RN and ZZ analyzed the results. All authors contributed to the article and approved the submitted version.

Funding

This project was funded by the Natural Science Foundation of China (Grant Nos. 31871772 and 31671832), the Beijing Natural Science Foundation (Grant No. 6192003), the Natural Science Foundation of Guangdong Province, China (Grant No. 2022A1515140021), and the Cultivation Project of Double First-Class Disciplines of Food Science and Engineering, Beijing Technology & Business University (Grant No. BTBUYXTD202208).

Conflict of interest

The authors declare that the research was conducted in the absence of any commercial or financial relationships that could be construed as a potential conflict of interest.

Publisher's note

All claims expressed in this article are solely those of the authors and do not necessarily represent those of their affiliated organizations, or those of the publisher, the editors and the reviewers. Any product that may be evaluated in this article, or claim that may be made by its manufacturer, is not guaranteed or endorsed by the publisher.

Supplementary material

The Supplementary Material for this article can be found online at: https://www.frontiersin.org/articles/10.3389/fmicb.2023.1111516/full#supplementary-material

References

Anders, S., Pyl, P. T., and Huber, W. (2015). HTSeq–a Python framework to work with high-throughput sequencing data. *Bioinformatics* 31, 166–169. doi: 10.1093/bioinformatics/btu638

Ariana, M., and Hamedi, J. (2017). Enhanced production of nisin by co-culture of *Lactococcus lactis* sub sp. lactis and *Yarrowia lipolytica* in molasses based medium. *J. Biotechnol.* 256, 21–26. doi: 10.1016/j.jbiotec.2017.07.009

Bolger, A. M., Lohse, M., and Usadel, B. (2014). Trimmomatic: a flexible trimmer for Illumina sequence data. *Bioinformatics* 30, 2114–2120. doi: 10.1093/bioinformatics/btu170

Bu, Y., Liu, Y., Li, J., Liu, T., Gong, P., Zhang, L., et al. (2021a). Analyses of plantaricin Q7 synthesis by *Lactobacillus plantarum* Q7 based on comparative transcriptomics. *Food Control* 124, 107909. doi: 10.1016/j.foodcont.2021.107909

Bu, Y., Yang, H., Li, J., Liu, Y., Liu, T., Gong, P., et al. (2021b). Comparative metabolomics analyses of plantaricin Q7 production by *Lactobacillus plantarum* Q7. *J. Agric. Food Chem.* 69, 10741–10748. doi: 10.1021/acs.jafc.1c03533

Buchfink, B., Xie, C., and Huson, D. H. (2015). Fast and sensitive protein alignment using DIAMOND. *Nat. Methods* 12, 59–60. doi: 10.1038/nmeth.3176

Calasso, M., Di Cagno, R., De Angelis, M., Campanella, D., Minervini, F., and Gobbetti, M. (2013). Effects of the peptide pheromone plantaricin A and cocultivation with *Lactobacillus sanfranciscensis* DPPMA174 on the exoproteome and the adhesion capacity of *Lactobacillus plantarum* DC400. *Appl. Environ. Microbiol.* 79, 2657–2669. doi: 10.1128/AEM.03625-12

Chaillou, S., Postma, P. W., and Pouwels, P. H. (2001). Contribution of the phosphoenolpyruvate:mannose phosphotransferase system to carbon catabolite repression in *Lactobacillus pentosus*. *Microbiology* 147, 671–679. doi: 10.1099/00221287-147-3-671

Chanos, P., and Mygind, T. (2016). Co-culture-inducible bacteriocin production in lactic acid bacteria. *Appl. Microbiol. Biotechnol.* 100, 4297–4308. doi: 10.1007/s00253-016-7486-8

Diep, D. B., Skaugen, M., Salehian, Z., Holo, H., and Nes, I. F. (2007). Common mechanisms of target cell recognition and immunity for class II bacteriocins. *Proc. Natl. Acad. Sci. U. S. A.* 104, 2384–2389. doi: 10.1073/pnas.0608775104

Goosen, N., and Moolenaar, G. F. (2001). Role of ATP hydrolysis by UvrA and UvrB during nucleotide excision repair. *Res. Microbiol.* 152, 401–409. doi: 10.1016/S0923-2508(01)01211-6

Ha, J.-H., Hauk, P., Cho, K., Eo, Y., Ma, X., Stephens, K., et al. (2018). Evidence of link between quorum sensing and sugar metabolism in *Escherichia coli* revealed *via* cocrystal structures of LsrK and HPr. *Sci. Adv.* 4, eaar7063. doi: 10.1126/sciadv.aar7063

Jeckelmann, J.-M., and Erni, B. (2020). The mannose phosphotransferase system (Man-PTS) - Mannose transporter and receptor for bacteriocins and bacteriophages. *Biochim. Biophys. Acta Biomembr.* 1862, 183412. doi: 10.1016/j.bbamem.2020.183412

Kern, L., Abdeen, S. K., Kolodziejczyk, A. A., and Elinav, E. (2021). Commensal inter-bacterial interactions shaping the microbiota. *Curr. Opin. Microbiol.* 63, 158–171. doi: 10.1016/j.mib.2021.07.011

Kieliszek, M., Pobiega, K., Piwowarek, K., and Kot, A. M. (2021). Characteristics of the proteolytic enzymes produced by lactic acid bacteria. *Molecules* 26, 1858. doi: 10.3390/molecules26071858

Kim, D., Paggi, J. M., Park, C., Bennett, C., and Salzberg, S. L. (2019). Graph-based genome alignment and genotyping with HISAT2 and HISAT-genotype. *Nat. Biotechnol.* 37, 907–915. doi: 10.1038/s41587-019-0201-4

Kjos, M., Nes, I. F., and Diep, D. B. (2009). Class II one-peptide bacteriocins target a phylogenetically defined subgroup of mannose phosphotransferase systems on sensitive cells. *Microbiology* 155, 2949–2961. doi: 10.1099/mic.0.030015-0

Kjos, M., Snipen, L., Salehian, Z., Nes, I. F., and Diep, D. B. (2010). The abi proteins and their involvement in bacteriocin self-immunity. *J. Bacteriol.* 192, 2068–2076. doi: 10.1128/JB.01553-09

Kumar, D., Bansal, G., Narang, A., Basak, T., Abbas, T., and Dash, D. (2016). Integrating transcriptome and proteome profiling: strategies and applications. *Proteomics* 16, 2533–2544. doi: 10.1002/pmic.201600140

Langdon, W. B. (2015). Performance of genetic programming optimised Bowtie2 on genome comparison and analytic testing (GCAT) benchmarks. *BioData Mining* 8, 1. doi: 10.1186/s13040-014-0034-0

Lee, J. M., Jang, W. J., Lee, E.-W., and Kong, I.-S. (2020). β-glucooligosaccharides derived from barley β-glucan promote growth of lactic acid bacteria and enhance nisin Z secretion by *Lactococcus lactis*. *LWT* 122, 109014. doi: 10.1016/j.lwt.2020.109014

Lengeler, J. W., and Jahreis, K. (2009). "Bacterial PEP-dependent carbohydrate: phosphotransferase systems couple sensing and global control mechanisms," in *Contributions to Microbiology*, eds. M. Collin and R. Schuch (Basel: KARGER), 65–87.

Leonard, B. A., Podbielski, A., Hedberg, P. J., and Dunny, G. M. (1996). *Enterococcus faecalis* pheromone binding protein, PrgZ, recruits a chromosomal oligopeptide permease system to import sex pheromone cCF10 for induction of conjugation. *Proc. Natl. Acad. Sci. U. S. A.* 93, 260–264. doi: 10.1073/pnas.93.1.260

Li, Y.-H., and Tian, X. (2012). Quorum sensing and bacterial social interactions in biofilms. *Sensors* 12, 2519–2538. doi: 10.3390/s120302519

Liu, G., Nie, R., Liu, Y., Li, X., Duan, J., Hao, X., et al. (2022). *Bacillus subtilis* BS-15 effectively improves plantaricin production and the regulatory biosynthesis in *Lactiplantibacillus plantarum* RX-8. *Front. Microbiol.* 12, 772546. doi: 10.3389/fmicb.2021.772546

Liu, W., Zhou, J., Tan, F., Yin, H., Yang, C., and Lu, K. (2021). Improvement of nisin production by using the integration strategy of co-cultivation fermentation, foam fractionation and pervaporation. *LWT* 142, 111093. doi: 10.1016/j.lwt.2021.111093

Ma, X., Wang, G., Zhai, Z., Zhou, P., and Hao, Y. (2018). Global transcriptomic analysis and function identification of malolactic enzyme pathway of *Lactobacillus paracasei* L9 in response to bile stress. *Front. Microbiol.* 9, 1978. doi: 10.3389/fmicb.2018.01978

Maldonado-Barragán, A., Caballero-Guerrero, B., Lucena-Padrós, H., and Ruiz-Barba, J. L. (2013). Induction of bacteriocin production by coculture is widespread among plantaricin-producing *Lactobacillus plantarum* strains with different regulatory operons. *Food Microbiol.* 33, 40–47. doi: 10.1016/j.fm.2012.08.009

Martín, J. F., and Liras, P. (2021). Molecular mechanisms of phosphate sensing, transport and signalling in streptomyces and related actinobacteria. *IJMS* 22, 1129. doi: 10.3390/ijms22031129

Miao, S., Wu, H., Zhao, Y., Caiyin, Q., Li, Y., and Qiao, J. (2018). Enhancing nisin yield by engineering a small noncodding RNA anti41 and inhibiting the expression of glnR in *Lactococcus lactis* F44. *Biotechnol. Lett.* 40, 941–948. doi: 10.1007/s10529-018-2550-3

Namrak, T., Raethong, N., Jatuponwiphat, T., Nitisinprasert, S., Vongsangnak, W., and Nakphaichit, M. (2022). Probing genome-scale model reveals metabolic capability and essential nutrients for growth of probiotic *Limosilactobacillus reuteri* KUB-AC5. *Biology* 11, 294. doi: 10.3390/biology11020294

Oun, S., Redder, P., Didier, J.-P., François, P., Corvaglia, A.-R., Buttazzoni, E., et al. (2013). The CshA DEAD-box RNA helicase is important for quorum sensing control in *Staphylococcus aureus*. *RNA Biol.* 10, 157–165. doi: 10.4161/rna.22899

Ponomarova, O., Gabrielli, N., Sévin, D. C., Mülleder, M., Zirngibl, K., Bulyha, K., et al. (2017). Yeast creates a niche for symbiotic lactic acid bacteria through nitrogen overflow. *Cell Syst.* 5, 345–357.e6. doi: 10.1016/j.cels.2017.09.002

Qian, Y., Li, Y., Tang, Z., Wang, R., Zeng, M., and Liu, Z. (2022a). The role of AI-2/LuxS system in biopreservation of fresh refrigerated shrimp: enhancement in competitiveness of *Lactiplantibacillus plantarum* for nutrients. *Food Res. Int.* 161, 111838. doi: 10.1016/j.foodres.2022.111838

Qian, Y., Li, Y., Xu, T., Zhao, H., Zeng, M., and Liu, Z. (2022b). Dissecting of the AI-2/LuxS mediated growth characteristics and bacteriostatic ability of *Lactiplantibacillus plantarum* SS-128 by integration of transcriptomics and metabolomics. *Foods* 11, 638. doi: 10.3390/foods11050638

Robinson, M. D., McCarthy, D. J., and Smyth, G. K. (2010). edgeR: a Bioconductor package for differential expression analysis of digital gene expression data. *Bioinformatics* 26, 139–140. doi: 10.1093/bioinformatics/btp616

Saier, M. H., and Roseman, S. (1976). Sugar transport. The crr mutation: its effect on repression of enzyme synthesis. *J. Biol. Chem.* 251, 6598–6605. doi: 10.1016/S0021-9258(17)32988-5

Straume, D., Johansen, R. F., Bjørås, M., Nes, I. F., and Diep, D. B. (2009). DNA binding kinetics of two response regulators, PlnC and PlnD, from the bacteriocin regulon of *Lactobacillus plantarum* C11. *BMC Biochem.* 10, 17. doi: 10.1186/1471-2091-10-17

Sturme, M. H. J., Nakayama, J., Molenaar, D., Murakami, Y., Kunugi, R., Fujii, T., et al. (2005). An agr-like two-component regulatory system in *Lactobacillus plantarum* is involved in production of a novel cyclic peptide and regulation of adherence. *J. Bacteriol.* 187, 5224–5235. doi: 10.1128/JB.187.15.5224-5235.2005

Teixeira, J. S., Seeras, A., Sanchez-Maldonado, A. F., Zhang, C., Su, M. S.-W., and Gänzle, M. G. (2014). Glutamine, glutamate, and arginine-based acid resistance in *Lactobacillus reuteri*. *Food Microbiol.* 42, 172–180. doi: 10.1016/j.fm.2014.03.015

Tian, S., Liang, X., Chen, J., Zeng, W., Zhou, J., and Du, G. (2020). Enhancement of 2-phenylethanol production by a wild-type *Wickerhamomyces anomalus* strain isolated from rice wine. *Bioresour. Technol.* 318, 124257. doi: 10.1016/j.biortech.2020.124257

Tian, Y., Wang, Y., Zhang, N., Xiao, M., Zhang, J., Xing, X., et al. (2022). Antioxidant mechanism of *Lactiplantibacillus plantarum* KM1 under H_2O_2 stress by proteomics analysis. *Front. Microbiol.* 13, 897387. doi: 10.3389/fmicb.2022.897387

Trappetti, C., McAllister, L. J., Chen, A., Wang, H., Paton, A. W., Oggioni, M. R., et al. (2017). Autoinducer 2 signaling *via* the phosphotransferase FruA drives galactose utilization by *Streptococcus pneumoniae*, resulting in hypervirulence. *mBio* 8, e02269–e02216. doi: 10.1128/mBio.02269-16

Tyanova, S., Temu, T., and Cox, J. (2016). The MaxQuant computational platform for mass spectrometry-based shotgun proteomics. *Nat. Protoc.* 11, 2301–2319. doi: 10.1038/nprot.2016.136

Wardani, A. K., Egawa, S., Nagahisa, K., Shimizu, H., and Shioya, S. (2006). Robustness of cascade pH and dissolved oxygen control in symbiotic nisin production process system of *Lactococcus lactis* and *Kluyveromyces marxianus*. *J. Biosci. Bioeng.* 101, 274–276. doi: 10.1263/jbb.101.274

Wick, R. R., Judd, L. M., Gorrie, C. L., and Holt, K. E. (2017). Unicycler: Resolving bacterial genome assemblies from short and long sequencing reads. *PLoS Comput. Biol.* 13, e1005595. doi: 10.1371/journal.pcbi.1005595

Wu, C., Zhang, J., Du, G., and Chen, J. (2013). Aspartate protects *Lactobacillus casei* against acid stress. *Appl. Microbiol. Biotechnol.* 97, 4083–4093. doi: 10.1007/s00253-012-4647-2

Yeom, E., Kwon, D.-W., Lee, J., Kim, S.-H., Lee, J.-H., Min, K.-J., et al. (2020). Asparaginyl-tRNA synthetase, a novel component of hippo signaling, binds to salvador and enhances yorkie-mediated tumorigenesis. *Front. Cell Dev. Biol.* 8, 32. doi: 10.3389/fcell.2020.00032

Yu, G., Wang, L.-G., Han, Y., and He, Q.-Y. (2012). clusterProfiler: an R package for comparing biological themes among gene clusters. *OMICS J. Integr. Biol.* 16, 284–287. doi: 10.1089/omi.2011.0118

Zhang, G., Qi, Q., Sadiq, F. A., Wang, W., He, X., and Wang, W. (2021). Proteomic analysis explores interactions between *Lactiplantibacillus plantarum* and *Saccharomyces cerevisiae* during sourdough fermentation. *Microorganisms* 9, 2353. doi: 10.3390/microorganisms91 12353

Zhao, D., Meng, F., Zhou, L., Lu, F., Bie, X., Sun, J., et al. (2021). Maltose effective improving production and regulatory biosynthesis of plantaricin EF in *Lactobacillus plantarum* 163. *Appl. Microbiol. Biotechnol.* 105, 2713–2723. doi: 10.1007/s00253-021-11218-w

Zhao, D., Wang, Q., Meng, F., Lu, F., Bie, X., Lu, Z., et al. (2022). TetR-Type regulator Lp_2642 positively regulates plantaricin EF production based on genome-wide transcriptome sequencing of *Lactiplantibacillus plantarum* 163. *J. Agric. Food Chem.* 70, 4362–4372. doi: 10.1021/acs.jafc.2c00206

frontiers | Frontiers in Microbiology

TYPE Original Research
PUBLISHED 06 March 2023
DOI 10.3389/fmicb.2023.1094671

OPEN ACCESS

EDITED BY
Paloma López,
Margarita Salas Center for Biological Research (CSIC), Spain

REVIEWED BY
Dave Siak-Wei Ow,
Bioprocessing Technology Institute (A*STAR), Singapore
Spiros Paramithiotis,
Agricultural University of Athens, Greece

*CORRESPONDENCE
Maria Rosaria Corbo
✉ mariarosaria.corbo@unifg.it
Antonio Bevilacqua
✉ antonio.bevilacqua@unifg.it

SPECIALTY SECTION
This article was submitted to Food Microbiology, a section of the journal Frontiers in Microbiology

RECEIVED 10 November 2022
ACCEPTED 20 February 2023
PUBLISHED 06 March 2023

CITATION
Racioppo A, Speranza B, Altieri C, Sinigaglia M, Corbo MR and Bevilacqua A (2023) Ultrasound can increase biofilm formation by *Lactiplantibacillus plantarum* and *Bifidobacterium* spp. *Front. Microbiol.* 14:1094671. doi: 10.3389/fmicb.2023.1094671

Ultrasound can increase biofilm formation by *Lactiplantibacillus plantarum* and *Bifidobacterium* spp.

Angela Racioppo, Barbara Speranza, Clelia Altieri, Milena Sinigaglia, Maria Rosaria Corbo* and Antonio Bevilacqua*

Department of Agriculture, Food, Natural Resources and Engineering, University of Foggia, Foggia, Italy

The main goal of this research was to study the effect of an Ultrasound (US) treatment on biofilm formation of *Lactiplantibacillus plantarum* (strains c19 and DSM 1055), *Bifidobacterium animalis* subsp. *lactis* DSM 10140, *Bifidobacterium longum* subsp. *longum* DSM 20219, and *Bifidobacterium longum* subsp. *infantis* DSM 20088. From a methodological point of view, each microorganism was treated through six US treatments, different for the power (10, 30, or 50% of the net power, 130 W), the duration (2, 6, or 10 min) and the application of pulses (0 or 10 s). After the treatment, a biofilm of the strains was let to form on glass slides and the concentration of sessile cells was analyzed for 16 days. Biofilms formed by untreated microorganisms were used as controls. As a first result, it was found that US significantly increased the concentration of sessile cells of *B. longum* subsp. *infantis*, while for some other strains US treatment could not affect the formation of biofilm while improving its stability, as found for *L. plantarum* DSM1055 after 16 days. The variable mainly involved in this positive effect of US was the duration of the treatment, as biofilm formation and stability were improved only for 2 min-treatments; on the other hand, the effect of power and pulses were strain-dependent. In conclusion, the results suggest practical implication of a US pre-treatment for various fields (improvement of adhesion of microorganisms useful in food or in the gut, biomedical and environmental industries), although further investigations are required to elucidate the mode of action.

KEYWORDS

ultrasound, functional microorganisms, biofilm formation, adhesion, stability

1. Introduction

Ultrasounds (US) are elastic waves that move through a medium producing compression (high pressure) or rarefaction (low pressure) and whose frequency is on average higher than that audible to the human ear (20 kHz) (Ojha et al., 2017). Depending on their use, US can be classified into high-power US (low frequency) and low-power US (high frequency) (Estivi et al., 2022). Low-power US are an excellent alternative to heat-based treatments because they avoid the negative effects of traditional processing (sensory and organoleptic

decay), assuring at the same time the inactivation of spoiling and pathogenic microorganisms (Moosavi et al., 2021). In food, US have been used for a wide range of products and with very interesting purposes, including inactivation of microorganisms and enzymes, production of emulsions and nano-emulsions, extraction of bioactive compounds and oils from plant cells, and removal of microorganisms from surfaces (Bevilacqua et al., 2019a; Soltani-Firouz et al., 2019).

Among others, food matrix properties (intended as kind of material, and viscosity), temperature, intensity, power, and treatment time are parameters that influence the effect of US on processed products (Chavan et al., 2022). Depending on the intensity and duration of treatment, US could exert a dual effect on the microbial cell. High-intensity US could damage membranes causing viability loss and release of cellular components, while low-intensity US could stimulate bacterial metabolism (Bevilacqua et al., 2019a). First, this dual effect was reviewed by Erriu et al. (2014) for microbial biofilms, while recent studies have shown the positive effect of US on biofilm stability of *Acidipropionibacterium jensenii*, *Propionibacterium freudenreichi* (Bevilacqua et al., 2019b), *Limosilactobacillus reuteri* (Racioppo et al., 2017), and *Lacticaseibacillus casei* (Giordano and Mauriello, 2023).

However, there are a few data and many times the effects on the same species are controversial. For example, the penetration effect of low-intensity/low-frequency US in *Staphylococcus aureus* biofilms was studied by Wang et al. (2020), thus they found that this type of US significantly increased biofilm permeability, depending on time and ultrasound intensity. On the other hand, Yu et al. (2021) evaluated the effectiveness of high-frequency US against *S. aureus* biofilm; the results clearly indicated that at high intensity and frequency US could disrupt *S. aureus* clusters and cause cell lysis.

Historically, biofilm have been considered with a strong negative impact for food quality and health, as spoilers or pathogens can grow in sessile form (Guéneau et al., 2022); however, recently, their impact and significance has been re-evaluated, because biofilm produced by positive microorganisms could contribute to safety by counteracting pathogen growth through a variety of effects (competition for nutrients, production of antimicrobial compounds, anti-adhesive effects, microbial interference, etc.) (Guéneau et al., 2022).

Indeed, the ability of probiotics to colonize biotic and abiotic surfaces by forming biofilms could have great potential for human health and food safety. In the biomedical field, for example, a biofilm formed by probiotic microorganisms could be useful in hindering the development of infection-causing microorganisms, while in the food industry biofilms can be used to ensure the health safety of food products and the extension of their shelf life. In a recent study, Speranza et al. (2020) focused on *in vivo* metabolism of *Bifidobacterium longum* subsp. *infantis* and *L. reuteri*, and showed that these probiotics form biofilms able to control the growth of harmful bacteria.

The question beyond this research is if biofilm formation by positive bacteria could be modulated and increased by physical approaches; therefore, this research examines biofilm formation by *Lactiplantibacillus plantarum* and *Bifidobacterium* spp. and the possibility of a modulation of adhesion properties through an US treatment, also assessing the effect of the main treatment variables (power, duration, pulse) on biofilm formation and stability.

2. Materials and methods

2.1. Microorganisms

This study focused on two strains of *L. plantarum*, labeled as c19 (a wild strain isolated from Bella di Cerignola table olives and with some functional properties; Bevilacqua et al., 2010) and DSM 1055 (from the German Collection of Microorganisms, Braunschweig, Germany), and on the collection isolates *B. animalis* subsp. *lactis* DSM 10140, *B. longum* subsp. *longum* DSM 20219, and *B. longum* subsp. *infantis* DSM 20088.

The strains of *L. plantarum* were stored at −20°C in MRS broth (Oxoid, Milan, Italy) added with 33% of sterile glycerol (J.T. Baker, Milan, Italy), while *Bifidobacterium* spp. were stored at −20°C in MRS broth supplemented with 0.5% cysteine (cMRS) (Sigma-Aldrich, Milan, Italy) added with 33% of sterile glycerol; cysteine creates a reducing environment for *Bifidobacteria*. Before each assay, the microorganisms were grown under anaerobic conditions either in MRS broth or cMRS broth, incubated at 37°C for 24 h in jars. Then, the cultures were centrifuged at 4,000 × *g* for 10 min at 4°C; the supernatant was discarded, and the pellet suspended in distilled water.

2.2. US—Treatment

Bacteria suspension at ~10^7 CFU/ml, prepared as reported in section "Microorganisms," were treated through a VC Vibra Cell Ultrasound equipment, model VC 130 (Sonics and Materials Inc., Newtown, CT, USA; net power, 130W) as follows. 20 ml of bacterial suspension were put in 50 ml sterile tubes; then, ultrasonic probe was placed 1–2 cm below the surface and in the middle of tube. Each strain was US-treated through 6 different combinations, different for power (from 10 to 50% of the net power of equipment, i.e., 130 W), pulse (from 0 to 10 s), and duration of the treatment (from 2 to 10 min). These three variables were combined through a centroid approach, as reported in **Table 1**. According to the centroid approach each variable was set to 3 different levels, identified by the codes 0 (minimum), 1 (maximum), 0.5 (mean value). **Table 1** shows the 6 combinations of the centroid and the control (i.e., an additional combination in which power, treatment time, and pulse were set to 0, that is microorganism not treated through US). US was done in aerobic conditions.

Before each treatment, the ultrasonic probe was washed with sterile distilled water, ethanol at 70% and again with distilled water;

TABLE 1 US treatments tested on *L. plantarum* and *Bifidobacterium* spp.

	Coded values			Real values		
	Power	Time	Pulse	Power (%)	Time (min)	Pulse (s)
1	1	0	0	50	2	0
2	0	1	0	10	10	0
3	0	0	1	10	2	10
4	0.5	0.5	0	30	6	0
5	0.5	0	0.5	30	2	5
6	0	0.5	0.5	10	6	5
Control	–	–	–	–	–	–

10.3389/fmicb.2023.1094671

immediately after processing, the sample was cooled in ice. After each US treatment, a plate count was performed on MRS agar (*Lactobacilli*) or cMRS agar (*Bifidobacteria*), incubated at 37°C for 48 h; plates were incubated under anaerobic conditions (jars and anaerobic kit).

2.3. Biofilm formation

Bacterial suspensions treated through US and control strains were used to inoculate broth containing glass slides (25.4 mm × 76.2 mm), as surface adhesion for biofilm formation. Before each experiment, it is important to perform a preliminary treatment on glass slides to remove any fingerprints, grease and other impurities that might be present on the material. Thus, the slides were washed with acetone for at least 30 min, rinsed in distilled water and immersed in 1 N NaOH for 1 h. After a final rinse in distilled water, the slides were allowed to air dry. Finally, the slides were autoclaved at 121°C for 15 min before use. After the treatment, the slides were placed in 50 ml-tubes (one slide per tube) containing 45 ml of MRS broth (*Lactobacilli*) or cMRS broth (*Bifidobacteria*). The final step for sample preparation is the inoculation of tubes with slides and broth with US bacteria, adding 200 µl of the suspensions prepared as reported in section "US—Treatment" (US-treated suspensions and untreated bacteria) to gain an initial inoculum of ~10^5 CFU/ml).

After preparation and inoculation, samples were incubated at 37°C in jars; for each microorganism 7 different combinations were tested (6 US combinations and untreated microorganism).

After 1, 5, 7, 9, 12, and 16 days, slides were aseptically removed from the culture medium, rinsed with sterile distilled water to remove unattached cells, and placed in a tube containing 40 ml of sterile saline solution (0.9% NaCl). Then, the samples were sonicated at 20% power for 3 min to promote detachment of cells from the surface (Speranza et al., 2009). Microbiological analyses were done on this saline solution on either MRS agar or cMRS agar, incubated at 37°C for 48 h in jars.

2.4. Statistical analysis

All tests were performed in duplicate on two independent samples for each combination and for each strain. Cell concentration recovered from saline solution (section "Biofilm formation") was converted to log CFU/cm^2 through the following formula:

$$C_1 = \frac{C_2 * VS}{SA}$$

where C_1 is the viable count expressed in log CFU/cm^2; C_2 is the viable count expressed as log CFU/ml; VS is the volume during the sonication treatment (40 ml) and SA the area of adhesion tested (39 cm^2, surface area of the slide considering both sides).

Data of *L. plantarum* were analyzed through a multifactorial Analysis of Variance, using strain (c19 or DSM 1055), age of biofilm or sampling time (1, 5, 7, 12, and 16 days) and combinations of US treatment (control, or combinations from 1 to 6) as categorical predictors; Fisher LSD test was used as the *post-hoc* test. Statistic was done through the software Statistica for Windows (Statsoft, Tulsa, OK, United States).

Afterwards, data at day 1 for *B. infantis* and after 16 days for *L. plantarum* DSM 1055 were analyzed through a multiple regression approach through the option DoE/mixture design of the software Statistica to assess the significance of the three parameters of US treatment (power, pulse, and duration).

3. Results

3.1. Effect of US treatment on biofilm of *Bifidobacterium* spp.

Table 2 shows the viable count of US-treated bacteria (log CFU/ml), compared to the control (CNT, untreated strains), immediately after the treatment; US did not reduce cell count, which was between 7.65 ± 0.068 log CFU/ml (*L. plantarum*) and 6.86 ± 0.02 log CFU/ml (*Bifidobacterium* spp.) in the control, against values of 7.71 ± 0.03 log CFU/ml (*L. plantarum*) and 6.23 ± 0.15 log CFU/ml (*Bifidobacterium* spp.) recovered after the most drastic treatment (combination 1, 50% of the net power, 2 min, pulses at 0 s), thus suggesting that US did not affect the viability of the test strains and could be used for a positive modulation of biofilm formation.

Generally, *Bifidobacteria* and *L. plantarum* showed different adhesion properties, with a very low stability of biofilm for *Bifidobacterium* spp.; therefore, the strains were separately analyzed to avoid a confounding effect due to the higher count of sessile cells in *L. plantarum*.

Ultrasound treatment did not affect the adhesion properties of *B. longum* subsp. *longum* and *B. animalis* subsp. *lactis* strains. After

TABLE 2 Viable count (log CFU/ml) of US-treated bacteria compared to the control (untreated microorganism, CNT) immediately after the treatment.

	Combination						
Strains	CNT	1	2	3	4	5	6
L. plantarum c19	7.59 ± 0.02	7.55 ± 0.0	7.66 ± 0.05	7.54 ± 0.07	7.48 ± 0.01	7.59 ± 0.00	7.52 ± 0.03
L. plantarum DSM 1055	7.65 ± 0.07	7.72 ± 0.03	7.69 ± 0.21	7.82 ± 0.12	7.58 ± 0.03	7.53 ± 0.05	7.88 ± 0.0
B. longum subsp. *infantis*	6.73 ± 0.11	6.63 ± 0.21	6.89 ± 0.40	7.10 ± 0.08	6.81 ± 0.47	7.28 ± 0.04	7.07 ± 0.13
B. longum susp. *longum*	6.47 ± 0.66	6.54 ± 0.60	6.07 ± 0.01	6.12 ± 0.11	6.17 ± 0.06	6.14 ± 0.01	6.97 ± 0.27
B. animalis subsp. *lactis*	6.86 ± 0.06	6.22 ± 0.15	7.24 ± 0.89	7.20 ± 0.26	7.23 ± 0.09	7.46 ± 0.03	7.19 ± 0.02

For each row, the differences were not significant (one-way ANOVA and Fisher LSD test, $P > 0.05$). Mean values ± standard deviation.

10.3389/fmicb.2023.1094671

TABLE 3 Concentration of sessile cells (log CFU/cm^2) of *B. longum* subsp. *infantis*, preliminary treated through US.

	Biofilm age			
Biofilm produced from US-treated strain	1 day	5 days	7 days	9 days
CNT (untreated microorganism)	5.01 ± 0.23a	4.36 ± 0.67	3.79 ± 0.0	ND**
1*	6.87 ± 1.03b	4.19 ± 0.28	3.69 ± 0.45	3.71 ± 0.0
2	6.24 ± 0.0a,b	ND	ND	ND
3	6.13 ± 0.27ab	ND	ND	ND
4	6.47 ± 0.0a,b	ND	ND	ND
5	5.80 ± 0.33a	ND	ND	ND
6	6.08 ± 0.01a	3.82 ± 0.0	ND	ND

CNT, control. Mean values ± standard deviation; in the column for the data at day 1, letters indicate significant differences (one-way ANOVA and Fisher LSD test, $P < 0.05$). *Combination of the centroid; **not detected.

TABLE 4 Standardized statistical effects related to individual and interactive terms of the strain, US treatment, and biofilm age of *L. plantarum* c19 and DSM 1055.

	Effects
Combination	3.09
Strain	130.19
Biofilm age	597.72
Combination × strain	5.61
Combination × age	3.40
Strain × age	99.90
Combination × strain × age	4.71

The results were obtained through a multifactorial ANOVA (analysis of variance).

24 h, the concentration of sessile cells was 6.3 and 5.85 log CFU/cm^2 for *B. longum* subsp. *longum* and *B. animalis*, respectively, and US treatment did not change this trend; in addition, the count of sessile cells experienced a strong reduction in all samples and was below the detection limit after 5–7 days (data not shown).

On the other hand, a significant effect was found for *B. longum* subsp. *infantis* (Table 3); after 1 day, biofilm produced by US-treated microorganism was at higher levels than the control (5.0 log CFU/cm^2 vs. 5.80–6.87 log CFU/cm^2) and the highest count was found in the combination 1 (treatment at 50% of power, for 2 min, no pulse). Moreover, this combination also resulted in a higher stability of biofilm, with a residual concentration of sessile cells at 3.70 log CFU/cm^2 after 9 days, while for untreated microorganism or for cells treated with other US combinations sessile cells were below the detection limit.

3.2. Effect on US treatment on biofilm of *Lactiplantibacillus plantarum*

As reported elsewhere *L. plantarum* strains showed different trends; moreover, the stability of biofilm was higher than that found for *Bifidobacteria*. Finally, the two strains behaved in a different way, thus requiring a preliminary standardization of data as biofilm detachment or reduction of biofilm count compared to the day 1; therefore, data for these two strains should be read as reduction of the count of sessile cells throughout time.

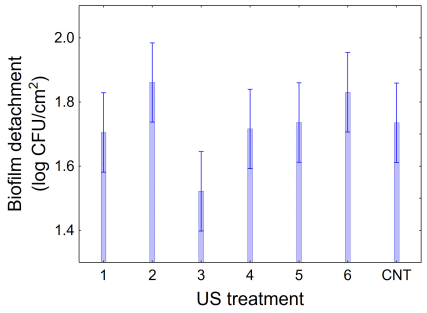

FIGURE 1
Decomposition of statistical hypothesis related to the individual term of US-treatment on the detachment of biofilm (log CFU/cm^2) of *L. plantarum* c19 and DSM 1055. Mean values ± 95% confidence interval.

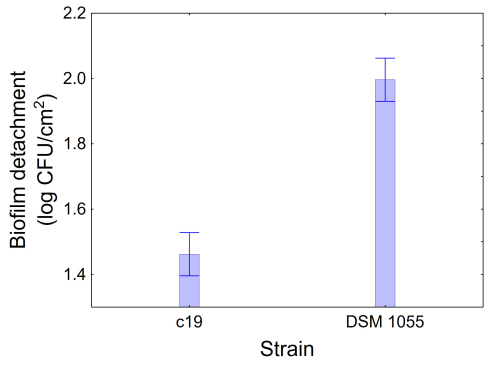

FIGURE 2
Decomposition of statistical hypothesis related to the individual term of strain on the detachment of biofilm (log CFU/cm^2) of *L. plantarum* c19 and DSM 1055. Mean values ± 95% confidence interval.

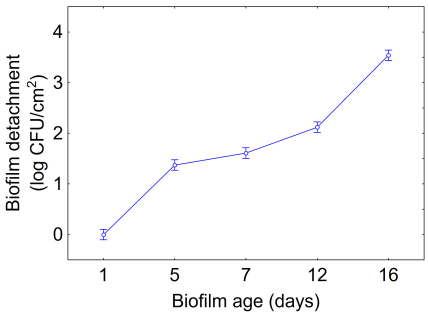

FIGURE 3
Decomposition of statistical hypothesis related to the individual term of biofilm age on the detachment of biofilm (log CFU/cm^2) of *L. plantarum* c19 and DSM 1055. Mean values ± 95% confidence interval.

Modeling was done through MANOVA; the table of standardized effects points out that all predictors, as individual or interactive terms (combination, strain, age of biofilm, combination × strain, combination × age of biofilm, strain × age of biofilm, combination × strain × age of biofilm), were found to be significant; however, their statistical weights were different.

10.3389/fmicb.2023.1094671

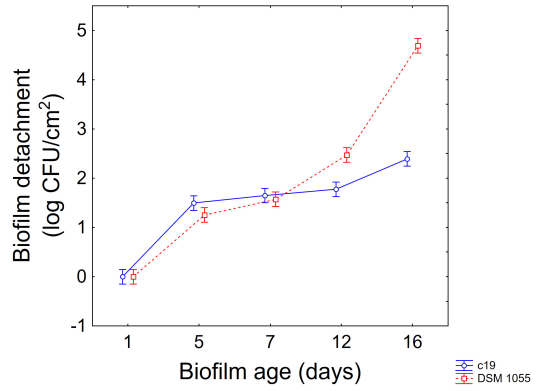

FIGURE 4
Decomposition of statistical hypothesis related to the interactive term "strain × biofilm age" on the detachment of biofilm (log CFU/cm^2) of *L. plantarum* c19 and DSM 1055. Mean values ± 95% confidence interval.

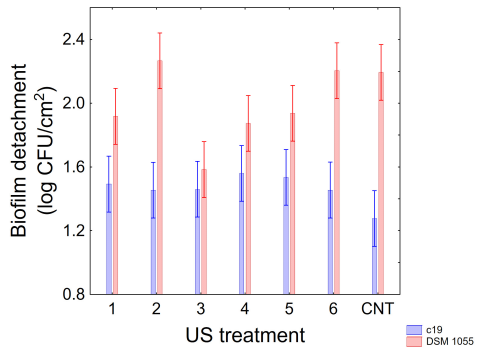

FIGURE 5
Decomposition of statistical hypothesis related to the interactive term "strain × US treatment" on the detachment of biofilm (log CFU/cm^2) of *L. plantarum* c19 and DSM 1055. Mean values ± 95% confidence interval.

The most important factor, as an individual term, was the age of biofilm, followed by the strain, and finally by the combination of US-treatment; on the other hand, the most important interactive term was "strain × age of biofilm" (Table 4).

The estimation of the quantitative effects of predictors is possible through the decomposition of the statistical hypothesis, which does not show real trends but the mathematical correlation of each predictor vs. the dependent variable.

Figures 1–3 show the decomposition of the statistical hypothesis for the individual effects of predictors (combination of US treatment, strain, and age of biofilm). Regarding the effect of the combination (Figure 1), the reduction of sessile cells (biofilm detachment) was minimum in combination 3 (power, 10%; duration of the treatment, 2 min; pulse, 10 s), while the other combinations did not show significant differences compared to control. The two strains produced a biofilm with a different stability, as generally *L. plantarum* DSM 1055 experienced a higher biofilm detachment (ca. 2.0 log CFU/cm^2) (Figure 2); as expected, biofilm age negatively affected its stability, as the detachment increased over time (Figure 3).

The approach of the decomposition of the statistical hypothesis was also used for the estimation of interactive terms. Figures 4, 5 show two-way interactions, namely for the interactions strain × age of biofilm (Figure 4) and combination of US treatment × strain (Figure 5).

The first interactive term highlights the higher stability of biofilm produced by the strain c19 mainly after 12 and 16 days, while for the different combinations the decomposition of the statistical hypothesis points out a higher stability of c19 biofilm in the control and in the combination 2 and 6.

Finally, Figure 6 shows 3-way interaction, that is the actual values; after 12 days significant differences were observed between the two strains in all combinations, showing a higher detachment of the biofilm for the strain DSM 1055. However, for this strain, a US treatment before biofilm formation is crucial, as biofilm detachment after 16 days was 5.5. log CFU/cm^2 in the control, 3.2 log CFU/cm^2 for the microorganism treated with the combination 3 and 4.4 log CFU/cm^2 when the microorganism had been treated with combinations 1, 4, and 5.

3.3. Significance of power, duration of US treatment and pulse on biofilm stability

Due to the significant effect of US on the viable count of sessile cells at day 1 for *B. longum* subsp. *infantis* and at day 16 for *L. plantarum* DSM 1055, the data for these sampling points were standardized as difference of sessile cells between US-treated microorganisms and untreated microorganisms and analyzed through a multiple regression procedure to understand how the three parameters of US (power, duration of the treatment, and pulse) could improve biofilm stability.

The first result of this approach is a set of standardized effects (Fisher-test values), which allows us to understand which variables were significant and which, among them, exerted the strongest effect. From a statistical point of view, for *B. longum* subsp. *infantis* the most important term was the power (*F*-test, 5.76), followed by the duration of the treatment (*F*-test, 3.81), and pulse (*F*-test, 3.47); the interactive terms (power × time, power × pulse, pulse × time) were not significant. In the case of *L. plantarum*, the most significant terms were power (*F*-test, 2.99) and pulse (*F*-test, 2.61).

However, the standardized effects show only the significance of the variables and do not allow the estimation of their quantitative effect. A better description can be obtained through the triangular plots; for *B. longum* subsp. *infantis* the triangular plot points out a higher value of biofilm for power-coded values around 1 (50% of net power), time 0 (treatment for 2 min), pulse 0 (0 s) (Figure 7). For *L. plantarum* DSM 1055 the highest difference US-treated strain vs. control (that is a higher stability of biofilm after US treatment) was found for the highest values of power or pulse (50% power and pulse at 10 s) or with the combination 0.5 power+0.5 pulse, as coded values, corresponding to real values of 30% of net power and 6 s of pulse, while an increase of the duration of the treatment exerted a detrimental effect on biofilm stability (Figure 8).

10.3389/fmicb.2023.1094671

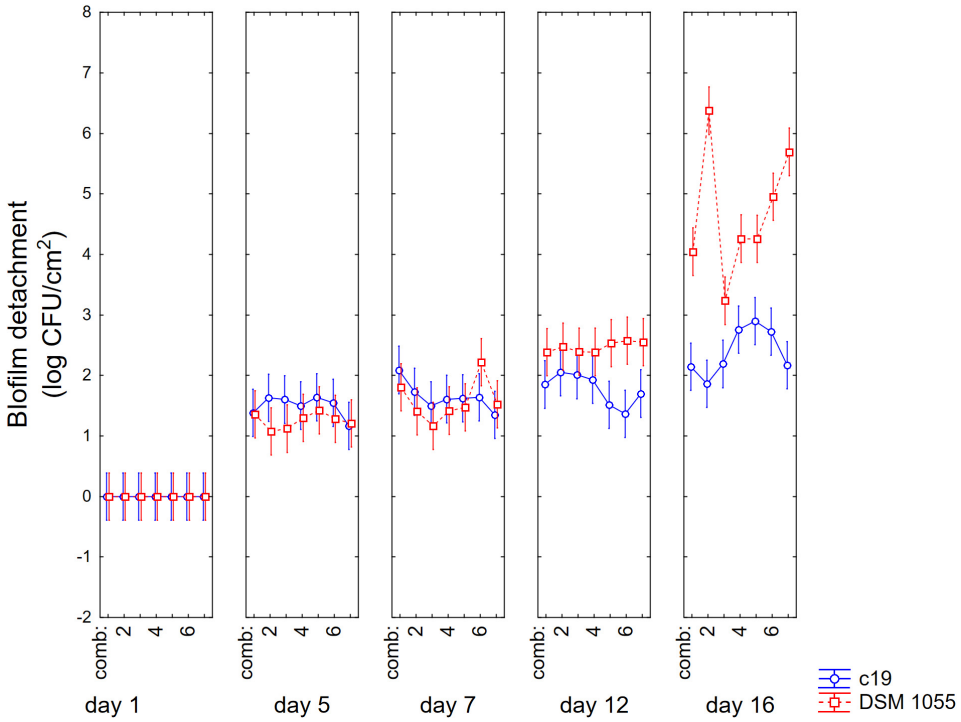

FIGURE 6
Decomposition of statistical hypothesis related to the interactive term "strain × biofilm age × US treatment" on the detachment of biofilm (log CFU/cm^2) of *L. plantarum* c19 and DSM 1055. Mean values ± 95% confidence interval.

4. Discussion

Bacterial adhesion could be strongly influenced by physical treatments such as US, as reviewed by Erriu et al. (2014) and Bevilacqua et al. (2019a). The first aspect to consider when applying US to probiotic or useful microorganisms is the effect on viability and the results of the first step showed that the treatments tested never reduced the viability of strains, even after the most drastic combination.

As reported elsewhere, US could produce different effects, mainly depending on the energy loaded in the system and the energy of US is a function of several parameters, including intensity, frequency, and pulses (Jomdecha and Prateepasen, 2010). US generally act through sonoporation and cavitation (Ojha et al., 2017); it is reliable to assume that low intensity US only produce sub-lethal injuries, which could promote the release of cellular components, and an increased rate of exchanges with environment, thus promoting microbial growth (Avhad and Rathod, 2015; Dai et al., 2017; Bevilacqua et al., 2019a); conversely, high-intensity

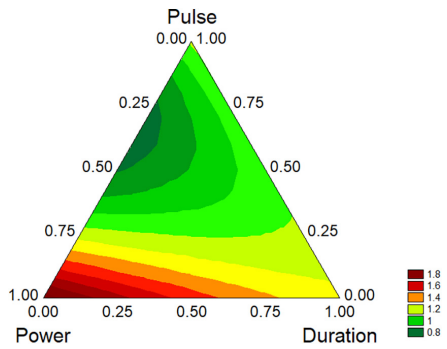

FIGURE 7
Triangular plots for the effect the factors of US-treatment (power, duration, and pulse) on biofilm stability compared to control (untreated microorganism) for *B. longum* subsp. *infantis* at day 1. The variables are reported as coded values (see **Table 1**).

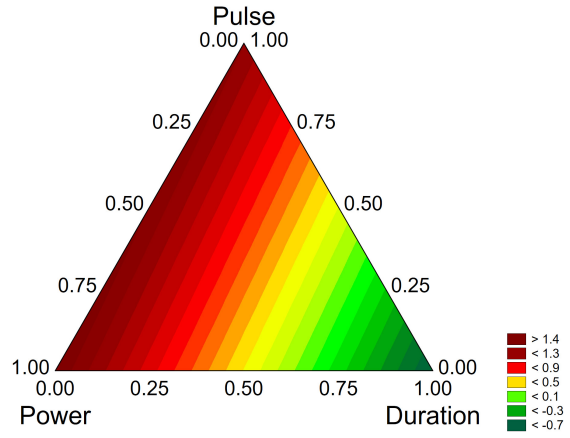

FIGURE 8
Triangular plots for the effect the factors of US-treatment (power, duration, and pulse) on biofilm stability compared to control (untreated microorganism) for *L. plantarum* DSM 1055 at day 16. The variables are reported as coded values (see **Table 1**).

treatments cause the formation of pores and cavities, resulting in an uncontrolled release of cell components and thus cell death (Ojha et al., 2017).

Erriu et al. (2014) reviewed the impact of US on bacterial biofilm, and they reported a positive modulation of this trait; however, there are a few data on this topic and the mechanisms beyond this phenomenon are still unknown.

The first evidence stressed by the results of this paper is the strong strain-dependence of the effect, as it was found only on *B. longum* subsp. *infantis* and on *L. plantarum* DSM 1055; moreover, strain dependence is also reflected in the combinations acting on the two microorganisms (50% power/2 min/no pulse for *B. longum*; 50% power/pulse at 10 s or 30% power/pulse at 6 s for *L. plantarum* DSM 1055).

Strain dependence is probably related to the effect of US on the outer layers of cells, as it is known that the first targets are capsule and cell wall (Gao et al., 2014a,b; Krasovitski et al., 2011); therefore, differences in the composition of these layers could result in a different effect of US or the need of different combinations to exert similar actions.

Apart from the positive effect, the different results on *Bifidobacteria* and *L. plantarum* also suggest that US could positively act on two different properties of biofilm: formation and stability.

Biofilm formation is the result of a complex phenomenon, also involving the interaction between bacterial and adhesion surfaces; in this mechanism, hydrophobicity plays a fundamental role as an unspecific adhesion to hydrophobic surfaces is the first phase for many processes of biofilm formation (de Wouters et al., 2015). This effect on hydrophobicity could be the reason beyond the action on *Bifidobacteria*, as in the past an increased cell surface hydrohobicity of *Limosilactibacillus reuteri* and *Propionibacteria* was found by authors after US treatments (Racioppo et al., 2017; Bevilacqua et al., 2019b). This effect on hydrophobicity was also reported for *Lacticaseibacillus casei* ATCC 393 (Giordano and Mauriello, 2023), also coupled with an increased membrane permeability.

In addition to the increased hydrophobicity, the positive effect on biofilm formation could be explained by an aggregating effect (increased aggregation) found in *Lactobacillus acidophilus*, *Lacticaseibacillus casei*, and *Lactococcus lactis* subsp. *cremoris* from Tabatabaie and Mortazavi (2008) after treatment with US. Autoaggregation is a desirable property since it results in increased adhesion of microbial cells to the intestinal mucosa, providing advantages in colonization of the gastrointestinal tract (García-Cayuela et al., 2014; Trunk et al., 2018), as well as in the ability to survive in harsh environments. However, this effect on auto-aggregation is controversial and conflicting results have been found in the literature, as stressed by Giordano and Mauriello (2023).

Finally, US is known to increase cell permeability, which results in the passive diffusion of quorum-sensing protein signaling molecules that can stimulate biofilm formation (Kamaraju et al., 2011; Fitzgerald et al., 2018).

On the other hand, the positive effect on biofilm stability, mainly found on *L. plantarum* DSM 1055, could also involve other phenomena, like the increased nutrients transport to deeper layers of the biofilm (Peterson and Pitt, 2000; Erriu et al., 2014), as well as by a probable effect on membrane permeability, and exopolysaccharide production (Khadem et al., 2020). In fact, it is reliable to assume that a good diffusion of nutrients across biofilm could delay cell aging, and consequently their detachment from the adhesion surface. Erriu et al. (2014) also postulated that ultrasound could increase the oxygen rate in the deeper layer of biofilm; this effect on oxygen rate could be related to the increased biofilm stability, at least in *L. plantarum*. In this species, in fact, it is possible the shift to an aerobic metabolism (Zotta et al., 2017), which could improve stress resistance (Guidone et al., 2013); another effect could be the improvement of viability after a long-term starvation (Zotta et al., 2012, 2013). Finally, a postulated effect of oxygen, indirectly linked to adhesion at least on a recombinant strain of *Lacticaseibacillus casei*, was an increased yield on EPS production (Li et al., 2015).

In conclusion, a low intensity US treatment could improve adhesion properties of *Lactobacilli* and *Bifidobacteria*, depending on the power of the treatment, its duration, and the use of pulse.

Concerning the duration, a short exposure (2 min) could positively affect biofilm formation, while the results on pulses were controversial, as biofilm was improved for pulsed treatments (6 or 10 s) in the case of *L. plantarum* and without pulse for *B. longum* subsp. *infantis*; concerning power, an intensity at 50% (or at 30% for *L. plantarum*) improved biofilm formation and/or stability.

The effect was strongly strain dependent, as it was found only on *B. longum* subsp. *infantis* and on a strain of *L. plantarum*. Moreover, the results also suggest two possible effects: improvement of adhesion for *Bifidobacteria* and positive modulation of biofilm stability for *L. plantarum*.

These results are promising, although they should be confirmed by other assays, such as biofilm formation and adhesion to intestinal model cell lines or to other abiotic surfaces. However, since a strain-dependence was found, further investigations are required to understand the mechanisms behind the recovered ultrasonic modulation of microbial cell properties.

Data availability statement

The raw data supporting the conclusions of this article will be made available by the authors, without undue reservation.

Author contributions

MS, MC, and AB designed the study. AR, BS, CA, and AB performed the experiments. AR and AB wrote the manuscript and analyzed the data. MS, MC, CA, and BS reviewed and edited the manuscript. MS and MC funded the research. AB supervised the experiments. All authors contributed to the article and approved the submitted version.

Conflict of interest

The authors declare that the research was conducted in the absence of any commercial or financial relationships that could be construed as a potential conflict of interest.

Publisher's note

References

Avhad, D. N., and Rathod, V. K. (2015). Ultrasound assisted production of a fibrinolytic enzyme in a bioreactor. *Ultrason. Sonochem.* 22, 257–264. doi: 10.1016/j.ultsonch.2014.04.020

Bevilacqua, A., Altieri, C., Corbo, M. R., Sinigaglia, M., and Ouoba, L. I. I. (2010). Characterization of lactic acid bacteria isolated from Italian Bella di Cerignola table olives: selection of potential multifunctional starter cultures. *J. Food Sci.* 75, M536–M544. doi: 10.1111/j.1750-3841.2010.01793.x

Bevilacqua, A., Campaniello, D., Speranza, B., Altieri, C., Sinigaglia, M., and Corbo, M. R. (2019a). Two nonthermal technologies for food safety and quality—Ultrasound and high pressure homogenization. effects on microorganisms, advances, and possibilities: a review. *J. Food Prot.* 82, 2049–2064. doi: 10.4315/0362-028X.JFP-19-059

Bevilacqua, A., Racioppo, A., Sinigaglia, M., Speranza, B., Campaniello, D., and Corbo, M. R. (2019b). A low-power ultrasound attenuation improves the stability of biofilm and hydrophobicity of *Propionibacterium freudenreichii* subsp. *freudenreichii* DSM 20271 and *Acidipropionibacterium jensenii* DSM 20535. *Food Microbiol.* 78, 104–109. doi: 10.1016/j.fm.2018.10.010

Chavan, P., Sharma, P., Sharma, S. R., Mittal, T. C., and Jaiswal, A. K. (2022). Application of high-intensity ultrasound to improve food processing efficiency: a review. *Microorganisms* 11:122. doi: 10.3390/foods11010122

Dai, C., Xiong, F., He, R., Zhang, W., and Ma, H. (2017). Effects of low-intensity ultrasound on the growth, cell membrane permeability and ethanol tolerance of Saccharomyces cerevisiae. *Ultrason. Sonochem.* 36, 191–197. doi: 10.1016/j.ultsonch.2016.11.035

de Wouters, T., Jans, C., Niederberger, T., and Rühs, P. A. (2015). Adhesion potential of intestinal microbes predicted by physico-chemical characterization methods. *PLoS One* 10:e0136437. doi: 10.1371/journal.pone.0136437

Erriu, M., Blus, C., Szmukler-Moncler, S., Buogo, S., Levi, R., Barbato, G., et al. (2014). Microbial biofilm modulation by ultrasound: current concepts and controversies. *Ultrason. Sonochem.* 21, 15–22. doi: 10.1016/j.ultsonch.2013.05.011

Estivi, L., Brandolini, A., Condezo-Hoyos, L., and Hidalgo, A. (2022). Impact of low-frequency ultrasound technology on physical, chemical and technological properties of cereals and pseudocereals. *Ultrason. Sonochem.* 86:106044. doi: 10.1016/j.ultsonch.2022.106044

Fitzgerald, N. J. M., Simcik, M. F., and Novak, P. J. (2018). Perfluoroalkyl substances increase the membrane permeability and quorum sensing response in *Aliivibrio fischeri*. *Environ. Sci. Technol. Lett.* 5, 26–31. doi: 10.1021/acs.estlett.7b00518

Gao, S., Lewis, G. D., Ashokkumar, M., and Hemar, Y. (2014a). Inactivation of microorganisms by low-frequency high-power ultrasound: effect of growth phase and capsule properties of the bacteria. *Ultrason. Sonochem* 21, 446–453. doi: 10.1016/j.ultsonch.2013.06.006

Gao, S., Lewis, G. D., Ashokkumar, M., and Hemar, Y. (2014b). Inactivation of microorganisms by low-frequency highpower ultrasound, 2: a simple model for the inactivation mechanism. *Ultrason. Sonochem.* 21, 454–460. doi: 10.1016/j.ultsonch.2013.06.007

García-Cayuela, T., Korany, A. M., Bustos, I., Gómez, de Cadiñanos, L. P., Requena, T., et al. (2014). Adhesion abilities of dairy *Lactobacillus plantarum* strains showing an aggregation phenotype. *Food Res. Int.* 57, 44–50. doi: 10.1016/j.foodres.2014.01.010

Giordano, I., and Mauriello, G. (2023). Ultrasound improves some surface properties of the probiotic strain *Lacticaseibacillus casei* ATCC 393. *Microorganisms* 11:142. doi: 10.3390/microorganisms11010142

Guéneau, V., Plateau-Gonthier, J., Arnaud, L., Piard, J. C., Castex, M., and Briandet, R. (2022). Positive biofilms to guide surface microbial ecology in livestock buildings. *Biofilm* 4:10075. doi: 10.1016/j.bioflm.2022.100075

Guidone, A., Ianniello, R. G., Ricciardi, A., Zotta, T., and Parente, E. (2013). Aerobic metabolism and oxidativestress tolerance in the *Lactobacillus plantarum* group. *Word J. Microbiol. Biotechnol.* 29, 1713–1722. doi: 10.1007/s11274-013-1334-0

Jomdecha, C., and Prateepasen, A. (2010). Effects of pulse ultrasonic irradiation on the lag phase of *Saccharomyces cerevisiae* growth. *Lett. Appl. Microbiol.* 52, 62–69. doi: 10.1111/j.1472-765X.2010.02966.x

Kamaraju, K., Smith, J., and Wang, J. (2011). Effects on membrane lateral pressure suggest permeation mechanisms for bacterial quorum signaling molecules. *Biochemistry* 50, 6983–6993. doi: 10.1021/bi200684z

Khadem, H., Tirtouil, A. M., Drabo, M. S., and Boubakeur, B. (2020). Ultrasound conditioning of *Streptococcus thermophilus* CNRZ 447: Growth, biofilm formation, exopolysaccharide production, and cell membrane permeability. *Bio Technol.* 101, 159–165. doi: 10.5114/bta.2020.94774

Krasovitski, B., Frenkel, V., Shoham, S., and Kimmel, E. (2011). Intramembrane cavitation as a unifying mechanism for ultrasound induced bioeffects. *Proc. Natl. Acad. Sci. U S A.* 108, 3258–3263. doi: 10.1073/pnas.1015771108

Li, N., Huang, Y., Liu, Z., You, C., and Buo, B. (2015). Regulation of EPS production in *Lactobacillus casei* LC2W through metabolic engineering. *Lett. Appl. Microbiol.* 61, 555–561. doi: 10.1111/lam.12492

Moosavi, M. H., Khaneghah, A. M., Javanmardi, F., Hadidi, M., Hadian, Z., Jafarzadeh, S., et al. (2021). A review of recent advances in the decontamination of mycotoxin and inactivation of fungi by ultrasound. *Ultrason. Sonochem.* 79:105755. doi: 10.1016/j.ultsonch.2021.105755

Ojha, K. S., Mason, T. J., O'Donnell, C. P., Kerry, J. P., and Tiwari, B. K. (2017). Ultrasound technology for food fermentation applications. *Ultrason. Sonochem.* 34, 410–417. doi: 10.1016/j.ultsonch.2016.06.001

Peterson, R. V., and Pitt, W. G. (2000). The effect of frequency and power density on the ultrasonically-enhanced killing of biofilm sequestered *Escherichia coli*. *Colloids Surf. B. Biointerfaces* 17, 219–227. doi: 10.1016/S0927-7765(99)00117-4

Racioppo, A., Corbo, M. R., Piccoli, C., Sinigaglia, M., Speranza, B., and Bevilacqua, A. (2017). Ultrasound attenuation of lactobacilli and bifidobacteria: effect on some technological and probiotic properties. *Int. J. Food Microbiol.* 243, 78–83. doi: 10.1016/j.ijfoodmicro.2016.12.011

Soltani-Firouz, M., Farahmandi, A., and Hosseinpour, S. (2019). Recent advances in ultrasound application as a novel technique analysis, processing and quality control fruits, juices and dairy product industries: a review. *Ultrason. Sonochem.* 57, 73–88. doi: 10.1016/j.ultsonch.2019.05.014

Speranza, B., Liso, A., Russo, V., and Corbo, M. R. (2020). Evaluation of the potential of biofilm formation of *Bifidobacterium longum* subsp. *infantis* and *Lactobacillus reuteri* as competitive biocontrol agents against pathogenic and food spoilage bacteria. *Microorganisms* 8:177. doi: 10.3390/microorganisms8020177

Speranza, B., Sinigaglia, M., and Corbo, M. R. (2009). Non starter lactic acid bacteria biofilms: A means to control the growth of *Listeria monocytogenes* in soft cheese. *Food Control* 20, 1063–1067. doi: 10.1016/j.foodcont.2009.01.006

Tabatabaie, F., and Mortazavi, A. (2008). Studying the effects of ultrasound shock on cell wall permeability and survival of some lactic acid bacteria in milk. *World Appl. Sci. J.* 3, 119–121.

Trunk, T., Khalil, H. S., and Leo, J. C. (2018). Bacterial autoaggregation. *AIMS Microbiol.* 4, 140–164. doi: 10.3934/microbiol.2018.1.140

Wang, T., Ma, W., Jiang, Z., and Bi, L. (2020). The penetration effect of HMME-mediated low-frequency and low-intensity ultrasound against the *Staphylococcus aureus* bacterial biofilm. *Eur. J. Med. Res.* 25:51. doi: 10.1186/s40001-020-00452-z

Yu, H., Liu, Y., Yang, F., Xie, Y., Guo, Y., Cheng, Y., et al. (2021). Combined an acoustic pressure simulation of ultrasonic radiation and experimental studies to evaluate control efficacy of high-intensity ultrasound against *Staphylococcus aureus* biofilm. *Ultrason. Sonochem.* 79:105764. doi: 10.1016/j.ultsonch.2021.105764

Zotta, T., Guidone, A., Ianniello, R. G., Parente, E., and Ricciardi, A. (2013). Temperature and respiration affect the growth and stress resistance of *Lactobacillus plantarum* C17. *J. Appl. Microbiol.* 115, 848–858. doi: 10.1111/jam.12285

Zotta, T., Parente, E., and Ricciardi, A. (2017). Aerobic metabolism in the genus *Lactobacillus*: impact on the stress response and potential application in the food industry. *J. Appl. Microbiol.* 122, 857–869. doi: 10.1111/jam.13399

Zotta, T., Ricciardi, A., Guidone, A., Sacco, M., Muscariello, L., Mazzeo, M. F., et al. (2012). Inactivation of ccpA and aeration affect growth metabolite production and stress tolerance of *Lactobacillus plantarum* WCFS1. *Int. J. Food Microbiol.* 155, 51–59. doi: 10.1016/j.ijfoodmicro.2012.01.017

frontiers | Frontiers in Microbiology

TYPE Original Research
PUBLISHED 06 April 2023
DOI 10.3389/fmicb.2023.1154130

OPEN ACCESS

EDITED BY
Christian Magni,
CONICET Instituto de Biología Molecular y Celular de Rosario (IBR), Argentina

REVIEWED BY
Ren-You Gan,
Agency for Science, Technology and Research, Singapore
Zhenshang Xu,
Qilu University of Technology, China

*CORRESPONDENCE
María Teresa Dueñas
mariateresa.duenas@ehu.eus
Paloma López
plg@cib.csic.es

SPECIALTY SECTION
This article was submitted to Food Microbiology, a section of the journal Frontiers in Microbiology

RECEIVED 30 January 2023
ACCEPTED 14 March 2023
PUBLISHED 06 April 2023

CITATION
Diez-Ozaeta I, Martín-Loarte L, Mohedano ML, Tamame M, Ruiz-Masó JÁ, del Solar G, Dueñas MT and López P (2023) A methodology for the selection and characterization of riboflavin-overproducing *Weissella cibaria* strains after treatment with roseoflavin. *Front. Microbiol.* 14:1154130. doi: 10.3389/fmicb.2023.1154130

A methodology for the selection and characterization of riboflavin-overproducing *Weissella cibaria* strains after treatment with roseoflavin

Iñaki Diez-Ozaeta[1,2], Lucía Martín-Loarte[1], Mari Luz Mohedano[1], Mercedes Tamame[3], José Ángel Ruiz-Masó[1], Gloria del Solar[1], María Teresa Dueñas[2]* and Paloma López[1]*

[1]Departamento de Biotecnología Microbiana y de Plantas, Centro de Investigaciones Biológicas Margarita Salas (CSIC), Madrid, Spain, [2]Departamento de Química Aplicada, Facultad de Química, Universidad del País Vasco (UPV/EHU), San Sebastián, Spain, [3]Instituto de Biología Funcional y Genómica, (IBFG) CSIC-Universidad de Salamanca, Salamanca, Spain

Fermentative processes by lactic acid bacteria can produce metabolites of interest to the health and food industries. Two examples are the production of B-group vitamins, and of prebiotic and immunomodulatory dextran-type exopolysaccharides. In this study, three riboflavin- and dextran-producing *Weissella cibaria* strains (BAL3C-5, BAL3C-7 and BAL3C-22) were used to develop a new method for selection and isolation of spontaneous riboflavin-overproducing *W. cibaria* mutants. This method was based on the selection of strains resistant to roseoflavin. The DNA sequencing of the FMN riboswitch of bacterial cell populations treated with various roseoflavin concentrations, revealed the existence of at least 10 spontaneous and random point mutations at this location. Folding and analysis of the mutated FMN riboswitches with the RNA fold program predicted that these mutations could result in a deregulation of the *rib* operon expression. When the roseoflavin-treated cultures were plated on medium supporting dextran synthesis, the most promising mutants were identified by the yellow color of their mucous colonies, exhibiting a *ropy* phenotype. After their isolation and recovery in liquid medium, the evaluation of their riboflavin production revealed that the mutant strains synthesized a wide range of riboflavin levels (from 0.80 to 6.50mg/L) above the wild-type level (0.15mg/L). Thus, this was a reliable method to select spontaneous riboflavin-overproducing and dextran-producing strains of *W. cibaria*. This species has not yet been used as a starter or adjunct culture, but this study reinforces the potential that it has for the food and health industry for the production of functional foods or as a probiotic. Furthermore, analysis of the influence of FMN present in the growth medium, on *rib* mRNA and riboflavin levels, revealed which mutant strains produce riboflavin without flavin regulation. Moreover, the BAL3C-5 C120T mutant was identified as the highest riboflavin-overproducer. Determination of its chromosomal DNA sequence and that of BAL3C-5, revealed a total identity between the 2 strains except for the C120T mutation at the FMN riboswitch. To our knowledge, this work is the first demonstration that only a single alteration in the genome of a lactic acid bacteria is required for a riboflavin-overproducing phenotype.

KEYWORDS

***Weissella cibaria*, lactic acid bacteria, vitamin B2 (riboflavin), FMN riboswitch, roseoflavin, riboflavin overproducing bacteria, regulation of rib operon**

1. Introduction

Lactic acid bacteria (LAB) have the metabolic capacity to synthesize B-group vitamins and dextran-type exopolysaccharides (EPS), which have a wide range of functionalities and properties. Dextran is an α-glucan polysaccharide mainly composed of D-glucopyranosyl residues with α-(1,6) linkages and varying percentages of α-(1,4), α-(1,3) or α-(1,2) branches (Bounaix et al., 2010). It is synthesized extracellularly by diverse LAB in a reaction catalyzed by dextransucrases (Dsr, enzymes belonging to the glycoside hydrolase GH 70 family) by hydrolysis of sucrose and transfer of glucose molecules to the growing chain of the polymer. Dextrans are potential new hydrocolloids with interesting rheological properties, improving the structure/texture of different foods (e.g., in the formulation of gluten-free bakery or low-fat dairy products; Lynch et al., 2018; Werning et al., 2022). In addition, the high molecular weight dextran produced by LAB strains could have also multiple beneficial properties for human health, since they can act as antiviral (Nácher-Vázquez et al., 2015), antioxidant, hypocholesterolemic (Nadzir et al., 2021) and prebiotic (Kim et al., 2022) agents. Moreover, they have shown immunomodulatory (Zarour et al., 2017), and anti-inflammatory (Soeiro et al., 2016; Zhou et al., 2022) properties.

Riboflavin (RF, vitamin B_2) is a water-soluble vitamin that is part of the vitamin B complex. It is the precursor of both flavin adenine dinucleotide (FAD) and flavin mononucleotide (FMN), which are essential coenzymes in many oxidation–reduction processes and play an important role in cell energy metabolism, and therefore is an essential micronutrient for human health and development. RF is not synthetized by the human body, and it must be obtained from ingested food and/or from the gut microbiota (Leblanc et al., 2015; Thakur et al., 2017). RF is mainly found in foodstuff of animal origin such as meat, eggs and dairy products, and in lower concentrations in legumes, cereals or other vegetables. The daily intake recommended by EFSA ranges from 0.3–1.5 mg/day depending on the population group (EFSA Panel on Dietetic Products, Nutrition and Allergies (EFSA NDA Panel), 2017). It is mainly absorbed in the proximal small intestine and excreted in the urine, and its deficiency is due to malabsorption or insufficient vitamin intake. RF deficiency (ariboflavinosis) is of worldwide concern. Although this health issue is common in developing countries, RF deficiency also occurs in developed countries, mainly in populations with low intake of animal origin foodstuff (vegans/vegetarians) or with a greater need for RF intake due to their physiological condition (pregnant women, young people or elderly; Gregory et al., 2000; Rohner et al., 2007; Titcomb and Tanumihardjo, 2019). Its deficiency can lead to various health disturbances, including migraine, cardiac and skin disorders or alterations in sugar metabolism. It plays a key role in the homeostasis of the human body (Dey and Bishayi, 2016), regulation of multiple metabolic pathways driven by redox reactions (Powers, 2003) or the metabolism of different vitamins (such as folic acid, niacin, pyridoxine, and cobalamin) through the action of FMN and FAD (Pinto and Rivlin, 2013). Besides its important role in maintaining human health, recently the antimicrobial activity of RF against parasites, fungi, viruses and bacteria has been demonstrated (Farah et al., 2022). Therefore, *in situ* biofortification of fermented foods through the use of LAB that overproduce vitamin B_2 and dextran-type EPS, is a promising strategy to strengthen the health of consumers and address different nutritional deficiencies.

With regard to large scale production of riboflavin, the biosynthesis by microbial fermentation is the most promising and the currently the best candidates as cell factories, beside some fungi, are a few bacteria including *Bacillus subtilis,* LAB and *Escherichia coli* (Zhang et al., 2021).

In most Gram-positive bacteria, including *Bacillus subtilis* and LAB, the synthesis of riboflavin is catalyzed by four proteins: RibG, RibB, RibA, and RibH (Figure 1A), whose coding genes constitute the *rib* operon (Figure 1B). The expression of this operon is regulated by transcriptional attenuation through the FMN riboswitch (also called the RFN element) located in the 5′-untranslated region of the *rib* mRNA (Figure 1C), The riboswitch contains the FMN-binding aptamer, thus, when the concentration of FMN in the bacterial cytosol reaches the necessary level for its role as cofactor, the compound binds to the riboswitch (Vitreschak et al., 2002; Winkler et al., 2002). This binding leads to the formation of a terminator hairpin (in the expression platform of the riboswitch) and repression of transcription occurs, inhibiting the synthesis of RF (Figure 1C). By contrast, in the absence of the flavin, transcription of the operon takes place (Abbas and Sibirny, 2011; Thakur et al., 2015; Figure 1C). This regulatory mechanism is conserved in many distinct species such as *Fusobacterium nucleatum, Bacillus subtilis, Lactococcus lactis, Propionibacterium freudenreichii, Leuconostoc mesenteroides,* and *Lactiplantibacillus plantarum* (Burgess et al., 2004, 2006; Serganov et al., 2009; Ripa et al., 2022).

Roseoflavin, is a toxic analog of RF that also has the capacity to interact with the FMN-binding aptamer provoking bacterial death, and therefore treatment with this compound has been classically used to discover riboflavin-overproducing LAB strains. Thus, this procedure has been successfully employed to select spontaneous roseoflavin-resistant and RF-overproducing LAB belonging to the *L. lactis, L. plantarum, Limosilactobacillus reuteri,* and *L. mesenteroides* species (Burgess et al., 2004, 2006; Capozzi et al., 2011; Russo et al., 2014; Mohedano et al., 2019; Ge et al., 2020; Kim et al., 2021). In all these cases, LAB were treated with roseoflavin by: (i) plating in the presence of a high concentration of the compound or (ii) successive exposures to increasing concentrations of the RF analog in liquid medium. In all cases DNA sequencing revealed changes in the upstream region of the *rib* operon. In the case of pickle-derived *L. plantarum*, Ge et al. (2020) found an insertion of 1,059-bp DNA fragment located between the FMN riboswitch and the ribosomal binding site of the first gene of the *rib* operon, which could be responsible for alterations in the *rib* operon expression. Besides that, in all the other cases, including *L. plantarum* roseoflavin-treated strains isolated from various habitats, point mutations or deletions in the FMN riboswitch were observed.

In addition, we have isolated from rye sourdough three *Weissella cibaria* strains (BAL3C-5, BAL3C-7, and BAL3C-22) which are able to produce dextran and RF (Llamas-Arriba et al., 2021), and selected three RF-overproducing mutants, each from one of the above parental strains, by treatment with increasing concentrations of roseoflavin (Hernández-Alcántara et al., 2022). Moreover, analysis of the mutants´ performance during experimental bread making revealed that indeed they were able to biofortify the bread with dextran and RF by *in situ* synthesis (Hernández-Alcántara et al., 2022). Therefore, these results indicated the potential interest of *W. cibaria* RF-overproducing strains for production of functional bread.

Against this background we here report a strategy for *in vitro* detection of spontaneous mutants, prior to their isolation, in roseoflavin-treated cultures of the previously characterized BAL3C-5,

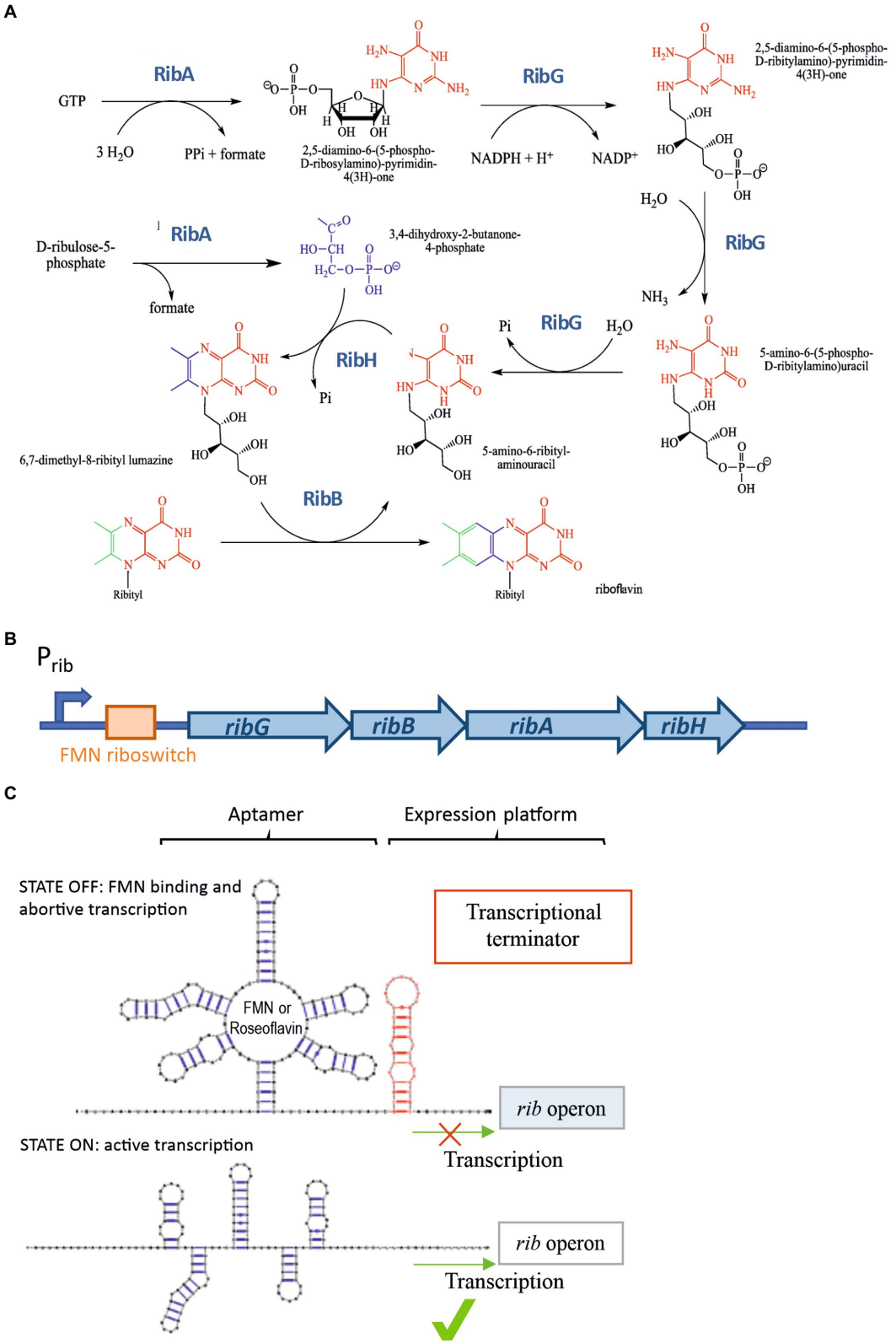

FIGURE 1
RF synthesis and regulation. **(A)** RF biosynthetic pathway. **(B)** The *rib* operon and its regulatory regions (promoter and FMN riboswitch). **(C)** Schematic representation of the *rib* operon riboswitch including the FMN binding sensing aptamer and the expression platform. Two alternative conformations of the regulatory domain. "OFF state" or FMN-bound state facilitating the formation of a ρ-independent transcriptional terminator in the regulatory element in the RNA, and the "ON state" in which an anti-terminator structure is formed in the absence of FMN enabling the transcription of the *rib* operon.

BAL3C-7, and BAL3C-22 strains and their further characterization. Prior to strain selection and isolation, molecular analyses and predictions of the consequences of point mutations in the regulatory region of roseoflavin treated cultures were carried out. Thereby, 8 mutants of interest were isolated, the changes in their FMN riboswitch characterized and their ability for RF overproduction validated under laboratory growth conditions. The influence of FMN and RF supplementation in the growth medium on RF production was also analyzed, as well as the effect of the FMN on the expression of the *rib* operon. Finally, determination of the DNA sequence of the genome of the parental BAL3C-5 strain and of its isogenic RF-overproducing mutant BAL3C-5 C120T revealed that indeed the mutation detected in the FMN-riboswitch was the only difference between the two chromosomal sequences. Thus, as far as we know, this is the first direct demonstration for a LAB strain that, in addition to the single mutation in the FMN riboswitch, no other molecular changes are required for its overproduction of RF.

2. Materials and methods

2.1. Bacterial strains and growth conditions

Weissella cibaria BAL3C-5, BAL3C-7, BAL3C-22 strains previously isolated from rye sourdough (Llamas-Arriba et al., 2021) and designated as parental or wild type (wt) as well as their corresponding RF-overproducing strains were used in this study and their characteristics are described in Table 1. The bacteria were grown at 30°C and propagated in liquid MRS medium (de Man et al., 1960) supplemented with either 2% sucrose (MRSS) or 2% glucose (MRSG). Also, the RF Assay Medium (RAM, Difco) containing 2% glucose, RAM supplemented with 2% sucrose (RAMS) or 2% maltose (RAMM) were used for the bacterial growth, when production of RF and dextran were investigated or during wt strain treatment with roseoflavin. Furthermore, RAMS plus 3 µM RF (RAMS + RF) and RAMS plus 3 µM FMN (RAMS + FMN) media were used to evaluate the influence of the presence of flavins during growth on RF production and *rib* operon expression.

2.2. Detection and isolation of RF-overproducing strains

The three parental *W. cibaria* strains were grown in MRSG medium to an optical density at 600 nm ($OD_{600\ nm}$) of 2.0. Afterwards, the bacterial cultures were diluted 1:100 in RAM medium and grown to mid exponential phase ($OD_{600\ nm}$ of 1.0). Then, the bacterial cultures were diluted in RAMM medium to give an $OD_{600\ nm}$ of 0.025 and four aliquots of 1 ml were supplemented each with a different roseoflavin concentration (100, 200, 300, or 400 µg/mL) and further grown at 30°C during approximately 60 h. Afterwards, cultures were sedimented by centrifugation at 9,300 × *g* for10 min at 4°C. The supernatants were removed, the bacterial cells were washed with phosphate-buffered saline (PBS) pH 7.3 and sedimented as above. After this step the cell pellets used for DNA extraction and further molecular analysis were stored at −20°C, whereas samples used for mutant isolation were resuspended in MRS supplemented with 20% glycerol and stored at −80°C. To isolate the mutants, selected roseoflavin-treated cultures were thawed and plated on MRSS agar plates. After 24 h incubation at 30°C, colonies were phenotypically selected (most of them yellowish), recovered from the plates by growth in MRSS and finally stored in MRS containing 20% glycerol at −80°C, until required.

2.3. Genomic DNA extraction, PCR amplification, and DNA sequencing of the FMN riboswitches' coding sequences

Genomic DNA (gDNA) extraction from *W. cibaria* strains was performed using the Wizard Genomic DNA Purification kit (Promega) following the instructions of the supplier but with modifications at three steps of the recommended protocol: (i) lysis step was carried out in the presence of lysozyme (30 mg/mL) and mutanolysin (25 U), (ii) DNA precipitation was performed with isopropanol and in the presence of Pellet Paint Coprecipitant NF (Merck), and (iii) after the isopropanol precipitation and supernatant removal, the washing step was performed through capillarity prior to drying the pellet with a vacuum pump and resuspension of the gDNA in 10 mM Tris HCl pH 8.0. DNA integrity was checked by electrophoresis in a 0.8% agarose gel with Tris-Acetate-EDTA buffer (Sigma-Aldrich) containing GelRed (Biotium). After that, gDNA was used as the template for amplification of the *W. cibaria* FMN riboswitch by the polymerase chain reaction (PCR).

PCR reactions were performed following the protocol of the recombinant Taq DNA polymerase (Thermo Fisher Scientific) in a final volume of 50 µL containing: 1x PCR buffer, 1.5 mM $MgCl_2$, 0.2 mM dNTPs mix, 0.5 µM from each of the primers, 1–500 ng of the DNA template, 1.0–2.5 U of the Taq DNA polymerase. The primers used were: ForRibo and ReverseRibo (Table 2). The reaction product was a 435 bp fragment including the *rib* operon regulatory region. PCR conditions were as follows: preheating at 94°C for 3 min, 15 PCR cycles of denaturing at 95°C for 45 s, annealing at 59°C for 30 s, extension at 72°C for 90 s and final extension for 10 min. The correct amplification was verified by analysis of the amplicons in 0.8% agarose gel and photographed using a Gel Doc 2000 Bio-Rad gel documentation system (Bio-Rad) and the Quantity One 4.5.2 Bio-Rad software. PCR products were purified with QIAquick PCR purification kit (Qiagen) and then, automated sequencing was performed through Sanger sequencing by Secugen (Madrid, Spain). The obtained sequences were analyzed with Chromas 2.6.6 (Technelysium Pty. Ltd.) and DNASTAR (Lasergene) software. The three parental strains (BAL3C-5, BAL3C-7, BAL3C-22) each carry an identical FMN riboswitch (Hernández-Alcántara et al., 2022) and its DNA sequence was compared with those of the roseoflavin treated cultures and isolates using the BLASTn software (Altschul et al., 1990). Predictions of the secondary structures of the FMN riboswitches were obtained by using the RNAfold web server (The ViennaRNA Web Services, version 2.4.18) and edited with VARNA 3.9 software (Darty et al., 2009).

2.4. Analysis of bacterial growth as well as RF and dextran production

Overnight cultures of the *W. cibaria* strains grown in MRSG were centrifuged at 9,300 × *g* for 10 min and the cells resuspended in fresh RAMS medium to give an $OD_{600\ nm}$ of 0.1. Then, cultures were grown to an $OD_{600\ nm}$ of 1.0, sedimented as above and resuspended in either RAMS + RF or RAMS + FMN. Aliquots of 200 µL in triplicate of each culture were analyzed in a sterile 96-well polystyrene optical bottom

TABLE 1 Bacterial strains used in this work.

Weissella cibaria strains	Characteristics	Source of isolation	FMN riboswitch	Reference
BAL3C-5	Riboflavin- and dextran-producer	Fermented rye dough	Wild-type	Llamas-Arriba et al. (2021)
BAL3C-7	Riboflavin- and dextran-producer	Fermented rye doughsdd	Wild-type	Llamas-Arriba et al. (2021)
BAL3C-22	Riboflavin- and dextran-overproducer	Fermented rye dough	Wild-type	Llamas-Arriba et al. (2021)
BAL3C-5 G15T (previously called BAL3C-5 B2)	Riboflavin-overproducer and dextran-producer	Spontaneous mutant of BAL3C-5 selected by roseoflavin treatment	G15T mutant	Hernández-Alcántara et al. (2022)
BAL3C-5 ΔG15	Riboflavin-overproducer and dextran-producer	Spontaneous mutant of BAL3C-5 selected by roseoflavin treatment	ΔG15 mutant	This work
BAL3C-5 A59C	Riboflavin-overproducer and dextran-producer	Spontaneous mutant of BAL3C-5 selected by roseoflavin treatment	A59C mutant	This work
BAL3C-5 A115G	Riboflavin-overproducer and dextran-producer	Spontaneous mutant of BAL3C-5 selected by roseoflavin treatment	A115G mutant	This work
BAL3C-5 C120T	Riboflavin-overproducer and dextran-producer	Spontaneous mutant of BAL3C-5 selected by roseoflavin treatment	C120T mutant	This work
BAL3C-7 G14T	Riboflavin-overproducer and dextran-producer	Spontaneous mutant of BAL3C-7 selected by roseoflavin treatment	G14T mutant	This work
BAL3C-7 G109A (previously called BAL3C-7 B2)	Riboflavin-overproducer and dextran-producer	Spontaneous mutant of BAL3C-7 selected by roseoflavin treatment	G109A mutant	Hernández-Alcántara et al. (2022)
BAL3C-22 C23T (previously called BAL3C-22 B2)	Riboflavin-overproducer and dextran-producer	Spontaneous mutant of BAL3C-22 selected by roseoflavin treatment	C23T mutant	Hernández-Alcántara et al. (2022)

TABLE 2 Primers used within the study.

Primers for amplification and sequencing of the FMN riboswitch		
Primer name	Primer sequence	Amplicon size (bp)
ForRibo	5′-GAAGTACCGGTATGACTGCTTT-3′	435
RevRibo	5′-TGGTTTCCCCTAACTACTACTCCGG-3′	
Primers for RT-PCR analyses		
Primer name	Primer sequence	Amplicon size (bp)
For1	5′-CCGGAGTAGTTAGGGGAAACA-3′	239
Rev1	5′-GACATACATCGTGGCCCCAA-3′	
For2	5′-GAAGTACCGGTATGACTGCTTT-3′	214
Rev2	5′-TCAACCGAATTGCTTAATCGCA-3′	
For*rpoB*	5′-GTCCATCAATGGAGCAAGGT-3′	224
Rev*rpoB*	5′-TAAACATCATCGCGGATCAA-3′	

plate (Thermo Fisher Scientific). Bacterial growth ($OD_{600\ nm}$) and fluorescence was monitored in real time, with measurements at 30 min intervals, at 30°C for 16 h using a Varioskan Flask System (Thermo Fisher Scientific), as previously described (Mohedano et al., 2019). RF fluorescence was measured using an excitation wavelength of 440 nm and detection of emission wavelength at 520 nm. RF concentration was calculated using a calibration curve (Mohedano et al., 2019). The growth rate and the doubling time of the strains was determined as previously described (Widdel, 2010).

Also, *W. cibaria* strains were inoculated in 5 ml of either RAMS or RAM to an OD_{600nm} of 0.1 and grown for 16 h at 30°C. Then, the concentration of RF was determined by measuring, as above: (i) the total fluorescence of the cultures and (ii) the fluorescence present in the culture supernatants after cell removal by centrifugation. Moreover, the dextrans present in the culture supernatants were recovered by ethanol precipitation as previously described (Besrour-Aouam et al., 2021) and their concentration determined by the phenol-sulfuric method (Dubois et al., 1956). Quantification was performed using a glucose calibration curve as a standard. Determinations were performed in triplicate.

2.5. Quantitative reverse transcription PCR analysis of expression of the *ribG* gene and the FMN riboswitch

Cultures of 5 mL of all *W. cibaria* strains were grown in RAMS or RAMS + FMN medium at 30°C in triplicate. Bacteria were

grown until the cultures reached an OD_{600nm} of 1.0. Then, RNA was rapidly stabilized by the addition of RNA Protect Bacteria Reagent (Qiagen) and cells were sedimented at 5,000 x *g* for 5 min. In parallel, aliquots of 1 mL cultures were withdrawn and used to determine the total RF concentration using the Varioskan equipment as described above.

To obtain total RNA, frozen bacterial cells were thawed, lysed by lysozyme (30 mg/mL) and mutanolysin (25 U) treatment, and further thermally disrupted at 80°C for 5 min. Total RNA was then purified following the instructions of the RNeasy Plus Mini kit, which includes on-column gDNA removal (Qiagen). Concentration and purity of extracted RNA was determined with a Nanodrop2000c spectrophotometer (ThermoFisher Scientific) and the integrity was confirmed through gel electrophoresis. Before cDNA synthesis, RNA was treated with ezDNAse (Invitrogen) to remove residual gDNA. Then, a 1 µg of RNA sample was used for cDNA synthesis which was carried out with the SuperScript IV First-Strand Synthesis System kit (Thermo Scientific) following the manufacturer's instructions. mRNA expression was monitored by real time qPCR carried out with SYBR Green PCR master mix (Roche Diagnostics) on a Roche LightCycler®96 instrument. The sequence of the primers used and the size of the amplicons generated during the qPCR analysis of the *ribG* gene (For1 and Rev1), the coding region of the FMN riboswitch (For2 and Rev2) and the housekeeping *rpoB* gene (For*rpoB* and Rev*rpoB*) are detailed in Table 2. For both assays, the reaction conditions were performed as follows: 95°C for 3 min followed by 40 cycles of 95°C for 20 s, 54°C for 40 s, and 72°C for 20 s and a dissociation step of 95°C for 10 s, 54°C for 60 s, and 97°C for 1 s. Reactions were performed in triplicate. The mean Cq value of each sample was normalized against the housekeeping *rpoB* gene and the corresponding control (see details in the Results section). The relative gene expression quantification was calculated with the $2^{-\Delta CT}$ method (Livak and Schmittgen, 2001).

2.6. Whole genome sequencing, assembly, annotation, and analysis

Weissella cibaria BAL3C-5 wt and BAL3C-5 C120T mutant strains were grown in MRS medium at 30°C to an $OD_{600\ nm}$ of 1.0. Genomic DNA extraction was performed as previously described using the Wizard® Genomic DNA Purification Kit (Promega). Extracted DNA was purified with NucleoSpin Gel and PCR Clean-up Kit (Macherey-Nagel), DNA concentration and quality was checked with Nanodrop and Qubit 2.0 fluorometer (Invitrogen).

Genome sequencing was achieved at Secugen (Madrid, Spain) combining Illumina Miseq technology with 2 × 150 paired-end reads and Oxford Nanopore MiniION technology. Libraries were prepared with the SQK-LSK109 ligation kit (Nanopore Technologies). A label was added to each sample (barcode) with the native barcoding kit EXP-NBD114 and the libraries were loaded in the flow cell FLO-MIN106 (Nanopore Technologies). The Illumina and Nanopore reads were analyzed with a high quality module (super accurate) of the MinKNOW software. The assembly was performed with Galaxy unicycler 0.5.0. software (Wick et al., 2017). Genome annotation was done with Prokka 1.14.6 tool through the Galaxy web-based platform.[1] Genome mapping visualization was performed through Proksee bioinformatic tool for genome assembly, annotation and visualization.[2]

The genomes were evaluated for the presence of antibiotic resistance genes using the BLAST and Resistance Gene Identifier (RGI) tools together with the Comprehensive Antibiotic Resistance Database (CARD, https://card.mcmaster.ca/; McArthur et al., 2013; Jia et al., 2017). Moreover, screening of resistance genes, genomic islands and virulence factors was assessed by Island4Viewer software[3] (Bertelli et al., 2017).

2.7. Statistical analysis

RF and dextran production as well as RT-PCR results were tested with one-way ANOVA analysis. A p-value ≤ 0.05 was considered significant. For each parental-mutants group, comparisons were computed with Dunnett test ($\alpha = 0.05$), and the comparison of all the strains together was performed by a Tukey's test. Means with a different letter are significantly different. All analyses were performed with the R software version 4.1.3 (R Foundation for Statistical Computing, Vienna, Austria).

3. Results

3.1. A method for specific detection and isolation of RF-overproducing LAB

A new methodology, including *in vivo*, *in vitro*, and *in silico* experiments and analysis, was devised as depicted in Figure 2.

Three RF and dextran-producing *W. cibaria* strains (BAL3C-5, BAL3C-7, and BAL3C-22) were used in the present work to detect and isolate RF-overproducing strains. The three strains were independently treated with various concentrations of roseoflavin (100, 200, 300, and 400 µg/mL). Then, prior isolation of mutants by plating and recovering individual colonies, with the aim to detect *in vitro* potential mutations in the bacterial pools, gDNAs of the treated as well as untreated control cultures were extracted, the DNAs encoding the FMN riboswitches of their *rib* operons were amplified and their sequences determined. Some of the chromatograms obtained from the gDNAs analysis are depicted in Figure 3. As expected from previous results (Hernández-Alcántara et al., 2022), the gDNAs from the untreated cultures of three parental strains carried identical FMN riboswitch encoding regions (data not shown). Furthermore, 9 single base substitutions at positions 14, 15, 16, 23, 59, 87, 109, 115, and 120;(the first ribonucleotide of the FMN riboswitch aptamer was considered position 1) and a single-nucleotide deletion at position 15 were detected in the DNA pools of the roseoflavin-treated cultures together with the wt sequence (Figure 3). In addition, minor and predominant mutations could be discerned. Predominant mutations were defined as having an equal or higher frequency than the corresponding wt strain DNA sequence, according to the intensity of their

1 https://usegalaxy.org
2 https://proksee.ca
3 https://www.pathogenomics.sfu.ca/islandviewer/

10.3389/fmicb.2023.1154130

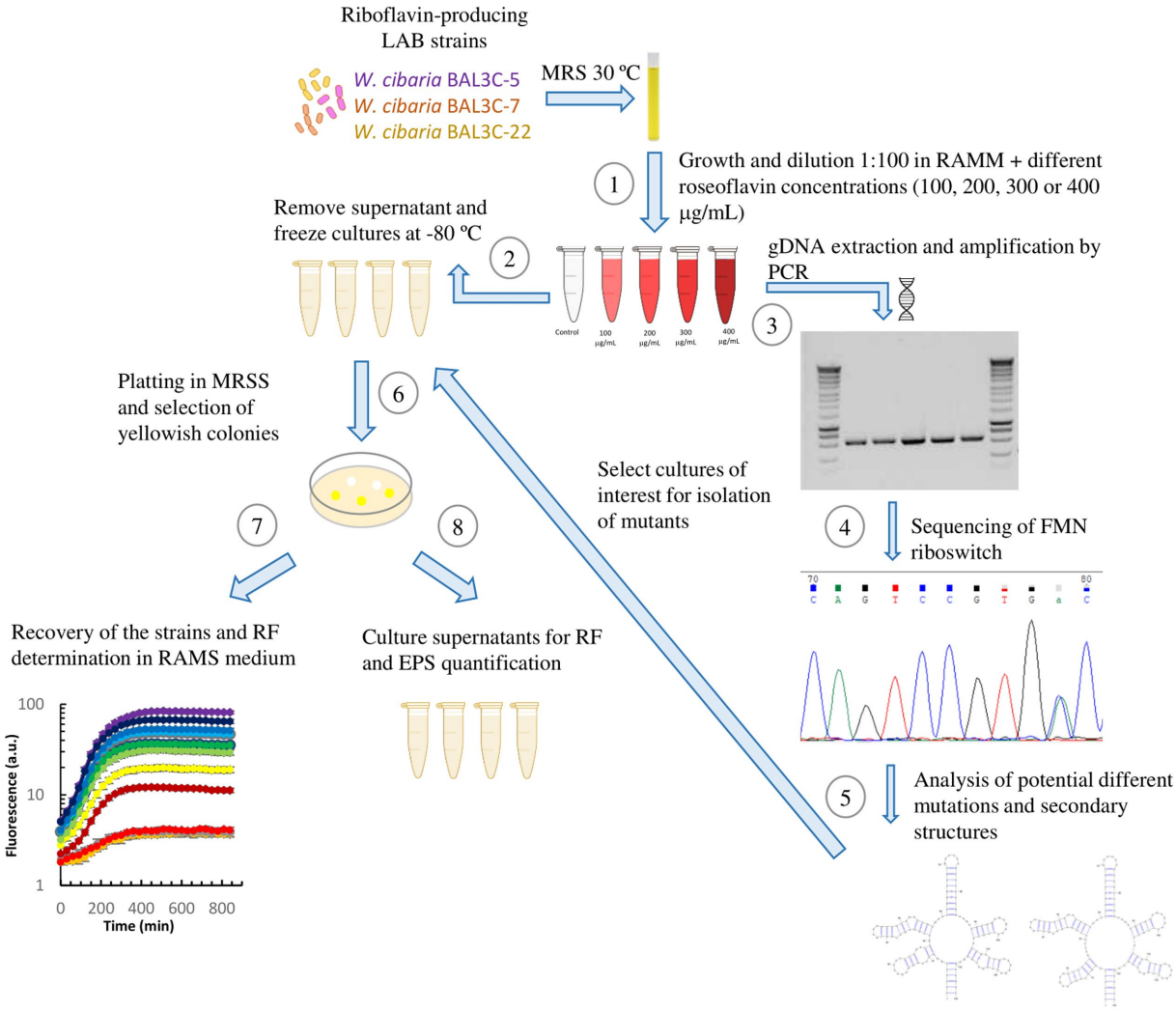

FIGURE 2
Schematic representation of the methodology followed for the selection and characterization of mutant strains. **(1)** Cultures reconstituted in MRS were grown in RAMM supplemented with different roseoflavin concentrations for 48h at 30°C. **(2)** Then, aliquots of the cultures were stored at −80°C. Another portion of bacterial cultures was used for gDNA extraction and amplification of the FMN riboswitch region. Amplified sequences were tested in agarose gels **(3)** and submitted to sequencing **(4)**. After, detection and location of point mutations in the FMN riboswitch aptamer by analysis of DNA sequencing chromatograms. **(5)** The predictive mutated aptamer structures were analyzed, and the *Weissella cibaria* roseoflavin-treated cultures, whose DNA showed the most promising mutations, were plated in MRSS and **(6)** yellow colonies were selected for isolation of the RF-overproducing strains. Then, the isolated mutant strains were subjected to analysis of RF production and growth in real time **(7)**, as well as quantification of RF and EPS production after 16h of growth **(8)**.

chromatographic peaks. For *W. cibaria* BAL3C-5, mutations with punctual substitutions G14T, G15T, T16G, C23T, A59C, A115G, and C120T, as well as a deletion at position 15 (ΔG15), were detected. The mutations G14T, T16G, A59C, G87A, and G109A were observed in treated cultures of *W. cibaria* BAL3C-7, and finally, a unique mutation C23T was detected in *W. cibaria* BAL3C-22 treated cultures. Moreover, it was also observed that the number and nature of the mutations was independent of the roseoflavin concentration.

The aim of this mutagenic analysis was to obtain the mutants with the highest constitutive RF production, and independent of FMN regulation. Therefore, before isolating the mutant strains, an *in silico* analysis of the wt and mutants FMN riboswitches was performed. The RNAfold program was used to predict the folding of the wt and mutants FMN aptamer domain (Figure 4). Moreover, the program allowed the calculation of the Gibbs free energy (ΔG) and the predicted values are also indicated in Figure 4. All the detected mutations were located in the aptamer of the riboswitch and only mutations A59C and G87A were located outside of the stem-loop structures. In addition, in 4 of the aptamers, the mutations (G14T, ΔG15, G15T y T16G) provoked changes in one of the stem loops structures (P2/L2, see details in Figure 5). Regarding to the ΔG required for formation of the FMN riboswitches, the folding of the structures built as a consequence of G14U, G15U, C23U, C120U and ΔG15 mutations showed higher ΔG (−45.0, −45.5, −45.5, −45.8, and −47.0 kcal/mol, respectively) than that of the wt folding structure (−47.9 kcal/mol). By contrast, the foldings of the A59C, G87A, and A115G aptamers, showed the same predicted ΔG as the wt, and the structure carrying the U16G, and G109A mutations, an even more favorable ΔG (both −48.6 kcal/mol) than the parental structure. With regard to the U16G, and G109A aptamer mutations, their low ΔG are

10.3389/fmicb.2023.1154130

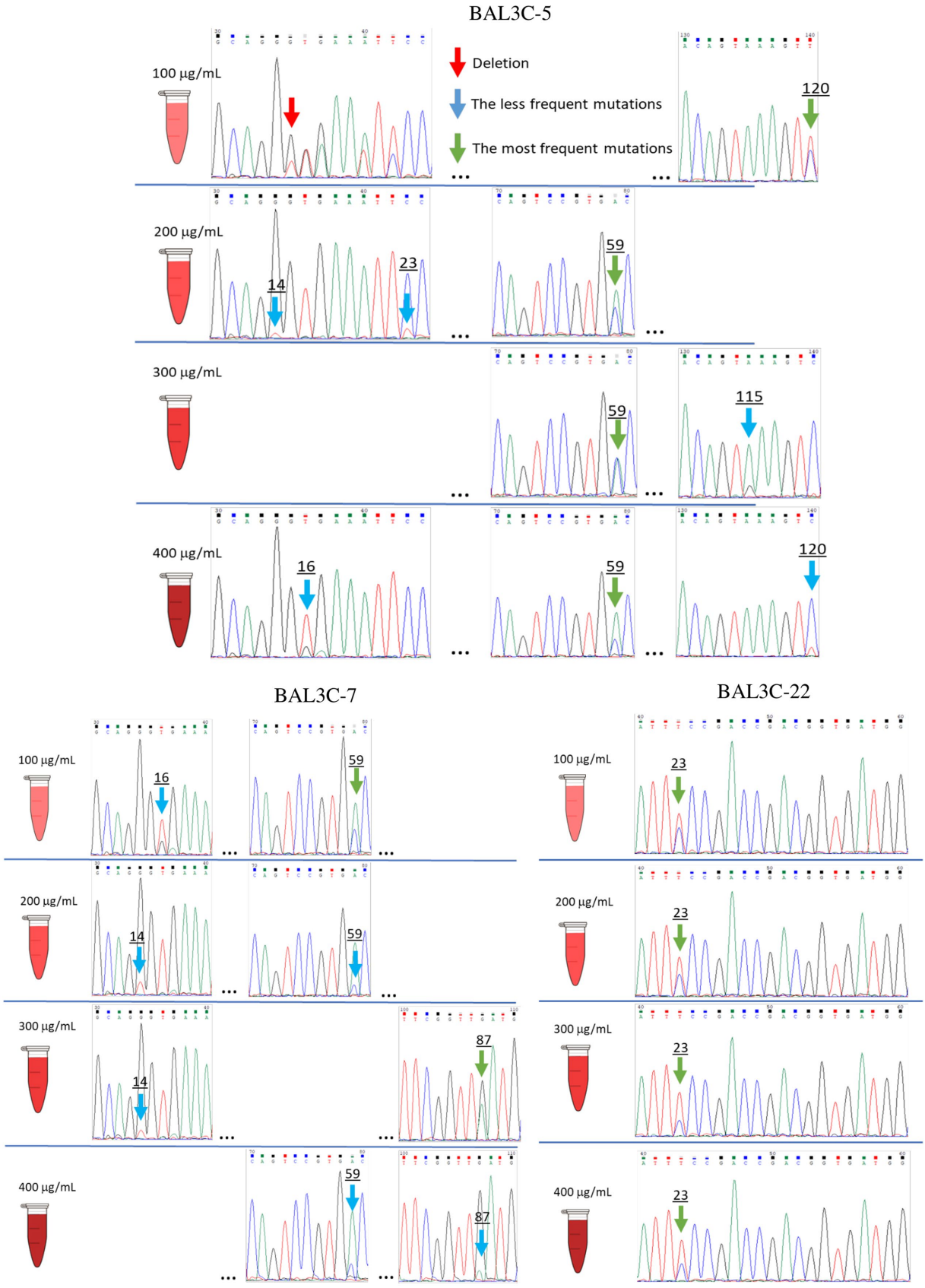

FIGURE 3
Identification of FMN riboswitch mutations present in roseoflavin treated *Weissella cibaria* cultures. Chromatograms of gDNA sequencing showing the *W. cibaria* BAL3C-5, BAL3C-7, and BAL3C-22 wt and mutants FMN riboswitches. The mutations were detected after various roseoflavin treatments.

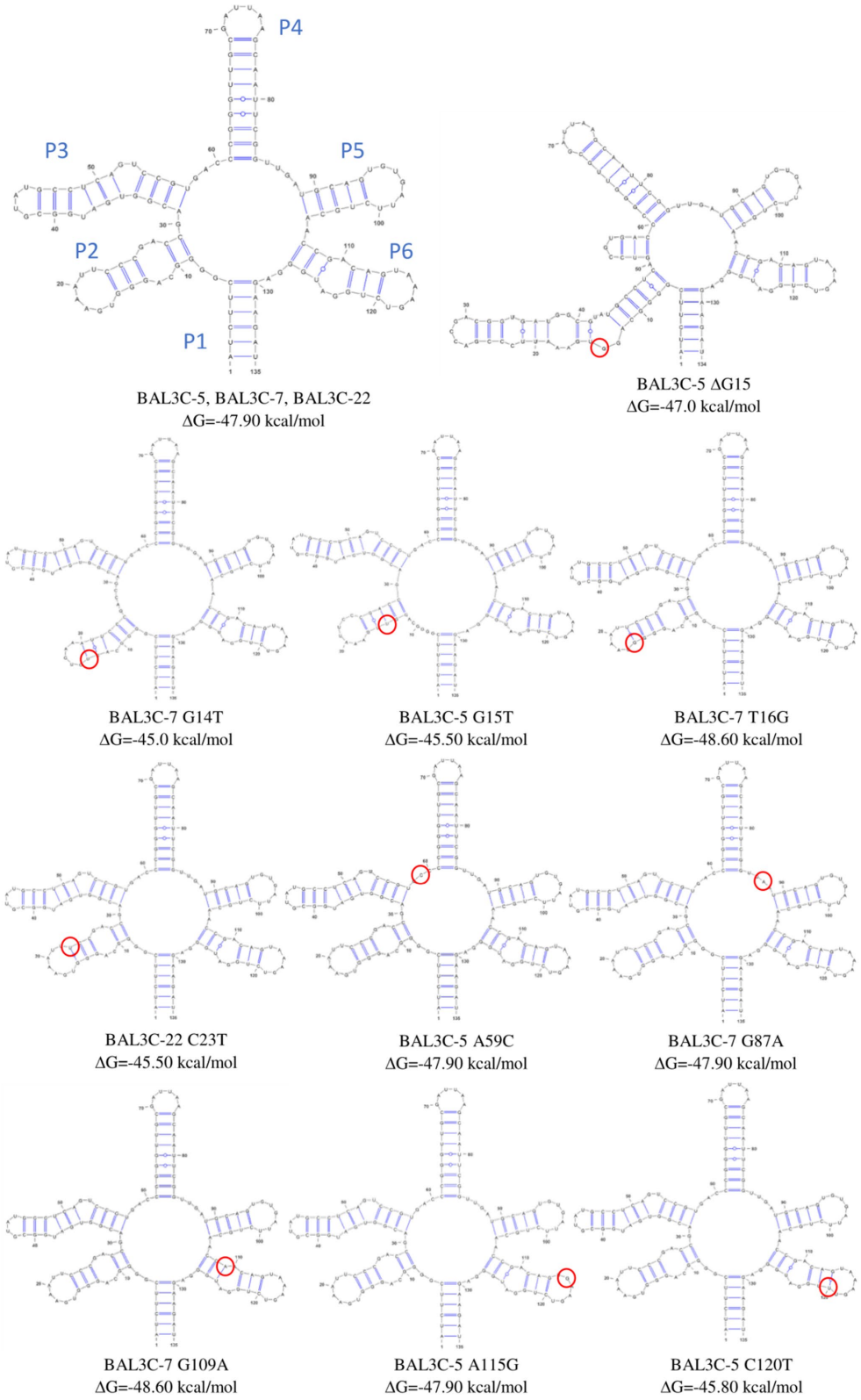

FIGURE 4
Predictive folding of the FMN riboswitch aptamer of the parental and of all the detected mutant strains. Change in Gibbs free energy (ΔG) for each secondary structure and location of each mutation (red circle) are also shown.

the consequence of the change in the strength of only one base pairing. This takes place by: (i) formation of hydrogen bonds between the G16 and U22 in the T16G mutant not present in the wt, which decreased the size of the P2 loop, and (ii) the interaction of A119 with U125 in the aptamer of the G109A mutant instead of the pairing of G109 with U125 in the structure of the wt strain (Figure 4).

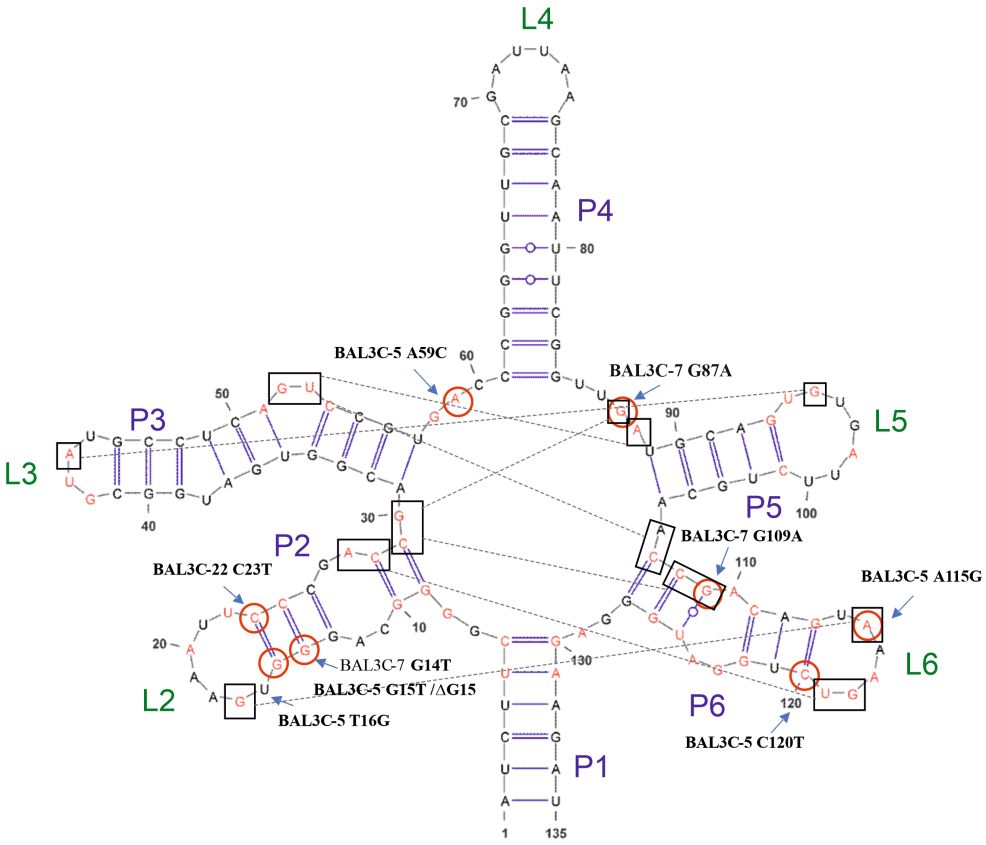

FIGURE 5
Model of the FMN riboswitch aptamer of *Weissella cibaria* based on the crystallographic studies performed by Serganov et al. (2009). Included in boxes are the nucleotides that could interact which each other for the conformation of the tertiary structure together with the FMN. In red, conserved nucleotides among distant species are depicted. Also, positions of detected mutations are shown.

Consequently, all the conformational and ΔG predicted changes of the FMN riboswitch aptamer indicated that the strains carrying most of the detected mutations should have altered regulation of the *rib* operon expression. Therefore, detection and isolation of strains carrying the mutations was approached by plating only the appropriate roseoflavin treated cultures for which the area of the mutated nucleotide was more prominent in the chromatograms, taking advantage of the fact that some RF-overproducing strains are qualitatively detectable by the turning of the colony and/or growth medium from white to yellow, due to the fluorescence of the flavin. However, when some of the treated cultures were plated in MRSG medium, no yellow colonies were detected. Consequently, we took into consideration that due to the production of dextran in MRSS solid medium, *W. cibaria* forms large mucous colonies, in which presumably even a pale yellow color of colonies from low RF-overproducer could be distinguished from the white colonies generated by the wt strains (Supplementary Figure S1). In fact, as part of the methodology used here by plating the selected roseoflavin-treated culture of the BAL3C-22 strain, colonies carrying the C23T mutation could be detected and isolated; strains harboring the G14T or G109A mutations were obtained from BAL3C-7 cultures and the other mutants were obtained from BAL3C-5 treated strain. Only A59C and A115G mutations, produced white colonies in MRSS. Finally, we could not recover the minor T16G and G87A mutations. A picture of liquid cultures of the BAL3C-5, BAL3C-7 and BAL3C-22 parental strains, as well as their mutant derivatives, is shown in Supplementary Figure S1A. A gradation of yellowish color was observed, with that of the BAL3C-5 C120T strain being the more intense. Thus, as an example of color differentiation of colonies, cultures in solid medium of the parental BAL3C-5, and mutant BAL3C-5 C120T strains alone or in a mixed culture are shown in Supplementary Figures S1B–D.

Production of dextran seems to be a common feature of *W. cibaria* species, since more than 50 strains represented in non-redundant protein sequences data bases (NCBI), carry dextransucrase proteins (annotated as glycosyl hydrolases). Therefore, the phenotypical method for selection of RF-overproducing strains by the yellowish color of their colonies in MRSS solid medium could be generally applied to various parental *W. cibaria* strains.

3.2. Analysis and quantification of RF production by the *Weissella cibaria* strains

An analysis of the bacterial growth and RF production of the isolated 8 mutants in comparison with their parental strains was performed. A fluorescent method was used to detect the RF production in real time (Mohedano et al., 2019). For this analysis, RAMS medium was used, since it only supports the growth of RF-producing strains, and it is suitable to detect quantitatively production of RF by *W. cibaria* (Llamas-Arriba et al., 2021). To confirm whether the different mutants obtained were

RF-overproducers, and whether flavin production was regulated, growth and production of the flavin in RAMS, RAMS + FMN, and RAMS + RF was monitored in real time by measurement the $OD_{600\,nm}$ and the fluorescence emitted by the bacterial cultures, respectively.

Regarding the growth in each tested medium, all the mutants and the wt strain behaved similarly (Figure 6A). The growth rate and doubling time of the different mutants and their parental strains were very similar. The growth rate ranged from 0.63 to 0.72 h^{-1} in RAMS, between 0.62 to 0.73 h^{-1} in RAMS + FMN, and from 0.69 to 0.77 h^{-1} in RAMS + RF. Regarding the RF production (Figure 6B), the 3 parental strains (BAL3C-5, BAL3C-7, and BAL3C-22) produced low levels of RF in RAMS medium, as previously observed (Llamas-Arriba et al., 2021; Hernández-Alcántara et al., 2022). In addition, all the mutant strains produced different levels of RF, which were higher than those synthesized by the parental strains. BAL3C-5 C120T was the highest producer and BAL3C-5 A59C the lowest. The addition of FMN or RF to the medium altered the basal levels of fluorescence of all strains, and resulted in a pronounced delay in fluorescence increase, ascribed to flavins, only in the cultures of the three parental strains (Figure 6B). In RAMS, RF production by the parental strains was detected from the beginning of growth, whereas in the media containing flavins, the fluorescence did not start to increase until the middle of the exponential phase (Figure 6B). This could be explained by an inhibition of the *rib* operon expression mediated by FMN internalized from the medium or synthesized from internalized RF. By contrast, the presence of either FMN or RF has little or no influence on the behavior of the mutant strains since increase of fluorescence due to the presence of flavins was observed almost from the beginning of the exponential growth phase. Also, the same pattern of RF production was detected among mutant strains.

To further characterize the production of RF by the *W. cibaria* strains, they were grown for 16 h at 30°C in either RAM (containing glucose) or RAMS (containing glucose plus sucrose). The final biomass of the LAB was assessed by plate counting. Their RF production was determined by measurement of: (i) the total fluorescence (total RF) and (ii) the fluorescence of the culture supernatants (free RF; Table 3). All the strains analyzed produced more RF in RAMS than in RAM (Table 3; Supplementary Figures S2–S5), and in addition the behavior of each one of the strains was the same in both media. Parental strains released a low proportion of the vitamin (between 25% and 54% in RAM and around 50% in RAMS) to the supernatant. By contrast, most of the total RF produced by the mutants (more than 90% in RAMS and more than 82% in RAM) was present in the culture supernatant, indicating that these bacteria externalize most of the RF, as previously observed for *L. plantarum* (Mohedano et al., 2019; Ripa et al., 2022). Nevertheless, regarding the RF concentration, wt strains did not show statistically significant differences among them, however, statistically significant differences ($p < 0.01$) were detected among all the mutant strains and between each wt and their mutant derivatives in both growth media tested (Table 3; Supplementary Figures S2–S5). The wt strains were the ones that produce less RF (0.16–0.18 and 0.02–0.03 mg/L in RAMS and RAM, respectively). Among the mutants, RF production by BAL3C-5 A59C was the lowest (1.42 and 0.73 mg/L in RAMS and RAM, respectively) in comparison with the rest of the mutants (Table 3). BAL3C-5 C120T produced the highest levels of total RF production (6.78 mg/L and 5.10 mL/L in RAMS and RAM, respectively). The increase in RF production between the wt and mutant strains was more pronounced in the case of RAM than in RAMS, presumably due to the low RF production observed in RAM for the wt strains. It is worth noting that BAL3C-5 C120T generated after 16 h of growth at 30°C almost 290-fold and 70-fold higher levels of RF than the parental strain in RAM and in RAMS, respectively. Thus, this strain will be the most interesting to be tested in the future for use in functional food production. BAL3C-7 G14T was the second highest RF producer (5.16 and 3.30 mg/L in RAMS and RAM, respectively) and their levels of production were also high compared with other overproducer mutants belonging to other species. Detection of the RF yellow color in strains grown in liquid and solid media also confirmed that BAL3C-5 C120T was the highest producer compared with the rest of the mutants and the wt strains (Supplementary Figure S1). In terms of the biomass in each medium, no significant differences between the wt and the mutant strains were observed. The CFU/L in RAMS ranged between 1.41×10^{11} and 2.16×10^{11} and in RAM from 8.23×10^{10} to 1.16×10^{11}.

3.3. Dextran production by the *Weissella cibaria* strains

The RF-overproducing phenotype could have a collateral influence in the dextran production of the mutant strains. Therefore, a comparative analysis of EPS production by the LAB strains was performed. The concentration of dextran, present in the supernatants of the parental and mutant strains grown 16 h at 30°C in RAMS, was determined, after ethanol precipitation, by the phenol sulfuric acid method (Table 3; Supplementary Figure S6). As expected, no production was detected in RAM, since it lacks sucrose, the substrate required for dextran synthesis by the dextransucrase. In RAMS all the strains produced similar dextran levels, ranging from 7.10 g/l to 5.60 g/l. The 3 parental strains BAL3C-5, BAL3C-7 and BAL3C-22 were the bacteria that produced the highest EPS yield (7.0, 6.8, and 7.1 g/L, respectively). Focusing on the mutant strains, BAL3C-5 A115G (6.73 g/L) and BAL3C-7 G14T (5.60 g/L) were the highest and the lowest EPS producers, respectively. Statistical analysis revealed that only the mutant BAL3C-7 G14T showed lower dextran production than its parental strain ($p < 0.05$; Table 3; Supplementary Figure S6). Nevertheless, although the mutant strain synthesized lower concentration of dextran than the parental bacteria, the EPS production was still high. Moreover, the above results confirmed that RAMS is suitable for the quantification of both RF and dextran production by *W. cibaria* strains.

Regarding dextran production, the good capability of BAL3C-5, BAL3C-7 and BAL3C-22 to produce dextran, as previously observed (Llamas-Arriba et al., 2021; Hernández-Alcántara et al., 2022), was confirmed here. In addition, no significant differences were detected among parental and mutant strains. Hence, dextran production was maintained in the mutants of interest.

3.4. Quantification of *ribG* gene expression in *Weissella cibaria* strains

The postulated mechanism of regulation of the *rib* operon expression made to predict that in the presence of FMN, this flavin

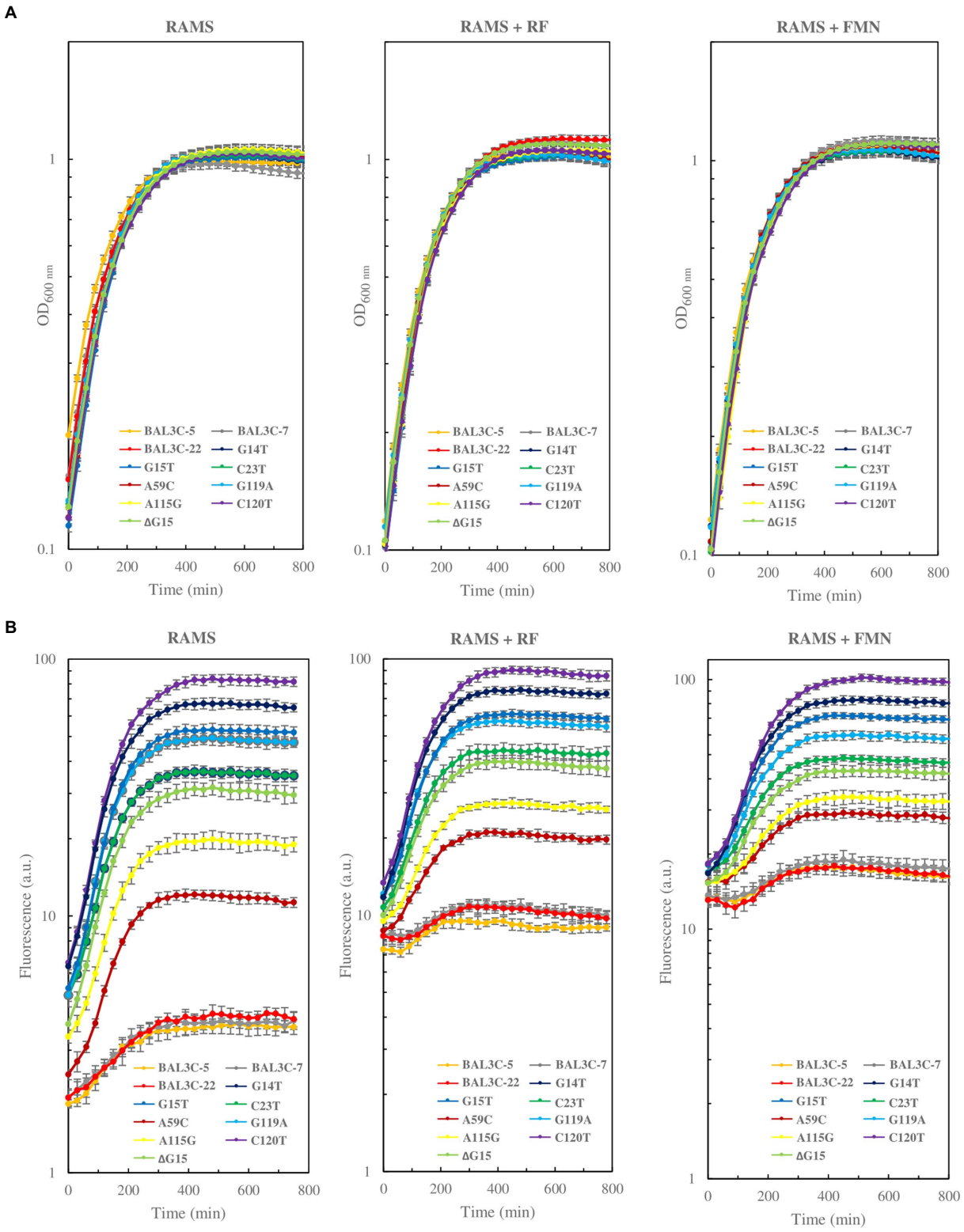

FIGURE 6
Comparative analysis of growth **(A)** and RF fluorescence **(B)** of the *Weissella cibaria* parental and mutant strains grown in RAMS, RAMS + FMN, and RAMS + RF.

will bind to the riboswitch aptamer and abortive transcription will take place, generating a transcript with its 3′-end at the ρ-independent terminator located upstream of *ribG* (Figures 1C, 7A).

To confirm that the different levels of transcription of the *rib* operon in the *W. cibaria* strains carrying mutant FMN riboswitches are related to the RF-overproducing phenotype, quantification of the

10.3389/fmicb.2023.1154130

TABLE 3 Analysis of riboflavin and dextran produced by the wt and mutant strains in RAM and RAMS.

Strains	Medium	Total RF (mg/L)[2]	Free RF (mg/L)[2]	Free RF/ Total RF (%)	Free RF mutant/ Free RF wt	$OD_{600\ nm}$	CFU/L	EPS (g/L)[2]	EPS/ $OD_{600\ nm}$ (g/L)
BAL3C-5	RAMS	0.16 ± 0.02^{I}	0.1 ± 0.01^{i}	59.66	-	3.23 ± 0.15	1.48E+11	$7.02 \pm 0.41^{\alpha\beta}$	2.04
BAL3C-7	RAMS	0.18 ± 0.01^{I}	0.09 ± 0.01^{i}	51.93	-	3.37 ± 0.06	2.11E+11	$6.80 \pm 0.45^{\alpha}$	2.02
BAL3C-22	RAMS	0.18 ± 0.02^{I}	0.09 ± 0.01^{i}	49.52	-	3.27 ± 0.12	1.68E+11	$7.10 \pm 0.68^{\alpha\beta}$	2.17
BAL3C-5 A59C	RAMS	1.42 ± 0.09^{C}	1.28 ± 0.06^{c}	90.22	13.25	3.47 ± 0.15	2.16E+11	$6.15 \pm 0.84^{\alpha\beta}$	1.83
BAL3C-5 A115G	RAMS	2.09 ± 0.12^{H}	1.99 ± 0.07^{h}	95.29	20.68	3.2 ± 0.10	1.23E+11	$6.73 \pm 0.57^{\alpha\beta}$	2.10
BAL3C-5 ΔG15	RAMS	2.3 ± 0.08^{G}	2.3 ± 0.07^{g}	98.70	23.89	3.5 ± 0.20	1.48E+11	$6.37 \pm 0.78^{\alpha\beta}$	1.82
BAL3C-22 C23T	RAMS	3.25 ± 0.12^{E}	3.16 ± 0.10^{e}	97.14	36.22	3.4 ± 0.17	1.96E+11	$6.01 \pm 0.84^{\alpha\beta}$	1.77
BAL3C-7 G109A	RAMS	3.69 ± 0.13^{B}	3.52 ± 0.11^{b}	95.27	37.77	3.1 ± 0.10	1.94E+11	$5.99 \pm 0.70^{\alpha\beta}$	1.93
BAL3C-5 G15T	RAMS	4.52 ± 0.21^{A}	4.16 ± 0.10^{a}	92.07	43.19	3.23 ± 0.15	2.12E+11	$6.23 \pm 0.82^{\alpha\beta}$	1.81
BAL3C-7 G14T	RAMS	5.16 ± 0.16^{D}	4.82 ± 0.17^{d}	89.94	51.75	3.4 ± 0.20	1.50E+11	$5.60 \pm 0.54^{\beta}$	1.65
BAL3C-5 C120T	RAMS	6.78 ± 0.13^{F}	6.67 ± 0.11^{f}	98.33	69.16	3.47 ± 0.12	1.41E+11	$6.29 \pm 0.70^{\alpha\beta}$	1.81
BAL3C-5	RAM	0.03 ± 0.01^{H}	0.02 ± 0.01^{h}	53.82	-	2.50 ± 0.10	1.02E+11	[1]n.d	-
BAL3C-7	RAM	0.03 ± 0.01^{H}	0.01 ± 0.00^{h}	33.46	-	2.47 ± 0.12	9.50E+10	[1]n.d	-
BAL3C-22	RAM	0.04 ± 0.01^{H}	0.01 ± 0.01^{h}	25.00	-	2.40 ± 0.10	8.23E+10	[1]n.d	-
BAL3C-5 A59C	RAM	0.73 ± 0.04^{C}	0.60 ± 0.03^{c}	82.23	37.18	2.53 ± 0.06	9.45E+10	[1]n.d	-
BAL3C-5 A115G	RAM	1.08 ± 0.06^{G}	0.94 ± 0.03^{g}	86.3	57.75	2.67 ± 0.12	9.98E+10	[1]n.d	-
BAL3C-5 ΔG15	RAM	1.46 ± 0.12^{D}	1.31 ± 0.07^{d}	90.05	80.97	2.53 ± 0.15	9.87E+10	[1]n.d	-
BAL3C-22 C23T	RAM	1.80 ± 0.10^{E}	1.52 ± 0.05^{e}	84.71	122.24	2.63 ± 0.06	1.05E+11	[1]n.d	-
BAL3C-7 G109A	RAM	2.81 ± 0.16^{B}	2.46 ± 0.14^{b}	87.65	215.01	2.5 ± 0.17	1.16E+11	[1]n.d	-
BAL3C-5 G15T	RAM	2.85 ± 0.09^{F}	2.47 ± 0.11^{f}	86.45	152.21	2.53 ± 0.15	9.68E+10	[1]n.d	-
BAL3C-7 G14T	RAM	3.30 ± 0.14^{C}	3.11 ± 0.09^{c}	94.13	271.23	2.63 ± 0.06	9.83E+10	[1]n.d	-
BAL3C-5 C120T	RAM	5.10 ± 0.16^{A}	4.66 ± 0.12^{a}	91.28	287.51	2.7 ± 0.10	1.13E+11	[1]n.d	-

[1]n.d., non-detected.

[2]Different letters mean statistically significant difference ($p \leq 0.01$).

rib mRNA levels was performed by RT-qPCR, and the changes in the expression of the first gene (*ribG*) of the *rib* operon in cultures grown in RAMS in the presence or absence of the effector FMN, were analyzed.

To this end, total RNA preparations were used to generate *rib* cDNA, and a fragment of the *ribG* gene located downstream of the putative riboswitch transcriptional terminator was quantitatively amplified by qPCR using the For1 and For2 primers (Figure 7A). Mean Ct values were calculated and fold changes in expression between each mutant and its corresponding parental strain are depicted in Figures 7B,C. The results showed different levels of abundance depending on the strain analyzed and the growth medium used. All the mutants exhibited a statistically significant increase of *ribG* expression compared to their corresponding parental strain

10.3389/fmicb.2023.1154130

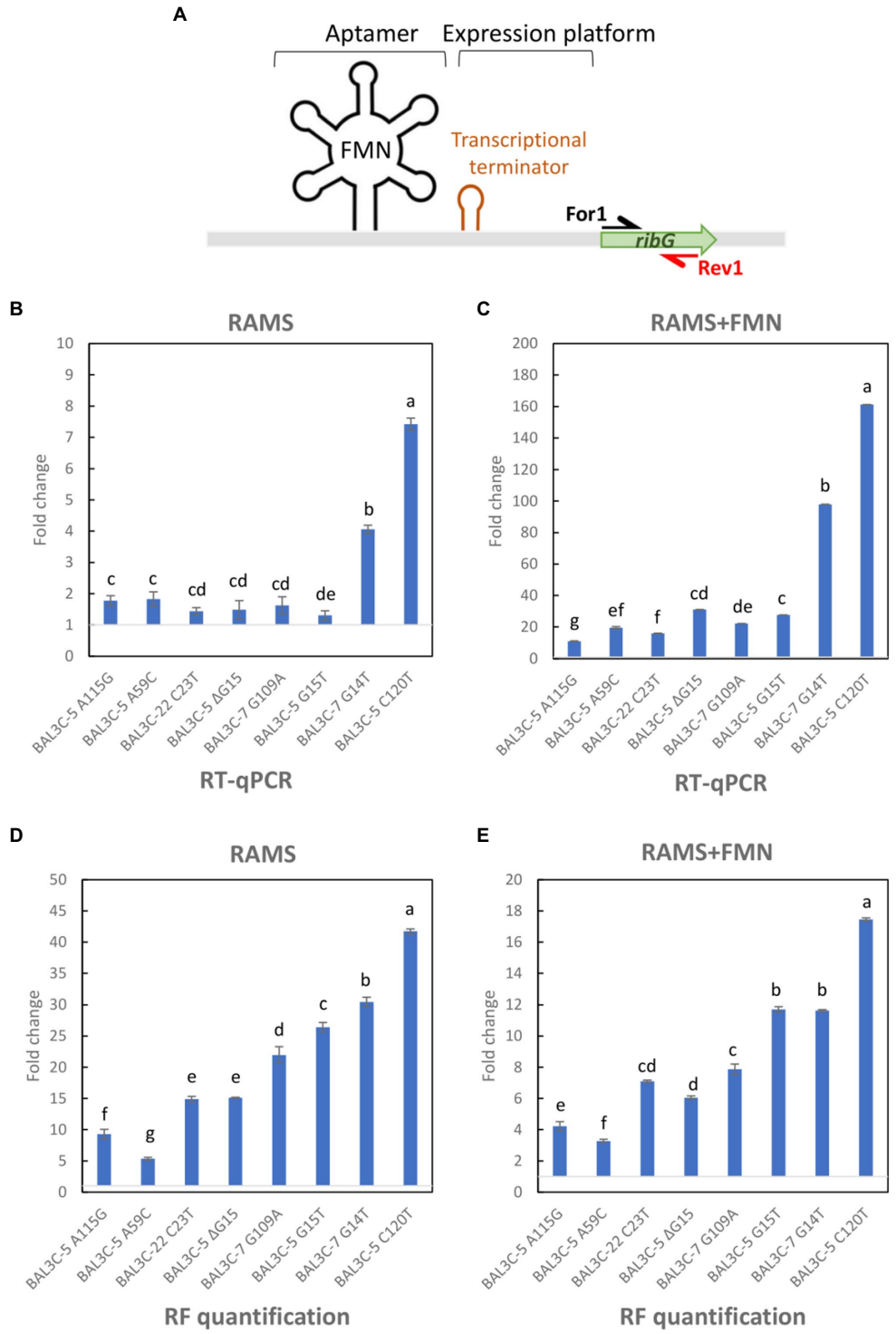

FIGURE 7
RT-qPCR analysis of *ribG* gene expression and evaluation of RF levels in *Weissella cibaria* cultures grown in RAMS or RAMS + FMN. **(A)** Schematic representation of the *rib* operon riboswitch including the FMN binding sensing aptamer and the expression platform in which a transcriptional terminator is formed in presence of FMN. The name and location of the primers used for the analysis are indicated. **(B,C)** Fold change of *ribG* gene expression in mutant strains compared with parental strains grown in RAMS **(B)** or RAMS + FMN **(C)**. **(D,E)** Fold change of RF production by mutant strains with regard to parental strains quantified from cultures submitted to RT-PCR in RAMS **(D)** or RAMS + FMN **(E)**. Different letters mean statistically significant difference ($p \leq 0.01$).

($p \leq 0.05$). The fold change values varied from 1.30 to 7.42 for mutant strains grown in RAMS (Figure 7B). In this case, BAL3C-5 C120T mutant strain showed the highest transcription level. A more pronounced increase of *ribG* expression was observed in cultures of the mutant strains compared to their parental strains when they were grown in RAMS + FMN. A 10.9- to 161.2-fold higher expression levels

were observed for the mutant strains (Figure 7C). Under this condition, it was also found that the BAL3C-5 C120T strain had the highest expression level of *ribG*. When the ratio of *ribG* expression in the presence vs. absence of FMN was analyzed for each strain independently, it was observed that the wt strains presented a very low level of *ribG* expression (0.05–0.09-fold) in the presence of the FMN effector (Figure 8). Although not so pronounced, the BAL3C-5 A115G and the BAL3C-5 A59C mutant strains also showed a significant drop in transcript abundance when the RAMS + FMN growth medium was used (0.33- and 0.58-fold; Figure 8), indicating that expression of the *rib* operon was still partially repressed by FMN-riboswitch aptamer interactions. This was not the case for the rest of the mutant strains, which presented a similar expression in the presence or absence of FMN in the growth medium (from 0.95- to 1.18-fold), with no significant statistical differences, beside BAL3C-7 G14T, which showed a slight but significant 1.86-fold higher level in RAMS + FMN medium than in RAMS medium (Figure 8), results that supported absence of post-transcriptional regulation mediated by the FMN effector.

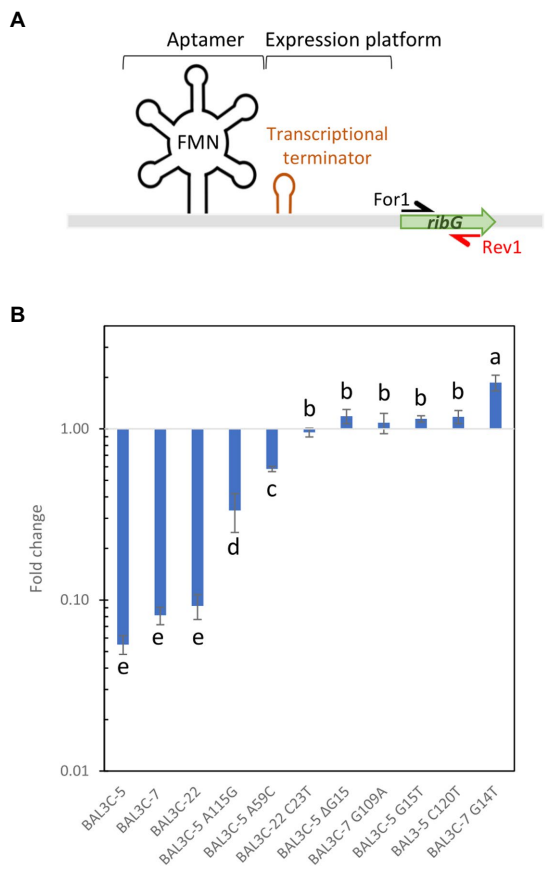

FIGURE 8
Analysis of the influence of FMN on transcription of the *ribG* gene in the *Weissella cibaria* parental and RF-overproducing strains. The bacteria were grown in RAMS and RAMS + 3μM FMN media and, using total RNA preparations, cDNA was synthesized and employed as substrate to perform RT-qPCR analysis. **(A)** Schematic representation of the *rib* operon riboswitch. See details in legend of Figure 7. The name and location of the primers used for the analysis are indicated. **(B)** The fold change of mRNA levels in the presence vs. absence of FMN are represented for each strain. Different letters mean statistically significant difference ($p \leq 0.01$).

In parallel, total RF concentration from cultures submitted to RT-qPCR was also evaluated. The RF production was expressed, as in the case of the RT-qPCR data depicted in Figures 7B,C, as fold change detected in the mutants with regard to their parental strains in RAMS (Figure 7D) and RAMS + FMN (Figure 7E). The results revealed, as shown in Table 3, that all the mutants produced statistically significant higher levels of RF in the two media tested ($p \leq 0.05$). Furthermore, the enhancement of production ranged from 5.3- to 41.7-fold for cultures grown in RAMS and from 3.2- to 17.4-fold for cultures grown in RAMS + FMN. In addition, in both media tested, BAL3C-5 A59C exhibited the lowest fold change value in comparison with the rest of the mutants and BAL3C-5 C120T showed the highest fold change in RF levels.

3.5. Expression profiling of the riboswitch region in presence and absence of FMN

Expression of the FMN riboswitch aptamer was quantified at the level of mRNA abundance. The aim of this analysis was to determine potential changes in the transcription of the untranslated lider region of the *rib* operon, upstream of the putative transcriptional terminator. Transcriptional analysis was carried out as above from cultures grown in both RAMS and RAMS + FMN, but using primers located upstream (For2) and within the aptamer (Rev2) for amplification during qPCR analysis (Supplementary Figure S7A). No statistically significant differences in mRNA levels between parental and mutant strains were observed (Supplementary Figure 7B), when cultures were grown in RAMS were analyzed. These results were expected, since nucleotide changes present in the mutant strains should not affect the transcriptional initiation signals of the *rib* operon. However, when cultures were grown in RAMS + FMN, the detected levels of the transcripts were significantly lower for the mutants compared with their corresponding parental strains (Supplementary Figure 7B). In addition, transcript abundance in the mutants showed a range of variation from 0.27- to 0.83-fold lower Ct values than that of the parental strains. Consequently, the overall RT-qPCR analysis indicated that, as expected, the untranslated leader region of the *rib* mRNA has a different fate to that of the coding one in both the parental and the mutant strains.

3.6. Determination of the complete DNA sequence of the chromosome of BAL3C-5 and BAL3C-5 C120T strains

Since BAL3C-5 C120T possesses the highest RF-overproducing phenotype among the studied strains, it was chosen, together with the parental BAL3C-5 strain, to carry out the sequencing of their genomes. A total of 83,974 (BAL3C-5) and 115,954 (BAL3C-5 C120T) mean raw reads comprising 397.4 and 473.2 Mb were obtained, indicating mean assembly coverage of 160X and 200X, respectively. Assembly resulted in 1 contig, with 2,406,256 bp of genome size and a GC% content of 45.15% for both strains. Annotation using prokka 1.14.6 revealed a total of 2,350 genes, distributed in 2,233 CDS, 88 tRNA, 28 rRNA and 1 tmRNA. Genome visualization is shown in Figure 9. The size of the circular chromosome of both stains was in accordance with the 13 complete genomes of *W. cibaria* available in the NCBI database which

range between 2,3 and 2,6 Mbp. Moreover, after comparing the genomes of the wt and the mutant strains analyzed only a single mutation was detected at position 446,494, which corresponds to the C120T alteration in the riboswitch of the mutant strain. These sequences were deposited in GenBank under the accession numbers CP116386 (BAL3C-5) and CP116385 (BAL3C-5 C120T).

The genomes were also screened against coding genes of antibiotic resistance and virulence factors. Antibiotic resistance evaluation using the CARD database confirmed that *W. cibaria* BAL3C5 and BAL3C5 C120T genomes did not harbor any specific resistance genes. In the same way, when virulence factors determination was carried out, Island4viewer software showed the absence of pathogen-associated genes, homologs of resistance genes, curated resistance genes, homologs of virulence factors and curated virulence factors (data not shown). Thus, safety parameters evaluated *in silico* support the potential use of the strain C120T for the development of functional foods.

4. Discussion

4.1. A strategy for identification of RF-overproducing strains

The FMN riboswitch regulatory element of the *rib* operon is composed of a FMN sensing domain and of the expression platform. It is thought that this RNA riboswitch presents two different conformations corresponding to the "OFF state" or FMN-bound state which facilitates the formation of the riboswitch aptamer and of a ρ-independent transcriptional terminator, and the "ON state" in which an anti-terminator structure is formed in the absence of FMN enabling the transcription of the *rib* operon (Vitreschak et al., 2002; Winkler et al., 2002 and Figure 1C). Moreover, roseoflavin-resistant strains usually harbor mutations in the riboswitch, which may lead to a reduction of production of RF in the presence of FMN.

Thus, in the present study a strategy for the *in vitro* identification and selection of mutant strains from *W. cibaria* species has been examined. Exposure to the selective pressure of high roseoflavin concentrations followed by the sequencing of the corresponding FMN riboswitch coding sequences of the resulting treated cultures was explored as an approach for the detection and selection of high RF-overproducing strains. The DNA sequencing of the *rib* operon leader region of the roseoflavin-treated cultures revealed a significant number of mutations (G14T, G15T, T16G, C23T, A59C, G87A, G109A, A115G, and C120T) and one deletion (ΔG15) located at the FMN riboswitch. The sensor domain of the FMN riboswitch is an aptamer, which contains five hairpins (from P2/L2 to P6/L6; P known as helix and L known as loop) and a P1 helix as the base of this element, which is predicted to be formed in the *rib* mRNA

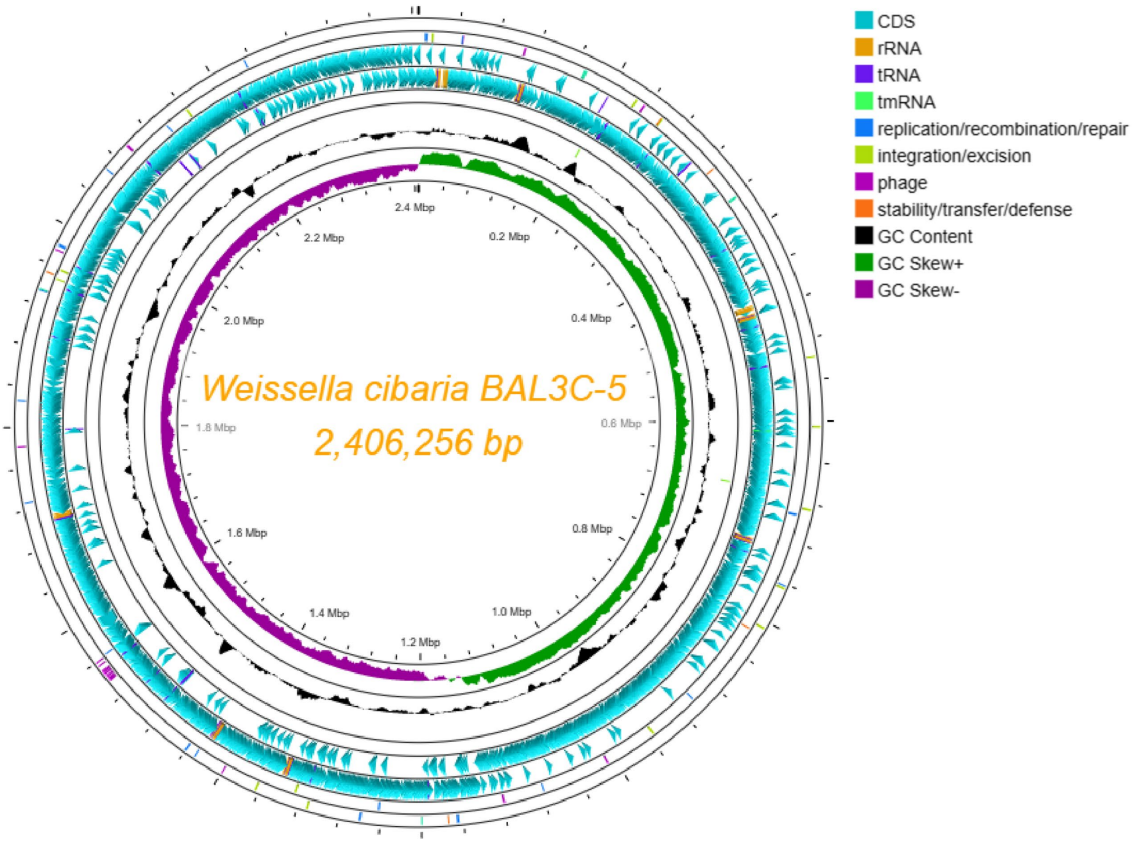

FIGURE 9
Circular genome representation of *Weissella cibaria* BAL3C-5. Each element color of each circle is shown in the legend. The different rings provide information about: forward CDS, reverse CDS, GC Skew, etc. rRNA, tRNA, and tmRNA are located in the same ring of CDS.

and interact with FMN (Figure 5). All the detected mutations were positioned in the aptamer and most of them were in peripheral locations, with P2 (containing positions 14, 15, 16, and 23) and P6 helices (containing positions 109, 115 and 120) being special hot-spots harboring most of the mutations. Only mutations A59C and G87A were located outside of the stem-loop structures. When comparing the position of these mutations with those detected in previous studies (Burgess et al., 2004, 2006; Serganov et al., 2009; Ripa et al., 2022), it was observed that most of them belong to conserved nucleotides among distant species (Figure 5), such as *B. subtilis, B. amyloliquefaciens, Fusobacterium nucleatum, L. mesenteroides, L. lactis*, *Propionibacterium freudenreichii.* or *L. plantarum.* Therefore, the location of these mutations may indicate that they are responsible for the RF-overproducing phenotype. According to the crystallographic study performed by Serganov et al. (2009) on the FMN riboswitch of *F. nucleatum* in the presence of FMN, the P2/L2 and P6/L6 structures as well as P3/L3 and P5/L5 interact with each other forming a tertiary structure. Consequently, mutations in these regions may lead to deregulation and overproduction of RF. Taking the model of the FMN riboswitch of Serganov et al. (2009), the proposed interactions between the nucleotides in the *W. cibaria* riboswitch are shown in Figure 5. In this regard, it is expected that the G115 ribonucleotide would interact with the ribonucleotide G17. The ribonucleotide C109 (together with C108) could interact forming a triplet with C29/G30 and G87, which are thought to interact with the phosphate group of the FMN. Also, ribonucleotides adjacent to C120 (whose mutation leads to the highest RF production) such as G118/T119 should interact with A26/C27 in the presence of FMN forming a tertiary structure. Consequently, mutations in these key positions may also be responsible for the overproducing phenotypes observed.

When the folding of the aptamer of each mutation was predicted with the RNA fold program, it was observed that some mutations resulted in conformational changes of the complex secondary structure (Figure 4). This was the case of ΔG15, G14U and G15U changes at the mRNA level, which may have an impact on the stability of the riboswitch aptamer, and thus, in the overproduction of RF. Moreover, the ΔG of each resulting secondary structure was also analyzed. The lower the thermodynamic energy of the structure, the more structured and stable it should be. Thus, the mutants ΔG15, G14T, G15T, C23T, C120T showed a higher value, accordingly a lower stable structure was expected. Indeed, these mutants, together with G109A (which takes part in key interactions in the riboswitch) were the higher RF producers. By contrast, the structures derived from A59C and A115G mutations, showed the same ΔG energy as the parental strains and they produced the lowest concentrations of RF, compared with the other mutants. These results show, as expected, that the mechanistic reason for an RF-overproducing phenotype is complex and diverse, since nucleotide mutations located at the riboswitch aptamer could affect interaction with other nucleotides/helices, and they could also lead to different secondary structures with different thermodynamic energy. Taking in account these features, sequence and folding structure analysis may be considered as tools for tentative prediction of overproducing phenotypes prior the *in situ* quantification of RF producing abilities and even isolation of mutant strains as shown in this work.

4.2. Selection and evaluation of RF-overproducing spontaneous mutants from RF-and dextran-producing *Weissella cibaria* populations

Once the mutations corresponding to the roseoflavin-treated cultures were detected *in vitro,* the next step was the selection of the mutants of interest. This approach was carried out by culture plating taking advantage of the EPS-producing capacity of the treated strains, and assuming that the overproducing phenotype would give the colonies a yellow color. This was evident when the LAB were plated in the presence of sucrose due to the large mucous colonies generated in which the yellow color was more amplified compared with the small colonies devised in the presence of glucose. With this strategy, we were able to recover and select the cited mutants. When the growth and RF-overproducing capabilities were analyzed in real time, no differences in growth performances were observed between the parental and their mutant derivatives. Hence, growth was not affected by the mutations detected neither the overproduction of RF. The mutant BAL3C-5 C120T showed the greatest overproduction phenotype while mutant BAL3C-5 A59C the least. Regarding the regulatory capacity of FMN or RF, it was observed that the mutant cultures presented an apparent production of RF independent of the presence of the flavins in the growth medium (Figure 6A), but not the parental strains in which the production of vitamin B_2 was delayed upon growth in RAMS + RF and RAMS + FMN, and reduction of the flavin levels was observed at the beginning of the bacterial growth (Figure 6B). Thus, it was confirmed that mutant strains could produce RF without consuming flavins present in the medium, and RF production in mutant strains seemed to be deregulated. In addition, it has been reconfirmed that the fluorescent detection of RF in real time described by us (Mohedano et al., 2019) is suitable for real-time quantification of the vitamin production.

Evaluation of the RF production in RAM and RAMS after 16 h of growth gave again the same results, and the same pattern of vitamin production by the mutants, with strain BAL3C-5 C120T being the highest RF overproducer and with no significant differences in viable cells (Table 3). The bacterial cultures showed further growth in RAMS, due to the fact that the RAM medium contains 2% glucose, whereas in RAMS, an additional 2% sucrose was also present. This fact would also support the higher RF production in RAMS compared with RAM. Another feature that should be highlighted is that the mutant strains externalize most of the RF produced. Given that overproduction of RF has no beneficial effects on mutant growth (Figure 4A), a possible explanation for the observed behavior is that high excess of unneeded RF in the cytosol of the mutants is released to the environment by active transport and/or diffusion to avoid toxic effects. In addition, independently of the mechanism, this release is a very desirable characteristic considering a possible application in the *in situ* biofortification of different fermented foods. Thus, in the present study the most promising *W. cibaria* BAL3C-5 C120T mutant strain was able to generate 6.70 mg/l extracellular RF.

Recently, we have described the selection, from BAL3C-5, BAL3C-7, and BAL3C-22, of three mutant strains named as BAL3C-5 B2, BAL3C-7 B2, and BAL3C-22 B2 (Hernández-Alcántara et al., 2022), and renamed in the present study as BAL3C-5 G15T, BAL3C-7 G109A, and BAL3C-22 C23T strains, respectively. Among them, the highest producer, BAL3C-5 B2, showed synthesis of RF in

concentrations up to 3.40 mg/L. Similar RF production has been obtained in the current work with this mutant (4.16 mg/L), which is 1.6-fold lower concentration than that observed with BAL3C-5 C120T (6.67 mg/L). Furthermore, to assess the RF-overproducing phenotype of BAL3C-5 C120T in a wider context, it was also compared with others RF-overproducing LAB obtained after roseoflavin treatment. This RF production of the mutant was higher than the maximum amount produced by previously obtained LAB mutant derivatives. Accordingly, it was found that *Lactobacillus fermentum* PBCC11 was able to produce approximately 1.20 mg/l (Russo et al., 2014), while this concentration dropped drastically to 0.90 mg/L for *L. lactis* (Burgess et al., 2004) and just about 0.60 mg/L in the case of *L. mesenteroides* and *L. plantarum* (Burgess et al., 2004; Capozzi et al., 2011). In addition, the ability of BAL3C-5 C120T strain was even higher than that of the recently identified high RF-overproducing *L. plantarum* strains showing 1.30–3.7 mg/L (Juarez del Valle et al., 2014; Mohedano et al., 2019; Yépez et al., 2019; Ripa et al., 2022). Recently, the characterization of two LAB species with high RF production capability has been carried out. Kim et al. (2021) highlighted the RF-overproducing phenotype of the *L. plantarum* HY7715 isolated from kimchi, selected under roseoflavin pressure, which was able to produce up to 14.50 mg/L. In the same way, Spacova et al. (2022) described a novel human isolate *L. reuteri* AMBV339, which showed a high natural RF overproduction of 18.16 mg/l. In both studies, it was also stated the resulting biomass of each strain after the RF production. Therefore, when we analyzed the RF concentration in reference to the biomass, considering the detected viable cells (CFU/L), the strain *W. cibaria* BAL3C-5 C120T showed the highest total RF production related to viable cells, since 1.41×10^{11} CFU/ml produced ≈ 6.78 mg/L, whereas approximately 10- or 60-fold higher biomass (1.55×10^{12} or 6×10^{12} CFU/L) of *L. plantarum* HY7715 or *L. reuteri* AMBV339 were required to produce ≈ 14.5 or 18.16 mg/L. Thus, it is expected that if we produce 10-fold higher biomass, we can reach levels of RF production of ≈ 67.8 mg/L. In addition, to our knowledge, and among the *W. cibaria* strains identified so far, *W. cibaria* BAL3C-5 C120T is the highest RF-overproducing strain currently available.

In addition, the determination of the DNA sequence of the BAL3C-5 C120T has revealed that a single change in the genome is solely responsible for an increase in RF production, which rose from 0.1 mg/L in the parental strain to almost 7 mg/L in the mutant strain. As far as we know this is the first time, that it has been certified that a single alteration in the genome is responsible for such a phenotypic change in RF production. Taking into account both its RF-overproducing and its dextran producing phenotypes, strain BAL3C-5 C120T has great potential in the production of *in situ* biofortified foods. Through this strategy, fermented foods with improved nutritional and functional properties, as well as suitable rheological and structural characteristics, could be developed. This supposes a great potential and interest of what this species can offer. In this regard, a first approach was performed by us (Hernández-Alcántara et al., 2022) in the development of experimental biofortified breads which may result of great interest for the manufacturing of functional breads. Indeed, *Weissella* genus include strains that are frequently present in spontaneously fermented food, among them *W. cibaria* strains are frequently isolated from sorghum. Furthermore, many *Weissella* strains have shown probiotic and biotechnological properties of interest for the food industry, but some clinical isolates belonging to this genus have been also isolated (Fusco et al., 2015). For this reason, currently none of the *Weissella* species has the *Qualified Presumption* of Safety (QPS) or the Generally Recognized as Safe (GRAS) status. Consequently, they have not been yet used as a starter or co-culture by the food industry. Nevertheless, due to the interest of these LAB, currently evaluation of the probiotic and safety properties of *Weissella* strains are investigated at the phenotypical and comparative genomic levels with the aim to identify potential starter or co-adjuvant strains for food fermentations (Falasconi et al., 2020; Apostolakos et al., 2022).

In this context, it has to be stated that although analysis of the genome of BAL3C-5 C120T did not reveal the existence of genes encoding virulent factors or resistance to antibiotics, before utilization of this *W. cibaria* strain for production of biofortified bread, it will be necessary to asses experimentally its safety status. Moreover, for the potential use of this strain to develop other types of fermented food, in which the bacteria will be alive, it will be necessary to assess his probiotic potential.

4.3. Transcriptional insights on RF production and expression profile comparison between mutants and their parental strains

After evaluating the different RF production of the selected mutants, we attempted to analyze its production at the transcriptional level and elucidate potential changes in the expression of *ribG*, the first gene in the *rib* operon. In the absence of FMN addition in the growth medium, most of the mutants presented only a slight increase of expression (1.3–1.8-fold) with respect to the corresponding parental strain, except the BAL3C-7 G14T and BAL3C-5 C120T strains, which presented a clearly higher expression (4.0- and 7.4-fold) than the rest of the mutant and wt strains (Figure 7B). The same type of results was observed in presence of FMN, although *ribG* gene expression levels in mutants compared with their respective parental strains were much higher (Figure 7C), BAL3C-7 G14T and BAL3C-5 C120T reaching values of 98 and 161-fold increase, respectively. This enhanced difference seems to be due to the low expression levels of *ribG* in the wt strains in presence of FMN, a conclusion inferred from the fact that the levels of transcription in the presence vs. in absence of FMN ranged from 0.05- to 0.09-fold for the 3 wt strains (Figure 8). When correlating the *ribG* expression and the RF production data, except for the two main producers (BAL3C-7 G14T and BAL3C-5 C120T strains), the order of transcript abundance did not match perfectly with RF synthesis measured in culture medium, since the production levels were much higher than those observed at the transcriptional level. Thus, other factors in the synthesis of RF should be considered. First, only the expression of the *ribG* has been evaluated and not of the downstream genes (*ribB*, *ribA*, and *ribH*) of the *rib* operon, whose products are also involved in the RF synthesis. For example, changes in the untranslated region of the *rib* operon might influence the folding of the total transcript, affecting its half-life and internal processing due to endoribonucleases. In addition, mRNA turnover rate for each strain may have also changed. Indeed, mRNA stability and the rate at which each mRNA is degraded and/or translated are important factors for gene expression control (Cooper, 2000). These

features may have also varied in the mutant strains and although transcription remains as the main level where gene expression is regulated, changes in mRNA degradation rate also have great influence in controlling the transcript levels, and subsequently protein levels, and finally, in this case, the RF production levels.

When comparing the behavior of the BAL3C-5, BAL3C-7, and BAL3C-22strains in the RAMS and RAMS + FMN environments (Figure 8), it was clear that the expression of *ribG* gene was almost insignificant in the presence of FMN. Thus, production of RF in the three wt strains seems to be properly regulated. However, in the case of BAL3C-5 A59C and BAL3C-5 A115G strains, which also showed lower transcript abundance in RAM + FMN grown cultures, *ribG* expression was partially regulated as they did not reach such an expression decay as that in the wt strains. It should be emphasized that both BAL3C-5 A59C and BAL3C-5 A115G showed the lowest RF production levels among all mutant strains. Furthermore, the Gibbs free energy of their FMN riboswitch aptamer was identical to that of the parental strains. Thus, the stability of their structures probably had not been compromised and therefore, the regulation in RF production would take place, at least partially due to the corresponding mutations, which could be the cause of the low levels of RF production compared to the rest of the mutants. Regarding to the remaining mutants, a similar expression was observed independent of the presence of FMN. These strains seem to be no longer subjected to regulatory response, which should lead to a RF production independent of FMN concentration. If attention is paid to the stability of the aptamer structures of the isolated strains (Figure 4), it can be seen that all of them (except the BAL3C-7 G109A strain) present less stability than their parental strains. This may be a possible explanation of the total deregulation in the production of RF, as the position of the mutation may be the main cause for the different levels of production observed. The BAL3C-7 G109A strain appears to have a more stable regulatory structure (according to its ΔG) than that of BAL3C-7, with the location of the mutation in a predicted key position for interaction of the phosphate group of the FMN with the riboswitch, it nevertheless results in a constitutive production of the vitamin that does not respond to transcriptional regulation by FMN.

Once the results corresponding to the expression of *ribG* gene were analyzed, it was decided to investigate the situation of expression of the FMN riboswitch region. Transcriptional analysis showed no significant differences between mutant strains in the absence of FMN (Supplementary Figure S7). However, when the bacterial cultures were grown in RAMS + FMN, differences were detected (Supplementary Figure S7). Under this condition, mutant strains presented lower abundance of transcript compared to their parental strains. A feasible hypothesis is that in the presence of FMN, in the case of the wt strains, the aptamer would be formed and stabilized by the binding of the flavin, a situation that could give greater stability to the leader region of the *rib* mRNA, since, as it has been observed in other studies (Richards and Belasco, 2021). The binding of the ligand to the riboswitch aptamer would be protecting the RNA from degradation by blocking the access of endo- and exo-nucleases to regions of the riboswitch susceptible to being attacked. On the contrary, in the case of the mutants, where it is predicted that the binding of FMN will be negligible or decreased, although the stability of the aptamer structure will be lower, it could still be formed and processing of the riboswitch aptamer and adjacent regions by nucleases could take place. Therefore, this could be the reason why a lower transcript signal is detected in mutants.

In this regard, those with the highest expression in the presence of FMN (apart from the wt strains), were BAL3C-5 A59C and BAL3C-5 A115G. These results correlated with the data previously observed. These are the mutant strains that showed lower *ribG* expression in the presence of FMN, the consequence of a partially regulated expression (Figure 8). These two bacteria are, among mutants, the strains with the highest expression of the regulatory region and could indicate stabilization of the riboswitch structure. Therefore, the formation of the A59C and the A115G aptamers would indicate a greater stability and abundance of transcript as well as more regulation compared with the rest of the mutants and thus, less RF production. On the contrary, the strain with the lowest expression carried the change G109A, mutation at a position that it has been previously observed to be key for the interaction with the FMN.

5. Conclusion

The method described here was found to be a suitable strategy for selecting spontaneous riboflavin-overproducing and dextran-producing mutants of *W. cibaria*. It has been possible to observe significant differences at the transcriptional level between the different strains, confirming the increase in *ribG* transcription in the highest overproducing strains compared to the rest of the strains. In this regard, it must be highlighted the selection of the BAL3C-5 C120T strain, as the highest RF overproducer. Above all, it has been ascertained that a single alteration in the genome is responsible for such a phenotypic change. Moreover, in the future, after evaluation of its probiotic potential and confirmation of its safety status of the BAL3C-5 C120T strain, new perspectives will be opened regarding the characterization of its potential use in the food and health industries, as an interesting strategy for the biofortification of potentially functional foods.

Data availability statement

The datasets presented in this study can be found in online repositories. The names of the repository/repositories and accession number(s) can be found at: https://www.ncbi.nlm.nih.gov/genbank/, CP116386 and https://www.ncbi.nlm.nih.gov/genbank/, CP116385.

Author contributions

MD and PL: conceptualization. ID-O, MM, and PL: methodology. ID-O, JR-M, and GdS: software. ID-O, LM-L, and MM: investigation. ID-O and PL: data curation. ID-O, MM, and PL: writing—original draft preparation. GdS, MD, MT, and PL: writing—review and editing. MD, MM, and PL: supervision. GdS, PL, and MD: funding acquisition. All authors contributed to the article and approved the submitted version.

Funding

This research was funded by the Spanish Ministry of Science, Innovation and Universities (grant RTI2018-097114-B-I00), CSIC (grant COOPA20488), the University of Basque Government (grants IT1662-22 and PIBA_2020_1_0032), and the University of Basque Country (UPV-EHU; GIU19/014). ID-O is the beneficiary of a postdoctoral grant Margarita Salas by UPV-EHU (MARSA21/25) in the framework of "the requalification of the Spanish university system" funded by the European Union-Next Generation EU.

Acknowledgments

We thank Guillermo Padilla Alonso for his valuable assistance in the biostatistical analysis and to Stephen Elson for the critical reading of the manuscript. We acknowledge support of the publication fee by the CSIC Open Access Publication Support Initiative through its Unit of Information Resources for Research (URICI). In addition, this work is also based upon the work from COST Action 18101 SOURDOMICS – Sourdough biotechnology network towards novel, healthier and sustainable food and bioprocesses (https://sourdomics.com/; https://www.cost.eu/actions/CA18101/#tabs|Name:overview), where the authors PL, GdS, ML-M, JR-M, MT, and MT are Members of the Working Groups WG2 and WG3.

Conflict of interest

The authors declare that the research was conducted in the absence of any commercial or financial relationships that could be construed as a potential conflict of interest.

Publisher's note

All claims expressed in this article are solely those of the authors and do not necessarily represent those of their affiliated organizations, or those of the publisher, the editors and the reviewers. Any product that may be evaluated in this article, or claim that may be made by its manufacturer, is not guaranteed or endorsed by the publisher.

Supplementary material

The Supplementary material for this article can be found online at: https://www.frontiersin.org/articles/10.3389/fmicb.2023.1154130/full#supplementary-material

References

Abbas, C. A., and Sibirny, A. A. (2011). Genetic control of biosynthesis and transport of riboflavin and flavin nucleotides and construction of robust biotechnological producers. *Microbiol. Mol. Biol. Rev.* 75, 321–360. doi: 10.1128/MMBR.00030-10

Altschul, S. F., Gish, W., Miller, W., Myers, E. W., and Lipman, D. J. (1990). Basic local alignment search tool. *J. Mol. Biol.* 215, 403–410. doi: 10.1016/S0022-2836(05)80360-2

Apostolakos, I., Paramithiotis, S., and Mataragas, M. (2022). Functional and safety characterization of Weissella paramesenteroides strains isolated from dairy products through whole-genome sequencing and comparative genomics. *Dairy* 3, 799–813. doi: 10.3390/dairy3040055

Bertelli, C., Laird, M. R., Williams, K. P., Simon Fraser University Research Computing GroupLau, B. Y., Hoad, G., et al. (2017). IslandViewer 4: expanded prediction of genomic islands for larger-scale datasets. *Nucleic Acids Res.* 45, W30–W35. doi: 10.1093/nar/gkx343

Besrour-Aouam, N., Fhoula, I., Hernández-Alcántara, A. M., Mohedano, M. L., Najjari, A., Prieto, A., et al. (2021). The role of dextran production in the metabolic context of *Leuconostoc* and *Weissella* Tunisian strains. *Carbohydr. Polym.* 253:117254. doi: 10.1016/j.carbpol.2020.117254

Bounaix, M. S., Robert, H., Gabriel, V., Morel, S., Remaud-Siméon, M., Gabriel, V., et al. (2010). Characterization of dextran-producing *Weissella* strains isolated from sourdoughs and evidence of constitutive dextransucrase expression. *FEMS Microbiol. Lett.* 311, 18–26. doi: 10.1111/j.1574-6968.2010.02067.x

Burgess, C., O'Connell-Motherway, M., Sybesma, W., Hugenholtz, J., and Van Sinderen, D. (2004). Riboflavin production in *Lactococcus lactis*: potential for *in situ* production of vitamin-enriched foods. *Appl. Environ. Microbiol.* 70, 5769–5777. doi: 10.1128/AEM.70.10.5769-5777.2004

Burgess, C. M., Smid, E. J., Rutten, G., and van Sinderen, D. (2006). A general method for selection of riboflavin-overproducing food grade micro-organisms. *Microb. Cell Fact.* 5:24. doi: 10.1186/1475-2859-5-24

Capozzi, V., Menga, V., Digesu, A. M., DeVita, P., van Sinderen, D., Cattivelli, L., et al. (2011). Biotechnological production of vitamin B2-enriched bread and pasta. *J. Agric. Food Chem.* 59, 8013–8020. doi: 10.1021/jf201519h

Cooper, G. M. (2000). *The cell: A molecular approach. 2nd* Edn. Sunderland (MA): Sinauer Associates.

Darty, K., Denise, A., and Ponty, Y. (2009). VARNA: Interactive drawing and editing of the RNA secondary structure. *Bioinformatics* 25, 1974–1975. doi: 10.1093/bioinformatics/btp250

de Man, J. C., Rogosa, M., and Sharpe, M. E. (1960). "A Medium for the Cultivation of Lactobacilli". *J. Appl. Bacteriol.* 23, 130–135. doi: 10.1111/j.1365-2672.1960.tb00188.x

Dey, S., and Bishayi, B. (2016). Riboflavin along with antibiotics balances reactive oxygen species and inflammatory cytokines and controls *Staphylococcus aureus* infection by boosting murine macrophage function and regulates inflammation. *J. Inflamm.* 13, 1–21. doi: 10.1186/s12950-016-0145-0

Dubois, M., Gilles, K. A., Hamilton, J. K., Rebers, P. A., and Smith, F. (1956). Colorimetric Method for Determination of Sugars and Related Substances. *Anal. Chem.* 28, 350–356. doi: 10.1021/ac60111a017

EFSA Panel on Dietetic Products, Nutrition and Allergies (EFSA NDA Panel)Turck, D., Bresson, J. L., Burlingame, B., Dean, T., Fairweather-Tait, S., Heinonen, M., et al. (2017). Dietary reference values for riboflavin. *EFSA J.* 15:e04919. doi: 10.2903/j.efsa.2017.4919

Falasconi, I., Fontana, A., Patrone, V., Rebecchi, A., Duserm Garrido, G., Principato, L., et al. (2020). Genome-assisted characterization of *lactobacillus fermentum*,*Weissella cibaria*,and *Weissella confusa* strains isolated from sorghum as starters for sourdough fermentation. *Microorganisms* 8:1388. doi: 10.3390/microorganisms8091388

Farah, N., Chin, V. K., Chong, P. P., Lim, W. F., Lim, C. W., Basir, R., et al. (2022). Riboflavin as a promising antimicrobial agent?. A multi-perspective review. *Curr Res Microbial Sci* 3:100111. doi: 10.1016/j.crmicr.2022.100111

Fusco, V., Quero, G. M., Cho, G. S., Kabisch, J., Meske, D., Neve, H., et al. (2015). The genus Weissella: taxonomy, ecology and biotechnological potential. *Front. Microbiol.* 6:155. doi: 10.3389/fmicb.2015.00155

Ge, Y.-Y., Zhang, J. R., Corke, H., and Gan, R.-Y. (2020). Screening and spontaneous mutation of pickle-derived *lactobacillus plantarum* with overproduction of riboflavin, related mechanism, and food application. *Foods* 9:88. doi: 10.3390/foods9010088

Gregory, J., Lowe, S., Bates, C. J., Prentice, A., Jackson, L., Smithers, G., et al. (2000). *National diet and nutrition survey: Young people aged 4 to 18 years: Report of the diet and nutrition survey*. London: The Stationery Office.

Hernández-Alcántara, A. M., Chiva, R., Mohedano, M. L., Russo, P., Ruiz-Masó, J. A., del Solar, G., et al. (2022). *Weissella cibaria* riboflavin-overproducing and dextran-producing strains useful for the development of functional bread. *Front. Nutr.* 9:978831. doi: 10.3389/fnut.2022.97883

Jia, B., Raphenya, A. R., Alcock, B., Waglechner, N., Guo, P., Tsang, K. K., et al. (2017). CARD 2017: expansion and model-centric curation of the comprehensive antibiotic resistance database. *Nucleic Acids Res.* 45, D566–D573. doi: 10.1093/nar/gkw1004

Juarez del Valle, M., Laino, J. E., Savoy de Giori, G., and LeBlanc, J. G. (2014). Riboflavin producing lactic acid bacteria as a biotechnological strategy to obtain bioenriched soymilk. *Food Res. Int.* 62, 1015–1019. doi: 10.1016/j.foodres.2014.05.029

Kim, G., Bae, J. H., Cheon, S., Lee, D. H., Kim, D. H., Lee, D., et al. (2022). Prebiotic activities of dextran from *Leuconostoc mesenteroides* SPCL742 analyzed in the aspect of the human gut microbial ecosystem. *Food Funct.* 13, 1256–1267. doi: 10.1039/d1fo03287a

Kim, J. Y., Choi, E. J., Lee, J. H., Yoo, M. S., Heo, K., Shim, J. J., et al. (2021). Probiotic potential of a novel vitamin B2-overproducing *lactobacillus plantarum* strain, HY7715, isolated from kimchi. *Appl. Sci.* 11:5765. doi: 10.3390/app11135765

LeBlanc, J. G., Laiño, J. E., del Valle, M. J., de Giori, G. S., Sesma, F., and Taranto, M. P. (2015). "B-group vitamins production by probiotic lactic acid bacteria," in *Biotechnology of lactic acid Bacteria: novel applications*. 2nd edn. eds. F. Mozzi, R. R. Raya and G. M. Vignolo (GM Wiley Blackwell, Ames), 279–296.

Livak, J. K., and Schmittgen, T. D. (2001). Analysis of relative gene expression data using real-time quantitative PCR and the $2^{-\Delta\Delta CT}$ method. *Methods* 25, 402–408. doi: 10.1006/meth.2001.1262

Llamas-Arriba, M. G., Hernández-Alcántara, A. M., Mohedano, M. L., Chiva, R., Celador-Lera, L., Velázquez, E., et al. (2021). Lactic acid bacteria isolated from fermented doughs in Spain produce dextrans and riboflavin. *Foods* 10:2004. doi: 10.3390/FOODS10092004

Lynch, K. M., Coffey, A., and Arendt, E. K. (2018). Exopolysaccharide producing lactic acid bacteria: their techno-functional role and potential application in gluten-free bread products. *Food Res. Int.* 110, 52–61. doi: 10.1016/J.FOODRES.2017.03.012

McArthur, A. G., Waglechner, N., Nizam, F., Yan, A., Azad, M. A., Baylay, A. J., et al. (2013). The comprehensive antibiotic resistance database. *Antimicrob. Agents Chemother.* 57, 3348–3357. doi: 10.1128/AAC.00419-13

Mohedano, M. L., Hernández-Recio, S., Yépez, A., Requena, T., Martínez-Cuesta, M. C., Peláez, C., et al. (2019). Real-time detection of riboflavin production by *lactobacillus plantarum* strains and tracking of their gastrointestinal survival and functionality *in vitro* and *in vivo* using mCherry labeling. *Front. Microbiol.* 10:1748. doi: 10.3389/fmicb.2019.01748

Nácher-Vázquez, M., Ballesteros, N., Canales, Á., Rodríguez Saint-Jean, S., Pérez-Prieto, S. I., Prieto, A., et al. (2015). Dextrans produced by lactic acid bacteria exhibit antiviral and immunomodulatory activity against salmonid viruses. *Carbohydr. Polym.* 124, 292–301. doi: 10.1016/j.carbpol.2015.02.020

Nadzir, M. M., Nurhayati, R. W., Idris, F. N., and Nguyen, M. H. (2021). Biomedical applications of bacterial exopolysaccharides: a review. *Polymers* 13:530. doi: 10.3390/POLYM13040530

Pinto, J., and Rivlin, R. (2013). "Riboflavin (vitamin B2)" in *Handbook of Vitamins*. (Boca Raton, FL, USA: RC Press), 191–266.

Powers, H. J. (2003). Riboflavin (vitamin B-2) and health. *Am. J. Clin. Nutr.* 77, 1352–1360. doi: 10.1093/ajcn/77.6.1352

Richards, J., and Belasco, J. G. (2021). Riboswitch control of bacterial RNA stability. *Mol. Microbiol.* 116, 361–365. doi: 10.1111/mmi.14723. Epub 2021 Apr 25

Ripa, I., Ruiz-Masó, J. A., De Simone, N., Russo, P., Spano, G., and del Solar, G. (2022). A single change in the aptamer of the *Lactiplantibacillus plantarum rib* operon riboswitch severely impairs its regulatory activity and leads to a vitamin B2-overproducing phenotype. *J. Microbial. Biotechnol.* 15, 1253–1269. doi: 10.1111/1751-7915.13919

Rohner, F., Zimmermann, M. B., Wegmueller, R., Tschannen, A. B., and Hurrell, R. F. (2007). Mild riboflavin deficiency is highly prevalent in school-age children but does not increase risk for anaemia in Côte d'Ivoire. *Br. J. Nutr.* 97, 970–976. doi: 10.1017/S0007114507665180

Russo, P., Capozzi, V., Arena, M. P., Spadaccino, G., Dueñas, M. T., López, P., et al. (2014). Riboflavin-overproducing strains of *lactobacillus fermentum* for riboflavin-enriched bread. *Appl. Microbiol. Biotechnol.* 98, 3691–3700. doi: 10.1007/s00253-013-5484-7

Serganov, A., Huang, L., and Patel, D. J. (2009). Coenzyme recognition and gene regulation by a flavin mononucleotide riboswitch. *Nature* 458, 233–237. doi: 10.1038/nature07642

Soeiro, V. C., Melo, K. R., Alves, M. G., Medeiros, M. J., Grilo, M. L., Almeida-Lima, J., et al. (2016). Dextran: influence of molecular weight in antioxidant properties and immunomodulatory potential. *Int. J. Mol. Sci.* 17:1340. doi: 10.3390/ijms17081340

Spacova, I., Ahannach, S., Breynaert, A., Erreygers, I., Wittouck, S., Bron, P. A., et al. (2022). Spontaneous riboflavin-overproducing *Limosilactobacillus reuteri* for biofortification of fermented foods. *Front. Nutr.* 9:916607. doi: 10.3389/fnut.2022.916607

Thakur, K., Tomar, S. K., and De, S. (2015). Lactic acid bacteria as a cell factory for riboflavin production. *J. Microbial. Biotechnol.* 9, 441–451. doi: 10.1111/1751-7915.12335

Thakur, K., Tomar, S. K., Singh, A. K., Mandal, S., and Arora, S. (2017). Riboflavin and health: a review of recent human research. *Crit. Rev. Food Sci. Nutr.* 57, 3650–3660. doi: 10.1080/10408398.2016.1145104

Titcomb, T. J., and Tanumihardjo, S. A. (2019). Global concerns with B vitamin statuses: biofortification, fortification, hidden hunger, interactions, and toxicity. *Compr Rev Food Sci Food Safe* 18, 1968–1984. doi: 10.1111/1541-4337.12491

Vitreschak, A. G., Rodionov, D. A., Mironov, A. A., and Gelfand, M. S. (2002). Regulation of riboflavin biosynthesis and transport genes in bacteria by transcriptional and translational attenuation. *Nucleic Acids Res.* 30, 3141–3151. doi: 10.1093/nar/gkf433

Werning, M. L., Hernández-Alcántara, A. M., Ruiz, M. J., Soto, L. P., Dueñas, M. T., López, P., et al. (2022). Biological functions of exopolysaccharides from lactic acid bacteria and their potential benefits for humans and farmed animals. *Foods* 11:1284. doi: 10.3390/foods11091284

Wick, R. R., Judd, L. M., Gorrie, C. L., and Holt, K. E. (2017). Unicycler: resolving bacterial genome assemblies from short and long sequencing reads. *PLoS Comput. Bio* 13:e100559. doi: 10.1371/journal.pcbi.1005595

Widdel, F. (2010). "Theory and measurement of bacterial growth" in *Grundpraktikum Mikrobiologie* (Bremen, Germany: Bremen University), 1–11.

Winkler, W. C., Cohen-Chalamish, S., and Breaker, R. R. (2002). An mRNA structure that controls gene expression by binding FMN. *Proc. Natl. Acad. Sci. U. S. A.* 99, 15908–15913. doi: 10.1073/pnas.212628899

Yépez, A., Russo, P., Spano, G., Khomenko, I., Biasioli, F., Capozzi, V., et al. (2019). In situ riboflavin fortification of different kefir-like cereal-based beverages using selected andean LAB strains. *Food Microbiol.* 77, 61–68. doi: 10.1016/j.fm.2018.08.008

Zarour, K., Llamas, M. G., Prieto, A., Rúas-Madiedo, P., Dueñas, M. T., Fernández de Palencia, P., et al. (2017). Rheology and bioactivity of high molecular weight dextrans synthesised by lactic acid bacteria. *Carbohydr. Polym.* 174, 646–657. doi: 10.1016/j.carbpol.2017.06.113

Zhang, J.-R., Ge, Y.-Y., Liu, P.-H., Wu, D.-T., Liu, H.-Y., Li, H.-B., et al. (2021). Biotechnological strategies of riboflavin biosynthesis in microbes. *Engineering* 12, 115–127. doi: 10.1016/j.eng.2021.03.018

Zhou, L., Zhou, L., Wei, C., and Guo, R. (2022). A bioactive dextran-based hydrogel promote the healing of infected wounds via antibacterial and immunomodulatory. *Carbohydr. Polym.* 291:119558. doi: 10.1016/j.carbpol.2022.119558

frontiers | Frontiers in Microbiology

TYPE Original Research
PUBLISHED 20 April 2023
DOI 10.3389/fmicb.2023.1165202

OPEN ACCESS

EDITED BY
Paloma López,
Spanish National Research Council (CSIC), Spain

REVIEWED BY
Pasquale Russo,
University of Milan, Italy
Christian Magni,
CONICET Instituto de Biología Molecular y Celular de Rosario (IBR), Argentina

*CORRESPONDENCE
Gaspar Pérez Martínez
✉ gaspar.perez@iata.csic.es

SPECIALTY SECTION
This article was submitted to Food Microbiology, a section of the journal Frontiers in Microbiology

RECEIVED 13 February 2023
ACCEPTED 20 March 2023
PUBLISHED 20 April 2023

CITATION
Pérez Martínez G, Giner-Pérez L and Castillo-Romero KF (2023) Bacterial extracellular vesicles and associated functional proteins in fermented dairy products with *Lacticaseibacillus paracasei*. *Front. Microbiol.* 14:1165202. doi: 10.3389/fmicb.2023.1165202

Bacterial extracellular vesicles and associated functional proteins in fermented dairy products with *Lacticaseibacillus paracasei*

Gaspar Pérez Martínez[1]*, Lola Giner-Pérez[1,2] and Keshia F. Castillo-Romero[1,3]

[1]Laboratory of Lactic Acid Bacteria and Probiotics, Department of Biotechnology, Instituto de Agroquímica y Tecnología de Alimentos (C.S.I.C.), Valencia, Spain, [2]Laboratory of Neurobiology, Centro de Investigación Príncipe Felipe, Valencia, Spain, [3]School of Engineering and Sciences, Tecnológico de Monterrey, Monterrey, Mexico

Cells of all kingdoms produce extracellular vesicles (EVs); hence, they are present in most environments and body fluids. *Lacticaseibacillus paracasei* produces EVs that have attached biologically active proteins (P40 and P75). In this study, EV and functional proteins were found in five different commercial dairy-fermented products carrying *L. paracasei*. Strains present in those products were isolated, and with one exception, all produced small EVs (24–47 d.nm) carrying P40 and P75. In order to winnow bacterial EV from milk EV, products were subjected to centrifugal fractionation at 15,000 × *g* (15 K), 33,000 × *g* (33 K), and 100,000 × *g* (100 K). P75 was present in all supernatants and pellets, but P40 was only found in two products bound to the 15 and 33 K pellets, and 16S rDNA of *L. paracasei* could be amplified from all 100 K EVs, indicating the presence of *L. paracasei* EV. To investigate the interactions of bacterial EV and proteins with milk EV, *L. paracasei* BL23 EV was added to three commercial UHT milk products. Small-size vesicles (50–60 d.nm) similar to *L. paracasei* BL23 EV were found in samples from 100 K centrifugations, but intriguingly, P40 and P75 were bound to EV in 15 and 33 K pellets, containing bovine milk EV of larger size (200–300 d.nm). Sequencing 16S rDNA bands amplified from EV evidenced the presence of bacterial EVs of diverse origins in milk and fermented products. Furthermore, *L. paracasei* 16S rDNA could be amplified with species-specific primers from all samples, showing the presence of *L. paracasei* EV in all EV fractions (15, 33, and 100 K), suggesting that these bacterial EVs possibly aggregate and are co-isolated with EV from milk. P40 and P75 proteins would be interacting with specific populations of milk EV (15 and 33 K) because they were detected bound to them in fermented products and milk, and this possibly forced the sedimentation of part of *L. paracasei* EV at lower centrifugal forces. This study has solved technically complex problems and essential questions which will facilitate new research focusing on the molecular behavior of probiotics during fermentation and the mechanisms of action mediating the health benefits of fermented products.

KEYWORDS

***Lacticaseibacillus paracasei*, extracellular vesicles, fermented products, P40, P75, milk, 16S rDNA**

1. Introduction

The discovery of extracellular vesicles (EVs) in biological fluids of all living organisms, including vegetables (Pérez-Bermúdez et al., 2017), prompted scientific interest on the likely role of EV in the deep interactions of food products with the host organism (Munir et al., 2020). Bovine and other ruminant's milk is rich in nutrients, immune and biologically active proteins, and generaly milk also contains abundant EV loaded with signaling proteins and miRNAs. Potential health benefits have been reported for milk EVs (Benmoussa et al., 2019a; García-Martínez et al., 2022); they are variable in size, proteomic profiles (Benmoussa et al., 2019b, 2020), and siRNAs content (Benmoussa et al., 2017). Nevertheless, industrial pasteurization and especially ultra-high temperature (UHT) treatment potentially alter the structure and composition of milk EV (Kleinjan et al., 2021). Fermented food products such as bread, fermented meats, olives, vegetables, and cheeses or fermented dairy products are essential for human nutrition. They require the presence and metabolic activity of conventional or unconventional microorganisms that provide pleasant organoleptic properties and extended shelf life, and in addition, they offer potential benefits for the consumer (host; Frias et al., 2016) and possibly contribute to enriching the gut microbiome (Milani et al., 2019). In particular, yogurt and fermented milk products are important references in healthy diets, which is supported by scientific evidence that showed that in addition to digestion and tolerance to lactose and improving the general gastrointestinal condition, yogurt and fermented milk products consumption reduced risks of breast and colon cancer, type 2 diabetes, weight control, and cardiovascular and bone health (Savaiano and Hutkins, 2021).

Bacteria also produce EVs with biological activity. EVs from gram-negative pathogenic bacteria showed virulence properties (Schwechheimer and Kuehn, 2015; Jan, 2017; Toyofuku et al., 2019) and pathogenic Firmicutes produce EVs with inflammatory effects, toxins, or virulence factors (Rivera et al., 2010; Gurung et al., 2011; Surve et al., 2016; Wagner et al., 2018). In contrast, EVs from probiotic bacteria have beneficial health properties, similar to the bacteria producing them, and these properties are related to their protein cargo, membrane-bound proteins, and lipoteichoic acids (LTA; Al-Nedawi et al., 2015; Domínguez Rubio et al., 2017; Grande et al., 2017; Bäuerl et al., 2020; Raftar et al., 2021; Fang et al., 2022). Probiotic species of the taxonomic group that includes *Lacticaseibacillus casei*, *Lacticaseibacillus paracasei*, and *Lacticaseibacillus rhamnosus* produce two characteristic and biologically active proteins, P40 and P75 (Bäuerl et al., 2019). These proteins have anti-inflammatory and tissue repair (anti-apoptotic) activities, and promote intestinal development in early life (Bäuerl et al., 2010; Yan et al., 2011, 2017; Wang et al., 2017; Lu et al., 2020). Furthermore, both proteins are externally bound to EVs (Bäuerl et al., 2020).

Given that *L. paracasei* (formerly *Lactobacillus casei*) is present in very popular and highly consumed fermented milk products, it was intriguing to know if commercial products had bacterial EVs and to what extent the functional proteins P40 and P75 were present and associated with bacterial vesicles. For this purpose, five commercial fermented milk products containing "*Lactobacillus casei*" were purchased. First *L. paracasei* strains were isolated and tested for the production of EV and the secretion of proteins P40 and P75. Unexpected results forced testing of the fate of these elements when EVs from the reference strain *L. paracasei* BL23 were mixed with sterilized milk. The results indicated that bacterial functional proteins—and possibly bacterial EV—combined with milk EVs and changed their sedimentation pattern.

2. Materials and methods

2.1. Bacterial culture, isolation, and identification

Isolation and regular culture of *Lacticaseibacillus* strains were carried out on Petri dishes with MRS medium and 1.8% agar or on liquid MRS, grown at 37°C under static conditions. For the isolation of *Lacticaseibacillus paracasei* strains from commercial products, fermented milk products of four different commercial brands that are labeled to contain probiotic strains of *Lactobacillus casei* (*Lacticaseibacillus paracasei*) were purchased. Product samples were arbitrarily encoded with letters A, Ca, Co, H, and Y. Serial dilutions of the five products were made on liquid MRS medium, and 100 μL of the 10^{-5}, 10^{-6}, and 10^{-7} surface inoculated dilutions on MRS agar plates was obtained in triplicate and incubated at 37°C for 48 h. Isolated colonies were purified and grown on MRS broth for 16S rDNA amplification and sequencing. An aliquot of this culture was preserved in 18% glycerol at −80°C.

For the identification of commercial isolates, the genomic DNA was isolated from a 5 mL MRS culture using the Real Pure SSS DNA Extraction kit (Real Durviz S.L., Valencia, Spain), following the manufacturer's instructions and described earlier (Bäuerl et al., 2019). Then, 16S rDNA was amplified with primers 27f (5'-AGAGTTTGATCCTGGCTCAG-3') and 558r (5'-GTATTCCGCGGCTG-3'), as described earlier (Marroki et al., 2011); next, amplicons (~500 bp) were purified with the Macherey–Nagel PCR Cleanup kit (Macherey-Nagel, CA, United States) and sequenced at Eurofins GATC Biotech (Eurofins Genomics, Germany). Sequences were compared with public databases through BLASTn.

Direct repeats in the gene encoding P75 (*cmu*B) from the isolated strains were sequenced together with BL23 as a reference. For this purpose, the chromosomal DNA of each of the strains was used as a template for the amplification of this region using two primers targeted 20 nt upstream, P75TR-for (5'-GCRAATGCTYCTAGCGCTGCTGC-3'), and 15 nt downstream, P75TR-rev (5'-GCCTGCCGTGACGGCGTAACAGG-3'), the satellite repeats. Then, sequences obtained were aligned to determine allele differences compared to those previously reported (Bäuerl et al., 2019).

2.2. Isolation of EV from bacteria and dairy samples

For EV isolation from dairy fermented products, samples were first neutralized with 0.75 M Tris pH 7.0 1:10 (v/v) and centrifuged at 4,000 × g to get rid of bacteria and other precipitates, as well as remaining fat. Then, supernatants were successively

centrifuged to recover pellet fractions at 15,000 × *g*, 33,000 × *g*, and 100,000 × *g*, as indicated in the general procedure for dairy products (Benmoussa et al., 2017). For the isolation of milk EV, filtered (0.22 μm pore membrane) 2% sodium citrate was mixed (1:1 vol/vol) with 200 mL of commercial semi-skimmed UHT milk samples. Samples were successively centrifuged at 15,000 × *g* (15 K) for 20 min; the pellet was collected and the supernatant was centrifuged at 35,000 × *g* (33 K); and again, the pellets were collected and the supernatant was ultracentrifuged at 100,000 × *g* (100 K) for 2 h. Centrifugations at 15 and 33 K were carried out in a Beckman Coulter Avanti J-26 XPI centrifuge, and ultracentrifugation at 100 K in a Beckman Coulter Optima L-70 Ultracentrifuge rotor type Ti70 (Beckman Coulter, Indianapolis, Indiana, USA). The 100 K pellets were washed with 0.22 μm filtered PBS by centrifugation for 1 h at 100,000 × *g*, and in all cases, the temperature was fixed at 4°C. After each step, the pellets were resuspended in 1 mL of 0.22 μm filtered sterile phosphate-buffered saline (PBS).

Large amounts of *L. paracasei* BL23 EV were prepared from 400 mL of MRS supernatant. It was first centrifuged at 10,000 × *g* for 20 min at 4°C in 250 mL polypropylene bottles using a type 16.250 JLA rotor (Avanti J-26 XPI centrifuge, Beckman Coulter, Indianapolis, Indiana, USA). The supernatant was then filtered through a 0.45 μm membrane (Sarstedt, Nümbrecht, Germany) and concentrated 10-fold by tangential flow filtration (TFF), using a 100 KDa molecular weight cutoff (MWCO) polyether sulfone (PES) membrane (Vivaflow 50, Sartorius, Göttingen, Germany). The flow-through was ultracentrifuged at 100 K, as described previously.

2.3. Western blot

Immunological detection of P40 and P75 in EV samples was performed by Western blot analysis, as previously described (Bäuerl et al., 2019). In brief, the equivalent of 2 μg of EV protein was separated in 10% SDS-PAGE gels and electrotransferred to Hybond-ECL membranes (GE Healthcare, Boston, Massachusets, USA). Membranes were blocked in a 5% (w/v) non-fat dry milk solution in 50 mM Tris–HCl, pH 7.6 and 150 mM NaCl (TBS) containing 0.1% (v/v) Tween-20. The primary antibodies used were polyclonal rabbit anti-P40N and anti-P75N. Then, membranes were incubated with secondary goat anti-rabbit HRP-conjugated antibodies, and signals were detected using ECL advance chemiluminescent reagents, following the supplier's instructions (GE Healthcare, Boston, Massachusetts, USA; Bäuerl et al., 2019).

Western blotting was also implemented for the detection of *L. paracasei* LTA using the previously described protocol (Bäuerl et al., 2020). Using an SDS-free loading buffer and electrophoresis in a 17.5% polyacrylamide gel (SDS-free) was a key step in the procedure. Then, an anti-*Staphylococcus aureus* LTA mouse monoclonal antibody (G43J; Invitrogen, Waltham, Massachusetts, USA) was used as the primary antibody, and the rest of the procedure was followed as mentioned earlier.

2.4. Light scattering determination of EV size

The average size of isolated EV from BL23, from the newly isolated *L. paracasei* strains, from fermented dairy products, as well as milk preparations, was determined by DLS using a Zetasizer NanoZS (Malvern Panalytical Ltd, Malvern, Worcestershire, U.K.), with similar settings to those reported previously (Bäuerl et al., 2020) and by others (Grande et al., 2017). All samples required a previous filtration through 0.20 μm filters (Filtropur S, Sarstedt AG, Nümbrecht, Germany). Measurement conditions, replicates, cycles, and consumables were described earlier (Bäuerl et al., 2020). The refraction index of the samples was fixed at 1.330 and the viscosity was fixed at 1.0031 mPa/s. The equipment software calculated the average particle size using a third-order fitting autocorrelation function, as described by the manufacturer (Malvern Panalytical Ltd, Malvern, Worcestershire, U.K.).

2.5. Amplification and sequencing of bacterial DNA from EV

For PCR amplification from EV, DNA was isolated following the procedure described earlier (Yoo et al., 2016; Chang et al., 2021), with some modifications. In brief, product pellets after centrifugations at 15, 33, and 100 K were heated at 100°C for 20 min, and then centrifuged at 11,000 rpm in an Eppendorf centrifuge for 20 min. DNA in the supernatants was purified with the Macherey–Nagel PCR Clean-up kit (MACHEREY-NAGEL GmbH & Co., Promega Corporation, Madison, Wisconsin, USA). Then, 16S rDNA was amplified by PCR with the conditions cited earlier, with general purpose 16S bacterial primers 27f and 558r. New primers were designed for the specific amplification of 16S rDNA of strains belonging to the genogroup *Lacticaseibacillus casei/paracasei/rhamnosus/zeae* (Lcas215for- CCGCATGGTTCTTGGCTGAAAGAT; Lcas462rev-CGCCGACAACAGTTACTCTGCCGACCA). These amplicons were also sequenced to check the full 16S rDNA identity of *L. paracasei*.

3. Results

3.1. Characterization of *L. paracasei* strains from commercial products

A total of five different dairy-fermented products have been studied, of which two are commercialized by independent brands and the other three were distributors' white brands. All of them were similar liquid (not set) fermented milk products in small bottles (65–100 g per unit) carrying *Lactobacillus casei* (*Lacticaseibacillus paracasei*). Possibly, for logistics or marketing reasons, the right taxonomic assignment of these strains has not been updated on their labels. A total of four products (A, Ca, H, and Co) described in the label that, in addition to *L. casei* (*L. paracasei*), they contained yogurt starters, dairy ferments, or specifically described the presence of *Streptococcus thermophilus* and *Lactobacillus delbruekii* subs *bulgaricus*. Only one of the

10.3389/fmicb.2023.1165202

TABLE 1 The average particle size of EVs obtained for the lactobacilli isolated from different commercial products found in 100 K pellets and determined by DLS.

Original product	EV	Pk 1 mean (d.nm; Sdev.)	Pk 2 mean (d.nm; Sdev.)	Pk 3 mean (d.nm; Sdev.)
	BL23	309.9 (55.6)	47.1 (9.9)	–
A	BL413	241.7 (142.4)	43.2 (17.9)	–
Ca	BL415	491.9 (187.9)	27.6 (5.9)	–
Co	BL416	301.0 (59.3)	–	–
H	BL417	234.8 (136.0)	39.6 (26.1)	–
Y	BL418	425.5 (6.6)	94.2 (17.2)	24.8 (2.0)

products (Y) mentioned the exclusive use of *L. casei* (*L. paracasei*). They all had low pHs between 3.80 and 4.65, and colony counts between 4.13×10^8 and 13.2×10^8 cfu/mL on MRS at 37°C (Supplementary Table 1). All strains were isolated and identified by sequencing the 500 nt 5' region of the 16S rDNA. Their sequences were almost identical and showed 99.6–100% identity to reference *L. paracasei* sequences, and then, they were given appropriate culture collection codes that corresponded to A, BL413; Ca, BL415; Co, BL416; H, BL417; and Y, BL418 (see also Supplementary Table 1). Furthermore, all five strains isolated were typed for the allele *cmu*B (encoding P75). Amplification and sequencing of the direct repeats containing the satellite region of this gene indicated that all strains had the same allele profile, identical to BL23 (*cmu*B1), with the exception of BL415 (FDP-Ca) which showed the deletion in allele *cmu*B3, following the pattern of strain *L. paracasei* TMV 1.1434 (Bäuerl et al., 2019; Supplementary Figure 1).

3.2. Isolation of EV and detection of associated P40 and P75 in commercial probiotics

All *L. paracasei* isolates were examined for the production of EV and associated P40 and P75 proteins. Supernatants of Lactobacilli grown on MRS were centrifuged at 15, 33, and 100 K successively, in order to follow the same procedure as with dairy products (see later). The presence and likely size of EV were determined by DLS in pellets recovered from the 100 K centrifugation. The amount and sizes of EV were variable between the strains. With the exception of BL416 (FDP-Co), all strains had two light scattering peaks corresponding to particles of 300–450 d.nm and much smaller size, between 24 and 67 d.nm [Table 1, which coincided with previously reported EV size reported for BL23 (Bäuerl et al., 2020)]. Larger particles detected on all samples could originate from EV aggregates (Table 1 and Supplementary Figure 2).

Then, the presence of P40 and P75 was monitored by Western blot in the EV obtained at 100 K and from pellets collected in previous 15 and 33 K centrifugations (Figure 1). All strains produced P40 and P75, and amounts detected in MRS had different intensities. They were found in the 100 K pellets, indicating that they were possibly bound to EV.

3.3. Identification of bacterial EV in fermented dairy products

EVs from fermented dairy products were isolated after successive centrifugations at 15 K, then the supernatant was centrifuged at 33 K, and this supernatant was centrifuged at 100 K. Pellets obtained after the different centrifugations were preserved at −80°C for further study. Due to the nature of those products, especially after 15 K centrifugations, pellets had a large volume and were difficult to dissolve in PBS, which made it difficult to analyze them by DLS. Only suspended vesicles from the 100 K pellets were stable and rendered good quality DLS signal intensity. The determination of the EV size showed that all the products had EVs of very similar size, yielding an average particle size of 147.26 d.nm (Sdev. 15.48; average z-value 120.95 d.nm, Sdev. 9.00; Supplementary Figure 3).

3.3.1. Detection of EV-bound proteins P40 and P75

In order to detect *L. paracasei* EV, pellets from 100 K ultracentrifugation were presumably carrying microbial EVs and the associated P40 and P75, but unexpectedly, P40 was not found in those samples. Then, Western blot was repeated for the inspection of P40 and P75 in all pellets and supernatants of fermented dairy products (15, 33, and 100 K; Figure 2). Due to the nature of the products, the 15 K pellets had a high volume and protein content, which saturated the nitrocellulose membrane blocking protein transfer in some samples. P40 could be clearly detected in product A (pellets of 15 and 33 K, and a very faint band in 100 K) as well as in product H (pellets of 33 K). In relation to P75, it was present in all the supernatants and pellets of all the products, normally yielding more intense bands in the corresponding pellet line. Products A, Ca, and Y had more intense bands than H and Co. In the case of product Y, it was particularly difficult to suspend the 15 K pellet in a small volume of buffer, and as a consequence, 15 K samples could not be analyzed.

3.3.2. Confirmation of the presence of microbial EV in the samples

In order to double-check the presence of bacterial EV in the different pellets, Western blots under special LTA electrophoresis conditions were run (Bäuerl et al., 2020), but no signals could be detected possibly low amounts of EV and low sensitivity of anti-LTA antibodies (data not shown). Bacterial EVs have been reported to carry bacterial DNA cargo (Biller et al., 2014); hence, we proceeded to confirm the presence of bacterial EV by PCR amplification and sequencing of the 100 K pellets of all fermented dairy products. Initially, all 100 K samples were tested for the presence of bacterial DNA by sequencing amplicons obtained with

10.3389/fmicb.2023.1165202

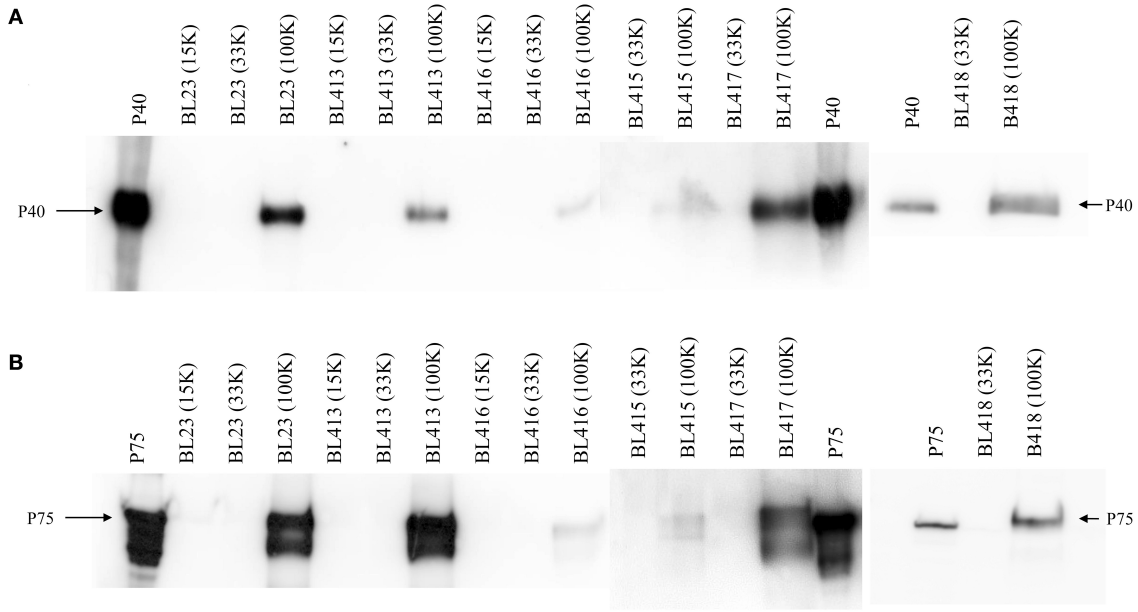

FIGURE 1
Western blot showing proteins P40 **(A)** and P75 **(B)** in EV isolated from the reference strain of *L. paracasei* BL23 and *L. paracasei* isolated from dairy fermented products (BL 413 from product A, BL 415 from product Ca, BL 416 from product Co, BL 417 from product H, and BL 418 from product Y). Control lines carry purified proteins P40 and P75 from BL23.

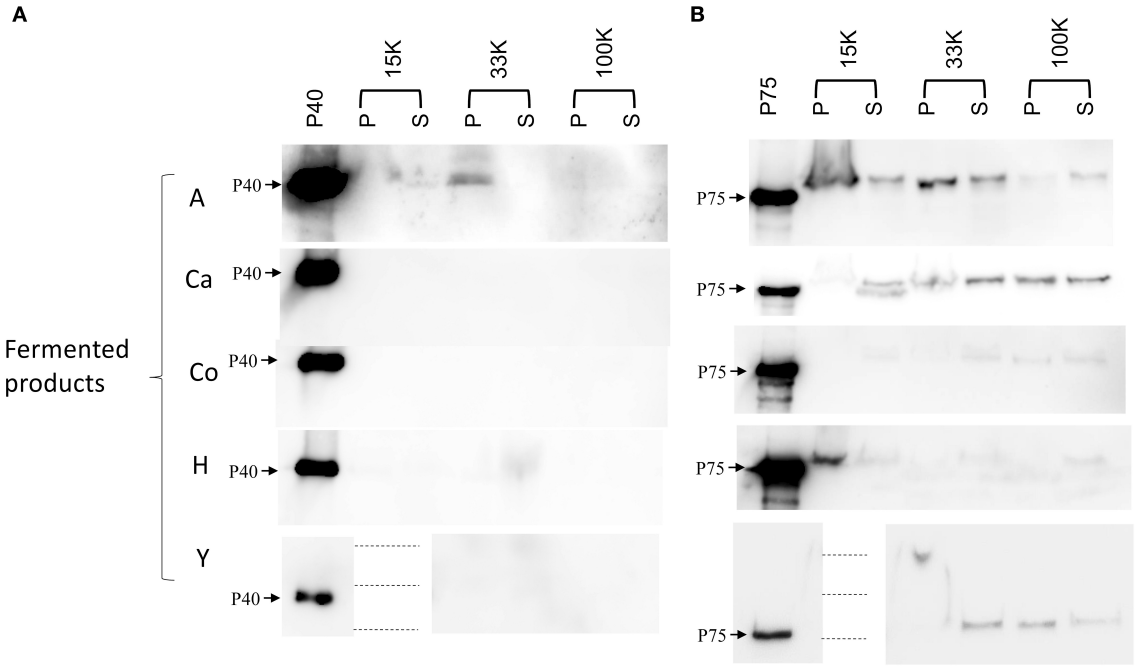

FIGURE 2
Detection of P40 and P75 in the pellets (P) and supernatants (S) of the sequential centrifugation (15, 33, and 100 K) of five fermented dairy products (A, Ca, Co, H, and Y). **(A)** Shows all samples detected with anti-P40 rabbit antibodies, and **(B)** shows samples detected with anti-P75 rabbit antibodies. Purified His-tag P40 and P75 were used as references for the corresponding blots. It was technically impossible to load on the PAGE samples of 15 K pellet of product Y; hence, both P and S samples of product Y were omitted, and the image has been split to align with the track annotations above.

general bacterial primers (Table 2). Sequencing of the amplicons indicated the presence of DNA from *Lactobacillus delbrueckii* subsp *bulgaricus* EV of two products (Co and H), *Streptococcus thermophilus* in product Ca, and *Pseudomonas gessardii* and *Pseudomonas aeruginosa*, respectively, in the 100 K EV fraction of products A and Y. Of note, with these universal 16S bacterial rDNA

10.3389/fmicb.2023.1165202

TABLE 2 Sequences obtained after the amplification of 16S rDNA from EV in the 100 K pellets of the different fermented dairy products.

EV from fermented dairy products	Universal bacterial 16S primers (27f-558r)	*L. paracasei* specific 16S primers (Lcas215for/ Lcas462rev)
100 K A	Low quality sequence (*Pseudomonas aeruginosa* 80% match)	*L. paracasei* 100%
100 K Ca	Low quality sequence (*Streptococcus thermophilus* 85.98% match)	*L. paracasei* 100%
100 K Co	*L. delbrueckii* subsp. *bulgaricus* 99% match	*L. paracasei* 100%
100 K H	*L. delbrueckii* subsp. *bulgaricus* 99% match	*L. paracasei* 99% match
100 K Y	*Pseudomonas gessardii* 99% match	*L. paracasei* 100% match

primers, all PCR reactions rendered a single high-intensity band at the expected size (~500 nt); however, quality of the sequences was low indicating that the amplicon had different DNA molecules. As a consequence, specific *L. paracasei* primers were designed to specifically detect EV of this probiotic species. Sequencing the corresponding amplicons showed that all the EVs analyzed contained *L. paracasei* 16S rDNA (Table 2).

3.4. Tracking added *L. paracasei* BL23 EV in milk

3.4.1. Size distribution

For this experiment, UHT skimmed milk from three different brands was purchased (coded as LA, PA, and PU), and the equivalent amount of EV isolated from *L. paracasei* BL23 grown in 200 mL of MRS was added to 200 mL of milk. Then, pellets from the successive centrifugations at 15, 33, and 100 K were collected in PBS and analyzed by DLS. In general, EVs of smaller size were recovered from centrifugations at slower speeds (Table 3), suggesting a higher EV density. In general terms, the size distribution of EV was very homogeneous within samples (Supplementary Figure 4), confirmed by the low standard deviations, particularly if compared to EV from the bacterial culture medium, possibly due to the low concentration of bacterial EV. Interestingly, peaks corresponding to possibly two different EV populations were recovered after ultracentrifugation at 100 K, the peak of smaller size EV, being on average 15–20 d.nm larger than the expected size of *L. paracasei* BL23 EV.

3.4.2. Distribution of L. paracasei BL23 proteins P40 and P75 in the EV fractions

After the addition of EV from *L. paracasei* to commercial UHT milks, small EVs of the approximate size of *L. paracasei* EVs were detected in the 100 K pellets (see Section 3.4.1). The next step was the detection of P40 and P75 in EV prepared from the different milk pellets in Western blot analysis. Interestingly, both proteins were mainly found associated with 15 and 33 K fractions in two of the milk products (PA and LA; Figure 3). Milk PU had an unusual behavior when centrifuged at 100 K, and a very large pellet was collected at 100 K ultracentrifugation, indicating the presence of a polymeric gel. If the manufacturing process of this milk used a large proportion of powdered milk, it could contain stabilizers as adjuncts that were found in the sediment at high centrifugal speed. Consequently, the results obtained from this commercial milk may not be representative of what could be happening during natural fermentation.

TABLE 3 EV size distribution, determined by DLS, of different milk samples with added *L. paracasei* EV recovered after 15, 33, and 100 K centrifugations.

	EV form 15 K pellet	EV from 33 K pellet	EV from 100 K pellet	
	Pk 1 mean (d.nm; Sdev.)	Pk 1 mean (d.nm; Sdev.)	Pk 1 mean (d.nm; Sdev.)	Pk 2 mean (d.nm; Sdev.)
LA	269.7 (11.5)	335.1 (2.2)	405.5 (35.42)	66.6 (19.0)
PU	188.4 (1.2)	183.6 (8.6)	302.3 (26.4)	57.9 (11.0)
PA	244.7 (15.1)	208.5 (9.3)	400.3 (89.7)	65.3 (18.6)
Total average	234.3 (37.3)	242.4 (70.7)	369.4 (70.9)	56.8 (25.7)

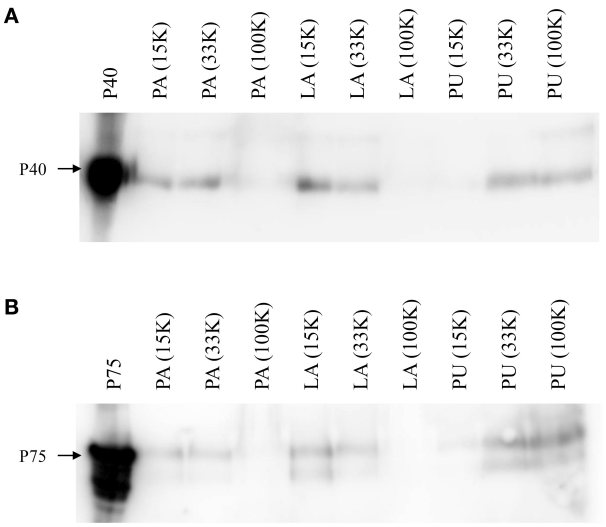

FIGURE 3
Detection of P40 **(A)** and P75 **(B)** by Western blot in EV isolated at different centrifugal pellets (15, 33, and 100 K), after the addition of *L. paracasei* EV to three different commercial UHT semi-skimmed milk products (PU, LA, and PU).

3.4.3. Presence of microbial DNA

As mentioned earlier, the presence of microbial DNA can be specifically associated with bacterial EV cargo. Hence, after the

10.3389/fmicb.2023.1165202

TABLE 4 Sequences obtained after the amplification of 16S rDNA from EV in the 100 K pellets of the different fermented dairy products.

Milk samples with added BL23 EV	Universal bacterial 16S primers (27f-558r)	*L. paracasei* specific 16S primers (Lcas215for/ Lcas462rev)
100 K LA	Uncultured bacterium 95–96% match	*L. paracasei* 100% match
33 K LA	*L. delbrueckii* subsp. *bulgaricus* 99.19% match	*L. paracasei* 99% match
15 K LA	Not quality sequence (contaminated)	*L. paracasei* 99% match
100 K PA	Uncultured bacterium/*L. delbrueckii* subsp. *bulgaricus* 94% match	*L. paracasei* 99% match
33 K PA	*L. delbrueckii* subsp. *bulgaricus* 99,59% match	*L. paracasei* 100% match
15 K PA	*L. delbrueckii* subsp. *bulgaricus* 99% match	*L. paracasei* 99% match
100 K PU	• *L. delbrueckii* subsp. *bulgaricus* 98% match • Contaminant: 26 nt 100% match *Staphylococcus epidermidis/ haemolyticus/ saprophyticus*	*L. paracasei* 99% match
33 K PU	Uncultured bacterium 94% match	*L. paracasei* 100% match
15 K PU	*L. delbrueckii* subsp. *bulgaricus* 97% match (low quality sequence)	No significant similarity found (contaminated)

addition of *L. paracasei* EV to three different commercial UHT skimmed milk products (PU, LA, and PU), PCR detection of microbial 16S rDNA was performed on EV isolated at different centrifugal speeds (15, 33, and 100 K). Universal 16S rDNA primer amplicons obtained from all milk samples were sequenced. Most of the sequences were not "clean," showing some background DNA sequences, and many of them had high homology to *Lactobacillus delbruekii* subsp. *bulgaricus* 16S rDNA, unknown bacteria, or were not quality sequences (Table 4). Then, 16S rDNA from *L. paracasei* was specifically amplified in all samples, and bands obtained were sequenced, indicating the presence of *L. paracasei* EV associated with all samples.

4. Discussion

The presence of EVs in all kingdoms of life suggests that they are present in food components; hence, higher organisms—including humans—would be regularly consuming large amounts of EVs of different natures. One of the main objectives of this study was to investigate the presence of *L. paracasei* EV in commercial fermented milk products. A previous article studied the presence of the anti-inflammatory and tissue-repairing proteins P40 and P75 in supernatants of some commercial fermented milk products prepared with *L. paracasei*, finding that P75 was always detected but not P40 (Bäuerl et al., 2019). Shortly after this, the same group showed that those proteins were adhered to the surface of EV from *L. paracasei* (Bäuerl et al., 2020). Some fermented dairy products contain probiotic strains of *L. paracasei;* therefore, it was interesting to know if *L. paracasei* could produce EV during milk fermentations, and what was the interaction between EV and P40 and P75 in commercial products. For that purpose, EVs were prepared from five different fermented drinks carrying *L. paracasei* strains, and the presence of P40 and P75 was investigated. Prior to further analysis, it was confirmed that commercial strains in the products produced EV, P40, and P75. EVs from fermented dairy products were prepared following conditions used from milk EVs, by successive centrifugations at 15, 33, and 100 K (Benmoussa et al., 2020). Some of the products rendered large lumpy pellets at lower speed centrifugations (15,000 × *g* and 33,000 × *g*), possibly due to the precipitation of milk proteins, as a consequence of the physicochemical changes occurring during the fermentation process. Given that the aim of this study was to find bacterial EV in fermented products, assays were initially focused on the 100 K centrifugal fractions and conditions used to recover EV from the bacterial culture supernatants. The particle size of EV from milk fermented products at 100 K had an average particle size by DLS of 147.26 d.nm (average *z*-value 120.95 d.nm), with no indication of the presence of small size *L. paracasei* EV (24.8–47.1 d.nm). This could be explained if the proportion of bacteria EV was small relative to milk EV, as large and more abundant EV may dissipate light more efficiently hampering the detection of smaller particles. In a preliminary assay, Western blot analysis of the 100 K pellets showed that a very small amount of P75 was present, and P40 was not detected. Therefore, pellets and supernatants from previous centrifugations were analyzed. It was previously shown that P75 can be attached to EV and also in solution, in contrast, P40 was always firmly attached to bacterial EV (Bäuerl et al., 2020). In agreement with this data, in fermented products, P75 was present in all pellets and supernatants, while P40 was detected only in the 33 K pellets and possibly 15 K pellets (faint signal) of two commercial products. These results suggested that both proteins may interact with membrane or perivesicular components of milk EV by electrostatic interactions, or alternatively, *L. paracasei* EV may be present in other centrifugal pellets when mixed with milk. In order to solve this question, a marker was required to detect bacterial EV in different pellets. LTA is a characteristic marker of the cell membranes of Firmicutes (Bäuerl et al., 2020), but here, the concentration of EV was below the sensitivity of the LTA antibodies used.

Empirical evidence showed that bacterial EV carry chromosomal DNA fragments (Biller et al., 2014; Bitto et al., 2017); in fact, new-generation sequencing techniques can be applied to study EV from bacterial gut populations and as health markers (Kameli et al., 2021; Park et al., 2021). In milk, the presence of indigenous nucleases (Stepaniak et al., 2003) in multifunctional proteins such as lactoferrin (Soboleva et al., 2019) could eliminate extravesicular DNA, for which PCR detection of bacterial 16S rDNA was implemented as a reliable cargo marker, and general bacterial 16S rDNA was used to detect bacterial EV. Total amplified bacterial DNA of 100 K pellets from fermented products rendered low-quality sequences where *L. paracasei* 16S rDNA was not found, but interestingly, sequences homologous to other bacterial

16S rDNAs were present (*L. delbrueckii* or *Pseudomonas* species). This indicated that these 100 K pellets contained a mixture of EV where *L. paracasei* EVs were underrepresented, but the technique could trace a previous microbiological history of the products, also observed in the EV from UHT milk. Then, specific *L. paracasei* primers were designed for the selective amplification of rDNA, and results showed that *L. paracasei* EVs were indeed present in all fermented products.

Since the concentration of *L. paracasei* EV was apparently very low in fermented products, large amounts of EV from *L. paracasei* BL23 were added to UHT milk in order to facilitate their detection in a milk environment and to test if P40 and P75 would bind to milk EV 15 and 33 K pellets, as suggested by the results from fermented products. After adding EV from *L. paracasei* to UHT milk samples, different fractions of EV were prepared by sequential centrifugations, and pellets were analyzed by DLS, Western blot, and 16S rDNA amplification and sequencing. UHT milk EVs have been reported to have large sizes (~200–230 nm) when determined by DLS (Benmoussa et al., 2017), which are normally larger than the sizes found by electron microscopy (Reinhardt et al., 2012), and this is possibly due to the presence of abundant perivesicular material (proteins and polysaccharides) that change the hydrodynamic diameter. In addition, UHT treatment structurally affects milk EV (Kleinjan et al., 2021). Vesicular properties cannot be extrapolated to the fermented products in this study because (heat) treatments used to prepare milk for the manufacture of commercial fermented milk could not be precisely determined from the product labels (Supplementary Table 1). Of note, it was not the scope of this article to study in detail UHT milk EVs because other fractionation methodologies should have been implemented (Kleinjan et al., 2021). The results showed that after adding *L. paracasei* BL23 EV to three UHT milk brands, the 100 K pellets showed dynamic light scattering populations of small EV (57.9–66.6 d.nm; Table 3), with a size similar to that found here for *L. paracasei* BL23 (41.9 ± 9.9 d.nm; Table 1). This, together with 16S rDNA analysis, supported the presence of *L. paracasei* EVs in the 100 K pellets, but P40 and P75 could not be found. As observed in the fermented products, P40 and P75 proteins were detected in EV from 15 and 33 K centrifugations. Bacterial DNA detection confirmed the presence of *L. paracasei* 16S rDNA in EV fractions obtained in all pellets, indicating that a fraction of *L. paracasei* EV was possibly isolated together with milk EV at 15 and 33 K centrifugations.

The general conclusions of this study underline that some of the commercial probiotics studied (A-BL413, H-BL417, and Y-BL418) produce P40 and P75 bound to EV at a high rate, much like reference probiotics such as *L. parcasei* BL23 or *L. rhamnosus* GG. In addition, different intensities of immunological signals for P40 and P75 in commercial fermented products could respond to fermentation parameters and environmental factors affecting the production of EV and functional proteins. Finally, other factors may possibly affect the functional benefits of P40 and P75 in these products, such as their likely association with milk EV. Most important is the fact that P40, and to a lesser extent P75, are not associated with native small-size bacterial EV, and they are probably complex to milk EV. Experimental data shown here would also support the aggregation or fusion of a fraction of *L. paracasei* EV with milk EV, including attached P40 and P75.

Data availability statement

The original contributions presented in the study are included in the article/Supplementary material, further inquiries can be directed to gaspar.perez@iata.csic.es.

Author contributions

KC-R and LG-P: experimental procedures and text editing. GP: planning, supervising, experimental procedures, and manuscript preparation. All authors contributed to the article and approved the submitted version.

Funding

This project was supported by the Spanish Ministry of Economy and Competitivity, grant RTI2018-097982-B-I00, a grant of the Spanish Ministry of Science and Innovation, Severo Ochoa Accreditation CEX2021-001189-S, KC-R was supported by a grant from the National Council on Science and Technology of Mexico (CONACyT) scholarship number (1018181), and LG-P was supported by a grant for Excellence groups form Generalitat Valenciana CIPROM/2021/082.

Acknowledgments

The authors would like to acknowledge the IATA (CSIC) for the support through APOYA-IATA.

Conflict of interest

The authors declare that the research was conducted in the absence of any commercial or financial relationships that could be construed as a potential conflict of interest.

Publisher's note

Supplementary material

The Supplementary Material for this article can be found online at: https://www.frontiersin.org/articles/10.3389/fmicb.2023.1165202/full#supplementary-material

References

Al-Nedawi, K., Mian, M. F., Hossain, N., Karimi, K., Mao, K., Forsythe, U., et al. (2015). Gut commensal microvesicles reproduce parent bacterial signals to host immune and enteric nervous systems. *FASEB J.* 29, 684–695. doi: 10.1096/fj.14-259721

Bäuerl, C., Abitayeva, G., Sosa-Carrillo, S., Mencher-Beltrán, A., Navarro-Lleó, N., Coll-Marqués, J. M., et al. (2019). P40 and P75 are singular functional muramidases present in the *Lactobacillus casei/paracasei/rhamnosus* taxon. *Front. Microbiol.* 10, 1420. doi: 10.3389/fmicb.2019.01420

Bäuerl, C., Coll-Marqués, J. M., Tarazona-González, C., and Pérez-Martínez, G. (2020). *Lactobacillus casei* extracellular vesicles stimulate EGFR pathway likely due to the presence of proteins P40 and P75 bound to their surface. *Sci. Rep.* 10, 19237. doi: 10.1038/s41598-020-75930-9

Bäuerl, C., Pérez-Martínez, G., Yan, F., Polk, D. B., and Monedero, V. (2010). Functional analysis of the p40 and p75 proteins from *Lactobacillus casei* BL23. *J. Mol. Microbiol. Biotechnol.* 19, 231–241. doi: 10.1159/000322233

Benmoussa, A., Diallo, I., Salem, M., Michel, S., Gilbert, C., Sévigny, J., et al. (2019a). Concentrates of two subsets of extracellular vesicles from cow's milk modulate symptoms and inflammation in experimental colitis. *Sci. Rep.* 9, 14661. doi: 10.1038/s41598-019-51092-1

Benmoussa, A., Gotti, C., Bourassa, S., Gilbert, C., and Provost, P. (2019b). Identification of protein markers for extracellular vesicle (EV) subsets in cow's milk. *J. Proteom.* 192, 78–88. doi: 10.1016/j.jprot.2018.08.010

Benmoussa, A., Ly, S., Shan, S. T., Laugier, J., Boilard, E., Gilbert, C., et al. (2017). A subset of extracellular vesicles carries the bulk of microRNAs in commercial dairy cow's milk. *J. Extracell. Vesicl.* 6, 1401897. doi: 10.1080/20013078.2017.1401897

Benmoussa, A., Michel, S., Gilbert, C., and Provost, P. (2020). Isolating multiple extracellular vesicles subsets, including exosomes and membrane vesicles, from bovine milk using sodium citrate and differential ultracentrifugation. *Bio-protocol* 10, e3636. doi: 10.21769/BioProtoc.3636

Biller, S. J., Schubotz, F., Roggensack, S. E., Thompson, A. W., Summons, R. E., and Chisholm, S. W. (2014). Bacterial vesicles in marine ecosystems. *Science* 343, 183–186. doi: 10.1126/science.1243457

Bitto, N. J., Chapman, R., Pidot, S., Costin, A., Lo, C., Choi, J., et al. (2017). Bacterial membrane vesicles transport their DNA cargo into host cells. *Sci. Rep.* 7, 7072. doi: 10.1038/s41598-017-07288-4

Chang, C.-J., Zhang, J., Tsai, Y.-L., Chen, C.-B., Lu, C.-W., Huo, Y.-P., et al. (2021). Compositional features of distinct microbiota base on serum extracellular vesicle metagenomics analysis in moderate to severe psoriasis patients. *Cells* 10, 2349. doi: 10.3390/cells10092349

Domínguez Rubio, A. P., Martínez, J. H., Martínez Casillas, D. C., Coluccio Leskow, F., Piuri, M., and Pérez, O. E. (2017). *Lactobacillus casei* BL23 produces microvesicles carrying proteins that have been associated with its probiotic effect. *Front. Microbiol.* 8, 1783. doi: 10.3389/fmicb.2017.01783

Fang, Z., Pan, T., Li, L., Wang, H., Zhu, J., Zhang, H., et al. (2022). Bifidobacterium longum mediated tryptophan metabolism to improve atopic dermatitis *via* the gut-skin axis. *Gut Microbes* 14, 2044723. doi: 10.1080/19490976.2022.2044723

Frias, J., Martinez-Villaluenga, C., and Peñas, E. (2016). *Fermented Foods in Health and Disease Prevention*. Ney York, NY: Academic press, Elsevier.

García-Martínez, J., Pérez-Castillo, Í. M., Salto, R., López-Pedrosa, J. M., Rueda, R., and Girón. M. D. (2022). Beneficial effects of bovine milk exosomes in metabolic interorgan cross-talk. *Nutrients* 14, 71442. doi: 10.3390/nu14071442

Grande, R., Celia, C., Mincione, G., Stringaro, A., Di Marzio, L., Colone, M., et al. (2017). Detection and physicochemical characterization of membrane vesicles (MVs) of *Lactobacillus reuteri* DSM 17938. *Front. Microbiol.* 8, 1040. doi: 10.3389/fmicb.2017.01040

Gurung, M., Moon, D. C., Choi, C. W., Lee, J. H., Bae, Y. C., Kim, J., et al. (2011). *Staphylococcus aureus* produces membrane-derived vesicles that induce host cell death. *PLoS ONE* 6, e27958. doi: 10.1371/journal.pone.0027958

Jan, A. T. (2017). Outer membrane vesicles (OMVs) of gram-negative bacteria: A perspective update. *Front. Microbiol.* 8, 1053. doi: 10.3389/fmicb.2017.01053

Kameli, N., Borman, R., López-Iglesias, C., Savelkoul, P., and Stassen, F. R. M. (2021). Characterization of feces-derived bacterial membrane vesicles and the impact of their origin on the inflammatory response. *Front. Cell. Infect. Microbiol.* 11, 667987. doi: 10.3389/fcimb.2021.667987

Kleinjan, M., van Herwijnen, M. J., Libregts, S. F., van Neerven, R. J., Feitsma, A. L., and Wauben, M. H. (2021). Regular industrial processing of bovine milk impacts the integrity and molecular composition of extracellular vesicles. *J. Nutr.* 151, 1416–1425. doi: 10.1093/jn/nxab031

Lu, R., Shang, M., Zhang, Y. G., Jiao, Y., Xia, Y., Garrett, S., et al. (2020). Lactic acid bacteria isolated from korean kimchi activate the vitamin D receptor-autophagy signaling pathways. *Inflamm. Bowel Dis.* 2020, izaa049. doi: 10.1093/ibd/izaa049

Marroki, A., Zúñiga, M., Kihal, M., and Pérez-Martínez, G. (2011). Characterization of *Lactobacillus* from Algerian goat's milk based on phenotypic, 16S rDNA sequencing and their technological properties. *Brazil. J. Microbiol.* 42, 158–171. doi: 10.1590/S1517-83822011000100020

Milani, C., Duranti, S., Napoli, S., Alessandri, G., Mancabelli, L., Anzalone, R., et al. (2019). Colonization of the human gut by bovine bacteria present in Parmesan cheese. *Nat. Commun.* 10, 1286. doi: 10.1038/s41467-019-09303-w

Munir, J., Lee, M., and Ryu, S. (2020). Exosomes in food: Health benefits and clinical relevance in diseases. *Adv. Nutr.* 11, 687–696. doi: 10.1093/advances/nmz123

Park, J., Kim, N.-E., Yoon, H., Shin, C. M., Kim, N., Lee, D. H., et al. (2021). Fecal microbiota and gut microbe-derived extracellular vesicles in colorectal cancer. *Front. Oncol.* 11, 650026. doi: 10.3389/fonc.2021.650026

Pérez-Bermúdez, P., Blesa, J., Soriano, J. M., and Marcilla, A. (2017). Extracellular vesicles in food: Experimental evidence of their secretion in grape fruits. *Eur. J. Pharmaceut. Sci.* 98, 40–50. doi: 10.1016/j.ejps.2016.09.022

Raftar, S. K. A., Ashrafian, F., Yadegar, A., Lari, A., Moradi, H. R., Shahriary, A., et al. (2021). The protective effects of live and pasteurized *Akkermansia muciniphila* and its extracellular vesicles against HFD/CCl4-induced liver injury. *Microbiol. Spectr.* 9, e00484–e00421. doi: 10.1128/Spectrum.00484-21

Reinhardt, T. A., Lippolis, J. D., Nonnecke, B. J., and Sacco, R. E. (2012). Bovine milk exosome proteome. *J. Proteom.* 75, 1486–1492. doi: 10.1016/j.jprot.2011.11.017

Rivera, J., Cordero, R. J. B., Nakouzi, A. S., Frases, S., Nicola, A., and Casadevall, A. (2010). *Bacillus anthracis* produces membrane-derived vesicles containing biologically active toxins. *Proc. Natl. Acad. Sci. U. S. A.* 107, 19002–19007. doi: 10.1073/pnas.1008843107

Savaiano, D. A., and Hutkins, R. W. (2021). Yogurt, cultured fermented milk, and health: A systematic review. *Nutr. Rev.* 79, 599–614. doi: 10.1093/nutrit/nuaa013

Schwechheimer, C., and Kuehn, M. J. (2015). Outer-membrane vesicles from Gram-negative bacteria: Biogenesis and functions. *Nat. Rev. Microbiol.* 13, 605. doi: 10.1038/nrmicro3525

Soboleva, S. E., Zakharova, O. G. D., Sedykh, S. E., Ivanisenko, N. V., Buneva, V. N., and Nevisky, G. A. (2019). DNase and RNase activities of fresh cow milk lactoferrin. *J. Mol. Recogn.* 32, e2777. doi: 10.1002/jmr.2777

Stepaniak, L., Fleming, C. M., Gobbetti, M., Corsetti, A., and Fox, P. F. (2003). "Indigenous nucleases in milk," in *Advanced Dairy Chemistry-—1 Proteins: Part A/Part B*, eds P. F. Fox and P. L. H. McSweeney (Boston, MA: Springer US), 545–561. doi: 10.1007/978-1-4419-8602-3_15

Surve, M. V., Anil, A., Kamath, K. G., Bhutda, S., Sthanam, L. K., Pradhan, A., et al. (2016). Membrane vesicles of group B streptococcus disrupt feto-maternal barrier leading to preterm birth. *PLoS Pathogens* 12, e1005816. doi: 10.1371/journal.ppat.1005816

Toyofuku, M., Nomura, N., and Eberl, L. (2019). Types and origins of bacterial membrane vesicles. *Nat. Rev. Microbiol.* 17, 13–24. doi: 10.1038/s41579-018-0112-2

Wagner, T., Joshi, B., Janice, J., Askarian, F., Škalko-Basnet, N., Hagestad, O. C., et al. (2018). *Enterococcus faecium* produces membrane vesicles containing virulence factors and antimicrobial resistance related proteins. *J. Proteom.* 187, 28–38. doi: 10.1016/j.jprot.2018.05.017

Wang, Y., Liu, L., Moore, D. J., Shen, X., Peek, R. M., Acra, S. A., et al. (2017). An LGG-derived protein promotes IgA production through upregulation of APRIL expression in intestinal epithelial cells. *Mucosal Immunol.* 10, 373–384. doi: 10.1038/mi.2016.57

Yan, F., Cao, H., Cover, T. L., Washington, M. K., Shi, Y., Liu, L., et al. (2011). Colon-specific delivery of a probiotic-derived soluble protein ameliorates intestinal inflammation in mice through an EGFR-dependent mechanism. *J. Clin. Invest.* 121, 2242–2253. doi: 10.1172/JCI44031

Yan, F., Liu, L., Cao, H., Moore, D. J., Washington, M. K., Wang, B., et al. (2017). Neonatal colonization of mice with LGG promotes intestinal development and decreases susceptibility to colitis in adulthood. *Mucosal Immunol.* 10, 117–127. doi: 10.1038/mi.2016.43

Yoo, J. Y., Rho, M., You, Y.-A., Kwon, E. J., Kim, M.-H., Kym, S., et al. (2016). 16S rRNA gene-based metagenomic analysis reveals differences in bacteria-derived extracellular vesicles in the urine of pregnant and non-pregnant women. *Exp. Mol. Med.* 48, e208. doi: 10.1038/emm.2015.110

frontiers | Frontiers in Microbiology

TYPE Original Research
PUBLISHED 24 May 2023
DOI 10.3389/fmicb.2023.1163662

OPEN ACCESS

EDITED BY
Giuseppe Spano,
University of Foggia, Italy

REVIEWED BY
Victor Sebastian Blancato,
CONICET Instituto de Biología Molecular y Celular de Rosario (IBR), Argentina
Serap Cosansu,
Sakarya University, Türkiye

*CORRESPONDENCE
Yuhong Lyu
✉ yuhonglyu@126.com
Changwu Yue
✉ changwuyue@126.com
Shanshan Deng
✉ dssjx@126.com

†These authors have contributed equally to this work

RECEIVED 11 February 2023
ACCEPTED 26 April 2023
PUBLISHED 24 May 2023

CITATION
Hu Y, Zhao Y, Jia X, Liu D, Huang X, Wang C, Zhu Y, Yue C, Deng S and Lyu Y (2023) Lactic acid bacteria with a strong antioxidant function isolated from "Jiangshui," pickles, and feces. *Front. Microbiol.* 14:1163662. doi: 10.3389/fmicb.2023.1163662

Lactic acid bacteria with a strong antioxidant function isolated from "Jiangshui," pickles, and feces

Yue Hu[1,2†], Yan Zhao[3†], Xu Jia[2,4], Dan Liu[5], Xinhe Huang[3], Cheng Wang[4], Yanhua Zhu[4], Changwu Yue[1*†], Shanshan Deng[2,4*†] and Yuhong Lyu[1*†]

[1]Yan'an Key Laboratory of Microbial Drug Innovation and Transformation, School of Basic Medicine, Yan'an University, Yan'an, Shaanxi, China, [2]Non-coding RNA and Drug Discovery Key Laboratory of Sichuan Province, Chengdu Medical College, Chengdu, Sichuan, China, [3]Life Science and Engineering, Southwest Jiaotong University, Chengdu, China, [4]School of Basic Medical Sciences, Chengdu Medical College, Chengdu, Sichuan, China, [5]Department of TCM, Sichuan Province People's Hospital, Sichuan Academy of Medical Sciences, Chengdu, China

Excessive free radicals and iron death lead to oxidative damage, which is one of the main causes of aging and diseases. In this field of antioxidation, developing new, safe, and efficient antioxidants is the main research focus. Lactic acid bacteria (LAB) are natural antioxidants with good antioxidant activity and can regulate gastrointestinal microecological balance and immunity. In this study, 15 LAB strains from fermented foods ("Jiangshui" and pickles) or feces were evaluated in terms of their antioxidant attributes. Strains with strong antioxidant capacity were preliminarily screened by the following tests: 2,2-diphenyl-1-picrylhydrazyl (DPPH), hydroxyl radical, superoxide anion radical scavenging capacity; ferrous ion chelating assay; hydrogen peroxide tolerance capacity. Then, the adhesion of the screened strains to the intestinal tract was examined using hydrophobic and auto-aggregation tests. The safety of the strains was analyzed based on their minimum inhibitory concentration and hemolysis, and 16S rRNA was used for molecular biological identification. Antimicrobial activity tests showed them probiotic function. The cell-free supernatant of selected strains were used to explore the protective effect against oxidative damage cells. The scavenging rate of DPPH, hydroxyl radicals, and ferrous ion-chelating of 15 strains ranged from 28.81–82.75%, 6.54–68.52%, and 9.46–17.92%, respectively, the scavenging superoxide anion scavenging activity all exceeded 10%. According to all the antioxidant-related tests, strains possessing high antioxidant activities J2-4, J2-5, J2-9, YP-1, and W-4 were screened, these five strains demonstrated tolerance to 2 mM hydrogen peroxide. J2-4, J2-5, and J2-9 were *Lactobacillus fermentans* and γ-hemolytic (non-hemolytic). YP-1 and W-4 were *Lactobacillus paracasei* and α-hemolytic (grass-green hemolytic). Although *L. paracasei* has been proven as a safe probiotic without hemolytic characteristics, the hemolytic characteristics of YP-1 and W-4 should be further studied. Due to the weak hydrophobicity and antimicrobial activity of J2-4, finally, we selected J2-5, J2-9 for cell experiment, J2-5 and J2-9 showed an excellent ability that resistant to oxidative damage by increasing SOD, CAT, T-AOC activity of 293T cells. Therefore, J2-5, and J2-9 strains from fermented foods "Jiangshui" could be used as potential antioxidants for functional food, health care, and skincare.

KEYWORDS

lactic acid bacteria, screening, ferroptosis, antioxidant activity, anti-aging, *Lactobacillus fermentans*

Introduction

Oxidation is an important physiological process in organisms. It can provide energy for the body, but a large number of free radicals and reactive oxygen species (ROS) are generated through exogenous chemistry or endogenous metabolism (Valko et al., 2006). Iron-dependent cell death (ferroptosis) has been widely investigated. Iron-dependent programmed cell death is accompanied by lipid peroxidation and high ROS production (Mancardi et al., 2021). Free radicals and ROS are highly unstable and can interact with carbohydrates, lipids, proteins, and DNA. When the amount of free radicals exceeds the ability of the antioxidant system to scavenge them, oxidative stress occurs, causing cell death and tissue damage. When free radicals accumulate, human aging and various chronic diseases, such as atherosclerosis, cancer, emphysema, liver cirrhosis, and arthritis, occur (Wang et al., 2017).

Antioxidants have been comprehensively studied, but the safety and long-term efficacy of synthetic chemical antioxidants, such as butylhydroxyanisole, butylhydroxytoluene, and propyl gallate, have been questioned (Wang W. et al., 2021). Therefore, effective, safe, and economical natural antioxidants have been developed. A good antioxidant choice includes lactic acid bacteria (LAB). LAB are Gram-positive bacteria that can ferment carbohydrates to produce large amounts of lactic acid, which widely exists in vegetables, fruits, and soil, and LAB also exist in the intestinal tract as essential and beneficial physiological flora. They form a protective barrier in the intestinal tract, inhibit harmful bacterial growth, and maintain the ecological balance of microorganisms in the body (Del Re et al., 2000). Moreover, they produce short-chain fatty acids, supplying nutrients to the body, reducing cholesterol, and enhancing immunity to maintain health. LAB are often used in fermented fruits and vegetables; grain, meat, and dairy products; breweries; and other industries (Chen et al., 2020). Their application field has also continuously expanded. Because of their probiotic properties, they are applied to healthcare and medical treatment. They can be used to treat diabetes, Alzheimer's disease, Parkinson's disease, obesity, liver diseases, and tumors (Lin et al., 2018; Yan et al., 2019).

Lactic acid bacteria (LAB) have excellent antioxidant properties (Lin and Yen, 1999). Shi et al. (2019) evaluated the antioxidant effect of 23 LAB strains that can scavenge free radicals, and the authors found that the superoxide dismutase (SOD) content is 0.53–8.62 U; these strains can also scavenge a certain amount of ROS. In Wang's study, the supernatants of *Bifidobacterium longum* CCFM752, *Lactobacillus plantarum* CCFM1149, and *L. plantarum* CCFM10 inhibit ROS production in A7R5 cells, and CCFM10 even inhibits 94.6 ± 5.9% of ROS production (Wang Y. et al., 2021). Zhao isolated *B. longum* K5 and K10 from infant feces and demonstrated their strong antioxidant activity (Zhao et al., 2021). Son screened *L. plantarum* Ln4 with a strong antioxidant activity through a 1,1-diphenyl-2-trinitrophenylhydrazine (DPPH) scavenging experiment and a β-carotene bleaching experiment (Son et al., 2017). Although the specific antioxidant mechanism of LAB remains unclear, researchers have found that LAB can produce antioxidant metabolites and scavenge ROS enzymes, upregulate the activity of host antioxidant enzymes, downregulate the activity of enzymes related to ROS production, and regulate the antioxidant signaling pathway in hosts and intestinal flora (Amaretti et al., 2013). Lipid peroxidation under ferrous catalysis produces large amounts of ROS, which induce cell ferroptosis (Zhang et al., 2021). LAB can chelate ferrous ions, inhibit lipid peroxidation, and scavenge free radicals, thereby alleviating aging-related damage caused by ferroptosis.

Fermented foods contain many beneficial microorganisms, which not only enrich the taste of fermented foods but also benefit human health. "Jiangshui" is a common traditional fermented food that has been known for more than 2,000 years and is especially popular in Shaanxi and Gansu provinces. Celery, cabbage, and mustard are boiled together for a few minutes for sterilization, and then flour is added to introduce yeast and LAB in "Jiangshui" (Wu et al., 2021). The ingredients are then soaked in sterile water for 4–5 days, giving the milky-white "Jiangshui" its characteristic smooth texture and slightly sour flavor. Moreover, Sichuan pickles have a long history of 1,000 years, and they have been selected in the first batch of protection lists of geographical indications in China and Europe, sold to the whole country, and even exported to foreign areas. Radish and cabbage peppered with salt are usually used for sterilization and water removal from Sichuan pickles. The processed vegetables and sterile water are then put into sealed jars and fermented for several months in an anaerobic environment. Unlike "Jiangshui", Sichuan pickles are crispier, saltier, and more sour (Luo et al., 2020). Different conditions affect the growth of LAB in fermented food, such as time, pH, and temperature (Yang et al., 2018). The optimum growth temperature of LAB is between 25 and 38°C. At the midpoint of the fermentation period, the pH gradually decreases. This elevated acidity leads to the death of miscellaneous bacteria, making *Lactobacillus* the dominant strain and delivering the optimal flavor and quality for the fermented food.

Studies have shown that elderly people have unique diets and living habits, highlighting the impact of diet on health and life expectancy (Hausman et al., 2011). Therefore, we screened antioxidant LAB from the famous Sichuan pickles and "Jiangshui" in Longevity Village, Hanzhong City, Shaanxi Province. "Jiangshui" is widely consumed by residents in Longevity Village. This study aimed to determine whether the local LAB have a strong antioxidant capacity to help people live longer; meanwhile, for testing the antioxidant properties of probiotics isolated from human intestines, feces preserved in the laboratory were also used as raw materials for screening. Finally, the five selected strains could chelate ferrous ions; tolerate hydrogen peroxide; and scavenge DPPH, hydroxyl radicals, and superoxide anions. After passing the safety test, antimicrobial activity assay, and the protective effects of strains against oxidative injury cells, two strains could be used in producing functional fermented food as well as medical or cosmetic skincare products.

Materials and methods

Strains and media

Test strains

A total of 15 experimental strains were tested. Among them, W-2 and W-4, which were isolated from human feces, were provided

by the Non-coding RNA and Drug Discovery Key Laboratory of Sichuan Province. J2-3, J2-4, J2-5, J2-7, and J2-9 were from "Jiangshui" in Shaanxi Longevity Village. Y2-1, Y2-6, YP-1, YP-8, GP-4, GP-7, GP-9, and WJ-6 were obtained from Sichuan pickles.

Indicator strains

Lactobacillus rhamnosus has been proven to have antioxidant activities. *L. rhamnosus GG (LGG)* ATCC7469 was used as a control. *LGG* ATCC7469, *Escherichia coli* ATCC25922, and clinical pathogenic bacteria *Acinetobacter baumannii (Ab)*, *Escherichia coli (Ec)*, *Klebsiella pneumoniae (Kp)*, and *Enterococcus faecalis (Efa)* were provided by the Non-coding RNA and Drug Discovery Key Laboratory of Sichuan Province.

MRS liquid and agar media (Solarbio Co., Ltd., Shanghai, China) and LB broth (Sangon Biotech, Co., Ltd. Shanghai, China) were used.

Other reagents and kits for screening antioxidant strains

DPPH, pyrogallic, L-ascorbic acid, potassium ferricyanide, diethylenetriaminepentaacetic acid, iron chloride hexahydrate, trichloroacetic acid (TCA), and 1,10-phenanthrolineall (Macklin Biomedical Co., Ltd., Shanghai) were used.

Isolation and purification of LAB strains

Lactic acid bacteria (LAB) in Sichuan pickles and "Jiangshui" were isolated in the MRS medium in accordance with the following steps. Fermentation products (5 mL) were added to 45 mL of sterile normal saline, mixed well, gradient-diluted 10^{-2}, 10^{-3}, 10^{-4}, 10^{-5}, and 10^{-6} times with sterile normal saline, and spread on the MRS agar media, which were placed at 37°C for 48 h under anaerobic conditions: N_2 (85%), CO_2 (5%), and H_2 (10%) (Luo et al., 2020).

After the isolates were cultured, single colonies were selected according to colony shape, size, and color. The selected strains were cultured, purified again, and streaked onto MRS agar containing bromocresol purple. Acid-producing strains were then chosen. The pure colonies were checked through gram staining and catalase testing. Gram-positive and catalase-negative strains were cultured at 37°C until they reached stability, maintained in a 25% glycerol solution, and stored in an ultra-low-temperature refrigerator at −80°C.

Preparation of sterile saline bacterial suspension

The bacterial suspension was prepared in accordance with previously described methods (Lin and Yen, 1999). LAB colonies obtained through the abovementioned steps were then used as the inoculation solution, inoculated in 50 mL of MRS liquid medium based on 2% volume, and incubated at 37°C for 18 h. The cells were collected through centrifugation at 7,000 rpm at 4°C for 10 min, washed twice with sterile saline, and adjusted to 10^9 CFU/mL for further antioxidant assay.

Analysis of DPPH scavenging capacity

DPPH scavenging by the tested strains was analyzed using previously described methods (Lin and Chang, 2000) with some modifications. In brief, 1 mL of a saline suspension of five strains was fully mixed with 1 mL of 0.2 mmol/L DPPH solution (dissolved in pure alcohol), reacted at room temperature in a dark environment for 30 min, and centrifuged at 9,000 × *g* for 10 min. The absorbance optical density at 517 nm (OD_{517}) of the supernatant was measured using a FlexStation 3 multifunctional microplate reader (Molecular Devices Co., Ltd., CA, USA). The control group samples were replaced with an equal volume of distilled water. In the blank group, DPPH was replaced with an equal volume of absolute alcohol. A mixture of an equal volume of distilled water and absolute ethanol was used as the calibration sample to adjust OD_{517} to zero. The experiments were performed in triplicates.

The scavenging rate was calculated using the following equation:

$$\text{Scavenging rate of DPPH} = [1 - (A1 - A2)/A0] \times 100\%$$

Where ODA1, ODA2, and ODA0 are equivalent to 1 mL DPPH + 1 mL sample, 1 mL pure alcohol + 1 mL sample, and 1 mL DPPH + 1 mL pure alcohol, respectively.

Determination of hydroxyl radical scavenging capacity

The hydroxyl radical scavenging ability of LAB was determined *via* the Fenton reaction system in accordance with previously described methods (Li et al., 2012). In brief, 1 mL of bright green (0.435 mM), 2 mL of ferrous sulfate (0.5 mM), 1.5 mL of hydrogen peroxide (3.0%, w/v), and 1 mL of LAB suspension were mixed and placed in a water bath at 37°C for 30 min. The supernatant was centrifuged at 9,000 rpm for 10 min, and the absorbance was measured at 525 nm. The blank sample was replaced with distilled water. The experiment was repeated thrice.

$$\text{Clearance rate \%} = [(AS - A0)/(A - A0)] \times 100\%$$

Where ODAS, ODA0, and ODA are equivalent to sample + bright green + Fenton reagent (the oxidation system of Fe^{2+} and H_2O_2 is Fenton reagent), bright green + Fenton reagent (without the sample), and only bright green, respectively.

Ferrous ion-chelating assay

Ferrous ion-chelating ability was determined using a previously described method (Li et al., 2012). In this assay, 0.5 mL of LAB was added to the mixture of 0.1 mL of ascorbic acid (mass fraction: 1%), 0.1 mL of ferrous sulfate (mass fraction: 0.4%), and 1 mL of

sodium hydroxide (concentration: 0.2 mol/L). The mixture was heated at 37°C for 20 min, and the protein was precipitated using trichloroacetic acid and centrifuged at 3,000 × *g* and 4°C for 10 min. Then, 0.2 mL of the supernatant was added to 2 mL of *o*-phenanthroline (mass fraction: 0.1%) and reacted for 10 min. The absorbance was measured at 510 nm, and phosphate buffer solution (PBS) was used as the blank control.

Determination of superoxide anion radical scavenging capacity

The superoxide anion radical scavenging capacity was assessed using the method reported by He et al. (2015). In this method, 1 mL of Tris-HCL solution (150 mmol/L, pH = 8.2), 1 mL of diethylenetriaminepentaacetic acid (DTPA) solution (3 mmol/L), 1 mL of pyrogallic solution (1.2 mmol/L), and 0.5 mL of bacterial suspension were mixed well and centrifuged; OD_{325} was measured after the mixture was placed in a water bath at 25°C for 10 min.

$$\text{Clearance rate of free radicals of super oxygen anion} = [1 - (A3 - A2)/(A1 - A0)] \times 100\%$$

Where ODA0, ODA1, ODA2, and ODA3 are equivalent to 1 mL Tris-HCL + 1 mL DTPA, 1 mL Tris-HCL + 1 mL DTPA + 1 mL pyrogallic, 1 mL Tris-HCL + 1 mL DTPA + 0.5 mL sample, and 1 mL Tris-HCL + 1 mL DTPA + 1 mL pyrogallic + 0.5 mL sample, respectively.

Based on the above experimental results, we selected the five strains with the strongest antioxidant activity (J2-4, J2-5, J2-9, YP-1, and W-4) for the next physiological tests.

Hydrogen peroxide tolerance

H_2O_2 tolerance was examined as described in previous studies (van Niel et al., 2002; Li et al., 2012) with some changes. The tested bacteria were inoculated in an MRS medium supplemented with H_2O_2 at concentrations of 1, 2, and 3 mmol/L based on the inoculation volume of 2%. They were then cultured at 37°C for 24 h. Afterward, the OD_{600} of the bacterial solution was determined. The blank control was prepared with an uninoculated medium.

Hydrophobicity of LAB

Hydrophobicity was assessed using a previously described assay (Zhao et al., 2021) with slight modifications. The LAB cultured in the MRS medium for 24 h were centrifuged at 6,000 rpm for 5 min and collected. After they were washed with 0.1 mM PBS thrice, the concentration of the bacterial solution was adjusted to 0.6 (OD_{600}). Then, 3 mL of the bacterial solution was mixed with 1 mL of xylene, placed at room temperature for 10 min, mixed completely, and placed in a vent for 30 min to separate the two phases.

The OD_{600} of the aqueous phase was measured and compared with the initial value, and the percentage of cell hydrophobicity was calculated using the following equation:

$$\text{Hydrophobicity\%} = (1 - A1/A0) \times 100\%$$

A1: OD_{600} of aqueous phase after adding xylene.
A0: Initial OD_{600}.

Auto-aggregation

Cells were auto-aggregated in accordance with previously described methods (Hojjati et al., 2020) with some modifications. Overnight grown cultures of J2-4, J2-5, J2-9, YP-1, and W-4 were harvested at 4,000 rpm for 10 min. The collected cells were washed with PBS (pH = 7.2) twice and diluted to OD_{600} = 1.1. Then, the resuspended solution was incubated at 37°C, and the upper suspension was read at 600 nm and at 0, 4, 8, and 12 h.

The auto-aggregation percentage of the four strains was calculated using the following equation (A0, OD_{600} at 0 h; Ax, OD_{600} at *x*h):

$$\text{Auto} - \text{aggregation\%} = [A0 - Ax/A0] \times 100\%$$

Hemolytic activity

J2-4, J2-5, J2-9, YP-1, and W-4 were streaked on Colombian blood plates (Macklin Co., Ltd., Shanghai) and incubated at 37°C. Hemolysis (α-, β-, and γ-hemolysis) was observed after 48 h.

Antibiotic susceptibility

The agar dilution method was used to evaluate the antibiotic sensitivity of the isolated strains. The minimum inhibitory concentration (MIC) of each drug was determined in accordance with the method recommended by the Clinical and Laboratory Standards Institute (M100) (Clinical and Laboratory Standards Institute, 2019). A total of five isolates and *E. coli* ATCC25922 as the control strain were diluted to 1 × 10^7 CFU/mL and inoculated with a sterile inoculation needle on MH agar plates containing meropenem, polymyxin, tetracycline, chloramphenicol, kanamycin, and gentamicin (Dalian Meilun Biotechnology Co., Ltd., Dalian, China). Each plate had a concentration gradient of 1–256 μg/mL. After incubation at 37°C for 48 h, the MIC was determined by observing the bacterial growth.

Strain identification via 16S rRNA gene sequencing and phylogenetic analysis

The DNA of the strains was extracted using a TIANamp Bacterial DNA kit (TIANGEN Biotechnology, China). The bacterial universal primers 27F (5′-AGAGTTTGATCCTGGCTCAG-3′) and 1492 R (5′-AAGGAGGTGATCCAGCCGCA-3′) were used. A PCR reaction system (31.5 μL) was prepared with Taq PCR Master Mix (15 μL), Primer 27 F (50 μmol/L) (0.3 μL), Primer 1492 R (50 μmol/L) (0.3 μL), sterilized ddH_2O (15 μL), and

DNA template (0.9 μL). Amplification was performed under the following parameters: predenaturation at 95°C for 5 min; 30 cycles of denaturation at 94°C for 30 s, annealing at 50°C for 30 s, and extension at 72°C for 1 min; and a final extension at 72°C for 10 min. The products were detected through 1% agarose gel electrophoresis. The amplified PCR products were sequenced at Tsingke Biotechnology Co., Ltd. by using the universal primers of 16S rDNA. The obtained sequence was submitted to the NCBI database (www.ncbi.nlm.nih.gov/blast/) and compared with the known sequence in the database (Shi et al., 2019).

Phylogenetic tree construction

The sequences were aligned with the corresponding model strains in MEGA 5.0, and the UPGMA method was used for 1,000 bootstrap tests to construct a phylogenetic tree.

Antimicrobial activity

Antimicrobial activity assays were examined as described in previous studies with some changes (Chen et al., 2020). LAB (J2-4, J2-5, and J2-9) were cultured in MRS medium at 37°C for 18 h. Clinical pathogenic bacteria stored in the laboratory, namely *Acinetobacter baumannii (Ab)*, *Escherichia coli (Ec)*, *Klebsiella pneumoniae (Kp)*, and *Enterococcus faecalis (Efa)*, were grown in LB broth (Sangon Biotech, Co., Ltd. Shanghai, China) at 37°C for 12 h, and then the pathogenic bacteria were diluted to 0.12 (OD_{600}), and they were flooded on LB agar plates. When the plates dried, three sterile iron pipettes (a depth of 6 mm and a diameter of 5 mm) were placed on the plate at an appropriate distance from each other, and then, 200 μL of bacterial (J2-4, J2-5, and J2-9) suspension was added to each well, with 200 μL MRS medium as the negative control. After incubation at 37°C for 24 h in an aerobic condition, the zone of inhibition was measured by a vernier caliper, and the experiment was repeated at least three times.

Oxidative damage model of 293T cell

The determination of cell viability of oxidative damage was performed according to a previous report with modifications (Sun et al., 2022).

Human embryonic 293T kidney cells were purchased from Boster Biological Technology Co., Ltd. The 293T cells were cultured in DMEM medium (Hyclone Biotechnology Co., Ltd, Beijing) with 10% fetal bovine serum (FBS) (Hyclone Biotechnology Co., Ltd, Beijing) and 1% penicillin–streptomycin double antibody (Hyclone Biotechnology Co., Ltd, Beijing) at 37°C, 5% CO_2 for 24 h. Cells were subcultured when they reached 80–90% confluency. The 293T cells were seeded in the wells of a 96-well plate, adjusted to 5×10^4 cells/well, and incubated at 37°C for 24 h, then, the DMEM medium was removed using a pipette, and finally, 0, 50, 100, 150, 200, 250, 300, 350, 400, and 450 μmol/L H_2O_2 was added to the cells and cultured at 37°C, 5% CO_2 for 4 h. After removing the H_2O_2, the 293T cell viability was measured using the CCK-8 kit, OD_{450} was measured after incubating at 37°C for 3 h, and the cell survival rate was calculated according to the following formula:

$$\text{Survival rate (\%)} = (A_2 - A_0)/(A_1 - A_0) \times 100\%$$

Where A_2 is the OD_{450} of 293T cells treated with different concentrations of H_2O_2,

A_1 is the OD_{450} of 293T cells without H_2O_2 treatment,

and A_0 is the OD_{450} without 293T cells added.

Analysis of antioxidant enzyme activity

The final selected LAB were inoculated in MRS liquid medium and incubated at 37°C for 24 h. The cells were washed twice with sterile saline, adjusted to 10^{10} CFU/mL, and added 1 mg/mL of lysozyme into it. After ultrasonic disruption (250 W, ultrasonic 10 min), the cell-free supernatant was collected through centrifugation at 8,000 rpm at 4°C for 10 min, and the cell-free supernatant was stored in an ultra-low-temperature refrigerator at −80°C.

The 293T cells in the logarithmic growth phase were seeded in the wells of a 6-well plate with 1×10^6 cells/well. Subsequently, the cells were cultured in a 2-mL medium with cell-free supernatant of J2-5 and J2-9 (ratio: 1.5:1) at 37°C in a 5% CO_2 atmosphere for 24 h. Then, based on the previous experimental result, 400 μL/mL H_2O_2 was added, the concentration that provided a 50% inhibitory survival rate to cells. After incubation for 4 h, 1% Triton-X 100 was added to lysate 293T cells.

The groups are as follows:

- Blank group (NegCon): without adding cell-free supernatant and H_2O_2.
- Oxidative damage model group (Con): added H_2O_2 without cell-free supernatant.
- Experiment groups (J2-5 + 293T): added both H_2O_2 and cell-free supernatant of J2-5.
- Experiment groups (J2-9 + 293T): added both H_2O_2 and cell-free supernatant of J2-9.

The oxidation resistance of different groups was determined according to the instructions of the T-SOD, CAT, and T-AOC reagent kits (Nanjing JianCheng Bioengineering Co., Ltd., Nanjing, China).

Statistical analysis

Each experiment was repeated thrice. Data were expressed as the mean ± standard deviation (SD). Statistical significance was determined via one-way ANOVA in SPSS v.20.0. Data with a *P*-value of <0.05 were considered to have statistically significant differences.

TABLE 1 Results of strains in different antioxidant experiments.

Strain	DPPH scavenging rate (%)	Hydroxyl clearance rate (%)	Fe^{2+} chelating ability (%)	Superoxide anion scavenging rate (%)
Y2-1	46.62 ± 1.09^{e}	21.07 ± 4.53^{i}	13.22 ± 1.14^{de}	13.30 ± 2.86^{ab}
Y2-6	41.76 ± 2.10^{f}	44.86 ± 2.89^{def}	15.23 ± 0.93^{bc}	12.50 ± 2.27^{ab}
YP-1	40.76 ± 0.77^{fg}	62.80 ± 5.72^{a}	15.77 ± 0.95^{abc}	10.22 ± 2.24^{b}
YP-8	37.80 ± 0.76^{fg}	30.36 ± 2.23^{h}	14.21 ± 1.00^{cd}	10.22 ± 2.23^{b}
J2-3	72.42 ± 0.79^{c}	27.41 ± 2.08^{hi}	15.92 ± 1.09^{abc}	10.96 ± 1.65^{b}
J2-4	82.41 ± 0.34^{a}	41.22 ± 7.02^{fg}	15.27 ± 1.27^{bc}	13.17 ± 2.45^{ab}
J2-5	76.32 ± 0.51^{b}	52.13 ± 2.48^{bc}	17.21 ± 0.71^{a}	15.52 ± 3.65^{a}
J2-7	48.91 ± 4.01^{de}	42.51 ± 4.02^{efg}	16.50 ± 1.10^{ab}	12.28 ± 0.24^{ab}
J2-9	83.97 ± 0.25^{a}	50.08 ± 2.52^{cd}	15.5 ± 0.46^{abc}	14.61 ± 1.31^{ab}
GP-4	29.20 ± 0.39^{i}	38.91 ± 1.43^{fg}	11.6 ± 1.05^{ef}	12.65 ± 1.1^{ab}
GP-7	51.92 ± 0.87^{d}	57.75 ± 6.77^{ab}	11.46 ± 0.49^{ef}	12.80 ± 2.15^{ab}
GP-9	37.46 ± 0.51^{gh}	48.98 ± 4.61^{cde}	13.19 ± 1.12^{de}	12.41 ± 4.36^{ab}
W-2	34.45 ± 0.78^{h}	37.81 ± 1.41^{g}	10.52 ± 1.06^{f}	12.76 ± 2.34^{ab}
W-4	74.65 ± 0.19^{c}	48.97 ± 1.66^{cde}	17.13 ± 1.1^{a}	13.32 ± 3.04^{ab}
WJ-6	38.86 ± 6.89^{fg}	25.54 ± 1.71^{hi}	12.26 ± 0.81^{ef}	12.53 ± 3.77^{ab}
ATCC7469	38.48 ± 1.91^{fg}	24.67 ± 1.91^{hi}	13.19 ± 1.18^{de}	11.62 ± 0.77^{ab}

Data are expressed as mean ± SD ($n = 3$). Values with different letter superscripts are significantly different. $P < 0.05$.

Results

DPPH scavenging ability of the isolated strains

The data in Table 1 show that the DPPH scavenging rates of 16 LAB strains were between 34.45 ± 0.78% and 83.97 ± 0.25%. Among them, J2-4 and J2-9 strains isolated from "Jiangshui" had the highest antioxidant activities, followed by J2-5. Furthermore, their clearance rates were significantly higher ($P < 0.05$) than those of the control strain *LGG* ATCC7469 (Table 1). The ability of J2-4, J2-5, and J2-9 to scavenge DPPH was significantly different. Moreover, J2-3 and W-4 also possessed evident scavenging abilities.

Hydroxyl-free radical scavenging capacity of the isolated strains

The hydroxyl radical scavenging rates of the strains in this study are shown in Table 1, and 16 strains of LAB exhibited different hydroxyl radical scavenging capacities ranging from 21.07 ± 4.53% to 62.80 ± 5.72%. The scavenging rates of 14 strains were higher than those of *LGG* ATCC7469, and the clearance rate of YP-1 (from Sichuan pickles) was the highest, reaching 68.52% ($P < 0.05$). In comparison, *LGG* had a clearance rate of 24.67 ± 1.91%, indicating that most of the strains screened in this study had a good ability to scavenge hydroxyl radicals.

Chelating ability of LAB with ferrous ion

The chelating ability result ranged from 10.52 ± 1.06% to 17.21 ± 0.71% (Table 1). Among them, the chelating capacities of J2-5 (isolated from "Jiangshui") and W-4 (from the laboratory) were the highest ($P < 0.05$) (17.21 ± 0.71% and 17.13 ± 1.1%, respectively). The results showed that different monoclonals had a chelating ability to iron ions, and the overall chelating ability slightly varied.

Superoxide anion radical scavenging capacity of the isolated strains

The ability of LAB to scavenge superoxide anion radicals is shown in Table 1. The results showed that the clearance rates of 16 strains were similar (10.96 ± 1.65%−15.52 ± 3.65%). Among them, J2-5 (from "Jiangshui") had the highest clearance rate of 15.52 ± 3.65% ($P < 0.05$). Most tested strains displayed a capacity of superoxide anion scavenging with no significant difference ($P > 0.05$).

Hydrogen peroxide tolerance

Lactic acid bacteria (LAB) were cultured in MRS with different H_2O_2 concentrations (1, 2, and 3 mM). The different strains had varying tolerance to H_2O_2, and the differences were evident at 2 mM ($P < 0.05$). J2-5 and YP-1 had relatively strong tolerance. One millimolar H_2O_2 had no inhibitory effect on the growth of J2-4 and J2-9; slightly higher strain growth rates were observed,

10.3389/fmicb.2023.1163662

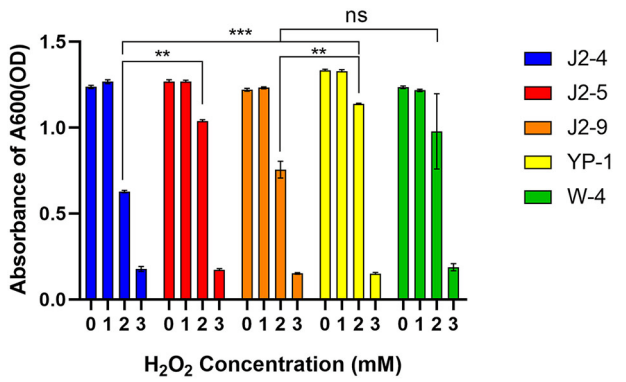

FIGURE 1
Tolerance of five strains to hydrogen peroxide. Lactic acid bacteria (LAB) were inoculated with 2% volume to a different MRS medium with different H_2O_2 concentrations (1, 2, and 3 mmol/L). The data shown correspond to the mean of independent experiments performed in triplicate. $^{**}P < 0.01$; $^{***}P < 0.001$, ns (no significance), $P > 0.05$.

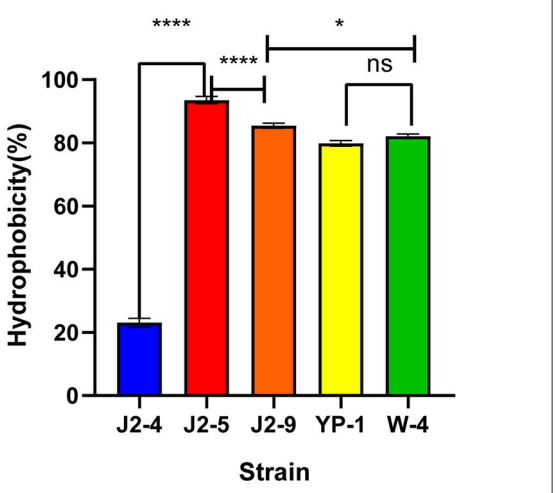

FIGURE 2
Hydrophobicity of five LAB (J2-4, J2-5, J2-9, YP-1, and W-4) in xylene. The data shown correspond to the mean of independent experiments performed in triplicate. $^{*}P < 0.05$, $^{****}P < 0.0001$, ns (no significance), $P > 0.05$.

and the inhibitory rates on YP-1, W-4 were 0.28 ± 0.24% and 1.48 ± 1.04%, respectively. The inhibitory rates of 2 mM H_2O_2 on J2-4, J2-5, J2-9, YP-1, and W-4 were 49.26 ± 0.71%, 18.09 ± 0.17%, 38.07 ± 3.66%, 14.66 ± 0.70%, and 31.80 ± 1.98%, respectively. The inhibitory rates of 3 mM H_2O_2 on J2-4, J2-5, J2-9, YP-1, and W-4 were 85.66 ± 1.06%, 86.44 ± 0.58%, 87.60 ± 0.26%, 88.77 ± 0.51%, and 86.66 ± 1.64%, respectively. Therefore, these strains, especially YP-1, had strong tolerance to hydrogen peroxide (Figure 1).

Hydrophobicity of LAB

The results showed that the hydrophobicity of J2-4, J2-5, J2-9, YP-1, and W-4 were 23.07 ± 1.38%, 93.53 ± 1.15%, 85.42 ± 0.80%, 79.86 ± 0.90%, and 82.12± 0.65% on average, respectively. Strain J2-5 showed the highest hydrophobicity, followed by J2-9, while that of YP-1 did not significantly differ ($P > 0.05$) from that of W-4. Moreover, the hydrophobicity of J2-4 significantly differed ($P < 0.05$) from that of the other strains. Thus, all strains, except J2-4, might be more likely to adhere to the intestine to form a beneficial biofilm (Figure 2).

Auto-aggregation of LAB

The auto-aggregation rates were different in each period, and the results are shown in Figure 3. At 12 h; the auto-aggregation rates of J2-4 and W-4 reached 61.52 ± 0.35% and 58.40 ± 0.51%, respectively. YP-1 had the lowest auto-aggregation rate of 38.07 ± 0.23% at 12 h. The difference between strains is symbolized by the letters a, b, c, and d ($P < 0.05$).

Hemolytic activity

The activated J2-4, J2-5, J2-9, YP-1, and W-4 were partitioned and lined on Colombian blood plates. After incubation at 37°C

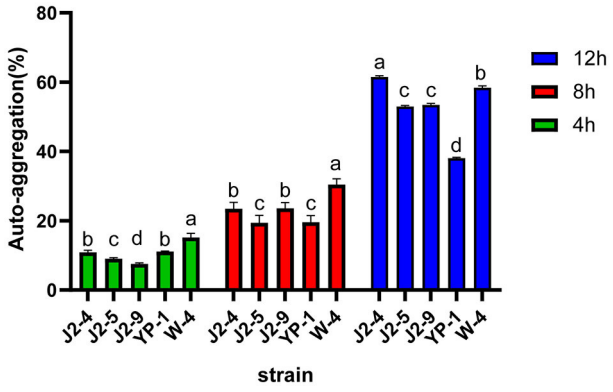

FIGURE 3
Auto-aggregation of five strains (J2-4, J2-5, J2-9, YP-1, and W-4) at 4, 8, and 12 h. The figure demonstrates the relatively strong auto-aggregation abilities of J2-4 and W-4. Values with different letter superscripts are significantly different ($P < 0.05$). The data are represented as mean ± SD of experiments repeated in triplicate.

for 48 h, no hemolytic zone was observed in J2-4, J2-5, and J2-9, indicating a γ-hemolytic activity (non-hemolytic). However, YP-1 and W-4 appeared dark green (α-hemolysis). These findings indicated that J2-4, J2-5, and J2-9 were safe probiotics. Conversely, YP-1 and W-4 might pose an opportunistic pathogenic risk (Figure 4).

Evaluation of antibiotic sensitivity

The drug sensitivity of five LAB isolates is shown in Table 2. All LAB strains were sensitive to chloramphenicol, kanamycin, and gentamicin. J2-4, J2-5, and J2-9 were moderately resistant to polymyxin and tetracycline but sensitive to meropenem. YP-1 and W-4 were sensitive to tetracycline but resistant to polymyxin

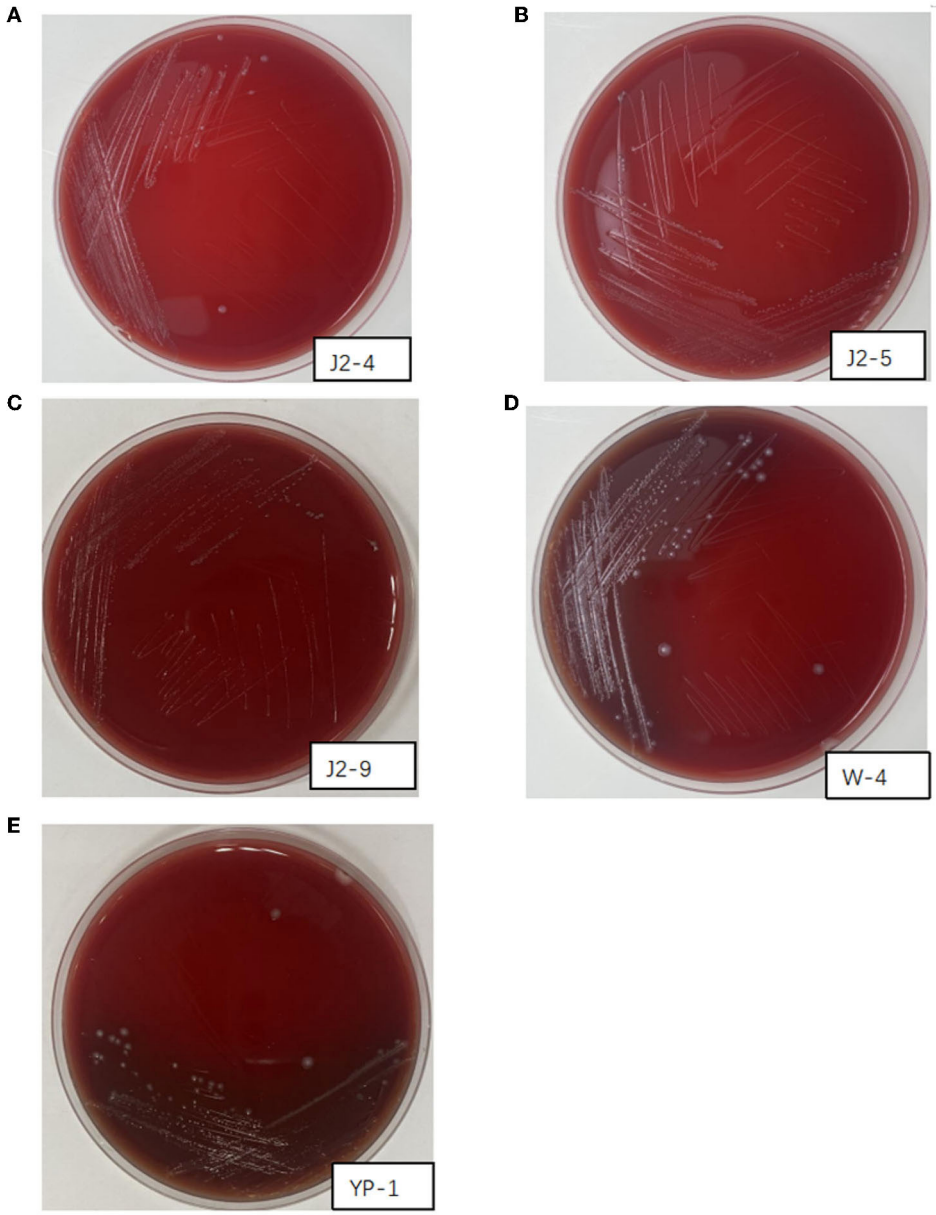

FIGURE 4
Hemolysis of J2-4, J2-5, J2-9, W-4, and YP-1. **(A)** J2-4 shows γ-hemolysis. **(B)** J2-5 shows γ-hemolysis. **(C)** J2-9 shows γ-hemolysis. **(D)** W-4 shows α-hemolysis. **(E)** YP-1 shows α-hemolysis.

and meropenem. Therefore, YP-1 and W-4 had relatively strong resistance to antibiotics.

Bacterial identification

The phylogenetic tree was constructed on the basis of the 16S rRNA gene by using the neighbor-joining method in MEGA5.0. J2-4, J2-5, and J2-9 were identified as *L. fermentans*, whereas YP-1 and W-4 were identified as *L. paracasei*, and the similarity between them was shown. Compared to J2-9 with J2-5, J2-5 exhibits the highest degree of genetic relationship with J2-4 (Figure 5).

Antimicrobial activity

The length of the antibacterial zones was measured for judging the inhibition degree of J2-4, J2-5, and J2-9 against pathogenic bacteria (Table 3). The results showed no inhibition effect of J2-4 on *Ab*, *Efa*, *Kp*, *and Ec*. J2-9 showed the strongest antimicrobial activity against *Ab* and *Efa*, with a zone of inhibition of two indicator bacteria: 13.61 ± 1.65 (mm) and 13.91 ± 0.77 (mm), respectively, and J2-5 showed a relatively weak antimicrobial activity against *Ab* and *Efa* with 10.79 ± 0.68 (mm) and 13.51 ± 1.40 (mm) inhibition zones, respectively. *Ab* was the most sensitive indicator bacteria against the J2-5 and J2-9 due to the most clear inhibition zone, and *Efa* is not more sensitive than *Ab* against these two *L. fermentum*

TABLE 2 Sensitivity of strains to antibiotics.

Isolates	J2-4	J2-5	J2-9	YP-1	W-4
Meropenem	S	S	S	R	R
Polymyxin	I	I	I	R	R
Tetracycline	I	I	I	S	S
Chloramphenicol	S	S	S	S	S
Kanamycin	S	S	S	S	S
Gentamicin	S	S	S	S	S

S, sensitive; R, resistant; I, moderately sensitive.

because of a small amount of Efa grown in the inhibition zone. J2-5 and J2-9 showed almost no inhibition against other indicator bacteria (*Kp and Ec*).

Analysis of antioxidant enzyme activity

Figure 6A shows that the 293T cell survival rate decreased as the concentration of H_2O_2 increased. To explore the probiotic protective effect against oxidative stress in cells, we selected 400 μL/mL H_2O_2 because at this concentration the survival rate of 239T cells decreased to ∼50%. Here, the antioxidant activities of 239T cells treated by J2-5 and J2-9 were analyzed. As shown in Figure 6B, the CAT content in the Con group significantly decreased, J2-9 showed a better protective effect than J2-5, and the CAT activities of four groups were 1.82 ± 0.25 (U/mL), 0.54 ± 0.48 (U/mL), 1.70 ± 0.12 (U/mL), and 1.31 ± 0.41 (U/mL), sequentially. As shown in Figure 6C, the T-AOC activities of J2-5- and J2-9-treated cells are significantly higher than the control group (Con). The result of the J2-5 + 293T group is 7.84 ± 0.04 (U/mL), J2-9 + 293T group is 7.90 ± 0.01 (U/mL), and both the probiotic-treated groups show a similar effect on T-AOC. Figure 6D shows the T-SOD activities of each group with different treatments. The protective effects of J2-5 and J2-9 against oxidative stress were explored, J2-9 demonstrates a superior antioxidant ability in this test, the SOD enzyme activity of each group are as follows, NegCon: 94.02 ± 5.84 (U/mL), Con: 30.72 ± 3.36 (U/mL), J2-5 + 293T: 39.25 ± 3.61 (U/mL), J2-9 + 293T: 50.81 ± 1.05 (U/mL). In general, the J2-5- and J2-9-treated groups showed strong antioxidant activities when compared with only the H_2O_2-treated group.

Discussion

Excessive free radicals produced by oxidative stress are one of the fundamental causes of aging and aging-related diseases (Cadenas and Davies, 2000). Meanwhile, ferroptosis is closely linked to oxidation precipitated by free radical generation catalyzed by iron ions. This is accompanied by a decrease in glutathione (GSH) activities and the inactivation of glutathione peroxidase (GPX). Moreover, lipid peroxidation causes an increase in ROS concentrations and elevates free radical accumulation, thereby aggravating the body's inflammatory responses (Zhang et al., 2021). Some studies in China and other countries reported that LAB could scavenge ROS. Although the specific mechanism via which LAB are able to scavenge reactive oxygen free radicals is not fully understood, a previous study attributed this scavenging capacity to the reducing activities of LAB and their chelation capacity with iron ions (Saide and Gilliland, 2005).

In this study, probiotics with strong antioxidant activity were isolated from the fermented food "Jiangshui" in Longevity Village in Shaanxi Province and from famous pickles in Sichuan Province. Fermented foods with rich probiotic content from both locations can be a guarantee for screening highly antioxidant bacteria. We also measured the antioxidative capacity of strains isolated from human feces. As assaying the antioxidant activity of each strain was determined through a specific target, limitations of the concept and technology of antioxidant *in vitro* experiments still exist as each strain shows different degrees of antioxidant properties in various experiments (Mu et al., 2018). The physiological functions of LAB may be more active and comprehensive *in vivo*. Therefore, we used various methods to compare their antioxidant properties and to evaluate the scavenging effects of LAB on several important reactive oxygen free radicals and metal ions in detail. Based on all of the results of free radical scavenging experiments and other antioxidant experiments, we selected the strongest five strains (J2-4, J2-5, J2-9, W-4, and YP-1) for the main analyses. These strains demonstrated evident antioxidant properties in all tests. Specifically, J2-4, J2-5, J2-9 (*L. fermentans*), and W-4 (*L. paracasei*) showed prominent DPPH radical scavenging abilities. The chelating power of J2-5 and W-4 to ferrous ions was remarkable as well. YP-1 (*L. paracasei*) showed the strongest scavenging capabilities regarding hydroxyl radicals.

DPPH scavenging is one of the most important indicators in determining the antioxidant activity of LAB *in vitro*. The results showed that the DPPH scavenging ability of the strains varied greatly among different strains. The clearance rates of *L. fermentans* J2-4, J2-5, and J2-9 were the highest (82.41 ± 0.34%, 76.32 ± 0.51%, and 83.97 ± 0.25%, respectively). The DPPH scavenging activities of the strains in our study were much higher than those of the strains obtained by Liu et al. (2020), Zeng et al. (2021), and Zhao et al. (2021). This difference was not due to using different species but was related to the heterogeneity of each strain.

Hydroxyl radicals are considered the most harmful ROS that cause oxidative damage. The Fenton reaction system was used to make iron ions catalyze hydrogen peroxide to produce hydroxyl, and the hydroxyl clearance rate of the tested strain was detected (Feng and Wang, 2020). The hydroxyl scavenging capacity of 15 experimental strains was between 21.07 ± 4.53% and 62.80 ± 5.72%, and that of *L. paracasei* YP-1 was the strongest. Consistent with the study of Mu et al. (2018), our study showed that the difference in the hydroxyl radical scavenging rate between strains reached ∼40%, and the significant difference might be related to their ability to chelate ferrous ions.

The Fenton reaction induced by iron ions is the key cause of ferroptosis (Mancardi et al., 2021). The chelating ability of LAB to iron ions can reduce the hydroxyl radicals produced by the Fenton reaction and directly reduce the damage caused by ferrous ions. The strongest chelating ability observed was that of J2-5 (17.21 ± 0.71%), followed by W-4 (17.13 ± 1.1%). Previous assays demonstrated that the cell-free extract

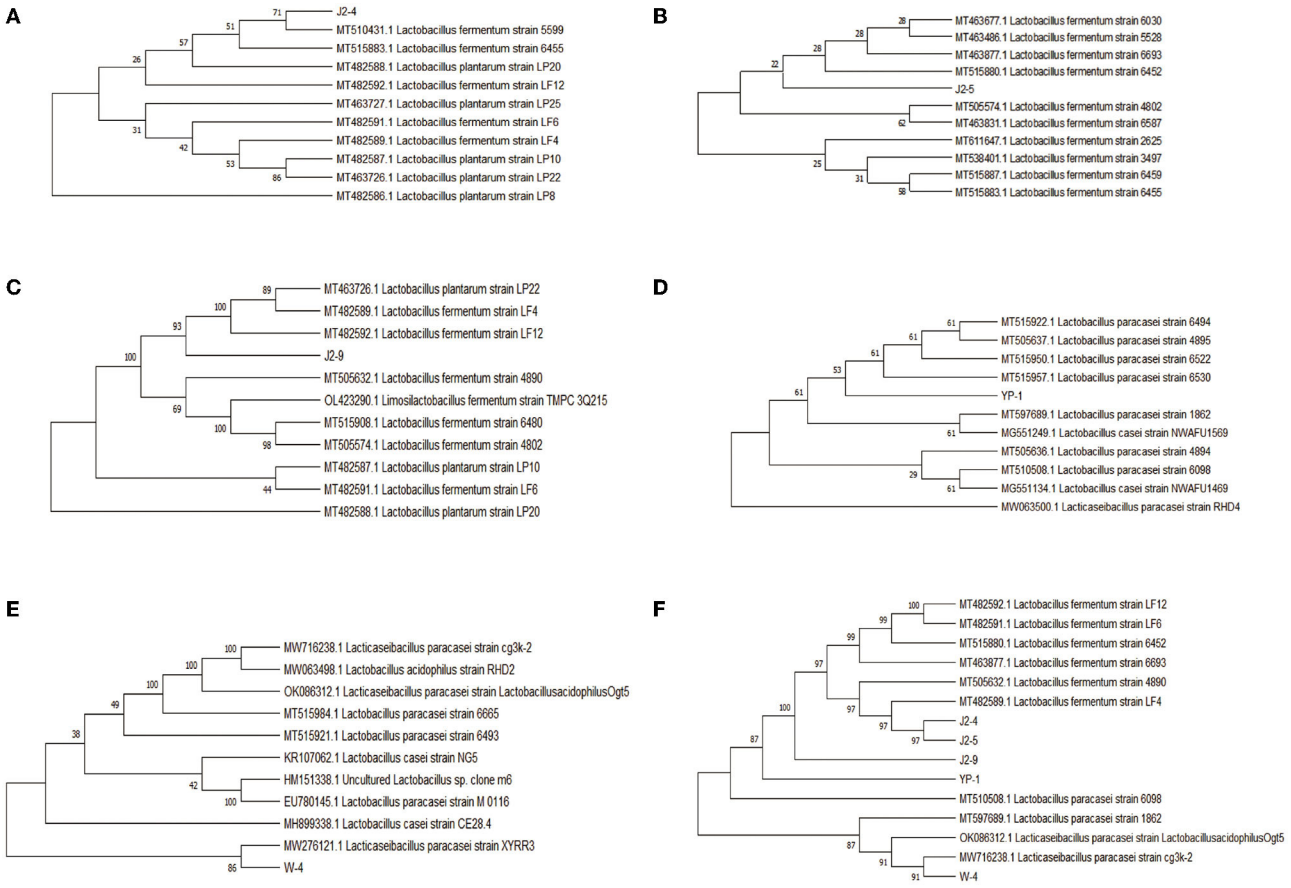

FIGURE 5
Phylogenetic tree showing the genetic relationships of the five isolates collected from "Jiangshui" and Sichuan pickles with the closest sequences identified in GenBank by the Basic Local Alignment Search Tool (BLAST). **(A)** J2-4 and related bacteria. **(B)** J2-5 and related bacteria. **(C)** J2-9 and related bacteria. **(D)** W-4 and related bacteria. **(E)** YP-1 and related bacteria. **(F)** Phylogenetic tree for similarity of five strains.

TABLE 3 Inhibition zone of *Lactobacillus fermentum* against pathogenic bacteria.

Strains	*Acinetobacter baumannii (Ab)*	*Escherichia coli (Ec)*	*Klebsiella pneumoniae (Kp)*	*Eenterococcus faecalis (Efa)*
J2-4	0 (mm)	0 (mm)	0 (mm)	0 (mm)
J2-5	10.79 ± 0.68 (mm)	0 (mm)	0 (mm)	13.51 ± 1.40 (mm)
J2-9	13.61 ± 1.65 (mm)	0 (mm)	0 (mm)	13.91 ± 0.77 (mm)

Data are mean ± SD ($n = 3$).

(CFE) of LAB exhibited stronger iron-chelating abilities, which was concentration-dependent. The antioxidant activity with 10^{10} CFU/mL was one time stronger than that with 10^{9} CFU/mL, accompanied by a strong difference among different strains (Li et al., 2012).

In this study, the superoxide anion scavenging capacity of J2-5 reached 15.52 ± 3.65%, which was relatively stronger and significantly different from that of *LGG* ($P < 0.05$). The scavenging rate of LAB against superoxide anions was weaker than that against hydroxyl radicals and DPPH. This could be possibly attributed to the weak binding of the antioxidant components of the intact cell (IC) surface to the superoxide anion target. It was reported that the antioxidant capacity of the cell-free supernatant (CFS) of LAB was much higher than that of ICs (Yan et al., 2019), possibly because of LAB-secreted metabolites, such as glutathione, butyric acid, folic acid, extracellular polysaccharide, antioxidant peptides, and isoflavone glycosides (Yamamoto et al., 2019). The antioxidant ability of CFE is often lower than the IC and CFS in antioxidant activities, indicating that the antioxidant components of LAB mainly exist in secretions and cell surfaces. Strains were screened by us, on which metabolites might show stronger physiological activities.

Hydrogen peroxide is a weaker oxidant than hydroxyl, but it has a high diffusion rate, can easily penetrate the cell membrane, and acts for a longer time, causing oxidative damage to DNA,

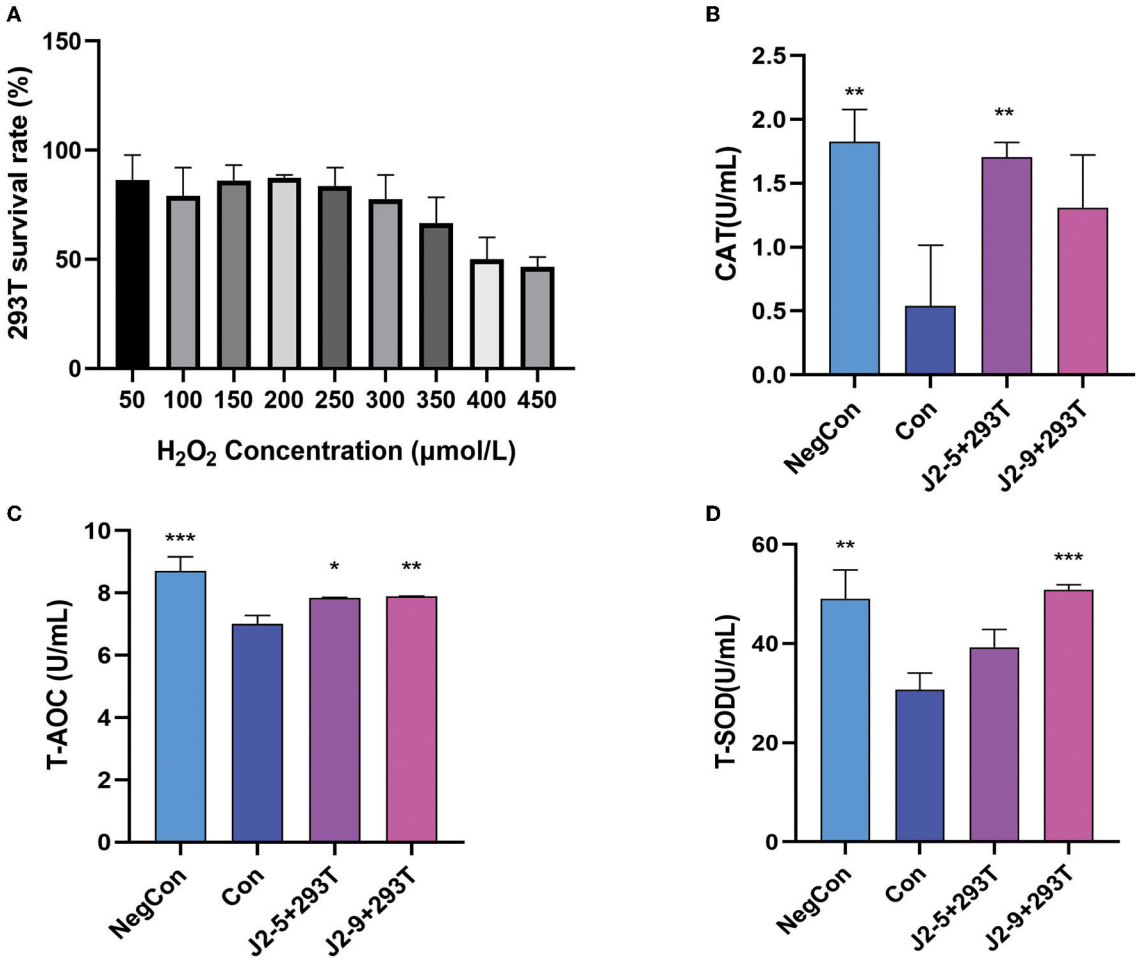

FIGURE 6
(A) Effect of different concentrations of H_2O_2 on the vitality of 293T cells. Effects of cell-free supernatant of J2-5 and J2-9 on antioxidant enzyme activity in 293T cells. **(B)** Catalase (CAT). **(C)** Total antioxidant capacity (T-AOC). **(D)** Total superoxide dismutase (T-SOD). Each group was compared with Con, $^*P < 0.05$, $^{**}P < 0.01$, $^{***}P < 0.001$.

proteins, and lipids (Cadenas and Davies, 2000). In this study, after 24 h, 1 mM H_2O_2 had no obvious inhibitory effect on bacterial growth; however, the inhibitory effect was evident at 2 mM H_2O_2. *L. fermentans* J2-5 and *L. paracasei* YP-1 had obvious tolerance to 2 mM hydrogen peroxide with inhibitory rates of 18.09 ± 0.17% and 14.6 ± 0.70%, respectively. All strains were inhibited by more than 80% when 3 mM was used, establishing that 3 mM H_2O_2 was a strong inhibitory concentration to the LAB. *L. fermentans* E-3, E-18, and Ee-338-1-1 isolated from the intestinal tract of children survived for 180 and 150 min in 1 mM H_2O_2 (Kullisaar et al., 2002). One millimolar H_2O_2 significantly inhibited all *L. plantarum* in the study of Li et al. (2012). The comparison revealed that the 24-h survival of the strains we tested under 1 mM H_2O_2 was almost not affected by oxidants, and a prominent growth efficiency was still maintained.

Hydrophobicity is linked to the colonization abilities of probiotics (Collado et al., 2006). The hydrophobicity index of only the J2-4 strain was <30%, while that of the extremely hydrophilic J2-5 strain reached 93.53%. Compared with *L. paracasei* C3 and most strains screened by Shi et al. (2019) and Reuben et al. (2020), J2-5, J2-9, YP-1, and W-4 had superior adhesion abilities to epithelial cells. The auto-aggregation ability of bacteria is an important factor affecting their intestinal adhesion (Del Re et al., 2000). The highest auto-aggregation ability observed in J2-4 reached 61.51% at 12 h, while that of W-4 was 58.97%, and J2-5 and J2-9 demonstrated relatively high auto-aggregation abilities. The extreme results between the two tests in the case of J2-4 are inconsistent with the view that there is a direct relationship between auto-aggregation and hydrophobicity (Del Re et al., 2000) but are consistent with the view of Vinderola et al. (2008). The difference in auto-aggregation percent also reflected the variation in physiological functions between strains. High hydrophobicity and strong auto-aggregation are more likely to produce protective barriers during adhesion, which can prevent pathogen attack (Del Re et al., 2000). However, some researchers believe that hydrophobicity is not related to intestinal adhesion and that strong hydrophobicity is not a necessary condition for adhesion (Lee et al., 2011). For example, *Lactobacillus acidophilus* (2% hydrophobic) has a high adhesion rate (40%) to HT29MTX cells (Schillinger and Wilhelm, 2005).

In the MIC test, *L. fermentans* J2-4, J2-5, and J2-9 showed moderate resistance to polypeptide and tetracycline antibiotics, while *L. paracasei* YP-1 and W-4 showed resistance to β-lactams and polypeptide antibiotics. All strains were sensitive to chloramphenicol and aminoglycosides. These results proved that sensitivity to different antibiotics depends on the species (Temmerman et al., 2003). This is in contradiction with the view that most Lactobacilli are resistant to aminoglycosides but is partially in accordance with the conclusion that *Lactobacilli* are naturally resistant to polypeptides and β-lactams (Li et al., 2020). Although acquired resistance in LAB can lead to better survival *in vivo*, their safety should also be considered. Resistance can be transferred from one bacteria to another, leading to widespread antibiotic risk (Hawkey, 1998). Hence, antibiotic-sensitive probiotics are preferred.

The hemolysis test showed no *L. fermentans* hemolysis. However, *L. paracasei* (W-4 from feces and YP-1 from pickles) were an α-hemolysin, indicating that they might have opportunistic pathogenicity. However, paradoxically, studies have confirmed that *L. paracasei* has no hemolytic activity and belongs to safe probiotics, such as CIDCA8339, CIDCA83123, and CIDCA83124 (Zhang et al., 2013). These results indicate that the heterogeneity among various strains may be related to gene or protein mutations; however, the specific reasons need further investigation. Future studies should determine the correlation between the MIC and hemolytic characteristics with the *L. paracasei* species.

LAB can produce bacteriocins and proteins which can inhibit pathogens' growth, and the organic acids secreted by LAB can decrease the pH, leading to a loss of a suitable growth environment for pathogens (Chen et al., 2020), and this is also the reason why fermented foods are not easily contaminated by other microbes. J2-5 and J2-9 had inhibitory effects against clinical strains *Efa* and *Ab*, the results of antimicrobial activity showed their probiotic ability, and J2-5 and J2-9 can inhibit the harmful flora in the intestine. J2-4 has no inhibitory activity to these clinic strains which might be due to the heterogeneity.

As a strong oxidant, H_2O_2 can damage cell membranes and enzymes, reducing cell activity. Therefore, we used an appropriate concentration of H_2O_2 (400 μL/mL) for inducing cell damage. Due to the weak hydrophobicity and antimicrobial ability of J2-4, we ultimately selected J2-5 and J2-9 through the above experiments and then treated the injury model with probiotics J2-5 and J2-9. Antioxidant enzymes, SOD and CAT, play an important role in the body's resistance to oxidative damage. SOD and CAT can balance the production of oxides and prevent tissue and cells from being damaged by peroxides. T-AOC is the total antioxidant index and is composed of various antioxidant substances and enzymes. Therefore, T-AOC was used to evaluate the antioxidant capacity of cells (Sun et al., 2022). Compared with the control group Con, the antioxidant activities of the groups treated with J2-5 or J2-9 were significantly increased. Antioxidant enzymes, polysaccharides, thioredoxin, and glutathione can be generated during the metabolism of LAB, and foods fermented by LAB also have strong antioxidant effects (Sun et al., 2022), with our results showing that J2-5 and J2-9 can restore cell vitality by increasing SOD, CAT, and T-AOC activity.

Conclusion

In summary, *L. fermentans* J2-4, J2-5, and J2-9 in "Jiangshui" from Longevity Village; *L. paracasei* YP-1 from Sichuan pickles; and W-4 from the intestine have relatively strong antioxidant activity. These five strains exhibited strong hydrogen peroxide tolerance, hydrophobicity, and auto-aggregation abilities. J2-4, J2-5, and J2-9 are γ-hemolytic, whereas YP-1 and W-4 are α-hemolytic. Due to the weak hydrophobicity and antimicrobial ability of J2-4, J2-5 and J2-9 were selected for 293T cell antioxidant experiments. The excellent probiotics J2-5 and J2-9 from Longevity Village are potential candidates for use in antioxidant supplements.

Data availability statement

The datasets presented in this study are deposited in the Genbank repository, accession numbers: SUB12873341 J2-4 OQ443145, SUB12873341 J2-5 OQ443146, SUB12873341 J2-9 OQ443147, SUB12873341 W-4 OQ443148, SUB12873341 YP-1 OQ443149.

Author contributions

YH: conceptualization, investigation, and writing—original draft. YL: methodology. YZha and DL: cell experiments. YZhu and CW: formal analysis. XJ, CY, SD, and XH: writing assistance. XH: providing language help. All authors have read and agreed to the published version of the manuscript. All authors contributed to the article and approved the submitted version.

Funding

This study was supported by the National Nature Science Foundation of China (grant numbers 32170119, 82060654, and 31870135) and the Yan'an Technology Project SL2020ZCSZ-001.

Conflict of interest

The authors declare that the research was conducted in the absence of any commercial or financial relationships that could be construed as a potential conflict of interest.

Publisher's note

References

Amaretti, A., di Nunzio, M., Pompei, A., Raimondi, S., Rossi, M., Bordoni, A., et al. (2013). Antioxidant properties of potentially probiotic bacteria: *in vitro* and *in vivo* activities. *Appl. Microbiol. Biotechnol.* 97, 809–817. doi: 10.1007/s00253-012-4241-7

Cadenas, E., and Davies, K. J. (2000). Mitochondrial free radical generation, oxidative stress, and aging. *Free Rad Biol Med.* 29, 222–230. doi: 10.1016/S0891-5849(00)00317-8

Chen, T., Wang, L., Li, Q., Long, Y., Lin, Y., Yin, J., et al. (2020). Functional probiotics of lactic acid bacteria from Hu sheep milk. *BMC Microbiol.* 20, 228. doi: 10.1186/s12866-020-01920-6

Clinical and Laboratory Standards Institute (CLSI). (2019). *M100 Performance Standards for Antimicrobial Susceptibility Testing, 29th Edn*. Clinical and Laboratory Standards Institute.

Collado, M. C., Jalonen, L., Meriluoto, J., and Salminen, S. (2006). Protection mechanism of probiotic combination against human pathogens: in vitro adhesion to human intestinal mucus. *Asia Pac. J. Clin. Nutr*. 15, 570–575.

Del Re, B., Sgorbati, B., Miglioli, M., and Palenzona, D. (2000). Adhesion, autoaggregation and hydrophobicity of 13 strains of *Bifidobacterium longum*. *Lett. Appl. Microbiol.* 31, 438–442. doi: 10.1046/j.1365-2672.2000.00845.x

Feng, T., and Wang, J. (2020). Oxidative stress tolerance and antioxidant capacity of lactic acid bacteria as probiotic: a systematic review. *Gut Microbes* 12, 1801944. doi: 10.1080/19490976.2020.1801944

Hausman, D. B., Fischer, J. G., and Johnson, M. A. (2011). Nutrition in centenarians. *Maturitas*. 68, 203–209. doi: 10.1016/j.maturitas.2011.01.003

Hawkey, P. M. (1998). The origins and molecular basis of antibiotic resistance. *BMJ.* 317, 657–660. doi: 10.1136/bmj.317.7159.657

He, Z., Wang, X., Li, G., Zhao, Y., Zhang, J., Niu, C., et al. (2015). Antioxidant activity of prebiotic ginseng polysaccharides combined with potential probiotic *Lactobacillus plantarum* C88. *Int. J. Food Sci. Technol.* 50, 1673–1682. doi: 10.1111/ijfs.12824

Hojjati, M., Behabahani, B. A., and Falah, F. (2020). Aggregation, adherence, anti-adhesion and antagonistic activity properties relating to surface charge of probiotic Lactobacillus brevis gp104 against Staphylococcus aureus. *Microb. Pathog.* 147, 104420. doi: 10.1016/j.micpath.2020.104420

Kullisaar, T., Zilmer, M., Mikelsaar, M., Vihalemm, T., Annuk, H., Kairane, C., et al. (2002). Two antioxidative lactobacilli strains as promising probiotics. *Int. J. Food Microbiol.* 72, 215–24. doi: 10.1016/S0168-1605(01)00674-2

Lee, H., Yoon, H., Ji, Y., Kim, H., Park, H., Lee, J., et al. (2011). Functional properties of Lactobacillus strains isolated from kimchi. *Int. J. Food Microbiol.* 145, 155–161. doi: 10.1016/j.ijfoodmicro.2010.12.003

Li, S., Zhao, Y., Zhang, L., Zhang, X., Huang, L., Li, D., et al. (2012). Antioxidant activity of *Lactobacillus plantarum* strains isolated from traditional Chinese fermented foods. *Food Chem*. 135, 1914–1919. doi: 10.1016/j.foodchem.2012.06.048

Li, T., Teng, D., Mao, R., Hao, Y., Wang, X., Wang, J. A., et al. (2020). critical review of antibiotic resistance in probiotic bacteria. *Food Res. Int.* 136, 109571. doi: 10.1016/j.foodres.2020.109571

Lin, M. Y., and Chang, F. J. (2000). Effect of intestinal bacteria *Bifidobacterium longum* ATCC 15708 *and Lactobacillus acidophilus* ATCC 4356. *Digest. Dis. Sci*. 45, 1617–22. doi: 10.1023/a:1005577330695

Lin, M. Y., and Yen, C. L. (1999). Antioxidative ability of lactic acid bacteria. *J. Agric. Food Chem.* 47, 1460–1466. doi: 10.1021/jf981149l

Lin, X., Xia, Y., Wang, G., Yang, Y., Xiong, Z., Lv, F., et al. (2018). Lactic acid bacteria with antioxidant activities alleviating oxidized oil induced hepatic injury in mice. *Front. Microbiol*. 9, 2684. doi: 10.3389/fmicb.2018.02684

Liu, N., Miao, S., and Qin, L. (2020). Screening and application of lactic acid bacteria and yeasts with l-lactic acid-producing and antioxidant capacity in traditional fermented rice acid. *Food Sci Nutr*. 8, 6095–6111. doi: 10.1002/fsn3.1900

Luo, Y., Liu, Y., Ren, T., Wang, B., Peng, Y., Zeng, S., et al. (2020). Sichuan paocai fermented by mixed-starter culture of lactic acid bacteria. *Food Sci. Nutr*. 8, 5402–5409. doi: 10.1002/fsn3.1833

Mancardi, D., Mezzanotte, M., Arrigo, E., Barinotti, A., and Roetto, A. (2021). Iron overload, oxidative stress, and ferroptosis in the failing heart and liver. *Antioxidants*. 10, 1864. doi: 10.3390/antiox10121864

Mu, G., Gao, Y., Tuo, Y., Li, H., Zhang, Y., Qian, F., et al. (2018). Assessing and comparing antioxidant activities of lactobacilli strains by using different chemical and cellular antioxidant methods. *J. Dairy Sci.* 101, 10792–10806. doi: 10.3168/jds.2018-14989

Reuben, R. C., Roy, P. C., Sarkar, S. L., Rubayet Ul Alam, A. S. M., and Jahid, I. K. (2020). Characterization and evaluation of lactic acid bacteria from indigenous raw milk for potential probiotic properties. *J. Dairy Sci.* 103, 1223–1237. doi: 10.3168/jds.2019-17092

Saide, J. A. O., and Gilliland, S. E. (2005). Antioxidative activity of lactobacilli measured by oxygen radical absorbance capacity. *Am. Dairy Sci. Assoc.* 88, 1352–7. doi: 10.3168/jds.S0022-0302(05)72801-0

Schillinger, U. G., and Wilhelm, H. (2005). *In vitro* adherence and other properties of lactobacilli used in probiotic yoghurt-like products: *Int. Dairy J.* 15, 1289–1297. doi: 10.1016/j.idairyj.2004.12.008

Shi, Y., Cui, X., Gu, S., Yan, X., Li, R., Xia, S., et al. (2019). Antioxidative and probiotic activities of lactic acid bacteria isolated from traditional artisanal milk cheese from Northeast China. *Probiotics Antimicrob. Proteins*. 11, 1086–1099. doi: 10.1007/s12602-018-9452-5

Son, S. H., Jeon, H. L., Jeon, E. B., Lee, N. K., Park, Y. S., Kang, D. K., et al. (2017). Potential probiotic *Lactobacillus plantarum* Ln4 from kimchi: evaluation of β-galactosidase and antioxidant activities. *LWT Food Sci. Technol*. 85, 181–186. doi: 10.1016/j.lwt.2017.07.018

Sun, Y., Xu, J., Zhao, H., Li, Y., Zhang, H., Yang, B., et al. (2022). Antioxidant properties of fermented soymilk and its anti-inflammatory effect on DSS-induced colitis in mice. *Front. Nutr*. 9, 1088949. doi: 10.3389/fnut.2022.1088949

Temmerman, R., Pot, B., Huys, G., and Swings, J. (2003). Identification and antibiotic susceptibility of bacterial isolates from probiotic products. *Int. J. Food Microbiol*. 81, 1–10. doi: 10.1016/S0168-1605(02)00162-9

Valko, M., Rhodes, C. J., Moncol, J., Izakovic, M., and Mazur, M. (2006). Free radicals, metals and antioxidants in oxidative stress-induced cancer. *Chem. Biol. Interact*. 160, 1–40. doi: 10.1016/j.cbi.2005.12.009

van Niel, E. W., Hofvendahl, K., and Hahn-Hagerdal, B. (2002). Formation and conversion of oxygen metabolites by *Lactococcus lactis* subsp. lactis ATCC 19435 under different growth conditions. *Appl Environ Microbiol*. 68, 4350–6. doi: 10.1128/AEM.68.9.4350-4356.2002

Vinderola, G., Capellini, B., Villarreal, F., Suárez, V., Quiberoni, A., Reinheimer, J., et al. (2008). Usefulness of a set of simple in vitro tests for the screening and identification of probiotic candidate strains for dairy use. *LWT Food Sci. Technol*. 41, 1678–88. doi: 10.1016/j.lwt.2007.10.008

Wang, W., Xiong, P., Zhang, H., Zhu, Q., Liao, C., Jiang, G., et al. (2021). Analysis, occurrence, toxicity and environmental health risks of synthetic phenolic antioxidants: a review. *Environ. Res*. 201, 111531. doi: 10.1016/j.envres.2021.111531

Wang, Y., Fang, Z., Zhai, Q., Cui, S., Zhao, J., Zhang, H., et al. (2021). Supernatants of *Bifidobacterium longum* and *Lactobacillus plantarum* strains exhibited antioxidative effects on A7R5 cells. *Microorganisms*. 9, 452. doi: 10.3390/microorganisms9020452

Wang, Y., Wu, Y., Wang, Y., Xu, H., Mei, X., Yu, D., et al. (2017). Antioxidant properties of probiotic bacteria. *Nutrients*. (2017) 9, 521. doi: 10.3390/nu9050521

Wu, Y., Ye, Z., Feng, P., Li, R., Chen, X., Tian, X., et al. (2021). *Limosilactobacillus fermentum* JL-3 isolated from "Jiangshui" ameliorates hyperuricemia by degrading uric acid. *Gut Microbes* 13, 1–18. doi: 10.1080/19490976.2021.1897211

Yamamoto, N. S. M., Hoshigami, H., Watanabe, K., Watanabe, K., Takatsuzu, T., Yasuda, S., et al. (2019). Antioxidant capacity of soymilk yogurt and exopolysaccharides produced by lactic acid bacteria. *Biosci. Microb. Food Health* 38, 97–104. doi: 10.12938/bmfh.18-017

Yan, F., Li, N., Yue, Y., Wang, C., Zhao, L., Evivie, S. E., et al. (2019). Screening for potential novel probiotics with dipeptidyl peptidase IV-inhibiting activity for type 2 diabetes attenuation *in vitro* and *in vivo*. *Front. Microbiol.* 10, 2855. doi: 10.3389/fmicb.2019.02855

Yang, E., Fan, L., Yan, J., Jiang, Y., Doucette, C., Fillmore, S., et al. (2018). Influence of culture media, pH and temperature on growth and bacteriocin production of bacteriocinogenic lactic acid bacteria. *AMB Exp*. 8, 10. doi: 10.1186/s13568-018-0536-0

Zeng, Z., He, X., Li, F., Zhang, Y., Huang, Z., Wang, Y., et al. (2021). Probiotic properties of bacillus proteolyticus isolated from Tibetan Yaks, China. *Front. Microbiol.* 12, 649207. doi: 10.3389/fmicb.2021.649207

Zhang, H., Wang, Y., Sun, J., Guo, Z., Guo, H., Ren, F., et al. (2013). Safety evaluation of *Lactobacillus paracasei* subsp. paracasei LC-01, a probiotic bacterium. *J. Microbiol.* 51, 633–8. doi: 10.1007/s12275-013-3336-x

Zhang, L., Jia, R., Li, H., Yu, H., Ren, K., Jia, S., et al. (2021). Insight into the double-edged role of ferroptosis in disease. *Biomolecules*. 11, 1790. doi: 10.3390/biom11121790

Zhao, L., Wang, S., Dong, J., Shi, J., Guan, J., Liu, D., et al. (2021). Identification, characterization, and antioxidant potential of *Bifidobacterium longum* subsp. longum strains isolated from feces of healthy infants. *Front. Microbiol.* 12, 756519. doi: 10.3389/fmicb.2021.756519

frontiers | Frontiers in Microbiology

TYPE Original Research
PUBLISHED 02 June 2023
DOI 10.3389/fmicb.2023.1174968

OPEN ACCESS

EDITED BY
Giuseppe Spano,
University of Foggia, Italy

REVIEWED BY
Chunlong Mu,
University of Calgary, Canada
Qi Wang,
Fujian Academy of Agricultural Sciences, China

*CORRESPONDENCE
Byung-Yong Kim
✉ bykim@ckdhc.com
Ki Tae Suk
✉ ktsuk@hallym.ac.kr

†These authors have contributed equally to this work

RECEIVED 27 February 2023
ACCEPTED 15 May 2023
PUBLISHED 02 June 2023

CITATION
Jeong J-J, Ganesan R, Jin Y-J, Park HJ, Min BH, Jeong MK, Yoon SJ, Choi MR, Choi J, Moon JH, Min U, Lim J-H, Lee DY, Han SH, Ham YL, Kim B-Y and Suk KT (2023) Multi-strain probiotics alleviate loperamide-induced constipation by adjusting the microbiome, serotonin, and short-chain fatty acids in rats. *Front. Microbiol.* 14:1174968. doi: 10.3389/fmicb.2023.1174968

Multi-strain probiotics alleviate loperamide-induced constipation by adjusting the microbiome, serotonin, and short-chain fatty acids in rats

Jin-Ju Jeong[1†], Raja Ganesan[1†], Yoo-Jeong Jin[2†], Hee Jin Park[1], Byeong Hyun Min[1], Min Kyo Jeong[1], Sang Jun Yoon[1], Mi Ran Choi[1], Jieun Choi[3], Ji Hyun Moon[3], Uigi Min[2], Jong-Hyun Lim[2], Do Yup Lee[3], Sang Hak Han[4], Young Lim Ham[5], Byung-Yong Kim[2]* and Ki Tae Suk[1]*

[1]Institute for Liver and Digestive Disease, Hallym University, Chuncheon, Republic of Korea, [2]R&D Center, Chong Kun Dang Healthcare, Seoul, Republic of Korea, [3]Department of Agricultural Biotechnology, Center for Food and Bioconvergence, Research Institute of Agricultural and Life Sciences, Seoul National University, Seoul, Republic of Korea, [4]Department of Pathology, Hallym University College of Medicine, Chuncheon, Republic of Korea, [5]Department of Nursing, Daewon University College, Jecheon, Republic of Korea

Constipation is one of the most common gastrointestinal (GI) disorders worldwide. The use of probiotics to improve constipation is well known. In this study, the effect on loperamide-induced constipation by intragastric administration of probiotics Consti-Biome mixed with SynBalance® SmilinGut (*Lactobacillus plantarum* PBS067, *Lactobacillus rhamnosus* LRH020, *Bifidobacterium animalis* subsp. *lactis* BL050; Roelmi HPC), *L. plantarum* UALp-05 (Chr. Hansen), *Lactobacillus acidophilus* DDS-1 (Chr. Hansen), and *Streptococcus thermophilus* CKDB027 (Chong Kun Dang Bio) to rats was evaluated. To induce constipation, 5mg/kg loperamide was intraperitoneally administered twice a day for 7days to all groups except the normal control group. After inducing constipation, Dulcolax-S tablets and multi-strain probiotics Consti-Biome were orally administered once a day for 14days. The probiotics were administered 0.5mL at concentrations of 2×10^8CFU/mL (G1), 2×10^9CFU/mL (G2), and 2×10^{10}CFU/mL (G3). Compared to the loperamide administration group (LOP), the multi-strain probiotics not only significantly increased the number of fecal pellets but also improved the GI transit rate. The mRNA expression levels of serotonin- and mucin-related genes in the colons that were treated with the probiotics were also significantly increased compared to levels in the LOP group. In addition, an increase in serotonin was observed in the colon. The cecum metabolites showed a different pattern between the probiotics-treated groups and the LOP group, and an increase in short-chain fatty acids was observed in the probiotic-treated groups. The abundances of the phylum *Verrucomicrobia*, the family *Erysipelotrichaceae* and the genus *Akkermansia* were increased in fecal samples of the probiotic-treated groups. Therefore, the multi-strain probiotics used in this experiment were thought to help alleviate LOP-induced constipation by altering the levels of short-chain fatty acids, serotonin, and mucin through improvement in the intestinal microflora.

KEYWORDS

constipation, probiotics, microbiome, serotonin, SCFAs

Introduction

Constipation is a common gastrointestinal (GI) disorder, and its prevalence is estimated to be 16% worldwide (Forootan et al., 2018). This symptom was reported more often in women than in men and in elderly people than in young people (Faigel, 2002). Various causes of constipation are known, but it can result from intestinal obstruction, lack of exercise, low fiber intake, or personal factors (Bosaeus, 2004). Laxatives that induce diarrhea are generally used for the treatment of constipation, and types include bulk-forming agents, chloride-channel activators, emollients, hyperosmotics, lubricants, saline laxatives, serotonin antagonists, and stimulants. However, they may have adverse effects such as diarrhea, cramping, and headache (Ambizas and Ginzburg, 2007). To overcome the side effects of laxatives, modulation of the intestinal microflora with probiotics might be necessary.

Probiotics are live microorganisms that can be ingested and have beneficial effects on health. Probiotics are effective in improving various diseases, such as GI diseases, allergies, respiratory diseases, neurological and psychiatric diseases, genitourinary tract infections, and oral diseases (Jeong et al., 2022). They have a variety of mechanisms, such as competition with pathogens, secretion of bacteriocins, fatty acid production, enzymatic activities, and microbiome changes (Plaza-Diaz et al., 2019). The genera *Bifidobacterium* and *Lactobacillus* are representative bacteria that are frequently used as probiotics (Koebnick et al., 2003; Yang et al., 2008; Li et al., 2015; Wang et al., 2019). Supplementation with *Bifidobacterium* not only increased the number of bowel movements per week in patients with chronic constipation in clinical trials but also significantly improved consistency (Yang et al., 2008). *Bifidobacterium* can alleviate constipation by improving fecal fluids, propionate and butyrate, and GI transit time (Wang et al., 2019). *Lactobacillus* improved self-diagnosed constipation severity and stool consistency in clinical trials (Koebnick et al., 2003). Similarly, *Bifidobacterium* and *Lactobacillus* relieved constipation by improving GI transit and increasing the production of fecal short-chain fatty acids (SCFAs) (Li et al., 2015). Chocolate made from *Lactobacillus* and *Streptococcus* also ameliorated constipation by increasing intestinal motility (Eor et al., 2019). Recently, the trend of using a mixture of individual probiotics is increasing. The reason is considered to be because of the possibility of synergy and additive effect rather than the use of a single strain (Kwoji et al., 2021). *Lactobacillus rhamnosus* GG (LGG) mixed with *Bifidobacterium animalis* subsp. *lactis* Bb12 was more effective in eliminating *Helicobacter pylori* and improving necrotizing enterocolitis than when LGG used alone (Myllyluoma et al., 2005; Hays et al., 2016).

Several mechanisms related to the amelioration of GI diseases by microorganisms have been identified. The gut microbiome is one of the most actively studied mechanisms in the last decade. In patients with constipation, a decrease in lactate- and butyrate-producing bacteria was observed (Dimidi et al., 2020). Butyrate belongs to the SCFA family of volatile fatty acids, with 1–6 carbon atoms attached to the aliphatic chain (Ríos-Covián et al., 2016). SCFAs were the major metabolites produced by the fermentation of anaerobic bacteria in the GI tract. Therefore, changes in the microbiome after treatment with microorganisms could be deeply related to changes in SCFAs. Among the SCFAs, acetate, butyrate, propionate, and valerate have been studied for their inhibitory effects on various diseases. Acetate is involved in cholesterol synthesis and shows a protective effect against infection by *Escherichia coli* O157:H7 (Arora and Sharma, 2011; Fukuda et al., 2011). Butyrate showed an immunoregulatory effect and was reported to have therapeutic and protective effects against distal ulcerative colitis (Böcker et al., 2003; Wang et al., 2018). SCFAs increased IL-18 production through a GPR109a-mediated pathway, which could sustain stomach homeostasis and prevent colorectal carcinogenesis (Kalina et al., 2002; Singh et al., 2014). Propionate inhibits cholesterol synthesis (Henningsson et al., 2001), and valerate has a positive effect on the pathogenesis of colitis (Yuille et al., 2018). In addition, SCFAs can stimulate the secretion of serotonin and mucin, which can improve constipation (Hatayama et al., 2007; Reigstad et al., 2015). It has been observed that serotonin is decreased in animal models of constipation, and its secretion is involved in GI motility and regulated by gut microbes (Gershon, 2004; Cao et al., 2017). Moreover, tryptophan, bile acids, lipopolysaccharide, methane, and hydrogen are known metabolites produced by microorganisms that are involved in gastrointestinal physiology (Jahng et al., 2012; Ao et al., 2013; Zelante et al., 2013; Ye et al., 2020).

Considering these factors, the use of probiotics is thought to contribute to alleviating the symptoms of constipation treatment without adverse effects caused by laxatives. In this study, the effect of multi-strain probiotics composed of *Bifidobacterium*, *Lactobacillus*, and *Streptococcus* on loperamide-induced constipation in rats was confirmed, and changes in the gut microbiome and metabolites were investigated.

Materials and methods

Multi-strain probiotics formulation

A multi-strain probiotics Consti-Biome containing a mixture of SynBalance® SmilinGut (*Lactobacillus plantarum* PBS067, *Lactobacillus rhamnosus* LRH020, *Bifidobacterium animalis* subsp. *lactis* BL050; Roelmi HPC), *L. plantarum* UALp-05 (Chr. Hansen), *Lactobacillus acidophilus* DDS-1 (Chr. Hansen), and *Streptococcus thermophilus* CKDB027 (Chong Kun Dang Bio) was obtained from Chong Kun Dang HealthCare (Seoul, Korea). The multi-strain probiotics Consti-Biome was adjusted to 2×10^{10} colony-forming unit (CFU), mixed in Dulbecco's phosphate-buffered saline (D-PBS), vortexed for 20 min, and diluted to the concentration required for the experiment.

Experimental animals and design

Five-week-old male Sprague Dawley (SD) rats were purchased from DooYeol Biotech (Seoul, Korea). Rats were bred under conditions of temperature of 20 ± 2°C, humidity of 55 ± 5%, and light and dark conditions for 12 h and given free access to drinking water and standard chow. After 1 week of adaptation, the rats were randomly divided into 6 groups with 7 animals in each group. They were grouped into normal control (NOR), loperamide administration

Abbreviations: GI, Gastrointestinal; SCFAs, Short-chain fatty acids; D-PBS, Dulbecco's phosphate-buffered saline.

(LOP), positive control (PC), low concentration multi-strain probiotics Consti-Biome administration (G1, 2×10^8 CFU), medium concentration Consti-Biome administration (G2, 2×10^9 CFU), and high concentration Consti-Biome administration (G3, 2×10^{10} CFU), respectively. As a positive control group, 5 mg/kg of constipation treatment drug called Dulcolax-S tablets (Boehringer Ingelheim, Alkmaar, Nederland) was used.

Constipation was induced by intraperitoneal administration of loperamide (Sigma, St. Louis, MO, United States) at a dose of 5 mg/kg body weight in all groups twice a day for 7 days except for NOR group. Dulcolax-S tablets and 0.5 mL of multi-strain probiotics were orally administered once a day for 14 days after induction of constipation. Body weight and food intake of the experimental animals were measured at weekly intervals. The feces of each group were collected 24 h after the bedding and feces in the cage were changed. Feces were collected at the end of the treatment. Animal sacrifice was performed by overdose of inhalational anesthesia overdose (isoflurane, Aerane; Baxter, Deerfield, IL, United States). Tissue of colon and intestine, and content of cecum were collected and stored at −80°C until required. All animal experiments were conducted in accordance with the regulations of the Animal Experimental Ethics Committee (IACUC) of Hallym University (Hallym 2021–79).

For pathological analysis of the intestine, intestinal specimens were fixed with 10% formalin, routinely embedded in paraffin; the tissue sections were processed with hematoxylin and eosin. All specimens were evaluated by the same pathologist (SHH), who was masked as to whether the specimens came from comparative or control groups. Mucosal thickness was measured by CellSens® (olympus imaging software).

pH, water content, and intestinal motility

At the end of the multi-strain probiotics' treatment, fecal samples were collected, then measured the number, pH, and water content, respectively. pH of diluted the fecal samples in distilled water was measured by a Ohause Starter300 pH meter (Chen et al., 2019). After drying the samples at 70°C for 24 h the water content was determined by measuring the dry weight and calculating the difference between the fresh weight, and the dry weight.

The effect of intestinal motility was measured after fasting 12 h before animal sacrifice. 1 mL of barium sulfate (1.4 g/mL; Daejung Chemicals & Metals Co. LTD., Siheung-si, Gyeonggi-do, Korea) was orally administered to the experimental animals, and after 30 min, the animals were sacrificed. Finally, by measuring the movement distance of barium sulfate in the intestine obtained from the animals, the intestinal movement rate was calculated as follows. Intestine transit rate (%) = distance moved by the barium sulfate (cm)/total intestine length (cm) × 100.

Serotonin- (5-HT1a, 5-HT1b, Sert, Tph1, and Tph2), cytokine- (Tnf-α), and mucin- (Muc2) related genes expression in the colon

To evaluate the ability of multi-strain probiotics to regulate intestinal immunity, cytokines, mucin-related genes, and serotonin-related markers were analyzed. The colons from animals were frozen using liquid nitrogen and stored at −80°C until use. For RNA extraction, 1,000 μL of trizol reagent (Lifetechnologies, Cardisbad, CA, United States) was added to 50 mg of colon tissue and it was homogenized. 200 μL of chloroform (Sigma Aldrich, St. Louis, MO, United States) was added to the sample, left at room temperature for 5 min, and then centrifuged at 14,000 rpm, 5 min, 4°C. 1 mL of 70% cold ethanol was added to the RNA pellet and centrifuged again at 7,500 rpm, 5 min, 4°C. After removing the supernatant and drying at room temperature for 10 min, 100 μL of diethyl pyrocarbonate (DEPC) water was added and vortexed. The purity and concentration of RNA were quantified by measuring absorbance at 260 nm. 5 μg of the isolated RNA and 2.5 μL of DEPC water were put into an RT premix (Bioneer, Deajeon, Korea), and 50 μL cDNA was synthesized using the Mastercycler gradient and used as a template for PCR amplification. In the reverse transcription temperature cycle, cDNA was synthesized at 42°C for 1 h, denatured at 94°C for 5 min, and cooled at 4°C for 5 min. For PCR, 10 pg. of cDNA, 10 pg. of sense primer, antisense primer, and DEPC water were added to a PCR premix (iNtron, Seongnam, Korea) and amplification was performed using a Mastercycler gradient. Primer information for each gene is described below (Table 1).

Serotonin (5-HT) in colon

Fifty milligrams of colonic tissue were washed with D-PBS followed by homogenizing in D-PBS. After centrifuging for 15 min at 1500 × g, the 5-HT concentration of homogenates was measured using a 5-HT ELISA kit (Abcam, ab133053) according to the manufacturer's instructions. Protein from the colonic tissue was quantified by the bicinchoninic assay. The result is presented as nanograms of serotonin per milliliter per microgram of protein.

TABLE 1 PCR primers used in this study.

Gene	Primer	Sequences 5′->3′
GAPDH	Forward	CCATCACCATCTTCCAGGAG
	Reverse	CCTGCTTCACCAACCTTCTTG
Muc2	Forward	GATAGGTGGCAGACAGGAGA
	Reverse	GCTGACGAGTGGTTGGTGATTG
Sert	Forward	ATCTCCTAGAACCCTGTAAC
	Reverse	GAAATGGACCTGGAGTATTG
Tph1	Forward	CACTCACTGTCTCTGAAAACGC
	Reverse	AGCCATGAATTTGAGAGGGAGG
Tph2	Forward	TAAATACTGGGCCAGGAGAGG
	Reverse	GAAGTGTCTTTGCCGCTTCTC
5-HT1a	Forward	TCCGACGTGACCTTCAGCTA
	Reverse	GCCAAGGAGCCGATGAGATA
5-HT1b	Forward	CCGGCTAACTACCTGATCGC
	Reverse	TATCCGACGACAGCCAGAAG
Tnf-α	Forward	TGCCTCAGCCTCTTCTCATT
	Reverse	GAGCCCATTTGGGAACTTCT

Metabolites in fecal samples

Analysis of metabolites of fecal samples was conducted followed by the previous study (Yu et al., 2021). In brief, each fecal sample was mixed with (acetonitrile:3′-dilstilled water, 1:1, volume:volume) and then homogenized with a Mixer Mill MM400 (Haan, Germany, Letsch GmbH & Co.). The homogenized samples were used for analysis of short-chain fatty acids (SCFAs) and untargeted metabolites.

SCFAs were analyzed using a Q-Exactive Plus Orbitrap MS-connected Ultimate-3,000 UPLC system. 40 μL of the supernatant of homogenized sample was mixed with 20 μL of 1-ethyl-3-(3-dimethylaminopropyl)carbodiimide hydrochloride (120 mM) dissolved in 6% pyridine solution and 200 mM 3-Nitrophenylhydrazine hydrochloride dissolved in 70% acetonitrile (ACN). These mixed samples were kept at 40°C for 30 min and diluted with 70% ACN to 2 mL (Han et al., 2015). For untargeted metabolites analysis, the cecal contents prepared above were chromatographically separated by Ultmate-3,000 UPLC system (Thermo Fisher Scientific,Waltham, MA, United States) equipped with 100 mm × 2.1 mm UPLC BEH 1.7 μm C18 column (Waters, Milford, MA, United States) and 5.0 mm × 2.1 mm UPLC BEH 1.7 μm C18 VanGuard Pre-Column (Waters, Milford, MA, United States). The mobile phase A and B was the same as used in SCFAs and flow rate was 0.300 mL/min. The MS analysis was performed on a Q-Exactive Plus Orbitrap MS instrument (Thermo Fisher Scientific, Waltham, MA, United States) in polarity switching ionization mode. Full MS scan was conducted on the metabolites (80–1,200 m/z) with resolution of 70,000 FWHM at m/z = 200 and with automatic gain control (AGC) target of 1e6 ions and maximum injection time (IT) of 100 ms. The data-dependent MS/MS analysis was performed on total pooled samples by each ionization mode (positive mode and negative mode). Data-dependent MS/MS setting was as follows: Top5 MS1 ions; resolution, 17,500 at 200 m/z; AGC target, 1e5; maximum IT, 50 ms; isolation window, 0.4 m/z; normalized collision energy (NCE), 30, 40 and 50; intensity threshold, 2e4 ions; apex trigger, 3–6 s; dynamic exclusion, 5 s.

Data acquisition and pre-processing were performed using Xcalibur software (Thermo Fisher Scientific, San José). The obtained raw data files were processed using Compound Discoverer software (version 3.2, Thermo Fisher Scientific, San José). The data processing was done following the workflow such as Select spectra, Align Retention times, Detect Unknown Compounds, Group Unknown Compounds, Fill Gaps and Search mzCloud. Align Retention Time node was set to 1 min to Maximum shift. Compound identification was done against mzCloud with criteria of 10 ppm (MS2 mass tolerance) and 70% of assignment threshold (Yu et al., 2021).

For untargeted metabolites analysis, the fecal samples prepared above were chromatographically separated by Ultmate-3,000 UPLC system (Thermo Fisher Scientific, Waltham, MA, United States) equipped with 100 mm × 2.1 mm UPLC BEH 1.7 μm C18 column (Waters, Milford, MA, United States) and 5.0 mm × 2.1 mm UPLC BEH 1.7 μm C18 VanGuard Pre-Column (Waters, Milford, MA, United States). The mobile phase A and B was the same as used in SCFAs and flow rate was 0.300 mL/min. The data were processed using Compound Discoverer software (version 3.2, Thermo Fisher Scientific, San José).

Microbiome in fecal samples

For metagenomic sequencing analysis, genomic DNA was extracted from rat stool and library construction was performed. Briefly, gDNA was extracted using the DNeasy Power Soil kit (Qiagen, Hilden, Germany) according to the manual provided by the manufacturer. To amplify the V3 and V4 regions, sequencing libraries were prepared according to the illumine 16S Metagenomic Sequencing Library protocols. The primers used for PCR amplification were forward 5'-TCGTCGGCAGCGTCAGATGTGTATAAGAGACAGCC TACGGGNGGCWG-CAG and reverse (5'-GTCTCGTGGGCTCGG AGATGTGTATAAGAGACAGGACTACHV-GGGTATCTAATCC). Cycle conditions were 95°C for 3 min, 25 cycles at 95°C for 30 s, 55°C and 72°C for 30 s, and final extension at 72°C for 5 min. The PCR product obtained here was purified with AMPure beads (Agencourt Bioscience, Beverly, MA). The purified PCR products were amplified for final library construction using NexteraXT Indexed Primer. All PCR conditions were the same described above, except that the number of cycles was 10 times. After purification the PCR products, they were quantified by qPCR using KAPA Library Quantification kits for Illumine Sequencing platforms, and qualified with TapeStation D1000 ScreenTape (Agilent Technologies, Waldbronn, Germany). Then, sequencing was performed using the MiSeq platform (Illumina, San Diego, United States); sequence analysis of the samples was conducted by the Macrogen Inc. (Macrogen, Seoul, Korea).

For amplicon sequence variants (ASV) analysis, the Cutadapt (v3.2) program was used to remove the sequencing adapter sequence and the F/R primer sequence of the target gene region (Martin, 2011). Error-correction of the amplicon sequencing process was performed using the DADA2 (v1.18.0) package of R (v4.0.3) (Callahan et al., 2016). After combining the corrected paired-end sequences into one sequence, the chimera was removed. Using QIIME (v1.9), subsampling was applied and normalized based on the number of reads of the sample with the minimum number of reads among all samples, and the microbial community was compared and analyzed (Caporaso et al., 2010).

The mafft (v7.475) was used for multiple alignment between SVs sequences (Katoh and Standley, 2013). With information of the ASV abundance and taxonomy, a comparative analysis of various microbial communities was performed using the QIIME. Shannon index and was obtained to confirm the species diversity and uniformity of the microbial community in the samples. Alpha diversity information was confirmed through the Chao1 value. Beta diversity between samples was calculated based on weighted and unweighted UniFrac distance. PCoA visualized the relationship between samples (Rambaut, 2009; Caporaso et al., 2010).

Statistical analysis

All data are expressed as mean ± standard error using Prism (Prism 8.0.3, GraphPad Software Inc., San Diego, United States), the significance of the system between the experimental group and the control group was verified using T-test or One way-ANOVA, and Tukey's post-test or Dunnett's multi comparisons test was performed. It was considered statistically significant at $p < 0.05$. Significant differences in SCFAs among six groups and in total metabolite features

compared to the LOP group were determined based on Kruskal-Wallis test and Mann–whitney u-test, respectively, using Multi Experimental Viewer (MeV, TIGR).

For principal component analysis (PCA) and partial least squares-discriminant analysis (PLS-DA) analysis of metabolites, SIMCA 17 (Umetrics AB, Umea, Sweden) was used.

Results

Food intake and body weight

When constipation was induced by injecting loperamide into 6-week-old experimental animals for 7 days, their body weight and food intake were not significantly different in any of the groups compared with the normal control group (NOR) (Table 2). In detail, no significant changes in body weight and food intake were observed before induction of constipation (1 week), after induction of constipation with loperamide (LOP) (2 weeks), and after administration of multi-strain probiotics (G1: 2×10^8 CFU; G2: 2×10^9 CFU; and G3: 2×10^{10} CFU) or Dulcolax-S tablets (PC) (3 and 4 weeks). These data indicate that loperamide-induced constipation has no effect on body weight or appetite.

Improvement of constipation-related indicators by the multi-strain probiotics

Figure 1A shows the overall animal experimental design. The average number of fecal pellets was 6 in the NOR, 5 in the LOP, 7 in the PC, 5 in the G1, and 7 in the G2 and G3 groups. However, compared to the LOP, there was no significant difference in the PC and G1 groups, and a significant difference was observed in the G2 and G3 groups (Figure 1B). In both groups, the number of fecal was increased about 1.3 times compared to LOP. In all probiotic groups, the pH and water content of the feces were improved similarly to PC and significantly improved compared with the LOP (Figure 1C). The water content reduced by constipation was increased by 2.7- to 2.9-fold and 2.8-fold in the G1-3 and PC groups, respectively, compared to the LOP group, which had a water content of 17.6%, and improved similarly to the NOR group (Figure 1D). In particular, the gastrointestinal (GI) transit rate, one of the most important indicators of constipation, was confirmed to be 63.8% on average in the NOR, 51.5% in the LOP, 62.4% in the PC, 66.6% in the G1, 60.1% in the G2, and 68.2% in the G3 group. In G3, which had the highest increase among all groups, it increased by about 1.3 times compared to LOP. The GI transit rate was significantly decreased in the LOP group compared to the NOR group and was significantly increased compared to the LOP group in both the PC and probiotic administration groups (Figure 1E).

Induction of constipation with loperamide is known to decrease the thickness of the intestinal mucosa and to delay the movement of contents in the intestine (Sin et al., 2010). Although, there was no significant difference in the mucosal thickness or length in all groups, both showed a tendency to increase in the multi-strain probiotics-treated groups G1, G2, and G3 compared to LOP (Supplementary Figure S1).

Serotonin-, cytokine-, and mucin-related mRNA expression

Secretion of serotonin can be stimulated in the intestinal tract, and serotonin relay peristalsis of the intestinal tract occurs (Park, 2011). Administration of multi-strain probiotics significantly increased the expression of serotonin-related genes (5-HT1a and 5-HT1b) and mucin-related gene (Muc2) in the colons of experimental animals (Figure 2). 5-HT1a was increased approximately 8-, 14-, and 7.1-fold in the G1, G2, and G3 groups, respectively, compared with LOP. The PC group also showed a tendency to increase approximately 3 times, but there was no statistically significant change in the PC and G3 groups compared to LOP. 5-HT1b was increased approximately 4 times in both the G1 and G2 groups and 2 times in the G3 group compared with LOP (Figure 2). Similar to 5-HT1a, the PC group showed a tendency to increase approximately 2-fold, but there was no significant change in the PC and G3 groups compared to LOP. *Sert*,

TABLE 2 Body weight and food intake by week of experimental animals.

	NOR*	LOP	PC	G1	G2	G3
1 week						
Body weight (g)	113.9 ± 2.3**	113.8 ± 1.5	113.4 ± 1.3	112.9 ± 1.0	112.7 ± 2.1	112.7 ± 2.7
2 weeks						
Body weight (g)	163.2 ± 3.3	156.56 ± 2.8	154.3 ± 3.4	154.3 ± 3.0	153.6 ± 3.4	155.2 ± 26
Feed intake (g/day)	16.3 ± 0.2	14.5 ± 0.2	14.0 ± 0.4	14.8 ± 0.4	14.1 ± 0.2	16.0 ± 0.2
3 weeks						
Body weight (g)	190.9 ± 3.9	184.0 ± 4.0	180.9 ± 3.2	182.3 ± 3.3	181.3 ± 5.3	188.7 ± 4.3
Feed intake (g/day)	15.4 ± 0.7	15.9 ± 0.1	15.6 ± 0.1	16.6 ± 0.3	16.3 ± 0.3	17.1 ± 0.3
4 weeks						
Body weight (g)	248.3 ± 12.6	255.4 ± 5.2	247.3 ± 5.0	254.0 ± 4.0	248.0 ± 7.1	255.3 ± 5.6
Feed intake (g/day)	22.2 ± 0.2	22.2 ± 0.2	21.1 ± 0.1	22.5 ± 0.4	22.5 ± 0.4	21.9 ± 0.3

*NOR, normal control; LOP, loperamide administration; PC, positive control; G1, low concentration multi-strain probiotics administration (2×10^8 CFU); G2, medium concentration multi-strain probiotics (2×10^9 CFU), and G3, high concentration multi-strain probiotics (2×10^{10} CFU) groups.
**Data are mean ± SEM of 7 animals.

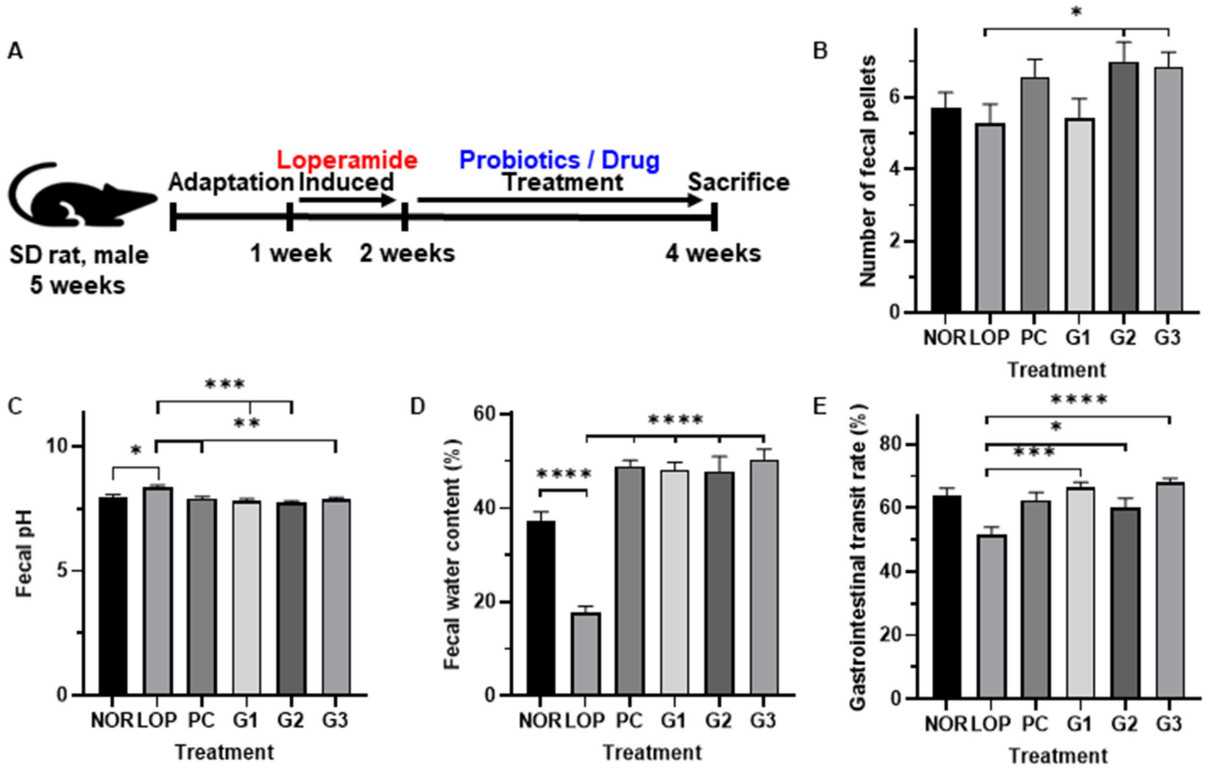

FIGURE 1
Changes in indicators related to constipation by multi-strain probiotics Consti-Biome. **(A)** Showed experimental scheme. **(B)**; number of fecal pellets, **(C)**; Fecal pH, **(D)**; Fecal water content, **(E)**; gastrointestinal transit rate of normal control (NOR), loperamide administration (LOP), positive control (PC), low concentration multi-strain probiotics administration (G1, 2×10^{8}cfu/mL), medium concentration multi-strain probiotics administration (G2, 2×10^{9}cfu/mL), and high concentration probiotic administration (G3, 2×10^{10}cfu/mL) groups. Data were collected 2weeks after treatment. Data are mean ± SEM of 7 animals. *p<0.05, **p<0.01, *** p<0.001, **** p<0.0001, significantly different from the LOP as per one-way ANOVA with the Tukey's multiple comparisons test.

Tph1, and *Tph2*, which are also related to serotonin, showed an increasing trend in the probiotic treatment groups, but a significant difference was not observed compared to the LOP group (Supplementary Figure S2). Mucin, which plays a role in protecting the intestine, is increased by laxatives (Kim et al., 2018). The expression of muc2, an oligomeric mucus/gel-forming protein coding gene, increased approximately 6-fold and 11-fold in the G1 and G2 groups, respectively, compared to the LOP (Figure 2). Tnf-α, which is known to be increased in inflammatory diseases, showed a tendency to increase in all constipation-induced groups. However, it tended to recover in the PC, G2, and G3 groups (Figure 2). This became evident with increasing probiotic concentrations. Taken together, the multi-strain probiotics used in this experiment have the effect of improving constipation by secreting serotonin and mucin and have anti-inflammatory potential.

Serotonin in the colon

Serotonin is known to play a pivotal role in gastrointestinal disorders, particularly lower functional gastrointestinal disorders (Camilleri, 2009). It is related to intestinal peristalsis and intestinal motility (Costedio et al., 2007). The multi-strain probiotics used in this experiment were found to significantly increase serotonin-related genes in the colons of experimental animals. Therefore, the amount of serotonin secreted in the colon was measured. In the NOR group, an average of 4.8 ng/mL serotonin was secreted. In the LOP group, a significant decrease in serotonin levels was observed at 2.3 ng/mL compared to the NOR group (Figure 3). The serotonin level of PC was 2.7 ng/mL, showing an increasing trend compared with the LOP group, but there was no statistically significant difference (Figure 3). On the other hand, the serotonin concentration in the G1 groups was 2.5 ng/mL, that of G2 was 4.1 ng/mL, and that of G3 was 4.0 ng/mL, and the low-concentration G1 group did not show significant changes; however, it showed a slight increase (Figure 3). In the G2 and G3 groups, a significant increase in the secretion of serotonin was observed in the colon compared to the LOP group (Figure 3). This result shows that multi-strain probiotics improve constipation by increasing the secretion of serotonin in the colon.

Metabolites

A total of 256 valid metabolites from all samples were identified through LC–MS analysis. As shown in Figure 4A, the predictive ability parameter Q2cum and goodness-of-fit parameter R2X of the first left principal component analysis (PCA) were 0.311 and 0.53, respectively. In PLS-DA, it was observed that each group was distinguished from

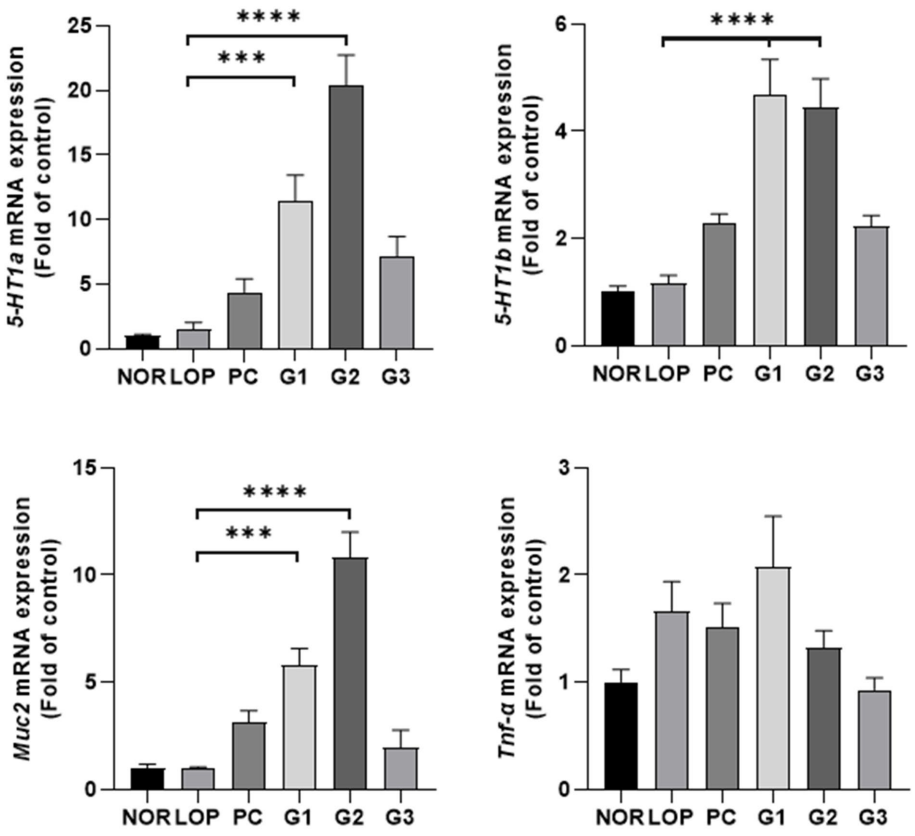

FIGURE 2
mRNA expression related to serotonin, cytokine, and mucin according to constipation induction and multi-strain probiotics Consti-Biome treatment. mRNA expression level in the colon of normal control (NOR), loperamide administration (LOP), positive control (PC), low concentration multi-strain probiotics administration (G1, 2×10^{8}cfu/mL), medium concentration multi-strain probiotics administration (G2, 2×10^{9}cfu/mL), and high concentration probiotic administration (G3, 2×10^{10}cfu/mL) groups were measured 2weeks after the multi-strain probiotics' treatment. Data are mean ± SEM of 7 animals. *p<0.05, **p<0.01, ***p<0.001, ****p<0.0001, significantly different from the LOP as per one-way ANOVA with the Tukey's post-test.

the LOP group as the concentration of multi-strain probiotics increased according to component 2. PLS-DA score plots discriminated between the constipation induction group and the probiotics treatment group after constipation induction with Q2cum (0.0826), R2X (0.51), and R2Y (0.344).

The common or unique metabolites are further examined that were regulated in the LOP and probiotics treatment groups (G1, G2, and G3 group). A total of common metabolites showed similar decreasing patterns among the three treatment groups compared to LOP group. Furthermore, it was confirmed that SCFAs (Acetate, Propionate, Butyrate, Valerate) increased significantly only in the G3 group, which was fed the highest dose (Supplementary Figure S3; Supplementary Tables S1–S3).

The six short-chain fatty acids (SCFAs) are listed in Figure 4B. Although the differences of SCFAs were not significant among the total 6 groups, acetate was significantly decreased in the LOP group compared to the NOR group, and the G3 group was shown to be able to significantly restore the concentration of acetate that was decreased by the induction of constipation. Butyrate, propionate, and valerate showed dose-dependent increasing trend in all the probiotic intake groups, but a significant change was observed only in the G3 group. Except for the isomers iso-butyrate and iso-valerate, no significant changes were observed among the groups, but their intensity increased with an increase in the concentration of multi-strain probiotics (Figure 4B; Supplementary Table S4).

Microbiome change

Changes in bacteria of stools were observed in the analysis of the microbiome (Supplementary Figure S5). At the phylum level, *Firmicutes* occupied the highest proportion in all groups (Figure 5A). Followed by the t-test not in ANOVA, the phylum *Verrucomicrobiota* decreased in abundance in the LOP group compared to the NOR group and significantly increased in the G3 group (Figure 5A; Supplementary Figure S4). At the family level, *Erysipelotrichaceae* belonging to the phylum *Firmicutes* (now *Bacillota*) was found to increase in abundance in the G2 and G3 groups compared to the LOP (Figure 5B). The genus *Akkermansia* belonging to *Verrucomicrobiota* increased in the G3 group (Figure 5C; Supplementary Figure S4). However, significant differences were not observed among the groups in alpha diversity and beta diversity (Figures 5D,F). In the PCoA analysis, each group was not clearly separated. In PCA for weighted, the percent variation explained for PC1 was 44.36% and for PC2 was 26.86%. In unweighted, 33.63% by PC1 and 8.51% by PC2 were explained (Figure 5E).

Discussion

Constipation is one of the most common gastrointestinal (GI) disorders worldwide. To alleviate this, probiotics are often used. In

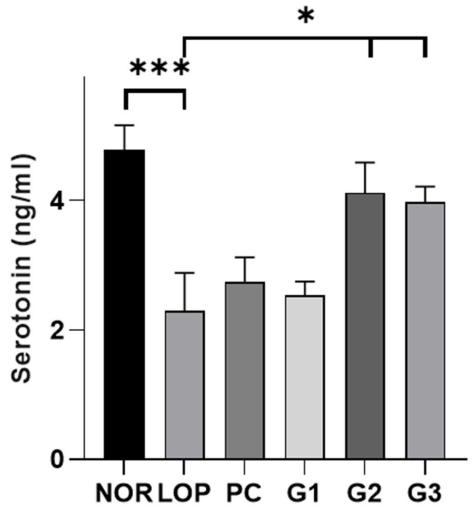

FIGURE 3
Serotonin (5-HT) levels (ng/ml) in colon samples. Colonic serotonin level of normal control (NOR), loperamide administration (LOP), positive control (PC), low concentration multi-strain probiotics administration (G1, 2×10^{8}cfu/mL), medium concentration multi-strain probiotics administration (G2, 2×10^{9}cfu/mL), and high concentration probiotic administration (G3, 2×10^{10}cfu/mL) groups were measured 5-HT ELISA kit. Data are mean ± SEM of 5 animals. *p<0.05, **p<0.01, significantly different from the LOP as per one-way ANOVA with the Dunnett's multi comparisons test.

this study, the relieving effect of a mixture of the genera *Lactobacillus, Bifidobacterium, and Streptococcus* on constipation was assessed. Multi-strain probiotics consisted of SynBalance® SmilinGut (*Lactobacillus plantarum, Lactobacillus rhamnosus*, *Bifidobacterium animalis* subsp. *lactis*; ROELMI), *L. plantarum* (UAS), *Lactobacillus acidophilus* (UAS), and *Streptococcus thermophilus* (Chong Kun Dang Bio). The probiotics improved constipation and increased the mRNA expression of genes related to serotonin and mucin in the colon. Cytokine-related genes tend to be decreased in G2 and G3. Increased colonic serotonin production and fecal short-chain fatty acids (SCFAs) were also observed. In fecal samples treated with the probiotics, the abundances of the phylum *Verrucomicrobiota*, the family *Erysipelotrichaceae*, and the genus *Akkermansia* were increased.

Previously, SmilinGut was used in a double-blind clinical trial with 50 subjects. Constipation was evaluated through self-symptom scoring. It was confirmed in the probiotic administration group that more than 30% of the subjects had improvement in their symptoms. It has been found to colonize well in the GI tract (Mezzasalma et al., 2016). However, clear mechanism has not been elucidated. Here, the mixture of the SmilinGut and other probiotics showed an improvement effect on symptoms related to constipation. The probiotic mixture used in this experiment improved constipation indicators such as the stool number, pH, and water content *in vivo* (Figures 1B–D). A high pH and low water content may be due to slow transit in GI. The probiotics also recovered the changes in the GI transit rate induced by loperamide (Figure 1E). Among these symptoms, GI transit time and water content are important risk factors for constipation (Burkitt et al., 1972). Several studies on the improvement in constipation by probiotics have been reported. *B. animalis* subsp. *lactis* exhibited an increase in the GI transit rate in both animal and clinical trials (Wang et al., 2021). Gut motility was increased after *Lactobacillus plantarum* was administered to subjects with constipation (Kusumo et al., 2019). In both of these strains, an increase in SCFAs was confirmed by changes in the gut microbiome. All things considered, the positive effect on constipation by the probiotic mixture used in this study could be due to the improvement in the GI tract.

5-HT (5-hydroxytryptamine; 5-HT) could be altered in disorders associated with changes in bowel function and sensation. Enterochromaffin cells use tryptophan hydroxylase (TPH) to synthesize 5-HT. TPH includes Tph1, which is mainly involved in peripheral serotonin synthesis, and TPH2, which is an isoenzyme involved in serotonin synthesis in the central nervous system, such as the raphe nucleus (Walther et al., 2003). 5-HT is removed from the interstitial space via the serotonin-selective reuptake transporter (Sert). Sert can induce chronic constipation by attenuating intestinal motility and circulatory muscle contractile activity (Guarino et al., 2011). 5-HT is known to decrease in the colonic mucosa of patients with chronic constipation (Coates et al., 2004). Increasing the concentration of 5-HT could decrease the colonic transit time of feces in rats and was associated with SCFAs (Fukumoto et al., 2003). Therefore, 5-HT is one of the important mechanisms for improving constipation. In a constipation rat model induced by loperamide, treatment with *Bifidobacterium bifidum* ameliorated symptoms of constipation, and increases in the 5-HT and Tph1 mRNA levels were observed (Makizaki et al., 2021). Treatment with *Bifidobacterium animalis* subsp. *lactis* in zebrafish could upregulate genes for 5-HT synthesis and downregulate Sert, which was associated with SCFAs (Lu et al., 2019). *B. animalis* was able to increase Muc2 as well as serotonin (Lu et al., 2021). This result was also observed when loperamide-induced constipation mice were treated with *Bifidobacterium lactis* (Tang et al., 2022). Similarly, in this study, an increase in serotonin and mucin in the colon was observed (Figures 2, 3). Muc2 is a mucin that forms a protective layer mucus that covers intestinal epithelial cells and helps maintain the integrity of the intestinal mucosal barrier (Wlodarska et al., 2014). An increase in mucin for constipation treatment has been continuously observed. This can be reduced by constipation (Kim et al., 2019a) and restored by probiotics or substances or a combination of probiotics and other substances (Kim et al., 2013, 2019b; Huang et al., 2022; Tang et al., 2022). Although significant results regarding intestinal mucosal length and thickness were not observed, they showed an increasing tendency (Supplementary Figure S1). In the long term, the results might support an improvement in intestinal mucosal length and thickness.

Constipation is related to impairment in the intestinal mucosal immune system (Collins, 1996). Cytokines are important mediators of inflammation and immune responses and include Tnf-α, Tnf-β, Il-8, and Il-10. These are known to increase in constipated patients (Zhou et al., 2015). *Bifidobacterium longum* reduced serum Tnf-α induced by loperamide in mice (Wang et al., 2022). Similarly, *Lacticaseibacillus paracasei* reduced serum Tnf-α in human experiments (Zhang et al., 2021). Although a significant difference was not observed, as the concentration of the probiotic mixture increased, Tnf-α expression was decreased in the colon of rats (Figure 2). This tendency might help avoid the disruption of tight junction proteins and the consequent increase in intestinal permeability (Zhou et al., 2015).

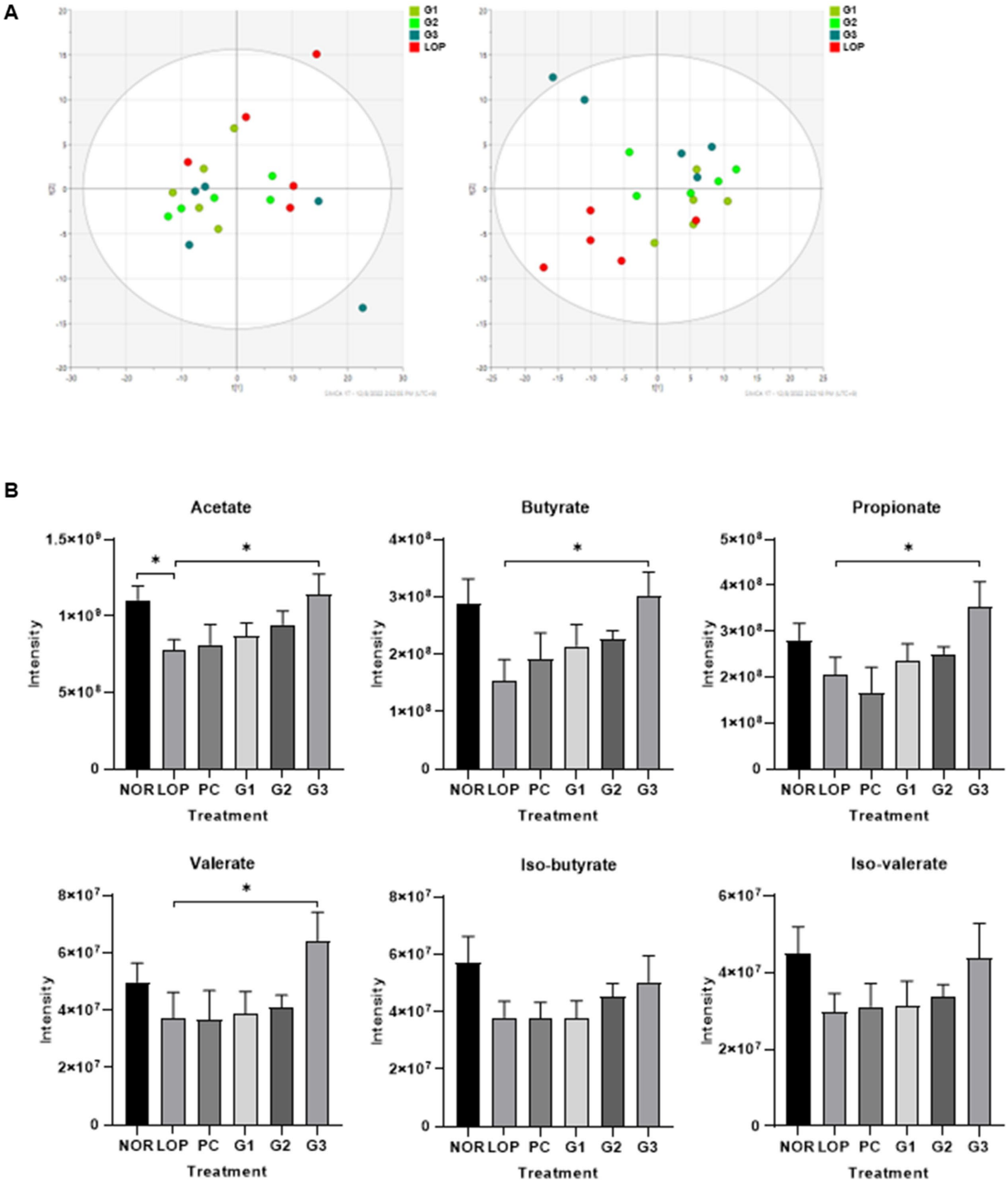

FIGURE 4
Changes in untargeted metabolites and short-chain fatty acids (SCFAs) by induction of constipation and administration of multi-strain probiotics Consti-Biome. **(A)** left indicate Principal Component Analysis (PCA) and right indicate Partial Least Squares Discriminant Analysis (PLS-DA) of metabolite profiling in fecal of loperamide administration (LOP), low concentration multi-strain probiotics administration (G1, 2×10^{8}cfu/mL), medium concentration multi-strain probiotics administration (G2, 2×10^{9}cfu/mL), and high concentration probiotic administration (G3, 2×10^{10}cfu/mL) groups. **(B)** Intensity of fecal SCFAs in normal control (NOR), LOP, positive control (PC), G1, G2, and G3. Data are mean ± SEM of 5 animals in **(B)**. *p<0.05, **p<0.01, significantly different from the LOP as per Mann–whitney u-test.

Alterations in metabolites are known to be caused by disease induction or the consumption of probiotics. *Lactobacillus* spp. and *Bifidobacterium* spp. can produce local metabolites (Wilms et al., 2021). Here, *in vivo*, changes in the metabolites in fecal samples by the mixture of probiotics that included *Lactobacillus* and *Bifidobacterium* were observed. Metabolites were clearly distinguished in partial squares discriminant analysis depending on the increasing concentration of probiotics (Figure 5A). A significant increase in

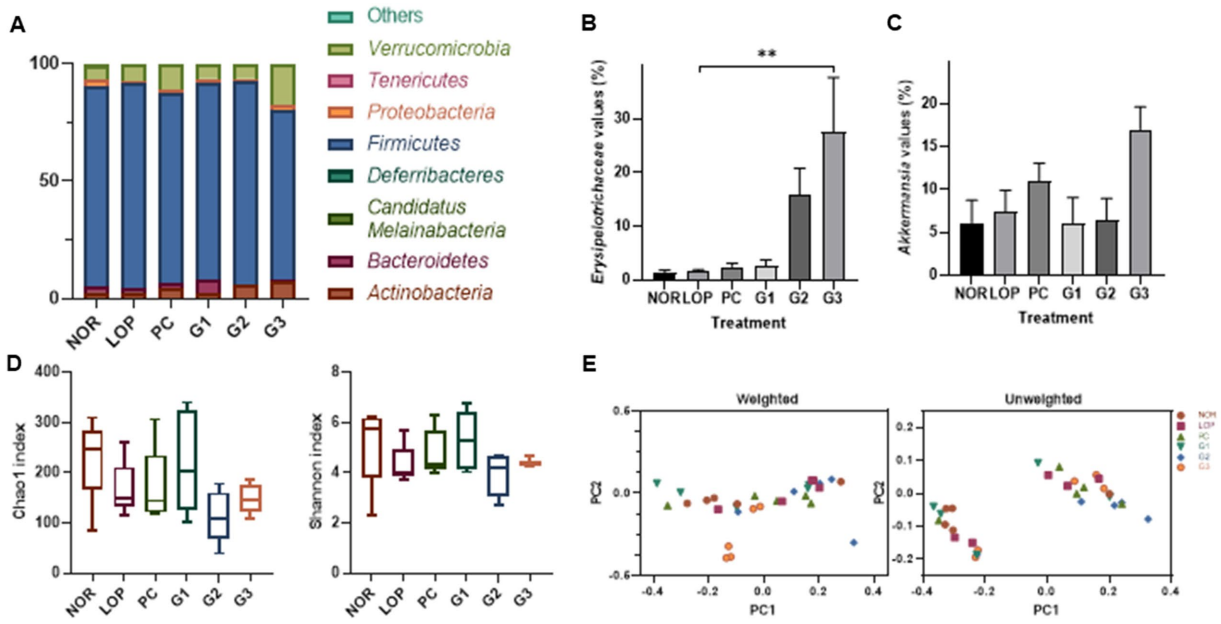

FIGURE 5
Microbiome changes by induction of constipation and intake of multi-strain probiotics Consti-Biome. **(A)** Is the representative phylum increase and decrease. **(B,C)** Are variations of the family *Erysipelotrichaceae* and the genus *Akkermansia*, respectively. **(D,E)** Exhibit the alpha-diversity beta-diversity, respectively. Microbiome of normal control (NOR), loperamide administration (LOP), positive control (PC), low concentration multi-strain probiotics administration (G1, 2×10^{8}cfu/mL), medium concentration multi-strain probiotics administration (G2, 2×10^{9}cfu/mL), and high concentration probiotic administration (G3, 2×10^{10}cfu/mL) groups were analyzed with fecal samples 2weeks after treatment with multi-strain probiotics. Data are mean ± SEM of 5 animals in **B** and **C**. *$p<0.05$, significantly different from the LOP as per one-way ANOVA with the Tukey's post-test.

SCFAs was observed, which are known to have positive effects on various diseases (Figure 4B). SCFAs are one of the key mechanisms by which probiotics improve chronic constipation. Among SCFAs, acetate, butyrate, propionate, and valerate were increased in rat cecal contents (Figure 4B). Treatment with probiotics for constipation has shown similar results (Wang et al., 2017; Zhao et al., 2022). In animal experiments, the absorption issue of SCFAs in the small intestine was resolved when acylated starches were fed for 1 month (Wang et al., 2020). These starches ameliorated constipation by increasing acetate-producing bacteria, which had a positive correlation with the small intestinal transit rate and water content of fecal samples (Wang et al., 2020). On the other hand, in the group consuming butylated starch, constipation was alleviated by butyrate-producing bacteria, which had a negative correlation with the first black stool defecation time (Wang et al., 2020). Although propionate did not directly relieve constipation, it was consistently observed in the feces of experimental groups fed probiotics in the constipation group (Zhuang et al., 2019; Wang et al., 2020, 2022). Its constipation-inhibiting effect might be due to an interaction control mechanism with butyrate (Zhuang et al., 2019). Valerate is also known to correlate with other SCFAs and the microbiome (Lu et al., 2022).

In addition, various constipation relief mechanisms of the SCFAs of probiotics have been studied. SCFAs can decrease luminal pH and improve gut motility by stimulating the contraction of colonic smooth muscle (Wilms et al., 2021). The activation of goblet cells and the increase in mucin-related gene expression are also closely related to SCFAs (Caballero-Franco et al., 2007). SCFAs have a local effect in the gut and affect intestinal immune cells (Ratajczak et al., 2019). In addition, they are also involved in colonic serotonin production (Reigstad et al., 2015). Therefore, SCFAs produced by probiotics could not only improve the pH and physical and chemical properties of the GI tract but could also stimulate the production of serotonin and mucin. These factors might contribute to constipation amelioration.

Numerous studies have shown that the microbiome affects host health through various mechanisms. It was observed that the phylum *Verrucomicrobiota*, the family *Erysipelotrichaceae*, and genus *Akkermansia* were significantly increased compared to the control group in this study (Figures 5A–C). An increase in *Erysipelotrichaceae* was observed in an animal model in which constipation was alleviated by Raffino-Oligosaccharide treatment (Liang et al., 2022). *Erysipelotrichaceae* are known to produce butyrate, one of the SCFAs. Butyrate can maintain barrier integrity by accelerating GI transit (Soret et al., 2010; Zhuang et al., 2019).

The genus *Akkermansia*, which was increased in this experiment (Figure 5C), was recently proposed as a next-generation probiotic (Liu Y. et al., 2022). The *Akkermansia* genus belongs to the phylum *Verrucomicrobiota*. Increasing levels of *Akkermansia* might significantly contribute to the increase in *Verrucomicrobiota* abundance identified by microbiome analysis here. Two species of *Akkermansia*, namely, *Akkermansia glycaniphila* and *Akkermansia muciniphila*, were reported at the time of writing (www.bacterio.net/index.html; Parte, 2018). Among them, studies on *A. muciniphila* have been relatively numerous. Mucosal health and mucosal immunity are proposed as the main potential mechanisms affecting host intestinal diseases (Liu M. J. et al., 2022). *A. muciniphila* is a commensal bacterium that could contribute to the maintenance of the integrity

(Reunanen et al., 2015) and dynamics (Kim et al., 2014; Singanayagam et al., 2022) of intestinal mucus. This bacterium is observed to decrease with the occurrence of various diseases and to increase with disease relief. An increase in *Akkermansia* abundance was observed following alleviation of irritable bowel syndrome (IBS) and inflammatory bowel disease (IBD) (Png et al., 2010; Rajilić-Stojanović et al., 2013). In animal studies, *A. muciniphila* and its extracellular vesicles alleviated colitis induced by dextran sulfate sodium (Kang et al., 2013; Zhai et al., 2019). *A. muciniphila* could reduce the expression of proinflammatory cytokines such as Tnf-α and IFN-γ in the colon (Zhai et al., 2019). Its outer membrane protein, Amuc-1,100 (Cani and Knauf, 2021), enhances intestinal barrier protection by activating Toll-like receptor 2 (TLR2)-mediated intracellular signaling in intestinal epithelial cells (Plovier et al., 2017). Furthermore, *Akkermansia* contributes to reducing the risk of metabolic syndrome, thereby alleviating complications of obesity and diabetes (Hagi and Belzer, 2021; Hasani et al., 2021; Yoon et al., 2021; Zhou et al., 2021). In addition, it can produce SCFAs (Swidsinski et al., 2009; Png et al., 2010; Arumugam et al., 2011; Rajilić-Stojanović et al., 2013). This suggests that the control of intestinal microflora by probiotics can help alleviate constipation.

The multi-strain probiotics used in this study showed improvement compared to the negative control group regardless of concentration in the number of fecal pellets, pH, and water content (Figures 1B–D). In addition, GI transit rate, one of the indicators related to constipation, showed a significant change at concentrations above G2 (Figure 1E). Based on the analyzed mechanisms for improving constipation, 5-HT1a and 5-HT1b, both serotonin-related factors, were significantly expressed in G1 and G2. Although the expression of these mRNA showed a tendency to increase in G3, no significant difference was observed compared to the LOP (Figure 2). However, the concentration of serotonin confirmed at the protein level did not increase in G1. On the other hand, an increase was observed in G3, which was not statistically significant at mRNA levels. Increased protein levels of serotonin were also observed in G2 (Figure 3). The difference between mRNA expression and protein expression may be caused by various factors. The relationship between mRNA levels and proteins can be influenced by steady state, long-term state, and short-term adaptation. Local availability of resources for protein biosynthesis and spatial and temporal mRNA variations also affect the relationship between protein levels and their coding transcripts. In addition, post-transcriptional processes in highly dynamic phases such as cell differentiation or stress response can lead to variation (Liu et al., 2016). Various factors can cause differences in protein and mRNA expression. In addition, supernatants of *Erysipelotrichaceae*, which were significantly observed in G2 and G3, were related to the serotonin pathway (Luna et al., 2017). Similarly, *Akkermansia* is associated with SCFAs (Koh et al., 2016). Therefore, microbiome changes may be closely involved in the expression of mRNAs, proteins, and SCFAs.

The multi-strain probiotics used in this study could modulate the microbiome and SCFAs and increase serotonin, mucin, and the GI transit rate. In addition, the number, pH, and water content in stools were improved. This treatment could relieve the symptoms of constipation. Taken together, the findings show that the bacterial mixture might increase the secretion of SCFAs, and as a result, constipation could be improved by increasing serotonin and mucin. Therefore, practically, this mixture could be applied to patients with constipation.

Conclusion

A multi-strain probiotics Consti-Biome containing a mixture of SynBalance® SmilinGut (*Lactobacillus plantarum, Lactobacillus rhamnosus*, *Bifidobacterium animalis* subsp. *lactis*; ROELMI), *L. plantarum* (UAS), *Lactobacillus acidophilus* (UAS), and *Streptococcus thermophilus* (Chong Kun Dang Bio) improved the number of fecal pellets, pH, and water content and gastrointestinal (GI) transit rate in rats with constipation induced by loperamide. The multi-strain probiotics could also increase the expression levels of serotonin and mucin-related genes. The improvement in constipation by the multi-strain probiotics could be a result of increasing the production of short-chain fatty acids (SCFAs) by altering the microbial composition, including the genus *Akkermansia*. These results showed the positive potential of using the probiotics in the treatment of constipation. However, clinical trials will be needed to evaluate the efficacy and effectiveness of the probiotics.

Data availability statement

The original contributions presented in the study are included in the article/Supplementary material, further inquiries can be directed to the corresponding authors.

Ethics statement

The animal study was reviewed and approved by Animal Experimental Ethics Committee (IACUC) of Hallym University (Hallym 2021-79).

Author contributions

B-YK and KTS contributed to conception and design of the study. J-JJ, RG, Y-JJ, HJP, BHM, MKJ, SJY, MRC, JC, and JHM organized the database and performed the statistical analysis. J-JJ wrote the first draft of the manuscript. RG, Y-JJ, MRC wrote sections of the manuscript. All authors contributed to manuscript revision, read, and approved the submitted version.

Funding

This research was supported by Hallym University Research Fund, the Basic Science Research Program through the National Research Foundation of Korea (NRF) funded by the Ministry of Education, Science and Technology (NRF-2020R1A6A1A03043026 and 2020R1I1A3073530), Korea Institute for Advancement of Technology (P0020622), and Bio Industrial Technology Development Program (20018494) funded by the Ministry of Trade, Industry and Energy (MOTIE, Korea).

Conflict of interest

The authors declare that the research was conducted in the absence of any commercial or financial relationships that could be construed as a potential conflict of interest.

Publisher's note

All claims expressed in this article are solely those of the authors and do not necessarily represent those of their affiliated organizations, or those of the publisher, the editors and the reviewers. Any product that may be evaluated in this article, or claim that may be made by its manufacturer, is not guaranteed or endorsed by the publisher.

Supplementary material

The Supplementary material for this article can be found online at: https://www.frontiersin.org/articles/10.3389/fmicb.2023.1174968/full#supplementary-material

References

Ambizas, E. M., and Ginzburg, R. (2007). Lubiprostone: a chloride channel activator for treatment of chronic constipation. *Ann. Pharmacother.* 41, 957–964. doi: 10.1345/aph.1K047

Ao, M., Sarathy, J., Domingue, J., Alrefai, W. A., and Rao, M. C. (2013). Chenodeoxycholic acid stimulates cl–secretion via cAMP signaling and increases cystic fibrosis transmembrane conductance regulator phosphorylation in T84 cells. *Am. J. Phys. Cell Phys.* 305, C447–C456. doi: 10.1152/ajpcell.00416.2012

Arora, T., and Sharma, R. (2011). Fermentation potential of the gut microbiome: implications for energy homeostasis and weight management. *Nutr. Rev.* 69, 99–106. doi: 10.1111/j.1753-4887.2010.00365.x

Arumugam, M., Raes, J., Pelletier, E., Le Paslier, D., Yamada, T., Mende, D. R., et al. (2011). Enterotypes of the human gut microbiome. *Nature* 473, 174–180. doi: 10.1038/nature09944

Böcker, U., Nebe, T., Herweck, F., Holt, L., Panja, A., Jobin, C., et al. (2003). Butyrate modulates intestinal epithelial cell-mediated neutrophil migration. *Clin. Exp. Immunol.* 131, 53–60. doi: 10.1046/j.1365-2249.2003.02056.x

Bosaeus, I. (2004). Fibre effects on intestinal functions (diarrhoea, constipation and irritable bowel syndrome). *Clin. Nutr. Suppl.* 1, 33–38. doi: 10.1016/j.clnu.2004.09.006

Burkitt, D. P., Walker, A., and Painter, N. S. (1972). Effect of dietary fibre on stools and transit-times, and its role in the causation of disease. *Lancet* 300, 1408–1411. doi: 10.1016/S0140-6736(72)92974-1

Caballero-Franco, C., Keller, K., De Simone, C., and Chadee, K. (2007). The VSL# 3 probiotic formula induces mucin gene expression and secretion in colonic epithelial cells. *Am. J. Physiol. Gastrointest. Liver Physiol.* 292, G315–G322. doi: 10.1152/ajpgi.00265.2006

Callahan, B. J., Mcmurdie, P. J., Rosen, M. J., Han, A. W., Johnson, A. J. A., and Holmes, S. P. (2016). DADA2: high-resolution sample inference from Illumina amplicon data. *Nat. Methods* 13, 581–583. doi: 10.1038/nmeth.3869

Camilleri, M. (2009). Serotonin in the gastrointestinal tract. *Curr. Opin. Endocrinol. Diabetes Obes.* 16, 53–59. doi: 10.1097/MED.0b013e32831e9c8e

Cani, P. D., and Knauf, C. (2021). A newly identified protein from *Akkermansia muciniphila* stimulates GLP-1 secretion. *Cell Metab.* 33, 1073–1075. doi: 10.1016/j.cmet.2021.05.004

Cao, H., Liu, X., An, Y., Zhou, G., Liu, Y., Xu, M., et al. (2017). Dysbiosis contributes to chronic constipation development via regulation of serotonin transporter in the intestine. *Sci. Rep.* 7:10322. doi: 10.1038/s41598-017-10835-8

Caporaso, J. G., Kuczynski, J., Stombaugh, J., Bittinger, K., Bushman, F. D., Costello, E. K., et al. (2010). QIIME allows analysis of high-throughput community sequencing data. *Nat. Methods* 7, 335–336. doi: 10.1038/nmeth.f.303

Chen, H.-J., Dai, F.-J., Chang, C.-R., Lau, Y.-Q., Chew, B.-S., and Chau, C.-F. (2019). Impact of dietary ingredients on the interpretation of various fecal parameters in rats fed inulin. *J. Food Drug Anal.* 27, 869–875. doi: 10.1016/j.jfda.2019.06.005

Coates, M. D., Mahoney, C. R., Linden, D. R., Sampson, J. E., Chen, J., Blaszyk, H., et al. (2004). Molecular defects in mucosal serotonin content and decreased serotonin reuptake transporter in ulcerative colitis and irritable bowel syndrome. *Gastroenterology* 126, 1657–1664. doi: 10.1053/j.gastro.2004.03.013

Collins, S. M. (1996). The immunomodulation of enteric neuromuscular function: implications for motility and inflammatory disorders. *Gastroenterology* 111, 1683–1699. doi: 10.1016/S0016-5085(96)70034-3

Costedio, M. M., Hyman, N., and Mawe, G. M. (2007). Serotonin and its role in colonic function and in gastrointestinal disorders. *Dis. Colon Rectum* 50, 376–388. doi: 10.1007/s10350-006-0763-3

Dimidi, E., Scott, S. M., and Whelan, K. (2020). Probiotics and constipation: mechanisms of action, evidence for effectiveness and utilisation by patients and healthcare professionals. *Proc. Nutr. Soc.* 79, 147–157. doi: 10.1017/S0029665119000934

Eor, J. Y., Tan, P. L., Lim, S. M., Choi, D. H., Yoon, S. M., Yang, S. Y., et al. (2019). Laxative effect of probiotic chocolate on loperamide-induced constipation in rats. *Food Res. Int.* 116, 1173–1182. doi: 10.1016/j.foodres.2018.09.062

Faigel, D. O. (2002). A clinical approach to constipation. *Clin. Cornerstone* 4, 11–18. doi: 10.1016/S1098-3597(02)90002-5

Forootan, M., Bagheri, N., and Darvishi, M. (2018). Chronic constipation: a review of literature. *Medicine* 97:e10631. doi: 10.1097/MD.0000000000010631

Fukuda, S., Toh, H., Hase, K., Oshima, K., Nakanishi, Y., Yoshimura, K., et al. (2011). Bifidobacteria can protect from enteropathogenic infection through production of acetate. *Nature* 469, 543–547. doi: 10.1038/nature09646

Fukumoto, S., Tatewaki, M., Yamada, T., Fujimiya, M., Mantyh, C., Voss, M., et al. (2003). Short-chain fatty acids stimulate colonic transit via intraluminal 5-HT release in rats. *Am. J. Phys. Regul. Integr. Comp. Phys.* 284, R1269–R1276. doi: 10.1152/ajpregu.00442.2002

Gershon, M. (2004). Serotonin receptors and transporters—roles in normal and abnormal gastrointestinal motility. *Aliment. Pharmacol. Ther.* 20, 3–14. doi: 10.1111/j.1365-2036.2004.02180.x

Guarino, M., Cheng, L., Cicala, M., Ripetti, V., Biancani, P., and Behar, J. (2011). Progesterone receptors and serotonin levels in colon epithelial cells from females with slow transit constipation. *Neurogastroenterol. Motil.* 23, 575–e210. doi: 10.1111/j.1365-2982.2011.01705.x

Hagi, T., and Belzer, C. (2021). The interaction of *Akkermansia muciniphila* with host-derived substances, bacteria and diets. *Appl. Microbiol. Biotechnol.* 105, 4833–4841. doi: 10.1007/s00253-021-11362-3

Han, J., Lin, K., Sequeira, C., and Borchers, C. H. (2015). An isotope-labeled chemical derivatization method for the quantitation of short-chain fatty acids in human feces by liquid chromatography–tandem mass spectrometry. *Anal. Chim. Acta* 854, 86–94. doi: 10.1016/j.aca.2014.11.015

Hasani, A., Ebrahimzadeh, S., Hemmati, F., Khabbaz, A., Hasani, A., and Gholizadeh, P. (2021). The role of *Akkermansia muciniphila* in obesity, diabetes and atherosclerosis. *J. Med. Microbiol.* 70:001435. doi: 10.1099/jmm.0.001435

Hatayama, H., Iwashita, J., Kuwajima, A., and Abe, T. (2007). The short chain fatty acid, butyrate, stimulates MUC2 mucin production in the human colon cancer cell line, LS174T. *Biochem. Biophys. Res. Commun.* 356, 599–603. doi: 10.1016/j.bbrc.2007.03.025

Hays, S., Jacquot, A., Gauthier, H., Kempf, C., Beissel, A., Pidoux, O., et al. (2016). Probiotics and growth in preterm infants: a randomized controlled trial, PREMAPRO study. *Clin. Nutr.* 35, 802–811. doi: 10.1016/j.clnu.2015.06.006

Henningsson, Ç. M., Margareta, E., Nyman, G., and Björck, I. M. (2001). Content of short-chain fatty acids in the hindgut of rats fed processed bean (*Phaseolus vulgaris*) flours varying in distribution and content of indigestible carbohydrates. *Br. J. Nutr.* 86, 379–389. doi: 10.1079/BJN2001423

Huang, J., Lin, B., Zhang, Y., Xie, Z., Zheng, Y., Wang, Q., et al. (2022). Bamboo shavings derived O-acetylated xylan alleviates loperamide-induced constipation in mice. *Carbohydr. Polym.* 276:118761. doi: 10.1016/j.carbpol.2021.118761

Jahng, J., Jung, I., Choi, E., Conklin, J., and Park, H. (2012). The effects of methane and hydrogen gases produced by enteric bacteria on ileal motility and colonic transit time. *Neurogastroenterol. Motil.* 24, 185–e92. doi: 10.1111/j.1365-2982.2011.01819.x

Jeong, J.-J., Park, H. J., Cha, M. G., Park, E., Won, S.-M., Ganesan, R., et al. (2022). The Lactobacillus as a probiotic: focusing on liver diseases. *Microorganisms* 10:288. doi: 10.3390/microorganisms10020288

Kalina, U., Koyama, N., Hosoda, T., Nuernberger, H., Sato, K., Hoelzer, D., et al. (2002). Enhanced production of IL-18 in butyrate-treated intestinal epithelium by stimulation of the proximal promoter region. *Eur. J. Immunol.* 32, 2635–2643. doi: 10.1002/1521-4141(200209)32:9<2635::AID-IMMU2635>3.0.CO;2-N

Kang, C.-S., Ban, M., Choi, E.-J., Moon, H.-G., Jeon, J.-S., Kim, D.-K., et al. (2013). Extracellular vesicles derived from gut microbiota, especially *Akkermansia muciniphila*,

protect the progression of dextran sulfate sodium-induced colitis. *PLoS One* 8:e76520. doi: 10.1371/journal.pone.0076520

Katoh, K., and Standley, D. M. (2013). MAFFT multiple sequence alignment software version 7: improvements in performance and usability. *Mol. Biol. Evol.* 30, 772–780. doi: 10.1093/molbev/mst010

Kim, B.-S., Song, M.-Y., and Kim, H. (2014). The anti-obesity effect of *Ephedra sinica* through modulation of gut microbiota in obese Korean women. *J. Ethnopharmacol.* 152, 532–539. doi: 10.1016/j.jep.2014.01.038

Kim, J. E., Lee, M. R., Park, J. J., Choi, J. Y., Song, B. R., Son, H. J., et al. (2018). Quercetin promotes gastrointestinal motility and mucin secretion in loperamide-induced constipation of SD rats through regulation of the mAChRs downstream signal. *Pharm. Biol.* 56, 309–317. doi: 10.1080/13880209.2018.1474932

Kim, J. E., Lee, Y. J., Kwak, M. H., Ko, J., Hong, J. T., and Hwang, D. Y. (2013). Aqueous extracts of Liriope platyphylla induced significant laxative effects on loperamide-induced constipation of SD rats. *BMC Complement. Altern. Med.* 13, 1–12. doi: 10.1186/1472-6882-13-333

Kim, J. E., Park, J. W., Kang, M. J., Choi, H. J., Bae, S. J., Choi, Y. S., et al. (2019a). Anti-inflammatory response and muscarinic cholinergic regulation during the laxative effect of *Asparagus cochinchinensis* in loperamide-induced constipation of SD rats. *Int. J. Mol. Sci.* 20:946. doi: 10.3390/ijms20040946

Kim, J. E., Yun, W. B., Lee, M. L., Choi, J. Y., Park, J. J., Kim, H. R., et al. (2019b). Synergic laxative effects of an herbal mixture of *Liriope platyphylla*, *Glycyrrhiza uralensis*, and *Cinnamomum cassia* in loperamide-induced constipation of Sprague Dawley rats. *J. Med. Food* 22, 294–304. doi: 10.1089/jmf.2018.4234

Koebnick, C., Wagner, I., Leitzmann, P., Stern, U., and Zunft, H. (2003). Probiotic beverage containing *Lactobacillus casei* Shirota improves gastrointestinal symptoms in patients with chronic constipation. *Can. J. Gastroenterol.* 17, 655–659. doi: 10.1155/2003/654907

Koh, A., De Vadder, F., Kovatcheva-Datchary, P., and Bäckhed, F. (2016). From dietary fiber to host physiology: short-chain fatty acids as key bacterial metabolites. *Cells* 165, 1332–1345. doi: 10.1016/j.cell.2016.05.041

Kusumo, P. D., Maulahela, H., Utari, A. P., Surono, I. S., Soebandrio, A., and Abdullah, M. (2019). Probiotic *Lactobacillus plantarum* IS 10506 supplementation increase SCFA of women with functional constipation. *Iran. J. Microbiol.* 11, 389–396. doi: 10.18502/ijm.v11i5.1957

Kwoji, I. D., Aiyegoro, O. A., Okpeku, M., and Adeleke, M. A. (2021). Multi-strain probiotics: synergy among isolates enhances biological activities. *Biology* 10:322. doi: 10.3390/biology10040322

Li, C., Nie, S.-P., Zhu, K.-X., Xiong, T., Li, C., Gong, J., et al. (2015). Effect of *Lactobacillus plantarum* NCU116 on loperamide-induced constipation in mice. *Int. J. Food Sci. Nutr.* 66, 533–538. doi: 10.3109/09637486.2015.1024204

Liang, Y., Wang, Y., Wen, P., Chen, Y., Ouyang, D., Wang, D., et al. (2022). The anti-constipation effects of raffino-oligosaccharide on gut function in mice using neurotransmitter analyses, 16S rRNA sequencing and targeted screening. *Molecules* 27:2235. doi: 10.3390/molecules27072235

Liu, M.-J., Yang, J.-Y., Yan, Z.-H., Hu, S., Li, J.-Q., Xu, Z.-X., et al. (2022). Recent findings in *Akkermansia muciniphila*-regulated metabolism and its role in intestinal diseases. *Clin. Nutr.* 41, 2333–2344. doi: 10.1016/j.clnu.2022.08.029

Liu, Y., Beyer, A., and Aebersold, R. (2016). On the dependency of cellular protein levels on mRNA abundance. *Cells* 165, 535–550. doi: 10.1016/j.cell.2016.03.014

Liu, Y., Yang, M., Tang, L., Wang, F., Huang, S., Liu, S., et al. (2022). TLR4 regulates RORγt+ regulatory T-cell responses and susceptibility to colon inflammation through interaction with *Akkermansia muciniphila*. *Microbiome* 10, 1–20. doi: 10.1186/s40168-022-01296-x

Lu, D., Pi, Y., Ye, H., Wu, Y., Bai, Y., Lian, S., et al. (2022). Consumption of dietary Fiber with different physicochemical properties during late pregnancy alters the gut microbiota and relieves constipation in sow model. *Nutrients* 14:2511. doi: 10.3390/nu14122511

Lu, Y., Yu, Z., Zhang, Z., Liang, X., Gong, P., Yi, H., et al. (2021). *Bifidobacterium animalis* F1-7 in combination with konjac glucomannan improves constipation in mice via humoral transport. *Food Funct.* 12, 791–801. doi: 10.1039/D0FO02227F

Lu, Y., Zhang, Z., Liang, X., Chen, Y., Zhang, J., Yi, H., et al. (2019). Study of gastrointestinal tract viability and motility via modulation of serotonin in a zebrafish model by probiotics. *Food Funct.* 10, 7416–7425. doi: 10.1039/C9FO02129A

Luna, R. A., Oezguen, N., Balderas, M., Venkatachalam, A., Runge, J. K., Versalovic, J., et al. (2017). Distinct microbiome-neuroimmune signatures correlate with functional abdominal pain in children with autism spectrum disorder. *Cell. Mol. Gastroenterol. Hepatol.* 3, 218–230. doi: 10.1016/j.jcmgh.2016.11.008

Makizaki, Y., Uemoto, T., Yokota, H., Yamamoto, M., Tanaka, Y., and Ohno, H. (2021). Improvement of loperamide-induced slow transit constipation by *Bifidobacterium bifidum* G9-1 is mediated by the correction of butyrate production and neurotransmitter profile due to improvement in dysbiosis. *PLoS One* 16:e0248584. doi: 10.1371/journal.pone.0248584

Martin, M. (2011). Cutadapt removes adapter sequences from high-throughput sequencing reads. *EMBnet. J.* 17, 10–12. doi: 10.14806/ej.17.1.200

Mezzasalma, V., Manfrini, E., Ferri, E., Sandionigi, A., La Ferla, B., Schiano, I., et al. (2016). A randomized, double-blind, placebo-controlled trial: the efficacy of multispecies probiotic supplementation in alleviating symptoms of irritable bowel syndrome associated with constipation. *Biomed. Res. Int.* 2016:4740907. doi: 10.1155/2016/4740907

Myllyluoma, E., Veijola, L., Ahlroos, T., Tynkkynen, S., Kankuri, E., Vapaatalo, H., et al. (2005). Probiotic supplementation improves tolerance to *Helicobacter pylori* eradication therapy–a placebo-controlled, double-blind randomized pilot study. *Aliment. Pharmacol. Ther.* 21, 1263–1272. doi: 10.1111/j.1365-2036.2005.02448.x

Park, M. I. (2011). Treatment of constipation. *Korean J. Med.* 80, 510–523.

Parte, A. C. (2018). LPSN–list of prokaryotic names with standing in nomenclature (Bacterio. Net), 20 years on. *Int. J. Syst. Evol. Microbiol.* 68, 1825–1829. doi: 10.1099/ijsem.0.002786

Plaza-Diaz, J., Ruiz-Ojeda, F. J., Gil-Campos, M., and Gil, A. (2019). Mechanisms of action of probiotics. *Adv. Nutr.* 10, S49–S66. doi: 10.1093/advances/nmy063

Plovier, H., Everard, A., Druart, C., Depommier, C., Van Hul, M., Geurts, L., et al. (2017). A purified membrane protein from *Akkermansia muciniphila* or the pasteurized bacterium improves metabolism in obese and diabetic mice. *Nat. Med.* 23, 107–113. doi: 10.1038/nm.4236

Png, C. W., Lindén, S. K., Gilshenan, K. S., Zoetendal, E. G., Mcsweeney, C. S., Sly, L. I., et al. (2010). Mucolytic bacteria with increased prevalence in IBD mucosa augmentin vitroutilization of mucin by other bacteria. *Am. J. Gastroenterol.* 105, 2420–2428. doi: 10.1038/ajg.2010.281

Rajilić-Stojanović, M., Shanahan, F., Guarner, F., and De Vos, W. M. (2013). Phylogenetic analysis of dysbiosis in ulcerative colitis during remission. *Inflamm. Bowel Dis.* 19, 481–488. doi: 10.1097/MIB.0b013e31827fec6d

Rambaut, A. (2009). *FigTree* v1.3.1. Available at: http://tree.bio.ed.ac.uk/software/figtree/.

Ratajczak, W., Rył, A., Mizerski, A., Walczakiewicz, K., Sipak, O., and Laszczyńska, M. (2019). Immunomodulatory potential of gut microbiome-derived short-chain fatty acids (SCFAs). *Acta Biochim. Pol.* 66, 1–12. doi: 10.18388/abp.2018_2648

Reigstad, C. S., Salmonson, C. E., Iii, J. F. R., Szurszewski, J. H., Linden, D. R., Sonnenburg, J. L., et al. (2015). Gut microbes promote colonic serotonin production through an effect of short-chain fatty acids on enterochromaffin cells. *FASEB J.* 29, 1395–1403. doi: 10.1096/fj.14-259598

Reunanen, J., Kainulainen, V., Huuskonen, L., Ottman, N., Belzer, C., Huhtinen, H., et al. (2015). *Akkermansia muciniphila* adheres to enterocytes and strengthens the integrity of the epithelial cell layer. *Appl. Environ. Microbiol.* 81, 3655–3662. doi: 10.1128/AEM.04050-14

Ríos-Covián, D., Ruas-Madiedo, P., Margolles, A., Gueimonde, M., De Los Reyes-Gavilán, C. G., and Salazar, N. (2016). Intestinal short chain fatty acids and their link with diet and human health. *Front. Microbiol.* 7:185. doi: 10.3389/fmicb.2016.00185

Sin, H.-J., Kim, K.-O., Kim, S.-H., Kim, Y.-A., and Lee, H.-S. (2010). Effect of resistant starch on the large bowel environment and plasma lipid in rats with loperamide-induced constipation. *J. Korean Soc. Food Sci. Nutr.* 39, 684–691. doi: 10.3746/jkfn.2010.39.5.684

Singanayagam, A., Footitt, J., Marczynski, M., Radicioni, G., Cross, M. T., Finney, L. J., et al. (2022). Airway mucins promote immunopathology in virus-exacerbated chronic obstructive pulmonary disease. *J. Clin. Invest.* 132:e120901. doi: 10.1172/JCI120901

Singh, N., Gurav, A., Sivaprakasam, S., Brady, E., Padia, R., Shi, H., et al. (2014). Activation of Gpr109a, receptor for niacin and the commensal metabolite butyrate, suppresses colonic inflammation and carcinogenesis. *Immunity* 40, 128–139. doi: 10.1016/j.immuni.2013.12.007

Soret, R., Chevalier, J., De Coppet, P., Poupeau, G., Derkinderen, P., Segain, J. P., et al. (2010). Short-chain fatty acids regulate the enteric neurons and control gastrointestinal motility in rats. *Gastroenterology* 138:e1774, 1772–1782.e4. doi: 10.1053/j.gastro.2010.01.053

Swidsinski, A., Loening-Baucke, V., and Herber, A. (2009). Mucosal flora in Crohn's disease and ulcerative colitis-an overview. *J. Physiol. Pharmacol.* 60, 61–71.

Tang, T., Wang, J., Jiang, Y., Zhu, X., Zhang, Z., Wang, Y., et al. (2022). *Bifidobacterium lactis* TY-S01 prevents Loperamide-induced constipation by modulating gut microbiota and its metabolites in mice. Frontiers. *Nutrition* 9:890314. doi: 10.3389/fnut.2022.890314

Walther, D. J., Peter, J.-U., Bashammakh, S., Hortnagl, H., Voits, M., Fink, H., et al. (2003). Synthesis of serotonin by a second tryptophan hydroxylase isoform. *Science* 299:76. doi: 10.1126/science.1078197

Wang, L., Cen, S., Wang, G., Lee, Y.-K., Zhao, J., Zhang, H., et al. (2020). Acetic acid and butyric acid released in large intestine play different roles in the alleviation of constipation. *J. Funct. Foods* 69:103953. doi: 10.1016/j.jff.2020.103953

Wang, L., Chai, M., Wang, J., Qiangqing, Y., Wang, G., Zhang, H., et al. (2022). *Bifidobacterium longum* relieves constipation by regulating the intestinal barrier of mice. *Food Funct.* 13, 5037–5049. doi: 10.1039/D1FO04151G

Wang, L., Chen, C., Cui, S., Lee, Y.-K., Wang, G., Zhao, J., et al. (2019). Adhesive Bifidobacterium induced changes in cecal microbiome alleviated constipation in mice. *Front. Microbiol.* 10:1721. doi: 10.3389/fmicb.2019.01721

Wang, L., Hu, L., Xu, Q., Yin, B., Fang, D., Wang, G., et al. (2017). *Bifidobacterium adolescentis* exerts strain-specific effects on constipation induced by loperamide in BALB/c mice. *Int. J. Mol. Sci.* 18:318. doi: 10.3390/ijms18020318

Wang, R., Sun, J., Li, G., Zhang, M., Niu, T., Kang, X., et al. (2021). Effect of *Bifidobacterium animalis* subsp. *lactis* MN-gup on constipation and the composition of gut microbiota. *Benefic. Microbes* 12, 31–42. doi: 10.3920/BM2020.0023

Wang, Y., Guo, Y., Chen, H., Wei, H., and Wan, C. (2018). Potential of *Lactobacillus plantarum* ZDY2013 and *Bifidobacterium bifidum* WBIN03 in relieving colitis by gut microbiota, immune, and anti-oxidative stress. *Can. J. Microbiol.* 64, 327–337. doi: 10.1139/cjm-2017-0716

Wilms, E., An, R., Smolinska, A., Stevens, Y., Weseler, A. R., Elizalde, M., et al. (2021). Galacto-oligosaccharides supplementation in prefrail older and healthy adults increased faecal bifidobacteria, but did not impact immune function and oxidative stress. *Clin. Nutr.* 40, 3019–3031. doi: 10.1016/j.clnu.2020.12.034

Wlodarska, M., Thaiss, C. A., Nowarski, R., Henao-Mejia, J., Zhang, J.-P., Brown, E. M., et al. (2014). NLRP6 inflammasome orchestrates the colonic host-microbial interface by regulating goblet cell mucus secretion. *Cells* 156, 1045–1059. doi: 10.1016/j.cell.2014.01.026

Yang, Y.-X., He, M., Hu, G., Wei, J., Pages, P., Yang, X.-H., et al. (2008). Effect of a fermented milk containing *Bifidobacterium lactis* DN-173010 on Chinese constipated women. *World J Gastroenterol: WJG* 14, 6237–6243. doi: 10.3748/wjg.14.6237

Ye, Y., Wang, Y., Yang, Y., and Tao, L. (2020). Aloperine suppresses LPS-induced macrophage activation through inhibiting the TLR4/NF-κB pathway. *Inflamm. Res.* 69, 375–383. doi: 10.1007/s00011-019-01313-0

Yoon, H. S., Cho, C. H., Yun, M. S., Jang, S. J., You, H. J., Kim, J.-H., et al. (2021). *Akkermansia muciniphila* secretes a glucagon-like peptide-1-inducing protein that improves glucose homeostasis and ameliorates metabolic disease in mice. *Nat. Microbiol.* 6, 563–573. doi: 10.1038/s41564-021-00880-5

Yu, J. S., Youn, G. S., Choi, J., Kim, C. H., Kim, B. Y., Yang, S. J., et al. (2021). *Lactobacillus lactis* and *Pediococcus pentosaceus*-driven reprogramming of gut microbiome and metabolome ameliorates the progression of non-alcoholic fatty liver disease. *Clin. Transl. Med.* 11:e634. doi: 10.1002/ctm2.634

Yuille, S., Reichardt, N., Panda, S., Dunbar, H., and Mulder, I. E. (2018). Human gut bacteria as potent class I histone deacetylase inhibitors *in vitro* through production of butyric acid and valeric acid. *PLoS One* 13:e0201073. doi: 10.1371/journal.pone.0201073

Zelante, T., Iannitti, R. G., Cunha, C., De Luca, A., Giovannini, G., Pieraccini, G., et al. (2013). Tryptophan catabolites from microbiota engage aryl hydrocarbon receptor and balance mucosal reactivity via interleukin-22. *Immunity* 39, 372–385. doi: 10.1016/j.immuni.2013.08.003

Zhai, R., Xue, X., Zhang, L., Yang, X., Zhao, L., and Zhang, C. (2019). Strain-specific anti-inflammatory properties of two *Akkermansia muciniphila* strains on chronic colitis in mice. *Front. Cell. Infect. Microbiol.* 9:239. doi: 10.3389/fcimb.2019.00239

Zhang, X., Chen, S., Zhang, M., Ren, F., Ren, Y., Li, Y., et al. (2021). Effects of fermented milk containing *Lacticaseibacillus paracasei* strain shirota on constipation in patients with depression: a randomized, double-blind, placebo-controlled trial. *Nutrients* 13:2238. doi: 10.3390/nu13072238

Zhao, Y., Liu, Q., Hou, Y., and Zhao, Y. (2022). Alleviating effects of gut micro-ecologically regulatory treatments on mice with constipation. *Front. Microbiol.* 13:956438. doi: 10.3389/fmicb.2022.956438

Zhou, Q., Costinean, S., Croce, C. M., Brasier, A. R., Merwat, S., Larson, S. A., et al. (2015). MicroRNA 29 targets nuclear factor-κB–repressing factor and Claudin 1 to increase intestinal permeability. *Gastroenterology* 148:e158, 158–169.e8. doi: 10.1053/j.gastro.2014.09.037

Zhou, Q., Pang, G., Zhang, Z., Yuan, H., Chen, C., Zhang, N., et al. (2021). Association between gut Akkermansia and metabolic syndrome is dose-dependent and affected by microbial interactions: a cross-sectional study. *Diabetes Metab. Syndr. Obes.* 14, 2177–2188. doi: 10.2147/DMSO.S311388

Zhuang, M., Shang, W., Ma, Q., Strappe, P., and Zhou, Z. (2019). Abundance of probiotics and butyrate-production microbiome manages constipation via short-chain fatty acids production and hormones secretion. *Mol. Nutr. Food Res.* 63:1801187. doi: 10.1002/mnfr.201801187

frontiers | Frontiers in Microbiology

TYPE Original Research
PUBLISHED 14 June 2023
DOI 10.3389/fmicb.2023.1192449

OPEN ACCESS

EDITED BY
Giuseppe Spano,
University of Foggia, Italy

REVIEWED BY
Nicola De Simone,
University of Foggia, Italy
Arun Karnwal,
Lovely Professional University, India

*CORRESPONDENCE
M. Y. Sreenivasa
✉ sreenivasamy@gmail.com;
✉ mys@microbiology.uni-mysore.ac.in

RECEIVED 23 March 2023
ACCEPTED 09 May 2023
PUBLISHED 14 June 2023

CITATION
Vanitha PR, Somashekaraiah R, Divyashree S, Pan I and Sreenivasa MY (2023) Antifungal activity of probiotic strain *Lactiplantibacillus plantarum* MYSN7 against *Trichophyton tonsurans*. *Front. Microbiol.* 14:1192449. doi: 10.3389/fmicb.2023.1192449

Antifungal activity of probiotic strain *Lactiplantibacillus plantarum* MYSN7 against *Trichophyton tonsurans*

P. R. Vanitha[1,2], Rakesh Somashekaraiah[1], S. Divyashree[1], Indranil Pan[3] and M. Y. Sreenivasa[1]*

[1]Department of Studies in Microbiology, University of Mysore, Mysuru, India, [2]Maharani's Science College for Women, Mysuru, India, [3]Department of Biosciences, School of Biosciences and Technology, Vellore Institute of Technology, Vellore, India

The primary objective of this study was to assess the probiotic attributes and antifungal activity of lactic acid bacteria (LAB) against the fungus, *Trichophyton tonsurans*. Among the 20 isolates screened for their antifungal attributes, isolate MYSN7 showed strong antifungal activity and was selected for further analysis. The isolate MYSN7 exhibited potential probiotic characteristics, having 75 and 70% survival percentages in pH3 and pH2, respectively, 68.73% tolerance to bile, a moderate cell surface hydrophobicity of 48.87%, and an auto-aggregation percentage of 80.62%. The cell-free supernatant (CFS) of MYSN7 also showed effective antibacterial activity against common pathogens. Furthermore, the isolate MYSN7 was identified as *Lactiplantibacillus plantarum* by 16S rRNA sequencing. Both *L. plantarum* MYSN7 and its CFS exhibited significant anti-*Trichophyton* activity in which the biomass of the fungal pathogen was negligible after 14 days of incubation with the active cells of probiotic culture (10^6 CFU/ml) and at 6% concentration of the CFS. In addition, the CFS inhibited the germination of conidia even after 72 h of incubation. The minimum inhibitory concentration of the lyophilized crude extract of the CFS was observed to be 8 mg/ml. Preliminary characterization of the CFS showed that the active component would be organic acids in nature responsible for antifungal activity. Organic acid profiling of the CFS using LC-MS revealed that it was a mixture of 11 different acids, and among these, succinic acid (9,793.60 μg/ml) and lactic acid (2,077.86 μg/ml) were predominant. Additionally, a scanning electron microscopic study revealed that CFS disrupted fungal hyphal structure significantly, which showed scanty branching and bulged terminus. The study indicates the potential of *L. plantarum* MYSN7 and its CFS to control the growth of *T. tonsurans*. Furthermore, *in vivo* studies need to be conducted to explore its possible applications on skin infections.

KEYWORDS

***L plantarum*, probiotic, *Trichophyton tonsurans*, antifungal activity, lactic acid bacteria**

Introduction

Dermatophytes are a group of pathogenic fungi that primarily cause superficial infections of hair, skin, and nails. The three genera of this group, i.e., *Trichophyton*, *Microsporum*, and *Epidermophyton*, cause significant diseases in human beings and other animals. *Trichophyton* is an anthropophilic species affecting only humans. Among the 40 species of dermatophytes that infect humans, the most common pathogens of scalp

infection–tinea capitis are *Trichophyton tonsurans* and *Microsporum canis* (White et al., 2014), and tinea capitis is considered to be the most infectious form of all tinea diseases (Müller et al., 2021).

According to the 2015 World Health Organization (WHO) report, dermatophytes affect ~25% of the world population (Petrucelli et al., 2020), affecting people of all age groups irrespective of whether they are immunocompromised or not (Segal and Elad, 2021). In the past 7–8 years, there has been an acute increase in difficult-to-treat, recurrent and chronic dermatophytosis in developing countries like India. Bongomin et al. (2017) estimated 21,073,423 cases of this infection in just 16 countries, with the majority of these cases in sub-Saharan Africa occurring predominantly in children (Hay, 2017; Nweze and Eke, 2018). In a study conducted in Sikkim, India, ~60.4% of patients gave a history of recurrent dermatophytosis (Sharma et al., 2017).

The infection can be effectively controlled with the use of antifungals, such as azoles and polyenes. However, most of these antifungals are known to cause side effects, such as liver damage, and elicit anaphylactic reactions (Chen et al., 2015). There are also many drug–drug interactions, which are potentially dangerous, especially in immunocompromised patients with conditions such as diabetes, renal failure, and liver dysfunction (Al-Khikani, 2020). In short, most of the clinically employed antifungals suffer from different drawbacks, such as toxicity, drug–drug interactions, no fungicidal effect, and high cost. In addition to this, there is an increase in the occurrence of resistance reported in clinically isolated strains from different regions of the world leading to failure in the treatment of mycoses. A unique multidrug-resistant *Trichophyton* species was isolated in North India showing a high rate of resistance to the three commonly used oral antifungal drugs, i.e., terbinafine, fluconazole, and griseofulvin (Singh et al., 2019). Similarly, terbinafine resistance was detected in the clinical isolates of *T. tonsurans* and *Trichophyton rubrum* at a rate of 2%, indicating the increasing number of antifungal-resistant dermatophytes (Salehi et al., 2018). In addition, there is a serious issue of cross-resistance noticed among the *Trichophyton* strains. For example, terbinafine-resistant *T. rubrum* exhibited cross-resistance to butenafine, tolnaftate, tolciclate, and naftifine (Sinha and Sardana, 2018). Hence, there is a persistent need for newer antifungal agents or formulations that are more effective and less toxic than those which are already in use (Iván et al., 2015; Bajpai et al., 2017).

In recent years, research on the possible use of natural products, such as plant products, beneficial microbes, namely PGPR and probiotics for clinical use, is gaining importance (Sreenivasa et al., 2011; Chennappa et al., 2016; Yooussef et al., 2016; Achar et al., 2020). Probiotics such as lactic acid bacteria (LAB) widely used in the food and pharmaceutical industries are proven to be beneficial and have been used for a number of disease applications and are generally regarded as safe for human use, making them ideal candidates for the development of new therapeutic formulations (Kleerebezem et al., 2017). LAB can potentially produce compounds such as enzymes, vitamins, organic acids, bacteriocins, and other metabolites (Arena et al., 2018). Several of these low molecular weight biomolecules have been isolated and shown to have the potential to inhibit fungal growth (Le Lay et al., 2016; Bukhari et al., 2020). Because LAB are naturally present in many foods (Rawat et al., 2018) and are also associated with health in the mammalian intestine, it is possible that antifungal agents from these do not induce side effects in humans, although this obviously warrants further investigation.

The antifungal activity of probiotic strains, specifically LAB, has been screened with promising results against tinea (Ajah, 2016; Mehdi-Alamdarloo et al., 2016). There are many cases in which probiotics are administered together with conventional drugs clinically for controlling fungal infections such as vulvovaginal candidiasis (Russo et al., 2018), and patents have been obtained for probiotic formulations to be used as topical applications (Angeles and Angeles, 2019). The results obtained from these studies are encouraging and confirm that probiotics and their products are a promising alternative for antifungal treatment.

One of the ideal sources to look for probiotics to fight against indigenous fungal pathogens is the traditional fermented foods prepared locally and have been in use for generations. Different *Lactiplantibacillus* spp isolated from such fermented foods have been examined with success for their antifungal activity (Arena et al., 2018) Although one of the best-known probiotic species, *Lactiplantibacillus plantarum*, has been explored for its antifungal activity against *Aspergillus* spp (Bukhari et al., 2020), *Penicillium* spp (Wang et al., 2012), *Fusarium proliferatum* (Deepthi et al., 2016), and *T. rubrum* (Danial et al., 2021), its effect on *Trichophyton tonsurans* is yet to be investigated.

In the present study, we have analyzed the *in vitro* antifungal activity of a specific probiotic isolate *L. plantarum* MYSN7 from a traditional fermented food, Haria, and have demonstrated the significant effect of the probiotic culture and its cell-free supernatant against *T. tonsurans*.

Materials and methods

Preparation of fungal spore suspension

The dermatophyte culture *Trichophyton tonsurans* (MTCC 8475) was procured for this study. The subcultures were grown on Sabouraud dextrose agar (SDA) plates at 30°C for 10 days and preserved at 4°C until further use. *Trichophyton tonsurans* spores were harvested from a 10-day-old culture plate by flooding it with phosphate-buffered saline and gently scraping the surface using a sterile inoculation loop. The spore concentration was adjusted to 10^6 spores/ml using a hemocytometer for further analysis.

Preparation of LAB suspension and freeze-dried cell-free supernatant

Haria, a fermented rice beverage that is popular among the rural tribe of West Bengal and East-Central India (Bengal et al., 2014), was prepared in the laboratory by inoculating cooked and dried rice with the starter culture bakhar, which is collected from five different sources. The inoculated rice sample was fermented for 14 days at room temperature. The fermented liquor was further used for the isolation of LAB adopting the method of Rao et al. (2015). The sample was first enriched in de Man Rogosa Sharpe (MRS) broth under anaerobic conditions at 37°C for 24 h. The enriched stock

was then serially diluted using phosphate-buffered saline, spread on MRS agar plates, and incubated under the same conditions. The discrete colonies were further sub-cultured onto MRS agar plates.

Each LAB strain was maintained in glycerol stock. To obtain the cell-free supernatant (CFS), 300 µl of LAB cell suspension (10^6 CFU/ml) was inoculated in 30 ml of MRS broth and incubated at 37°C for 48 h. The CFS was obtained by centrifuging the broth at 3,000 rpm for 15 min at 4°C. It was then sterilized by filtration using a 0.2-µm syringe filter (AXIVA) and freeze-dried aseptically (Danial et al., 2021).

LAB preliminary identification and characterization

Preliminary identification was performed through microscopic analysis and biochemical tests including gram staining, catalase test, bile salt hydrolysis (0.3% ox gall), osmotic stress tolerance (3, 5, and 7% NaCl), and carbohydrate fermentation. The growth of the isolates at different temperatures (4, 10, 37, and 45°C) was conducted and recorded (Ni et al., 2015).

Screening of LAB for its antifungal activity

The antifungal activity of the LAB isolates was examined using the agar overlay method against *T. tonsurans*, as per the procedure of Quattrini et al. (2018). Log phase MYSN7 culture was streaked as 2-cm lines on MRS agar plates and incubated at 37°C for 24 h. Then, 1 ml of conidial suspension (10^6 spores/ml) was mixed with 100 ml molten and cooled SDA medium containing 0.7% agar. The medium containing spore suspension was gently overlaid on the MRS plates with bacterial streaks, maintained undisturbed for solidification, and then incubated at 30°C for 7 days. The activity was graded based on the diameter of the zone of inhibition (+++ >8%−10% area of the plate showing zone of inhibition, ++ 3–8% of the plate showing zone of inhibition, + visible inhibition only above the streak, and – no visible inhibition). The bacterial isolate showing the maximum zone of inhibition was taken for further studies.

Molecular characterization

The LAB isolate MYSN7 with potential antifungal activity was identified by 16S rRNA amplification followed by Sanger sequencing. DNA isolation was carried out using the phenol–chloroform–isoamyl alcohol method. The purified DNA was amplified by PCR using the primer pairs 8F-(5′GAGTTTGATCCTGGCTCAG3′) and 1391R-(5′GACGGGCGGTGWGTRCA3′) (Lane et al., 1985). Following identification, a phylogenetic tree was constructed using the MEGA-X software by neighbor-joining method. The sequence has been submitted to NCBI GenBank and an accession number was obtained.

Determination of growth kinetics

The isolate MYSN7 was inoculated in 15 ml MRS broth and incubated overnight. Furthermore, it was transferred to a fresh medium in a 96-well plate, and the absorbance was measured every 2 h for 24 h at 600 nm. The readings were taken and graphically represented (Somashekaraiah et al., 2021).

Determination of probiotic activity assays

Acid tolerance and bile tolerance

The isolate's ability to tolerate the gastric pH and bile was tested as per the protocol of Yadav et al. (2016) with minor modifications. For this, overnight culture of the LAB was inoculated in two sets of MRS broth tubes, which have been adjusted to pH 2 and pH 3. Similarly, broth containing 0.3% ox gall was inoculated with the same culture. All the tubes were incubated at 37°C. Samples were withdrawn each hour for 3 h, and OD_{600} was measured. The survival percentage of MYSN7 was calculated using the formula (OD test/OD control) × 100.

Auto-aggregation

The isolate grown overnight was centrifuged at 8,000 rpm for 10 min, and the pellet was resuspended in 5 ml of PBS adjusting the OD to 0.25 ± 0.05 at 600 nm. The sample was allowed to stand at 37°C, and the upper suspension was checked for absorbance (OD_{600}) at intervals of 0, 1, 2, 3, and 4 h. The aggregation was measured by applying the formula auto-aggregation % = $[1 - (A_t/A_0) \times 100]$, where A_t represents the absorbance at a particular time and A_0 represents the initial absorbance (Somashekaraiah et al., 2019).

Cell surface hydrophobicity

MYSN7 overnight culture was suspended in 3 ml of PBS and adjusted to OD_{600} of 0.25 ± 0.05. Then, 1 ml of xylene was added, mixed gently, and kept undisturbed at 37°C for phase separation. After every hour for 3 h, the lower aqueous phase was drawn and OD_{600} was measured. The percent of hydrophobicity was calculated using the formula $[(A_0 - A_t/A_0)] \times 100$, where A_0 is the initial absorbance and A_t is the absorbance of the aqueous phase at time t (Rokana et al., 2018).

Antibiotic susceptibility profile

Probiotic isolates should meet the safety standards for application in food and humans. One such assay that is routinely carried out is the antibiotic susceptibility profile to the commonly used antibiotic as given in EFSA guidelines. The sensitivity pattern of the MYSN7 to these antibiotics was tested by the Kirby–Bauer disc diffusion procedure. The diameter of the zone of inhibition (ZOI) was measured, and the antibiotic sensitivity pattern was interpreted as sensitive, intermediate, or resistant following the CLSI (2014) guidelines.

Antibacterial activity

This was assessed by the microtiter plate technique using the method described by Somashekaraiah et al. (2019). The CFS of the isolate MYSN7 was tested against the common pathogens *Escherichia coli* (ATCC 25922), *Pseudomonas aeruginosa* (ATCC 15422), *Staphylococcus aureus* (ATCC 6538), *Klebsiella pneumoniae* (MTCC 7407), and *Salmonella paratyphi* (ATCC 9150). Then, 50 µl of the sterile CFS and 50 µl of the bacterial suspension were added to the wells with the final cell concentration of ~10^8 CFU/ml. It was made up to 200 µl using the Luria–Bertani broth and incubated at 37°C. Wells having uninoculated LB broth and broth inoculated with bacterial suspension were maintained as negative and positive controls, respectively. OD was recorded at 600 nm after 24 h of incubation, and the percentage inhibition of growth was calculated using the formula $[(OD_{Control} - OD_{Test})/OD_{Control}] \times 100$.

Hemolytic activity

This test was performed for observing the hemolytic activity of the isolate. The overnight culture was streaked on the blood agar plate (5% sheep blood) and incubated at 37°C for 24 h. *Staphylococcus aureus* (MTCC 87) was streaked on another blood agar plate as a positive control. The plates were observed for α (partial), β (complete), or γ (no) hemolysis (Yadav et al., 2016).

Analysis of antifungal activity

Co-inoculation assay

To determine the effect of MYSN7 on the growth kinetics of *T. tonsurans*, the co-inoculation assay as described by Deepthi et al. (2016) was performed. Modified MRS medium (mMRS) was prepared according to the composition given (bacteriological peptone 5 g/L, mycological peptone 5 g/L, beef extract 10 g/L, yeast extract 5 g/L, dextrose 20 g/L, $MgSO_4$ 0.10 g/L, $MnSO_4$ 0.05 g/L, and K_2HPO_4 2 g/L). The medium is devoid of antifungal substances, such as sodium acetate, polysorbate 80, and ammonium citrate. Then, 100 µl of overnight LAB culture (10^6 cfu/ml) and 100 µl of conidial suspension (10^6 spores/ml) were inoculated in 50 ml of mMRS broth. At different intervals of incubation (3, 7, 10, and 14 days), the mycelial mass was separated by filter paper and the weight was measured after drying at 80°C. Then, 50 ml of mMRS broth with only the mold spores was kept as a control. The experiment was performed in triplicates.

Fungal biomass inhibition by CFS-MYSN7

A biomass inhibition assay was determined using the protocol described by Quattrini et al. (2018). Then, 50 ml of sterile SDB was supplemented with different concentrations of sterile CFS (2%, 4%, 6%, 8%, and 10%), inoculated with *T. tonsurans* spores (10^6 spores/ml), and incubated at 30°C. Then, 50 ml of SDB inoculated with spores was maintained as a control. After 10 days, the percentage of inhibition was calculated by comparing the weight of the mycelial mat with that of the control.

Conidial germination inhibition assay

The effect of CFS-MYSN7 on the conidial germination of *T. tonsurans* was determined using a 24-well microtiter plate adopting the method of Guo et al. (2011) with some modifications. In the well, 200 µl of CFS-MYSN7 and 100 µl of conidial suspension (10^6 spores/ml) were added and made up to 1 ml using SDB. The well containing the fungal spores and the broth medium without CFS was kept as a control. The plate was incubated at 30°C, and the conidial germination was observed at 2, 4, 8, 16, 24, 48, and 72 h by mounting 10 µl of sample on a microscopic slide and observed under the phase contrast microscope (Carl Zeiss AXIO, Germany) with bright-field illumination. Germinated conidia were counted using a hemocytometer, and the percentage of conidial germination was calculated by applying the formula: [number of germinated conidia/total conidia counted] × 100.

Determination of MIC

Freeze-dried CFS powder (CFSp) of LpMYSN7 was prepared to find the minimum inhibitory concentration against *T. tonsurans*. The standard antifungal drug ketoconazole (HI Media, Mumbai, CMS4322) was used as a positive control. Minimum inhibitory concentration (MIC) determination of the CFSp-LpMYSN7 was carried out following the procedure of EUCAST antifungal MIC methods for molds (EUCAST E.DEF 9.3 December 2015) using the broth microdilution method. For MIC determination, 10 µl of conidial suspension (10^4 spores/ml) was taken in a 96-well microtiter plate, and 190 µl of different concentrations of CFSp (8 mg/ml—0.0625 mg/ml) prepared using the serial double dilution method was added. Similarly, the procedure was repeated for the standard drug ketoconazole with concentrations of 8–0.065 µg/ml. The plate was incubated at 30°C for 72 h before observing the growth inhibition. MIC was determined as the lowest concentration of the extract inhibiting visual growth of the test cultures. Three replications were conducted to confirm antifungal activity (Arasu et al., 2014).

Residual bioactivity of CFS-MYSN7

To understand the chemical nature of the antifungal compound in the CFS, the effect of different factors such as heat, pH, proteases, extended storage, and freeze–thaw cycle on the CFS-LpMYSN7 was performed following the method of Kang et al. (2011) with modifications. To determine the effect of heat, the CFS was kept in an 80°C water bath for 20 min and cooled. To nullify the effect of bacteriocin-like compounds, 5 ml of CFS was treated with proteinase-K (1 mg/ml) and incubated for 3 h at 37°C and the enzyme was then heat-inactivated at 80°C for 5 min (Jamwal et al., 2019). The pH of the CFS was adjusted to 7 using sterile 1 M NaOH to neutralize the antifungal activity of organic acids present. To test the effect of freeze–thaw cycle, 1 ml of CFS was frozen at −20°C for 24 h and thawed for 20 min at 4°C (Ponce et al., 2008). To know the efficiency of the antifungal activity of CFS after long-term storage, it was kept stored at −20°C for 2 months before use.

10.3389/fmicb.2023.1192449

TABLE 1 Preliminary characterization of LAB strains.

Assays	Isolates		
	MYSN6	MYSN7	MYSY1
Gram's staining	+	+	+
Morphology	Rod	Rod	Rod
Catalase test	–	–	–
Citrate utilization test	–	–	–
Bile salt hydrolysis (0.3%)	+	+	+
Growth at NaCl			
3%	+	+	+
5%	+	+	+
7%	+	+	+
Growth of isolates at various temperature			
4°C	–	–	–
10°C	+	+	+
37°C	++	++	++
45°C	+	+	+
Fermentation of sugars	Hetero	Hetero	Hetero
D-Glucose	++	++	+
D-Arabinose	+++	+++	+++
Lactose monohydrate	+++	+++	+++
D-Sorbitol	+++	+++	+++
D-Raffinose	+++	+++	+++
Mannitol	+++	+++	++
D-Xylose	++	++	+
L-Arabinose	++	++	++
D-Maltose	+++	+++	+++
D-Fructose	+++	+++	+++

+ (weak growth); ++ (good growth); + + + (very good growth); – (no growth); hetero, heterofermentative.

All the above-treated CFS were tested for residual anti-*Trichophyton* activity using the microdilution method using 24-well polystyrene flat-bottomed cell culture plate (NEST Biotechnology Co., Ltd, China). Then, 200 µl of treated CFS was mixed with 100 µl conidial suspension (10^6 spores/ml) and made up to 1 ml using SDB medium. The well containing conidial suspension with SDM alone was kept as control. The plate was incubated at 30°C and observed visually for growth inhibition after 7 days.

Organic acid profiling of the CFS-MYSN7 using LC-MS/MS

The extraction of organic acids was performed as described by Ribeiro et al. (2007). An aliquot of 500 µl of the sample was made up to 5 ml using 80% methanol. From this, 0.1 ml was taken and made up to 1 ml with mobile phase and then filtered, and 4 µl of this was injected into the LC-MS/MS (Waters UPLC H class system fitted with TQD-MS/MS system) for further analysis. The analytical column used was a 2.1 × 50 mm UPLC BEH-Amide column (Waters) with 1.7 µm particles, protected by a Vanguard 2.1 × 5 mm BEH-Amide with 1.7 µm particle size guard column (Waters). The column temperature was maintained at 25°C. The sample injection volume was 4 µl. The eluted organic acids were monitored using the TQD-MS/MS (Waters, USA) system, which was optimized for the detection and quantification of organic acids analysis (Kuwaki et al., 2002).

Scanning electron microscopic analysis

To observe the effect of MYSN7 on the mycelial morphology of *T. tonsurans,* SEM analysis was performed on treated and untreated fungal mycelial structures (Chandra, 2013). Fungal mycelia were picked from both treated and control plates for the study. The dehydrated mycelia were mounted on an aluminum stub with carbon tape, coated with gold–palladium alloy, and observed under the EVO LS 15 Scanning Electron Microscope (Carl Zeiss, Germany).

Statistical analysis

The data obtained from this study were the mean of three replicates expressed as mean ± standard deviation and analyzed using two-way analysis of variance (ANOVA) using the software GraphPad Prism version 8.0.2 (263) (GraphPad Software Inc.). Values of $p < 0.05$ were considered to be statistically significant.

Results

Preliminary identification and characterization of LAB

A total of 20 LAB strains were isolated from Haria—the fermented rice beverage. The chosen LAB isolates were Gram-positive, rod-shaped, and catalase negative. The three strains that survived the preliminary screening for LAB included MYSN6, MYSN7, and MYSY1. The physiological characteristics of these three strains have been tabulated (Table 1).

Screening of antifungal activity

The antifungal activity of the chosen strains was examined using the agar overlay method and was graded based on the diameter of the inhibition zone. The activity of MYSN7 against *T. tonsurans* was graded as +++ as the zone of inhibition covering the area of >8%−10% of the agar plate, whereas the activity of MYSN6 and MYSY1 was graded as ++ as the zone of inhibition covered was 3%−8% of the agar plate. Based on the observation, the LAB isolate MYSN7 was selected for further analysis (Figure 1).

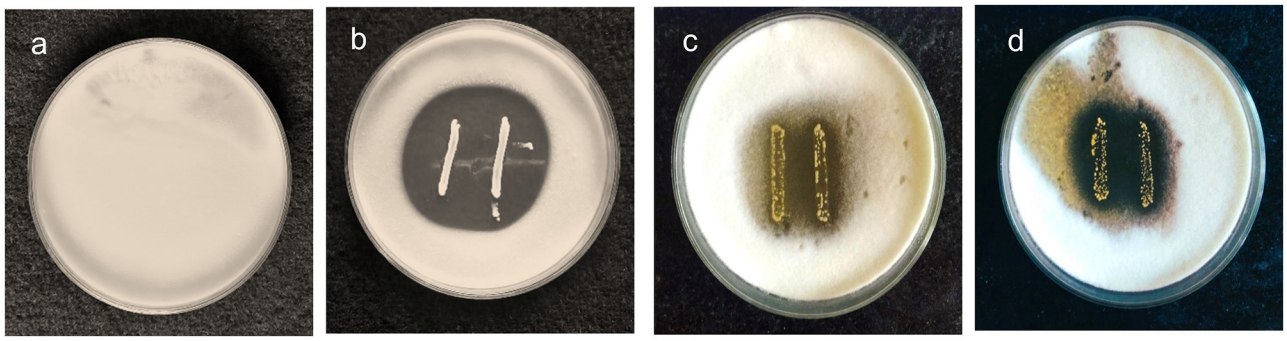

FIGURE 1
Agar overlay plates showing the growth inhibition of *T. tonsurans* in the presence of probiotic isolates. **(a)** Control plate of *T. tonsurans*. **(b)** Antifungal activity of MYSN7. **(c)** Antifungal activity of MYSN6. **(d)** Antifungal activity of MYSY1.

FIGURE 2
Molecular characterization and phylogenetic analysis of MYSN7. Phylogenetic tree showing the relationship between different *Lactobacillus* spp. The dendrogram was constructed based on the neighbor-joining method.

Molecular characterization

MYSN7 isolate showing maximum antifungal activity was identified using a molecular method. The isolated genomic DNA was quantified using nanodrop and found to be 733 ng/μl. The quality of the PCR amplified product was checked with agarose gel electrophoresis. By 16S rRNA sequencing, the isolate MYSN7 was found to be *L. plantarum,* and the sequence was deposited in NCBI GenBank with the accession number MZ470276. The phylogenetic tree constructed using the neighbor-joining method is shown in Figure 2.

Growth kinetics of *Lp*MYSN7

The growth pattern of the identified strain *L. plantarum* MYSN7 (LpMYSN7) was analyzed by plotting the graph with the *Y*-axis showing the OD of the growing culture at 600 nm and the *X*-axis showing the time of incubation in hours (Figure 3D). For the first 2–3 h, there was no increase in the OD value, and after 4 h of incubation, there was a logarithmic increase in the growth of this bacterium that continued for 14 h. After this, there was a stationary period of 6 h and a subsequent decrease in the OD for the last 2 h of incubation.

Probiotic attributes of LpMYSN7

Studying the probiotic attributes of the LAB isolates helps in the *in vitro* assessment of the survival and colonization of the isolate in the digestive system. LpMYSN7 showed an average survival percentage of 75% in pH 3 and a 70% survival percentage in pH 2 after 3 h of incubation when compared to the control (Figure 3A). The percentage of tolerance to 0.3% ox gall after 3 h of incubation was 68.73% (Figure 3B). The isolate showed moderate hydrophobicity of 48.87% after 3 h of incubation with the hydrocarbon xylene, and the auto-aggregation percentage was 80.62% after 4 h of incubation.

10.3389/fmicb.2023.1192449

Antibiotic susceptibility of LpMYSN7

The susceptibility profile of the LAB isolate to the commonly used antibiotics needs to be assessed before it is employed for human use. The antibiotics that were used for this study and the sensitivity pattern of LpMYSN7 are shown in Table 2. The sensitivity characteristic of the organism was determined by measuring the diameter of the ZOI and referring to the interpretative chart given in the catalog. It was found to have sensitivity toward ampicillin, gentamycin, kanamycin, chloramphenicol, erythromycin, clindamycin, tetracycline, and tylosine. There is moderate sensitivity for streptomycin, and the organism is resistant to vancomycin (Figure 4).

Antibacterial activity

The cell-free supernatant of LpMYSN7 shows strong antibacterial activity against common enteric pathogens as shown in Figure 3C. The inhibition percentages were 88.01%, 77.45%, 76.59%, 94.68%, and 93.17% against *S. aureus, S. paratyphi, K. pneumoniae, E. coli, and P. aeruginosa,* respectively.

Safety evaluation

Hemolytic activity of the probiotic isolate was observed on the blood agar plate to confirm its safety. It showed no hemolysis, which

TABLE 2 Antibiotic sensitivity profile of *L. plantarum* MYSN7.

Antibiotic used	Zone of inhibition (mm)	Sensitivity pattern
Ampicillin (10 μg/disc)	38.5	Sensitive
Vancomycin (30 μg/disc)	0	Resistant
Gentamycin (10 μg/disc)	17	Sensitive
Kanamycin (30 μg/disc)	13	Sensitive
Streptomycin (10 μg/disc)	17.5	Moderately sensitive
Chloramphenicol (30 μg/disc)	30.5	Sensitive
Erythromycin (15 μg/disc)	30.5	Sensitive
Clindamycin (2 μg/disc)	24.5	Sensitive
Tetracycline (30 μg/disc)	21.5	Sensitive
Tylosine (15 μg/disc)	27.5	Sensitive

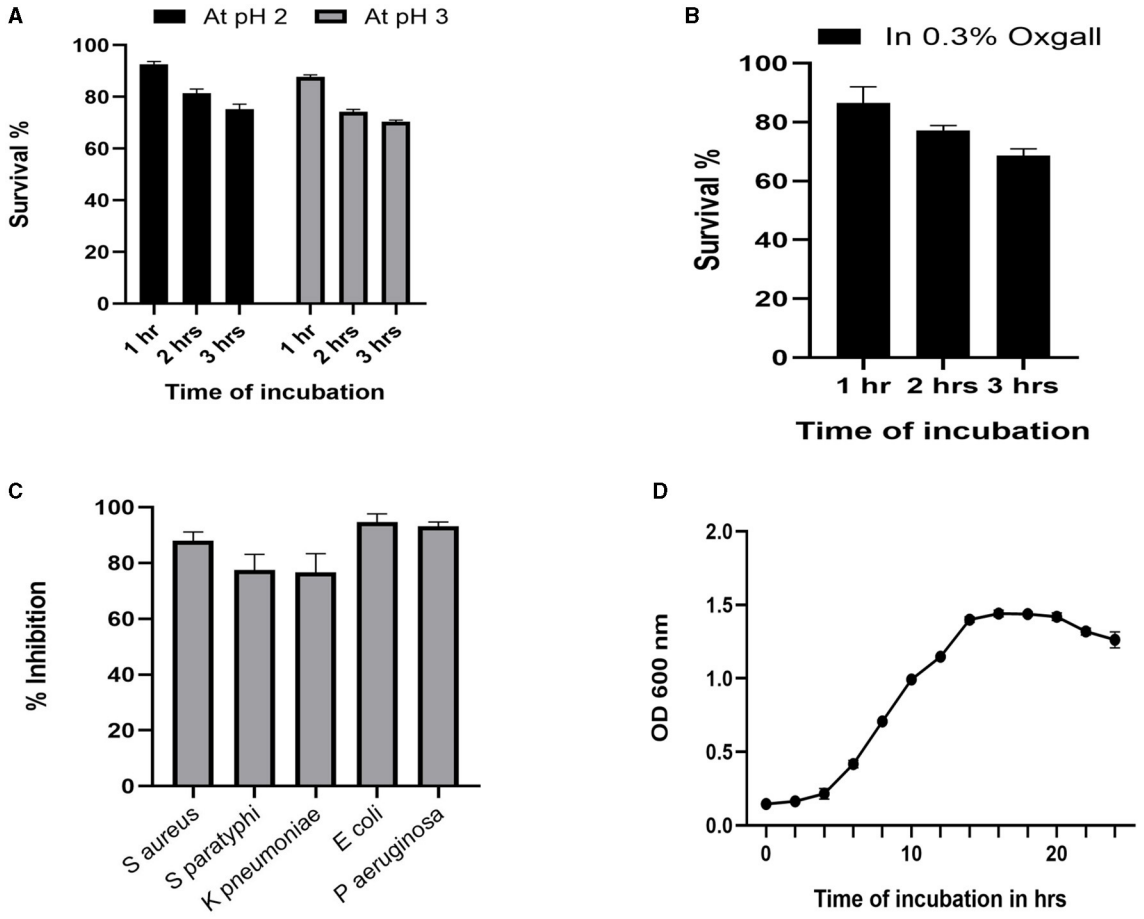

FIGURE 3
Probiotic properties of *Lp*MYSN7. **(A)** Survival percentage of the isolate at pH2 and pH3. **(B)** Survival percentage of the isolate in the presence of 0.3% ox gall. **(C)** Antibacterial activity of LpMYSN7 CFS against the common pathogens. **(D)** Growth curve of LpMYSN7 with logarithmic growth phase from 4 to 14 h. Data shown are mean ± SE of triplicate values of independent experiments and differ significantly ($p < 0.0001$).

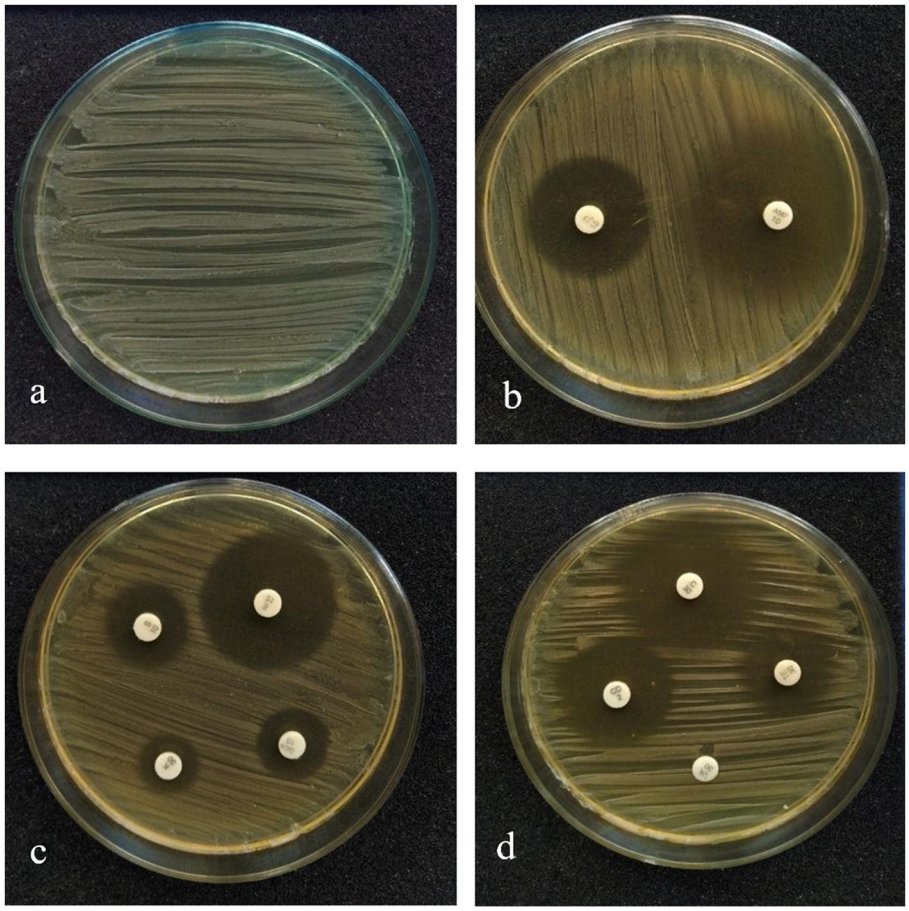

FIGURE 4
Antibiotic sensitivity pattern of LpMYSN7. **(a)** Control plate. **(b)** ZOI for ampicillin and gentamycin. **(c)** ZOI for kanamycin, tylosine, and clindamycin. **(d)** ZOI for tetracycline, erythromycin, chloramphenicol, and streptomycin.

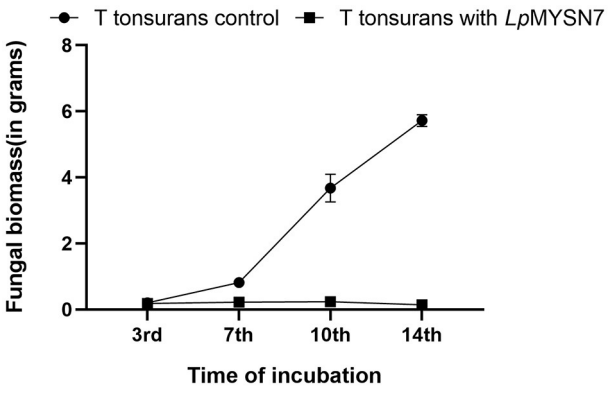

FIGURE 5
Growth rate of *T. tonsurans* with and without LpMYSN7 at different time intervals: 3, 7, 10, and 14 days of incubation. Data shown are mean ± SE of triplicate values of independent experiments and differ significantly ($p < 0.0001$).

is an indication of its avirulent character when compared to the control strain *S. aureus* (MTCC 87), which showed β hemolysis on the blood agar plate (Figure 5).

Anti-*Trichophyton* activity of LpMYSN7

Trichophyton tonsurans inhibition by LpMYSN7 in co-inoculation

Growth inhibition studies in liquid culture were carried out by co-inoculation of the *T. tonsurans* spores and the cells of LpMYSN7 in modified MRS broth. Biomass of fungal culture was measured after 3, 7, 10, and 14 days. It was found that *T. tonsurans* culture biomass increased constantly over the 14-day incubation period from 0.201 to 5.720 g in the control flask but showed no significant growth ($p < 0.001$) when grown with *Lactiplantibacillus* culture (Figures 5, 6), whereas the bacteria were found to survive throughout the incubation period with an initial increase in the concentration of cells followed by a steady decline of cells with increasing incubation time (Table 3).

Biomass inhibition of *T. tonsurans* by CFS-LpMYSN7

When the biomass of dermatophyte culture grown in SDB with different concentrations of CFS of the LpMYSN7 was weighed after 10 days of incubation, a gradual reduction in mycelial growth of

10.3389/fmicb.2023.1192449

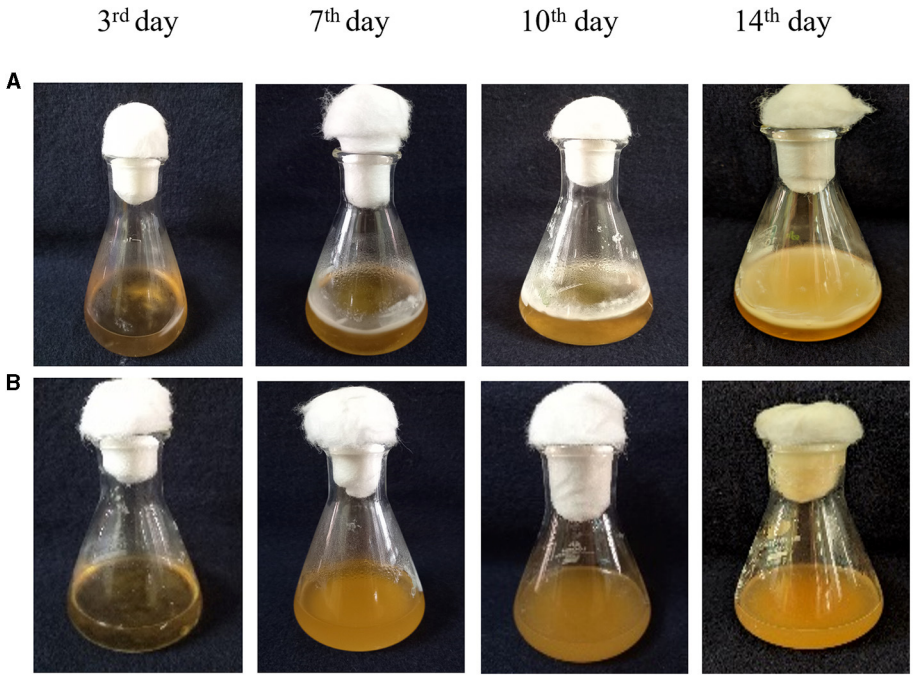

FIGURE 6
Co-inoculation of LpMYSN7 with *Trichophyton tonsurans* spores. **(A)** Growth of *T. tonsurans* (control) showing a dense mycelial mat after 14 days of incubation. **(B)** *T. tonsurans* showing no significant increase in growth when inoculated with LpMYSN7.

TABLE 3 Growth kinetics of *T. tonsurans* and LpMYSN7 co-inoculated in modified MRS broth.

Days	Biomass (g)		Log CFU ml^{-1}	
	Tt control	Tt + LpMYSN7	LpMYSN7 control	Tt + LpMYSN7
3	0.20 ± 0.01	0.18 ± 0.01	9.22 ± 0.05	9.16 ± 0.04
7	0.82 ± 0.01	0.22 ± 0.02	9.23 ± 0.07	9.09 ± 0.18
10	3.67 ± 0.42	0.24 ± 0.00	6.09 ± 0.10	5.91 ± 0.18
14	5.72 ± 0.17	0.14 ± 0.03	4.09 ± 0.05	3.97 ± 0.11

n = 3.
Mean ± SD; Tt, Trichophyton tonsurans; LpMYSN7, Lactiplantibacillus plantarum MYSN7.

1.058, 0.594, 0.125, 0.123, and 0.089 g was observed with 2%, 4%, 6%, 8%, and 10% CFS, respectively, whereas the biomass of the control was 1.632 g after the same period of incubation (Figure 7).

Conidial germination inhibition

This assay showed inhibition of conidial germination with CFS-LpMYSN7 when observed at different intervals of time for 3 days. In the control, the germination of conidia was initiated at 16 h and reached a maximum of more than 95% after 48 h of incubation, and at 72 h, 100% germination was observed (Figure 8A), whereas, in CFS-treated conidia, the germination was negligible even after 72 h of incubation exhibiting the effective control of conidial germination ($p < 0.001$) by CFS-LpMYSN7 (Figure 8B). The percentage of conidial germination of *T. tonsurans* conidiospores inoculated in CFS-treated SDB was negligible with 0, 8.69 ± 0.9, 3.92 ± 0.3, 6.67 ± 0.3, 4.55 ± 0.7, 4.76 ± 0.3, and 2.22 ± 1.4 germination percentage at 2, 4, 8, 16, 24, 48, and 72 h, respectively (Figure 9).

MIC determination

The anti-*Trichophyton* activity of lyophilized extract of CFS-LpMYSN7 (CFSp) was carried out with different concentrations of the dried extract (8–0.0625 mg/ml). CFSp showed promising activity, with a MIC value of 8 mg/ml against *T. tonsurans*. At this concentration, visual growth of the fungi could not be observed in the microtiter plate, and the conidial germination inhibition was found to be ~88.6 ± 1.6%. The inhibition percentage kept decreasing at increasing dilutions of the lyophilized extract, which has been plotted in the graph (Figure 10). The anti-*Trichophyton* activity of CFSp was compared with the standard antifungal drug ketoconazole with concentrations of 8–0.06 μg/ml, and the MIC value for the same was 1.0 μg/ml, showing conidial germination inhibition of 92.9 ± 2.3%.

Characterization of CFS-LpMYSN7

When the CFS was subjected to heat treatment, proteinase-K treatment, freeze–thaw cycle, or long-term storage, its antidermatophytic activity was unaffected as we could observe no growth in the wells filled with treated CFS and inoculated with spores of *T. tonsurans*. On the contrary, profuse growth could be observed in the well containing pH-neutralized CFS of LpMYSN7 and in the control (Figure 11). This indicates that the antifungal metabolites in the CFS are acidic in nature, which prompted further investigation of CFS for its organic acid content.

Organic acid profiling

During LC-MS/MS analysis of the CFS-LpMYSN7, a mixture of organic acids was detected (Table 4). They were identified as succinic acid, lactic acid, pyruvic acid, malonic acid, maleic

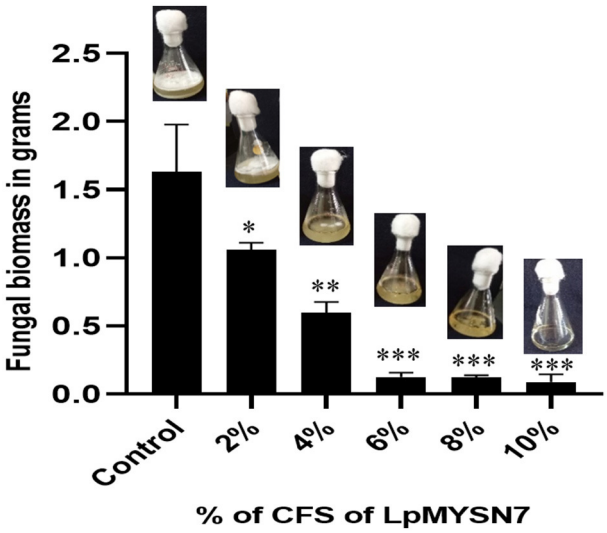

FIGURE 7
Biomass inhibition of *Trichophyton tonsurans* after 10 days of incubation in the presence of different concentrations (2%, 4%, 6%, 8%, and 10%) of sterile CFS-LpMYSN7 compared with the positive control. Data shown are mean ± SE of triplicate values of independent experiments and differ significantly (*$p < 0.05$; **$p < 0.01$; ***$p < 0.001$).

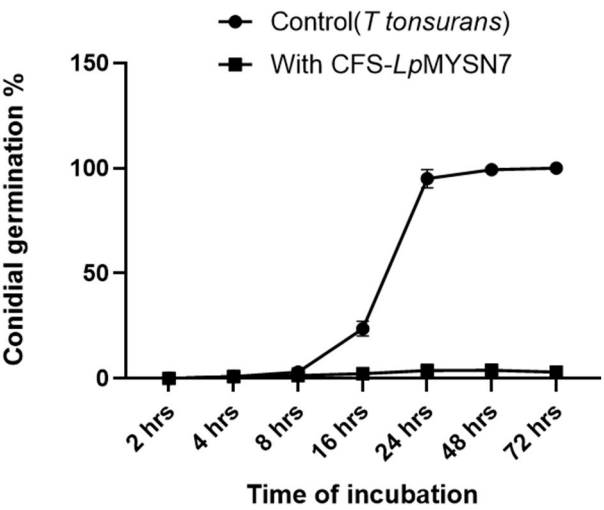

FIGURE 9
Percentage of conidial germination of *T. tonsurans* control and the conidia treated with CFS-LpMYS7 at different time intervals of 2, 4, 8, 16, 24, 48, and 72 h. Data shown are mean ± SE of triplicate values of independent experiments and differ significantly ($p < 0.0001$).

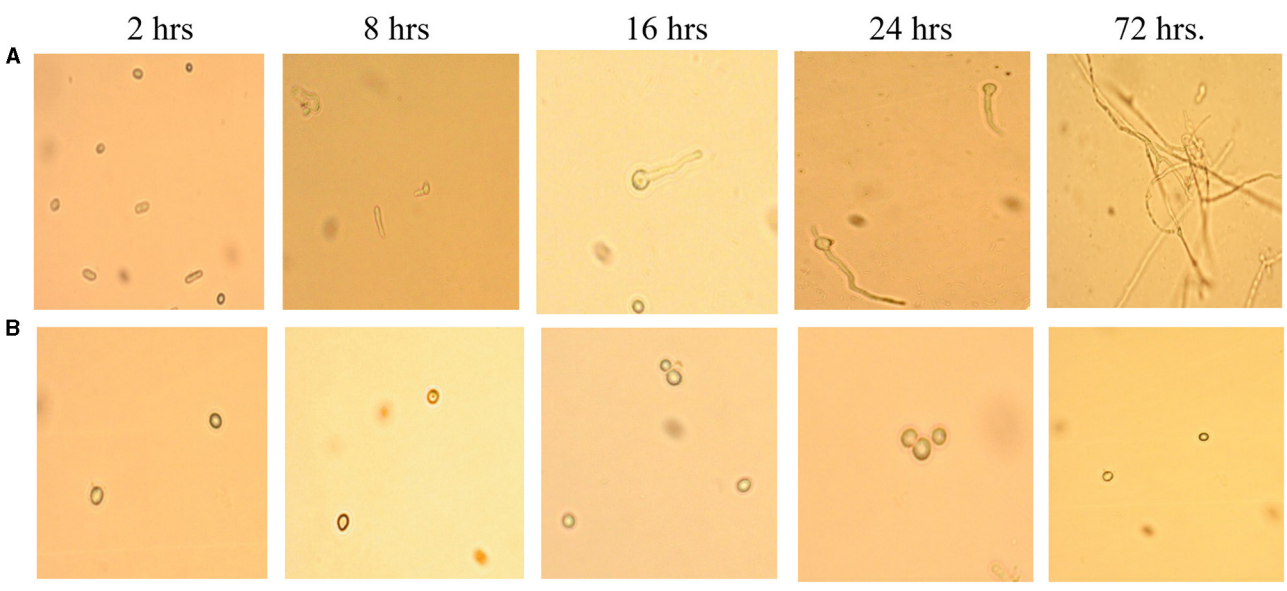

FIGURE 8
Effect of CFS-LpMYS7 on the conidial germination of the fungal pathogen. **(A)** Control—Conidia of *T. tonsurans* showing germination at 2, 8, 16, 24, and 72 h. **(B)** Conidia treated with CFS-LpMYSN7 showing retarded germination at the same time intervals.

acid, fumaric acid, malic acid, shikimic acid, citric acid, and hydroxycitric acid. Among these, the predominant acids were succinic and lactic acid at a concentration of 9,793.60 and 2,077.86 μg/ml, respectively.

SEM analysis of LpMYSN7 effect on *T. tonsurans*

Antifungal compounds present in the CFS of LpMYSN7 had an observable effect on the hyphal morphology as can be observed in the SEM images (Figure 12). Evident mycelial disintegrations were observed in the hyphal wall taken from the inhibited zone (Figure 12c), and the extent of hyphal branching was also significantly retarded (Figure 12d) when compared to the control. Mycelia were less healthy with constrictions and bulged termini (Figures 12b, d), whereas, in the case of the control, no such effects could be detected. The mycelia were intact and healthy (Figure 12a).

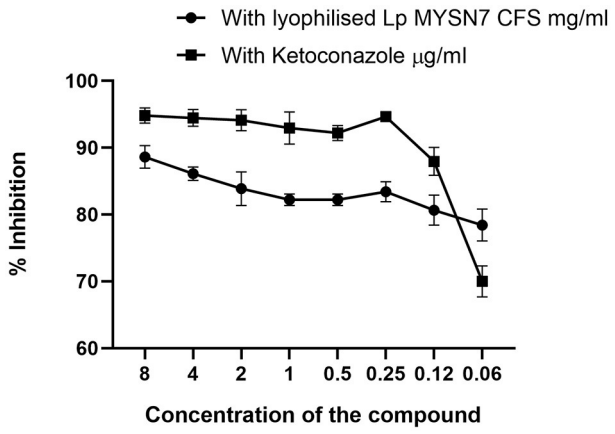

FIGURE 10
Inhibition of *T. tonsurans* in different concentrations of lyophilized CFS-LpMYSN7 and ketoconazole. Data shown are mean ± SE of triplicate values of individual experiments and differ significantly ($p < 0.0001$).

Discussion

This study focussed on the screening of antifungal activity of *Lactiplantibacillus* spp. isolated from the fermented rice beverage, Haria. Previously, the same ethnic food was investigated for the composition of microbial consortia that developed during fermentation. It was found that molds and yeasts were present in

TABLE 4 Organic acid profiling of the cell-free supernatant of *Lp*MYSN7.

Organic acids	IUPAC name	Concentration (μg/ml)
Lactic acid	2-Hydroxypropanoic acid	2077.86
Pyruvic acid	2-oxopropanoic acid	201.66
Malonic acid	propanedioic acid	93.96
Maleic acid	(2*Z*)-But-2-enedioic acid	11.06
Fumaric acid	(2*E*)-But-2-enedioic acid	9.67
Succinic acid	Butane-1,4-dioic acid	9793.60
Malic acid	2-Hydroxybutanedioic acid	11.66
Tartaric acid	2,3-Dihydroxybutanedioic acid	3.60
Shikimic acid	3*R*,4*S*,5*R*)-3,4,5-Trihydroxy cyclohex-1-ene-1-carboxylic acid	10.27
Citric acid	2-Hydroxypropane-1,2,3-tricarboxylic acid	11.72
Hydroxycitric acid	1,2-Dihydroxypropane-1,2,3-tricarboxylic acid	15.07

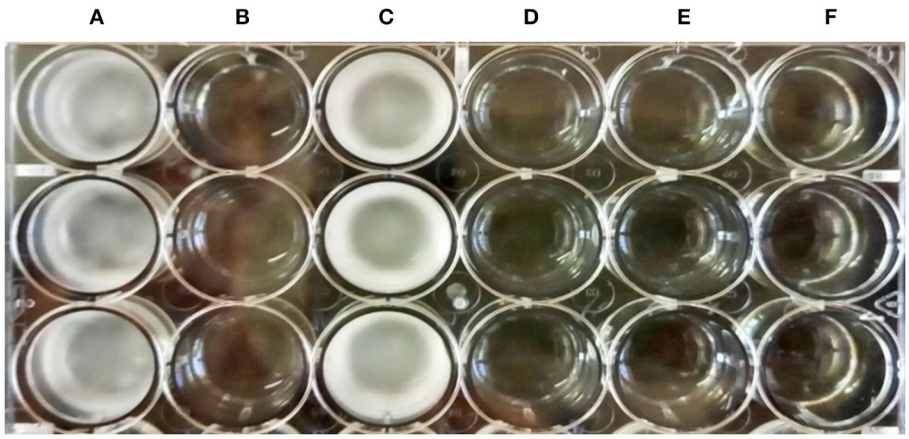

FIGURE 11
Antifungal activity of the treated CFS-LpMYSN7 against *T. tonsurans*. **(A)** Control well with SDB inoculated with the pathogen. **(B)** Heat-treated CFS + Pathogen showing no growth. **(C)** Neutralized CFS + Pathogen. **(D)** Proteinase-K-treated CFS + Pathogen. **(E)** Frozen and thawed CFS + Pathogen. **(F)** Long-term-stored CFS + Pathogen.

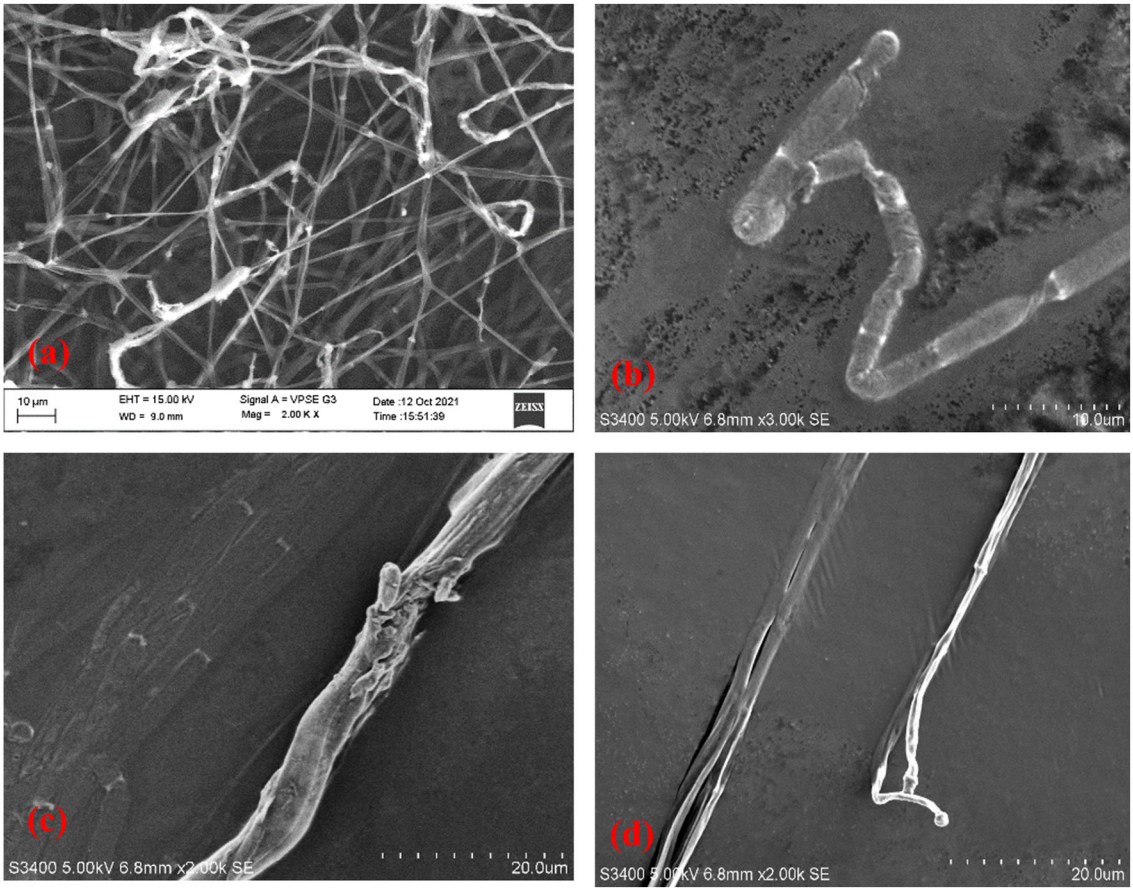

FIGURE 12
Scanning electron micrographs of *T. tonsurans*. **(a)** Control—profusely branched hyphae. **(b–d)** Scanty branching and twisting of the hyphae, disruption in the cell wall, and a bulged terminus.

high numbers during the early fermentation period followed by *Lactobacillus* and *Bifidobacteria,* which were predominant at the end (Ghosh et al., 2015). Ray et al. (2017) further investigated the probiotic attributes of *Bifidobacterium* sp MKK4 isolated from Haria and suggested its use as a potent probiotic agent. In our study, we have made an attempt to isolate and study the probiotic characteristics of *Lactiplantibacillus* spp. from this beverage and also studied the antifungal activity of one of the strains LpMYSN7 against the dermatophytic fungi *Trichophyton tonsurans,* an emerging pathogen of tinea capitis (Müller et al., 2021).

Of the 20 LAB strains that were isolated, the MYSN7 strain later identified as *L. plantarum* exhibited maximum antifungal activity during the preliminary screening. This strain was selected to further evaluate its probiotic and anti-*Trichophyton* activity. The purpose of doing such a study is to explore the application of a probiotic isolate with potential antifungal activity that could be used against skin infections. LAB have long been proven to have different types of antimicrobial activity and are regarded safe owing to their presence in fermented foods (Rawat et al., 2018) and their association with the mammalian intestine (Reale et al., 2015). Studies have convincingly shown that the intake of probiotics helps to stop and treat skin conditions (Fabbrocini et al., 2016). Some early studies recommend the advantages of probiotics, e.g. that they introduce healthy microorganisms to the gut and make a barrier to prevent inflammation, which may trigger certain skin conditions (Holz et al., 2017). The World Health Organization has researched the result of probiotics on skin diseases and stated that there is strong proof of the role of probiotics in treating skin diseases. Thus, the development of probiotic formulations that could be applied topically is an exciting area of analysis, and also many makers are currently exploring the idea of adding either cells or extracts of probiotics in skin care products such as moisturizers, lotions, cleansers, and peels (Bernard and Fr, 2017; Angeles and Angeles, 2019).

L. plantarum MYSN7 strain, which was identified by 16S rRNA sequencing, has indicated potential probiotic characteristics with an acid tolerance of 75% and 70% survival percentage in pH 3 and pH 2, respectively. This acid tolerance character of *L. plantarum* was attributed to the transcriptional and physiological response of the species under acid stress. There is an upregulation of gene expression involved in the production of alkali and synthesis of saturated fatty acids and cyclopropane fatty acids of cell membranes in acid-challenged cells, causing a significant reduction in membrane fluidity (Huang et al., 2016). Our study displayed

the bile salt tolerance level of LpMYSN7 as 68.73% in 0.3% ox gall after 3 h of incubation. This is a moderately bile-tolerant strain as shown by Hamon et al. (2011) who compared the bile salt tolerance properties of nine *L. plantarum* strains. The investigation led to the identification of six proteins that may play a key role in the bile salt response and adaptation in *L. plantarum*: two glutathione reductase enzymes involved in protection against oxidative stress caused by bile salts, a cyclopropane fatty acyl-phospholipid synthase protein implicated in maintaining cell envelope integrity, a bile salt hydrolase enzyme, an ABC transporter, and an F0F1-ATP synthase that play a part in the active removal of bile-related stress factors (Argyri et al., 2013). The study further proves that this tolerance character is strain-dependent as some of the strains of *L. plantarum* were highly resistant to bile, showing a survival percentage of 85%−97%, while some strains had a moderate tolerance of 66 to 81%. Hence, the study of bile tolerance needs to be carried out for any new isolate.

Cell surface hydrophobicity is an important property of the adhesion capacity of probiotics to the intestinal mucosa. Microbial adhesion to hydrocarbons (MATH) analysis of *L. plantarum* strains by Yadav et al. (2013) indicated that while 40% of the strains have a low percentage of hydrophobicity (<25%), only 20% have a higher percentage of hydrophobicity (>35%). The strain *Lp91* has exhibited the maximum hydrophobicity of 37.9 and 39.4% to toluene and hexadecane, respectively. All these were fecal isolates. In another study, 18 strains of *L. plantarum* isolated from various sources were analyzed for their adhesion capacity to xylene and chloroform. The five strains from infant feces show extraordinarily high hydrophobicity, ranging from 65% to 80%, while the remaining strains from traditional fermented fish and shrimp intestines had hydrophobicity ranging from 30% to 50%. This indicates that the adhesion capacity of the strains depends on their isolation habitats (Buntin et al., 2017). Comparatively, our strain LpMYSN7 isolated from fermented rice beverage has shown strong cell surface hydrophobicity of 48.87% and an auto-aggregation percentage of 80.62%. Furthermore, the organism has exhibited effective antibacterial activity against common human pathogens, such as *S. aureus, S. paratyphi, K. pneumoniae, E. coli,* and *P. aeruginosa*. There are several mechanisms through which this biological activity can be accomplished, the principal of which include competition for nutrients and adhesion sites, inducing changes in environmental conditions that are unfavorable to pathogenic bacterial growth, production of antimicrobial metabolites, and finally modulating the host immune responses (Nair et al., 2017). Comparative analysis of the antimicrobial activity of different probiotic strains has shown that *L. plantarum* often displays a broad capacity to inhibit pathogens among *Lactobacilli* species (Davoodabadi et al., 2015; Divyashree et al., 2021, 2022).

In addition, knowing about the isolate's susceptibility to commonly used antibiotics is essential to find the risk of transfer of antibiotic resistance genes (Argyri et al., 2013). LpMYSN7 has shown sensitivity to most of the commonly used antibiotics. This sensitivity pattern gives assurance that the organism is totally safe as a probiotic agent. Though the isolate shows resistance to vancomycin, it is detected to be an intrinsic resistance character (Delcour et al., 1999). In addition, mutations in chromosomes leading to drug resistance have been detected in lactobacilli (Taylor et al., 2015). However, the risk of transfer is considered very low in both intrinsic resistance and acquired resistance due to chromosomal mutations (Gueimonde et al., 2013).

The anti-*T. tonsurans* activity of LpMYSN7 was tested in both solid and liquid media. In the agar overlay assay, the isolate showed strong inhibition of + + + (inhibition zone covering 8–10% of the agar plate) when compared to the other two strains selected for the study. This prompted us to select this strain to proceed with further analysis. When the chosen strain was tested against the fungi in a liquid medium (modified MRS broth), the result was encouraging as the antifungal activity was found to be comparable to that of the agar overlay assay. During the 14-day incubation period, the growth of *T. tonsurans* in the presence and absence of LpMYSN7 was measured by fungal biomass gain. The biomass of the fungi did not show any increase at the end of the incubation period with LpMYSN7 cells when compared to the control in which the weight of the mycelial mat increased exponentially from 0.201 to 5.720 g after 14 days. In a similar study by Guo et al. (2012), five LAB strains, namely *Lactobacillus reuteri R2, Lactobacillus reuteri ee1p, Lactobacillus brevis JJ2P, Lactobacillus arizonensis R13,* and *Lactobacillus casei R20,* which had shown strong antifungal activity during preliminary screening, were tested against *T. tonsurans,* and among those, *L. reuteri* R2 was found to be the most active against the fungi, affirming that the antifungal activity of the LAB is strain specific.

To see the antifungal activity of the cell-free supernatant of LpMYSN7 (CFS-LpMysN7), different concentrations of the sterile CFS were added to the medium inoculated with *T. tonsurans* spores. At a minimum of 6% concentration, the fungal growth was inhibited almost fully with negligible biomass of the fungi (0.125 ± 0.03 g) when compared to the control, which gave 1.632 ± 0.3 g after the same period of incubation. Such biomass assays were usually not performed with dermatophytic fungi, and for the first time, we tested the effect of LAB cells and their CFS on the growth of such fungi by studying the effect on biomass. However, the biomass assay has been performed for studying the control of other fungi, such as *Aspergillus parasiticus*, *F. proliferatum,* and *Aspergillus ochraceus* (Rao et al., 2019; Deepthi et al., 2016; Adithi et al., 2022).

The germination of the microconidia of *T. tonsurans* and mycelial growth was examined in the presence of CFS and compared with the control. At 6% concentration, the percentage of conidial germination was between 4 and 6% even after 72 h of incubation. However, at the same incubation period, 100% germination was seen with the control. This is comparable with another study carried out by Guo et al. (2012) in which it was detected that in the control, maximum germination (95%) of *T. tonsurans* microconidia was obtained after the incubation period of 21 h and in the presence of 10% freeze-dried CFS of the *L. reuteri* producer strain (cfsp), the germination and mycelial growth were completely inhibited. Interestingly, we could obtain the same effect with our crude extract.

A study of the MIC of freeze-dried CFS powder (CFSp-LpMYSN7) was carried out, which showed visual inhibition of the fungi in the microtiter plate at a concentration of 8 mg/ml with a conidial germination inhibition of approximately 90%, whereas the standard antifungal drug showed the same level of inhibition at 1.0 μg/ml with a conidial inhibition percentage of

92.9%. This difference in concentration could be because of the crude nature of our CFS powder when compared to the highly purified standard antifungal drug. To know the exact nature of the antifungal compound that is the crude extract, CFS characterization was performed, and from this, it was inferred that the antifungal effect is mainly because of the acidic nature of the extract. In organic acid profiling, the predominant acids found included succinic acid (9,793.60 μg/ml) and lactic acid (2,077.86 μg/ml). Previously, *L. plantarum* has been shown to produce organic acids, such as phenyl lactic acid (Maikhan and Researcher, 2018), benzene acetic acid, 2-propenyl ester (Wang et al., 2012), oleic acid (Rao et al., 2019), 10-octadecenoic acid, palmitic acid, heptadecanoic acid, stearic acid, and lauric acid (Deepthi et al., 2016). Nevertheless, the antifungal effect seemed to be maximal with the use of a mixture of organic acids rather than any single acid (Danial et al., 2021).

In addition to this, we wanted to see the effect of LpMYSN7 on the morphology of *T. tonsurans*. SEM analysis of the treated fungal hyphae showed different morphological anomalies when compared to the untreated control. The same anomalies have been detected in *T. tonsurans* when it was made to grow in the presence of a plant product, i.e., chicory extracts in which the hyphae become warped, with amorphous fibrillar extruded material and twisted hyphae (Mares et al., 2005).

Future experiments will be focussed on studying the effect of LpMYSN7 cells and its CFS in *in vivo* conditions to know the prospects of using it as a potential antidermatophytic formulation.

Conclusion

This study demonstrated that *L. plantarum* MYSN7 has been identified as a new probiotic candidate with antifungal attributes against *Trichophyton tonsurans*. The *L. plantarum* MYSN7 and its CFS were able to control *T. tonsurans* at the hyphal level, biomass production inhibition, and the inhibition of conidial germination. It will further be tested for the isolate's ability to control biofilm formation in the dermatophyte, which has been implicated as the important virulence factor in causing infection. This study highlighted the occurrence of probiotic *Lactiplantibacillus* spp. in this type of rice-based fermented beverage, and there is enough scope to exploit their bio-therapeutic potential in the future.

Data availability statement

The datasets presented in this study can be found in online repositories. The names of the repository/repositories and accession number(s) can be found in the article/Supplementary material.

Author contributions

PRV analyzed the data and wrote the manuscript. PRV and IP carried out the research activities. MYS, SD, and RS gave technical guidance during the experiment and assisted in software handling. MYS and PRV designed the research and edited and submitted the final version of the manuscript. All authors read and approved for publication.

Acknowledgments

We are grateful to the Institution of Excellence, University of Mysore, for their support in carrying out the SEM analysis. We acknowledge the help from ICAR-IIHR, Bangalore, India, with the antimicrobial compound analysis.

Conflict of interest

The authors declare that the research was conducted in the absence of any commercial or financial relationships that could be construed as a potential conflict of interest.

Publisher's note

Supplementary material

The Supplementary Material for this article can be found online at: https://www.frontiersin.org/articles/10.3389/fmicb.2023.1192449/full#supplementary-material

FIGURE S1
Hemolytic activity on blood agar plate **(a)** MYSN7 showing no hemolysis **(b)** Control showing beta hemolysis.

References

Achar, P. N., Quyen, P., Adukwu, E. C., Sharma, A., Msimanga, H. Z., Nagaraja, H., et al. (2020). Investigation of the antifungal and anti-aflatoxigenic potential of plant-based essential oils against *Aspergillus flavus* in peanuts. *J. Fungi.* 6, 383. doi: 10.3390/jof6040383

Adithi, G., Somashekaraiah, R., Divyashree, S., Shruthi, B., and Sreenivasa, M. Y. (2022). Assessment of probiotic and antifungal activity of *Lactiplantibacillus plantarum* MYSAGT3 isolated from locally available herbal juice against mycotoxigenic *Aspergillus* species. *Food Biosci.* 50, 102118. doi: 10.1016/j.fbio.2022.102118

Ajah, H. A. (2016). *In vitro* and *in vivo* studies on the antifungal activity of probiotics and seaweed extract (*Ascophyllum nodosum*). *Int. J. Innov. Sci. Eng. Technol.* 3, 306–312.

Al-Khikani, F. (2020). Dermatophytosis a worldwide contiguous fungal infection: Growing challenge and few solutions. *Biomed. Biotechnol. Res. J.* 4, 117–122. doi: 10.4103/bbrj.bbrj_1_20

Angeles, L., and Angeles, L. (2019). *Probiotic Treatment of Skin Diseases, Disorders, and Infections: Formulations, Methods and Systems*. United States Patent. 2. Patent No: US 10, 238, 597 B2.

Arasu, M. V., Al-Dhabi, N. A., Rejiniemon, T. S., Lee, K. D., Huxley, V. A. J., Kim, D. H., et al. (2014). Identification and characterization of *Lactobacillus brevis* P68 with antifungal, antioxidant and probiotic functional properties. *Indian J. Microbiol.* 55, 19–28. doi: 10.1007/s12088-014-0495-3

Arena, M. P., Capozzi, V., Russo, P., Drider, D., Spano, G., Fiocco, D., et al. (2018). (2018). Correction to: Immunobiosis and probiosis: antimicrobial activity of lactic acid bacteria with a focus on their antiviral and antifungal properties (Applied Microbiology and Biotechnology, 10.1007/s00253-018-9403-9). *Appl. Microbiol. Biotechnol.* 102, 9871. doi: 10.1007/s00253-018-9441-3

Argyri, A. A., Zoumpopoulou, G., Karatzas, K. A. G., Tsakalidou, E., Nychas, G. J. E., Panagou, E. Z., et al. (2013). Selection of potential probiotic lactic acid bacteria from fermented olives by in vitro tests. *Food Microbiol.* 33, 282–291. doi: 10.1016/j.fm.2012.10.005

Bajpai, V. K., Yoon, J. I., and Kang, S. C. (2017). Antifungal potential of essential oil and various organic extracts of Nandina domestica Thunb. against skin infectious fungal pathogens. *Appl. Microbiol. Biotechnol.* 33, 1127–1133. doi: 10.1007/s00253-009-2017-5

Bengal, L. W., Ghosh, K., Maity, C., Adak, A., Halder, S. K., Jana, A., et al. (2014). Ethnic preparation of Haria, a rice-based fermented beverage, in the province of lateritic West Bengal, India. *Ethnobot. Res. Appl.* 12, 39–49.

Bernard, D., and Fr, V. (2017). *Treatment of Greasy Skin With a Bacterial Lystate*. 2.

Bongomin, F., Gago, S., Oladele, R. O., and Denning, D. W. (2017). Global and multi-national prevalence of fungal diseases-estimate precision. *J. Fungi* 3, 57. doi: 10.3390/jof3040057

Bukhari, S. A., Salman, M., Numan, M., Javed, M. R., Zubair, M., Mustafa, G., et al. (2020). Characterization of antifungal metabolites produced by *Lactobacillus plantarum* and *Lactobacillus coryniformis* isolated from rice rinsed water. *Mol. Biol. Rep.* 47, 1871–1881. doi: 10.1007/s11033-020-05281-1

Buntin, N., de Vos, W. M., and Hongpattarakere, T. (2017). Variation of mucin adhesion, cell surface characteristics, and molecular mechanisms among *Lactobacillus plantarum* isolated from different habitats. *Appl. Microbiol. Biotechnol.* 101, 7663–7674. doi: 10.1007/s00253-017-8482-3

Chandra, N. (2013). Production and partial characterisation of an inducer-dependent novel antifungal compound (s) by Pediococcus acidilactici LAB 5. *J. Sci. Food Agric.* 93, 2455–2453. doi: 10.1002/jsfa.6055

Chen, J., Song, X., Yang, P., and Wang, J. (2015). Appearance of anaphylactic shock after long-term intravenous itraconazole treatment. *Ann. Pharmacother.* 43, 537–541. doi: 10.1345/aph.1L343

Chennappa, G., Naik, M. K., Adkar-Purushothama, C. R., Amaresh, Y. S., and Sreenivasa, M. Y. (2016). PGP, abiotic stress tolerant and antifungal activity of *Azotobacter* sp. isolated from paddy soils. *Indian J. Exp. Biol.* 54, 322–331.

CLSI (2014). *Clinical and Laboratory Standards Institute, M100-S24 Performance Standards for Antimicrobial Susceptibipity Testing; 24th Informational Supplement*.

Danial, A. M., Medina, A., and Magan, N. (2021). *Lactobacillus plantarum* strain HT-W104-B1: potential bacterium isolated from Malaysian fermented foods for control of the dermatophyte *Trichophyton rubrum*. *World J. Microbiol. Biotechnol.* 37, 1–11. doi: 10.1007/s11274-021-03020-7

Davoodabadi, A., Soltan Dallal, M. M., Rahimi Foroushani, A., Douraghi, M., Sharifi Yazdi, M. K., and Amin Harati, F. (2015). Antibacterial activity of *Lactobacillus* spp. isolated from the feces of healthy infants against enteropathogenic bacteria. *Anaerobe* 34, 53–58. doi: 10.1016/j.anaerobe.2015.04.014

Deepthi, B. V., Rao, K. P., Chennapa, G., Naik, M. K., and Chandrashekara, K. T. (2016). Antifungal attributes of *Lactobacillus plantarum* MYS6 against fumonisin producing *Fusarium proliferatum* associated with poultry feeds. *PLoS ONE.* 11, e0155122. doi: 10.1371/journal.pone.0155122

Delcour, J., Ferain, T., Deghorain, M., Palumbo, E., and Hols, P. (1999). The biosynthesis and functionality of the cell-wall of lactic acid bacteria. *Antonie Van Leeuwenhoek* 76, 159–184. doi: 10.1023/A:1002089722581

Divyashree, S., Anjali, P. G., Deepthi, B. V., Somashekaraiah, R., Walid, M., Hammami, R., et al. (2022). Black cherry fruit as a source of probiotic candidates with antimicrobial and antibiofilm activities against Salmonella. *S. Afr. J. Bot.* 150, 861–872. doi: 10.1016/j.sajb.2022.08.045

Divyashree, S., Anjali, P. G., Somashekaraiah, R., and Sreenivasa, M. Y. (2021). Probiotic properties of *Lactobacillus casei* – MYSRD 108 and *Lactobacillus plantarum*-MYSRD 71 with potential antimicrobial activity against *Salmonella paratyphi*. *Biotechnol. Rep.* 32, e00672. doi: 10.1016/j.btre.2021.e00672

Fabbrocini, G., Bertona, M., Picazo, Pareja-Galeano, H., Monfrecola, G., and Emanuele, E. (2016). Supplementation with *Lactobacillus rhamnosus* SP1 normalises skin expression of genes implicated in insulin signalling and improves adult acne. *Benef. Microbes* 7, 625–630. doi: 10.3920/BM2016.0089

Ghosh, K., Ray, M., Adak, A., Dey, P., Halder, S. K., Das, A., et al. (2015). Microbial, saccharifying and antioxidant properties of an Indian rice based fermented beverage. *Food Chem.* 168, 196–202. doi: 10.1016/j.foodchem.2014.07.042

Gueimonde, M., Sánchez, B., de los Reyes-Gavilán, C., and Margolles, A. (2013). Antibiotic resistance in probiotic bacteria. *Front. Microbiol.* 4, 1–6. doi: 10.3389/fmicb.2013.00202

Guo, J., Brosnan, B., Furey, A., Arendt, E. K., Murphy, P., Coffey, A., et al. (2012). Antifungal activity of *Lactobacillus* against *Microsporum canis*, *Microsporum gypseum* and *Epidermophyton floccosum*. *Bioeng. Bugs* 3, 104–113. doi: 10.4161/bbug.19624

Guo, J., Mauch, A., Galle, S., Murphy, P., Arendt, E. K., and Coffey, A. (2011). Inhibition of growth of Trichophyton tonsurans by Lactobacillus reuteri. *J. Appl. Microbiol.* 111, 474–483. doi: 10.1111/j.1365-2672.2011.05032.x

Hamon, E., Horvatovich, P., Izquierdo, E., Bringel, F., Marchioni, E., Aoudé-Werner, D., et al. (2011). Comparative proteomic analysis of Lactobacillus plantarum for the identification of key proteins in bile tolerance. *BMC Microbiol.* 11. doi: 10.1186/1471-2180-11-63

Hay, R. J. (2017). Tinea capitis: current status. *Mycopathologia* 182, 87–93. doi: 10.1007/s11046-016-0058-8

Holz, C., Benning, J., Schaudt, M., Heilmann, A., Schultchen, J., Goelling, D., et al. (2017). Novel bioactive from *Lactobacillus brevis* DSM17250 to stimulate the growth of *Staphylococcus epidermidis*: a pilot study. *Benef. Microbes* 8, 121–131. doi: 10.3920/BM2016.0073

Huang, R., Pan, M., Wan, C., Shah, N. P., Tao, X., Wei, H., et al. (2016). Physiological and transcriptional responses and cross protection of *Lactobacillus plantarum* ZDY2013 under acid stress. *J. Dairy Sci.* 99, 1002–1010. doi: 10.3168/jds.2015-9993

Iván, D., Salazar, O., Alberto, R., Sánchez, H., Sánchez, F. O., Arteaga, M. A., et al. (2015). Antifungal activity of neem (Azadirachta indica: meliaceae) extracts against dermatophytes. *Acta Biol. Colomb.* 20, 201–207. doi: 10.15446/abc.v20n3.45225

Jamwal, A., Sharma, K., Chauhan, R., Bansal, S., and Goel, G. (2019). Evaluation of commercial probiotic lactic cultures against biofilm formation by Cronobacter Sakazakii. *Intest. Res.* 17, 192–201. doi: 10.5217/ir.2018.00106

Kang, M. S., Oh, J. S., Lee, H. C., Lim, H. S., Lee, S. W., Yang, K. H., et al. (2011). Inhibitory effect of Lactobacillus reuteri on periodontopathic and cariogenic bacteria. *J. Microbiol.* 49, 193–199. doi: 10.1007/s12275-011-0252-9

Kleerebezem, M., Kuipers, O. P., and Smid, E. J. (2017). Editorial: Lactic acid bacteria—a continuing journey in science and application. *FEMS Microbiol. Rev.* 41, S1–S2. doi: 10.1093/femsre/fux036

Kuwaki, S., Ohhira, I., Takahata, M., Murata, Y., and Tada, M. (2002). Antifungal activity of the fermentation product of herbs by lactic acid bacteria against tinea. *J. Biosci. Bioeng.* 94, 401–405. doi: 10.1016/S1389-1723(02)80216-X

Lane, D. J., Pace, B., Olsen, G. J., Stahl, D. A., Sogin, M. L., Pace, N. R., et al. (1985). Rapid determination of 16S ribosomal RNA sequences for phylogenetic analyses. *Proc. Natl. Acad. Sci. U. S. A.* 82, 6955–6959. doi: 10.1073/pnas.82.20.6955

Le Lay, C., Coton, E., Le Blay, G., Chobert, J. M., Haertlé, T., Choiset, Y., et al. (2016). Identification and quantification of antifungal compounds produced by lactic acid bacteria and propionibacteria. *Int. J. Food Microbiol.* 239, 79–85. doi: 10.1016/j.ijfoodmicro.2016.06.020

Maikhan, H. K., and Researcher, I. (2018). Study the Effect of *Lactobacillus* spp. on the growth of *Trichophyton rubrum*. *Online Int. Interdiscip. Res. J. VI*, 24–36.

Mares, D., Romagnoli, C., Tosi, B., Andreotti, E., Chillemi, G., Poli, F., et al. (2005). Chicory extracts from *Cichorium intybus* L. as potential antifungals. *Mycopathologia* 160, 85–91. doi: 10.1007/s11046-004-6635-2

Mehdi-Alamdarloo, S., Ameri, A., Moghimipour, E., Gholipour, S., and Saadatzadeh, A. (2016). Formulation development of a topical probiotic gel for antidermatophytosis effect. *Jundishapur J. Nat. Pharm. Prod.* 11. doi: 10.17795/jjnpp-35893

Müller, V. L., Kappa-Markovi, K., Hyun, J., Georgas, D., Silberfarb, G., Paasch, U., et al. (2021). Tinea capitis et barbae caused by *Trichophyton tonsurans*: a retrospective cohort study of an infection chain after shavings in barber shops. *Mycoses* 64, 428–436. doi: 10.1111/myc.13231

Nair, M. S., Amalaradjou, M. A., and Venkitanarayanan, K. (2017). *Antivirulence Properties of Probiotics in Combating Microbial Pathogenesis*. Amsterdam: Elsevier Ltd

Ni, K., Wang, Y., Li, D., Cai, Y., and Pang, H. (2015). Characterization, identification and application of lactic acid bacteria isolated from forage paddy rice silage. *PLoS ONE* 10, e0121967. doi: 10.1371/journal.pone.0121967

Nweze, E. I., and Eke, I. E. (2018). Dermatophytes and dermatophytosis in the eastern and southern parts of Africa. *Med. Mycol.* 56, 13–28. doi: 10.1093/mmy/myx025

Petrucelli, M. F., de Abreu, M. H., Cantelli, B. A. M., Segura, G. G., Nishimura, F. G., Bitencourt, T. A., et al. (2020). Epidemiology and diagnostic perspectives of dermatophytoses. *J. Fungi* 6, 1–15. doi: 10.3390/jof6040310

Ponce, A. G., Moreira, M. R., del Valle, C. E., and Roura, S. I. (2008). Preliminary characterization of bacteriocin-like substances from lactic acid bacteria isolated from organic leafy vegetables. *LWT* 41, 432–441. doi: 10.1016/j.lwt.2007.03.021

Quattrini, M., Bernardi, C., Stuknyt, M., Masotti, F., Passera, A., Ricci, G., et al. (2018). Functional characterization of *Lactobacillus plantarum* ITEM 17215 : a potential biocontrol agent of fungi with plant growth promoting traits, able to enhance the nutritional value of cereal products. *Food Res. Int.* 106, 936–944. doi: 10.1016/j.foodres.2018.01.074

Rao, K. P., Chennappa, G., Suraj, U., Nagaraja, H., Raj, A. P. C., Sreenivasa, M. Y., et al. (2019). Probiotic potential of *Lactobacillus* strains isolated from

sorghum-based traditional fermented food. *Probiotics Antimicrob. Proteins* 7, 146–156. doi: 10.1007/s12602-015-9186-6

Rao, K. P., Deepthi, B. V, Rakesh, S., Ganesh, T., Achar, P., and Sreenivasa, M. Y. (2015). Anti-aflatoxigenic potential of cell free supernatant from Lactobacillus plantarum MYS44 against Aspergillus parasiticus. *Probiotic. Antimicro. Prot.* 11, 55–64. doi: 10.1007/s12602-017-9338-y

Rawat, K., Kumari, A., Kumar, S., Kumar, R., and Gehlot, R. (2018). Traditional fermented products of India. *Int. J. Curr. Microbiol. Appl. Sci.* 7, 1873–1883. doi: 10.20546/ijcmas.2018.704.214

Ray, M., Hor, P. K., Singh, S. N., and Mondal, K. C. (2017). Screening of health beneficial microbes with potential probiotic characteristics from the traditional rice-based alcoholic beverage, haria. *Acta Biol. Szeged.* 61, 51–58. Available online at: http://www2.sci.u-szeged.hu/ABS

Reale, A., Di Renzo, T., Rossi, F., Zotta, T., Iacumin, L., Preziuso, M., et al. (2015). Tolerance of *Lactobacillus casei*, *Lactobacillus paracasei* and *Lactobacillus rhamnosus* strains to stress factors encountered in food processing and in the gastro-intestinal tract. *LWT* 60, 721–728. doi: 10.1016/j.lwt.2014.10.022

Ribeiro, B., Rangel, J., Valentão, P., Andrade, P. B., Pereira, J. A., Bölke, H., et al. (2007). Organic acids in two Portuguese chestnut (Castanea sativa Miller) varieties. *Food Chem.* 100, 504–508. doi: 10.1016/j.foodchem.2005.09.073

Rokana, N., Singh, B. P., Thakur, N., Sharma, C., and Gulhane, R. D. (2018). Screening of cell surface properties of potential probiotic lactobacilli isolated from human milk. *J. Dairy Res.* 85, 347–354. doi: 10.1017/S0022029918000432

Russo, R., Edu, A., and De Seta, F. (2018). Study on the effects of an oral lactobacilli and lactoferrin complex in women with intermediate vaginal microbiota. *Arch. Gynecol. Obstet.* 298, 139–145. doi: 10.1007/s00404-018-4771-z

Salehi, Z., Shams-ghahfarokhi, M., and Razzaghi-abyaneh, M. (2018). Antifungal drug susceptibility profile of clinically important dermatophytes and determination of point mutations in terbinafine-resistant isolates. *Eur. J. Clin. Microbiol. Infect Dis.* 37, 1841–1846. doi: 10.1007/s10096-018-3317-4

Segal, E., and Elad, D. (2021). Human and zoonotic dermatophytoses: epidemiological aspects. *Front. Microbiol.* 12, 1–10. doi: 10.3389/fmicb.2021.713532

Sharma, R., Adhikari, L., and Sharma, R. L. (2017). Recurrent dermatophytosis: a rising problem in Sikkim, a Himalayan state of India. *Indian J. Pathol. Microbiol.* 60, 541–545. doi: 10.4103/IJPM.IJPM_831_16

Singh, A., Masih, A., Monroy-nieto, J., Kumar, P., Bowers, J., Travis, J., et al. (2019). A unique multidrug-resistant clonal *Trichophyton population* distinct from *Trichophyton mentagrophytes*/*Trichophyton interdigitale* complex causing an ongoing alarming dermatophytosis outbreak in India: genomic insights and resistance profile. *Fungal Genet. Biol.* 133, 103266. doi: 10.1016/j.fgb.2019.103266

Sinha, S., and Sardana, K. (2018). Antifungal efficacy of amphotericin B against dermatophytes and its relevance in recalcitrant dermatophytoses: a commentary. *Indian Dermatol. Online J.* 9, 120–122. doi: 10.4103/idoj.IDOJ_103_17

Somashekaraiah, R., Mottawea, W., Gunduraj, A., and Joshi, U. (2021). Probiotic and antifungal attributes of *Levilactobacillus brevis* MYSN105, isolated from an Indian traditional fermented food pozha sampling and isolation of lactic acid. *Front. Microbiol.* 12, 696267. doi: 10.3389/fmicb.2021.696267

Somashekaraiah, R., Shruthi, B., Deepthi, B. V., and Sreenivasa, M. Y. (2019). Probiotic properties of lactic acid bacteria isolated from neera: a naturally fermenting coconut palm nectar. *Front. Microbiol.* 10, 1382. doi: 10.3389/fmicb.2019.01382

Sreenivasa, M. Y., Dass, R. S., Adkar-Purushothama, C. R., Nagendra Prasad, M. N., Achar, P., Ramanayaka, G. J., et al. (2011). Assessment of the growth inhibiting effect of some plant essential oils on different *Fusarium* species isolated from sorghum and maize grains. *J. Plant Dis. Protect.* 118, 208–213. doi: 10.1007/BF03356405

Taylor, P., Georgieva, R., Yocheva, L., Tserovska, L., Zhelezova, G., Atanasova, A., et al. (2015). Biotechnology and biotechnological equipment antimicrobial activity and antibiotic susceptibility of *Lactobacillus* and *Bifidobacterium* spp. intended for use as starter and probiotic cultures. *Biotechnol. Biotechnol. Equip.* 29, 84–91. doi: 10.1080/13102818.2014.987450

Wang, H. K., Yan, Y. H., Wang, J. M., Zhang, H. P., and Qi, W. (2012). Production and characterization of antifungal compounds produced by *Lactobacillus plantarum* IMAU10014. *PLoS ONE* 7, 1–7. doi: 10.1371/journal.pone.0029452

White, T. C., Findley, K., Dawson, T. L., Scheynius, A., Boekhout, T., Cuomo, C. A., et al. (2014). Fungi on the skin: dermatophytes and malassezia. *Cold Spring Harb. Perspect. Med.* 4, a019802. doi: 10.1101/cshperspect.a019802

Yadav, A. K., Tyagi, A., Kaushik, J. K., Saklani, A. C., Grover, S., and Batish, V. K. (2013). Role of surface layer collagen binding protein from indigenous Lactobacillus plantarum 91 in adhesion and its anti-adhesion potential against gut pathogen. *Microbiol. Res.* 168, 639–645. doi: 10.1016/j.micres.2013.05.003

Yadav, R., Puniya, A. K., and Shukla, P. (2016). Probiotic properties of *Lactobacillus plantarum* RYPR1 from an indigenous fermented beverage raabadi. *Front. Microbiol.* 7, 1683. doi: 10.3389/fmicb.2016.01683

Yooussef, M. M., Quyen, P., Achar, P. N., and Sreenivasa, M. Y. (2016). Antifungal activity of essential oils on *Aspergillus parasiticus* isolated from peanuts. *J. Plant Protect. Res.* 56, 139–142. doi: 10.1515/jppr-2016-0021

Frontiers in Microbiology

Explores the habitable world and the potential of microbial life

The largest and most cited microbiology journal which advances our understanding of the role microbes play in addressing global challenges such as healthcare, food security, and climate change.

Discover the latest Research Topics

See more →

Frontiers

Avenue du Tribunal-Fédéral 34
1005 Lausanne, Switzerland
frontiersin.org

Contact us

+41 (0)21 510 17 00
frontiersin.org/about/contact